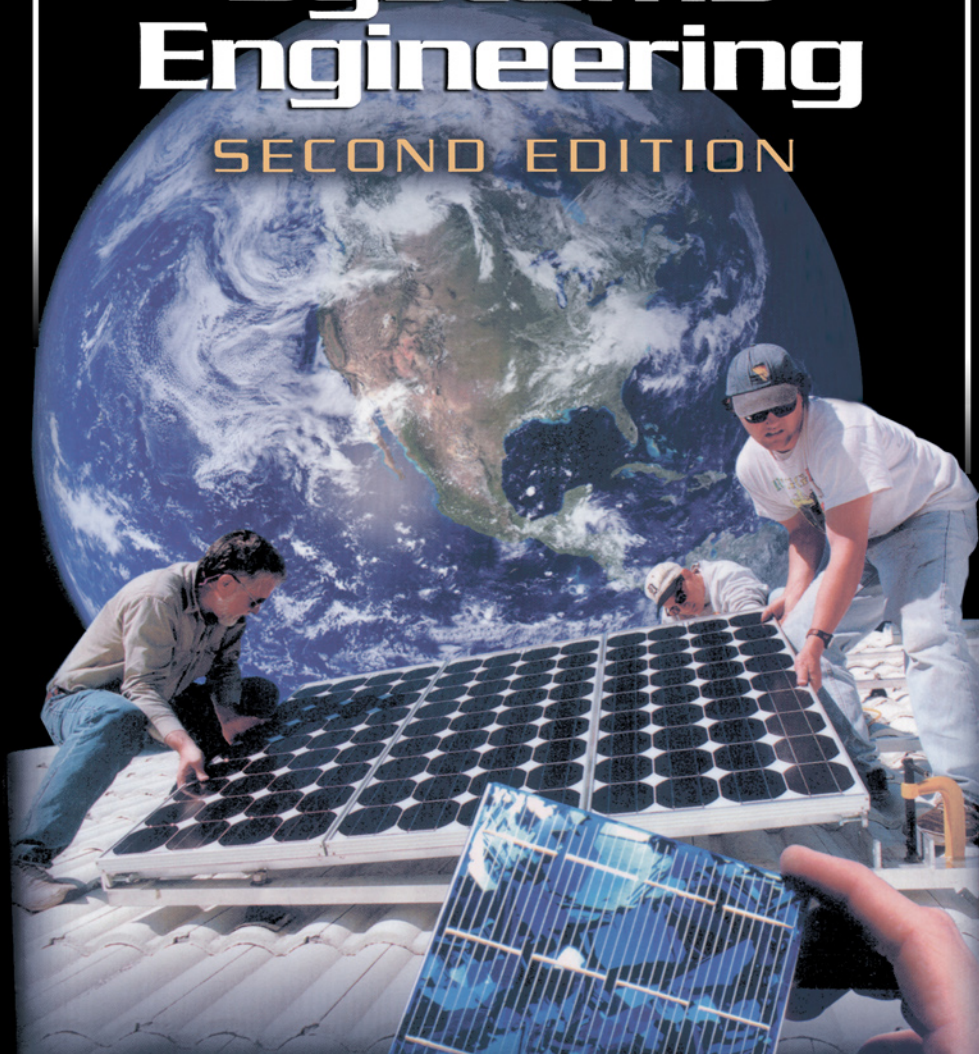


Photovoltaic Systems Engineering

SECOND EDITION



Roger A. Messenger
Jerry Ventre

 CRC PRESS

**Also available as a printed book
see title verso for ISBN details**

Photovoltaic Systems Engineering

SECOND EDITION

Photovoltaic Systems Engineering

SECOND EDITION

**Roger A. Messenger
Jerry Ventre**



CRC PRESS

Boca Raton London New York Washington, D.C.

This edition published in the Taylor & Francis e-Library, 2005.

“To purchase your own copy of this or any of Taylor & Francis or Routledge’s collection of thousands of eBooks please go to www.eBookstore.tandf.co.uk.”

Photo Illustration: Steven C. Spencer, Florida Solar Energy Center

View of the Earth From Space, Western Hemisphere: NASA Goddard Space Flight Center Image by Reto Stöckli. Enhancements by Robert Simmon. Data and technical support: MODIS Land Group; MODIS Science Data Support Team; MODIS Atmosphere Group; MODIS Ocean Group, USGS EROS Data Center, USGS Terrestrial Remote Sensing Flagstaff Field Center..

Library of Congress Cataloging-in-Publication Data

Messenger, Roger.

Photovoltaic systems engineering / Roger Messenger, Jerry Ventre.—
2nd ed.

p. cm.

Includes bibliographical references and index.

ISBN 0-8493-1793-2 (alk. paper)

1. Photovoltaic power systems. 2. Dwellings—Power supply. 3.
Building-integrated photovoltaic systems. I. Ventre, Jerry. II. Title.

TK1087 .M47 2003

621.31'244—dc21

2003053063

This book contains information obtained from authentic and highly regarded sources. Reprinted material is quoted with permission, and sources are indicated. A wide variety of references are listed. Reasonable efforts have been made to publish reliable data and information, but the author and the publisher cannot assume responsibility for the validity of all materials or for the consequences of their use.

Neither this book nor any part may be reproduced or transmitted in any form or by any means, electronic or mechanical, including photocopying, microfilming, and recording, or by any information storage or retrieval system, without prior permission in writing from the publisher.

The consent of CRC Press LLC does not extend to copying for general distribution, for promotion, for creating new works, or for resale. Specific permission must be obtained in writing from CRC Press LLC for such copying.

Direct all inquiries to CRC Press LLC, 2000 N.W. Corporate Blvd., Boca Raton, Florida 33431.

Trademark Notice: Product or corporate names may be trademarks or registered trademarks, and are used only for identification and explanation, without intent to infringe.

Visit the CRC Press Web site at www.crcpress.com

© 2004 by CRC Press LLC

No claim to original U.S. Government works

International Standard Book Number 0-8493-1793-2

Library of Congress Card Number 2003053063

ISBN 0-203-50629-4 Master e-book ISBN

ISBN 0-203-58847-9 (Adobe eReader Format)



**We did not inherit this world from our parents. . . .
We are borrowing it from our children.**
(Author unknown)

**It is our fervent hope that the engineers who read this book
will dedicate themselves to the creation of a world
where children and grandchildren will be left
with air they can breathe and water they can drink,
where humans and the rest of nature
will nurture one another.**

PREFACE

The goal of the first edition of this textbook was to present a comprehensive engineering basis for photovoltaic (PV) system design, so the engineer would understand the *what*, the *why* and the *how* associated with electrical, mechanical, economic and aesthetic aspects of PV system design. The first edition was intended to *educate* the engineer in the design of PV systems so that when engineering judgment was needed, the engineer would be able to make intelligent decisions based upon a clear understanding of the parameters involved. This goal differentiated this textbook from the many design and installation manuals that are currently available that *train* the reader *how* to do it, but not *why*.

Widespread acceptance of the first edition, coupled with significant growth and new ideas in the PV industry over the 3 years since its publication, along with 3 additional years of experience with PV system design and installation for the authors, has led to the publication of this second edition. This edition includes updates in all chapters, including a number of new homework problems and sections that cover contemporary system designs in significant detail. The book is heavily design-oriented, with system examples based upon presently available system components (2003).

While the primary purpose of this material is for classroom use, with an emphasis on the electrical components of PV systems, we have endeavored to present the material in a manner sufficiently comprehensive that it will also serve the practicing engineer as a useful reference book.

The *what* question is addressed in the first three chapters, which present an updated background of energy production and consumption, some mathematical background for understanding energy supply and demand, a summary of the solar spectrum, how to locate the sun and how to optimize the capture of its energy, as well as the various components that are used in PV systems. A section on shading has been added to Chapter 2, and Chapter 3 has been updated to include multilevel H-bridge inverters and linear current boosters.

The *why* and *how* questions are dealt with in the remaining chapters in which every effort is made to explain why certain PV designs are done in certain ways, as well as how the design process is implemented. Included in the *why* part of the PV design criteria are economic and environmental issues that are discussed in Chapters 5 and 9. Chapter 6 has been embellished with additional practical considerations added to the theoretical background associated with mechanical design. Chapters 7 and 8 have been nearly completely reworked to incorporate the most recently available technology and design and installation practice.

Appendix A has been extended to include horizontal and vertical array orientations along with the three array orientations covered in the first edition. Web sites have been updated in Appendix B, and a new Appendix C has been added that presents a recommended format for submittal of a PV design package for permitting or for design review.

A modified top-down approach is used in the presentation of the material. The material is organized to present a relatively quick exposure to all of the building blocks of the PV system, followed by design, design and design. Even the physics of PV cells of Chapter 10 and the material on present and future cells of Chapter 11 are presented with a design flavor. The focus is on adjusting the parameters of PV cells to optimize their performance, as well as on presenting the physical basis of PV cell operation.

Homework problems are incorporated that require both analysis and design, since the ability to perform analysis is the precursor to being able to understand how to implement good design. Many of the problems have multiple answers, such as ‘Calculate the number of daylight hours on the day you were born in the city of your birth.’ We have eliminated a few homework problems based on old technology and added a number of new problems based upon contemporary technology. Hopefully there is a sufficient number to enable students to test their understanding of the material.

We recommend that the course be presented so that by the end of Chapter 4, students will be able to think seriously about a comprehensive design project, and by the end of Chapter 7, they will be able to begin their design. We like to assign two design projects—a stand-alone system based on Chapter 7 material and a utility interactive system based on Chapter 8 material.

While it is possible to cover all the material in this textbook in a 3-credit semester course, it may be necessary to skim over some of the topics. This is where the discretion of the instructor enters the picture. For example, each of the design examples of Chapter 4 introduces something new, but a few examples might be left as exercises for the reader with a preface by the instructor as to what is new in the example. Alternatively, by summarizing the old material in each example and then focusing on the new material, the *why* of the new concepts can be emphasized.

The order of presentation of the material actually seems to foster a genuine reader interest in the relevance and importance of the material. Subject matter covers a wide range of topics, from chemistry to circuit analysis to electronics, solid state device theory and economics. The material is presented at a level that can best be understood by those who have reached upper division at the engineering undergraduate level and have also completed coursework in circuits and in electronics.

We recognize that the movement to reduce credit toward the bachelor’s degree has left many programs with less flexibility in the selection of undergraduate elective courses, and note that the material in this textbook can also be used for a beginning graduate level course.

One of the authors has twice taught the course as an internet course using the first edition of the book. Those students who were actually sufficiently motivated to keep up with the course generally reported that they found the text to be very readable and a reasonable replacement for lectures. We highly recommend that if the internet is tried, that quizzes be given frequently to coerce the student

into feeling that this course is just as important as her/his linear systems analysis course. Informal discussion sessions can also be useful in this regard.

The photovoltaic field is evolving rapidly. While every effort has been made to present contemporary material in this work, the fact that it has evolved over a period of a year almost guarantees that by the time it is adopted, some of the material will be outdated. For the engineer who wishes to remain current in the field, many of the references and web sites listed will keep him/her up-to-date. Proceedings of the many PV conferences, symposia and workshops, along with manufacturers' data, are especially helpful.

This textbook should provide the engineer with the intellectual tools needed for understanding new technologies and new ideas in this rapidly emerging field. The authors hope that at least one in every 4.6837 students will make his/her own contribution to the PV knowledge pool.

We apologize at the outset for the occasional presentation of information that may be considered to be practical or, perhaps, even interesting or useful. We fully recognize that engineering students expect the material in engineering courses to be of a highly theoretical nature with little apparent practical application. We have made every effort to incorporate heavy theory to satisfy this appetite whenever possible.

ACKNOWLEDGMENTS

We are convinced that it is virtually impossible to undertake and complete a project such as this without the encouragement, guidance and assistance from a host of friends, family and colleagues.

In particular, Jim Dunlop provided a diverse collection of ideas for us to develop and Neelkanth Dhere provided insight into the material in Chapters 10 and 11. Paul Maycock was kind enough to share his latest data on worldwide PV shipments and installations. Iraida Rickling once again gave us invaluable library reference support and Dianne Wood did an excellent job on the new Chapter 6 illustrations. And, of course, student feedback on the first edition provided significant insight to the authors on how to make the material easier to understand. We hope we have accomplished this goal.

We asked many questions of many people as we rounded up information for the wide range of topics contained herein. A wealth of information flowed our way from the National Renewable Energy Laboratory (NREL) and Sandia National Laboratories (SNL) as well as from many manufacturers and distributors of a diverse range of PV system components. Special thanks to Dave Collier, Don Mayberry, Jr., John Wiles, Dale Tarrant, Martin Green, Ken Zweibel, Tom Kirk and Brad Bunn for the information they provided.

And, once again, Nancy Ventre was willing to forego the pleasure of Jerry's company while he engaged in his rewrite. We thank her for her support and understanding.

Roger Messenger
Jerry Ventre
2003

ABOUT THE AUTHORS

Roger Messenger is professor of Electrical Engineering at Florida Atlantic University in Boca Raton, Florida. He received his Ph.D. in Electrical Engineering from the University of Minnesota and is a Registered Professional Engineer and a Certified Electrical Contractor, who enjoys working on a field installation as much as he enjoys teaching a class or working on the design of a system or contemplating the theory of operation of a system. His research work has ranged from electrical noise in gas discharge tubes to deep impurities in silicon to energy conservation. He worked on the development and promulgation of the original Code for Energy Efficiency in Building Construction in Florida and has conducted extensive field studies of energy consumption and conservation in buildings and swimming pools.

During his tenure at Florida Atlantic University he has worked his way through the academic ranks and has also served in administrative posts for 11 years, including Department Chair, Associate Dean and Director of the FAU Center for Energy Conservation. He has received three university-wide awards for teaching over his 34 years at FAU, and currently advises half the undergraduate EE majors. Recently he has been actively involved with the Florida Solar Energy Center in the development of courses, exams and study guides for voluntary certification of PV installers.

Jerry Ventre is director of the Photovoltaics and Distributed Generation Division of the Florida Solar Energy Center (FSEC), a research institute of the University of Central Florida. He received his B.S., M.S., and Ph.D. degrees in aerospace engineering from the University of Cincinnati and has more than 30 years of experience in various aspects of engineering, including research, development, design and systems analysis. He served on the aerospace engineering faculties of both the University of Cincinnati and the University of Central Florida, is a Registered Professional Engineer, and, among many courses, taught photovoltaic systems at the graduate level. He has designed solid rocket motors and jet engines for the Advanced Engine Technology Department of the General Electric Company, and has performed research for numerous agencies, including NASA, Sandia National Laboratories, Oak Ridge National Laboratory, U.S. Navy, the FAA and the U.S. Department of Energy. He has been active in technical societies and has been the recipient of a number of awards for contributions to engineering and engineering education.

TABLE OF CONTENTS

Chapter 1 BACKGROUND

1.1 Introduction	1
1.2 Energy Units	2
1.3 Current World Energy Use Patterns	2
1.4 Exponential Growth	6
1.4.1 Introduction	6
1.4.2 Compound Interest	7
1.4.3 Doubling Time.	7
1.4.4 Accumulation	9
1.4.5 Resource Lifetime in an Exponential Environment	10
1.4.6 The Decaying Exponential	12
1.4.7 Hubbert's Gaussian Model	12
1.5 Net Energy, Btu Economics and the Test for Sustainability	14
1.6 Direct Conversion of Sunlight to Electricity with Photovoltaics	15
Problems	17
References	19
Suggested Reading	20

Chapter 2 THE SUN

2.1 Introduction	21
2.2 The Solar Spectrum	21
2.3 The Effect of Atmosphere on Sunlight	23
2.4 Insolation Specifics	25
2.4.1 Introduction	25
2.4.2 The Orbit and Rotation of the Earth	26
2.4.3 Tracking the Sun.	29
2.4.4 Measuring Sunlight	31
2.5 Capturing Sunlight	35
2.5.1 Maximizing Irradiation on the Collector	35
2.5.2 Shading	38
2.5.3 Special Orientation Considerations	39
Problems	42
References	45
Suggested Reading	45

Chapter 3 INTRODUCTION TO PV SYSTEMS

3.1 Introduction	47
3.2 The PV Cell	47
3.3 The PV Module	52
3.4 The PV Array	56

3.5 Energy Storage	57
3.5.1 Introduction	57
3.5.2 The Lead-Acid Storage Battery.	57
3.5.3 The Nickel Cadmium Storage Battery	64
3.5.4 Other Battery Systems	66
3.5.5 Hydrogen Storage	67
3.5.6 The Fuel Cell	68
3.5.7 Other Storage Options	70
3.6 PV System Loads	70
3.7 PV System Availability	72
3.8 Associated System Electronic Components	75
3.8.1 Introduction	75
3.8.2 Charge Controllers	76
3.8.3 Maximum Power Trackers and Linear Current Boosters	80
3.8.4 Inverters	83
3.9 Generators	92
3.9.1 Introduction	92
3.9.2 Types and Sizes of Generators	93
3.9.3 Generator Operating Characteristics	94
3.9.4 Generator Maintenance	97
3.9.5 Generator Selection	97
3.10 Wiring and Code Compliance	98
3.10.1 Introduction	98
3.10.2 The <i>National Electrical Code</i>	98
3.10.3 IEEE Standard 929-2000.	103
3.11 Balance of System Components	105
Problems	105
References	109
Suggested Reading	110

Chapter 4 PV SYSTEM EXAMPLES

4.1 Introduction	111
4.2 Example 1: A Simple PV-Powered Fan	111
4.2.1 The Simplest Configuration: Module and Fan	111
4.2.2 PV Fan with Battery Backup	114
4.3 Example 2: A PV-Powered Water Pumping System with Linear Current Booster	116
4.3.1 Determination of System Component Requirements	116
4.3.2 A Simple Pumping System	119
4.3.3 Alternative Design Approach for Simple Pumping System	121
4.4 Example 3: A PV-Powered Area Lighting System	122
4.4.1 Determination of the Lighting Load	122
4.4.2 An Outdoor Lighting System.	124
4.5 Example 4: A PV-Powered Remote Cabin	126

4.6 Example 5: A Hybrid System	128
4.7 Example 6: A Utility Interactive System	130
4.7.1 Introduction	130
4.7.2 A Simple Utility Interactive System with No Battery Storage	132
4.8 Example 7: A Cathodic Protection System	134
4.8.1 Introduction	134
4.8.2 System Design	135
4.9 Example 8: A Portable Highway Advisory Sign	138
4.9.1 Introduction	138
4.9.2 Determination of Available Average Power	139
Problems	141
References	143
Suggested Reading	143

Chapter 5 COST CONSIDERATIONS

5.1 Introduction	145
5.2 Life Cycle Costing	145
5.2.1 The Time Value of Money	145
5.2.2 Present Worth Factors and Present Worth	148
5.2.3 Life Cycle Cost	149
5.2.4 Annualized Life Cycle Cost	151
5.2.5 Unit Electrical Cost	152
5.3 Borrowing Money	152
5.3.1 Introduction	152
5.3.2 Determination of Annual Payments on Borrowed Money	152
5.3.3 The Effect of Borrowing on Life Cycle Cost	154
5.4 Externalities	155
5.4.1 Introduction	155
5.4.2 Subsidies	156
5.4.3 Externalities and Photovoltaics	157
Problems	157
References	158
Suggested Reading	158

Chapter 6 MECHANICAL CONSIDERATIONS

6.1 Introduction	159
6.2 Important Properties of Materials	159
6.2.1 Introduction	159
6.2.2 Mechanical Properties	161
6.2.3 Stress and Strain	163
6.2.4 Strength of Materials.	166
6.2.5 Column Buckling	167
6.2.6 Thermal Expansion and Contraction	167

6.2.7 Chemical Corrosion and Ultraviolet Degradation	169
6.2.8 Properties of Steel	172
6.2.9 Properties of Aluminum	173
6.3 Establishing Mechanical System Requirements	174
6.3.1 Mechanical System Design Process	174
6.3.2 Functional Requirements	175
6.3.3 Operational Requirements	176
6.3.4 Constraints	176
6.3.5 Tradeoffs	177
6.4 Design and Installation Guidelines	177
6.4.1 Standards and Codes	177
6.4.2 Building Code Requirements	179
6.5 Forces Acting on Photovoltaic Arrays	179
6.5.1 Structural Loading Considerations	179
6.5.2 Dead Loads	180
6.5.3 Live Loads	181
6.5.4 Wind Loads	181
6.5.5 Snow Loads	189
6.5.6 Other Loads	189
6.6 Array Mounting System Design	190
6.6.1 Introduction	190
6.6.2 Objectives in Designing the Array Mounting System	190
6.6.3 Enhancing Array Performance	193
6.6.4 Roof-Mounted Arrays	194
6.6.5 Ground-Mounted Arrays	197
6.6.6 Aesthetics	199
6.7 Computing Mechanical Loads and Stresses	200
6.7.1 Introduction	200
6.7.2 Withdrawal Loads	200
6.7.3 Tensile Stresses	201
6.7.4 Buckling	202
6.8 Summary	203
Problems	204
References	207
Suggested Reading	208

Chapter 7 STAND-ALONE PV SYSTEMS

7.1 Introduction	209
7.2 A Critical Need Refrigeration System	210
7.2.1 Design Specifications	210
7.2.2 Design Implementation	210
7.3 A PV-Powered Mountain Cabin	224
7.3.1 Design Specifications	224
7.3.2 Design Implementation	225

7.4 A Hybrid Powered Residence	235
7.4.1 Design Specifications	235
7.4.2 Design Implementation	236
7.5 Seasonal or Periodic Battery Discharge	248
7.6 Battery Connections	249
7.7 Computer Programs	253
Problems	254
References	257
Suggested Reading	257

Chapter 8 UTILITY INTERACTIVE PV SYSTEMS

8.1 Introduction	259
8.2 Nontechnical Barriers to Utility Interactive PV Systems	260
8.2.1 Cost of PV Arrays	260
8.2.2 Cost of Balance of System Components	261
8.2.3 Standardization of Interconnection Requirements	262
8.2.4 PV System Installation Considerations	262
8.2.5 Metering of PV System Output	263
8.3 Technical Considerations for Connecting to the Grid	264
8.3.1 Introduction	264
8.3.2 IEEE Standard 929-2000 Issues	265
8.3.3 <i>National Electrical Code</i> Considerations	271
8.3.4 Other Issues	279
8.4 Small (<10 kW) Utility Interactive PV Systems	281
8.4.1 Introduction	281
8.4.2 Array Installation	283
8.4.3 PCU Selection and Mounting	283
8.4.4 Other Installation Considerations	284
8.4.5 A 2.5 kW Residential Rooftop Utility Interactive PV System . .	285
8.4.6 A Residential Rooftop System Using AC Modules	289
8.4.7 A 4800 W Residential Rooftop System with Battery Storage .	290
8.5 Medium Utility Interactive PV Systems	299
8.5.1 Introduction	299
8.5.2 A 16 kW Commercial Rooftop System	299
8.6 Large Utility Interactive PV Systems	303
8.6.1 Introduction	303
8.6.2 A Large Parking Lot PV System	303
Problems	312
References	316
Suggested Reading	317

Chapter 9 EXTERNALITIES AND PHOTOVOLTAICS

9.1 Introduction	319
9.2 Externalities	319
9.3 Environmental Effects of Energy Sources	321
9.3.1 Introduction	321
9.3.2 Air Pollution.	322
9.3.3 Water and Soil Pollution	323
9.3.4 Infrastructure Degradation	324
9.3.5 Quantifying the Cost of Externalities.	324
9.3.6 Health and Safety as Externalities	328
9.4 Externalities Associated with PV Systems.	328
9.4.1 Environmental Effects of PV System Production	328
9.4.2 Environmental Effects of PV System Deployment and Operation	330
9.4.3 Environmental Effects of PV System Decommissioning	331
Problems	332
References	332

Chapter 10 THE PHYSICS OF PHOTOVOLTAIC CELLS

10.1 Introduction	335
10.2 Optical Absorption.	335
10.2.1 Introduction	335
10.2.2 Semiconductor Materials	335
10.2.3 Generation of EHP by Photon Absorption	337
10.2.4 Photoconductors	339
10.3 Extrinsic Semiconductors and the pn Junction	341
10.3.1 Extrinsic Semiconductors	341
10.3.2 The pn Junction	343
10.4 Maximizing PV Cell Performance	352
10.4.1 Introduction	352
10.4.2 Minimizing the Reverse Saturation Current	352
10.4.3 Optimizing Photocurrent	353
10.4.4 Minimizing Cell Resistance Losses	362
10.5 Exotic Junctions	364
10.5.1 Introduction	364
10.5.2 Graded Junctions	364
10.5.3 Heterojunctions.	366
10.5.4 Schottky Junctions	366
10.5.5 Multijunctions	369
10.5.6 Tunnel Junctions	369
Problems	371
References	372

Chapter 11 PRESENT AND PROPOSED PV CELLS

11.1 Introduction	373
11.2 Silicon PV Cells	374
11.2.1 Production of Pure Silicon	375
11.2.2 Single Crystal Silicon Cells	376
11.2.3 Multicrystalline Silicon Cells	383
11.2.4 Buried Contact Silicon Cells	384
11.2.5 Other Thin Silicon Cells	386
11.2.6 Amorphous Silicon Cells	386
11.3 Gallium Arsenide Cells	389
11.3.1 Introduction	389
11.3.2 Production of Pure Cell Components	389
11.3.3 Fabrication of the Gallium Arsenide Cell	392
11.3.4 Cell Performance	394
11.4 Copper Indium (Gallium) Diselenide Cells	394
11.4.1 Introduction	394
11.4.2 Production of Pure Cell Components	395
11.4.3 Fabrication of the CIS Cell	398
11.4.4 Cell Performance	400
11.5 Cadmium Telluride Cells	401
11.5.1 Introduction	401
11.5.2 Production of Pure Tellurium	402
11.5.3 Production of the CdTe Cell	402
11.5.4 Cell Performance	404
11.6 Emerging Technologies	404
11.6.1 New Developments in Silicon Technology	404
11.6.2 CIS-Family-Based Absorbers	406
11.6.3 Other III-V and II-VI Emerging Technologies	407
11.6.4 Other Technologies	408
11.6.5 Summary	410
Problems	410
References	411
Suggested Reading	413
Appendix A Average Daily Irradiation for Selected Cities	415
Appendix B A Partial Listing of PV-Related Web Sites	431
Appendix C Design Review Checklist	433
Index	437

Chapter 1

BACKGROUND

The Million Solar Roofs Initiative

On June 26, 1997, U.S. President Bill Clinton announced the Million Solar Roofs Initiative (MSRI) to the United Nations Special Session on Environment and Development in New York [1]. ‘Now we will work with businesses and communities to use the sun’s energy to reduce our reliance on fossil fuels by installing solar panels on 1 million more roofs around our nation by 2010. Capturing the sun’s warmth can help us to turn down the Earth’s temperature.’

The following day, U.S. Secretary of Energy Federico Peña commented on the projected accomplishments of the Million Solar Roofs Initiative [2]:

- Slow greenhouse gas emissions
- Expand our energy options
- Create high-technology jobs
- Build on existing momentum
- Keep U.S. companies competitive
- Rely on market forces and consumer choice
- Marshal existing federal resources

Implementation of this ambitious program requires engineers who are knowledgeable in photovoltaic system design. These engineers need to understand the why of photovoltaic systems in order to be able to make intelligent system design choices. Success of the million solar roofs program should provide the momentum for a sustained effort in the deployment of solar technologies well beyond the year 2010. In fact, the MSRI may need to be extended to a 100 Million Solar Roofs Initiative to meet the sustainable energy needs of future generations. This book is dedicated to the engineers and technicians who have been and may become involved in turning this dream into reality.

1.1 Introduction

The human population of the earth has now passed 6 billion [3], and all of these inhabitants want the energy necessary to sustain their lives. Exactly how much energy is required to meet these needs and exactly what sources of energy will meet these needs will be questions to be addressed by the present and by future generations. One certainty, however, is that developing nations will be increasing their per capita energy use significantly. For example, in 1997, the Peoples Republic of China was building electrical generating plants at the rate of 300 megawatts per week. These plants have been using relatively inexpensive, old, inefficient, coal-fired technology and provide electricity to predominantly inefficient end uses [4]. The potential consequences to the planet of continua-

tion of this effort are profound. Before we proceed with the details of photovoltaic power systems, a promising source of energy for the future, it is instructive to look at the current technical and economic energy picture. This look will enable the reader to better assess the contributions that engineers will need to make toward a sustainable energy future for the planet.

1.2 Energy Units

Energy is measured in a number of ways, including the calorie, the Btu, the quad, the foot-pound and the kilowatt hour. For the benefit of those who may not have memorized the appendices of their freshman physics books, we repeat the definitions of these quantities for an earth-based system at or about a temperature of 27°C [5].

1 calorie is the heat needed to raise the temperature of 1 ml of water 1°C.

1 Btu is the heat needed to raise the temperature of 1 lb of water 1°F.

1 quad is 1 quadrillion (10^{15}) Btus.

1 foot-pound is the energy expended in raising 1 lb through a distance of 1 ft.

1 kilowatt hour is the energy expended by 1 kilowatt operating for 1 hour.

With these definitions, the following equivalencies can be determined:

$$\begin{aligned}1 \text{ Btu} &= 252 \text{ calories} \\1 \text{ kWh} &= 3413 \text{ Btu} = 2,655,000 \text{ ft-lb} \\1 \text{ ft-lb} &= 0.001285 \text{ Btu} \\1 \text{ quad} &= 2.930 \times 10^{11} \text{ kWh}\end{aligned}$$

Since the emphasis of this text will be on electrical generation, and since the kWh is the common unit for electrical energy, the equivalence between kWh and ft-lb is especially noteworthy. For example, suppose a 150-lb person wished to generate 1 kWh, assuming a system with 100% efficiency. One way would be to climb to the top of a 17,700-ft mountain to create 1 kWh of potential energy. Then, by returning to sea level by way of a chair, connected via a pulley system to a generator, the person's potential energy could be converted to electrical energy. This kWh could then be sold at wholesale for about 3 cents. Another somewhat simpler method is to burn approximately 11 fluid ounces of petroleum to produce steam to turn a steam turbine as shown in Figure 1.1.

Still another method is to deploy about 2 m² of photovoltaic (PV) cells. This system will produce about 1 kWh per day for 20 years or more with no stops for refueling, no noise, minimal maintenance and no release of CO₂, SO₂ or NO₂ while the electricity is being produced.

1.3 Current World Energy Use Patterns

Figure 1.2 shows the increase in worldwide energy production by source since 1970. In 2000, worldwide annual primary energy consumption reached 397.40 quads [6]. The developed countries of the world consumed approxi-



Figure 1.1 Several ways to produce a kWh of electricity.

mately 75% of this energy, while nearly 2 billion people in developing countries, mostly within the tropics, remained without electricity.

The petroleum curve in Figure 1.2 shows how price can affect energy consumption. It also shows that there can be a time delay between market forces and market responses. Note that the production of petroleum continues upward after the 1973 oil embargo and the subsequent significant petroleum price in-

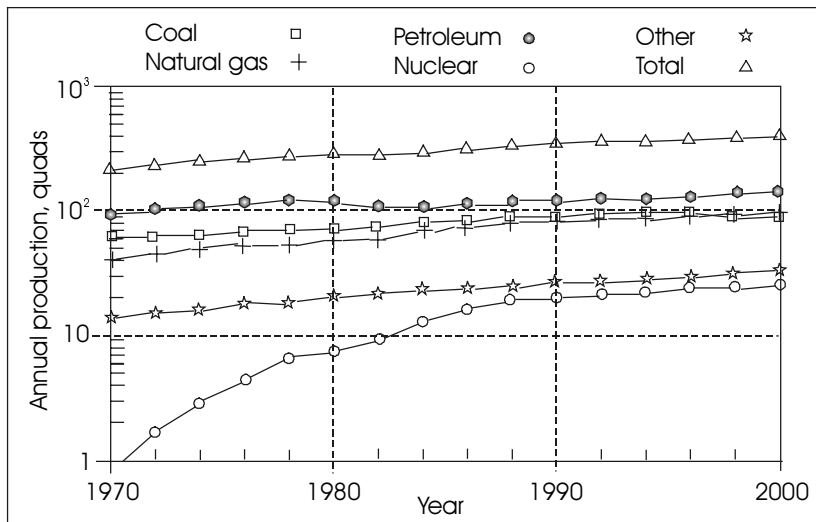


Figure 1.2 Growth of worldwide energy production by source, 1970–2000 (Data from [6]).

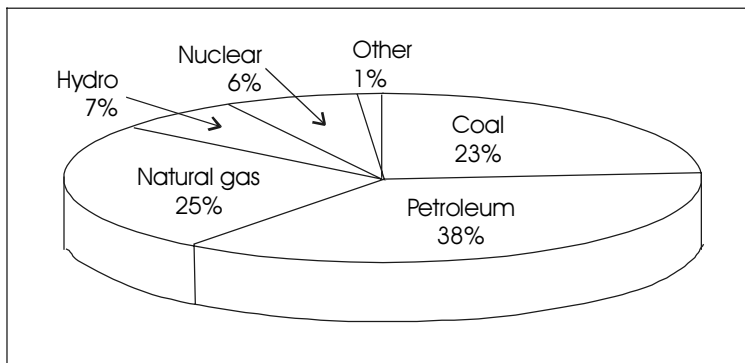


Figure 1.3 2000 Global energy production mix by fuel type (Data from [6]).

creases during the remaining 1970s and early 1980s. During this period, high petroleum prices spurred the development of energy efficiency legislation, such as the National Energy Conservation and Policy Act, codes for energy efficiency in building construction and increased vehicle fleet mileage requirements. Consumers also responded by reducing energy use by lowering thermostats and installing insulation and other energy conservation measures. The result was lower petroleum production for a period in the mid-1980s, since the demand was lower. During this same period, more efficient use of electricity resulted in the cancellation of nuclear plant construction, resulting in a significant decrease in the growth rate of nuclear-produced electricity. Finally, concern over oil price control and embargoes prompted a switch from petroleum to coal and natural gas for use in fossil-fired electrical generation. Figure 1.3 shows the global mix of energy sources in the year 2000. The “other” category includes sources such as wind, biomass, geothermal and photovoltaics.

Figures 1.4 and 1.5 illustrate that the world faces a challenge of mammoth proportions as developing countries strive to achieve energy equity with the de-

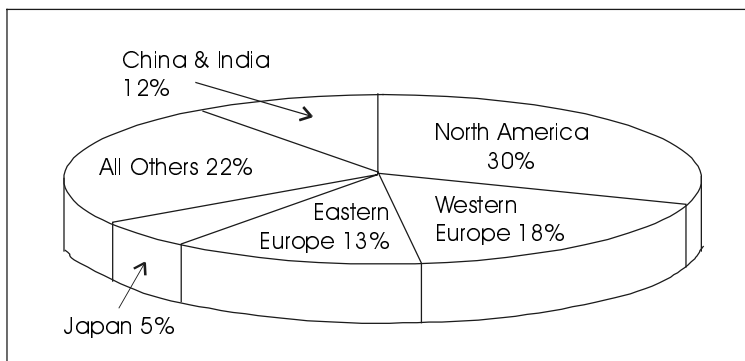


Figure 1.4 2000 Distribution of energy users (Data from [7]).

veloped countries. Note that energy equity is simply another term for the attempt to achieve comparable standards of living. But achieving a higher standard of living can carry with it a price. The price includes not only monetary obligations, but also the potential for significant environmental degradation if energy equity is pursued via the least expensive, first-cost options. Regrettably, this is the most probable scenario, since it is already underway in regions such as Eastern Europe and Asia. In fact, it is probably more likely that use of least-cost energy options may lead to comparable per capita energy use, but may simultaneously degrade the standard of living by producing air not suitable for breathing and water not suitable for drinking. These issues will be dealt with in more detail in Chapter 9.

Figure 1.4 shows that North America, with slightly more than 5% of the world population, consumes 30% of the world's energy, while China and India, with nearly one third of the world's population, consume 12% of the world's energy. What is missing in Figure 1.4 is the efficiency with which the energy is consumed in these regions.

Figure 1.5 is particularly interesting, because it clearly shows examples of countries where energy is used least and most efficiently. Those countries with the highest Btu/gross domestic product-ratios are typically engaged in inefficient-large-scale manufacturing with the use of energy produced in inefficient generation plants. Those with lower Btu/gdp ratios generally produce and use energy more efficiently. Some have shifted from predominantly manufacturing economies to predominantly information economies, with the result of a smaller fraction of energy use for manufacturing. Countries at the low end of the scale tend to be farming-oriented with the use of mostly manual labor.

As developing countries increase their manufacturing capabilities, using cheap but polluting local energy sources, there may be pressure to relax pollution

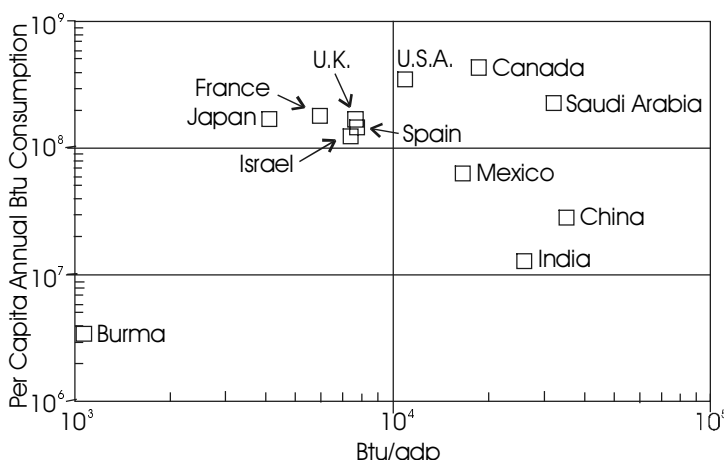


Figure 1.5 Worldwide variations in per capita energy consumption vs energy efficiency (Data from [8, 9]).

control standards within the developed world in order to maintain the ability to compete with production from developing countries. Opposition to free trade agreements has been partially based on such environmental concerns, since such agreements forbid any country to impose import tariffs on goods produced in countries having weak environmental standards. So the developed countries are challenged to export efficiency to the developing countries.

But what does this discussion have to do with photovoltaic power production? Simple. As will be shown in Chapter 9, photovoltaic energy sources are very clean, but current photovoltaic deployment costs cannot compete with the initial installed costs of fossil sources of electrical generation in most cases. It means that the consumer must be familiar with life-cycle costing and that the engineer must be able to create the most cost-effective photovoltaic solution. It also means that a significant amount of research and development must be done to ensure the continuation of the decrease in the price of photovoltaic generation. It also means that work must continue in the effort to put a price tag on environmental degradation caused by energy sources, so this price can be factored into the total cost to society of any energy source.

The bottom line is that there remains a significant amount of work in research, development and public education to be done in the energy field, and particularly in the field of photovoltaics. And much of this work can best be done by knowledgeable engineers who, for example, understand the concept of exponential growth.

1.4 Exponential Growth

1.4.1 Introduction

Exponential growth is probably most familiar to the electrical engineer in the diode equation, which relates diode current, I , to diode voltage, V

$$I = I_o (e^{\frac{qV}{kT}} - 1). \quad (1.1)$$

While this equation is fundamental to the performance of photovoltaic cells, many other physical processes are also characterized by exponential growth.

Exponential growth is commonly referred to as compound interest. Almost everyone has heard about it, but few understand the ramifications of constant annual percentage increase in a quantity, whether it be money, population, or energy supply or demand. One of the first to warn of the dangers of exponential growth was Malthus in 1798 [10]. He warned that population growth would exceed the ability to feed the population. The Malthusian theory is often the subject of ridicule of growth enthusiasts [11]. The intent of this discussion is neither to support nor discount the predictions of Malthus, but merely to illustrate an important mathematical principle that engineers often overlook. The application of the principles of exponential growth is widespread in society, so

the principles of exponential growth should be just as important to a well-informed engineer as is the second law of thermodynamics. For those who may have missed the second law of thermodynamics in either chemistry or thermodynamics class, it is a statement that in every process less energy comes out than what is put in. In other words, there is no free lunch.

1.4.2 Compound Interest

Compound interest is the process of compounding simple interest. If a quantity N_0 is subject to an interest rate i , with i expressed as a fraction (i.e., $i = \%/100$), the quantity will increase (or decrease, if $i < 0$) to a value of

$$N(I) = N_0(1+i) \quad (1.2)$$

after one prescribed time period has elapsed. If the quantity present after the prescribed time period is allowed to remain and to continue to accumulate at the same rate, then the quantity is subject to compound interest and the amount present after n time periods will be

$$N(n) = N_0(1+i)^n. \quad (1.3)$$

To show that this formula is a form of the exponential function, one need only recall that

$$y^x = e^{x \ln y}.$$

Hence,

$$N(n) = N_0 e^{n \ln(1+i)}. \quad (1.4)$$

Some special properties of the exponential function can now be considered.

1.4.3 Doubling Time

To determine the time, D , it will take for the original quantity to double, one need only set $N(n) = 2N_0$ and solve for n . The result (and the answer to problem 1.1) is

$$n = \frac{\ln 2}{\ln(1+i)} = D. \quad (1.5)$$

For small values of i , $\ln(1+i)$ can be approximated as $\ln(1+i) \cong i$. Noting that $\ln 2 = 0.693$ leads to the formula so popular in the financial world, i.e.,

$$D = n \cong 0.7/i. \quad (1.6)$$

Hence, for an interest rate of 7% per year ($i = 0.07$), the doubling time will be 10 years. For an interest rate of 10%, the doubling time will be approxi-

mately 7 years. However, as the interest rate exceeds 10%, the approximation becomes less valid, and the exact expression should be used for accurate results. In the case where the interest rate is negative, it should be obvious that no doubling can occur. The authors have proven this to be the case with various investments in the stock market.

An important property of the exponential function is that the doubling process continues for all time. Hence, if the doubling time is 10 years, then the quantity will double again in another 10 years, so it will now be 4 times its original value. In another 10 years it will double again to 8 times its original value. After 40 years, the quantity will be 16 times its original value. Figure 1.6 shows this exponential increase.

Note that if the function $y = Ae^{bx} = A10^{bx\log e}$ is plotted with linear coordinates, the familiar exponential curve appears, as in Figure 1.6a. If the logarithm of each side is taken, the result is

$$\log y = \log A + (b \log e)x . \quad (1.7)$$

Hence, if $\log y$ is plotted as a function of x , the graph will be linear with slope $b \log e$, as shown in Figure 1.6b. Figure 1.6b shows that plotting $\log y$ vs. x is a convenient way to check for an exponential relationship between two variables. Notice also that the vertical axis can be labeled either in terms of $\log y$ or, simply, in terms of y . When the axis is labeled in terms of y , it is understood that the axis is linear in the logarithm of y .

The values of A and b can be determined easily from the semilog plot. The intercept of the function and the y -axis ($x = 0$) yields the value of A , provided that the y -axis is labeled in terms of y . The slope can be calculated from a semilog plot by evaluating

$$\text{slope} = \frac{\log y_2 - \log y_1}{x_2 - x_1} = \frac{\log A + (b \log e)x_2 - [\log A + (b \log e)x_1]}{x_2 - x_1} = (b \log e) . \quad (1.8)$$

For the person who prefers to let computers do the work, either Excel or Matlab can conveniently plot data and produce a least mean square curve fit to the data along with an estimate of the goodness of the fit. When a set of data is available, all one needs to do is to list the independent and dependent variables side-by-side on an Excel spreadsheet and then use the Chart Wizard to plot an x - y scatter plot of the data. Selection of the chart option with the plot of the data but no connecting lines and following through to the placement of the chart on the spreadsheet, one can then click on the data points, go to “Chart” on the pull-down menu, and select “Add Trendline.” This opens a dialog box that offers a

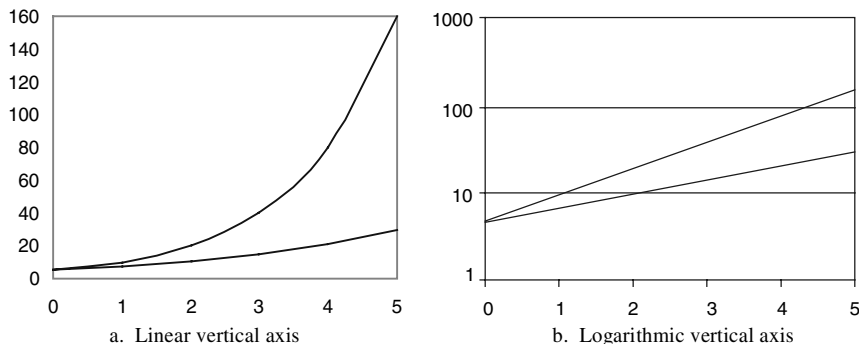


Figure 1.6 Examples of exponential functions plotted on linear and on semilogarithmic coordinates.

choice of six trend/regression types. To obtain the best fit, select a regression type, then select ‘Options’ and choose to add the equation and the R^2 value to the graph. An R^2 value of 1 indicates a perfect fit of the data to the curve, the equation to which is displayed. Low R^2 values suggest choosing a different regression type. Several good user guides for Excel are available for those who would like to further explore the use of Excel as a convenient analysis tool for use in photovoltaic system design or other technical endeavors [12, 13]. Matlab and other math programs are also powerful tools.

For the reader who has not had the pleasure of using Excel to find the least mean square fit to a data set, several problems are available at the end of this chapter. It is anticipated that the reader will use Excel frequently as a tool for the design of PV systems in later chapters.

1.4.4 Accumulation

Another important property of the exponential function is the amount of accumulation (or depletion) of a quantity in a doubling time. It is a straightforward math exercise to show that *the amount accumulated (or depleted) in a doubling time is equal to the amount accumulated in all previous history*. To demonstrate this, assume that D represents a doubling time. Next, calculate the amount present after $m+1$ doubling times and the amount present after m doubling times. The difference is ACC, the amount accumulated in a doubling time. This difference is given by

$$ACC = N[(m+1)D] - N[mD] = N_o e^{(m+1)D \ln(1+i)} - N_o e^{mD \ln(1+i)}.$$

A bit of manipulating on this formula yields the simple, and hopefully not too surprising, result that

$$ACC = N_o e^{m \ln 2} = N_o 2^m. \quad (1.9)$$

In order to compare this with the amount accumulated in all previous history, all that is necessary is to observe the amount present after m doubling times. Doing so yields

$$N(mD) = N_o e^{mD \ln(1+i)} = N_o e^{m \ln 2} = N_o 2^m. \quad (1.10)$$

Hence, *the amount accumulated in a doubling time equals the amount accumulated in all previous history*. The implications of this result are far reaching. For example, a prominent political figure once noted that there was still as much oil underground in the U.S. as what had been pumped out since pumping first started more than 140 years ago [14]. This was at a time when oil extraction was increasing at a rate of approximately 7% per year. If the extraction had continued to increase at 7% per year, which has a doubling time of approximately 10 years, in the next doubling time all of the remaining petroleum would have been extracted. Many other important public figures have made similar statements that tend to assign a linear nature to the exponential function [14]. Could this be an argument for engineers to run for public office?

In fact, extraction did not continue to increase at this rate. With regard to the use of resources, M. King Hubbert [15] developed a model that incorporates a Gaussian function for depletion, which seems to have more validity than the exponential model. The rising edge of the Gaussian function, however, is conveniently approximated by an exponential.

The accumulation formula, of course, may also apply to the deployment of new technology. For example, if the use of photovoltaic cells for generation of power increases at the rate of 10% per year, the power produced by photovoltaics will double every 7 years, and the cumulative amount of power production over a doubling time will equal the power production capability of all photovoltaic cells deployed in all previous history. Since the early 1990s, photovoltaic power production has been increasing at a very impressive rate. Problems 1.15 and 1.16 offer an opportunity to explore the relevance of this observation if this rate of increase continues.

1.4.5 Resource Lifetime in an Exponential Environment

The previous discussion of exponential growth has been based on total amounts of a quantity at any given time. If the time derivative of the exponential expression for quantity is taken, the rate of change of the quantity is obtained. Since the derivative of an exponential is also an exponential, the same rules apply to the derivative as to the function. Distinguishing between amount present and rate of use (or increase) is important when determining the lifetime of a resource. Hence, when considering an exponential expression, one needs to establish whether it refers to barrels or barrels per day, or, perhaps, megawatts or megawatts per year of photovoltaic deployment.

The final concept to explore relating to the exponential function is the lifetime of a resource under conditions of exponential increase. It is common to predict the lifetime of a resource under the current rate of consumption. This involves simple arithmetic, since if there are Z (quantity) widgets left to use and if we use X (rate of use) of them per year, then the widgets will last for Y years, where $Y = Z/X$. But what happens to the expected lifetime of the widget if people decide that they really like widgets and they decide to use them at an increasing rate of $100i\%$ per year? This problem can be solved by assuming that C_o represents the present rate of consumption of a resource and Y_o represents the estimated lifetime of the resource at the present rate of consumption. Then, if consumption increases by $100i\%$ per year, the rate of consumption at any point in time, x , is given by

$$C(x) = C_o(1+i)^x. \quad (1.11)$$

The accumulated consumption over a period of m years, TOT, can be found from previous formulas, or, more formally, by evaluating

$$\begin{aligned} TOT &= \int_0^m C(x)dx = \int_0^m C_o e^{x \ln(1+i)} dx \\ &= \frac{C_o}{\ln(1+i)} (e^{m \ln(1+i)} - 1). \end{aligned}$$

Next, set the total to equal the estimated amount remaining ($C_o Y_o$) and solve for m , since this will yield the number of years for the total consumption to equal the amount remaining. The result is

$$m = \frac{\ln[Y_o \ln(1+i) + 1]}{\ln(1+i)}. \quad (1.12)$$

As an example of the use of this result, assume that a resource is estimated to last for another 100 years at present consumption rates ($Y_o = 100$), but that consumption will increase at the rate of 5% per year ($i = .05$). Using these numbers in the above formula gives $m = 36.31$ years. If the estimate is off by a factor of 10, and there is really a 1000-year supply left at current consumption rates, then $m = 80.09$ years.

As a perhaps more reassuring example of the use of this result, it is also possible that the consumption of a resource might decline at a constant percentage per year. This could happen if the resource was replaced by another resource, for example. For the above example, with $Y_o = 100$ years and an annual decrease of 0.5% (i.e., $i = -0.005$), the new lifetime becomes 139 years, and if $i = -0.01$, the resource will last forever.

Hence, two important observations emerge from the lifetime formula:

1. *If annual consumption of a resource increases exponentially, it is not important how much is thought to remain; it will be consumed much faster than one can imagine.*
2. *If annual consumption decreases exponentially, it is possible to extend the lifetime of a resource to forever.*

1.4.6 The Decaying Exponential

The engineering student is probably more familiar with the decaying exponential, such as decaying voltages and currents in R-L and R-C circuits. When $i < 0$, the compounding process becomes one of decay rather than of growth. Many natural processes experience exponential decay, such as radioactive isotopes, attenuation of light as it enters a uniform medium and various forms of chemical decay. Exponential decay is displayed by any process for which the rate of change of the amount present is proportional to the amount present at a given time. This is expressed mathematically as

$$\frac{dN}{dt} = -KN(t). \quad (1.13)$$

The solution to this equation is the familiar $N = N_0 e^{-Kt}$, where N_0 is the value of the parameter N at $t = 0$. Most electrical engineers recognize the reciprocal of K as the time constant of the process, where the time constant represents the time for the transition to $e^{-1} = 0.3679$ of the initial value. It is also useful to determine the time to decay to half the initial value. This time is known as the half-life. To find the half-life in terms of the time constant, one need only set $N = \frac{1}{2}N_0$. Doing so, and solving for t , yields the result

$$t_{\frac{1}{2}} = \tau \ln 2, \quad (1.14)$$

where $\tau = K^{-1}$. After each half-life, half of the quantity remains. Hence, after two half-lives, 25% remains; after three, 12.5% remains; after four, 6.25% remains, etc. In general, after m half-lives, $2^{-m}N_0$ remains. Thus, if $m = 10$, only 0.000977 of the original amount remains. Note that if the original amount was a large number, however, that 0.000977 times a large number may still be a relatively large number.

Finally, the cumulative amount used in an environment of exponential decay is still given by integrating from 0 to the desired time. Regardless of the desired time, the result of integration remains finite.

1.4.7 Hubbert's Gaussian Model

In 1956, M. King Hubbert, who was employed by the Shell Oil Company, published his now acclaimed theory of resource depletion [15]. Simply put,

Hubbert reasoned that the life of a finite resource follows a Gaussian curve described by the equation, often referred to as the error function or normal curve,

$$R(t) = R_m e^{\frac{-(t-t_0)^2}{2s^2}}, \quad (1.15)$$

where $R(t)$ represents the consumption rate at a given time, t ,

R_m represents the maximum consumption rate, and

s represents a shape factor for the curve, commonly known as the standard deviation.

Figure 1.7 shows a plot of (1.15), and Figure 1.8 shows Hubbert's 1971 curves relating to petroleum production. The rising edge represents a nearly exponential function, until it nears the peak of the curve, where leveling occurs, followed by nearly exponential decay. Since the curve of Figure 1.7 plots consumption rate, note that according to Hubbert's theory, when half a resource is consumed, the consumption will have leveled at its maximum value and then will begin its nearly exponential decline. According to Hubbert's model, domestic petroleum production in the U.S. would peak near 1970 and world petroleum production would peak near the turn of the century. Indeed, it appears that the domestic prediction has been confirmed. According to projections of the U.S. Department of Energy, Energy Information Agency, both domestic and Alaskan petroleum production will continue to decline through the year 2015.

Interestingly enough, it also turns out with the Hubbert theory that if an error is made in estimating the amount of a resource present, the peak of the curve will not be shifted by a significant amount. Perhaps the most significant conclusion of the Hubbert theory, however, is that the consumption of a resource follows a smooth curve rather than an abrupt one that involves unabated consumption until suddenly no more is left. Hopefully, approaching the peak sends a message to find a replacement.

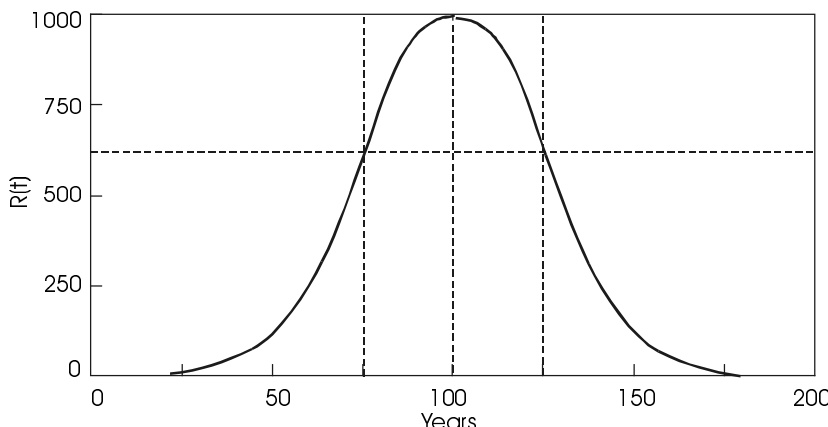


Figure 1.7 Gaussian function with $R_m = 1000$, $t_o = 100$ and $s = 25$.

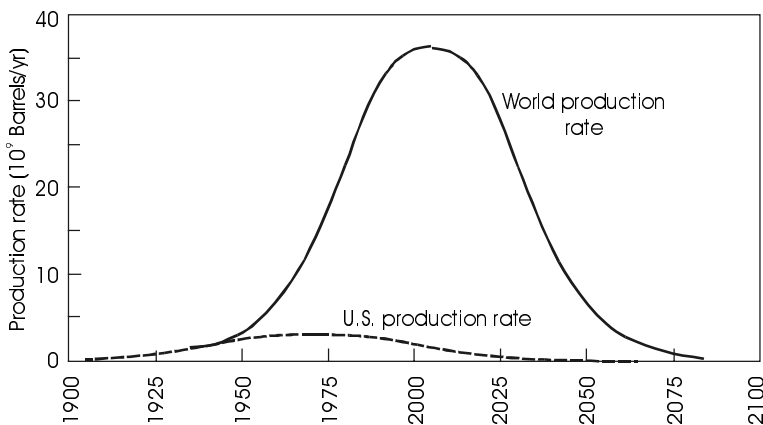


Figure 1.8 Hubbert's predictions for U.S. and world petroleum production.
(Adapted from Hubbert [15] with permission.)

1.5 Net Energy, Btu Economics and the Test for Sustainability

The net energy associated with an energy source is simply the difference between the energy required to obtain and convert the source to useful energy and the actual useful energy obtained from the source. For example, in order to be able to burn a barrel of oil, it is necessary to find the oil, extract the oil, transport the oil, refine the oil and construct the facility for burning the oil. The refined oil must then be transported to the burning site and, presumably, after the oil is burned, any environmental damage resulting from the extraction, transportation, refining and burning should be repaired. Energy is involved in all of these steps. The bottom line is that if it takes more than a barrel of oil worth of energy to obtain and convert the energy available in a barrel of oil, one should question seriously whether it makes sense to burn the oil in the first place.

In some cases, it may make sense to expend the energy to get the resource. Suppose, for example, that another use was discovered for oil such as providing an essential chemical for the cure of cancer. Then it would make sense to expend energy from sources other than oil, even if the energy exceeded the energy value of the oil, in order to make the oil available for the more important use. Another situation would be to use a lower grade or quality form of energy to produce a higher grade or quality form of energy. Sometimes such an action might make energy sense.

For example, burning coal to produce electricity takes about three units of coal energy to produce one unit of electrical energy. Until television sets that run directly from coal are invented, this inefficient process of converting coal energy to electrical energy will probably continue.

The concept of net energy was introduced by Odum and Odum in 1976 [16, 17]. They incorporated the net energy concept into a new standard for econom-

ics that they felt made better sense than the gold standard. They called it the Btu standard. The Btu standard simply recognizes that everything has an energy content. Henderson [18] has written extensively on the concept of Btu economics. The reader is encouraged to read Odum and Odum and Henderson during a term break for enlightening discussions of how the economic system might be changed to an energy-based standard.

For the purposes of this book, the test for sustainability for an energy source will include two factors. The first will be whether the source is finite. A finite source is generally termed nonrenewable, while an infinite source is termed renewable. The second will be whether the source has positive net energy. That is, once energy is expended to produce the source, will the source then generate more energy than was required for its production?

The idea that a source can produce more energy than was used to create the source may seem inconsistent with the second law of thermodynamics. However, if we allow the use of energy from a very large reservoir as a supply of energy to be converted by the source, then the source becomes nearly infinite. In the case of the sun, which is expected to survive for another 4 billion years or so [19], we have such a reservoir. Thus, for example, if a photovoltaic cell can generate more electrical energy over its lifetime than was expended in its production and deployment and ultimately in its disposal, including environmental energy costs, then the cell would be considered to have positive net energy.

The concept of net energy will be considered in the context of photovoltaic cell production and in discussion of environmental effects of energy sources.

1.6 Direct Conversion of Sunlight to Electricity with Photovoltaics

Becquerel [20] first discovered that sunlight can be converted directly into electricity in 1839, when he observed the photogalvanic effect. Then, in 1876, Adams and Day found that selenium has photovoltaic properties. When Planck postulated the quantum nature of light in 1900, the door was opened for other scientists to build on this theory. It was in 1930 that Wilson proposed the quantum theory of solids, providing a theoretical linkage between the photon and the properties of solids. Ten years later, Mott and Schottky developed the theory of the solid state diode, and in 1949, Bardeen, Brattain and Shockley invented the bipolar transistor. This invention, of course, revolutionized the world of solid state devices. The first solar cell, developed by Chapin, Fuller and Pearson, followed in 1954. It had an efficiency of 6%. Only four years later, the first solar cells were used on the Vanguard I orbiting satellite.

One might wonder why it took so long to develop the photovoltaic cell. The answer lies in the difficulty in producing sufficiently pure materials to obtain a reasonable level of cell efficiency. Prior to the development of the bipolar transistor and the advent of the space program, there was little impetus for concentrating on preparing highly pure semiconductor materials. Coal and oil were meeting the world's need for electricity and vacuum tubes were meeting the

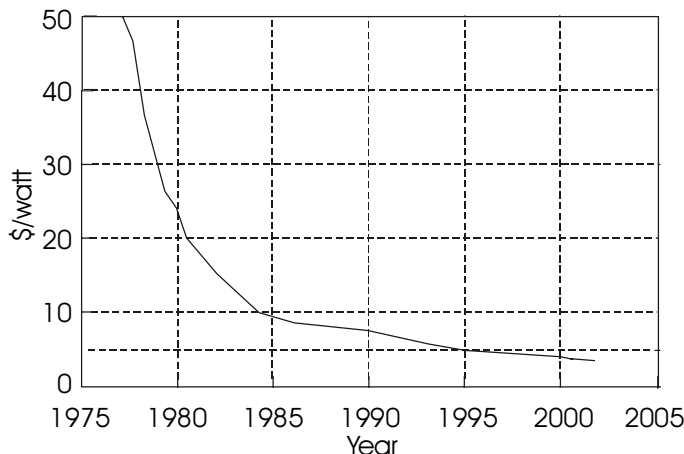


Figure 1.9 The decline in cost per watt for photovoltaic modules. (Data from [21, 22, 23])

needs of the electronics industry. But since vacuum tubes and conventional power sources were impractical for space use, solid state gained its foothold.

Photovoltaic cells are made of semiconductor materials and are assembled into modules of approximately 36 cells. This observation is significant, since this means the same industry that has, in the past 50 years, progressed from the development of the bipolar transistor to integrated circuits containing millions of transistors is also involved in the development of photovoltaic cells. Figure 1.9 shows the decline in cost of photovoltaic modules over the past 25 years. Much of the initial cost reduction has been due to process improvement in the production of the cells. At this point, the limiting factor is becoming the energy cost of the cells. Hence, the challenge of the future will be to reduce the energy content of the cell production process while maintaining or increasing cell performance, efficiency and reliability.

Figure 1.10 shows world PV shipments in megawatts from 1971 to 2002. Note that the data is plotted on semilogarithmic coordinates. The actual data since 1994 are given in Problem 1.16 so the reader can generate a plot and determine the goodness of fit and the rate of growth over this period. As will be seen, the growth rates during both periods are impressive. A further important observation is that in 1995, 45% of the world's PV modules were manufactured in the U.S., while Europe, Japan and the rest of the world manufactured 80% of the world's PV modules in 2002 [23]. Just as the U.S. has allowed the manufacture of consumer electronics to transfer to other countries, it appears that the U.S. is also allowing the same to happen with the PV industry. It will be interesting to observe this trend in the future.

As an initial test as to whether to continue with this book, it is useful to determine whether the net energy associated with photovoltaic cells is positive. Indeed, photovoltaic cells can produce more than a 4:1 return on the energy invested in their production, and future improvements in production technology

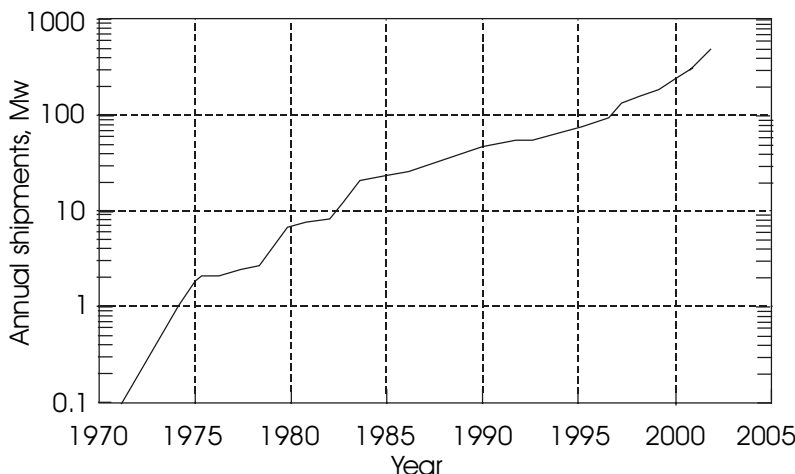


Figure 1.10 Worldwide PV shipments, 1971–2002 (Data from [22, 23, 24])

and practice will likely result in exceeding this value. Hence, it appears to be worth investigating this technology in more detail.

Problems

- 1.1 Prove equation 1.5.
- 1.2 Calculate the approximate and exact doubling times for annual percentage increases of 5%, 10%, 15% and 20%.
- 1.3 The human population of the earth is approximately 6 billion and is increasing at approximately 2% per year. The diameter of the earth is approximately 8000 miles and the surface of the earth is approximately two-thirds water. Calculate the population doubling time, then set up a spreadsheet that will show a) the population, b) the number of square feet of land area per person, and c) the length of the side of a square that will produce the required area per person. Carry out the spreadsheet for 15 doubling times, assuming that the rate of population increase remains constant. What conclusions can you draw from this exercise?
- 1.4 Assume there is enough coal left to last for another 300 years at current consumption rates.
 - a. Determine how long the coal will last if its use is increased at a rate of 5% per year.
 - b. If there is enough coal to last for 10,000 years at current consumption rates, then how long will it last if its use increases by 5% per year?
 - c. Can you predict any other possible consequences if coal burning increases at 5% per year for the short or long term?

- d. Determine the annual percent reduction in coal consumption to ensure that coal will last forever, assuming the 300-year lifetime at present consumption rates.
- 1.5 If the half-life of a radioactive isotope is 500 years, how many years will it take for an amount of the isotope to decay to 1% of its original value?
- 1.6 If a colony of bacteria lives in a jar and doubles in number every day, and it takes 30 days to fill the jar with bacteria,
- How long does it take for the jar to be half full?
 - How long before the bacteria notice they have a problem? (You may want to pretend you are a bacterium.)
 - If on the 30th day, 3 more jars are found, how much longer will the colony be able to continue to multiply at its present rate?
- 1.7 An enterprising young engineer enters an interesting salary agreement with an employer. She agrees to work for a penny the first day, 2 cents the second, 4 cents the third, and so on, each day doubling the amount of the previous day. Set up a spreadsheet that will show her daily and cumulative earnings for her first 30 days of employment.
- 1.8 Burning a gallon of petroleum produces approximately 25 pounds of carbon dioxide and burning a ton of coal produces approximately 7000 pounds of carbon dioxide.
- If a barrel of petroleum contains 42 gallons, if the world consumes 70 million barrels of petroleum per day and if the atmosphere weighs 14.7 pounds per square inch of earth surface area, calculate the weight of carbon dioxide generated each year from burning petroleum and compare this amount with the weight of the atmosphere.
 - If a total of 14 million tons of coal are burned every day on the earth, calculate the weight of carbon dioxide generated each year from coal burning and compare it with the weight of the atmosphere.
- 1.9 Assume a world population of 6 billion and a U.S. population of 270 million.
- Using the data in Figures 1.2-1.4, determine the total world energy consumption in quads if the rest of the world were to use the same per capita energy as in the U.S.
 - If the energy source mix were to remain the same as the present mix in achieving the scenario of part a, what would be the percentage increase in CO₂ emissions?
- 1.10 Obtain data on worldwide energy consumption by sector from the United States Department of Energy, Energy Information Administration website.

Plot the data and estimate annual percentage growth rates for the seven regions reported and then for the world.

- 1.11 The following measurements of $x(t)$ are made:

t	0	1	2.3	3.0	4.5	5.2	6.5	8.0
x	2.1	8.4	31	65	360	850	3700	20,000

Construct a semilog plot of $x(t)$ either manually or with a computer, and determine whether the function appears to have an exponential dependence. If so, determine $x(t)$.

- 1.12 a. What does the area under the Gaussian curve represent?
 b. Show that 68% of the area under the Gaussian curve lies within one standard deviation, s , of maximum value of the function.
 c. What percentage of the area lies within $2s$?
- 1.13 Determine R_m , t_o and s for the worldwide graph of Figure 1.7.
- 1.14 Look up actual U. S. and world petroleum production figures and plot them on Hubbert's curves to compare the actual production with the theoretical production.
- 1.15 Based on the data of Figure 1.10,
 a. Estimate the year when PV shipments will reach 1000 MW.
 b. Estimate the year when PV shipments will reach 10,000 MW.
 c. Estimate the year when PV shipments will reach 2700 GW.
- 1.16 Paul Maycock [23, 24] reports the following worldwide PV production figures. Plot the data on an Excel graph, establish an equation to represent the data, and then answer the three questions posed in Problem 1.15. Compare the results of the two problems.

Year	1994	1995	1996	1997	1998	1999	2000	2001	2002
MW	69.4	77.6	88.6	126	155	201	288	391	513

References

- [1] Remarks by President William Clinton in Address to the United Nations Special Session on Environment and Development, June 26, 1997.
- [2] Peña, F. F., U. S. Secretary of Energy, 'Remarks on President Clinton's Address of June 26, 1997,' June 27, 1997.
- [3] Bos, E., et al., *World Population Projections, 1994-95*, The Johns Hopkins University Press, Baltimore, 1994.
- [4] Lindley, D., An overview of renewable energy in China, *Renewable Energy World*, November 1998, 65-69.
- [5] Fishbane, P. M., Gasiorowicz, S. and Thornton, S. T., *Physics for Scientists and Engineers, 2nd Ed.*, Prentice Hall, Upper Saddle River, NJ, 1996.

- [6] Annual Energy Review, 2001, U.S. Department of Energy, Energy Information Administration, Washington, D.C. (www.eia.doe.gov/emeu/aer).
- [7] International Energy Annual 2000: World Overview, U.S. Department of Energy, Energy Information Administration, Washington, D.C. (www.eia.doe.gov/emeu).
- [8] World per capita Primary Energy Consumption, U.S. Department of Energy, Energy Information Administration, Washington, D.C. (www.eia.doe.gov/emeu).
- [9] World Primary Energy Consumption per GDP, U.S. Department of Energy, Energy Information Administration, Washington, D.C. (www.eia.doe.gov/emeu)
- [10] Malthus, T. R., *An Essay on the Principle of Population, as It Affects the Future Improvement of Society, with Remarks on the Speculations of Mr. Godwin, M. Condorcet, and Other Writers*, Printed for J. Johnson in St. Paul's Church-Yard, London, 1798.
- [11] Bahr, H. M., Chadwick, B. A. and Thomas, D. L., Eds., *Population, Resources, and the Future: Non-Malthusian Perspectives*, Brigham Young University Press, Provo, UT, 1974.
- [12] Bloch, S. C., *Excel for Engineers and Scientists*, 2nd Ed., John Wiley & Sons, Hoboken, N. J., 2003.
- [13] Gottfried, B., *Spreadsheet Tools for Engineers Using Excel, Including Excel 2002*, McGraw-Hill, New York, 2003.
- [14] Bartlett, A. A., Forgotten fundamentals of the energy crisis, *Am. J. Phys.* Vol 46, No 9, September 1978, 876-888.
- [15] Hubbert, M. K., The energy resources of the earth, *Scientific Am.*, Vol 225, No 3, September 1971, 60-70.
- [16] Odum, H. T. and Odum, E. C., *Energy Basis for Man and Nature*, McGraw-Hill, New York , 1976.
- [17] Odum, H. T. and Odum, E. C., *Energy Basis for Man and Nature*, 2nd Ed., McGraw-Hill, New York, 1981.
- [18] Henderson, H., *The Politics of the Solar Age: Alternatives to Economics*, Anchor Press/Doubleday, Garden City, NY, 1981.
- [19] Foukal, P., *Solar Astrophysics*, John Wiley & Sons, New York, 1990.
- [20] Markvart, T., Ed., *Solar Electricity*, John Wiley & Sons, Chichester, U.K., 1994.
- [21] Maycock, P. D., Ed., *Photovoltaic News*, Vol 18, No 1, January 1999.
- [22] *International Marketing Data and Statistics*, 22nd Ed., Euromonitor PIC, London, 1998.
- [23] Maycock, P. D., The world PV market, production increases 36%, *Renewable Energy World*, July-August 2002, 147-161.
- [24] Maycock, P. D., *PV News*, Vol 22, No 3, March 2003.

Suggested Reading

- Aubrecht, G. J., *Energy*, 2nd Ed., Prentice Hall, Upper Saddle River, NJ, 1995.
- Kerr, R. A., The next oil crisis looms large and perhaps close, *Science*, Vol 281, August 21, 1998, 1128-1131.
- 'President Clinton Announces Million Solar Roofs by 2010,' *FEMP Focus*, August/September 1997, 7.
- Silberberg, M., *Chemistry: The Molecular Nature of Matter and Change*, Mosby, St. Louis, 1996.
- Starke, L., Ed., *Vital Signs 1998: The Environmental Trends That Are Shaping Our Future*, W. W. Norton, New York, London, 1998.

Chapter 2

THE SUN

2.1 Introduction

Optimization of the performance of photovoltaic and other systems that convert sunlight into other useful forms of energy is contingent on knowledge of the properties of sunlight. This chapter provides a synopsis of important solar phenomena, including the solar spectrum, atmospheric effects, solar radiation components, determination of sun position, measurement of solar parameters and positioning of the solar collector. In this chapter, an attempt is made to quantify the obvious and, perhaps, some not-so-obvious observations: Why is it light during the day and dark at night? Why are there more daylight hours in summer than in winter? Why is the sun higher in the sky in summer than in winter? Why are there more summer sunlight hours in northern latitudes than in latitudes closer to the equator? Why does less energy reach the surface of the Earth on cloudy days? Why is it better for a solar collector to face the sun? What happens if a solar collector does not face the sun directly? How much energy is available from the sun? Why is the sky blue?

2.2 The Solar Spectrum

The sun provides the energy needed to sustain life in our solar system. In one hour, the Earth receives enough energy from the sun to meet its energy needs for nearly a year. In other words, this is about 5000 times the input to the Earth's energy budget from all other sources. In order to maximize the utilization of this important energy resource, it is useful to understand some of the properties of this "ball of fire" in the sky.

The sun is composed of a mixture of gases with a predominance of hydrogen. As the sun converts hydrogen to helium in a massive thermonuclear fusion reaction, mass is converted to energy according to Einstein's famous formula, $E = mc^2$. As a result of this reaction the surface of the sun is maintained at a temperature of approximately 5800 K. This energy is radiated away from the sun uniformly in all directions, in close agreement with Planck's blackbody radiation formula

$$w_{\lambda} = \frac{2\pi hc^2 \lambda^{-5}}{e^{\lambda kT} - 1} \text{ (W/m}^2/\text{unit wavelength in meters),} \quad (2.1)$$

where $h = 6.63 \times 10^{-34}$ watt sec² (Planck's constant), and
 $k = 1.38 \times 10^{-23}$ joules/K (Boltzmann's constant).

Equation 2.1 yields the energy density at the *surface* of the sun in W/m²/unit wavelength in m. By the time this energy has traveled 150 million km to the

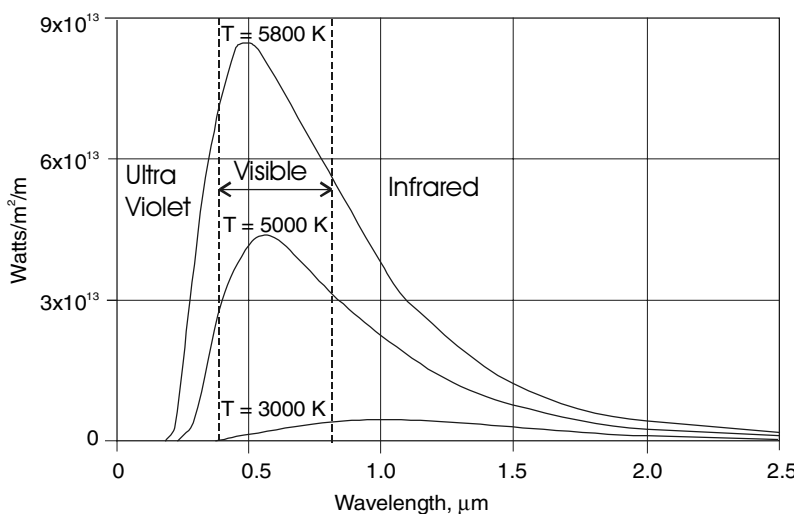


Figure 2.1 Blackbody radiation spectra for temperatures 3000 K, 5000 K and 5800 K.

Earth, the total extraterrestrial energy density decreases to 1367 W/m^2 and is often referred to as the solar constant (see Problem 2.1) [1].

Figure 2.1 shows plots of Planck's blackbody radiation formula for several different temperatures, along with the extraterrestrial solar spectrum. Note that at lower temperatures, nearly all of the spectrum lies outside the visible range in the infrared range, whereas at 5800 K, the characteristic white color of the sun is obtained due to the mix of wavelengths in the visible spectral range. At even higher temperatures, the color shifts toward blue, and at lower temperatures, the color shifts toward red. Incandescent lamp filaments, for example, typically are operated at temperatures of approximately 3000 K and, hence, emit a blackbody spectrum characteristic of 3000 K. Depending on the color temperature of the light source, photographic film must be compensated to obtain true colors, unless appropriate filters are used. The extraterrestrial solar spectrum indicates that the sun can be reasonably approximated as a blackbody radiator.

Most sources of light are not perfect blackbody sources. Reasonable approximations of blackbody spectra are obtained from sources that emit light as a result of heating a filament to a high temperature. But to be a perfect radiator, the object must also be a perfect absorber of light, which is not the case for common light sources. Gas discharge lamps, for example, emit either the discrete spectra characteristic of the specific gas, or, alternatively, emit light containing many discrete spectral lines from emission from phosphorescent materials. Thus fluorescent, high pressure sodium and high intensity discharge lamps have spectra characteristic of gas discharge systems. This is an important fact to recognize, since in the testing of photovoltaic systems, it is important to be able to produce standardized spectral testing conditions.

Knowledge of the spectral composition of the sun is important for understanding the effects of the atmosphere on the radiation from the sun and for understanding which materials should offer the best performance in the conversion of sunlight to electricity.

2.3 The Effect of Atmosphere on Sunlight

As sunlight enters the Earth's atmosphere some is absorbed, some is scattered and some passes through unaffected by the molecules in the atmosphere and is either absorbed or reflected by objects at ground level.

Different molecules do different things. Water vapor, carbon dioxide and ozone, for example, have several significant absorption wavelengths. Ozone plays an important role by absorbing a significant amount of radiation in the ultraviolet region of the spectrum, while water vapor and carbon dioxide absorb primarily in the visible and infrared parts of the spectrum. These absorption lines are shown in Figure 2.2.

Absorbed sunlight increases the energy of the absorbing molecules, thus raising their temperature. Scattered sunlight is responsible for light entering north-facing windows when the sun is in the south. Scattered sunlight, in fact, is what makes the sky blue. Without atmosphere and its ability to scatter sunlight, the sky would appear black, such as it does on the moon. Direct sunlight consists of parallel rays, which are necessary if the light is to be focused. The reader has probably experimented with a magnifying glass and found that it is not possible to burn holes in paper when a cloud covers the sun. This is because the diffuse light present under these conditions cannot be focused.

All of these components of sunlight have been given names of their own. Sunlight that reaches the Earth's surface without scattering is called **direct** or **beam** radiation. Scattered sunlight is called **diffuse** radiation. Sunlight that is reflected from the ground is called **albedo** radiation, and the sum of all three components of sunlight is called **global** radiation.

The amount of sunlight either absorbed or scattered depends on the length of path through the atmosphere. This path length is generally compared with a vertical path directly to sea level, which is designated as **air mass = 1** (AM1). Hence, the air mass at a higher altitude will be less than unity for sun directly overhead and the air mass generally will be more than unity for nonvertical sun angles. In general, the air mass through which sunlight passes is proportional to the secant of the zenith angle, θ_z , which is the angle measured between the direct beam and the vertical. At AM1, after absorption has been accounted for, the intensity of the global radiation is generally reduced from 1367 W/m^2 at the top of the atmosphere to just over 1000 W/m^2 at sea level. Hence, for an AM1 path length, the intensity of sunlight is reduced to 70% of its original AM0 value. In equation form, this observation can be expressed as

$$I = 1367(0.7)^{\text{AM}} . \quad (2.2)$$

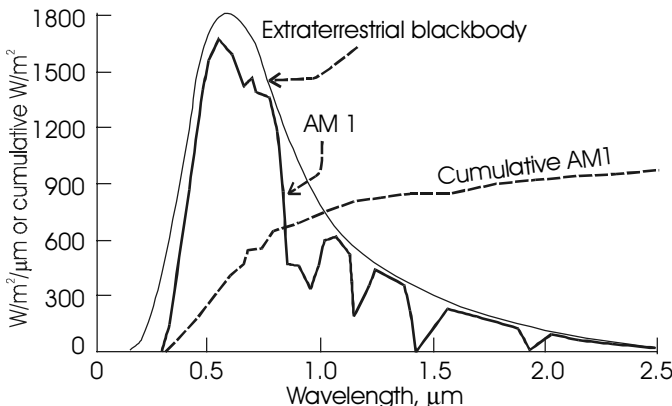


Figure 2.2 AM 1 solar spectrum after atmospheric absorption effects, including plots of extraterrestrial blackbody spectrum plus cumulative incident energy vs. wavelength.

This equation is, of course, obvious for AM1. But does it hold for air masses different from unity? According to Meinel and Meinel [2], a better fit to observed data is given by

$$I = 1367(0.7)^{(\text{AM})^{0.678}}. \quad (2.3)$$

On the average, over the surface of the Earth, an amount of heat is reradiated into space at night that is just equal to the amount absorbed from the sun during the day. As long as this steady state condition persists, the average temperature of the Earth will remain constant. However, if for any reason the amount of heat absorbed is not equal to the amount reradiated, the planet will either cool down or heat up. This delicate balance can be upset by events such as volcanoes that fill the atmosphere with fine ash that reflects the sunlight away from the Earth, thus reducing the amount of incident sunlight. The balance can also be upset by gases such as carbon dioxide and methane, which are mostly transparent to short wavelength (visible) radiation, but more absorbing to long wavelength (infrared) radiation. Since the incident sunlight is dominated by short wavelengths characteristic of the 5800 K sun surface temperature, and since the reradiated energy is dominated by long wavelengths characteristic of the Earth surface temperature of approximately 300 K, these greenhouse gases tend to prevent the Earth from reradiating heat at night. In order to reach a new balance, it is necessary for the Earth to increase its temperature, since radiation is proportional to T^4 , where T is the temperature in K.

The natural compensation mechanism is green plants on land and under water. Through the process of photosynthesis, they use sunlight and carbon dioxide to produce plant fiber and oxygen, which is released to the atmosphere. Hence, replacement of green plants with concrete and asphalt and adding carbon dioxide to the atmosphere by burning fossil fuels have a combined negative effect on the

stability of the concentration of carbon dioxide in the atmosphere. Global warming has been discussed extensively in other literature, some of which is listed in the chapter references.

2.4 Insolation Specifics

2.4.1 Introduction

Nearly everyone has noticed that the sun shines longer in the summer than in the winter. Nearly everyone also knows that the Sahara Desert receives more sunshine than does London. Another obvious observation is that cloudy places receive less sunlight than sunny places. It may be less evident, however, that the hours of sunlight over a year are the same for every point on the Earth, provided that only the hours between sunrise and sunset are counted, regardless of cloud cover. Those regions of the Earth closer to the poles that have long winter nights also have long summer days. However, since the sun, on the average, is lower in the sky in the polar regions than in the tropics, sunlight must traverse greater air mass in the polar regions than in the tropics. As a result, polar sunlight carries less energy to the surface than does tropical sunlight. Not surprisingly, the polar regions are colder than the tropics.

In this section, quantitative formulas will be presented that will enable the reader to determine exactly how long the sun shines in any particular place on any particular day, and to determine how much sunlight can be expected, on the average, during any month at various locations. Means will also be presented for determining the position of the sun at any time on any day at any location. Finally, the effects of varying the orientation of a photovoltaic array on the power and energy produced by the array will be discussed.

Irradiance is the measure of the power density of sunlight and is measured in W/m^2 . Irradiance is thus an instantaneous quantity. The solar constant for Earth is the irradiance received by the Earth from the sun at the top of the atmosphere, i.e., at AM0, and is equal to 1367 W/m^2 . After passing through the atmosphere with a path length of AM1, the irradiance is reduced to approximately 1000 W/m^2 , and has a modified spectral content due to atmospheric absorption. The irradiance for AM1.5 is accepted as the standard calibration spectrum for photovoltaic cells.

Irradiation is the measure of energy density of sunlight and is measured in kWh/m^2 . Since energy is power integrated over time, irradiation is the integral of irradiance. Normally, the time frame for integration is one day, which, of course, means during daylight hours.

Irradiation is often expressed as *peak sun hours* (psh). The psh is simply the length of time in hours at an irradiance level of 1 kW/m^2 needed to produce the daily irradiation obtained from integration of irradiance over all daylight hours.

Irradiance and irradiation both apply to all components of sunlight. Hence, at a given time, or for a given day, these quantities will depend on location,

weather conditions and time of year. They will also depend on whether the surface of interest is shaded by trees or buildings and whether the surface is horizontal or inclined. The daily irradiation is numerically equal to the daily psh.

In order to determine the amount of irradiation available at a given location at a given time for conversion to electricity, it is useful to develop several expressions for the irradiance on surfaces, depending on the angle between the surface and the incident beam. It is also interesting to be able to determine the number of hours of sunlight on a given day at a given location.

2.4.2 The Orbit and Rotation of the Earth

The Earth revolves around the sun once per year in an elliptical orbit with the sun at one of the foci, so the distance from sun to Earth is given by

$$d = 1.5 \times 10^{11} \left\{ 1 + 0.017 \sin \left[\frac{360(n - 93)}{365} \right] \right\} \text{ m}, \quad (2.4)$$

where n represents the day of the year with January 1 as day 1. Since the deviation of the orbit from circular is so small, it is normally adequate to express this distance in terms of its mean value.

The Earth also rotates about its own polar axis once per day. The polar axis of the Earth is inclined by an angle of 23.45° to the plane of the Earth's orbit about the sun. This inclination is what causes the sun to be higher in the sky in the summer than in the winter. It is also the cause of longer summer sunlight hours and shorter winter sunlight hours. Figure 2.3 shows the Earth's orbit around the sun with the inclined polar axis. Note that on the first day of Northern Hemisphere summer, the sun appears vertically above the Tropic of Cancer, which is latitude 23.45° N of the equator. On the first day of winter, the sun appears vertically above the Tropic of Capricorn, which is latitude 23.45° S of the equator. On the first day of spring and the first day of fall, the sun is directly above the equator. From fall to spring, the sun is south of the equator and from spring to fall the sun is north of the equator. The angle of deviation of the sun from directly above the equator is called the **declination**, δ . If angles north of the equator are considered as positive and angles south of the equator are considered negative, then at any given day of the year, n , the declination can be found from

$$\delta = 23.45^\circ \sin \left[\frac{360(n - 80)}{365} \right]. \quad (2.5)$$

This formula, of course, is only a good approximation, since the year is not exactly 365 days long and the first day of spring is not always the 80th day of the year. In any case, to determine the location of the sun in the sky at any time of

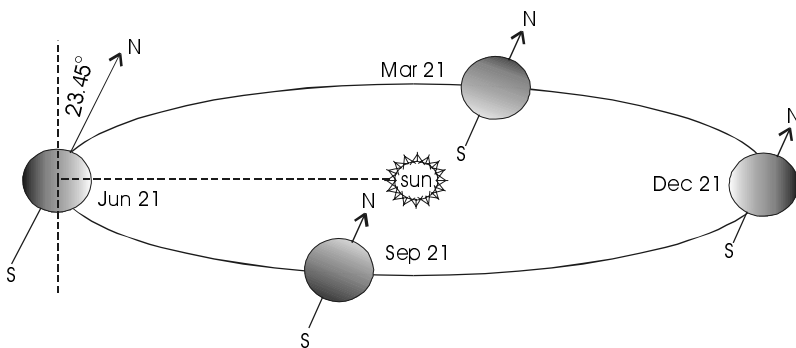


Figure 2.3 The orbit of the earth and the declination at different times of the year.

day at any time of year at any location on the planet, the declination is an important parameter.

The **zenith** is a line perpendicular to the Earth (i.e., straight up). The **zenith angle**, θ_z , is defined as the angle between the sun and the zenith. The declination can be related to the zenith angle at solar noon by noting that the sun is at its highest point in the sky at solar noon.

Solar noon occurs at 12 noon at only one longitude, L_1 , within any time zone. At longitudes east of L_1 , solar noon will occur before 12 noon and at longitudes west of L_1 , solar noon will occur after 12 noon. On a sunny day, solar noon can be determined as that time when a shadow points directly north or south, depending on the latitude.

Fortunately, if the longitude is known, it is straightforward to determine the relationship between clock noon and solar noon. Since there are 24 hours in a day and since the Earth rotates 360° during this period, this means that the Earth rotates at the rate of 15°/hr. It is also convenient that longitude zero corresponds to clock noon at solar noon. As a result, solar noon occurs at clock noon at multiples of 15° east or west longitude. Furthermore, since it takes the Earth 60 minutes to rotate 15°, it is straightforward to interpolate to find solar noon at intermediate longitudes.

For example, at a longitude of 80° west, solar noon can be found by noting that 80° is between 75° and 90°, where solar noon occurs at clock noon *standard time*. Since 80° is west of 75°, when the sun is directly south at 75°, the sun will be east of south at 80°. The clock time at which the sun will be south at 80° (solar noon for 80°) is thus found by interpolation to be

$$t = 12 + \frac{80 - 75}{15} \times 60 = 12 + 20 \text{ min} = 12 : 20 \text{ p.m.}$$

Note that this time is standard time relative to the time zone for which solar noon occurs at 75° W. If 90° W is used as the solar noon reference, then solar noon at 80° will occur 40 minutes before solar noon occurs at 90°. Note that the answer

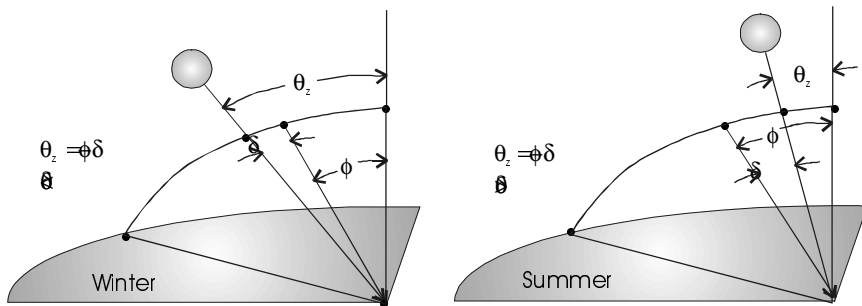


Figure 2.4 Relationships among θ_z , ϕ , and δ at solar noon in winter and summer.

is still the same. At 80° W, solar noon occurs at 12:20 p.m. Eastern Standard Time or at 11:20 a.m. Central Standard Time.

The one glitch in the solar noon argument involves those unique locations on the Earth such as Newfoundland, Canada or India, where there is only half an hour shift between adjacent time zones, or Alaska, where a single clock time zone covers nearly 30° of longitude.

Since the sun is directly overhead on the first day of summer at solar noon on the Tropic of Cancer, it becomes evident that

$$\theta_z = \phi - \delta, \quad (2.6)$$

where ϕ represents the latitude, or angular distance from the equator, since when the declination and latitude are the same, the zenith angle is zero. Note that this relationship only holds true at a given latitude at solar noon, since both ϕ and δ are constant for any given day in any given location. However, as the time differs from solar noon, it is evident that the sun will no longer be overhead, and, hence, the zenith angle is no longer zero.

Equation 2.6, however, is useful for determining the highest point in the sky reached by the sun on any particular day of the year at any particular latitude. It is also useful in determining that the highest point of the sun in the sky will be at $\theta_z = \phi - 23.45^\circ$ and the lowest point of the solar noon sun in the sky will be at $\theta_z = \phi + 23.45^\circ$, provided that $\phi > 23.45^\circ$. It is particularly interesting to note that if $\phi > 90^\circ - 23.45^\circ = 66.55^\circ$, then the lowest point of the sun in the sky is below the horizon, meaning that the sun does not rise or set that day. This, of course, is the situation in polar regions, which are subject to periods of 24 hours of darkness. These same regions, of course, are also subject to equal periods of 24 hours of sun six months later. If $\phi < 23.45^\circ$, θ_z will at some time during the summer be negative. This simply means that the sun will appear north of directly overhead at solar noon. The relationships among θ_z , ϕ and δ are illustrated in Figure 2.4.

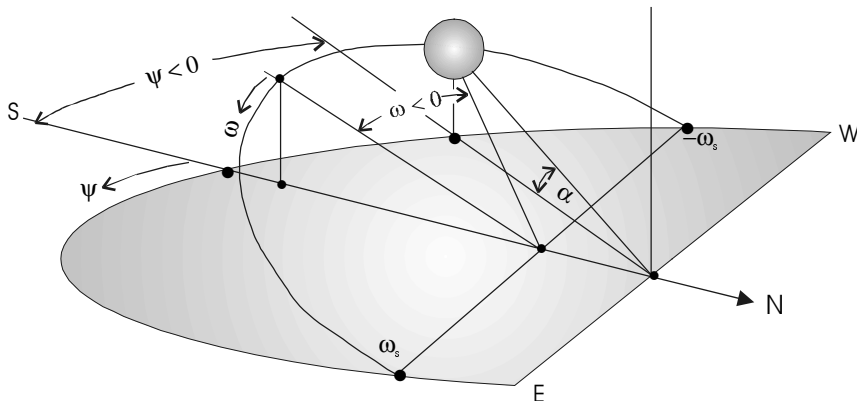


Figure 2.5 Sun angles, showing altitude, azimuth and hour angle.

2.4.3 Tracking the Sun

To completely specify the position of the sun it is necessary to specify three coordinates. However, if one assumes the distance from the sun to the Earth to be constant, the position of the sun can be specified using two coordinates. Two common choices are the solar altitude and the azimuth.

The complement of the zenith angle, θ_z , is called the **solar altitude**, α , and represents the angle between the horizon and the incident solar beam in a plane determined by the zenith and the sun, as shown in Figure 2.5. It has already been noted that the air mass is proportional to $\sec\theta_z$. Hence,

$$AM = AM(90^\circ) \csc \alpha \quad (2.7)$$

The angular deviation of the sun from directly south can be described by the **azimuth angle**, ψ , which measures the sun's angular position east or west of south. The azimuth angle is zero at solar noon and increases toward the east. It is the angle between the intersection of the vertical plane determined by the observer and the sun with the horizontal and the horizontal line facing directly south from the observer, assuming the path of the sun to be south of the observer. *The reader should note that in many publications, the azimuth angle is referenced to north, such that solar noon appears at $\psi = 180^\circ$.*

Another useful, albeit redundant, angle in describing the position of the sun is the angular displacement of the sun from solar noon in the plane of apparent travel of the sun. The **hour angle** is the difference between noon and the desired time of day in terms of a 360° rotation in 24 hours. In other words,

$$\omega = \frac{12-T}{24} \times 360^\circ = 15(12-T)^\circ, \quad (2.8)$$

where T is the time of day expressed with respect to solar midnight, on a 24-hour clock. For example, for $T = 0$ or 24 (midnight), $\omega = \pm 180^\circ$ and for $T = 9$ a.m., $\omega = 45^\circ$. By relating ω to the other angles previously discussed, it is possible to show [1] that the sunrise angle is given by

$$\omega_s = \cos^{-1}(-\tan \phi \tan \delta), \quad (2.9)$$

which, in turn, implies that the sunset angle is given by $-\omega_s$. This formula is useful because it enables one to determine the number of hours on a specific day at a specific latitude that the sun is above the horizon. Converting the sunrise angle to hours from sunrise to solar noon, and then multiplying by 2 to include the hours from solar noon to sunset, yields the number of hours of daylight to be

$$DH = \frac{48}{360} \times \omega_s = \frac{\cos^{-1}(-\tan \phi \tan \delta)}{7.5} \text{ hr.} \quad (2.10)$$

Two very important relationships among α and ψ can be determined by the reader who enjoys trigonometry. If δ , ϕ and ω are known, then the position of the sun, in terms of α and ψ at this location at this date and time, can be determined from:

$$\sin \alpha = \sin \delta \sin \phi + \cos \delta \cos \phi \cos \omega \quad (2.11)$$

and

$$\cos \psi = \frac{\sin \alpha \sin \phi - \sin \delta}{\cos \alpha \cos \phi} \quad (2.12)$$

Note that in all above expressions, angles are measured in degrees.

Since (2.11) and (2.12) are somewhat difficult to visualize, it is convenient to plot α vs. ψ for specific latitudes and days of the year. Figure 2.6 shows a series of plots of altitude vs. azimuth at a latitude of 30° N. The curves show approximately how high in the sky the sun will be at a certain time of day during a particular month, with the azimuth angle determined by the time of day. With the irradiance following (2.3), the mathematical challenge is to calculate the daily irradiation that falls on a surface mounted at either a fixed angle with respect to the sun or that falls on a surface designed to remain perpendicular to the direct radiation. This means that an expression must be derived that will describe the position of the sun during all daylight hours, and then the irradiance must be expressed in terms of this position. Finally, the irradiance must be integrated over all daylight hours, taking into account the angle between the solar altitude and the plane of the collecting surface.

Interestingly enough, when all of the mathematical work just described is finished, one ends up with an answer that does not take into account cloud cover. Markvart [1] gives detailed formulas for sun position and the components of global irradiance. The interested reader is encouraged to review them. The most

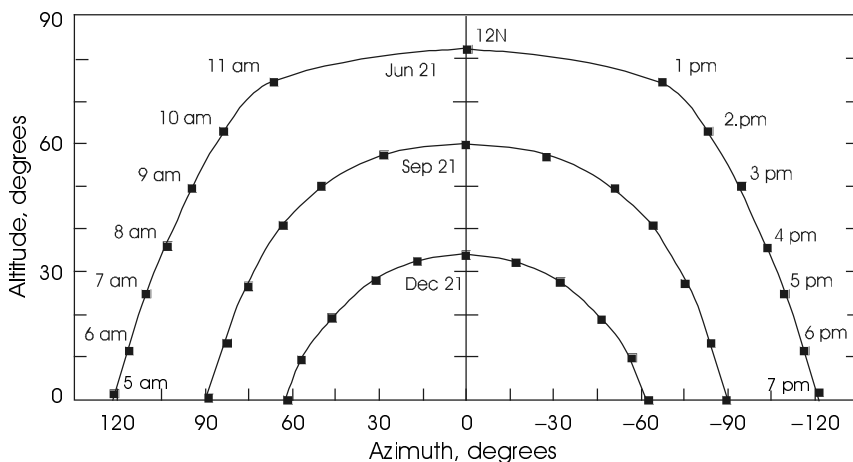


Figure 2.6 Plot of solar altitude vs. azimuth for different months of the year at a latitude of 30° N.

reliable means of accounting for cloud cover is to make measurements over a long period of time in order to determine average figures. Figure 2.7 shows average daily irradiation over the Earth for summer (a) and winter (b). Appendix A shows average daily irradiation for a number of locations on a monthly basis.

2.4.4 Measuring Sunlight

Since all the calculations and approximations in the world cannot yield exact predictions of the amount of sunlight that will fall on a given surface at a given angle at a given time at a given day in a given place, the design of photovoltaic power systems is dependent upon the use of data based on measurements averaged over a long time. Since irradiance data is still being accumulated, the engineer should be familiar with the instrumentation used in acquiring sunlight data. In addition, many photovoltaic systems installed on an experimental basis require instrumentation to determine the system performance parameters.

Depending whether it is desired to measure global, beam, diffuse or albedo components of irradiance, or whether it is simply desired to measure when sunlight exceeds a certain brightness level, different types of instrument are used. Figure 2.8 shows the a) Black and white pyranometer, b) Pyrheliometer with tracker, and c) Pyranometer mounted on a shadow band stand.

Precision Measurements

The **pyranometer** is designed to measure global radiation. It is normally mounted horizontally to collect general data for global radiation on a horizontal surface. However, it is also often mounted in the plane of a photovoltaic collector in order to measure the global radiation incident on the inclined surface.

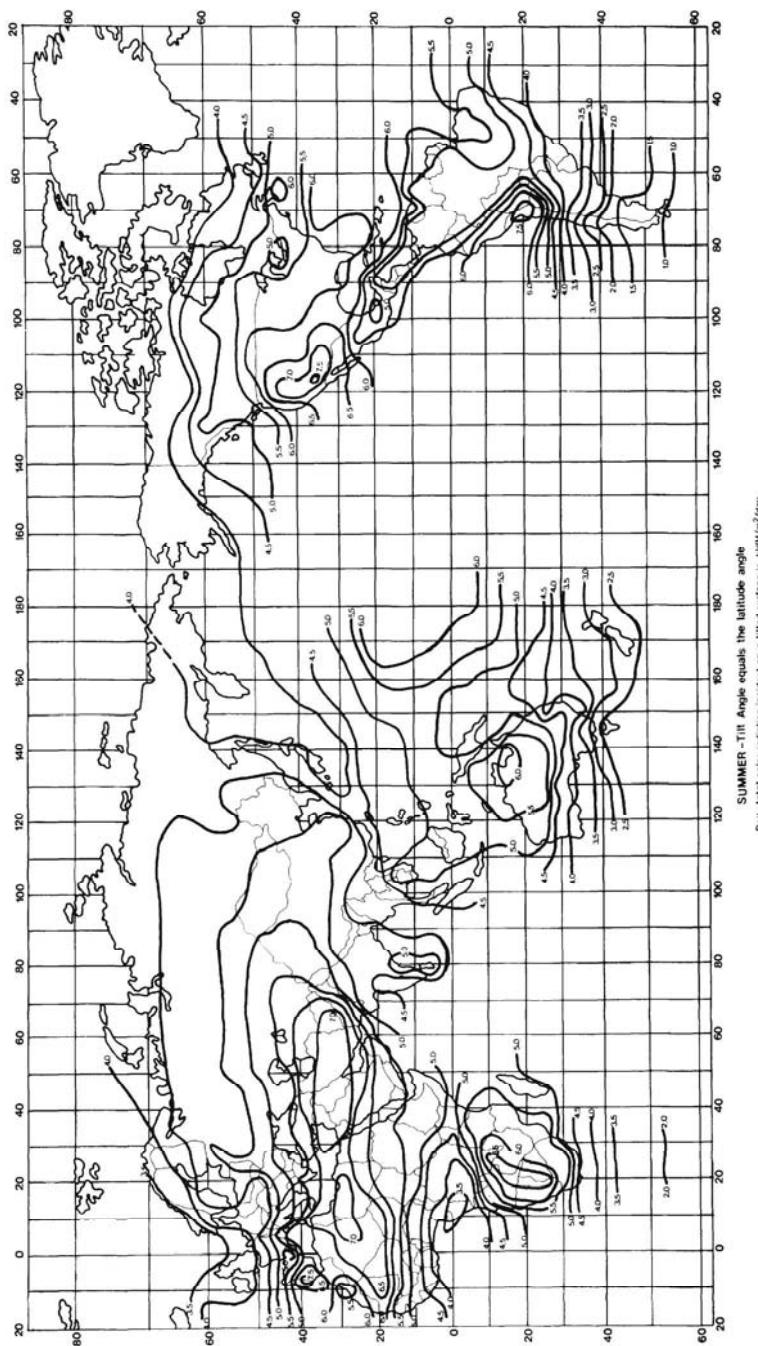


Figure 2.7a Worldwide average daily irradiation (kWh/m³) for summer. (Courtesy National Renewable Energy Laboratory [3].)

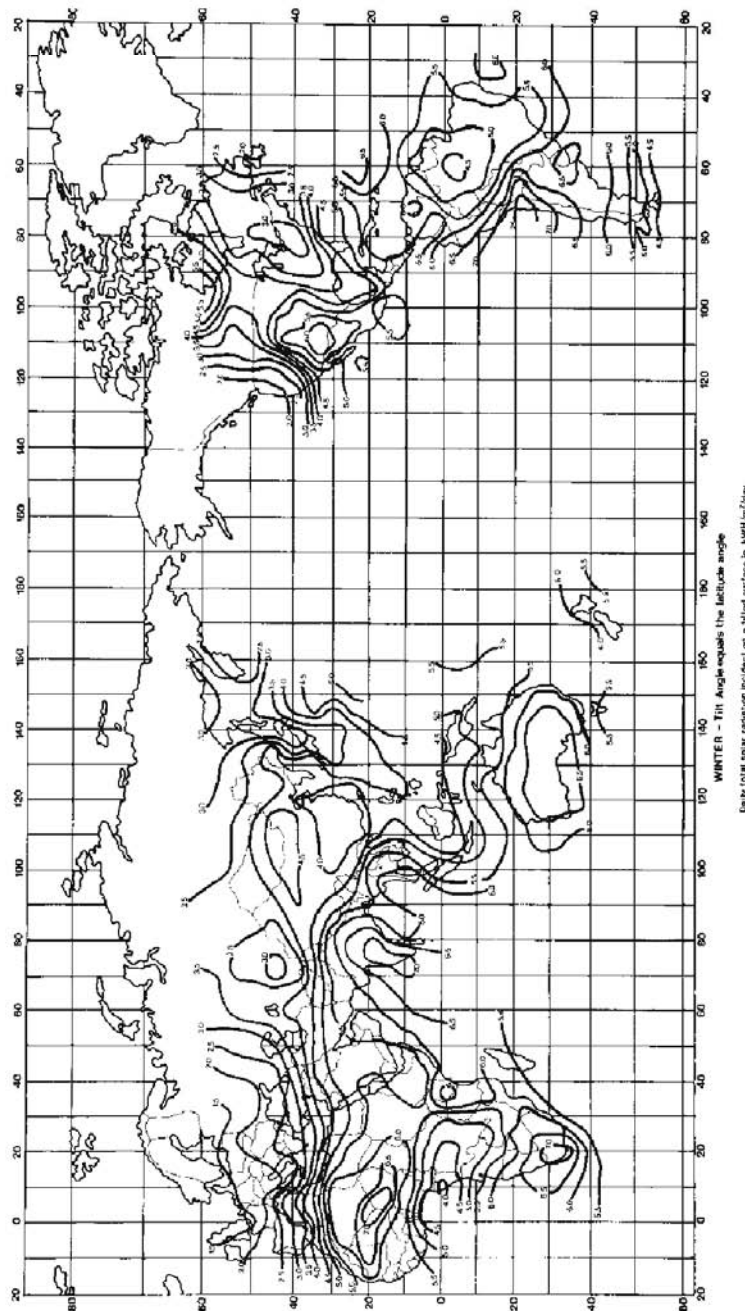
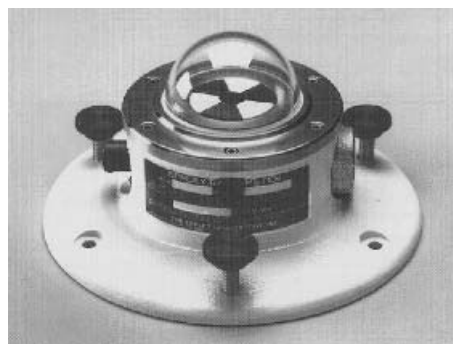


Figure 2.7b Worldwide average daily irradiation (kWh/m^2) for winter. (Courtesy National Renewable Energy Laboratory [3].

The pyranometer is designed to respond to all wavelengths and, hence, it responds accurately to the total power in any incident spectrum. The precision spectral pyranometer contains a circular, multijunction, wire-wound thermopile. This instrument is capable of withstanding mechanical vibration in excess of 20 g. Its lens is transparent between 0.285 and 2.8 micrometers, and it is accurate within 1% for solar altitudes higher than 20°. The instrument has an output voltage of approximately $9 \mu\text{V}/\text{W}/\text{m}^2$ and an output impedance of 650Ω .

The black and white pyranometer operates on the principle of differential heating of a series of black and white wedges, as shown in the photo in Figure 2.8. The temperatures of each wedge are measured with thermocouples that yield voltage differences dependent on the temperature differences. The output voltage, approximately $10 \mu\text{V}/\text{W}/\text{m}^2$, is then calibrated with respect to incident energy. This instrument is somewhat less accurate than the precision unit.

The **normal incidence pyrheliometer** uses a long, narrow tube to collect beam radiation over a narrow beam solid angle, generally about 5.5°. The inside of the tube is blackened to absorb any radiation incident at angles outside the



a. Black and white pyranometer



b. Pyrheliometer with tracker



c. Pyranometer on shadow band stand

Figure 2.8 Instruments for measuring sunlight. (Courtesy of Eppley Laboratory.)

collection solid angle. The tube is sealed with dry air to eliminate absorption of incident radiation within the tube by water vapor. The sensor is a wire-wound thermopile at the base of the tube that has a sensitivity of approximately $8\mu\text{V}/\text{W}/\text{m}^2$ and an output impedance of approximately $200\ \Omega$. Since the instrument is only sensitive to beam radiation, a tracker is needed if continuous readings are desired.

The pyranometer can be mounted on a **shadow band stand** to block out beam radiation so that it will respond only to the diffuse component. The stand is mounted so the path of the sun will be directly above the band during daylight hours. Because δ changes from day to day and because the band blocks out only a few degrees, it is necessary to readjust the band every few days. Obviously the north-south orientation of the device is important to ensure symmetry of the ring about solar noon. If the beam component of sunlight is desired, the instrumentation needs to be installed where the albedo component is negligible. Subtracting the diffuse from the global component yields the beam component.

Less Precise Measurements

Many inexpensive instruments are also available for measuring light intensity, including instruments based on cadmium sulfide photocells and silicon photodiodes. These devices give good indications of relative intensity, but are not sensitive to the total solar spectrum and thus cannot be accurately calibrated to measure total energy. These devices also do not normally have lenses that capture incident radiation from all directions. Devices that capture solid angles from a few degrees to upwards of 90° are available.

2.5 Capturing Sunlight

2.5.1 Maximizing Irradiation on the Collector

The designer of any system that collects sunlight must decide on a means of mounting the system. Perhaps the easiest mounting of most systems is to mount them horizontally. This orientation, of course, does not optimize collection, since the beam radiation component collected is proportional to the cosine of the angle between the incident beam and the normal to the plane of the collector, as shown in Figure 2.9. Depending on the ratio of diffuse to beam irradiance components, the fraction of available energy collected will be between $\cos\gamma$ and unity. Of course, in a highly diffuse environment, the beam irradiance will be only a small fraction of the global irradiance. Several alternatives to horizontal mounting exist. Equation 2.6 shows that if a collector is mounted with its plane perpendicular to θ_z at solar noon, it will be perpendicular to the sun at solar noon. This is the point at which the sun is highest in the sky, resulting in its minimum path through the atmosphere and corresponding lowest air mass for the day. Since the sun travels through an angle of 15° per hour, it will be close to perpendicular to the collector for a period of approximately two hours. Beyond

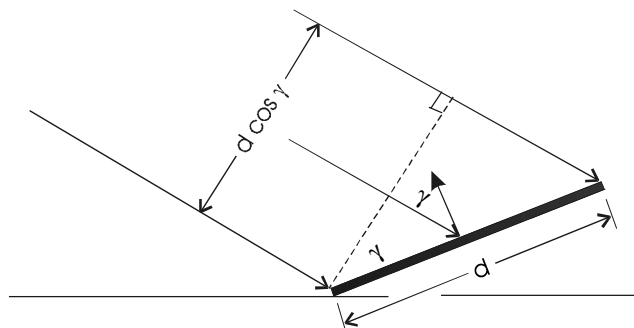


Figure 2.9 Two-dimensional illustration of effect of collector tilt on effective area presented to beam component of radiation.

this time, the intensity of the sunlight decreases due to the increase in air mass, and the angle between incident sunlight and the normal to the collector increases. These two factors cause the energy collected by the collector to decrease relatively rapidly during the hours before 10 a.m. and after 2 p.m. Figure 2.10 shows the approximate cumulative irradiation received by a south-facing collector tilted at the latitude angle in a region where the beam radiation component is significantly stronger than either the diffuse or the albedo components.

If the collector is mounted so it can track the sun, then the incident irradiance is affected only by the increasing air mass as the sun approaches the horizon. Figure 2.10 also shows the additional cumulative irradiation under direct beam conditions received by a tracking collector. Approximately 50% more energy can be collected in the summer in a dry climate such as that found in Phoenix, AZ, by using a tracking collector. During winter months, however, only about 20% more energy is collected using a tracker. In Seattle, WA, which receives somewhat more diffused sunlight than does Phoenix, a tracking collec-

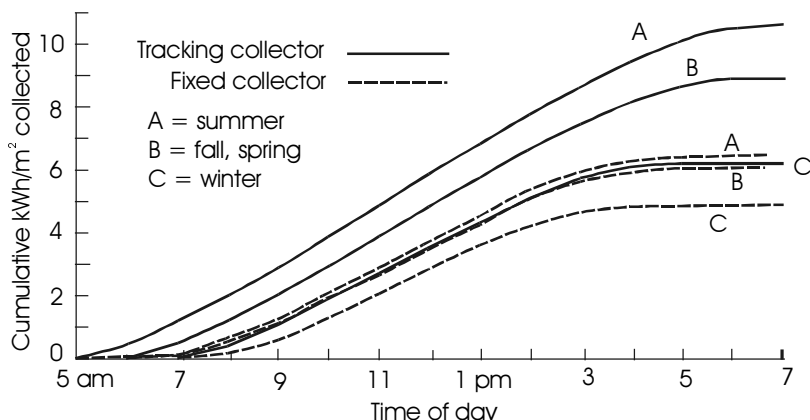


Figure 2.10 Cumulative daily irradiation received by fixed and tracking collectors for different seasons, direct beam contribution only.

tor will collect about 35% more in the summer but only 9% more energy compared to an optimized fixed collector in the winter (See Appendix A). Whether to use a two-axis tracking collector then becomes an important economic decision for the engineer, since a tracking mount is more costly than a fixed mount.

To make the mounting selection even more interesting, one can consider a single-axis tracker, which rotates about an axis fixed with respect to θ_z . One can then also consider mountings that can be adjusted manually several times per day or, perhaps, several times per year. Each of these options will enable the collection of an amount of energy that lies somewhere between the optimized fixed collector and the 2-axis tracking collector results.

Collector orientation may also be seasonally dependent. For example, a remote cabin, used only during summer months, will need its collector oriented for optimal summer collection. However, if the cabin is used in the winter as a ski lodge, or in the fall as a hunting base, then the collector may need to be optimized for one of these seasons. For optimal performance on any given day, a fixed collector should be mounted with its plane at an angle of $\phi - \delta$ with respect to the horizontal, as shown in Figure 2.11. This will cause the plane of the collector to be perpendicular to the sun at solar noon.

For optimal seasonal performance, then, one simply chooses the average value of δ for the season. For summer in the northern hemisphere, δ varies sinusoidally between 0° on March 21 to 23.45° on June 21 and back to 0° on September 21. If this variation is plotted as half a sine wave with amplitude of 23.45° , those who have evaluated the average value of a sine wave in conjunction with the output of a rectifier circuit may recall that the average value of half a sine wave having amplitude A , is $2A/\pi$. Hence, the average declination between March 21 and September 21 is 14.93° . Similarly, the average declination for the period from September 21 to March 21 is -14.93° . Hence, for best average summer performance, a collector should be mounted at approximately $\phi - 15^\circ$, and for best average winter performance, it should be mounted at $\phi + 15^\circ$. For optimum spring or fall performance or optimum annual performance, the

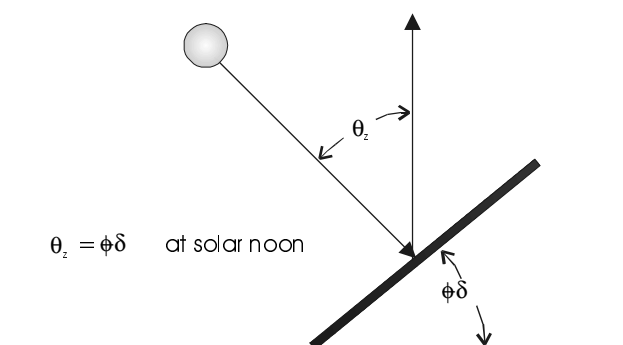


Figure 2.11 Optimizing the mounting angle of a fixed collector.

collector should be mounted at about $0.9\phi^{\circ}$. Since normally it is acceptable to orient a collector for optimal seasonal or, perhaps, annual performance, many tables of irradiation on collectors are available for collector tilts of either ϕ , $\phi + 15^{\circ}$, or $\phi - 15^{\circ}$ at various locations on the globe. Examples of these tables as compiled by the National Renewable Energy Laboratory are presented in Appendix A. Figure 2.12 shows how monthly performance depends on collector tilt angle. Different locations will show different relative monthly performance, depending on local weather seasonal behavior.

2.5.2 Shading

Even a small amount of shade on a PV module can significantly reduce the module output current. It is thus of paramount importance to select a site for a PV system where the PV array will remain unshaded for as much of the day as possible. This is easy if there are no objects that might shade the array, but it is probably more likely that a site will have objects nearby that shade the array at some time of the day on some day of the year. The PV system designer must thus be able to use her knowledge of sun position to determine the times at which a PV array might be shaded.

Figure 2.13 shows a device that incorporates plots of altitude vs. azimuth for selected latitudes. The device is used at the proposed site to determine when the array will be shaded by observing the position of reflected objects on the screen of the device. By sketching the outlines of shading objects on the screen with the device at the proposed location of the collector, the user can then determine when the collector will be shaded. For the example in Figure 2.13, the collector will be free of shade during May, June, July and August. In September, the collector will be unshaded between about 9:15 a.m. and 3:15 p.m. sun time, while in November, December and January, the collector is shaded most of the day except for a short period around 1 p.m. sun time. This proposed collector location is thus acceptable if the collector is to be used only during the summer months.

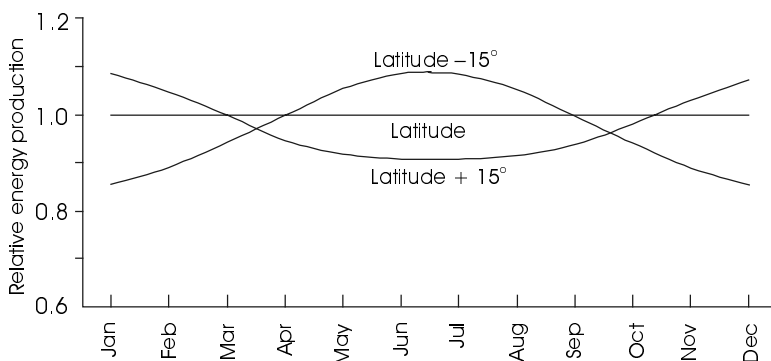


Figure 2.12 Monthly collector performance as a function of collector tilt angle.

The device also provides a measure of the fraction of available solar energy that will be collected under various shading conditions. For example, in September, 7% of the total daily insolation arrives between 11:00 and 11:30 a.m. on a south-facing surface, while in December, 8% of the total daily insolation arrives between 11:00 and 11:30 a.m. sun time. For the example shown in Figure 2.13, during March about 67% of the daily available sun will arrive at the collector during the unshaded period between 9:30 a.m. and 2:45 p.m.

The inclinometer is another device that can be used to determine potential shading problems. The inclinometer simply measures the angle between the horizontal at the height of the PV array and the top of objects that might present shading problems. This angle, along with an azimuth angle measured with a compass, corrected to true north, can then be compared with the altitude vs. azimuth chart for the sun for the location of the installation for different months of the year.

2.5.3 Special Orientation Considerations

It should be noted that all previous discussion about collector orientation has assumed fixed collectors to be facing directly south (or north if in the southern hemisphere). Sometimes it is not practical to orient a collector directly to the

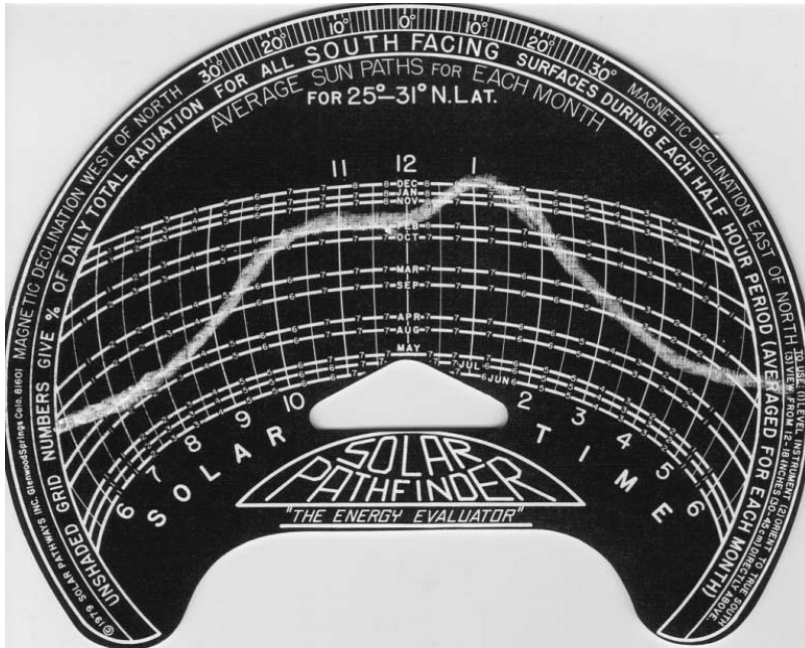


Figure 2.13 Solar Pathfinder showing region of shading. Shading occurs at points above the white line on the pattern. (Florida Solar Energy Center Photo.)

south and sometimes it may even be desirable to use a different orientation. In other situations, a horizontal mount is preferable. The question is to what extent collection is sacrificed by a non-south facing collector, or, alternatively, what may be gained with an alternate orientation.

Horizontal Mounting

In some PV installations, notably on floating buoys or watercraft, the orientation of the collector changes as the direction of travel of the watercraft changes. If a buoy has a single anchor, it will rotate. In these or similar cases, the collectors are normally mounted horizontally.

An estimate of average daily available irradiation can be made by determining whether a collector mounting of latitude $+15^\circ$, latitude -15° or latitude will yield the angle closest to horizontal. Then find the average daily peak sun hour data for this tilt angle, γ , for the location closest to the point of interest from a table similar to the tables in Appendix A. Multiplication of each peak sun hour data point in the table by $\cos\gamma$ then yields a corrected set of data that will more closely represent the irradiation to be received by the collector. This operation assumes all radiation to be beam radiation. Considering that in different locations, different fractions of global radiation are due to the beam component, this correction represents a worst-case estimate.

An alternate (and preferable) method of obtaining the irradiation on a horizontal surface is to use National Renewable Energy Laboratory tables [3] or contour maps of global irradiation on a horizontal surface.

The loss in performance with a horizontal mount depends mostly on the latitude of the installation and the season of the year, but also depends on the specific location and the ratio of beam to diffuse components of irradiance for that location. Since the optimal seasonal performance of collectors is obtained somewhere between $\phi \pm 15^\circ$, if the installation is in the tropics, a relatively small amount of annual collection is lost with a horizontal mount.

Non-South Facing Mounting

Sometimes it is not possible or convenient to install a collector facing directly south. If south-facing is the preferred orientation, Morse and Czarnecki [11] have reported that the collector can be facing up to 22.5° away from south with less than a 2% reduction in annual collection at latitudes up to 45° .

In other cases, maximum PV system output may be desirable at a time of day other than solar noon. For example, in many regions, peak utility electrical generation occurs between the hours of 3 and 6 p.m. If a PV system is connected to the utility grid, it may be desirable to maximize system output during the utility peak. For a fixed mounting, this would require having the collector face the sun at the midpoint of this time period on a date near the middle of the period during which maximum collector output is desired. This orientation will produce peak output when the sun path is at a higher air mass than at solar noon, resulting in a slightly lower peak output than would be obtained with a south-facing collector.

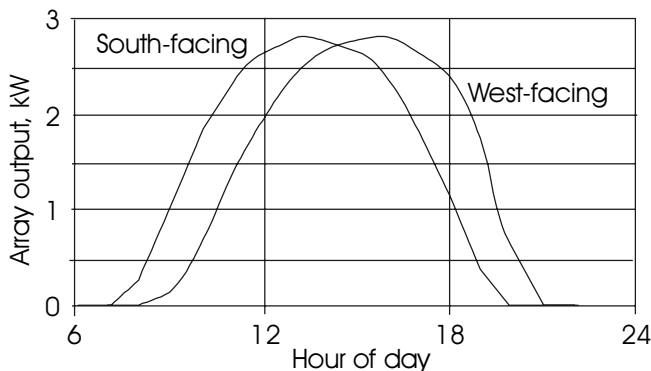


Figure 2.14 Comparison of power and energy output for south-facing and west-facing PV systems in Sacramento, CA, in summer. The south-facing system produced 22,417 Wh and the west-facing system produced 22,192 Wh. (Courtesy of Collier [4]).

Figure 2.14 shows a comparison of PV output for south-facing and west-facing PV systems. Note the appreciable increase in system output later in the afternoon for the west-facing system. During utility peak time, the system power output is increased by 70% for the west-facing system, but the west-facing system develops 14.6% less total annual energy than the south-facing system. Although the total energy output of the west-facing system is lower than that of the south-facing system, the loss of total energy may be acceptable if the added power output during utility peak hours will offset the need to use more expensive peaking generation. This observation holds particularly if it will offset the need to install the peaking generation in the first place.

Computation of the desired orientation for maximum output in a direction other than south is straightforward:

1. Determine the latitude of the location.
2. Calculate the declination for the design day, using (2.5).
3. Determine the time of day (local time) for peak PV system output.
4. Convert the local time to solar time, based upon site longitude.
5. Calculate the hour angle using (2.8).
6. Use (2.11) and (2.12) to determine α and ψ .

Example: Suppose it is desired to determine the position of the sun over Atlanta, GA, at 2 p.m. on July 1. Starting with step 1 of the 6 steps outlined above, the latitude of Atlanta is found in Appendix A to be $33^{\circ}39' = 33.65^{\circ}$ N. Then (2.5) is used to determine the declination for July 1. Since July 1 is the 181st day of the year, (2.5) gives

$$\delta = 23.45 \sin \left[\frac{360(181 - 80)}{365} \right] = 23.12^{\circ} .$$

With 2 p.m. local time (Eastern Daylight Time) at the longitude of Atlanta ($84^{\circ}36' \text{W} = 84.60^{\circ}\text{W}$) as the time of day for peak system output, the solar time is found to be 1 p.m. (Eastern Standard Time) plus an additional

$$t = \frac{84.6 - 75}{15} \times 60 = 38.4 \text{ minutes,}$$

or 1:38 p.m.

Next, substituting the solar time in (2.8) yields the hour angle as

$$\omega = \frac{12 - 13.64}{24} (360^{\circ}) = -24.60^{\circ}.$$

The solar altitude is next found from (2.11) with the result

$$\sin \alpha = \sin 23.12^{\circ} \sin 33.65^{\circ} + \cos 23.12^{\circ} \cos 33.65^{\circ} \cos (-24.6^{\circ}) = 0.9161.$$

Next, the azimuth is found from (2.12) to be

$$\cos \psi = \frac{0.9161 \sin 33.65^{\circ} - \sin 23.12^{\circ}}{\cos[\sin^{-1} 0.9161] \cos 33.65^{\circ}} = 0.3445.$$

So, finally, $\alpha = \sin^{-1} 0.9161 = 66.36^{\circ}$ and $\psi = \cos^{-1} 0.3445 = 69.85^{\circ}$.

Problems

- 2.1 Show that, for a surface temperature of 5800 K, the sun will deliver 1367 W/m² to the Earth. This requires integration of the blackbody radiation formula over all wavelengths to determine the total available energy at the surface of the sun in W/m². Numerical integration is recommended. Be careful to note the range of wavelengths that contribute the most to the spectrum. Then note that the energy density decreases as the square of the distance from the source, similar to the behavior of an electric field emanating from a point source. The diameter of the sun is 1.393×10^9 m, and the mean distance from sun to Earth is 1.5×10^{11} m.

- 2.2 If the diameter of the sun is 1.393×10^9 m, and if the average density of the sun is approximately $1.4 \times$ the density of water, and if 2×10^{19} kg/yr of hydrogen is consumed by fusion, how long will it take for the sun to consume 25% of its mass in the fusion process?
- 2.3 Calculate the zenith angles needed to produce AM 1.5 and AM 2.0 if AM 1.0 occurs at zero degrees.
- 2.4 Calculate the zenith angle at solar noon at a latitude of 40° north on May 1.
- 2.5 Calculate the number of hours the sun was above the horizon on your birthday at your birthplace.
- 2.6 Calculate the irradiance of sunlight for AM 1.5 and for AM 2.0, assuming no cloud cover, using (2.2) and (2.3). Then write a computer program that will plot irradiance vs. AM for $1 \leq \text{AM} \leq 10$ for each equation.
- 2.7 Assume no cloud cover, and, hence, that the solar irradiance is predominantly a beam component. If a nontracking collector is perpendicular to the incident radiation at solar noon, estimate the irradiance on the collector at 1, 2, 3, 4, 5 and 6 hours past solar noon, taking into account air mass and collector orientation. Then estimate the total daily irradiation on the collector in kWh. Assume AM 1.0 at solar noon and a latitude of 20° N.
- 2.8 Write a computer program using Matlab, Excel or something similar that will plot solar altitude vs. azimuth. Plot sets of curves similar to Figure 2.6 for the months of March, June, September and December for Denver, CO, Mexico City, Mexico, and Fairbanks, AK.
- 2.9 Write a computer program that will generate a plot of solar altitude vs. azimuth for the 12 months of the year for your home town. It would be nice if each curve would have time-of-day indicators.
- 2.10 Calculate the time of day at which solar noon occurs at your longitude. Then compare the north indicated by a compass with the north indicated by a shadow at solar noon and estimate the error in the compass reading.
- 2.11 Noting the dependence of air mass on θ_z ,
- Generate a table that shows α , ψ and I (using 2.3) vs. time for a latitude of your choice on a day of your choice.
 - Assuming a tracking collector and no cloud cover, estimate the total energy available for collection during your chosen day.
- 2.12 Plot I vs. AM and then plot I vs. α .

- 2.13 Calculate the collector orientation that will produce maximum summer output between 2 p.m. and 5 p.m. in Tucson, AZ. Use July 21 as the assumed midpoint of summer and correct for the longitude of the site.
- 2.14 Calculate the collector orientation that will produce maximum summer output at 9 a.m. Daylight Savings Time in Minneapolis, MN, using July 21 as the assumed midpoint of summer and using a longitude correction.
- 2.15 A collector in Boca Raton, FL ($\phi = 26.4^\circ$ N, $\psi = 80.1^\circ$ W) is mounted on a roof with a 5:12 pitch, facing 30° S of W. Determine the time of day and days of the year that the direct beam radiation component is normal to the array.
- 2.16 Determine the location (latitude and longitude) where, on May 29, sunrise is at 6:30 a.m. and sunset is at 8:08 p.m. EDT. At what time does solar noon occur at this location?
- 2.17 Using Figure 2.13, make a table of unshaded collector times for each month of the year.
- 2.18 An array of collectors consists of three rows of south-facing collectors as shown in Figure P2.1. If the array is located at 40° N latitude, determine the spacing, x , between the rows needed to prevent shading of one row by another row.

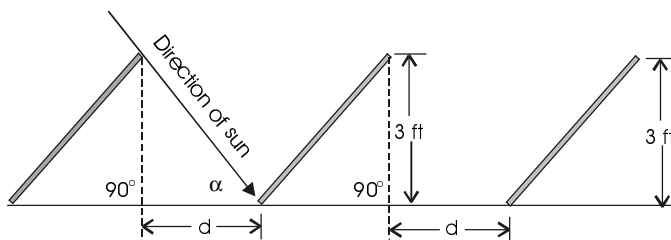


Figure P2.1 Rows of rack-mounted modules.

- 2.19 The top of a tree is found to be at an angle of 15° between the horizontal and the corner of a collector and at an azimuth angle of -30° . If the site is at a latitude of 30° N, determine the months (if any) when the tree will shade the array at the point from which the measurements are taken.
- 2.20 A residence has a 5:12 roof pitch and is located at latitude 27° N and longitude 83° W, facing 15° west of south. If two rows of 66 cm x 142 cm collectors are to be mounted on the back roof so they will have a tilt of latitude, as shown in Figure P2.2,

- a. How far apart will the rows need to be if collectors are to remain unshaded for 6 hours on December 21?
- b. Assuming Eastern Standard Time, over what time period on December 21 will the collectors be unshaded, assuming the collectors are facing 15° west of south.
- c. Assuming no other shading objects, over what time period will the collectors be unshaded on March 21?

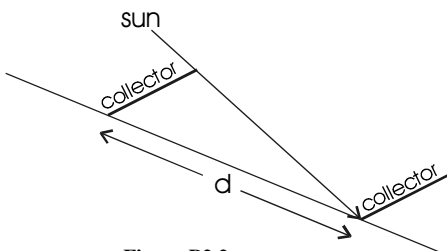


Figure P2.2

References

- [1] Markvart, T., Ed., *Solar Electricity*, John Wiley & Sons, Chichester, U.K., 1994.
- [2] Meinel, A. B. and Meinel, M. P., *Applied Solar Energy, an Introduction*, Addison-Wesley, Reading, MA, 1976.
- [3] http://rredc.nrel.gov/solar/old_data/nsrdb/redbook/sum2/. National Renewable Energy Laboratory, 30-Year Average of Monthly Solar Radiation, 1961-1990, Spreadsheet Portable Data Files.
- [4] Collier, D. E., ‘Photovoltaics in the Sacramento Municipal Utility District,’ Interconnecting Small Photovoltaic Systems to Florida’s Utility Grid, A Technical Workshop for Florida’s Utilities, Cocoa, FL, October 22, 1998.

Suggested Reading

- Howell, J. R., Bannerot, R. B. and Vliet, G. C., *Solar-Thermal Energy Systems, Analysis and Design*, McGraw-Hill, New York, 1982.
- Hu, C. and White, R. M., *Solar Cells, From Basics to Advanced Systems*, McGraw-Hill, New York, 1983.
- Hubbert, M. K., The energy resources of the Earth, *Scientific Am.*, Vol 225, No 3, September 1971, 60-70.
- McCluney, W. R., Sun position in Florida, Design Note, Florida Solar Energy Center, Cocoa, FL, (FSEC-DN-4-83), 1985.
- Morse, R. N. and Czarnecki, J. T., Report E.E. 6 of Engineering Section, Commonwealth Scientific and Industrial Res. Org., Melbourne, Australia, 1958.
- Stand-Alone Photovoltaic Systems: A Handbook of Recommended Design Practices*, Sandia National Laboratories, Albuquerque, NM, 1995.
- Water Pumping: The Solar Alternative*, Sandia National Laboratories, Albuquerque, NM, 1996.

Chapter 3

INTRODUCTION TO PV SYSTEMS

3.1 Introduction

Photovoltaic systems are designed around the photovoltaic cell. Since a typical photovoltaic cell produces less than 3 watts at approximately 0.5 volt dc, cells must be connected in series-parallel configurations to produce enough power for high-power applications. Figure 3.1 shows how cells are configured into modules, and how modules are connected as arrays. Modules may have peak output powers ranging from a few watts, depending upon the intended application, to more than 300 watts. Typical array output power is in the 100-watt-to-kilowatt range, although megawatt arrays do exist.

Since PV arrays produce power only when illuminated, PV systems often employ an energy storage mechanism so the captured electrical energy may be made available at a later time. Most commonly, the storage mechanism consists of rechargeable batteries, but it is also possible to employ more exotic storage mechanisms. In addition to energy storage, storage batteries also provide transient suppression, system voltage regulation and a source of current that can exceed PV array capabilities.

When a battery storage mechanism is employed, it is common to also incorporate a charge controller into the system, so the batteries can be prevented from reaching either an overcharged or overdischarged condition. It is also possible that some or all of the loads to be served by the system may be ac loads. If this is the case, an inverter will be needed to convert the dc from the PV array to ac. If a system incorporates a backup system to take over if the PV system does not produce adequate energy, then the system will need a controller to operate the backup system.

It is also possible that the PV system will be interconnected with the utility grid. Such systems may deliver excess PV energy to the grid or use the grid as a backup system in case of insufficient PV generation. These grid interconnected systems need to incorporate suitable interfacing circuitry so the PV system will be disconnected from the grid in the event of grid failure. Figure 3.2 shows the components of several types of photovoltaic systems.

This chapter will emphasize the characteristics of PV system components in order to pave the way for designing systems in the following chapters. The physics of PV cells, with an emphasis on the challenges to the cell innovator, are covered in Chapter 10, and current specific cell technologies are discussed in Chapter 11.

3.2 The PV Cell

The PV cell is a specially designed pn junction or Schottky barrier device. The well-known diode equation describes the operation of the shaded PV cell.

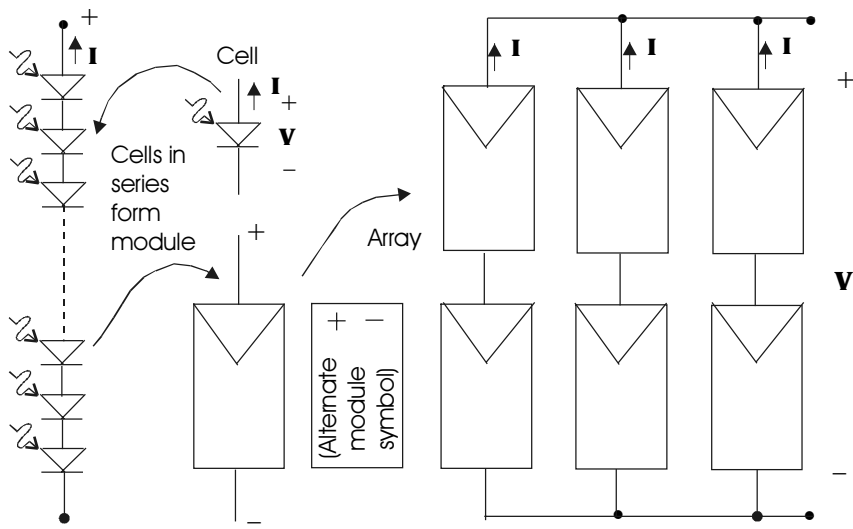


Figure 3.1 Cells, modules and arrays.

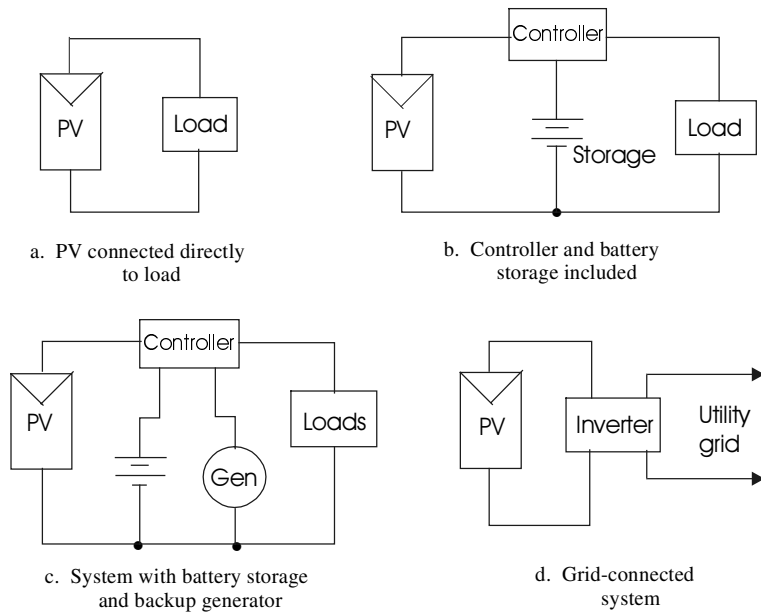


Figure 3.2 Examples of PV systems.

When the cell is illuminated, electron-hole pairs are produced by the interaction of the incident photons with the atoms of the cell. The electric field created by the cell junction causes the photon-generated-electron-hole pairs to separate, with the electrons drifting into the n-region of the cell and the holes drifting into the p-region. This process will be discussed in detail in Chapter 10. For the purposes of this chapter, knowledge of the terminal properties of the PV cell is all that is needed.

Figure 3.3 shows the I-V characteristics of a typical PV cell. Note that the amounts of current and voltage available from the cell depend upon the cell illumination level. In the ideal case, the I-V characteristic equation is

$$I = I_\ell - I_o \left(e^{\frac{qV}{kT}} - 1 \right) \quad (3.1)$$

where I_ℓ is the component of cell current due to photons, $q = 1.6 \times 10^{-19}$ coul, $k = 1.38 \times 10^{-23}$ J/K and T is the cell temperature in K. While the I-V characteristics of actual PV cells differ somewhat from this ideal version, (3.1) provides a means of determining the ideal performance limits of PV cells.

Figure 3.3 shows that the PV cell has both a limiting voltage and a limiting current. Hence, the cell is not damaged by operating it under either open circuit or short circuit conditions. To determine the short circuit current of a PV cell, simply set $V = 0$ in the exponent. This leads to $I_{SC} = I_\ell$. To a very good approximation, the cell current is directly proportional to the cell irradiance. Thus, if the cell current is known under standard test conditions, $G_o = 1 \text{ kW/m}^2$ at AM 1.5, then the cell current at any other irradiance, G , is given by

$$I_\ell(G) = (G/G_o)I_\ell(G_o). \quad (3.2)$$

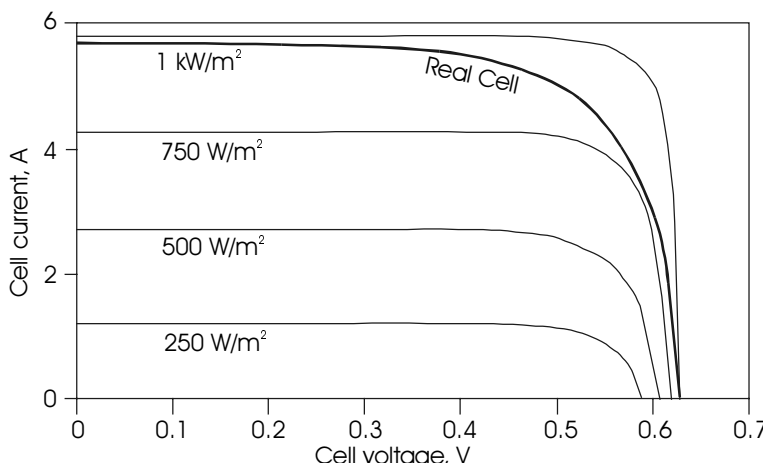


Figure 3.3 I-V characteristics of real and ideal PV cells under different illumination levels.

To determine the open circuit voltage of the cell, the cell current is set to zero and (3.1) is solved for V_{OC} , yielding the result

$$V_{OC} = \frac{kT}{q} \ln \frac{I_\ell + I_o}{I_o} \approx \frac{kT}{q} \ln \frac{I_\ell}{I_o}, \quad (3.3)$$

since normally $I_\ell \gg I_o$. For example, if the ratio of photocurrent to reverse saturation current is 10^{10} , using a thermal voltage (kT/q) of 26 mV, yields $V_{OC} = 0.6$ V. Note that the open circuit voltage is only logarithmically dependent on the cell illumination, while the short circuit current is directly proportional to cell illumination.

Multiplying the cell current by the cell voltage yields the cell power. In order to obtain as much energy as possible from the rather costly PV cell, it is desirable to operate the cell to produce maximum power. Referring to Figure 3.4, note that there is one point on the cell I-V characteristic where the cell produces maximum power. Note also that the voltage at which maximum power occurs is dependent upon the cell illumination level. The maximum power point can be obtained by plotting a set of hyperbolas defined as $IV = \text{constant}$, and noting the power associated with the hyperbola that is tangent to the cell I-V curve at only one point, as opposed to missing the curve or intersecting the curve in two points. The maximum power point may also be determined by differentiating the cell power equation and setting the result equal to zero. After finding the voltage for which this condition is satisfied, and checking to verify that this voltage represents a maximum, the maximum power point is known. The

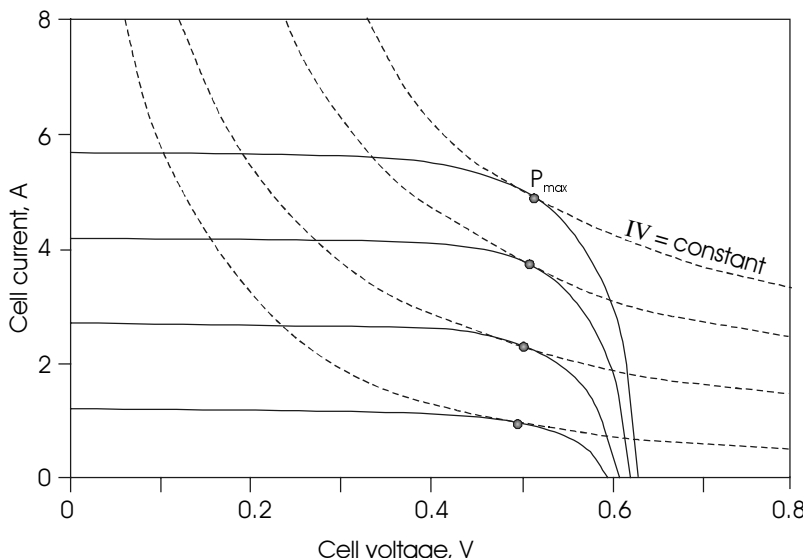


Figure 3.4 Determination of the maximum power point on a PV cell operating characteristic.

maximum power point is also readily found by simply plotting cell power vs. cell voltage, as shown in Figure 3.5.

If I_m represents the cell current at maximum power, and if V_m represents the cell voltage at maximum power, then the cell maximum power can be expressed as

$$P_{\max} = I_m V_m = FF I_{SC} V_{OC}, \quad (3.4)$$

where FF is defined as the cell **fill factor**. The fill factor is a measure of the quality of the cell. Cells with large internal resistance will have smaller fill factors, while the ideal cell will have a fill factor of unity. Note that a unity fill factor suggests a rectangular cell I-V characteristic. Such a characteristic implies that the cell operates as either an ideal voltage source or as an ideal current source. Although a real cell does not have a rectangular characteristic, it is clear that it has a region where its operation approximates that of an ideal voltage source and another region where its operation approximates that of an ideal current source.

For the cell having an ideal I-V characteristic governed by (3.1), with $V_{OC} = 0.596$ V and $I_{SC} = 2.0$ A, the fill factor will be approximately 0.83. Typical fill factors for real PV cells, depending on the technology, may vary from 0.5 to 0.82. The secret to maximizing the fill factor is to maximize the ratio of photocurrent to reverse saturation current while minimizing series resistance and maximizing shunt resistance within the cell.

The cell power vs. cell voltage curve is especially important when considering maximizing power transferred to the cell load. This topic will be investigated in more detail in Section 3.6, where methods of matching the load to the source are discussed.

The PV cell I-V curve is also temperature sensitive. A quick look at (3.3) might suggest that the open circuit voltage is directly proportional to the absolute temperature of the cell. A longer look, however, will reveal that the reverse saturation current is highly temperature dependent also. The net result, which

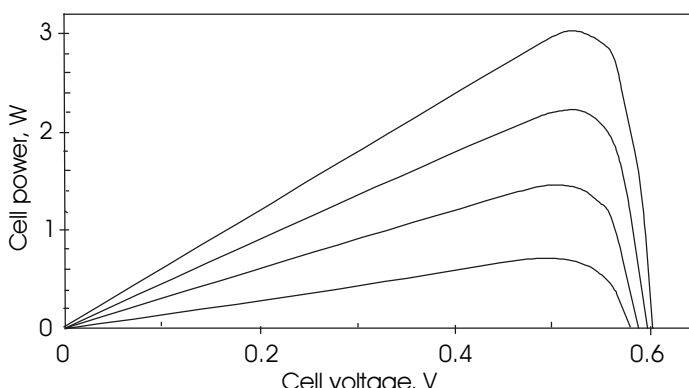


Figure 3.5 Power vs. voltage for a PV cell for 4 illumination levels.

will be covered in detail in Chapter 10, is that the open circuit voltage of a silicon PV cell decreases by $2.3 \text{ mV}/^\circ\text{C}$ increase in temperature, which amounts to approximately $0.5\%/\text{ }^\circ\text{C}$. The short circuit current, on the other hand, remains nearly constant. As a result, the cell power also decreases by approximately $0.5\%/\text{ }^\circ\text{C}$. Figure 3.6 shows the temperature dependence of the PV cell power vs. voltage characteristic.

It is important to remember that when a cell is illuminated, it will generally convert less than 20% of the irradiance into electricity. The balance is converted to heat, resulting in heating of the cell. As a result, the cell can be expected to operate above ambient temperature. If the cell is a part of a concentrating system, then it will heat even more, resulting in additional temperature degradation of cell performance.

The photocurrent developed in a PV cell is dependent on the intensity of the light incident on the cell. The photocurrent is also highly dependent on the wavelength of the incident light. In Chapter 2 it was noted that terrestrial sunlight approximates the spectrum of a 5800 K blackbody source. PV cells are made of materials for which conversion to electricity of this spectrum is as efficient as possible. Depending on the cell technology, some cells must be thicker than others to maximize absorption. Cells are often coated with an antireflective coating to minimize reflection of sunlight away from the cells.

3.3 The PV Module

In order to obtain adequate output voltage, PV cells are connected in series to form a PV module. Since PV systems are commonly operated at multiples of 12 volts, the modules are typically designed for optimal operation in these systems. The design goal is to connect a sufficient number of cells in series to keep V_m of the module within a comfortable range of the battery/system voltage un-

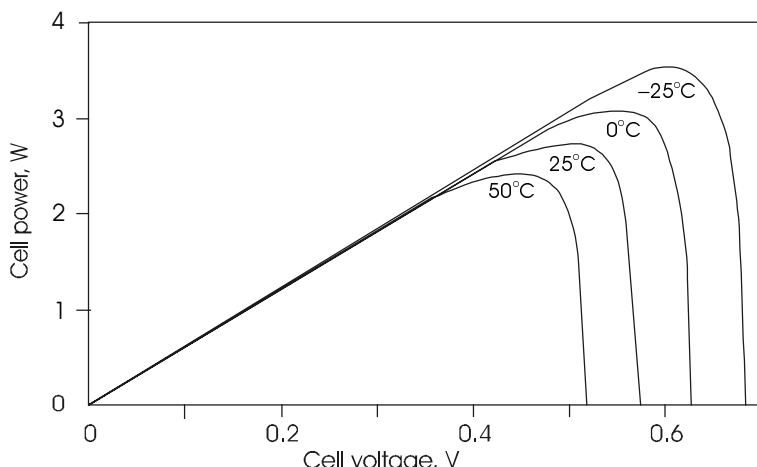


Figure 3.6 Temperature dependence of the power vs. voltage curve for a PV cell.

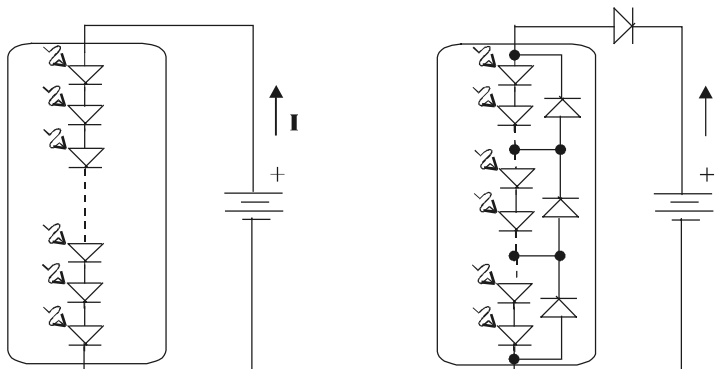
der conditions of average irradiance. If this is done, the power output of the module can be maintained close to maximum. This means that under full sun conditions, V_m should be approximately 16–18 V. Since V_m is normally about 80% of V_{OC} , this suggests designing the module to have a V_{OC} of about 20 volts. With silicon single cell open-circuit voltages typically in the range of 0.5–0.6 volts, this suggests that a module should consist of 33–6 cells connected in series. With each individual cell capable of generating approximately 2–3 watts, this means the module should be capable of generating 70–100 watts.

When connecting a module into a system, one consideration is what happens when the module is not illuminated. This can happen at night, but can also happen during the day if any cell or portion of a cell is shaded by any means.

Under nighttime conditions, when none of the cells are generating appreciable photocurrent, it is necessary to consider the module as a series connection of diodes that may be forward biased by the system storage batteries, as shown in Figure 3.7. For example, suppose the module consisted of 33 cells, each of which has a reverse saturation current of 10^{-10} A. Suppose also that the system battery voltage is 12.8 volts, and that this voltage is uniformly distributed across the series cells. This means that each cell will have 0.388 volts across it in the forward bias direction. Equation 3.1 shows this will result in a current of 0.32 mA flowing from the batteries into the PV module.

If the module consisted of 28 cells, this might result in more efficient battery charging during peak sun, since V_m would be approximately 14.6 V, which is closer to the battery voltage. However, under no sun, each cell would have 0.457 V across it and a battery discharge current of 4.63 mA would flow. Furthermore, under weak sun or high temperatures, the module output voltage could be less than the battery voltage and no charging would occur.

If another diode is connected in series with the module to prevent current from flowing in the reverse direction, this **blocking diode** will then have a forward voltage drop and associated power loss of more than 1 watt when the mod-



a. Module without blocking or bypass diodes b. Module with blocking and bypass diodes

Figure 3.7 Battery discharge path through PV module with and without blocking diode.

ule is providing photocurrent. If the module is only providing 50 watts, this loss represents 2–3% of the total module output power. The bottom line is that it is more efficient to simply have more cells in the series connection. In fact, blocking diodes are rarely used in PV systems. The exact number of cells will depend on the performance characteristics of the individual cell. Manufacturers of modules specify the open circuit voltage and short circuit current of the modules along with the module maximum power rating under full sun test conditions. These parameters are shown in Figure 3.4 for individual cells.

Another important observation relating to the series connection of PV cells relates to shading of individual cells. If any one of the cells in a module should be shaded, the performance of that cell will be degraded. Since the cells are in series, this means that the cell may become forward biased if other unshaded modules are connected in parallel, resulting in heating of the cell. This phenomenon can cause premature cell failure. To protect the system against such failure, modules are generally protected with **bypass diodes**, as shown in Figure 3.7. If PV current cannot flow through one or more the PV cells in the module, it will flow through the bypass diode instead.

When cells are mounted into modules, they are often covered with antireflective coating, then with a special laminate to prevent degradation of the cell contacts. The module housing is generally metal, which provides physical strength to the module. When the PV cells are mounted in the module, they can be characterized as having a **nominal operating cell temperature** (NOCT). The NOCT is the temperature the cells will reach when operated at open circuit in an ambient temperature of 20°C at AM 1.5 irradiance conditions, $G = 0.8 \text{ kW/m}^2$ and a wind speed less than 1 m/s. For variations in ambient temperature and irradiance the cell temperature (in °C) can be estimated quite accurately with the linear approximation that

$$T_C = T_A + \left(\frac{\text{NOCT} - 20}{0.8} \right) G. \quad (3.5)$$

The combined effects of irradiance and ambient temperature on cell performance merit careful consideration. Since the open circuit voltage of a silicon cell decreases by 2.3 mV/°C, the open circuit voltage of a module will decrease by $2.3n \text{ mV/}^\circ\text{C}$, where n is the number of series cells in the module.

Hence, for example, if a 36-cell module has a NOCT of 40°C with $V_{OC} = 19.40 \text{ V}$, when $G = 0.8 \text{ kW/m}^2$, then the cell temperature will rise to 55°C when the ambient temperature rises to 30°C and G increases to 1 kW/m^2 . This 15°C increase in cell temperature will result in a decrease of the open circuit voltage to 18.16 V, a 6% decrease. Furthermore, excessive temperature elevation may cause the cell to fail prematurely.

Finally, a word about module efficiency. It is important to note that the efficiency of a module will be determined by its weakest link. Since the cells are series connected, it is important that cells in the module be matched as closely as possible. If this is not the case, while some cells are operating at peak efficiency, others may not be optimized. As a result, the power output from the

module will be less than the product of the number of cells and the maximum power of a single cell.

Figure 3.8 shows how individual cell operating characteristics must be combined to produce the composite operating characteristic of the module. Note that since all cells carry the same current, the voltages of individual cells must adjust accordingly to meet the current constraint imposed by the external load. The composite I-V characteristic for n cells in series is thus obtained by adding the individual cell voltages that result for each cell to deliver the required current. The maximum current available from the module is affected by the cell with the lowest current under specific load conditions at the operating irradiance. Hence, it is desirable for all cells in the module to have identical I vs. V vs. irradiance curves. It is not difficult to imagine circumstances where the power output of one cell may differ from the power output of other cells, especially if the module is operated in a location where flocks of birds find it to be a convenient rest stop.

To arrive at the composite I-V curve for two cells in series, simply add the corresponding voltages required to produce the required current, as shown in Figure 3.8. Note that if one cell has a larger I_{sc} than the other cell, as indicated, while the voltage across the combination is zero, the voltage of each cell will not necessarily be zero. In Figure 3.8, cell #2 has a lower I_{sc} than cell #1, and thus its voltage goes negative until its current equals the current of cell #1. This means that cell #1 is generating power and cell #2 is dissipating this power.

When approximately 30 cells are connected in series, if they do not have identical I-V curves, then when the module is short-circuited, some of the cells will be generating power while others will be dissipating power. The greater the mismatch among cells in the module, the greater the level of power dissipated in the weaker cells. If all cells are perfectly matched, no power is dissipated within the module under short circuit conditions.

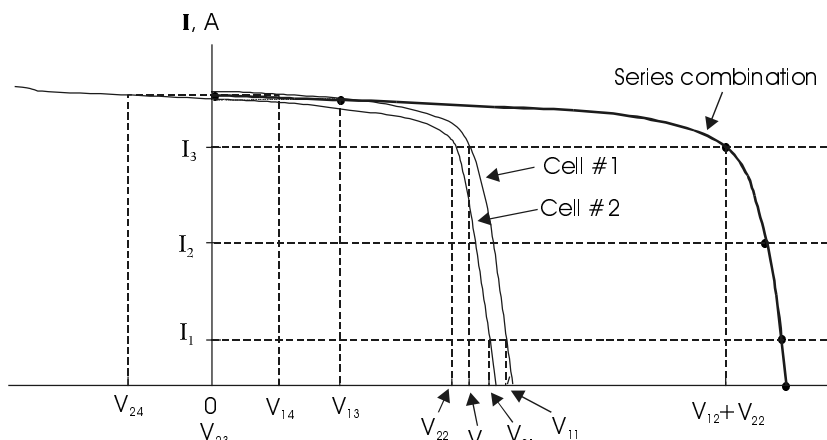


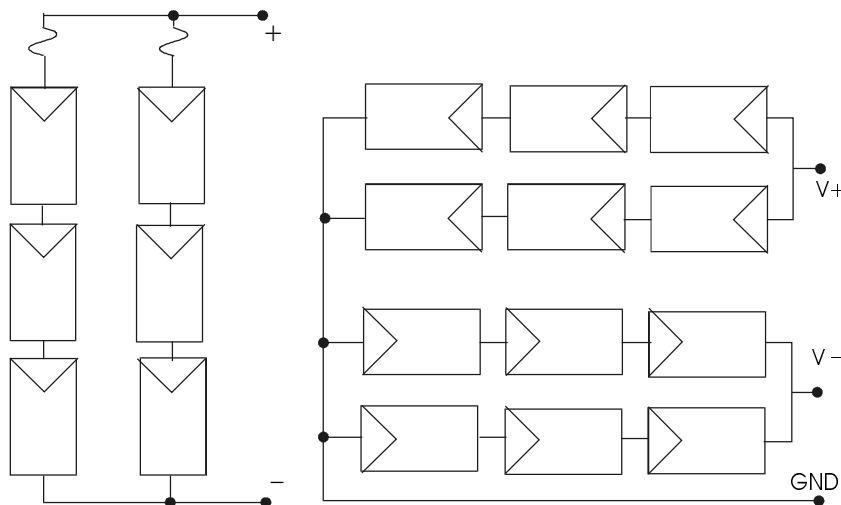
Figure 3.8 Determination of composite operating characteristic for a PV module.

3.4 The PV Array

If higher voltages or currents than are available from a single module are required, modules must be connected into arrays. Series connections result in higher voltages, while parallel connections result in higher currents. When modules are connected in series, it is desirable to have each module's maximum power production occur at the same current. When modules are connected in parallel, it is desirable to have each module's maximum power production occur at the same voltage. Thus, when mounting and connecting modules, the installer should have this information available for each module.

Figure 3.9 shows two common module configurations. In Figure 3.9a, modules are connected in series-parallel. In the parallel connection of Figure 3.9a, fuses are connected in series with each series string of modules, so that if any string should fail, any excess current from the remaining series strings that might otherwise flow in the reverse direction through the failed string will be limited by the fuse in the failed string. Individual modules will normally have several internally connected bypass diodes, as shown in Figure 3.7.

In Figure 3.9b, the modules are connected to produce both positive and negative voltages with respect to ground. If three sets of modules are connected in this manner, the combined output conveniently feeds the input of a 3-phase inverter system. A 15 kW 3-phase system sometimes uses three 5 kW inverters and three arrays of modules connected to produce approximately ± 250 volts under maximum power conditions.



a. Series-Parallel with internal bypass diodes and series fuses

b. Series-Parallel with center grounded to provide + and - supplies (fuses and diodes not shown)

Figure 3.9 Examples of PV arrays.

3.5 Energy Storage

3.5.1 Introduction

Most electrical engineers have some familiarity with batteries, especially the ones used in flashlights, toys, laptop computers, watches, calculators, video cameras, automobiles and golf carts. The extent of familiarity normally extends to the decision as to whether to purchase C-Zn batteries or whether to buy the more expensive, but longer lasting, alkaline cells. Remembering to get the correct size, whether a 9-volt or a 1.5-volt AA battery is another of life's energy storage dilemmas. In this section, considerations in battery selection for PV systems are presented. Alternatives to battery energy storage are also presented, so the PV design engineer will be able to make educated choices, based on sound economic and engineering principles, as to which type of energy storage to incorporate into a specific PV system design.

Many different types of rechargeable batteries suitable for PV applications are currently available. Although several rather exotic technologies are now available, the lead-acid battery is still the most common for relatively economical storage of relatively large quantities of electrical energy, and will probably remain so for at least the next few years. However, unless improvements in energy density, cost and lifetime are made with lead-acid technology, other promising technologies may surpass lead-acid technology. For example, *Ni-Cd* batteries are in common use in applications that require sealed batteries capable of operating in any position, and still require high energy density. But they are more expensive per joule stored than lead-acid units. Nickel metal hydride and several lithium technologies may also one day provide cost effective storage.

But, then, batteries are not the only way to store energy. It is also possible to store energy by producing hydrogen, by pumping water uphill, by spinning a flywheel or by charging a large chemical capacitor. This section explores the applications, advantages and disadvantages of some of the storage methods currently in use as well as some of the new ideas that have been proposed.

3.5.2 The Lead-Acid Storage Battery

Chemistry of the Lead-Acid Cell

Figure 3.10 shows the basics of lead-acid cell operation. In simple terms, the battery consists of a lead cathode and a lead oxide (PbO_2) anode immersed in a sulfuric acid solution. The discharging reaction at the anode consists of the exchange of oxygen ions from the anode with sulfate ions of the electrolyte. At the cathode, the discharge involves sulfate ions from the electrolyte combining with lead ions to form lead sulfate. Removal of sulfate ions from the solution reduces the acidity of the electrolyte. To maintain charge neutrality, two electrons must enter the anode terminal and two electrons must leave the cathode terminal via the external circuit for each two sulfate ions that leave the electrolyte. This corresponds to a positive current leaving the anode terminal, which is

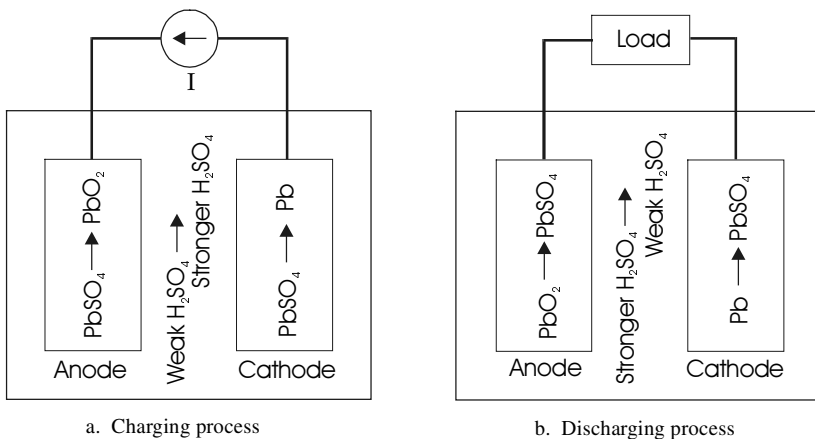
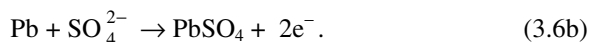


Figure 3.10 Charge and discharge of the lead-acid cell.

consistent with the passive sign convention for power being delivered. Specifically, the chemical process at the anode and cathode during discharge are represented by the respective equations

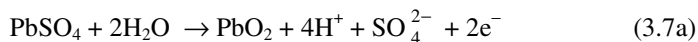


and



The oxygen ion, which enters the solution from the anode, combines with two hydrogen ions from the sulfuric acid electrolyte to form water.

When an external voltage source greater than the voltage produced by the reactions at the anode and cathode is applied across the battery terminals, the discharge process is reversed, and current flows into the anode rather than out of the anode, thus charging the battery. The chemical processes are then reversed at the anode and cathode to



and



To maintain charge balance, the two electrons shown in (3.7a) and (3.7b) must leave the anode via the external connection and travel to the cathode. As the electrons leave the anode, they are replaced by an oxygen ion, which combines with a lead ion in the anode, which was created by a sulfate ion entering the electrolyte. As these two electrons are added to the cathode, a sulfate ion is liberated from the cathode to the solution. The two electrons combine with a lead ion, producing a lead atom. The sulfate ions liberated from the cathode and

the anode to the solution increase the concentration of sulfuric acid in the electrolyte solution by balancing with hydrogen ions in the solution, while the oxygen ion left behind by the dissociated water molecule is left alone in solution. The positive potential difference between anode and cathode causes the negatively charged oxygen ion to migrate to the anode, where it becomes a part of the anode reaction, ultimately being converted to lead oxide at the anode, as previously indicated.

When the battery discharges, ultimately the surfaces of both electrodes are converted to lead sulfate. If excessive lead sulfate is allowed to build up on the electrodes, the effective surface area of the electrodes is reduced and cell performance may be affected. It is thus important to avoid fully discharging a lead-acid battery. During the charging process, some of the hydrogen ions combine with free electrons and are converted into gaseous hydrogen. At a certain point during charging, when the cathode is fully converted back to lead, there is no more sulfate at the cathode to maintain continuity in the charging current. At this point, if charging is continued, the electrons entering the cathode can no longer release sulfate ions, so the electrons continue into the electrolyte, combine with hydrogen ions, and produce hydrogen gas. This phenomenon is called gassing, and it is generally not desirable to charge a battery beyond this point, since the hydrogen gas can present a safety hazard. Occasional charging of a battery to the gassing stage so the gas bubbles up through the electrolyte can be useful, however, since the bubbling action tends to perform a cleaning action on the electrodes and a mixing action on the electrolyte.

The potential difference between electrodes in the lead-acid system is approximately 2.12 volts when the cell is fully charged. As cells are connected in series, multiples of 2.12 volts can be achieved. Most commonly, either three or six cells are connected in series, producing nominal voltages of 6 or 12 volts.

Properties of the Lead-Acid Storage Battery

Ideally, the charging and discharging processes of the lead-acid system should be reversible. In reality, however, they are not. The temperature of operation, the rate of discharge and the rate of charge all affect the performance of the battery. Since the electrical path of the battery presents ohmic resistance, some of the electrical energy intended for charging, i.e., storage, is converted to heat. When hydrogen is lost, it also represents an energy loss. Typically, the charging process is about 95% efficient. The discharge process also results in some losses due to internal resistance of the battery, so only about 95% of the stored energy can be recovered. The overall efficiency of charging and discharging a lead-acid battery is thus about 90%.

Since battery losses to internal resistance are proportional to the square of the current, this means that high current charging or high current discharging will tend to result in higher internal losses and less overall performance efficiency. This effect is offset somewhat by the increase in temperature of the battery during charging or discharging at high rates due to the higher I^2R losses. It turns out that a warmer battery can hold more charge. It also turns out that if a

battery is too warm for too long, its life expectancy is shortened, so charging and discharging rates need to be carefully observed so they will not exceed rated values for a specific battery.

The amount of energy stored in a battery is commonly measured in ampere hours. While ampere hours are technically not units of energy, but, rather, units of charge, the amount of charge in a battery is approximately proportional to the energy stored in the battery. If the battery voltage remains constant, then the energy stored is simply the product of the charge and the voltage.

The capacity of a battery is often referred to as C . Thus, if a load is connected to a battery such that the battery will discharge in x hours, the discharge rate is referred to as C/x . The charging of a battery is measured in a similar fashion. Figure 3.11 indicates the effect of discharging rates on the relative amount of charge that can be obtained from a lead-acid battery. Note that higher discharge rates result in less charge being available as energy to a load. At higher charging rates, a smaller fraction of the charging energy is used for charging and a larger fraction is used to heat up the battery. The battery can be fully charged at higher charging rates, but it takes more energy at higher charging rates to obtain full charge.

These phenomena can be explained on the basis of the Thevenin equivalent circuit of the battery, which includes a resistance in series with the open circuit cell voltages. Since the charging or discharging current must pass through the internal (Thevenin) resistance of the battery, a power loss equal to I^2R occurs. For constant current charging or discharging, the charge delivered to or removed from the battery is given by $Q = It$. Since Q is proportional to energy storage, the energy stored is thus proportional to I , whereas the energy lost is proportional to I^2 . Hence, at higher charging or discharging rates, a larger fraction of available charging energy is lost to resistive heating. This effect is compensated for somewhat by the fact that warm batteries are capable of storing more charge than cold batteries, as is shown in Figure 3.12.

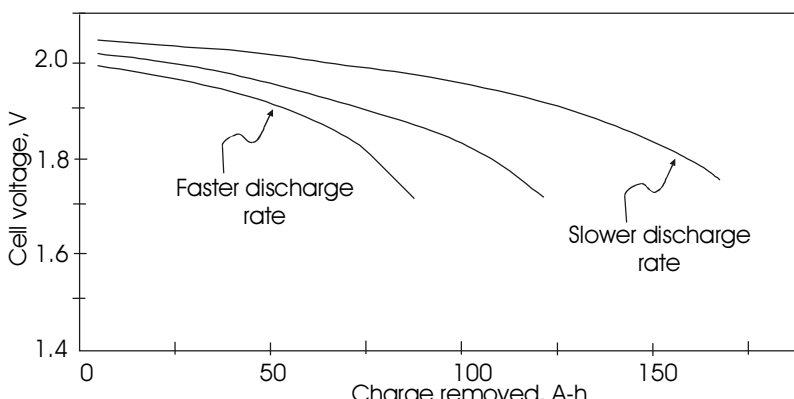


Figure 3.11 Effect of discharge rate on available energy from a lead-acid battery.

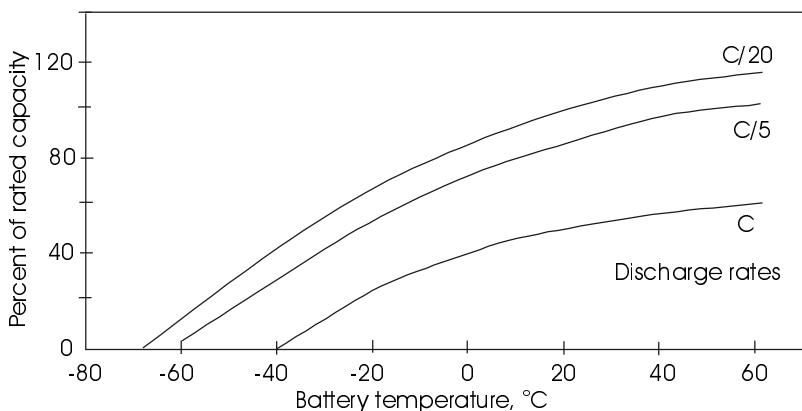


Figure 3.12 Effect of temperature and discharge rate on available energy from a lead-acid battery.

Figure 3.12 shows the effect of discharge rates and temperature on the relative amount of charge that a battery can deliver. Again, slower discharge rates result in a higher overall amount of charge being delivered by the battery. This figure is especially notable to those readers who live in northern latitudes and find it difficult to start their automobiles in subzero weather.

Depending upon specific composition of the electrodes, lead-acid batteries may be optimized for shallow discharge or for deep discharge operation. The shallow discharge units typically have a small amount of calcium combined with the lead to impart greater strength to the otherwise pure lead. The plates can then be made thinner with greater area to produce higher starting currents. These units should not be discharged to less than 75% of their capacity. In automobile applications, these are satisfactory operating conditions, since the battery is needed primarily for operation of the starter motor until the engine starts. After this point, the alternator takes over, recharging the battery and operating the automobile electrical systems. The shallow discharge units have a smaller quantity of lead and are correspondingly less expensive.

Deep discharge lead-acid batteries use antimony to strengthen the lead and can be cycled down to 20% of their initial capacity. The plates are thicker, with less area and are hence designed for sustained lower level currents. These batteries are designed for use in golf carts, marine applications, electric forklifts and for PV system use. Although the deep discharge batteries are designed for deep discharge applications, their lifetime in cycles depends on the depth of discharge during normal operation. Figure 3.13 shows how the depth of discharge affects the number of operating cycles of a deep discharge battery. The PV system designer must carefully consider the trade-off between using more batteries operating at shallower discharge rates to extend the overall life of the batteries vs. using fewer batteries with deeper discharge rates and the correspondingly lower initial cost. Life cycle costing of systems will be considered in Chapter 5.

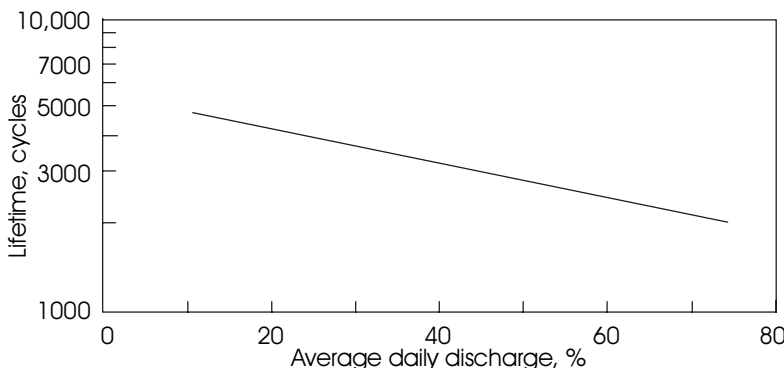


Figure 3.13 Lead-acid battery lifetime in cycles vs. depth of discharge per cycle [1].

Lead-acid batteries are available in vented and nonvented enclosures. There is a trade-off between lead-antimony and lead-calcium batteries when venting is considered. In certain lead-calcium batteries, minimal hydrogen and oxygen are lost during charging. This means minimal water is lost from the electrolyte. As a result, it is possible to seal off the cells of these batteries, making them essentially maintenance free. The trade-off, however, is that if these batteries are either purposely or inadvertently discharged to less than 75% of their maximum charge rating, their expected lifetime may be significantly shortened.

Lead-antimony electrodes, on the other hand, may be discharged to 20% of their maximum charge rating. This means that a 100 Ah lead-calcium battery has only 25 Ah available for use, while a 100 Ah lead-antimony battery has 80 Ah available for use, or more than 3 times the availability of the lead-calcium unit. However, the lead-antimony unit produces significantly more hydrogen and oxygen gas from dissociation of water in the electrolyte, and thus water must be added to the battery relatively often to prevent the electrolyte level from falling below the top of the electrodes.

Water loss can be reduced somewhat by the use of cell caps that catalyze the recombination of hydrogen and oxygen back into water, which returns to the cell. Other cell caps have a flame-retardant structure that prevents any flame external to the battery from entering the cell. In any case, the bottom line is that nonsealed, deep-discharge batteries have open vents and require relatively frequent addition of water for maintenance, depending upon cycle time and depth.

An advantage of removable cell caps on batteries is that it is possible to measure the specific gravity of the cells of these batteries. Since one of the most accurate measures of the state of charge of a battery is the specific gravity of the electrolyte, this provides a convenient means of finding faulty battery cells. Figure 3.14 shows how the electrolyte specific gravity and voltage vary during charging and discharging of the battery. Note particularly the effect of the voltage drop across the internal cell resistance during charging and discharging.

For applications where maintenance of batteries is inconvenient, maintenance free, sealed deep-cycle batteries exist, but are generally at least double the

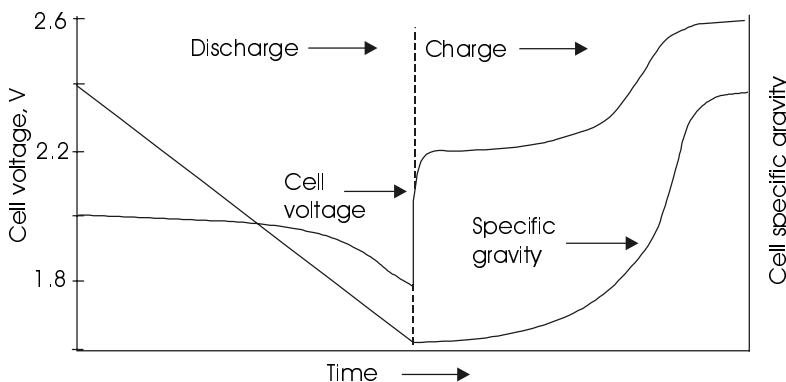


Figure 3.14 Variation of cell electrolyte specific gravity and cell voltage during charge and discharge at constant rate [1].

price of equivalent capacity nonsealed lead-acid units. These batteries are valve regulated to recombine gases, with additional treatment to immobilize the electrolyte. *Gel Cells* are sealed, lead-acid deep-cycle batteries that have silica gel added to the electrolyte. Absorbed Glass Mat (AGM) batteries have highly absorbent glass mat separators between plates to bind the electrolyte. In addition to being maintenance free, sealed deep-discharge units do not leak and have long life and low self-discharge. Charging requirements for sealed lead acid batteries differ somewhat from nonsealed units. While nonsealed units are designed for occasional overcharge, sealed units should not be overcharged.

Once a battery type has been selected, a suitable enclosure must be selected or designed and appropriate safety precautions must be taken during installation, operation and maintenance of lead-acid batteries. Two important references are the *National Electrical Code (NEC)* [2] and the *IEEE Recommended Practice for Installation Design and Installation of Valve-Regulated Lead-Acid Storage Batteries for Stationary Applications* (IEEE 1187-2002 [3]). Annex C of IEEE 1187-2002 provides information on the degree to which the life of lead-acid batteries is shortened if the batteries are operated at temperatures above 25°C. For example, at a temperature of 35°C, the battery lifetime will be shortened to 44% of its expected lifetime at 25°C. This means that it is important to provide adequate ventilation for batteries, not only to vent any hydrogen or other gases, but also to maintain a battery operating temperature close to 25°C. The serious PV system designer should be sure to have access to the *NEC* and IEEE 1187.

As a final note on lead-acid batteries, it is important to be aware of the temperatures at which the electrolytes of batteries will freeze. As the electrolyte becomes more acidic, the freezing temperature is depressed. Hence, fully charged batteries may be operated at low temperatures, while batteries in some state of discharge will need to be kept warmer. Table 3.1 summarizes the relationships between state of charge, specific gravity, cell voltage and electrolyte freezing point.

Table 3.1 Typical deep-cycle, lead-acid battery cell properties vs. state of charge [1].

State of Charge, %	Specific Gravity	Cell Voltage, V	Voltage of 12V Battery	Freezing Point, °F
100	1.265	2.12	12.70	-71
75	1.225	2.10	12.60	-35
50	1.190	2.08	12.45	-10
25	1.155	2.03	12.20	+3
0	1.120	1.95	11.70	+17

3.5.3 The Nickel Cadmium Storage Battery

Chemistry of the Nickel Cadmium Storage Battery

Ni-Cd batteries use nickel hydroxide for the anode plates and cadmium oxide for the cathode plates, in a structure similar to that of the lead-acid system. The electrolyte in the Ni-Cd system is potassium hydroxide. The NiOH anode is generally made of nickel fibers mixed with graphite- or nickel-coated plastic fibers. Small quantities of other materials such as barium and cobalt compounds are also added to improve performance. The cathode is also frequently made of a cadmium-coated plastic fiber. If the cathode is not a coated plastic, then it is commonly mixed with iron or nickel. The fiber structures of anode and cathode maximize the surface area while minimizing the amount of relatively expensive nickel and cadmium required for the electrodes.

The overall discharge reaction at the electrodes is given by



The reaction is reversed in the charging direction. The voltage of the fully charged cell is 1.29 V. Unlike the lead-acid system where the specific gravity of the electrolyte changes measurably during discharge or charge, the KOH electrolyte of the Ni-Cd system changes very little during battery operation. In some batteries, LiOH is also added to the electrolyte to improve cycle life and also to improve higher temperature operation.

Properties of the Nickel Cadmium System

Ni-Cd batteries are more robust than lead-acid batteries. They can survive freezing and high temperatures, they can be fully discharged and they are less affected by overcharging. As a result, in some applications, Ni-Cd batteries may be a better choice because their robust nature may enable the elimination of the system charge controller. If the batteries are to be used in a location where access for maintenance is difficult, the higher cost of these batteries can also often be justified.

The most common industrial Ni-Cd batteries are of the vented pocket plate type. These batteries are in use in industrial, military and space applications where the previously mentioned properties are important. Capacities range from small sizes up to more than 1200 Ah. Three different thicknesses are used

for electrodes, depending on whether the battery is designed for high, medium or low discharge rates.

Energy densities range from 20 Wh/kg for the pocket plate batteries to more than 50 Wh/kg when cells are made of the plastic-bonded plates.

Unlike the lead-acid system, which loses capacity under conditions of heavy discharge, the Ni-Cd system can be discharged at rates up to C over a wide temperature range, while still providing more than 90% of its capacity to the load. This is partially attributable to the very low internal resistance of the cells, which, depending on cell area, can be less than a milliohm.

If Ni-Cd batteries are charged and then left unused, they will lose charge at the rate of approximately 2% per day for the first few days, but then stabilize to a relatively low loss rate. Over a 6-month period, the total loss is typically about 20%, depending on whether the battery is a high, medium or low discharge rate battery. The higher the discharge rating of the battery, the greater the loss of charge over time.

Loss of charge is also temperature dependent. The loss rate is greater at higher temperatures, but at a temperature of -20 °C, there is almost no loss at all.

The lifetime of a Ni-Cd battery depends on how it is used, but is less dependent on depth of discharge than that of lead-acid batteries. A lifetime of at least 2000 cycles can be expected for a battery when it is not used extensively at elevated temperatures. As a result, under certain applications and operating conditions, a battery may last as long as 25 years, while under more frequent cycling, the lifetime may be reduced to 8 years. It is not unreasonable to expect a Ni-Cd battery to last twice as long as its lead-acid counterpart.

Ni-Cd batteries may be charged at either constant current, constant voltage or somewhere in between. This makes them especially useful in PV applications, since a PV array tends to act as a constant current source, depending on the cloud cover at the moment. If Ni-Cd batteries are overcharged, gassing will occur and the water in the electrolyte will decompose, creating a need for more maintenance. Normally, charging from full discharge to full charge should be accomplished in 5 to 7 hours, with a charging voltage between 1.50 and 1.65 volts per cell. The ampere-hour charging efficiency of the most efficient Ni-Cd batteries approaches 85%.

Those proud owners of camcorders, computers or electric toothbrushes with Ni-Cd batteries are probably familiar with the memory effect. If the battery is not fully discharged prior to recharge, the battery will tend to discharge only to the point where it was most recently discharged, and then lose cell voltage. This is manifested in the 1-hour battery lasting only for 15 minutes before the charge light comes on and the camcorder shuts down. Fortunately, the memory effect is predominant in sealed batteries and is not a problem in a battery with either pocket, fiber or plastic-bonded plate cells.

Sealed Ni-Cd batteries are also available, but their cost is higher. Their advantages over the vented units include maintenance-free operation, high discharge rates and high charge rates, along with wide temperature range. However, presently they are only available in sizes under 35 Ah.

Disadvantages of Ni-Cd batteries include difficulty in determining the state of charge of the batteries and the toxicity of the cadmium, which creates an environmental concern during production and disposal.

3.5.4 Other Battery Systems [4]

A number of other battery systems are currently in use, and others seem to show promise for future use. The **nickel-zinc** battery is a combination of the Ni-Cd system and the Cu-Zn system, which provides some attractive features, including long life and a capacity advantage. The specific energy of the Ni-Zn system is double the specific energy of the Ni-Cd system. The overall discharge chemical reaction is given by



If the battery is allowed to overcharge, it dissociates the water in the KOH electrolyte, resulting in gassing and the release of hydrogen and oxygen. Hence, charging must be controlled to avoid overcharging. Fully charged cell voltage is approximately 1.73 V.

Ni-Zn battery systems can be made in sizes in excess of 200 Ah. At normal operating temperatures ($\geq 20^\circ\text{C}$) and reasonable discharge rates ($\leq \text{C}/3$) the cell voltage remains quite stable at about 1.6 volts over most of the discharge range.

Another technology that is becoming very popular, particularly in smaller applications such as camcorders and laptop computers, is the **nickel-metal hydride** (NIMH) battery. This battery replaces the cadmium cathode with an environmentally benign metal hydride cathode, allowing for higher energy density at the cathode and a correspondingly longer lifetime or higher capacity, depending on the design goal. The anode is the same as in the Ni-Cd cell and KOH is used as the electrolyte. The overall discharge reaction is



The NIMH cell requires clever use of an oxygen recombination system to prevent loss of oxygen during the charging cycle. Electrodes are also carefully sized to ensure that the useful capacity of the battery is determined by the anode electrode to ensure that the cathode will moderate any overcharge or overdischarge condition.

A number of additional battery types are currently under investigation for PV and similar uses, such as electric vehicles. A partial listing of these batteries includes zinc/silver oxide, metal/air, iron/air, zinc/air, aluminum/air, lithium/air, zinc/bromine, lithium-aluminum/iron sulfide, lithium-aluminum/iron disulfide, sodium/sulfur, sodium/metal chloride and several variations of lithium ambient temperature batteries.

The lithium technologies appear quite attractive due to energy densities up to 150 Wh/kg, cell voltages up to 4 V and long charge retention and shelf life. Other problems must be overcome, however, before use of these batteries becomes widespread. For example, they have low cycle life, relatively poor high-

rate performance, relatively poor low-temperature performance, capacity fading and potential safety problems. It should be remembered that metallic lithium is highly reactive and presents a danger if it contacts water or humans.

The young engineer can expect to see progress in these new technologies during his/her path toward becoming an older engineer. In addition to battery storage, which is presently the most common method of energy storage for PV systems, a number of other energy storage methods are either in use or have been proposed. Many of these methods will also require a significant research effort to bring them into cost-effective, production scale use.

3.5.5 Hydrogen Storage [5]

Aside from using batteries to store energy produced by PV systems, it is also possible to use hydrogen as a storage medium. The advantage of using hydrogen for energy storage is when it is desired to recover the stored energy, the hydrogen is reacted with oxygen to form water, which is an exothermic reaction that does not have any carbon byproducts. If the hydrogen is burned in air to produce steam to turn a turbine to generate electricity, water is still produced as the byproduct, with a relatively minimal amount of nitrogen oxides. Of course, the hydrogen does not need to be used to produce electricity. It can also be used as an engine fuel to power a vehicle, such as an automobile, bus or space shuttle. Indirectly, the result is a solar-powered vehicle that stores energy in hydrogen rather than in batteries. The engineering community has not yet developed a battery-powered, space shuttle booster engine.

Perhaps the most important advantage of hydrogen storage is the energy density of hydrogen. One of the highest energy densities in conventional fuels is that of gasoline, which contains approximately 1,047,000 Btu/ft³. To store the same amount of energy in high capacity storage batteries would require approximately 120 batteries having approximately 2000 Btu/ft³ storage capacity. The storage capacity of liquid hydrogen is close to 240,000 Btu/ft³, and gaseous hydrogen can store approximately 47,000 Btu/ft³. Since water cannot be decomposed into gasoline, however, and since gasoline burning produces CO₂, among other undesirable combustion products, clean burning hydrogen is a more attractive alternative for combustion. Aside from liquid and gaseous hydrogen storage, other means of obtaining relatively high energy density, including various hydrides, are also available.

Hydrogen is normally obtained by the electrolysis of water. The output of a PV system is conveniently dc at a level consistent with that needed for relatively efficient electrolysis. Production of hydrogen by electrolysis may seem to be simply a matter of passing a current through water to produce hydrogen and oxygen, just as many readers have already done in chemistry lab. The challenge is to produce hydrogen efficiently with a system whose power output varies significantly whenever a cloud passes over the PV array.

First of all, pure water is not a good conductor. Thus, to increase efficiency, something needs to be dissolved in the water to increase the conductivity. Sev-

eral electrolytes are in common use, and others have been proposed that seem to show promise for higher efficiency conversion.

Once the hydrogen is produced, it can be used on site or it can be transported to other locations. Hydrogen proponents have suggested that hydrogen be produced in tropical latitudes having greater annual insolation and shipped to regions having less sun. Thus, after the production of hydrogen, storage and transport of the gas also present engineering challenges.

Recent interest in fuel cells for use in automotive applications has once again piqued interest in the efficient and convenient production of hydrogen. The same technology that may emerge for automotive fuel cell applications may very well spin off into PV energy storage applications as well.

3.5.6 The Fuel Cell

Fuel cells provide a convenient means of reacting hydrogen and oxygen directly to produce electricity and water. They utilize essentially the inverse of the electrolysis process. The first fuel cell was built in 1839 by Sir William Grove [6]. The high cost of fuel cells, however, had kept them out of practical use until NASA decided to use them on space flights to provide power and water. Table 3.2 summarizes the five types of fuel cells currently in use.

Fuel cells are being constructed in a wide range of power output capabilities. The smaller cells are sized to power video cameras and laptop computers. On a larger scale, The Southern California Gas Company had ten 200-kW plants on line in 1993 and experimental units in the megawatt range are now in operation [6]. The fuel cell reaction is exothermic, so if cleverly applied, the cells can supply both heat and electricity to a building. By capturing the heat, the overall system efficiency is increased, provided that the heat can be put to good use, such as for district heating or other space or water heating application.

The alkaline cell (AFC) contains a 30% solution of KOH as the electrolyte. The proton exchange (or polymer electrolyte) membrane cell (PEMFC) incorporates a semipermeable membrane that will pass hydrogen ions, resulting in a proton exchange. The phosphoric acid cell (PAFC) is based on a 103% phosphoric acid solution. The molten carbonate cell (MCFC) is based on a eutectic mixture of molten lithium carbonate and potassium carbonate. The solid oxide cell (SOFC) is based on a stabilized zirconium oxide electrolyte.

The low temperature cells are approximately twice as efficient as conventional heat engines in the conversion of energy stored in hydrogen to electricity. This makes fuel cells a very attractive possibility for energy storage and conversion to electricity in an electric vehicle, since electric motors can be operated at very high efficiency, especially with modern solid-state controllers. The present disadvantage, of course, is that fuel cells remain quite costly and will require further development to reduce their cost. Fuel cells also require a source of hydrogen, so a means for providing fuel for vehicular applications of fuel cells will need to be created.

Table 3.2 Basic fuel cell properties [7]. (Adapted from Roland, B. et al., *Hydrogen and Fuel Cells: The Clean Energy System*, 1992, Elsevier Sequoia. Reproduced with permission.)

Type	Cell Operating Temperature	Primary Cell Gas	Oxidant	System Components	Theoretical Electrical Efficiency	Achieved Electrical Efficiency	Overall System Efficiency
Alkaline	60–90°C	Pure H ₂	Pure O ₂	Cell, water, removal unit	83%	60%	
Membrane	80°C	H ₂ with C(CO) < 300 ppm	O ₂ , air	Cell, water, removal unit	83%	60%	
Phosphoric acid	160–220°C	CH ₄ or H ₂ with C(CO) < 1%	O ₂ , air	Reformer, cell, inverter, heat exchange system	80%	55%	40%
Molten carbonate	660°C	CH ₄ , H ₂ or coal gas	O ₂ , air	Coal gasifier or reformer, cell, inverter and GuD-unit	78%	55–65% 47–50% for H ₂	48–55% 60%
Solid oxide	800–1000°C	CH ₄ , H ₂ or coal gas	O ₂ , air		73%	60–65% 44–47% for H ₂	55–60%

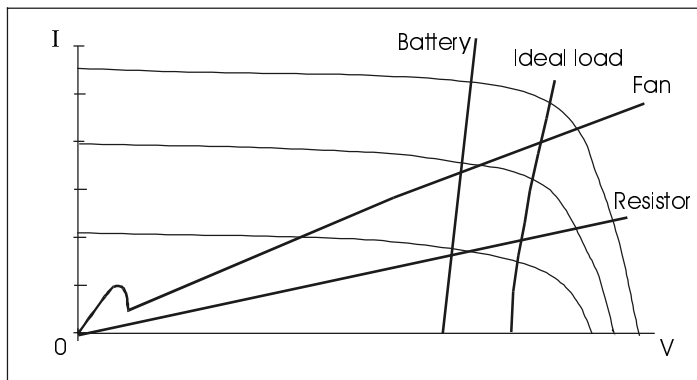


Figure 3.15 I-V characteristics for several common loads along with ideal load I-V characteristic for maximum power operation of a PV system.

3.5.7 Other Storage Options

Perhaps one of the simplest means of storing energy from the sun is to fill a water storage tank so the water can be used after sundown. Maybe the use will be for drinking or irrigation, or maybe the water will be used to turn a turbine to generate electricity before it is used for some other purpose. It is not difficult to calculate the amount of potential energy stored in a gallon of water raised to a height of 10 feet above ground.

Other possible storage mechanisms include compressed air, flywheels, superconducting magnets and chemical capacitors. All of these can be shown to be useful for certain end uses, but, in general, the cost per kWh stored is quite high at present.

3.6 PV System Loads

The importance of operating PV modules near their maximum power points has already been discussed. Maximum power operation is a challenging problem, since it requires that the system load be capable of using all power available from the PV system at all times. Not only does this mean that the system load needs to be maximum when PV system output is maximum, but it means the system load must adjust itself rather quickly at the onset or dispersion of cloud cover. In any case, the I-V characteristic of the ideal load will intersect the locus of maximum power points on the I-V characteristics of the PV array for varying illumination levels. The I-V characteristic for this ideal load is shown in Figure 3.15 along with the I-V characteristics of several other common PV system loads.

If the intersection of the I-V characteristic of a load with that of a PV source departs significantly from the maximum power point of the PV source, it may be desirable to employ an electronic maximum power tracker between the array

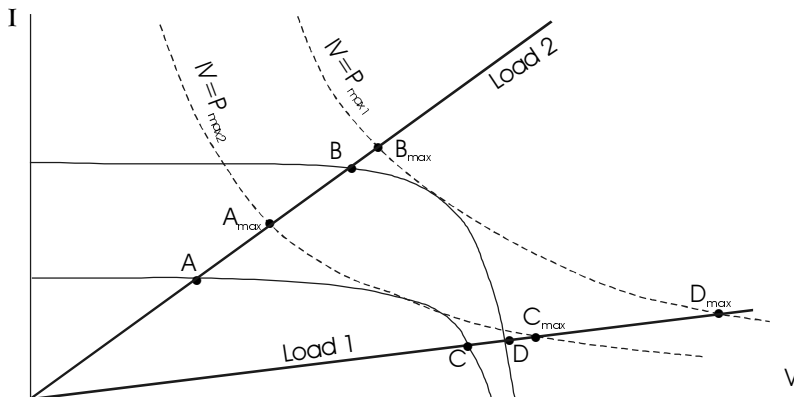


Figure 3.16 Operation of the MPT.

and the load. Maximum power trackers (MPT) generally employ pulse-width modulation techniques to switch from an input dc voltage to an output dc voltage at a different level, similar to a switching dc power supply. The MPT employs a feedback loop to sense the output power and change the output voltage accordingly until the output power is maximized.

Figure 3.16 shows how the MPT moves the operating point along the maximum power hyperbola associated with the PV array until it intersects the load I-V characteristic. The price paid for this MPT is not just the dollar price, since there is also some power loss in the MPT. It is thus necessary to justify that the expense of the MPT will be recovered by the value of the additional energy made available by the device.

A variation of the MPT involves varying the load to absorb maximum power as opposed to adjusting the source. For example, an adjustable resistive load can be adjusted until the I-V characteristic of the load intersects the source maximum power point, as shown in Figure 3.17. Another consideration for loads on PV systems is the trade-off between lifetime operating cost of a load

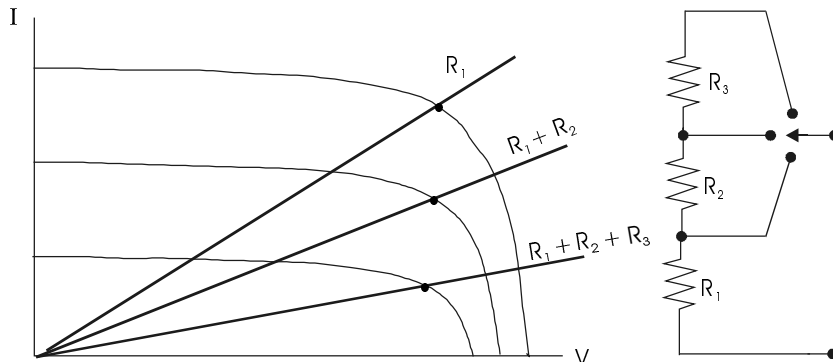


Figure 3.17 Varying a resistive load to track maximum power from a PV array.

and initial cost of the load. Often a more efficient load is available at a higher initial cost. It is then necessary for the PV system designer to perform an economic analysis of both system options to determine which load is a better choice. In particular, the choice between relatively inexpensive first-cost incandescent lamps and more expensive but more efficient fluorescent lamps involves an interesting cost analysis. Also, the cost difference between dc refrigerators and ac refrigerators is considerable, but the efficiency of the dc units is generally significantly higher than the ac units, so the purchase of a \$2500 dc refrigerator may be justified. These considerations will be accounted for in Chapter 5.

3.7 PV System Availability

Critical loads are defined as loads for which power is required at least 99% of the time. Noncritical loads require power for at least 95% of the time. It is important to recognize that these definitions involve a statistical distribution of downtime over the expected lifetime of the system. In other words, a critical system may have availability during any given month or year of its operation that may be less than 99%, while it will have availability during other years in excess of 99%. The 99% figure is considered to be an average over the lifetime of the system.

The reader is probably familiar with causes of downtime on conventional grid-connected systems. Sometimes it is a failure of an electrical generator. Sometimes it is a system overload that requires parts of the system to be shut down selectively to prevent generator overload. Sometimes a tree falls and breaks a power line. About every 100 years, an ice storm of the century causes long-term power outages for millions of utility customers, and sometimes a short circuit occurs and causes a circuit breaker to trip. Clearly, many other situations may occur that will result in the loss of power.

Photovoltaic systems are subject to similar failure modes. Loose or corroded connections, battery failure, controller failure and module failure represent a few of the things that might go wrong in a PV system. However, a good preventive maintenance program can keep these failure modes at a minimum.

Photovoltaic systems do have a factor that affects system performance to which conventional systems are not subjected—unpredictable cloud cover. As a result of unpredictable cloud cover, it is necessary to provide battery backup not only for hours of nighttime operation, but for those days when the sun either does not shine at all or when it shines too little to make sufficient electricity to meet the required daily need. Most readers are aware that different geographical locations have different seasons when cloudy days are more common. The reader in the north will be familiar with the winter weeks when the sun almost never peeks through the cloud cover. The reader in the south will be familiar with the rainy summer days when little sun is available. The bottom line is that for different geographical locations, different amounts of battery backup are required for critical and noncritical loads.

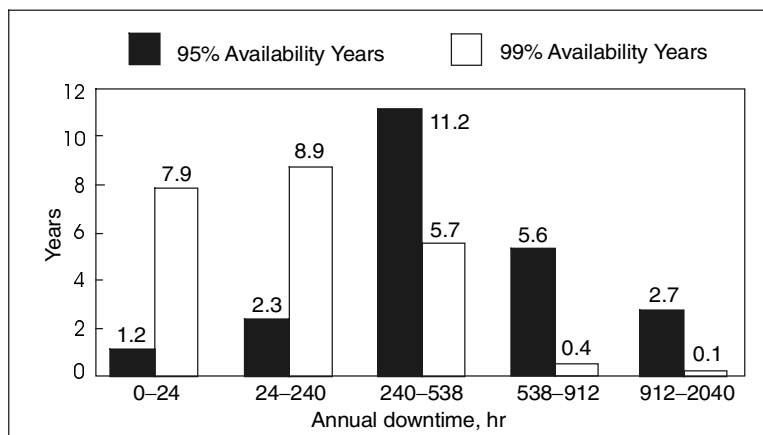


Figure 3.18 Statistical distribution of annual downtime for critical and noncritical PV systems over a 23-year system lifetime. [8]

Figure 3.18 shows the statistical distribution of downtimes due to weather over a 23-year system lifetime for critical and noncritical systems. Note that a 95% available system is allowed 438 hours of downtime per year, but that for 3.5 years of the 23 years, the system will be down for less than 240 hours and for 8.3 years the system will be down for somewhere between 538 and 2040 hours per year. The critical system is allowed to be down for 88 hours per year, but will be down for less than 24 hours per year for 7.9 years and will be down for more than 240 hours per year for 6.2 years out of the 23-year lifetime.

Figure 3.19 shows a comparison of necessary days of battery backup for critical and *noncritical* operation as a function of available peak sun hours. Days

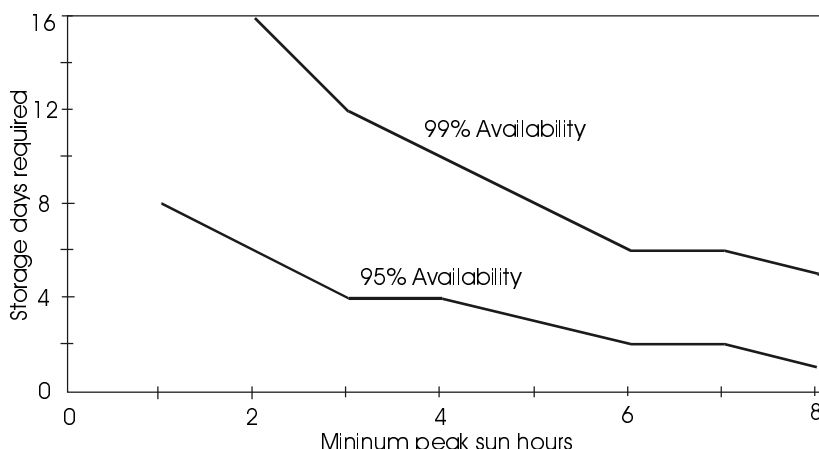


Figure 3.19 Necessary days of autonomy for critical and noncritical PV systems operation vs. minimum available peak sun hours [8].

of battery backup are also known as storage days or **days of autonomy**. A linear approximation to the data in Figure 3.19 yields the following equations for estimating necessary storage days, based on minimum average peak sun hours over the year, T_{\min} , as determined from insolation data for the listed sites.

$$D_{\text{crit}} = -1.9T_{\min} + 18.3 \quad (3.11a)$$

for critical applications, and

$$D_{\text{non}} = -0.48T_{\min} + 4.58 \quad (3.11b)$$

for *noncritical* applications, provided that $T_{\min} > 1$ hr. These equations should be used only if the critical and *noncritical* storage times have not already been determined for a site, since site-specific cloud cover or sunlight availability may differ from the averages assumed in arriving at (3.11).

Not only will there be daily variations in battery depth of discharge, but there will likely also be seasonal variations. Since there is typically more sunlight available in the summer than in the winter, it is possible to configure the battery storage system to store energy from the summer and fall for use in the winter. This involves a trade-off between the purchase of batteries and the purchase of PV modules. Suppose, for example, that a location has summer sun availability three or more times the winter sun availability. In such cases, the PV modules can be expected to produce three times as much energy in the summer as in the winter. If some of the summer energy is saved for the winter, then each winter day of sunshine need not necessarily fully recharge the battery system. Seasonal discharge of a battery system is shown in Figure 3.20 along with the daily variations for a battery system designed for seasonal cycling.

Extending the availability of a PV system from 95% to 99% may at first appear to be a simple, linear extension of the 95% system. Such a linear extension would involve only an additional 4% in cost. However, this is far from the case, and should obviously be so considering that essentially no systems can provide

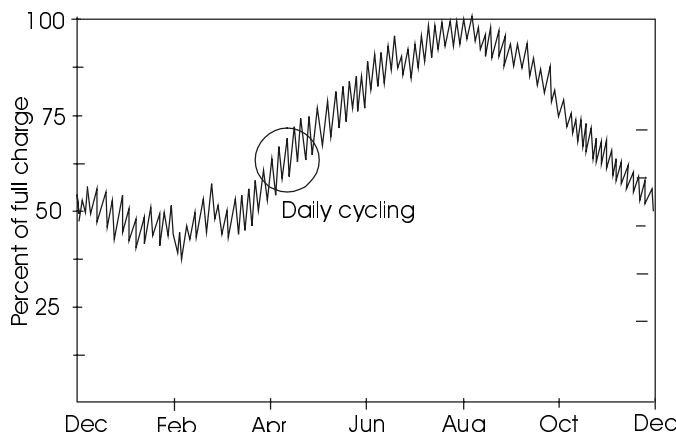


Figure 3.20 Seasonal battery cycling.

100% availability at any cost. Figure 3.21 shows the sharp increase in system cost as the availability of the system approaches 100%.

The cost of extending the availability of a system toward 100% depends on the ratio of available sun during the worst time of the year to available sun during the best time of the year. The extreme of this situation is represented by the polar latitudes, where no sun at all is available during the winter. Thus, near-100% availability would require enough batteries to store enough energy to meet all the no-sun load needs, plus a sufficient number of PV modules to charge up the batteries. This situation is further complicated by the probability that the winter loads would be larger than the summer loads. Clearly a system with 180 days of autonomy should be more costly than a system with 10 days.

In the less extreme situation, such as found in Seattle, to provide the winter system needs, the system must be overdesigned with respect to the summer needs, resulting in excess power from the array during the summer. There is a good chance that this excess availability will be wasted unless a creative engineer figures out a way to put it to use.

3.8 Associated System Electronic Components

3.8.1 Introduction

This section introduces the basic electronic components of PV systems. These components include charge controllers, maximum power trackers, linear current boosters and inverters. All of these components handle relatively large amounts of power, and are thus classified under the realm of power electronics. In each case, a simplistic explanation of the operation of the component will be given, with an emphasis on system performance requirements and how to best achieve them. Readers are encouraged to extend their understanding of these systems by consulting a power electronics text.

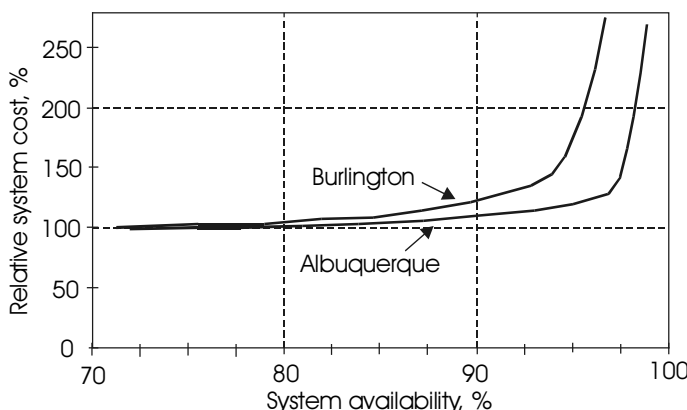


Figure 3.21 Relative cost vs. availability for PV systems in Burlington, VT, and Albuquerque, NM [8].

3.8.2 Charge Controllers

In nearly all systems with battery storage, a charge controller is an essential component. The charge controller must shut down the load when the battery reaches a prescribed state of discharge and must shut down the PV array when the battery is fully charged. When the ‘battery’ is really a system of batteries connected in series and parallel as needed to meet system needs, the control process becomes somewhat of a challenge. The controller should be adjustable to ensure optimal battery system performance under various charging, discharging and temperature conditions.

Battery terminal voltage under various conditions of charge, discharge and temperature has been presented in Figure 3.14 and Table 3.1. These results can be used to determine a Thevenin equivalent circuit for the battery system as shown in Figure 3.22. The key is that during charging, the battery terminal voltage will exceed the battery cell voltage, since the terminal voltage is the sum of the cell voltage and the voltage drop across the internal battery resistance. During discharge, the terminal voltage will be less than the cell voltage, since under discharge conditions, the terminal voltage is equal to the cell voltage minus the internal battery voltage drop. The battery cell voltage is simply the battery open circuit voltage.

The requirements for charging and discharging are made more complicated by the fact that the Thevenin equivalent circuit for the battery system is temperature dependent for both the open circuit voltage and for the resistance. As temperature decreases, open circuit voltage decreases and resistance increases. Furthermore, the Thevenin equivalent circuit for an old battery is different from that of a new battery of the same type. Hence, in order for a charge controller to handle all of these parameters, it should incorporate several important features. Depending upon the specific application, it may be possible to omit one or more of the following features.

Charging Considerations

First, consider the charging part of the process. Assume that the battery is fully charged when the terminal voltage reaches 15 volts with a specific charging current. Assume also that when the terminal voltage reaches 15 volts, the array will be disconnected somehow from the batteries and that when the termi-

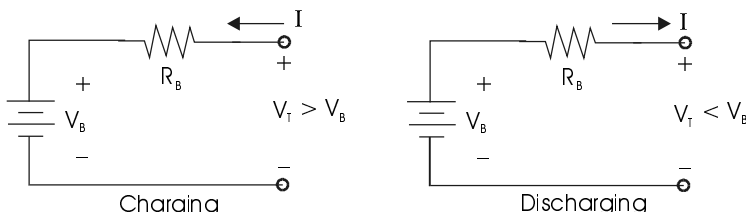


Figure 3.22 Thevenin equivalent circuit for a battery under charging and discharging conditions.

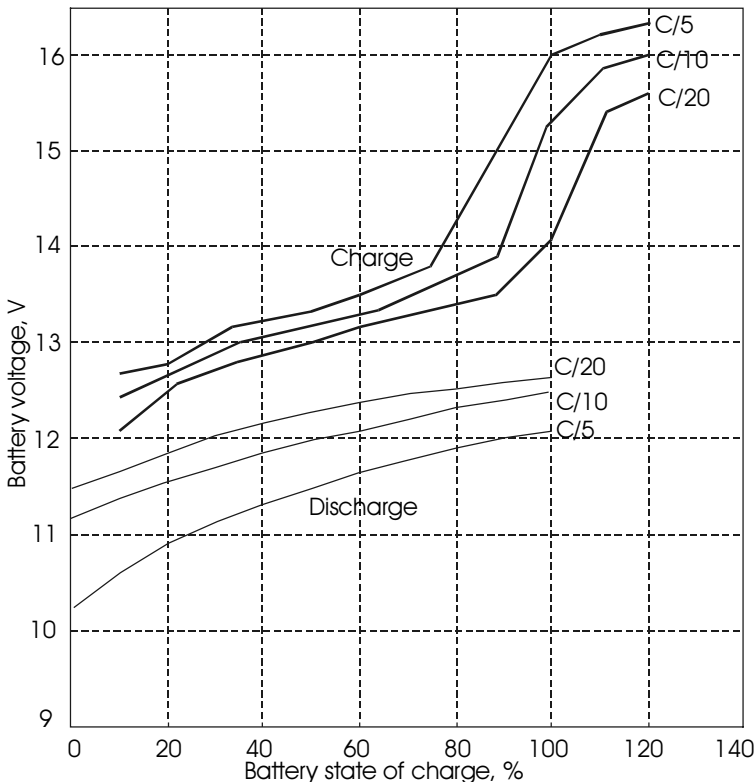


Figure 3.23 Terminal voltage as a function of charging or discharging rate and state of charge [1].

nal voltage falls below 15 volts, the array will be reconnected. Now note that when the array is disconnected from the terminals, the terminal voltage will drop below 15 volts, since there is no further voltage drop across the battery internal resistance. The controller thus assumes that the battery is not yet charged and the battery is once again connected to the PV array, which causes the terminal voltage to exceed 15 volts, which causes the array to be disconnected. This oscillatory process continues until ultimately the battery becomes overcharged or until additional circuitry in the controller senses the oscillation and decreases the charging current. Figure 3.23 shows how the terminal voltage of a battery depends on the charge or discharge rate and the state of charge for a typical battery. Note, for example, that if the battery is charged at a C/5 rate, full charge will be reached at a terminal voltage of 16 V, whereas if the battery is charged at C/20, then the battery will reach full charge at a terminal voltage of 14.1 V. If the charging current is then reduced to zero, the terminal voltage will drop to below 13 volts.

One way to eliminate overcharging resulting from the oscillatory process would be to reduce the turnoff set point of the controller. This, however, may

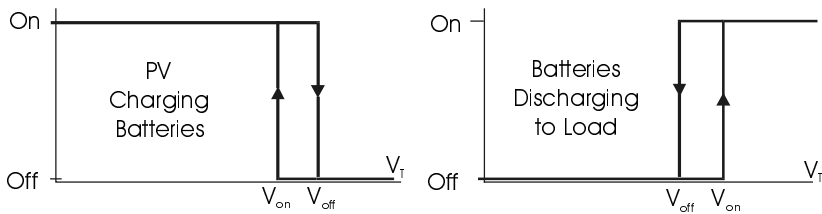


Figure 3.24 Hysteresis loops in charge controller using regenerative comparator for voltage sensing.

result in insufficient charging of the battery. Another method is to introduce hysteresis into the circuit, as shown in Figure 3.24, so that the array will not reconnect to the batteries until the batteries have discharged somewhat. The reader who has been wondering what to do with the regenerative comparator circuit that was presented in an electronics course now may have a better idea of a use for this circuit.

A more careful examination of Figure 3.23 suggests that an even better charging algorithm might be to initially charge at a relatively high rate, such as C/5. When the terminal voltage reaches about 15 V, indicating approximately 85% of full charge, the charging rate is then decreased, taking temperature into account, until the battery ultimately reaches 100% charge at a very low charging rate and a correspondingly lower voltage. This method is employed in many of the charge controllers currently being marketed for use with PV systems.

Figure 3.25 shows the regions of charge associated with the algorithm suggested in the previous paragraph. Initially, the charge controller acts as a current source. If the charging mechanism is a PV array, then presumably full array current will be used for charging. This is the bulk stage. When the charging voltage reaches a preset level, the *bulk voltage*, the charging mode is switched to constant voltage, during which the charging current decreases nearly linearly. This is called the *absorption* stage. The absorption mode is continued for a time

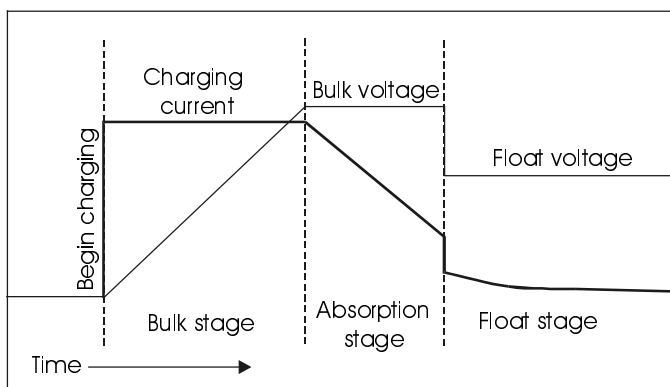


Figure 3.25 Three-stage battery charge control.

preprogrammed into the controller, after which the charging voltage is decreased to the *float* voltage. The float voltage is then maintained by the charge controller. The float voltage must be set to a level that will not result in damage to the battery. In fact, since battery temperature affects battery terminal voltage and state of charge, modern charge controllers incorporate battery temperature sensor probes that provide temperature information to the controller that results in automatic adjustment of charging set points for the charging modes.

A further mode that is available in modern chargers is the equalization mode. The equalization mode involves application of a voltage higher than the bulk voltage for a relatively short time after the batteries are fully charged. This interval of overcharging causes gassing, which mixes the electrolyte as a result of the turbulence caused by the escaping gases. This mixing helps prevent sulfate buildup on the plates and brings all individual cells to a full state of charge.

Only unsealed or vented batteries need equalization. For specific equalization recommendations, manufacturers' literature on the battery should be consulted. Some charge controllers allow for automatic equalization every month or so, but often it is also possible to set the controllers for manual equalization.

The battery disconnect may result in the array's being short-circuited, open circuited, or, perhaps, connected to an auxiliary load that will use excess array energy. If the array is short-circuited to disconnect it from the batteries, the controller is called a shunt controller. Open circuiting the array is done by a series controller. One advantage of the shunt controller is that it maintains a constant battery terminal voltage at an acceptable level by bypassing enough charging current to achieve this result. The disadvantage is the amount of power that must be dissipated by the shunt and the heat sinking necessary to remove this heat from the shunt device.

Discharging Considerations

Now consider the discharge part of the cycle. Assume the battery terminal voltage drops below the prescribed minimum level. If the controller disconnects the load, the battery terminal voltage will rise above the minimum and the load will turn on again, and once again an oscillatory condition exists. Thus, once again an application for hysteresis is identified, and another regenerative comparator circuit is justified for the output of the controller.

Now, all that remains is to make the set points of the charging regenerative comparator temperature sensitive with the correct temperature correction coefficient and the controller is complete. Of course, if the controller is designed to reduce charging current in order to bring the batteries up to exactly full charge before shutting down, and if the controller selectively shuts down loads to ensure the battery is optimally discharged, then the overall system efficiency will be improved over the strictly hysteresis-controlled system.

New designs continue to emerge for controllers as engineers continue their quest for the optimal design. Figure 3.26 shows the block diagram for a controller that employs temperature sensing, hysteresis on charge and discharge, selective load disconnect and reduced current final charging by employing

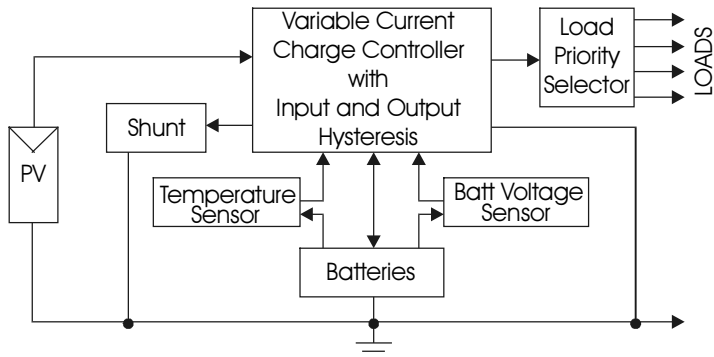


Figure 3.26 Block diagram of a fancy charge controller.

shunt-linear disconnect means. Ideally, a charge controller will make full use of the output power of the PV array, charge the batteries completely and stop the discharge of the batteries at exactly the prescribed set point, without using any power itself.

3.8.3 Maximum Power Trackers and Linear Current Boosters

Electronic maximum power trackers (MPT) have already been mentioned in Section 3.6. Linear current boosters (LCB) are special-purpose maximum power trackers designed for matching the PV array characteristic to the characteristic of dc motors designed for daytime operation, such as in pumping applications. In particular, a pump motor must overcome a relatively large starting torque. If a good match between array characteristic and pump characteristic is not made, it may result in the pump operating under locked rotor conditions and may result in shortening of the life of the pump motor due to input electrical energy being converted to heat rather than to mechanical output.

Figure 3.27 shows a typical pump I-V characteristic, along with a set of PV array I-V curves for different illumination levels. The fact that the pump characteristic is relatively far from the array characteristic maximum power point for lower illumination levels shows why an LCB can enable the pump to deliver up to 20% more fluid. The LCB input voltage and current track V_{mp} and I_{mp} of the PV array. The LCB output voltage and current levels maintain the same power level as the input, except for relatively small conversion losses, but at reduced voltage and increased current levels to satisfy the pump motor characteristic. The fact that the LCB increases current to the load accounts for the name of the device. This result will be used later in the design of PV pumping systems.

Maximum power trackers and linear current boosters are generally adaptations of dc-to-dc switching voltage regulators, as indicated in Section 3.6. Coupling to the load for maximum power transfer may require providing either a higher voltage at a lower current or a lower voltage at a higher current. Either a buck-boost or a boost-buck conversion scheme is commonly used in conjunction with load voltage and current sensors tied into a feedback loop using a micro-

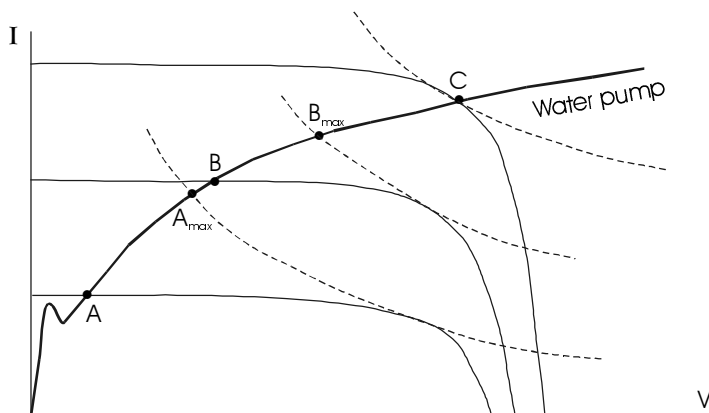


Figure 3.27 Pump and PV I-V characteristics, showing the need for use of MPT.

controller to vary the switching times on the switching device to produce optimal output voltage.

The LCB is used in special cases where only a boost of current is needed. This means a decrease in voltage will accompany the current boost in order to keep output power equal to input power. Since only a decrease in voltage is required, no boost is needed in the converter. Hence, a simple buck converter with associated tracking and control electronics will meet the design requirements of the device.

Figure 3.28a shows a simplified diagram of a buck converter circuit. When the MOSFET is switched on, current from the PV array can only flow through the inductor into the parallel RC combination, where the capacitor voltage increases. When the MOSFET is off, current must remain flowing in the inductor, so the inductor current is now supplied by the capacitor through the diode, causing the capacitor to discharge. The extent to which the capacitor charges or discharges depends upon the duty cycle of the MOSFET. If the MOSFET is on continuously, the capacitor will charge to the array voltage. If the MOSFET is not on at all, the capacitor will not charge at all. In general, the output voltage and current of an ideal buck converter are given by

$$V_{\text{out}} = DV_{\text{in}}, \quad (3.12a)$$

$$\text{and} \quad I_{\text{out}} = I_{\text{in}}/D, \quad (3.12b)$$

where D is the duty cycle of the MOSFET, expressed as a fraction ($0 < D < 1$). Note that the polarity of the output voltage is the same as the polarity of the input voltage, so there is no problem keeping the same grounded conductor at the input and the output of the converter.

Figure 3.28b shows the basic elements of a buck-boost converter that might be used in an MPT. Note that in this system, the polarity of the output voltage is opposite the polarity of the input voltage. This can be a problem if a common

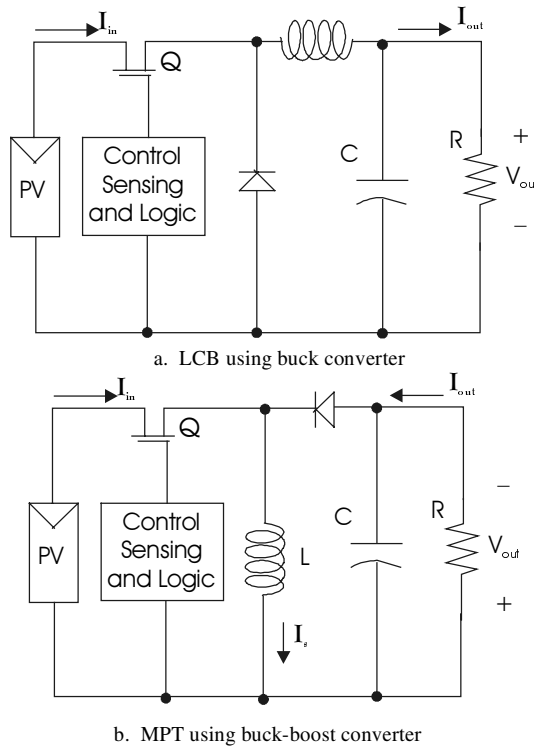


Figure 3.28 Maximum power tracker and linear current booster.

negative (grounded) conductor is required for the PV circuit and the output of the converter. In this case, the circuit needs to be somewhat more sophisticated.

The output voltage and current of the ideal buck-boost converter are given by

$$V_{\text{out}} = \frac{D}{1-D} V_{\text{in}}, \quad (3.12c)$$

$$I_{\text{out}} = \frac{1-D}{D} I_{\text{in}}. \quad (3.12d)$$

where again, D is the duty cycle of the MOSFET. Note that if $D < 0.5$, $V_{\text{out}} < V_{\text{in}}$, and if $D > 0.5$, $V_{\text{out}} > V_{\text{in}}$. Hence, the MPT is capable of either increasing or decreasing its output voltage in order to track an array maximum power point. Of course, if the MPT output voltage decreases, then its output current will increase, and vice versa, such that, in the ideal case, the output power will equal the input power.

During the time Q is on, energy is stored in the inductor. When Q turns off, the inductor current must continue to flow, so it then flows through R and C and the diode, charging C to V_{out} , since the capacitor voltage equals the output

voltage. When Q turns on again, the diode becomes reverse biased, and current is built up again in the inductor while the capacitor discharges through the resistor. Finally, when Q turns off, the cycle repeats itself. The values of L and C and the switching frequency determine the amount of ripple in the output voltage. Since no energy is lost in ideal inductors and capacitors, and since Q and the diode approximate ideal switches, essentially all power extracted from V_{in} must be transferred to the load. Of course, in reality, these components will have some losses, and the efficiency of the MPT will be less than 100%. However, a well-designed MPT will have an overall efficiency greater than 90%, with many units currently being marketed having advertised efficiencies that are close to 95% [9, 10].

Another application of the MPT is to ensure optimal charging of batteries. The MPT charge controller tracks the PV array maximum power point to ensure that maximum charging current is delivered to the battery bank. Problem 3.14 explores this concept further.

3.8.4 Inverters

Depending on the requirements of the load, a number of different types of inverters are available. Selection of the proper inverter for a particular application depends on the waveform requirements of the load and on the efficiency of the inverter. Inverter selection will also depend on whether the inverter will be a part of a grid-connected system or a stand-alone system. Many opportunities still exist for the design engineer to improve on inverters, since inverter failure remains one of the primary causes of PV system failure.

Table 3.3 Summary of inverter performance parameters [1, 11, 12].

Parameter	Square Wave	Modified Sine Wave	Pulse Width Modulated	Sine Wave*
Output power range (watts)	Up to 1,000,000	Up to 2,500	Up to 20,000	Up to 100,000
Surge capacity (multiple of rated output power)	Up to 20x	Up to 4x	Up to 2.5x	Up to 4x
Typical efficiency over output range	70-98%	>90%	>90%	>90%
Harmonic distortion	Up to 40%	>5%	<5%	<5%

* Multilevel H-Bridge or similar technology to yield utility grade sine wave output.

Table 3.3 summarizes inverters presently available. Inverter performance is generally characterized in terms of the rated power output, the surge capacity, the efficiency and the harmonic distortion. Since maximum efficiency may be achieved near rated output, it is important to consider the efficiency vs. output power curve for the inverter when selecting the inverter. Certain loads have significant starting currents, so it is important to provide adequate surge current capacity in the inverter to meet the load surge requirements. Other loads will

either overheat or introduce unwanted noise if the harmonic distortion of their power supply is not below a specific level.

In general, the square wave inverter is the least expensive and is relatively efficient, but has limitations on its applications. It has the best surge capacity but the highest harmonic distortion. The modified sine inverter is more complicated, but still relatively efficient. The pulse width modulated inverter has higher cost, high efficiency and minimal distortion. The pure sine inverter has the least distortion, but the lowest efficiency for stand-alone applications.

Square Wave Inverters

The simplest inverters are square wave inverters. These inverters employ solid state switches connected as either astable multivibrators or as externally controlled switches. Use of astable multivibrators enables the inverter to be used in a self-contained PV system, whereas externally synchronized switches are used when the inverter is to be synchronized with an external ac power source. Figure 3.29a shows how a single source can be switched alternatively in a positive direction, then in a negative direction. Figure 3.29b shows how a center-tapped array can be alternatively switched positive or negative to produce a square wave.

The key to efficient switching is to have current flowing from the array at all times while maintaining zero volts across the switching element when it passes current, and zero current through the switching element when it has voltage across it. This can be approximated reasonably well either with insulated gate bipolar transistors, power MOSFETs or silicon-controlled rectifiers. Once the dc is converted into a square wave, its amplitude normally needs to be increased to produce a 120 V rms ac waveform. Since the rms value of a square wave is simply the amplitude of a square wave, a system with a 12-volt dc input will need a transformer with a 10:1 turns ratio.

It is important, however, to realize that the transformer must be designed with a sufficient number of turns so the time constant determined by the mag-

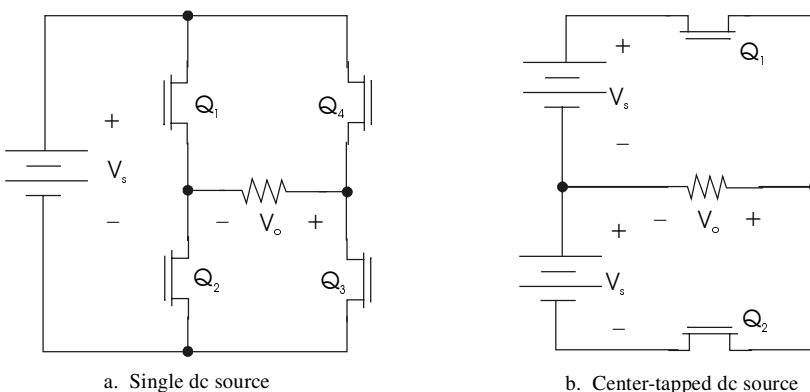


Figure 3.29 Converting dc sources to square waves.

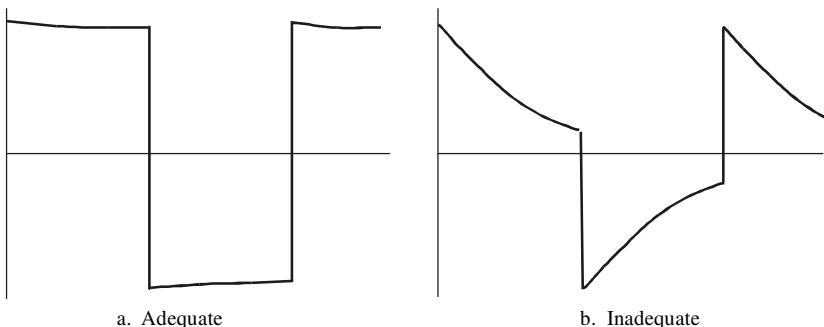


Figure 3.30 Output waveforms for square wave inverter with adequate and with inadequate number of transformer turns.

netizing inductance of the transformer and the source resistance will be long enough to maintain the square wave. Too few turns on the transformer will cause the output waveform to droop as shown in Figure 3.30. When specifying the transformer for this application, it is easy to assume that transformers are ideal and to simply try to use a 120:12 volt transformer backwards. The 120:12 volt transformer, however, probably would have been designed for use with a sinusoidal signal, and thus would not have enough turns to handle the square wave effectively. A square wave inverter with a good transformer and efficient switching can operate at efficiencies in the 90% range.

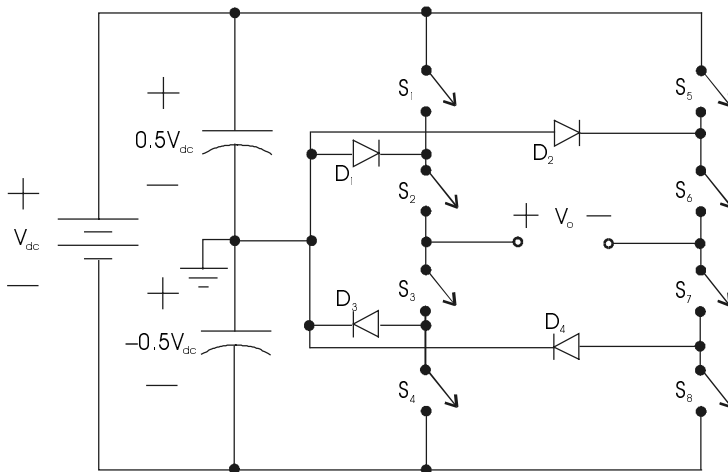
Modified Sine Wave Inverters

For a number of applications, a square wave is inadequate for meeting the harmonic distortion requirements of the load. For example, since square waves have significant harmonic content, and since hysteresis and eddy current losses in magnetic materials increase significantly with increase in frequency, square wave excitation may cause some motors or fluorescent ballasts to overheat.

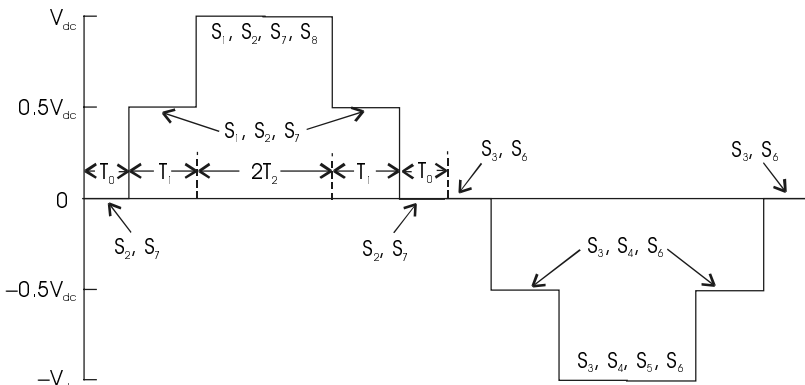
Square wave harmonics can also introduce noise into a system. Thus, before selecting an inverter, it is important to verify that the proposed load will operate with square wave excitation.

If square wave excitation is not suitable for a load, it is possible that a modified sine wave will work. A number of methods are available to convert the output of a dc source into some approximation of a sine wave. One such method involves using a multilevel H-bridge as shown in Figure 3.31a to generate a waveform such as the one shown in Figure 3.31b. The idea is to time the individual voltage levels so that harmonic distortion will be minimized and that the rms value of the output voltage will remain constant in the event that the input dc voltage should vary.

The sequence for closing switches to obtain portions of the waveform in Figure 3.31b is shown on the waveform diagram. The actual switches may be bipolar transistors, MOS transistors, SCRs or insulated gate bipolar transistors. As an example of how the various voltage levels in v_o are obtained, consider the interval T_1 , where, according to the output voltage waveform, $v_o = 0.5V_{dc}$. If S_1



a. Switching configuration



b. Output voltage waveform

Figure 3.31 Multilevel H-bridge modified sine wave inverter..

is closed, diode D_1 becomes reverse biased and appears as an open circuit. If S_7 is closed, then the positive terminal of v_o is connected to $0.5V_{dc}$. Closing S_7 provides a path to ground from the negative terminal of v_o through forward biased D_4 . Hence, if voltage drops across diodes and electronic switches are neglected, $v_o = 0.5V_{dc}$. Next, consider the interval where v_o is shown as $-V_{dc}$. During this interval, when S_3 and S_4 are closed, D_3 becomes reverse biased and appears as an open circuit and the positive terminal of v_o is thus connected to $-0.5V_{dc}$. Closing S_5 and S_6 reverse biases D_2 and connects the negative terminal of v_o to $+0.5V_{dc}$. Hence, $v_o = -V_{dc}$. It is left as an exercise for the reader to verify the remaining switching combinations.

Noting the symmetry of v_o , and recognizing that $T_0 + T_1 + T_2 = 0.25T$, where T is the period of the waveform, it is possible to determine the rms value of v_o from the first quarter cycle by solving

$$\begin{aligned} V_{rms} &= \left[\frac{4}{T} \int_0^{\frac{T}{4}} v_o^2(t) dt \right]^{\frac{1}{2}} = \left[\frac{4}{T} \left\{ \int_0^{T_0} 0 dt + \int_{T_0}^{T_0+T_1} (0.5V_{dc})^2 dt + \int_{T_0+T_1}^{T_0+T_1+T_2} V_{dc}^2 dt \right\} \right]^{\frac{1}{2}} \\ &= V_{dc} \left[\frac{T_1}{T} + \frac{4T_2}{T} \right]^{\frac{1}{2}}. \end{aligned} \quad (3.13)$$

As an example, assume that $V_{dc} = 160$ V, and it is desired to produce $V_{rms} = 120$ V by keeping $T_0 = T_1$ and solving for T_2 . The result is that $T_0 = T_1 = T/16$ and $T_2 = T/8$. Problem 3.18 offers the reader a chance to solve for T_0 , T_1 and T_2 for different values of V_{dc} . Note that since $T_1 + 4T_2 < T$, if $V_{dc} < V_{rms}$, there is no solution for T_0 , T_1 and T_2 .

H-Bridges can be designed with $2n + 1$ levels, where n is an integer. The more levels, the closer v_o can be made to approximate a sine wave. In addition, the voltage drop across any individual switch is reduced as the number of levels is increased. Problem 3.21 involves the design of a 7-level H-bridge.

Most computer uninterruptible power supplies produce a 5-level modified sine wave, so it is safe to say that this waveform is acceptable for use in providing backup ac power to a computer. However, IEEE Standard 929-2000 [13] requires that any source connected to the utility line must have less than 5% total harmonic distortion (THD). For those who haven't memorized the formula for THD from their electronics textbook, recall that THD is the percentage ratio of the sum of the rms values of all the harmonics above the fundamental frequency to the rms value of the fundamental frequency. It is unlikely that a 5-level modified sine wave inverter will meet the 5% THD rule, especially if V_{dc} is allowed to vary while keeping V_{rms} constant. This is the reason for the existence of pure sine inverters. Using higher level H-Bridges to approximate pure sine waves is one method. Another method is to use pulse width modulation techniques.

Pulse Width Modulated Inverters

The pulse width modulated (PWM) inverter produces a waveform that has an average value at any instant equivalent to the level of a selected wave at that instant. PWM inverters are perhaps among the most versatile of the family of inverters. They are similar to the PWM described in the discussion of the MPT with the exception that the MPT PWM signal is designed to have a constant average value to produce a regulated dc output, while the inverter PWM signal is designed to have a time-dependent average value that can have any arbitrary waveform at any arbitrary frequency at any arbitrary amplitude. For use in PV applications, it is generally desirable to have a sinusoidal waveform with a predictable amplitude and frequency.

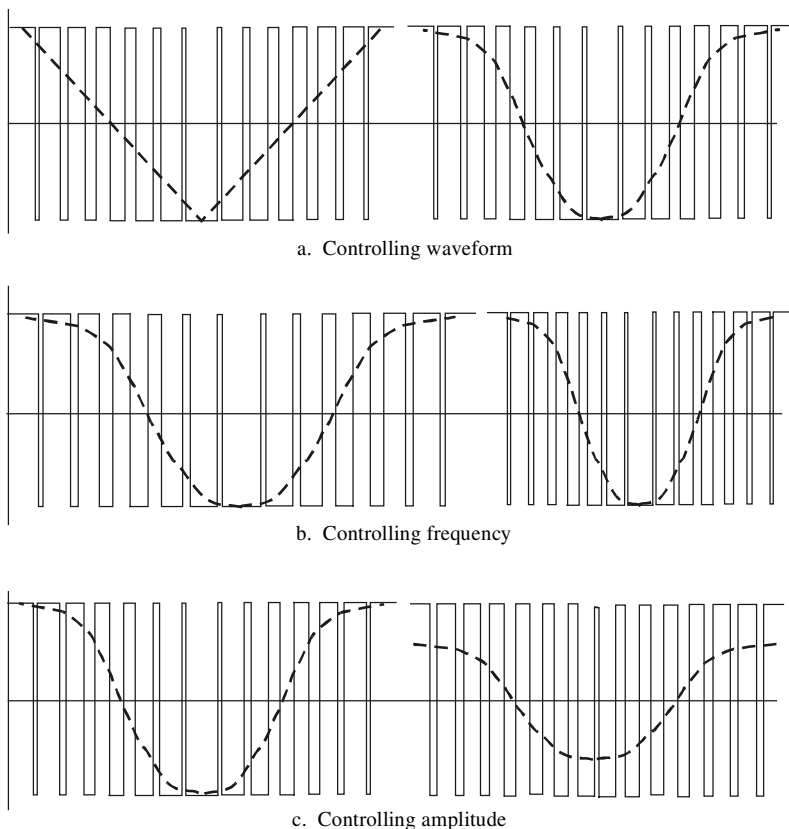


Figure 3.32 PWM control of waveform, frequency and amplitude.

Figure 3.32 shows how a PWM waveform can produce waveforms of differing amplitudes and frequencies by controlling the on-and-off time of a pulse waveform. The waveform is controlled by controlling the relative duty cycle of successive pulses. The amplitude is controlled by controlling the overall duty cycle and the frequency is determined by controlling the repetition time for the pulse sequence.

By switching the pulse between a positive level and a negative level, it is possible to construct waveforms with zero average value, which is particularly important when driving loads for which a dc component in the excitation may cause losses in the load. This includes applying dc to an ac motor or to a magnetic fluorescent lighting ballast. Application of dc to such loads can result in significant I^2R heating with possible failure of the winding insulation and subsequent catastrophic failure of the motor or the ballast, including the possibility of fire. For this reason, elimination of any dc component in the output of an inverter is important regardless of the type of inverter.

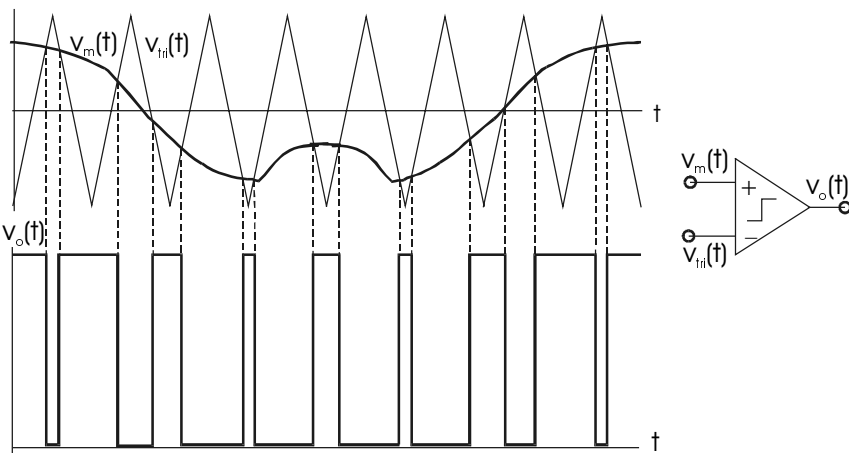


Figure 3.33 Generation of a PWM waveform.

PWM inverters are particularly useful when used as ac motor controllers, since the speed of an ac motor can be controlled by adjustment of the frequency of the motor excitation. It must be recalled, however, that the flux developed in the motor is inversely proportional to the excitation frequency, and that every motor has a saturation flux above which the motor draws significant current without further flux increase. Hence, as a motor excitation frequency is decreased, the peak value of the applied voltage must also decrease proportionally to keep the motor out of saturation. A PWM controller coupled with MPT capability can be a very efficient means of maximizing the efficiency of a PV pumping system.

Figure 3.33 shows one means of generating a PWM waveform. The process begins with a triangle wave at the frequency of the pulse waveform applied to one input of a voltage comparator. Next, the desired waveform is applied as a modulating waveform at the other input of the comparator. Whenever the modulating signal exceeds the triangle waveform, the comparator output goes high, and whenever the modulating signal is less than the triangle waveform, the comparator output goes low. The comparator output is then used to switch the output pulse on and off. The result is an output PWM waveform that has a moving average value proportional to the modulating signal.

The average value of the PWM output is obtained in a manner similar to the detection process used to pick off the modulation signal of an amplitude modulated communications signal. A filter needs to be incorporated that will not allow the voltage (or current) of the load to change instantaneously, but will allow it to change quickly enough to follow the moving average of the PWM waveform. This can be achieved with inductive and/or capacitive filtering, depending on whether it is desired to smooth the current, the voltage or both.

The harmonic content of the two-level PWM waveform can be significantly reduced through the use of a three-level PWM waveform. A three-level PWM

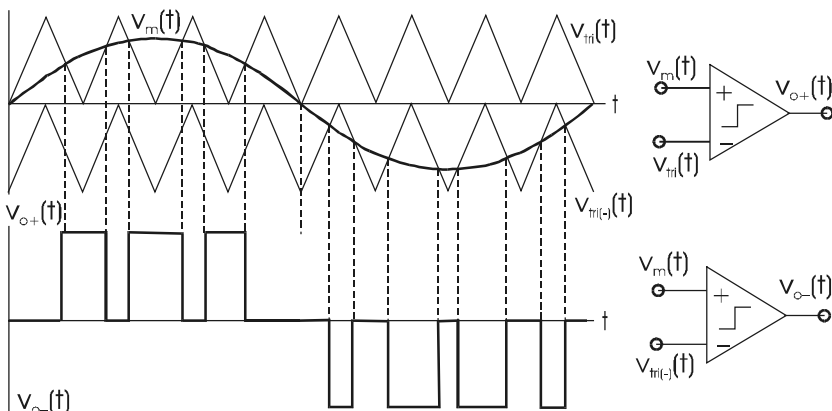


Figure 3.34 Three-level PWM inverter configuration and output signal.

waveform can be generated by incorporating a second comparator into the circuit, so that one comparator will control the positive-going pulse when the modulating signal is positive and the other comparator will control the negative-going pulse when the modulating signal is negative. The challenge here, however, is to switch the PV input so the array is never turned off if the inverter is powered directly from the array. If a storage mechanism is used for array current, so the array is continuously supplying dc power to the storage mechanism, then the storage mechanism can be switched on and off to meet the load requirements without interrupting the power flow from the array. Figure 3.34 shows a three-level PWM inverter output signal derived from dc input from battery storage.

Figure 3.35 shows a PWM inverter circuit using a full-bridge switching network for the dc source, including MPT. This is an adaptation of the full-bridge that was shown for the generation of a square wave. The inverter can be fixed frequency, line commutated (synchronized) or variable frequency, depending on the source of the modulation signal. The controller generates the triangle waveform and the modulating waveform, v_m , with the amplitude and/or frequency of v_m determined by the PV array output voltage and current as sensed by the MPT. Switches Q_1 and Q_3 of the bridge are switched on during the positive pulse excursions and Q_2 and Q_4 are switched on during the negative excursions. This provides a continuous power drain on the PV array, thus enabling maximum power tracking.

Keeping the switching elements as close to ideal as possible, along with minimal loss in the filtering elements, can yield very high overall efficiencies for these units. When a switching element has either zero voltage or zero current, it does not dissipate power. During a switching transition, however, switching elements have both voltage and current and, hence, dissipate power. The tradeoff in a PWM inverter, then, is to have the frequency as high as possible to give adequate waveform reproduction, but not so high as to increase

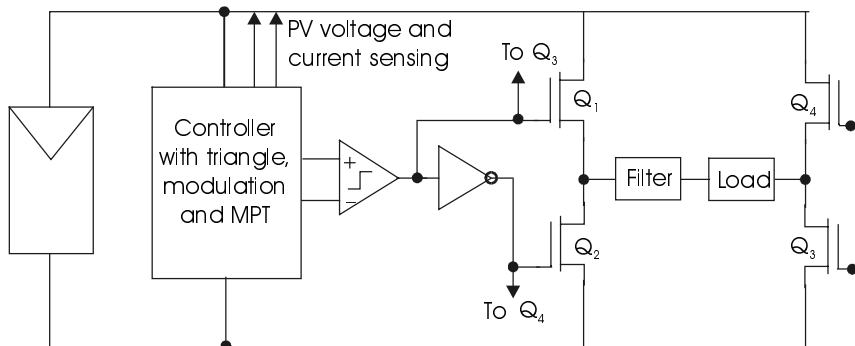


Figure 3.35 Full-bridge PWM converter showing controller and PV connections.

losses to unacceptable levels. Most manufacturers now advertise PWM inverters with efficiencies above 90% over a wide range of inverter output power.

Other Desirable Inverter Features

Modern inverters for PV applications often incorporate very sophisticated features to optimize inverter performance. In fact, the instruction and installation manuals for some of these inverters are nearly as long as this textbook [14].

For stand-alone inverters and for grid-connected inverters with stand-alone option, a ‘search’ mode is often incorporated into the design. In the search mode, the inverter uses minimal energy to keep its electronics operational when no loads are connected. In the search mode, approximately once every second, the inverter sends out an ac voltage pulse a few cycles long. If the inverter senses that no current flows as a result of the pulse, it concludes that no load is connected and waits to send another pulse. On the other hand, if current flows at a magnitude greater than a preprogrammed value, the inverter then recognizes that a load has been connected and supplies a continuous output voltage. If the inverter is not producing an output voltage on a continuous basis, power losses in the inverter are minimized.

In some cases, however, an inverter in the search mode can be confused. For example, if the inverter is set to provide power as long as more than 25 watts is connected, it can be confused by a 20-watt incandescent light bulb. The reason is that when the lamp filament is cold, it has a lower resistance and a surge of current flows until the filament is heated. Hence, a 20-watt incandescent light bulb will appear to be a higher wattage load when it first turns on, and then will drop back to 20 watts when the filament is hot. This, then, will cause the inverter to turn off and resume the search mode, where it will find the same light bulb and will turn it on again until it gets hot, resulting in a light that flashes on and off. Other confusing loads include the remote receivers in electronic equipment such as televisions, VCRs and CD players. When they are on, they draw very small amounts of power, so when an inverter is in the search mode, it is quite possible that the remote receivers will shut down.

For stand-alone inverters, it is necessary that the output appear as a voltage source, preferably as close to ideal as possible. For utility interactive inverters, however, it is more convenient to let the grid voltage fulfill the voltage source role and to have the inverter act as a current source that feeds current into the utility grid. Utility interactive inverters with battery backup that are capable of supplying power to emergency loads if the utility grid is disconnected must be capable of switching over from grid-synchronized current source to internally synchronized voltage source to power emergency loads.

Utility interactive inverters must be designed so that if the utility goes down, the inverter output to the utility also shuts down. This safety feature is relatively easy to design into an inverter if no other distributed electrical source is connected to the utility. However, if another nonutility source is connected to the line it is important that the PV system inverter will not recognize this source as a utility source and continue to supply power to the line. This is called ‘islanding’ and will be discussed later in this chapter and also in Chapter 8.

Many utility interactive inverters that have an emergency backup feature also incorporate a battery charger in the inverter so the utility can be used to charge the batteries in the event that the PV system has not fully charged the batteries. This feature only works, of course, when the utility grid is energized. Fortunately, this is generally most of the time.

Another convenient feature found in many inverters is a generator start option. This allows for a separate ac generator to be used as a backup to the PV system in either a utility interactive or a stand-alone system. When the battery level of charge drops to a prescribed level, the inverter will send a starting signal to the generator. If the inverter has a real-time clock, the time of day for generator starting can also be controlled, so the generator will not come on just before the sun is about to charge the batteries.

Finally, most high quality inverters that are connected to a PV array will incorporate maximum power tracking circuitry at their dc input so that the PV array will deliver power at its maximum power level to the inverter.

3.9 Generators

3.9.1 Introduction

In some cases, where either a large discrepancy between seasonal loads exists or where seasonal sun availability varies greatly, a system designed completely around PV components will result in the deployment of a large PV array to meet the needs of one season. Meanwhile, during other seasons, much of the energy available from the array is not used. This is similar to the problem of meeting critical system needs with PV, where the cost generally increases rapidly as the system availability exceeds 95%. In such cases, it is often more cost effective to employ an alternate source of electricity to be available when the PV array is not meeting system needs. While it is conceivable that the backup source for a stand-alone system may be wind or other renewable source, it is

more common to employ either a gasoline, diesel or propane generator as a system backup. In a grid-connected system, the utility grid provides any needed backup power, unless, of course, the grid goes down.

With relatively low acquisition costs of small and portable generators, it may appear that it would make better economic sense to simply use the generator without the PV array. However, life-cycle cost analysis, as is discussed in Chapter 5, often shows the use of a mix of PV and conventional generation to be more economical than an engine-powered generator. Furthermore, the fact that PV generation is quiet and clean adds further appeal to using a maximum practical amount of PV generation in the system.

When it makes economic sense to use a generator, it is important for the engineer to have some knowledge of generator options. This section deals with some of the considerations in selecting a generator.

3.9.2 Types and Sizes of Generators

While most small electrical generators use a gasoline engine as the mechanical prime mover, methane, propane and diesel powered engines are also available. A number of factors will enter the selection process, including initial cost, power requirements, fuel availability and maintenance requirements.

While it is possible to obtain dc generators for use in battery charging applications, dc generators are generally not recommended because of maintenance requirements. They have brushes and commutators that require frequent replacement and cleaning. Many years ago, automotive batteries were charged with dc generators, but now all batteries are charged with alternators, which are simply ac generators that are connected to rectifiers to convert their output to dc. Similarly, ac generators are used in PV systems, even if the systems are dc systems, to minimize maintenance costs.

Table 3.4 lists a few common generator sizes and approximate costs, based on 2002 data. The smaller units are normally used as portable units, while larger sizes are intended for use as fixed units. Rated output is generally about 90% of maximum output.

Table 3.4 Common generator sizes, features and approximate costs [15, 16].

Max KW	Engine HP	Duty Rating	Voltage Regulation	Noise Level	\approx kWh/gal @ Rated Load	Approx Cost
0.65	2.2	Economy	no	67 dB	\approx 4.6	\$500
2.5	5.5	Economy	yes	70 dB	\approx 6.0	\$600
5.0	11.0	Economy	yes	76 dB	\approx 5.4	\$1300
1.8	5.5	Deluxe	yes	64 dB	\approx 4.7	\$1000
3.5	8.0	Deluxe	yes	68 dB	\approx 5.5	\$1500
5.0	11.0	Deluxe	yes	72 dB	\approx 5.6	\$1900
2.5	5.5	Industrial	yes	69 dB	\approx 7.1	\$1300
5.0	11.0	Industrial	yes	72 dB	\approx 5.6	\$1800
11.0	20.0	Industrial	yes	80 dB	\approx 5.5	\$3400

3.9.3 Generator Operating Characteristics

Factors other than peak power output will enter the selection process if a generator is carefully chosen. Generator specifications also include rotation speed, efficiency, fuel type, altitude effects, waveform harmonic content, frequency stability, noise levels, type of starting and overload characteristics.

Rotation Speed

Normally, 60 Hz generators operate at either 3600 rpm or 1800 rpm. Corresponding speeds for 50 Hz generators are 3000 rpm and 1500 rpm. The 3600 rpm units are 2-pole machines and are of simpler construction, resulting in lower acquisition cost. The 1800-rpm machines are 4-pole machines and are somewhat more expensive, but more common in the larger sizes or heavy duty units.

In general, the higher the rpm, the more wear and tear on the bearings, which means more frequent maintenance requirements. Two-pole generators are thus most convenient for use in relatively light duty applications that require less than 400 hours per year of operation. Four-pole generators are recommended when more than 400 hours of operation per year are anticipated.

Efficiency

Electrical and mechanical losses are present in all generators. However, the greatest losses in a generator system are attributable to the prime mover engine. Since the prime mover and electrical generator will each generally have a particular load at which they will operate at maximum efficiency, manufacturers endeavor to carefully match the two components to produce maximum efficiency at somewhere between 80 and 90% of rated full load. Figure 3.36 shows approximate plots of efficiency vs. percent of rated electrical load and kWh per gallon vs. percent of rated electrical load for typical small generators [21].

As generator size increases, the overall maximum efficiency also increases. Figure 3.37 shows maximum efficiency vs. generator size. Whether or not to use a larger, more expensive generator, operating at higher efficiency for shorter intervals, presents an interesting design challenge to the design engineer.

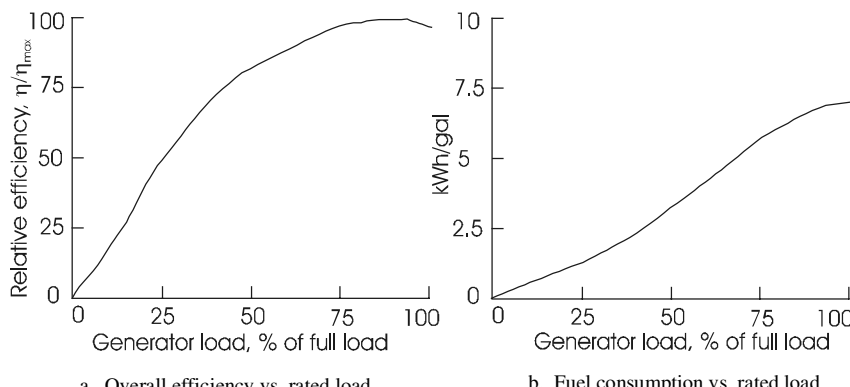


Figure 3.36 Two means of characterizing generator efficiency.

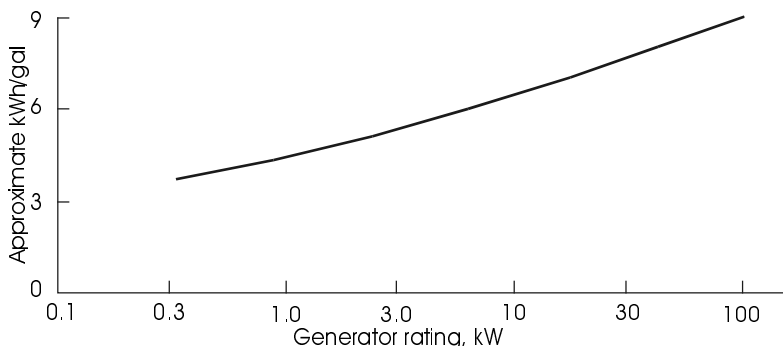


Figure 3.37 Approximate efficiency vs. generator size at rated output.

Maximum generator size is limited in most cases by maximum allowable charging rates for the system batteries, assuming the generator is incorporated into a system with batteries. For systems with highly variable electrical loads, it is particularly inefficient to incorporate a generator unless battery storage is provided to present a nearly constant load on the generator.

Fuel Types

Choice of fuel for a generator will depend on several factors. Although diesel generators tend to be the most efficient, diesel fuel is sometimes more difficult to obtain and is more likely to become contaminated with water or other contaminants than are other fuel choices. In cold temperatures, diesel engines tend to be more difficult to start, so they need to be used under adequately controlled temperature conditions if they are to be started and stopped. Diesel is probably not the best choice for remote locations for these reasons, especially if the site is unattended and reliability is important.

Gasoline is probably the easiest fuel to obtain and will be the fuel of choice for many applications, since gasoline engines can be started and run under relatively adverse conditions. In some situations, however, when either natural gas or propane is used on site for other purposes, such as cooking or space heating, it is convenient to also use it as a fuel for backup electrical generation. This eliminates the need to keep track of more than one supply of fuel. However, as will be noted in the next section, natural gas efficiency decreases more rapidly with increase in altitude than gasoline or propane efficiency, so this observation may need to be taken into account.

Altitude Effects

Many engineers have observed that their automobiles do not respond as well at high altitudes as they do at lower altitudes. As altitude increases, less air is available for the combustion process, and combustion engines thus degrade in performance with increase in altitude.

The design engineer should first check manufacturers' specifications for altitude derating on generators. If manufacturers' specifications do not list

derating factors, then it is reasonable to derate gasoline, diesel and propane generators by 3% per 1000 ft of altitude above sea level and to derate natural gas engines by 5% per 1000 ft of altitude above sea level.

Waveform Harmonic Content

Generally the output waveform of an electrical generator is adequate for nearly all applications. For battery charging, almost any waveform is satisfactory, depending on whether the battery charger contains a transformer.

If the charger contains a transformer, there is a remote possibility that excessive dc or harmonic content in the generator waveform may damage the transformer. If the generator is connected directly to the PV system ac loads at any time, then it is a good idea to be sure the generator output waveform is sufficiently "clean" to meet the requirements of the loads. Normally, the only loads with possible sensitivity to waveform quality will be electronic systems.

Frequency Stability

Again, depending on load requirements and whether the generator is connected to ac loads with critical power frequency requirements, the frequency stability of a generator may need to be taken into account. It is generally desirable to maintain frequency fluctuations at less than ± 0.5 Hz for ac loads, but this degree of frequency stability is not necessary for many PV system loads.

Amplitude Stability

It is generally desirable to have the generator output voltage amplitude remain within 5% of its no-load value. This implies a voltage regulation figure of 5%. Depending on whether the load is inductive or capacitive, the load voltage under full-load conditions may actually exceed the no-load voltage. The voltage regulation of the generator is defined by

$$VR = \frac{V_{nl} - V_{fl}}{V_{fl}}, \quad (3.14)$$

where V_{nl} and V_{fl} are the no-load and full-load voltages, respectively. Hence, if $V_{fl} > V_{nl}$, VR will be negative.

Again, voltage regulation requirements will depend on the specific application. If the PV system is designed to operate the generator at maximum efficiency, the load will remain nearly constant and the output amplitude and frequency will remain quite stable.

Noise Level

Some generators are noisy and others are less noisy. Local ordinances should be checked, but normally the noise level demands of the user will be more stringent than local ordinances. National parks, for example, have relatively strict noise regulations.

Type of Starting

If the generator is to be controlled by the system controller, then it will need to be equipped with electric starting. Otherwise, it may be satisfactory to use a generator with manual starting.

Overload Characteristics

A synchronous generator can suffer serious consequences if it is overloaded. Overloads can occur with the application of excessive steady-state loads, but also can occur as the result of transient loads, such as motor starting.

For example, if the generator is to operate an electric motor, the starting current of the motor can place the generator in an overload condition that can cause the generator to slow down, resulting in reduced generator output. This, in turn, can result in insufficient starting current for the motor and slow the generator even more. This can result in damage to the prime mover and possibly to the generator armature winding and lead to an expensive repair bill.

Power Factor Considerations

The generator must be able to meet the real power requirements of the load as well as the reactive power requirements of the load. Since I^2R copper losses in the generator armature winding depend on the magnitude of the armature current, generators are rated in kVA rather than in watts. It is also possible that the generator will have a minimum power factor rating under full-load conditions. If so, the minimum power factor anticipated for the load must also be considered when the generator is selected.

3.9.4 Generator Maintenance

Table 3.5 shows cost and maintenance information on 3600-rpm gasoline generators, 1800-rpm gasoline generators and diesel generators. Note that gas includes gasoline, natural gas and propane. Note also that ‘sm all’ is defined as sizes less than 100 kW. Diesel generators up to 5 MW are not uncommon, but are not typically intended for home or recreational vehicle use.

Table 3.5 Cost and maintenance information on small electrical generators [8].

Type	Size Range (kW)	Application	Cost (\$/W)	Maintenance Intervals		Engine Rebuild, hr
				Oil Ch, hr	Tune-Up, hr	
3600 rpm gas	1-20	Light use	.50	25	300	2000-5000
1800 rpm gas	5-20	Heavy use	.75	50	300	2000-5000
Diesel	3-100	Industrial	1.00	125-750	500-1500	6000

3.9.5 Generator Selection

Selection of a generator for a system may involve all the previous considerations. If the generator is not expected to be used very much, a light duty or port-

able unit may suffice. If it is to be an essential, reliable system component, capable of running for long periods and for a significant number of hours per year, then a heavy duty unit is preferable. The interesting challenge for the engineer is to determine the dividing line between light duty and heavy duty. After this choice is made, then all the other items previously listed may be considered. Generally the unit with the lowest life-cycle cost will be the best unit for the application, provided that all operating parameters have been incorporated into the analysis.

3.10 Wiring and Code Compliance

3.10.1 Introduction

A number of codes and standards have been created to ensure the safety of electrical systems. These codes and standards also generally address the efficiency and reliability of systems. Since a PV system is capable of generating sufficiently high voltages to present a potential electrical safety hazard, PV systems are included in these codes. Perhaps the two most common codes and standards that deal with PV systems are the *National Electrical Code®* [2] and IEEE 929-2000 Standard for utility interfacing [13]. The PV engineer should be familiar with both. But the list does not end here. PV systems have a mechanical component as well as an electrical component, and, hence, a number of mechanical codes also apply. If the PV system is to be integrated into the construction of a building, the list of codes and standards becomes even longer.

Table 3.6 provides a partial listing of the many codes and standards that may be applicable to any particular PV installation.

3.10.2 The *National Electrical Code*

Introduction

The *National Electrical Code* (*NEC*) is published by the National Fire Protection Association and is updated approximately every three years. The *NEC* consists of a collection of articles that apply to considerations such as wiring methods, grounding, motor circuits and nearly every conceivable topic in which electrical safety and efficient utilization is a consideration, including Article 690, which deals specifically with PV systems.

The *NEC* specifies the sizes and types of switches, fuses and wire to be used, and specifies where these items must be located in the system. These components are necessary, not only to protect the end user, but also to protect the maintenance technician. In later chapters, when specific PV system design examples are discussed, compliance with the *NEC* will be incorporated into the design process discussion. In particular, proper wire sizing to limit voltage drop in connecting wires to acceptable limits, proper use of switches, circuit breakers and fuses and proper grounding will be considered.

Normally, copper wire will be used in PV system wiring. Aluminum wire is allowed by the *NEC*, but generally it is used only over longer distances for car-

rying higher currents when the cost of using copper would be prohibitive. For example, since copper is significantly heavier than aluminum, the insulators on power poles would need to be considerably stronger if copper wire is used instead of aluminum. Aluminum has a lower conductivity than copper, it oxidizes faster than copper and unless torqued properly, it is more likely to loosen in a connector. Furthermore, aluminum oxide is not readily visually distinguishable from aluminum.

Table 3.6 Partial listing of codes and standards that may apply to PV systems [2, 9, 10, 13, 17-20].

Reference #	Title/Contents
NEC 2002	National Electrical Code /Wiring methods (comprehensive)
IEEE 928	IEEE Recommended Criteria for Terrestrial Photovoltaic Power Systems
IEEE 929	IEEE Recommended Practice for Utility Interface of Residential and Intermediate Photovoltaic Systems
IEEE 937	IEEE Recommended Practice for Installation and Maintenance of Lead-Acid Batteries for Photovoltaic Systems
IEEE 937	Installation and Maintenance of Lead-Acid Batteries for PV Systems
IEEE 1013	IEEE Recommended Practice for Sizing Lead-Acid Batteries for Photovoltaic Systems
IEEE 1013	Recommended Practice for Sizing Lead-Acid Batteries for PV Systems
IEEE 1144	Sizing of Industrial Nickel Cadmium Batteries for PV Systems
IEEE 1145	IEEE Recommended Practice for Installation and Maintenance of Nickel Cadmium Batteries for Photovoltaic Systems
IEEE 1187	Recommended Practice for Design and Installation of Valve-Regulated Lead-Acid (VRLA) Storage Batteries for Stationary Applications
IEEE 1262	Recommended Practice for Qualification of Photovoltaic Modules
IEEE 1361	Recommended Practice for Determining Performance Characteristics and Suitability of Batteries in Photovoltaic Systems
IEEE 1373	Recommended Practice for Field Test Methods and Procedures for Grid-Connected Photovoltaic Systems
IEEE 1374	Guide for Terrestrial Photovoltaic Power System Safety
IEEE 1479	Recommended Practice for the Evaluation of Photovoltaic Module Energy Production
IEEE 1513	Recommended Practice for Qualification of Concentrator Photovoltaic Receiver Sections and Modules
IEEE 1526	Recommended Practice for Testing the Performance of Stand-Alone Photovoltaic Systems
IEC TC-82	A compendium of 25 standards relating to the electrical and mechanical performance testing and measurement of PV systems
ISO 9001	An international quality standard, comprised of 20 segments, dealing with all aspects of design, manufacturing and delivery of service
UL 1741	Standard for Static Inverters and Charge Controllers for use in Photovoltaic Power Systems
ANSI Z97.1	Relates to safety relating to potential glass breakage
ASTM	A compendium of tests and standards that may apply to building integrated photovoltaic systems
ASCE 7-02	Minimum Design Loads for Buildings and Other Structures

Since aluminum oxide is a good insulator, special care must be taken when terminating aluminum to ensure that the exposed aluminum is free of oxidation. If aluminum wire is used in a system, devices with terminations approved for use with aluminum must be used.

The intent of this section is to highlight several *NEC* requirements. The reader who goes beyond the walls of the classroom into the design of PV systems, should invest in the latest edition of the *NEC* to be sure to have all the latest requirements on items such as ground fault detection and interruption, source and output circuit maximum voltage ratings, acceptable conductor placement and storage batteries.

Voltage Drop and Wire Sizing

Table 3.7 shows the dc resistance per 1000 feet and rated current (ampacity) for copper conductors with insulation rated at 90°C. The ampacities are for no more than three current-carrying conductors in conduit at a temperature of 30°C or less. If more than three current-carrying conductors are in a conduit, or if the conductors are operated in an ambient that exceeds 30°C, their ampacity must be derated. Ampacities for single conductors in free air are higher than those listed in Table 3.7. While many different types of insulation exist, as shown in *NEC* Article 310, type THWN-2 is a high temperature (90°C), moisture and oil resistant, thermoplastic insulation that is commonly in use. Frequently, type THHN insulation is also rated as THWN-2.

Table 3.7 Properties of copper conductors with 90°C insulation. (Data from *NEC*, [2]).

Size	18	16	14	12	10	8	6	4
dc Ω/kft	7.77	4.89	3.07	1.93	1.21	0.764	0.491	0.308
I_{\max}, A	14	18	25	30	40	55	75	95
Size	3	2	1	0	00	000	0000	250 kcm
dc Ω/kft	0.245	0.194	0.154	0.122	0.0967	0.0766	0.0608	0.0515
I_{\max}, A	110	130	150	170	195	225	260	290

Single conductor wire sizes 18-8. Stranded for larger sizes.

The *NEC* requires that the total voltage drop in feeder and branch circuits be less than 5%, with the drop in either feeder or branch circuit limited to no more than 3%. A feeder circuit is a circuit that provides power to an electrical distribution panel. In a common residential electrical service, the feeder circuit is the wiring between the electric meter and the circuit breaker panel. The branch circuits are the circuits that provide power to the individual electrical loads, such as lighting, refrigerators, dishwashers, air conditioners, etc., that are connected to the distribution panel.

Many tables exist in various design manuals that list the maximum distance a certain size conductor can be run with a given current and still not produce excessive voltage drop. For the engineer with a calculator, however, all one needs to do is to recognize that a circuit consists of wire in both directions, so that a load located 50 feet from a battery will need 100 feet of wire to carry the current

to and from the load. If d is the distance from source to load and V_s is the source voltage, the percent voltage drop in the wire is thus given by

$$\%VD = 100 \frac{I}{V_s} \left(\frac{\Omega}{kft} \right) \left(\frac{2d}{1000} \right) = \frac{0.2Id}{V_s} \left(\frac{\Omega}{kft} \right). \quad (3.15)$$

Example 3.10.1: A 20-watt, 12-VDC fluorescent lamp is located 50 feet from a 12 V battery. Specify the wire size needed to keep the voltage drop between battery and lamp under 2%.

Solution. First solve equation (3.15) for (Ω/kft) to obtain

$$\Omega / kft = \frac{(\%VD)V_s}{0.2Id} .$$

Then, determine the load current from $P = IV$, assuming the load voltage to be essentially equal to the supply voltage. Substituting the known values on the right hand side yields $\Omega/kft = (2 \times 12) / (0.2 \times 1.67 \times 50) = 1.437$. Table 3.7 shows that #12 wire has too much resistance, so it is necessary to use #10. The actual voltage drop with #10 wire can now be found from (3.15) to be 1.68%.

Note that although #10 wire will carry 40 amperes, the current in the circuit is limited to 1.67 amperes due to the voltage drop problem. It is very important to be aware of the need for larger wire in low voltage systems. Equation (3.15) and Table 3.7 will find considerable use in examples to follow in later chapters.

Because of the problem with voltage drop at low voltages, and the correspondingly larger wire sizes necessary, it is generally desirable to operate PV systems that deliver any significant amounts of power over any reasonable distances at voltages higher than 12 volts. If the previous 20-watt load were connected to a 24-volt system, the load current would be halved, and the load voltage would be doubled. This allows the resistance of the wiring to be four times higher, or as much as 5.648 Ω/kft , which means that #16 wire is now adequate. From a total cost standpoint, however, the cost of the additional 12-V battery will exceed the difference in cost between #10 wire and #16 wire. Presumably the cost of the PV modules will be the same, since the amount of power required has not changed.

For concealed wiring, the minimum wire size is #14. Smaller wire sizes are normally used only for portable cords or for attaching single loads.

Switches, Circuit Breakers, Fuses and Receptacles

All switches, circuit breakers and fuses used in the dc sections of PV systems must be rated for use with dc. Switches, circuit breakers and fuses used in ac circuits must be rated for ac use. Switches have both current and voltage ratings. If a switch is used to control a motor, it must be rated to handle the horsepower of the motor at the operating voltage of the motor.

Circuit breakers must be sized in accordance with *NEC* requirements. Although the maximum current ratings for #14, #12 and #10 THHN wire are 25, 30 and 40 amperes, respectively, the maximum fuse or circuit breaker sizes allowed for use with these wire sizes are 15, 20 and 30 amperes, respectively. Larger wire sizes may be fused at their rated ampacities (i.e., I_{max}).

For motors, it may be necessary to install a fuse or a circuit breaker with a rating that exceeds the circuit ampacity in order to accommodate the starting current of a motor. When this is the case, the motor must have a form of overload protection that will disconnect the motor if the motor current exceeds approximately 125% of its rated running current, depending on the size and type of motor. Details of wiring for motors and motor controllers are covered in great detail in *NEC Article 430*.

Different voltages require different receptacles. While it is not very likely that 12 VDC will damage a piece of 120 VAC equipment, except possibly a motor or transformer, it is almost certainly true that 120 VAC will damage a piece of 12 VDC equipment. It is thus necessary to use different attachment cap and receptacle configurations for different voltages.

Since the *NEC* will be referenced in nearly all the design examples in Chapters 4, 7 and 8, specific applications of *NEC* requirements will become more clearly evident as the examples are developed. Further discussion of overcurrent protection, disconnects and wire sizing in accordance with *NEC* requirements will be covered in detail in these examples.

Ground Fault, Surge and Lightning Protection

Presumably, current will leave the PV array via the positive conductor and the same amount of current will return to the array via the negative conductor. This will be the case, provided that no alternate return paths are present.

The *NEC* requires that metallic frames and other metal parts of PV systems be connected to ground. The conductors used for this purpose are called **grounding conductors**. Generally, the negative conductor is also connected to ground at some point along the system. If so, then the negative conductor is called the **grounded conductor**. Since the negative conductor is connected to ground at only one point, current will flow in the grounded conductor, but will not flow in any of the grounding conductors, since there is no closed circuit in which the current can flow.

However, if for some reason the positive conductor were connected to ground, then there would be an alternate closed path in which current would be able to flow through the grounding conductors. If this is the case, then Kirchhoff's current law requires that the current in the positive conductor will equal the sum of the currents in the grounded and grounding conductors. The net result is that no longer will the currents in the positive and negative (grounded) conductors be equal. The greatest danger in dc ground fault currents in a PV system is the means by which they are established. If the ground fault results from a loose connection, the connection may begin to arc and become a fire hazard.

The *NEC* requires that if an array is rooftop mounted on a dwelling, then ground fault protection must be provided to disconnect the array in the event of a difference in current between the positive and negative array conductors leading to the controller/inverter.loads.

Another important component used to provide protection to the array and inverter is the surge protector. Surge protectors are similar to zener diodes in that they are made of material that is essentially insulating until a predetermined voltage appears across the material. At this point, avalanche breakdown occurs and the surge protector acts as a current shunt. Metal oxide varistor (MOV) types of surge protector respond in nanoseconds and can bypass many joules of surge energy. However, a disadvantage of MOV surge protectors is that they draw a small current at all times and generally the failure mode of a MOV device is a short circuit. SiO (SOV) surge protectors are an improvement in terms of the MOV disadvantages. It is good practice to incorporate surge protection into system design at a location close to the common system ground point.

Additional protection from lightning strikes can be obtained with lightning rod systems. Contrary to popular belief, lightning rods do not attract lightning. Rather, they present a sharp point (or points) that are connected to ground. If a potential difference should appear between the rod and the surrounding atmosphere, a very high electric field builds up around the point to the extent that a corona discharge takes place, equalizing the charge between the air and the ground. Corona discharge is also known as glow discharge. Lightning is known as arc discharge. Arc discharge is violent, but glow discharge is essentially harmless since the charge is equalized over a much longer period of time.

3.10.3 IEEE Standard 929-2000

IEEE 929-2000 deals with the utility interface of grid-connected systems. It addresses concerns of utilities regarding quality of power delivered to the grid and the need to disconnect the PV system from the utility grid in the event of utility power failure. IEEE 929-2000, while specific to grid-connected PV systems, incorporates the general requirements of several other standards, including UL 1741 on the testing of grid-connected inverters, IEEE 519-1992 on harmonic control and ANSI C84.1-1995 on voltage and voltage ratings in 60 Hz systems.

IEEE 929-2000 establishes standards relating to voltage disturbances, frequency disturbances, islanding protection, power factor, reconnect after grid failure and restoration, injection of dc into an ac system, grounding, surge protection and dc and ac disconnects.

Voltage at the inverter output, for example, should not be more than 5% higher than the voltage at the point of utility connection. The inverter should be able to sense grid voltage abnormalities and shut down the inverter when indicated. Shutdown should occur within 6 cycles if the utility voltage, V , drops below 50% of its nominal value. If $50\% < V < 88\%$ or if $110\% < V < 137\%$ of nominal, then the inverter must shut down within 120 cycles. For $V > 137\%$ of nominal, shutdown must occur within 2 cycles. If the line frequency falls below

59.3 or goes above 60.5 Hz, the inverter should also disconnect from the line within 6 cycles. The operation of a PV system also should not cause excessive flicker on the utility line, and the power factor of the utility interactive PV inverter should not be less than 0.85 leading or lagging.

One item of particular concern to utilities is what happens if a number of PV systems are connected to the grid when for some reason the grid loses power. If one PV system remains on longer than others, it may be feeding power into the grid, and the remaining PV systems may then operate as though the grid were energized by the utility. If the grid appears to be energized by the utility, the PV systems may not disconnect from the grid as required. Hence, a mechanism must be built into PV systems, most likely into the inverters, which will prevent this islanding phenomenon.

If an islanded load occurs and an inverter senses either a) a 50% mismatch in real power load to inverter power output, or b) an islanded load power factor less than 0.95 leading or lagging, then the inverter must shut down within 10 cycles of sensing the mismatch. In the case where the mismatch is less than 50% and the islanded-load power factor is greater than 0.95 and the Q of the load is less than 2.5, then the inverter must disconnect from the utility within 2 seconds. This topic will be discussed in greater detail in Chapter 8.

After a grid is restored, the PV inverter should remain disconnected until normal grid operation has been established for a minimum of 5 minutes. For large inverters, the inverter is often designed to undergo a soft start, in which the inverter output increases gradually to its maximum in accordance with whatever agreement may be in effect between the PV owner and the utility. For small systems, the inverter may switch on to full power immediately. The dividing line between large and small systems is generally in the range of 10 kW, but may vary from utility to utility.

The quality of power entering the utility grid from a PV system inverter is also of concern to utilities, since if too many harmonics are present in the inverter output, they may cause interference in loads at other locations that require pure, or, at least, better, sinusoidal power. IEEE 929 references IEEE 519-1992 (©1992, IEEE), which sets the harmonics as shown in Table 3.8.

Table 3.8 Harmonic distortion limits for grid-connected PV inverters. Even harmonics should be less than 25% of the odd harmonics in the listed ranges [13, 19].

Odd Harmonics	Distortion Limit
3rd through 9th	< 4.0 %
11th through 15th	< 2 %
17th through 21st	< 1.5 %
23rd through 33rd	< 0.6 %
Above 33rd	< 0.3 %

Another important component of the inverter output that must be limited is any dc component, since dc can be very harmful to transformers and motors in

an ac system. Inverter dc output current must be no greater than 0.5% of rated inverter output current.

Discussions of optimal protection from islanding and allowable inverter output harmonic levels are ongoing. Inverters that supply utility interactive loads are of particular interest, especially those that provide for battery backup of grid power. Until more field data is available, the discussions will continue, based on limited theoretical studies and limited testing. Perhaps the reader of this text will one day also contribute to the discussion if he or she is not already doing so.

3.11 Balance of System Components

The balance of system (BOS) components include mounting materials for the modules, wire and all wiring components, lightning protectors, grounding connections and battery containers. In some cases, the connected loads are considered to be part of the BOS and in other cases the loads are not considered to be a part of the system. The distinction is generally made when the system is installed to operate a specific load, as opposed to being installed to be one contributor to the operation of any load.

Certain BOS components are regulated by codes or standards. Array mounts, for example, must meet any windloading requirements of applicable building codes. Battery compartments are covered in the *NEC*.

In certain environments, BOS components may need to be resistant to corrosion from exposure to salt air or may need to be appropriate for other environmental considerations. If a PV system is part of a building integrated structure, then a number of other codes and standards may become applicable.

Problems

- 3.1 If $I_\ell = 2 \text{ A}$, $I_o = 10^{-10} \text{ A}$ and $T = 300 \text{ K}$ for a PV cell, determine the maximum power point of the cell by differentiating the expression obtained by multiplying Equation (3.1) by the cell voltage.
- 3.2 Determine the range of operating voltages for which a 36-cell module will have power output within 90% of maximum power. You may assume $I_o = 10^{-10} \text{ A}$ and $V_{oc} = 0.596 \text{ V}$ at an operating temperature of 300 K. Assume all cells in the module to be identical.
- 3.3 A PV module is found to operate at a temperature of 60°C under conditions of $T_A = 30^\circ\text{C}$ and $G = 980 \text{ W/m}^2$. Determine the NOCT of the module.
- 3.4 Plot V_m vs. T for $-25 < T < +75^\circ\text{C}$ for a 36-cell Si module for which each cell has $V_m = 0.5 \text{ V}$ at 25°C.

- 3.5 Plot P_m vs. T for the module of Problem 3.4 if $I_m = 5.85 \text{ A}$ at 25°C .
- 3.6 Two 36-cell PV modules are connected in series. One is shaded and one is fully illuminated, such that the I-V characteristics of each module are as shown in Figure P3.1.
- If the output of the two series modules is shorted, estimate the power dissipated in the shaded module.
 - If the two modules are equipped with bypass diodes across each 12 series cells, estimate the power dissipated in the shaded module.
-
- Figure P3.1** I-V characteristics of two modules, one shaded and one fully illuminated.
- 3.7 Rewrite the chemical equations of the Ni-Cd and NIMH systems showing the half-reactions at the anodes and at the cathodes. Determine the charge transfer mechanism.
- 3.8 How many gallons would have to be pumped into a tank raised 10 feet from the ground in order to be able to recover 1 kWh of electricity at a conversion efficiency of 100%, assuming the water is allowed to fall the entire 10 feet to operate the electrical generator?
- 3.9 Determine the capacitance of a capacitor needed to store 1 kWh if it is charged to 500 V.
- 3.10 Determine the inductance needed to store 1 kWh if the inductor is carrying a reasonable current, to be determined by the problem solver.
- 3.11 Determine the size and rotation speed of a flywheel designed to store 1 kWh of energy.
- 3.12 Describe two additional charging algorithms that will result in a fully charged battery and minimal waste of PV array energy.

- 3.13 If a maximum power tracker operates at 90% efficiency, determine the additional power available to each load if the PV source and load characteristics are as shown in Figure p.3.2. For each load, how long would the system need to operate under the conditions described in order to recover the cost of the MPT if the MPT cost \$200 and the PV-generated electricity has a value of \$.50/kWh?
- 3.14 A battery charge controller incorporates a MPT to optimize charging of the batteries. Assume the maximum power voltage of a PV array to be 64 volts and the bulk charge voltage level of a 48-V vented lead-acid battery bank to be 58 V. If the conversion efficiency of the MPT is 93%, determine the percentage increase in charge delivered to the battery under these conditions over that which would be delivered by a controller that causes the array to operate at 58 V rather than 64 V. You may assume the PV array consists of 4 modules as described in Figure P3.2 connected in series and that V_{mp} is independent of irradiance levels.

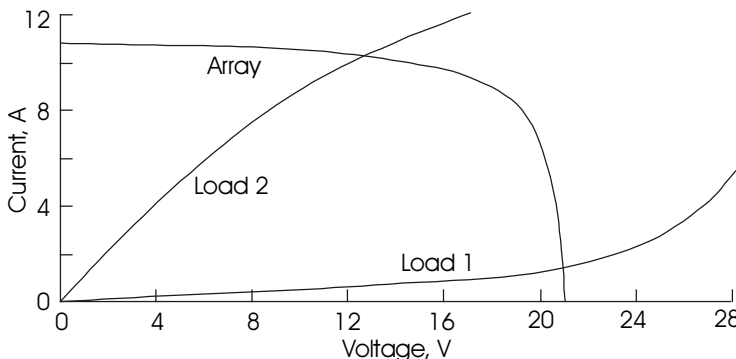


Figure P3.2 I-V characteristic for PV array and 2 loads.

- 3.15 For the circuits of Figures 3.28a and 3.28b,
- Explain the on-off sequencing of the MOSFET switches in Figure 3.28a to produce a symmetrical square wave output. Sketch the result.
 - Explain the on-off sequencing of the MOSFET switches in Figure 3.28b to produce a symmetrical square wave output. Sketch the result.
- 3.16 Determine whether the dc sources in Figures 3.28a and 3.28b remain on constantly during the switching. If not, explore modifications to the circuitry to ensure that the dc sources are delivering constant dc current.
- 3.17 Show how a dc-dc converter can be used as a part of an inverter designed to have a square wave output of 120 V with a 12-V dc input. The idea is to design the inverter without a transformer. Sketch a block diagram, showing some components to clearly express your design.

- 3.18 For the 5-level H-Bridge of Figure 3.31, determine T_2 if $T_1 = T_0$, $V_{rms} = 120$ V, and

- $V_{dc} = 150$ V
- $V_{dc} = 155$ V
- $V_{dc} = 160$ V
- $V_{dc} = 165$ V

Note that Excel or MATLAB can be very useful for this problem.

- 3.19 For the 5-level H-Bridge of Figure 3.31, determine a set of values of T_0 , T_1 and T_2 that will minimize the total harmonic distortion of the waveform if $V_{dc} = 160$ V and $V_{rms} = 120$ V. A convenient tool is to construct the waveform in PSPICE using series pulse voltage sources and then to run a Fast Fourier Transform of the resulting waveform.

- 3.20 For the 5-level H-Bridge of Figure 3.31, determine the maximum value for V_{dc} if the design requires $T_2 > 0.025T$ and $T_0 > 0.025T$.

- 3.21 Referring to Figure 3.31a, design a 7-level H-Bridge, using 4 capacitors and an appropriate number of series switches in each string. Show the waveform and the switching needed to obtain each of the 7 levels of the output voltage.

- 3.22 For the 7-level H-Bridge output waveform, derive a formula for the rms value of the output voltage.

- 3.23 Construct the 7-level H-Bridge output waveform using series pulse voltage sources in PSPICE and perform a Fast Fourier Transform on the waveform to explore the harmonic distortion of the waveform. Keep V_{dc} and V_{rms} constant, while varying the duration of the different levels of the waveform in order to minimize the total harmonic distortion (THD) of the waveform.

- 3.24 Make a list of loads that might confuse an inverter that is in the ‘sleep’ mode. Explain why each load causes a problem.

- 3.25 The following data are given for a series of gasoline-powered electrical generators:

Rated output	1500 W	2300 W	3000 W	4500 W
Fuel tank size	2.9 gal	2.9 gal	4.5 gal	4.5 gal
Run time/ tankful	9 hr	9 hr	8.3 hr	5.6 hr

Calculate the kWh/gal for each of these generators under rated load conditions.

3.26 Refer to Table 3.7 or to the *NEC* in order to:

- a. Determine the wire size needed to limit voltage drop to 3% for a 100-watt, 24-volt load at a distance of 75 feet from the voltage source.
- b. Using the wire size determined in part a, determine the actual voltage drop for the wiring.

References

- [1] *Maintenance and Operation of Stand-Alone Photovoltaic Systems*, Sandia National Laboratories, Albuquerque, NM, 1991.
- [2] *NFPA 70 National Electrical Code , 2002 Ed.*, National Fire Protection Association, Quincy, MA, 2002. [1] Markvart, T., Ed., *Solar Electricity*, John Wiley & Sons, Chichester, U.K., 1994.
- [3] IEEE Standard 1187-2002, *IEEE Recommended Practice for Installation Design and Installation of Valve-Regulated Lead-Acid Storage Batteries for Stationary Applications*, Institute of Electrical and Electronics Engineers, Inc., New York, 2002.
- [4] Linden, D., Ed., *Handbook of Batteries*, 2nd Ed., McGraw-Hill, New York, 1994.
- [5] Hancock, Jr., O. G., Hydrogen storage: the hydrogen alternative, *Photovoltaics International*, March, 1986.
- [6] Skerrett, P. J., Fuel UPD, *Pop. Science*, June, 1993.
- [7] Roland, B., Nitsch, J. and Wendt, H., *Hydrogen and Fuel Cells-the Clean Energy System*, Elsevier Sequoia, Oxford, U.K., 1992.
- [8] *Stand-Alone Photovoltaic Systems: A Handbook of Recommended Design Practices*, Sandia National Laboratories, Albuquerque, NM, 1995.
- [9] UL 1741: 1999, Standard for Static Inverters and Charge Controllers for Use in Photovoltaic Power Systems, Underwriters Laboratories, Inc., Northbrook, IL, May 1999.
- [10] ANSI C84.1-1995, Electric Power Systems and Equipment –Voltage Ratings (60 Hertz), American National Standards Institute, New York, 1995.
- [11] <http://www.xantrex.com/> (Information on Trace/Xantrex Power Electronics Equipment.)
- [12] <http://www.ommion.com/> (Information on Omnion Power Electronics Equipment.)
- [13] IEEE 929-2000, *IEEE Recommended Practice for Utility Interface of Residential and Intermediate Photovoltaic (PV) Systems*, IEEE Standards Coordinating Committee 21, Photovoltaics, 2000.
- [14] Trace Engineering Company, Inc., ‘SW Series Inverter/Chargers With Revision 4.01 Software Owner’s Manual,’ Arlington, WA, September 1999.
- [15] <http://www.mayberrys.com/> (Additional information on Honda generators from Don Mayberry, Jr., Mayberry Sales and Service, Inc., Port Murray, NJ).
- [16] Onan Corporation, Minneapolis, MN, sales literature on Onan generators, including ‘Gensize™ ’96” software for sizing generator sets.

- [17] Wohlgemuth, J., "Testing for BIPV," *Proc. Photovoltaic Performance and Reliability Workshop*, Cocoa Beach, FL, November 1998, 113.
- [18] DeBlasio, R., "Status of IEEE Standards Coordinating Committee (SCC 21) and IEC Standards Technical Committee 82 (TC82)," *Proc. Photovoltaic Performance and Reliability Workshop*, Cocoa Beach, FL, November 1998, 236.
- [19] IEEE Standard 519-1992, *Recommended Practices and Requirements for Harmonic Control in Electrical Power Systems*, Institute of Electrical and Electronics Engineers, Inc., New York, 1992.
- [20] Zgonena, T., "Safety Considerations for Static Grid-Tied Photovoltaic Inverters," *Interconnecting Small PV Systems to Florida's Utility Grid*, A Technical Workshop for Florida's Utilities, Cocoa, FL, October 22, 1998.
- [21] Danley, D. R., Orion Energy Corporation, Ijamsville, MD, Personal communication regarding fuel efficiency of fossil-fueled generators, August, 1999.

Suggested Reading

- ASCE Standard 7-02, *Minimum Design Loads for Buildings and Other Structures*, American Society of Civil Engineers, Reston, VA, 2000.
- Hoogers, G., Ed., *Fuel Cell Technology Handbook*, CRC Press, Boca Raton, FL, 2002.
- Hu, C. and White, R., *Solar Cells: From Basics to Advanced Systems*, McGraw-Hill, New York, 1983.
- Krein, Philip T., *Elements of Power Electronics*, Oxford University Press, New York, 1998.
- Roden, M. S. and Carpenter, G. L., *Electronic Design: From Concept to Reality*, Discovery Press, Burbank, CA, 1997.
- Sedra, A. S. and Smith, K. C., *Microelectronic Circuits*, 4th Ed., Oxford University Press, New York, 1998.
- Silberberg, M., *Chemistry: The Molecular Nature of Matter and Change*, Mosby, St. Louis, 1996.
- Skvarenina, T. L., ed, *The Power Electronics Handbook*, CRC Press, Boca Raton, FL, 2002.
- Vithayathil, J., *Power Electronics: Principles and Applications*, McGraw-Hill, New York, 1995.

Chapter 4

PV SYSTEM EXAMPLES

4.1 Introduction

Analysis is the next stop on the road to design. In this chapter, several PV systems will be analyzed in order to acquaint the reader with some of the considerations used in the design of systems. Analysis of the systems should encourage the reader to think of alternative means of achieving the desired end result, since normally there is no single best solution to a design problem. If there were, the world would be a boring place, with only one model of automobile, one model of computer, one model of television, and, perhaps worst of all, everyone would be wearing the same uniform. The engineer can thus be grateful for diversity in the world.

In each example, an effort will be made to point out the areas where the PV system is open to the discretion of the designer. Perhaps reliability, performance and cost are among the items of most common concern. It is often the case that there will be a trade-off among these three parameters. Chapter 5 has been included to provide the designer with quantitative means of dealing with cost considerations. Other considerations commonly overlooked include environmental impact, safety and aesthetics. These topics are discussed in greater detail with regard to energy systems in Chapter 9.

The first few examples in this chapter are relatively simple systems. In each case, the systems could be made more complicated to increase performance, but it should be remembered that complexity often results in a sacrifice in reliability, and almost certainly involves an increase in price. Simplicity, thus, should be acknowledged as having an elegance of its own, and should not necessarily be discarded as an option.

The final examples are more complex, and are intended to demonstrate the wide range of applications of PV power systems. In these examples, it will become evident that there are many options and tradeoffs involved in reaching the final system design.

4.2 Example 1: A Simple PV-Powered Fan

4.2.1 The Simplest Configuration: Module and Fan

Figure 4.1 shows the simplest of PV systems, a fan motor connected to a PV module. The figure also shows the superimposed performance (I-V) characteristics of the fan and the module. The operation is simple: as the sun shines brighter, the fan turns faster. If the designer has no concern for the exact quantity of air moved, the design becomes nearly trivial. However, if the amount of air moved must meet a code requirement or other constraint, then it will be necessary to consider the design in more detail.

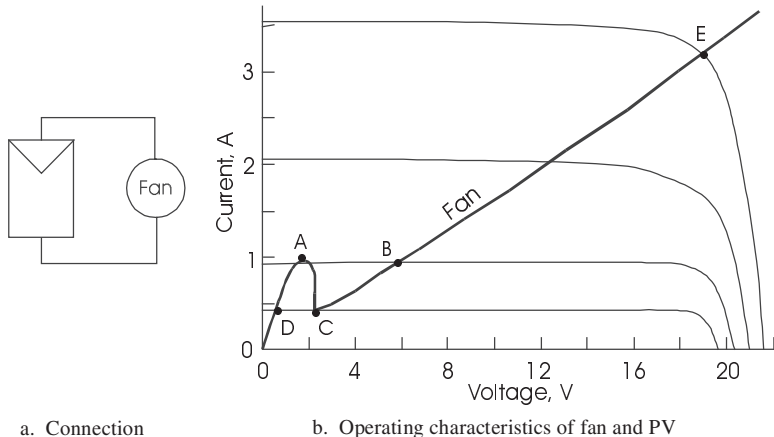


Figure 4.1 A simple PV-powered fan, showing performance characteristics for fan and PV module.

The system operation point is determined by the intersection of the performance characteristics. Note that as the sun shines brighter, making more PV current and voltage available, the fan consumes more power. It is reasonable to assume that as the fan consumes more power it will move more air.

Perhaps the second observation the reader will make regarding the performance characteristics intersections in Figure 4.1 is that the module is not operating anywhere near maximum power at low light levels. If a module having higher short circuit current is used, the fan will remain at nearly constant speed over a wider range of light levels, but at high illumination levels, the module is delivering only a fraction of its maximum power capability. Hence, the designer must decide how much air movement is needed at various irradiance levels, and choose the module accordingly. So, even in this relatively simple design example, the designer must use discretion. Larger modules will cost more, but will deliver more air at lower irradiance levels.

Figure 4.1b also shows the hysteresis effect encountered in starting the fan. Under stalled rotor conditions, the fan motor does not produce a back EMF and thus the fan will draw stalled rotor current until sufficient armature current is present to overcome the starting torque. The irradiance level at point A on the curve is just adequate to provide this current, and the operating point then jumps to point B. As the irradiance level continues to increase, the operating point moves toward point E. When irradiance levels decrease, fan performance follows the fan characteristic to point C, after which the fan stalls and the operating point jumps to point D and eventually approaches the origin as darkness falls.

Another question for the designer to ask is whether it would be better to use a different fan to meet the design requirements. The obvious answer is “maybe.” And that is what makes the design of PV systems so much fun. It should be clear from Figure 4.1b that regardless of the choice of fan or module, there will be a significant power mismatch over a relatively wide range of irradiance. Thus, no

matter what the choice, there will be some portion of the fan or PV characteristic where maximum power will not be transferred to the fan. If it is desired to optimize fan power for all illumination levels, a maximum power tracker will need to be incorporated into the design.

The MPT can be particularly useful at irradiance levels between the start and stop irradiance levels of Figure 4.1b, where it will enable the fan to start at a lower irradiance level and to stop at a lower irradiance level, with greater air flow at irradiance levels between these points. Here the interesting part of the trade-off is whether including an MPT with a smaller module will cost less than using a larger module to obtain comparable system performance.

Another possible concern is whether the fan will start at low irradiance levels. If the fan motor draws current, but does not start, it may overheat in this stalled rotor condition, depending on the design of the motor. While this is an unlikely possibility, the thorough engineer will want to check the motor specifications to be sure the PV module is not capable of damaging the motor in stalled rotor condition.

To determine the air moved by the fan, it is necessary to extend the set of performance characteristics to include an air volume vs. fan voltage curve, as shown in Figure 4.2. This figure shows a family of curves that depend on the resistance to air flow to which the fan is exposed. If the fan has a long or constricted intake or exhaust port, there will be higher resistance to air flow, and the actual volume of air moved by the fan will be reduced. In effect, the fan must produce pressure, for which the trade-off is loss of flow. Note that in many systems, the power consumed is obtained by multiplying a flow variable by a pressure variable. If flow is the desired output, then pressure must be minimized to maximize flow and vice versa.

The reader is encouraged to envision situations that would be adequately served with the various system performance possibilities shown in this example.

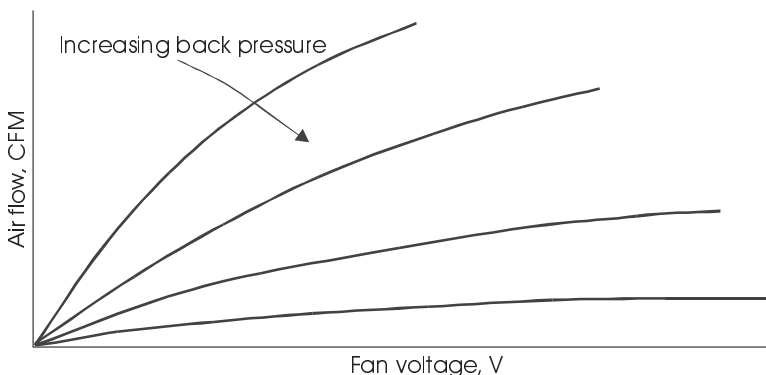


Figure 4.2 Air flow vs. fan motor voltage with pressure developed as a parameter.

4.2.2 PV Fan with Battery Backup

It is not difficult to imagine a situation where it is desired to use a fan at times when the sun is not shining. For that matter, it is perhaps even easier to envision a situation where it is desired to use a light when the sun is not shining. In either case, it will be necessary to store energy for later use. Figure 4.3 shows a PV fan system that includes storage batteries in the system. In this system, it is necessary to match the fan to the batteries as well as to the module(s). This is done by first determining the hours of operation of the fan as well as the energy to be used by the fan. Once again, the range of choices may be limitless.

Suppose that it has been determined that the fan must run continuously, and, since the fan will be operating from the battery, the fan voltage will be the battery voltage, which will presumably remain relatively constant. In this case, it is a simple matter to determine the daily energy consumption of the fan, since constant fan voltage will produce constant fan power. For example, if the fan motor consumes 24 watts when run from a nominal 12-volt battery, then in one day the fan will consume $(24 \text{ watts}) \times (24 \text{ hours}) = 576 \text{ Wh}$ of electrical energy.

The battery capacity, however, will be measured in ampere-hours (Ah). To determine the **connected load** in Ah for the fan, simply divide the energy by the voltage. In this case, the result is 48 Ah. Note that this result is also determined by multiplying the load current by the run time, or, if the load current is not constant, then the load current must be integrated over the time of operation.

Since neither the battery charging and discharging nor the wiring are 100% efficient, it is not adequate to consider only the connected load Ah requirements. The **corrected load** is determined by dividing the **connected load** by the battery efficiency and by the wiring efficiency. Typically, 90% of the charging energy can be recovered, and wiring losses are about 2%. So the **corrected load** becomes $48 \div 0.9 \div 0.98 = 54.4 \text{ Ah}$.

Next, it must be determined how critical it is that the fan run all the time. If fan operation is critical, then sufficient battery storage must be provided to power the fan during long periods of darkness or cloudy weather. The anticipated duration of such periods will depend on the geographical location of the fan and on whether the use of the fan is seasonal. Suppose this has all been worked out and that it has been determined that three days of storage is adequate. This means that a total storage capacity of 163 Ah is needed.

At this point, a decision must be made as to what type of battery to use. Suppose a lead-antimony storage battery is chosen. Since the lead-antimony system will allow deep discharge, suppose the battery (or batteries) is allowed to discharge to 20% of full charge. This means that only 80% of the battery rating is available for use. The capacity needed for this design is thus $163 \div 0.8 = 204 \text{ Ah}$. This capacity might be obtained with a single 12-volt, 204 Ah battery, but more likely would be obtained with two 6-volt batteries connected in series, since a 12-volt, 204 Ah lead-acid battery would be heavy and difficult to handle. Smaller units will usually be a more practical choice, as long as no more than 4

sets of batteries need to be connected in parallel. If more than 4 sets of batteries are connected in parallel, the chance of unbalance in battery charging and discharging currents is increased. This can cause premature battery failure.

Next, it is necessary to specify the PV power needs. This is done by determining the times when the least amount of sunlight is available during the months in which the fan is to operate. Suppose this has been done and it has been determined that the equivalent of 4 hours of full sun is available in the worst case. This does not imply that the sun shines at maximum intensity for 4 hours and then sets beyond the horizon, but that the average intensity over daylight hours is the same as peak intensity for 4 hours. It means that on some days, more than 4 hours of peak sun will be available and on some days, less than 4 hours of peak sun will be available.

During this 4-hour period, the PV array must produce all the electricity needed to operate the fan for a day. If a PV array with a nominal 12 V output is used, then the array must produce the needs of the batteries in ampere hours. However, it must be taken into account that the PV modules may not always operate at peak efficiency, such as if they get dusty. Operation at cell temperatures higher than 25°C may reduce maximum output power by an additional 15% by reducing the module maximum power voltage by 15%. Thus, rather than designing the PV system to produce the daily corrected load of 54.4 Ah, the system should be designed to produce $54.4 \div 0.9 = 60.4$ Ah. This amount allows for a 10% degradation of PV module output and assumes the module will then produce the necessary charging current at the charging voltage of the batteries, which is normally approximately 15 volts.

Since the available full sun is 4 hours, this means the PV module output must be $(60.4 \text{ Ah}) \div (4 \text{ hr}) = 15.1 \text{ A}$. So, finally, assuming the use of modules capable of producing 5.04 A at 15 V, a total of 3 modules will need to be connected in parallel to produce the necessary 15.1 A.

The design of the system is now nearly complete. In the event that the sun is hidden for more than 3 days, the batteries may discharge below the 20% level. Secondly, during the months of the year when more than 4 peak sun hours are available, the batteries may overcharge. These situations are mitigated somewhat by the fact that the fan motor runs faster and consumes more energy when the battery voltage is higher and conversely runs more slowly and consumes less energy when the battery voltage is lower. Yet, both situations can result in shortening of the life of the batteries. So good design practice would include a charge controller to prevent overcharge or overdischarge of the batteries. The charge controller must be capable of handling at least 125% of the total PV short-circuit output current on a continuous basis. It must also handle the fan current on a continuous basis.

Additional BOS components may also be considered, such as lightning surge protectors. More details on these items will follow in Chapter 7. Figure 4.3 shows the fan system with batteries and charge controller.

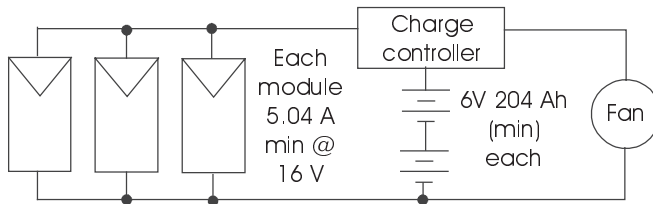


Figure 4.3 PV fan with battery storage.

4.3 Example 2: A PV-Powered Water Pumping System with Linear Current Booster

4.3.1 Determination of System Component Requirements

One of the most common PV applications is water pumping, especially when the water to be pumped is a long distance from a utility grid. Water pumping applications do not normally require battery backup unless the water source will not produce an adequate supply of water to meet the pumping needs during the period of peak sun. Under these circumstances, it is common practice to charge a battery so the pump can run for an extended period. When the water supply can meet the pumping capacity of the system, then it is generally desirable to pump all the water the pump is capable of delivering and store any excess in a storage tank. In effect, the storage of water replaces the storage of electricity in batteries. It still represents conversion of kinetic to potential energy. In fact, it is conceivable that the pumped water could be used during dark periods to turn a generator to generate electricity while the water is being delivered to its final use. The sacrifice is loss of pressure at the final delivery point.

When designing a water pumping system, it is necessary to determine a number of parameters in order to properly size the system components. First of all, the daily water needs must be determined. Secondly, the source must be characterized in terms of available water and vertical distance over which the water must be pumped. Once these factors are known, along with the number of hours per day available for pumping, the pumping rate can be determined. The pumping rate along with the pumping height equates to the pumping power, once again the product of a pressure quantity with a flow quantity. The pumping power can then be converted to horsepower so the size of the pump motor can be determined. It should be noted that this approach is somewhat simplified, since a pump motor does not produce constant horsepower as the flow and pressure are varied. Normally, depending on the exact type of pump, higher volumes at lower pressures involve higher horsepower than higher pressures and lower volumes from the same pump. These relationships will be discussed further in the examples presented in Chapter 7.

Once the size of the pump motor is known, the ampere-hour requirements of the motor can be determined, and, finally, the size of the PV array needed to

provide the ampere-hours can be determined. Inclusion of a linear current booster (LCB) extends the useful pumping time of the pump motor and enables the use of a smaller motor and a smaller array that is utilized more efficiently.

To quantify the pumping problem, it is useful to note that a gallon of water weighs 8.35 pounds and that one horsepower = 550 ft-lb/sec = 746 watts, assuming 100% conversion efficiency. This means that pumping a gallon of water to a height of one foot involves 8.35 ft-lb of work. In the MKS system, converting gallons to liters and feet to meters, gives the result that pumping a liter of water to a height of one meter requires 7.23 ft-lb = 9.83 J. If the pumping time is given in hours, and it is desired to determine the pump horsepower, then the pump horsepower can be determined from

$$HP = (4.22 \times 10^{-6}) \frac{(GPD)(h)}{(PT)(PTF)(\eta)} , \quad (4.1a)$$

where GPD is the gallons per day to be pumped, PT is the pumping time, PTF is the pumping time factor, h is the effective height and η is the wire-to-water efficiency of the pump-motor combination. In MKS, the horsepower is given by

$$HP = (3.66 \times 10^{-6}) \frac{(LPD)(h)}{(PT)(PTF)(\eta)} , \quad (4.1b)$$

where now LPD is the pumping requirement in liters per day and h is the effective pumping height in meters.

The effective height is the sum of the distance from the top of the water supply to the delivery point, including piping friction losses, which, in a properly designed system will be limited to about 5% of the total effective height. The pumping time will normally be the same as the peak sun hours and the pumping time factor is a modifier to account for the use of either batteries, a LCB or a tracking array mount. The product of PT and PTF then represents an effective pumping time.

If batteries are used, then the PTF is simply the ratio of the actual time the pump operates each day to the peak sun hours. Then, expressing PT as the peak sun hours and multiplying by this PTF gives the actual operating hours per day. If an LCB is used, so that the pump performance curve more closely matches the PV performance curve maximum power point, then more water will be pumped during low sun hours than would otherwise have been pumped. Use of an LCB in the system normally increases the daily volume pumped by an additional 20%. Hence, a reasonable default value for PTF when an LCB is used is 1.2. If the pump is connected directly to the PV array, then the PTF is 1.0.

The wire-to-water efficiency, η , will be specified by the pump manufacturer. For fractional horsepower pumps, it is typically about 25%, while larger pumps will be more efficient.

Piping friction loss is determined by the type and diameter pipe used, just as voltage drop is determined by the size and material of the wire used, although

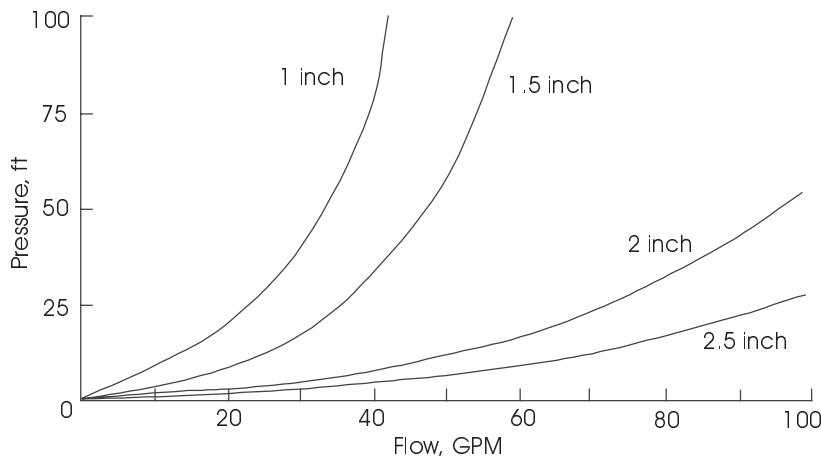


Figure 4.4 Pressure vs. flow curves for equal lengths of piping of different diameters.

the relationship between pressure and flow for a water pipe tends to be somewhat more nonlinear than the I-V relationship for a wire. However, at relatively low flow rates, the flow vs. pressure curve for a piping system can be approximated by a linear relationship. Figure 4.4 shows pressure vs. flow curves for several sizes of piping.

Although it is reasonably straightforward to select the horsepower for a pump, it is somewhat more involved to select the pumping system that will perform at maximum efficiency. The reason is that some pumps are designed to deliver higher pressure than others. The pumps that can deliver higher pressure are needed for lifting water to greater heights. Figure 4.5 shows performance curves for two pumps of equal horsepower, one of which is a high head (pres-

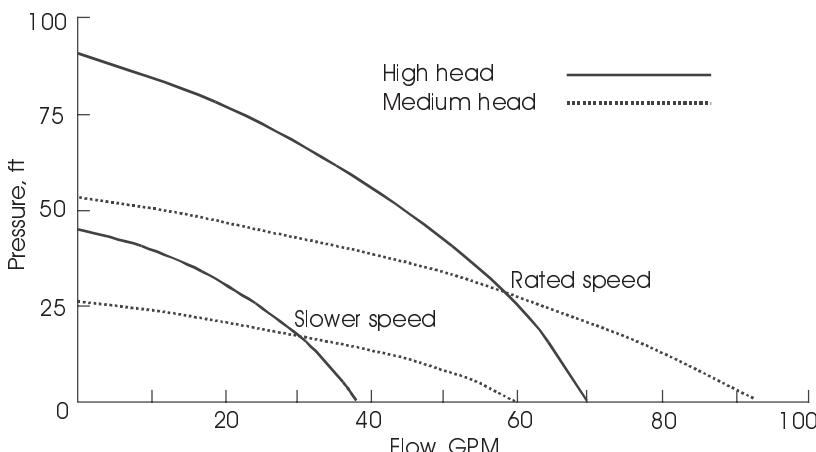


Figure 4.5 High head and medium head pump performance characteristics at two operating speeds.

sure) pump and the other is a medium head pump.

Note that the medium head pump will deliver more volume than the high head pump at low pressure, but the high head pump will overcome a greater pumping height. Note also that the performance of a pump depends on the speed at which the pump is operated. If the pump speed decreases, both pressure and flow capacity decrease. It is thus important to select a pump that will be able to overcome the lift requirement under low sun conditions.

4.3.2 A Simple Pumping System

Suppose a volume of 2000 gallons per day is required for irrigation purposes. Suppose also that the reservoir from which the water is to be pumped is very large, but located 200 feet underground, and that the worst case peak sun hours during the irrigation period is 6 hours. The problem is to determine the necessary components for a PV water pumping system to supply this water.

First, from (4.1a), the pump HP can be determined, assuming PTF = 1, peak sun of 6 hours and 25% pump efficiency, along with 5% piping friction losses. Taking the 5% piping losses into account, the effective height becomes $1.05 \times 200 = 210$ ft. Note that it is assumed that the water is being distributed at ground level with no storage. Using this value of h in (4.1a) along with the other system variables yields HP = 1.18. Of course, pumps do not come in 1.18 HP sizes, so the system designer now must choose from available sizes, meaning either a 1 HP or a 1.5 HP pump.

This is where the notion of service factor is useful. Motors are designed with service factor ratings. The service factor represents the amount of overload to which a motor may be subjected on a continuous basis without damaging the motor. A service factor of 1.25 for a 1 HP motor is not unusual. Hence, a 1 HP motor with a service factor of 1.25 can deliver the needed 1.18 HP. It should also be remembered that the pump motor will only be delivering maximum HP for at most a few hours near solar noon. Prior to and after this period, the pump will receive less power from the PV array and will thus operate at a lower HP.

Since the pump is connected directly to the array, the array size can thus be determined by installing the same current at full sun as the pump requirement, taking into account a 10% PV array degradation factor. Using a 10% degradation factor, the array current would be $(1.18 \text{ HP}) \times (746 \text{ watts/HP}) \times (1.1) \div (24 \text{ V}) = 40.3 \text{ A}$, assuming a 24 V pump motor. Note that the motor efficiency has already been accounted for in the overall wire-to-water efficiency estimate, so no further increase in array current is required for the pump motor.

Assuming 7 A at peak sun modules, a total of 12 modules will be needed to supply 42 A at a nominal voltage of 24 V, which should be close enough to the design requirement. If an LCB is used, then the PTF will be 1.2, and the new required HP is 20% less, since the pump operates 20% more efficiently. This will require only $0.8 \times 42 = 35 \text{ A}$, which will require 10 modules. The question then is whether the price of the two additional modules is greater than the cost of

an LCB. A 7 A module produces about 120 W maximum power, so at \$4/watt, this comes to \$960, so if an MPT can be purchased for less than \$960, it may be a good investment. In the next chapter, the possibility that the LCB may need more maintenance than the modules will be taken into account in determining whether the LCB will be a good choice. In choosing the pump, it is important to choose a pump that will lift the water the 200-foot distance over the full range of sun conditions. In the case of the LCB system, the pump can now use a 3/4 HP motor, which will cost slightly less than the 1 HP motor of the direct system.

The next step is to check the voltage for the pump motor and select a type for the pump. The assumption in each case is that the motor will be a dc motor. To determine the motor voltage, it is useful to calculate the motor current required at different voltages. Assuming an 880-watt power level, a 12-volt motor would draw $880 \div 12 = 73.4$ amperes. Depending on the distance from array to motor, this could result in the use of very large wire size to prevent excessive voltage drop. A higher voltage is thus advisable. At 24 V, the motor current will be 36.7 A, and at 48 V, the motor current will be 18.3 A.

As the system voltage is increased above 12 volts, however, one must consider the total number of modules needed for the system. For example, if 12 modules are used, they could be connected as 12 in parallel, 6 parallel sets of 2 in series, 3 parallel sets of 4 in series, 2 parallel sets of 6 in series, or one set of 12 in series. This offers nominal system voltages of either 12, 24, 48, 72 or 144 volts. But if 10 modules were required, they could be connected in 5 parallel sets of 2 in series to achieve a 24 V nominal system. However, 12 modules would be required for a 48 V system, since with 10 modules, there would be 2 series sets of 4 modules and 2 modules left over. Thus, even though only 10 modules may be needed to supply the needed power, they can not be conveniently connected to supply 48 V. So if an LCB is used with 10 modules, then either 12 V, 24 V, 60 V or 120 V system voltages could be obtained with 12 V nominal modules.

The type of pump will normally depend on the application. There are above ground pumps and submersible pumps. There are ac pumps and dc pumps. There are so many different kinds of pumps that it is an absolute necessity for the engineer facing the optimization of a pumping system design to obtain as many manufacturer specification sheets as possible to become acquainted with the available options. Figure 4.6 shows the two pumping systems discussed.

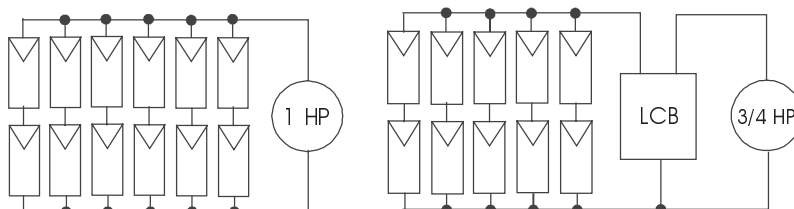


Figure 4.6 24 V dc water pumping systems.

4.3.3 Alternative Design Approach for Simple Pumping System

The previous pumping system design example involved calculating a number of system parameters that are often tabulated by pump manufacturers. If such data are available, then all the designer needs to know is the daily amount of water needed and the overall pumping height. The daily water needs can be converted to gallons or liters per minute over the time the pump will operate and a suitable pump can be selected from manufacturers' tables.

Using the 2000 gallons per day, 200 ft pumping height and 6 hours of sun-light figures of the previous example means that 2000 gallons must be pumped in 6 hours. This means $2000 \div 6 \div 60 = 5.56$ gallons per minute must be pumped a height of $200 \times 1.05 = 210$ ft to account for piping losses. Table 4.1 tabulates the GPM delivered at specific pumping heights at specific current and voltage levels for one model of dc submersible pump. Since 5.56 GPM and 210 ft are not on the table, it is necessary to interpolate to determine the appropriate pump voltage to deliver the required GPM. The PV power is 125% of the product of the pump current and pump voltage for this sizing algorithm.

Table 4.1 Pumping characteristics of a typical dc submersible pump. (Data courtesy AEE[1].)

Lift, ft	GPM	Pump Current	Pump Voltage	PV watts
150	6.4	6.00	90	675
150	12	8.95	120	1340
175	6.2	5.56	90	625
175	13.7	8.82	120	1320
200	7.6	6.64	105	875
200	11.0	8.42	120	1260
250	6.4	7.76	120	1164

It would be nice if a linear interpolation could be used. Since hydraulic power is proportional to the product of lift and GPM, one might expect electrical input power would be proportional to hydraulic power. A look at the figures for pumping lifts of 150, 175 and 200 ft shows this to be approximately the case, since the ratio of electrical powers is approximately equal to the ratio of GPM for these values of lift. In fact, a convenient normalization involves determining W/GPM at each lift. At 200 ft, the result is 115 W/GPM and at 250 ft the result is 182 W/GPM. Linear interpolation between 200 and 250 ft then yields a W/GPM ratio at 210 ft to be

$$\frac{W}{GPM} = \frac{210 - 200}{250 - 200} (182 - 115) + 115 = 128 .$$

Since the pumping requirement is 5.56 GPM, the PV power required is $128 \times 5.56 = 712$ watts.

Next the voltage necessary to produce 712 watts must be determined. One might expect the ratios of the powers to be proportional to the square of the ratios of the voltages. Testing this hypothesis gives $1260 \div 875 = 1.44$ whereas

$(120 \div 105)^2 = 1.31$, suggesting perhaps a different power relationship. If it is true that

$$\frac{P_2}{P_1} = \left(\frac{V_2}{V_1} \right)^n, \quad (4.2)$$

then one can solve for n, using 1260 and 875 for P_2 and P_1 and 120 and 105 for V_2 and V_1 . The result (see Problem 4.3) is $n = 2.73$. Now, $n = 2.73$ is used in estimating the operating voltage associated with the 712 watts of PV power needed to pump the 5.56 GPM through the 210-ft lift. The voltage, V_2 , can be determined by substituting $P_2 = 712$ W, $P_1 = 875$ W and $V_1 = 105$ V into (4.2), with $n = 2.73$. The result (see Problem 4.3) is $V_2 = 97.4$ V. Hence, if $V_2 = 97.4$ V, the PV current must be $712 \div 97.4 = 7.31$ A.

For modules rated at $V_{mp} = 17$ V and $I_{mp} = 7.3$ A, one might expect that connecting 6 of these modules in series would be adequate, since the output at maximum power should be 7.3 A at 102 V, or 745 W. In a perfect world, this would be true, but because of temperature and other degradation factors, pump manufacturers generally recommend oversizing the PV array by 25%. Hence, to ensure adequate current, it would be better to connect 7 modules in series. Furthermore, pump manufacturers generally recommend using an LCB with the pump, so the final system should probably also use a LCB for better performance at lower light levels and to better match the array characteristic to the pump characteristic.

One should note, however, that the cost of this 1 HP pump is over \$1800, whereas a 1/4 HP pump that will deliver 2.15 GPM while consuming 186 watts can be purchased for \$495. This suggests the entire system, including the battery storage needed for the slower pumping rate should probably be evaluated when a serious design exercise is in progress.

Other manufacturers provide tables for their pumps that list lift, GPM and power consumed for a fixed pump voltage. These tables are very convenient and result in simple interpolations and reliable results, especially if pump voltage is maintained nearly constant with batteries.

4.4 Example 3: A PV-Powered Area Lighting System

4.4.1 Determination of the Lighting Load

The design of a PV-powered area lighting system follows closely the design of the fan system with battery backup. The first step is to determine the lighting load, followed with battery selection and, finally, the number and type of PV modules to use. In order to determine the lighting load in watts, it is first necessary to determine the amount of light needed and the area over which the light is needed. Hence, the design begins with the determination of the necessary illumination level.

While illumination levels could be measured in watts/m², in the U.S., illumination levels are most commonly measured in foot candles. A foot-candle is the amount of light received at a distance of one foot from a standard candle. A standard candle is a candle that emits a total amount of light equal to 4π lumens. The lumen is thus the basic quantity of light in the foot-candle system of measurement of light intensity. It compares to the coulomb in the electrostatic realm.

If a closed surface surrounds the standard candle, then all of the 4π lumens of light must ultimately pass through the surface. If the light from the source is emitted uniformly in all directions, and if a sphere of radius 1 ft is centered on the light source, then the light will be uniformly distributed over the surface of the sphere with a density of $(4\pi \text{ lumens})/(4\pi \text{ ft}^2)$. This light intensity of 1 lumen/ft² defines the foot-candle (f-c).

The Illumination Engineering Society publishes guidelines for illumination levels for various spaces [2]. For example, parking lot lighting should normally be lighted to an average illumination level of approximately 1 f-c, depending on the degree of security desired. A desk for normal work is generally adequately lighted with 50 f-c. Direct sunlight provides about 10,000 f-c [3].

The **luminous efficacy** of a source is a measure of the efficiency with which the source transforms electrical energy to light energy. It is measured in lumens per watt. Table 4.2 shows the luminous efficacies for several light sources.

Table 4.2 Approximate luminous efficacy for several light sources [4, 5, 6].

Source	Luminous Efficacy, l/w	Lamp Lifetime, hr
25 W incandescent	8.6	2500
100 W incandescent	17.1	750
100 W long-life incandescent	16.0	1125
50 W quartz incandescent	19.0	2000
T-8 fluorescent	75–100	12,000–24,000+
Compact fluorescent	27–80	6,000–10,000
Metal halide	80–115	10,000–20,000
High-pressure sodium	90–140	10,000–24,000+
3.6 W LED array	~130	100,000+

Determination of the wattage of light needed to accomplish a specific lighting task, then, will depend on the required illumination level and the area to be lighted. It also depends on the luminous efficacy of the source. Other factors include whether the available light can be directed only to the area where the light is needed and whether some of the light will be absorbed by walls or other absorbers, such as the light fixture itself, before it reaches the surface to be illuminated. Dust on the fixture and lamp also absorbs useful light output.

In addition to the intensity of light, the color temperature of light is sometimes also a factor to be considered. The color temperature of light refers to the equivalent spectral content of radiation from a blackbody at a particular temperature. The color temperatures with which the reader is most familiar are the

5800 K temperature of the sun, which produces its characteristic white color, and the 3000 K temperature of a tungsten incandescent light filament, which is more toward orange. Not all light sources can be characterized by a color temperature, since the concept is based on blackbody radiators. Sources with discrete spectral components, such as lasers or gas discharge lamps, can be assigned equivalent color temperatures to indicate the temperature to which the spectrum of the source is most closely matched, but the color temperature is not a precise measure of the color of the source. For example, xenon produces a very white flash, which, on photographic film, appears to be close to the color of daylight. Although the output spectrum of a xenon lamp differs from the AM 1.5 solar spectrum, xenon lamps are commonly used in solar simulators with appropriate correction factors.

Consideration of color temperature can be an important factor in the choice of light sources. For example, low pressure sodium has a very high luminous efficacy, but the light is comprised primarily of the sodium d₂ lines. When low pressure sodium sources are used, anything not yellow in color will not be accurately perceived, since, if a source does not contain a particular color, then that color cannot be reflected back to the eye to be perceived as such. For PV applications, generally the most popular and efficient sources are fluorescent, metal halide and high pressure sodium. Occasionally incandescent sources are used for special purpose applications.

4.4.2 An Outdoor Lighting System

Suppose it is desired to provide nominal lighting in an area to enable people to see a walkway and any animals that may have come into the area. An average illumination level of approximately 1 f-c can do this. Suppose the area to be lighted is 15 feet wide and 1000 feet long and suppose a sharp cut-off fixture has been found that will provide coverage for an area measuring 15 feet by 40 feet if mounted on a 10-foot pole. The fixture has a **coefficient of utilization** (CU) of 0.80, which means that 80% of the light produced by the lamp will emerge from the fixture. Note that this CU is valid provided that the fixture remains clean. The **maintenance factor** (MF) ($0 < MF < 1$) accounts for dirt on the lamp, lens and reflector. One could thus estimate further reduction in light directed toward the designated space with another correction factor.

First, the number of fixtures must be determined. This is simple in this case, since each fixture will light 40 feet of the total length. Thus 25 fixtures will be needed, spaced at 40-foot intervals. Note that this spacing, four pole heights apart, is common for area lighting systems. Since the fixtures will be PV powered, each will be self-contained and can be specified separately. Hence, the solution for a 15-by-40-foot area will simply be repeated 25 times.

The total lumen requirement for each fixture is determined by the product of the area lighted and the average illumination level. In this case the result is $600 \text{ ft}^2 \times 1 \text{ f-c} = 600 \text{ lumens}$. Since the CU of the fixture is 0.8, the lumen output of

the lamp must be $600 \div 0.8 = 750$ lumens. This is close to the light output of a 9-watt compact fluorescent tube, which will produce approximately 600 lumens. Since the illumination level is not critical, the 9-watt tube should be adequate.

If the walkway is to remain lighted all night, it is necessary to determine the longest night of the year. Suppose the longest winter night is 15 hours. This means the shortest summer night will be 9 hours. It also means that the PV modules on the shortest day of the year must produce enough electricity to operate the fixtures through the longest night of the year. On the other hand, during the longest day, the PV array only need produce enough electricity for the shortest night. Clearly, if the longest night demand is to be met, the system will waste electricity during the longest day. Depending on the application or the location, it may be possible to either turn off the lights for a few hours during the longest night or to find an alternate use for the excess energy during the longest days.

Next, suppose a 12-volt system is selected. This means the lamps will draw 0.75 A when they are operating. The worst case daily corrected load is thus $15 \times 0.75 \div 0.9 \div 0.98 = 12.76 \text{ Ah}$. Suppose 3 days of storage are required and deep-cycle batteries are used. This means that $12.76 \times 3 \div 0.8 = 47.9 \text{ Ah}$ of storage is needed, assuming a depth of discharge of 80%. So a single 12 V battery with a minimum capacity of 48 Ah can be used.

To size the PV array, the peak sun hours of the shortest day are needed. Suppose the winter peak sun is 4 hours and the summer peak sun is 6 hours. Thus, in 4 hours, the array must produce $12.76 \div 0.9 = 14.2 \text{ Ah}$. This means an hourly production rate of $3.55 \text{ Ah/h} = 3.55 \text{ A}$. This can be done with a standard module rated at approximately 50 watts at maximum power, since the charging will be done at approximately 15 to 16 volts. A very straightforward system is thus possible, with a readily obtainable fixture, lamp, battery and module. Of course, a means of switching the light on and off between dusk and dawn needs to be incorporated into the system. This may be a relay in series with the module, which keeps the light off as long as the battery is charging, but turns the light on when the battery is no longer charging. A CdS photocell may be a more efficient choice of sensor, however, since the power loss in the relay coil during charging will probably exceed any minimal power loss in the photocell. The careful engineer will check both options.

It is interesting to look at the summer performance of the system. Since the lamp is on for only 9 hours per night, the daily corrected load is reduced to $9/15$ of the winter consumption, or 7.66 Ah. The module, on the other hand, will produce $3.55 \times 6 \times 0.9 = 19.2 \text{ Ah}$. This means an excess of 11.5 Ah per day is produced by the system. If this additional energy is directed to the battery, the battery will soon become overcharged and its lifetime will be shortened. It is thus important to either employ another use for the excess summer energy or else to employ a charge controller to limit the state of charge of the battery. It is also interesting to note that since the battery needs are nominal, a somewhat larger battery can be obtained at a nominal additional cost, so that the winter storage can be increased beyond 3 days.

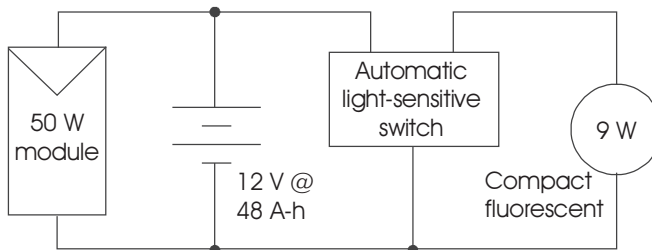


Figure 4.7 PV outdoor walkway lighting system.

It should also be noted that it may be possible to adjust the module tilt to obtain more sunlight in the winter. Tilting the module at an angle of latitude $+ 15^\circ$ in most regions will result in greater winter collection than summer collection, so it is important to choose the proper module tilt to match the annual system output needs as closely as possible. Module tilt will be discussed in detail when stand-alone system design is covered in Chapter 7. The lighting system is shown in Figure 4.7.

4.5 Example 4: A PV-Powered Remote Cabin

Another common PV application is to supply electricity to buildings located far from the nearest utility grid. Normally these applications involve only a few, relatively small, electrical loads. In this example a mountain cabin will be discussed which has a few lights, a refrigerator and a water pump. It will be assumed that the cabin is used only on weekends (with a few 3-day weekends) during the summer months. A listing of loads with their average *weekly* Ah consumption is shown in Table 4.3. Assume that the minimum peak sun hours during the season is 5 and that one week of battery storage is required, noting that all discharging will be on weekends. All loads are 12 V dc.

Table 4.3 Summary of loads for remote mountain cabin.

Load	Power, W	Current, A	Hr/Day	Ah/wk
Kitchen light	18	1.5	3	13.5
Dining room light	18	1.5	4	18
Living room lights	18	1.5	3	13.5
Bedroom lights	18	1.5	1	4.5
Bathroom light	9	0.75	1	2.25
Bedroom fan	24	2	4	24
Refrigerator	84	7	9	189
TV	36	3	3	27
Water pump	36	3	1	9

The total connected *weekly* load is thus 300.75 Ah. Notice that the *weekly* cycle of this system differs from the *daily* cycle of previous systems. Although

the loads are relatively constant during the times of occupancy, the system is provided with 3 days of battery storage, so that the PV array will have 7 days to provide 3 days of energy. During four of the charging days, there is no load on the batteries while during three days there is a load. The batteries will thus presumably be fully charged as the cabin is initially occupied and will then be simultaneously charging and discharging for three days. At the end of three days, depending upon the amount of sunlight available over the weekend, the batteries may become discharged to the design discharge value. This particular system has been designed to allow a maximum system discharge of 80%.

The system weekly corrected *load* in this case will be $300.75 \div 0.9 \div 0.97 = 344.5$ Ah, assuming a battery charging and discharging efficiency of 90% and wiring efficiency of 97%.

To determine the battery requirements, assuming 90% temperature correction factor and 80% depth of discharge, the battery requirements are found to be $344.5 \div 0.8 \div 0.9 = 478.5$ Ah. One way to provide this amount of storage would be to use four 6-volt golf cart batteries rated at 240 Ah each.

Next, to determine the PV array requirements, begin by converting the daily peak sun hours to weekly peak sun hours. Assuming 5 hours of peak sun per day gives 35 hours of peak sun per week. Hence, the PV requirements are $(344.5 \text{ Ah}) \div (35 \text{ hr}) \div 0.9 = 10.94 \text{ A}$. If 2 modules, each with $I_{mp} = 5.85 \text{ A}$ are used, then the system needs will be easily met.

The system, of course, will consist of more than the loads, the batteries and the PV array. The array must be mounted securely, the wiring must be properly sized and adequate disconnecting, fusing, switching, battery protection, lightning protection and distribution must be provided. Wire sizing will depend on the load currents and the distances of the loads from the source. These details will be covered in Chapter 7. Figure 4.8 shows the system block diagram, except for balance of system components (BOS).

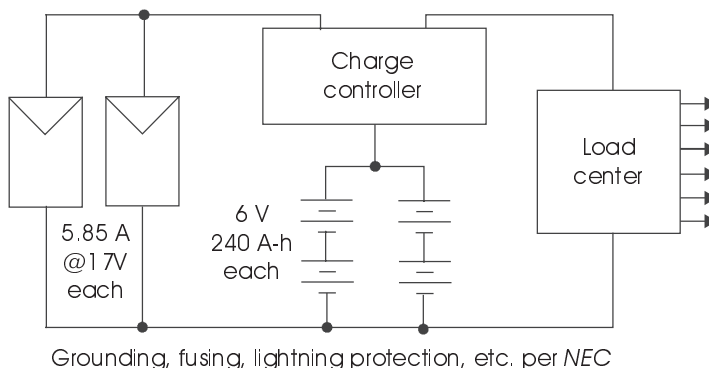


Figure 4.8 PV-powered remote cabin.

4.6 Example 5: A Hybrid System

Sometimes it is not economical or practical to provide all energy with PV modules. For example, when loads are relatively constant during summer and winter, or, perhaps even greater in winter, and if winter peak sun is very low, it may take a large number of modules to meet winter requirements. This may result in significant waste of energy produced by the modules during the summer months. In such cases, it may be more economical to provide some of the system energy needs by another means, such as a gasoline or diesel generator. A system that uses PV for part of its energy production and other means for the balance of the production is called a hybrid system. The best cost-effectiveness is generally obtained when none of the PV-generated energy is wasted.

Consider, for example, a radio repeater system at a high northern latitude that receives 7 hours of summer peak sun but only 1 hour of winter peak sun, with 3 hours average peak sun for spring and fall. Assume the system requires a constant 2 kW for 24 hours per day all year long, and that a PV system is to handle the summer load with 3 days of battery backup. Assume also that a gasoline generator will deliver the balance of system needs and that the generator will generate 6 kWh per gallon of fuel, and the system will only be refueled twice per year. The battery backup is important, since the system need is critical, and if the generator should fail, 3 days of battery power are needed to allow time for generator repair. The radio equipment operates on 120 V ac, so an ac generator and an inverter will be used. The inverter will have internal provisions for charging the batteries from the generator at an efficiency of 90%.

First, the corrected load is determined to be $2 \times 24 \div 0.9 \div 0.98 \div 0.9 = 60.5$ kWh/day, where 90% battery utilization efficiency, 98% wiring efficiency and 90% inverter efficiency are used. So the 60.5 kWh/day is the energy that must be delivered to the batteries. If the batteries operate at 48 volts, then this amounts to a daily corrected load of $(60,500 \text{ Wh}) \div 48 \text{ V} = 1260 \text{ Ah}$.

Assuming a 90% PV array degradation factor and 7 peak sun hours, the array current must be $1260 \div 0.9 \div 7 = 200 \text{ A}$. Note that if the array were sized to meet the winter load, then the array current would need to be 1400 A.

One popular larger module will deliver 17.4 A at 17.2 V [7]. Hence, to produce 200 A at 17.2 V, it will take $200 \div 17.4 = 12$ modules. Since it will take 4 modules in series to produce the needed battery charging voltage of approximately 56–58 V, 48 modules will be needed. Note that 48 modules will produce 14,400 W if operated at maximum power at standard test conditions, whereas in this system, with an output voltage of 56 V, the modules will only be producing 11,700 W, or 81.2% of their rated output. This power loss is due to the fact that the modules are expected to operate at approximately 10–12 V below the standard test condition V_{mp} .

Battery storage requirements are determined by dividing 60.5 kWh by the nominal system voltage, resulting in 1260 Ah per day of storage. Assuming use of deep-cycle batteries, but allowing for the batteries to cool down some in the

winter, resulting in less available charge, the total battery capacity required becomes $1260 \times 3 \div 0.9 \div 0.8 = 5250$ Ah. The 0.9 factor represents the winter charge degradation factor. If 6 V, 350 Ah batteries are used, then a total of 15 batteries in parallel will be needed, and since it takes 8 batteries in series to produce 84 volts, the total number of batteries increases to 120. Obviously this system is a bit larger than the systems previously discussed. For this system, it makes much better sense to use larger, sealed, maintenance-free batteries, such as a 1055 Ah @ 12 V unit [14]. The system will require 20 of these batteries.

The total energy requirement of the battery system is $(5250 \text{ Ah}) \times (48 \text{ V}) = 252,000 \text{ Wh} = 252 \text{ kWh}$. If the generator is to charge the batteries at a rate of C/10, the generator must be rated at $(252 \text{ kWh}) \div (10 \text{ hr}) = 25.2 \text{ kW}$. Taking into account a 90% conversion efficiency from generator ac output to battery dc input, a 28 kW generator will just meet the desired C/10 rate. Since the C/10 rate is not critical, a 25 kW generator will be adequate for the job.

The next items to be determined are the annual fuel usage and generator running time. To do so involves estimating the fraction of the total energy needs that should be produced by the PV array.

With the information given, the assumption is that for 3 months, the PV system produces all of the system electrical needs. Then, for 6 months the PV system provides only 3/7 of the system needs, since the peak sun hours are reduced from 7 to 3 during spring and fall. During the winter 3 months, the PV system will only supply 1/7 of the system needs.

Hence, for 182 days, the generator must produce $(4/7) \times 60.5 \div 0.9 = 38.4$ kWh/day, which results in $182 \times 38.4 = 6989$ total kWh production. The 0.9 factor is included to compensate for the loss in conversion of ac to dc for charging. For the winter months, the generator must provide $(6/7) \times 60.5 \div 0.9 = 57.6$ kWh/day for 91 days. This amounts to 5242 kWh. The total annual generator electrical output is thus 12,231 kWh.

Now, since the generator will produce 6 kWh/gal, the generator annual gasoline consumption will be 2039 gallons. If the tank is filled twice per year, then a tank half that size will suffice. To provide a slight safety margin, a 1200 gallon tank would be a reasonable choice. At a worst-case consumption rate of $57.6 \div 6 = 9.6$ gal/day, this provides about an 18.8-day leeway in case of bad weather or other problems in accessing the site for gasoline delivery.

To determine the generator run time per year for maintenance purposes, note that the generator produces 25 kW while it is operating, on the average. For example, depending on the control system, if the PV system is providing part or most of the power needed by the repeater system, depending on the state of charge of the batteries, the generator may or may not be running. Without this information on the control algorithm, it is only possible to deal with averages. Hence, dividing the kWh by the kW yields the hours of operation. The result is 489 hours of operation per year.

Without the PV system, the generator would have to generate $365 \times 60.5 \div 0.9 = 24,536$ kWh/yr. The PV system thus saves 12,305 kWh of generation by the

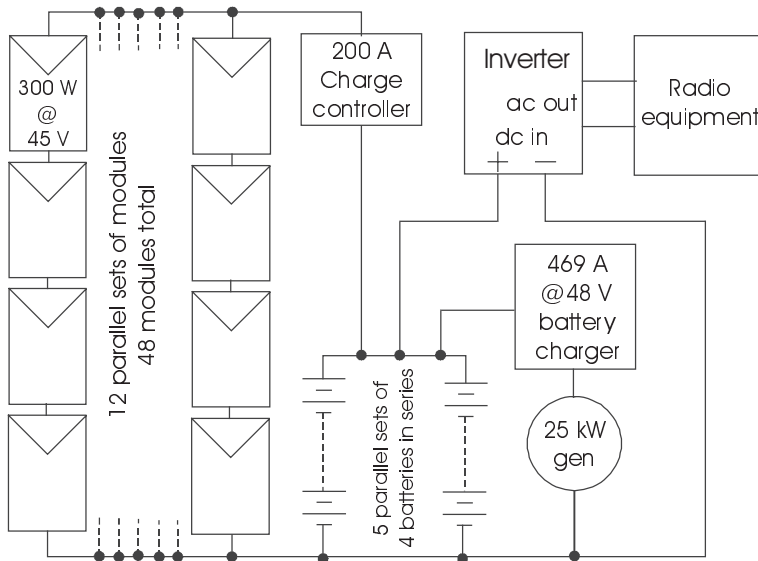


Figure 4.9 Hybrid radio repeater system. Disconnects, fusing and grounding not shown.

generator. If fuel for the generator costs \$1.50 per gallon, then the PV system saves over \$3076 in fuel costs per year. Of course, the assumption is that the system is pretty remote and the cost of getting fuel to the generator is fairly high. Hence, adding an additional transportation cost for the gasoline may add a significant additional amount to the fuel cost. Furthermore, the generator will probably require maintenance each time fuel is delivered, and that may add another \$200 or more per year to the cost of the generator. These costs will be dealt with in detail in the next chapter.

The 25 kW generator will require a battery charger capable of converting 25 kW at 120 Vac to 48 Vdc. It will thus have an input current rating of 208 A and an output current rating of 469 A, assuming 90% efficiency. With 5 sets of batteries in parallel, this results in a charging current of 93.75 A per series set of batteries. If the charger is near the batteries, the heat from the charger might be used to keep the batteries warm. The system, including inverter, battery charger and charge controller, is shown in Figure 4.9.

4.7 Example 6: A Utility Interactive System

4.7.1 Introduction

Utility interactive systems can range from the 1 kW range to the megawatt range. Residential systems typically are about 1.5 to 5 kW peak, while commercial installations tend to be in the 15 kW range, while central power installations exist in excess of a megawatt. Regardless of size, the systems are quite similar, except in the care taken to disconnect the system from the grid in the event of a

grid failure. IEEE 929 distinguishes systems under 10 kW as small systems. The simplest utility interactive system uses an inverter between the PV array and the utility grid. When the sun is shining, the PV system generates power. If the feed is on the user side of the revenue meter, the PV system supplies its maximum output and the grid supplies any additional power needed by the user. Depending on load requirements and PV array size, during some times of day, the PV system may feed power to the grid, causing the meter to run backwards.

If the grid loses power, the PV system must disconnect from the grid until the grid power is once again stable. In some locations, where grid power may be lost for prolonged periods, it may be desirable to provide battery backup with an inverter that continues to power the system load while the system is disconnected from the grid. In these systems, the inverter also acts as a battery charger/controller. When grid power is lost, the inverter switches in the battery system and keeps it on until the grid is restored or until the batteries are discharged to the allowed limit. If the inverter switches fast enough, it can act as an uninterruptible power supply.

The inverter may be connected on the utility side of the meter, or the customer side of the meter such that it will supply all user loads, supplemented as needed by utility power. The inverter may also be connected as an emergency source for certain user loads. When it serves as an emergency source, it must disconnect from the utility while the utility is down, even though it remains on to supply the emergency loads. When the inverter is used as an emergency, or uninterruptible power source, it must be capable of maintaining its frequency and output waveform in the absence of a synchronizing utility signal. For 24-hour emergency service, battery backup will also be needed, so the inverter also will serve as a charge controller. Figure 4.10 shows these three possible connections.

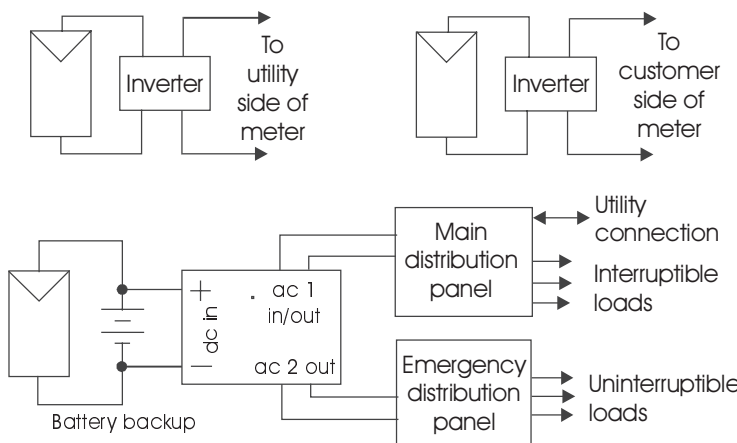


Figure 4.10 Three possible configurations for utility interactive PV systems.

4.7.2 A Simple Utility Interactive System with No Battery Storage

One nice feature of a utility interactive system is that if it does not have a specific backup function, the amount of PV installed depends upon the space available for the array and the budget of the system owner. If the PV array is connected to the customer side of the meter and if the array is generating in excess of customer needs, the excess is fed into the grid. If the PV is not meeting the needs of the customer, then the grid meets these needs. The origin of the electricity is transparent to the customer.

As long as the PV system does not generate more energy than the customer uses at any moment, the presence of the PV system will be similar to the implementation of a conservation measure—it simply lowers the customer's monthly electric bill. An interesting situation occurs, however, if the PV system generates more than the customer's needs at any moment during a metering period. In this case, the utility must determine a price for which to purchase the excess PV energy. If the utility does not own the PV system, then the question becomes whether to purchase the excess electrical energy at wholesale or retail prices. Herein lies a question, that of net metering, that may remain unanswered until various regulatory bodies study the pros and cons of each possibility. As this edition goes to press, 34 states have enacted net metering laws that require the utility to purchase the power from the PV power producer at the same rate that is charged the producer for electricity used from the utility [8].

From a technical perspective, however, the installation is simple, provided that the inverter is listed to comply with UL 1741, meaning that it meets IEEE 929 standards and that it complies with the requirements of the *National Electrical Code*, which requires all utility interactive inverters to be UL 1741 listed. The system also needs to be installed in accordance with all *NEC* requirements, including fusing, switching, ground fault protection and disconnects. Note that these conditions apply to PV arrays less than 10 kW.

As an example system, consider a 2400 W PV array, connected appropriately to a 2500 W inverter. The PV array has 20 modules rated at 120 W each, with module $V_{mp} = 16.9$ V, $V_{OC} = 21.5$ V, $I_{mp} = 7.10$ A and $I_{SC} = 7.45$ A. The modules are connected in a single series source circuit that delivers 7.10 A at 338 V dc under standard test conditions, provided that the inverter tracks array maximum power.

The inverter is line commutated so it depends on the utility voltage for synchronism. It has a 240 V, single phase, output voltage and feeds into the main panel of a dwelling through a 2-pole 20 A circuit breaker. The inverter input tracks maximum array power over an input voltage range of 225 to 550 V dc at a maximum inverter input current of 10.5 A.

Note that the inverter output is connected to the load side of the circuit breaker, since the line side of the breaker is connected to the bus bar of the main panel that is fed from the utility connection. Thus, when the circuit breaker is turned off, it is still conceivable that both sides of the breaker may be live, since

neither the utility nor the PV has necessarily been disconnected. However, since the inverter is designed to shut down in the absence of utility power, if the breaker is turned off, then the inverter loses its connection with utility power and shuts down.

The system is thus comprised of the PV array, the inverter and the circuitry to connect into the main panel. Most inverters now incorporate many of the *NEC*-required BOS components, so all that is needed may be source circuit fuses and a dc disconnect in the PV output circuit. If the array is roof mounted on a dwelling, then ground fault protection is also required per *NEC* Article 690–5. The inverter of this system incorporates all required NEC components. Figure 4.11 shows the system in detail, including a surge arrestor and system grounding.

The monthly and annual electrical energy production of the 2.5 kW system will depend upon the location and the orientation of the array. Allowing for 20% derating of the array for dust and elevated cell temperature and 94% efficiency of the inverter, the usable array output power, P , can be estimated to be $20 \times 120 \times 0.8 \times 0.94 = 1804$ W, assuming an average array temperature of 45°C. Monthly kWh can then be computed from

$$\text{kWh}/\text{mo} = P \times (\text{days}/\text{mo}) \times (\text{pk sun hr}/\text{day}) \div 1000. \quad (4.3)$$

Using the monthly figures for an array tilted at latitude for Seattle, WA, Denver, CO, and Albuquerque, NM, as tabulated in Appendix A, the monthly and annual kWh production of the array can be computed for these locations. The results are tabulated in Table 4.4. If the cost of electricity is known for these areas, the annual value of the electricity produced can be calculated. If the cost of the system is divided by the annual savings, a rough estimate of the time to pay back the system cost can be made. In Chapter 5, a more refined method that takes into account the time value of money will be introduced.

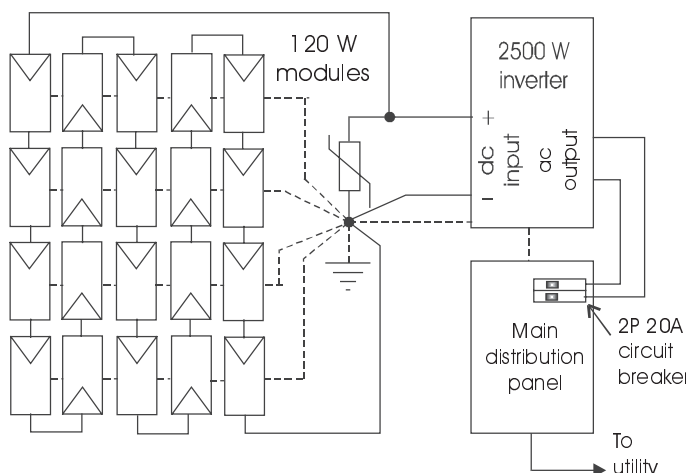


Figure 4.11 A 2.4-kW utility interactive system connected on the customer side of the utility meter.

Table 4.4 Monthly and annual kWh production of 2400 W array for three locations.

Seattle, WA							
Month	Jan	Feb	Mar	Apr	May	Jun	
Peak sun hr	1.39	2.22	3.87	4.56	5.12	5.14	
kWh/mo	78	112	216	247	286	278	
Month	Jul	Aug	Sep	Oct	Nov	Dec	Ann Total
Peak sun hr	6.06	5.75	4.69	3.07	1.65	1.16	
kWh/mo	339	322	254	172	89	65	2458
Denver, CO							
Month	Jan	Feb	Mar	Apr	May	Jun	
Peak sun hr	5.07	5.54	6.80	6.65	6.69	6.67	
kWh/mo	284	280	380	360	374	361	
Month	Jul	Aug	Sep	Oct	Nov	Dec	Ann Total
Peak sun hr	6.84	6.66	7.02	6.53	5.05	4.81	
kWh/mo	383	372	380	365	273	269	4081
Albuquerque, NM							
Month	Jan	Feb	Mar	Apr	May	Jun	
Peak sun hr	5.27	6.31	6.91	7.84	7.75	7.40	
kWh/mo	295	319	386	424	433	400	
Month	Jul	Aug	Sep	Oct	Nov	Dec	Ann Total
Peak sun hr	7.27	7.42	7.35	7.13	6.19	5.28	
kWh/mo	407	415	398	399	335	295	4506

4.8 Example 7: A Cathodic Protection System

4.8.1 Introduction

Material can be electroplated onto another material by immersing the two materials in a suitable electrolyte and applying a voltage between an anode composed of the desired plating substance and a cathode consisting of the material to which the material is to be plated. The result is transfer of material from the anode to the cathode.

When a metal is buried in the ground, it is highly likely that it will become a part of an electroplating system resulting from galvanic action between two dissimilar metals. If the metal assumes a higher potential than its surroundings, i.e., becomes an anode, then metal will be removed as a result of ion loss from the metal. However, if the metal is deliberately connected as the cathode of a system, then electrons will flow from the voltage source negative terminal to the metal. The positive terminal of the voltage source is connected to a buried anode material so electrons flow from the anode material to the positive terminal of the voltage source. Removal of electrons from the anode material creates positive ions that can enter the electrolyte (i.e., the ground) and flow toward the cathode. The process is shown in Figure 4.12.

The U.S. government requires that any underground storage of toxic materials or petrochemicals must have cathodic protection. Cathodic protection in-

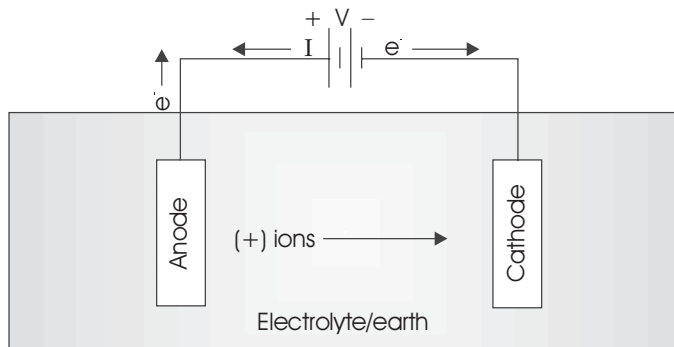


Figure 4.12 Schematic diagram of flow of current and charge carriers in an electrolyte system.

volves using the material to be protected, usually steel, as a cathode, while an anode (or anodes), typically of graphite, is buried nearby. In addition to protection of toxic waste containers, billions of dollars of infrastructure are built with steel reinforced concrete, much of which is under water. Cathodic protection of the steel in the concrete can prolong the life of buildings, bridges and other important infrastructure components.

To prevent ion loss from the cathode, different current densities are required for different materials, ranging generally from a fraction of a mA/ft^2 to several mA/ft^2 . The total current needed to protect a cathode is thus the product of the necessary current density and the surface area of the cathode. The voltage needed to supply this current is thus determined by the product of the current and the resistance from anode to cathode. In this example, the methods for determining current density, resistance and voltage are explored, along with determining necessary battery storage and array size.

If all soils were identical, cathodic protection system design would be nearly trivial. Fortunately for the corrosion engineer, the earth has been blessed with a wide range of soil types, often with diversity in a small area. This relatively wide range of soil conditions, sometimes varying with time in the same location, makes the job of protection of critical systems sufficiently challenging to warrant the high fees of the corrosion engineer. Considering the fines and/or lost revenues that can result from a spill of petrochemicals or toxics, design of systems to protect these systems cannot be left to amateurs. While this example will not convert the reader into a professional cathodic protection designer, it will at least convey some background needed for cathodic protection design.

4.8.2 System Design

The first step in the design of a cathodic protection system is to determine the system current needs. Suppose the item to be protected is an uncoated steel tank in sandy soil. Suppose the tank has an exposed surface area of 100 ft^2 . The current density required for use in this environment for exposed steel is $1 \text{ mA}/\text{ft}^2$, so

the total current needed will be 100 mA. If more current is generated, the cathode will remain protected, but the anode will be sacrificed at a higher rate.

The next step is to choose an anode. A typical anode will carry a maximum current of 2 A, so the choice of anodes will presumably not be significantly affected by current. The other consideration in choosing an anode is the resistance between the anode and the cathode. This resistance depends on the soil resistivity and on the size of the anode. Since the anode is generally cylindrical, the current from the anode travels more or less radially outward. The reader may recall from an electromagnetics course that a cylindrical geometry with an infinitely long charged cylinder produces an electric field that varies inversely with the distance from the cylinder. This results in a logarithmic variation in voltage and a nice, nonlinear relationship between the length and diameter of the anode and the resistance from anode to ground. Fortunately the resistance to ground for anodes of different diameter and length in a uniform soil with resistivity, $\rho = 1000 \Omega\text{-cm}$, are tabulated. The resistance to ground for different soil resistivity is then in proportion to the resistance at standard conditions. The resistance to ground for the anode is used as the resistance between anode and cathode.

In this case, suppose a 3-in diameter, 5-ft long anode is chosen. Table 4.5 shows the resistance to ground for such an anode in 1000 $\Omega\text{-cm}$ soil to be 4.3 Ω . But the resistivity of sandy soil is closer to 25,000 $\Omega\text{-cm}$, so the resistance to ground of this anode at the tank location will be approximately 25 times higher, or $25 \times 4.3 = 107.5 \Omega$.

Table 4.5 Anode resistance to ground in standard 1000 $\Omega\text{-cm}$ soil [9].

Anode Diameter, In	Anode Length, Ft				
	4	5	6	7	8
3	5.0 Ω	4.3 Ω	3.7 Ω	3.3 Ω	3.0 Ω
4	4.7 Ω	4.0 Ω	3.5 Ω	3.1 Ω	2.8 Ω
6	4.1 Ω	3.5 Ω	3.1 Ω	2.8 Ω	2.5 Ω
8	3.7 Ω	3.2 Ω	2.9 Ω	2.6 Ω	2.3 Ω
10	3.5 Ω	3.0 Ω	2.7 Ω	2.4 Ω	2.2 Ω

The required voltage is thus the product of the current and resistance, which, in this case, is $0.1 \times 107.5 = 10.75 \text{ V}$, which can readily be supplied by a standard nominal 12 V module (i.e., $V_{OC} \approx 20 \text{ V}$). Assuming the current is needed on a 24 hr/day basis, a 12 V storage battery will be needed.

Using a battery charging efficiency factor of 0.9 and a wire efficiency factor of 0.98, the daily corrected system load is determined to be $(0.1 \text{ A}) \times (24 \text{ hr}) \div 0.9 \div 0.98 = 2.72 \text{ Ah}$.

The next step is to determine the size of the battery needed, along with the current rating of the PV array. Assuming deep discharge batteries with 5 days of storage time and an allowable discharge of 80%, the battery needs will be $(2.72 \text{ Ah}) \times (5 \text{ days}) \div 0.8 = 17 \text{ Ah}$. This is about the size of the battery in a small uninterruptible power supply for computer backup power.

Finally, if the minimum daily insolation for the location of the tank is 4 hours, using a module derating of 90%, the module current is found to be $(2.72 \text{ Ah})/(4 \text{ hr}) \cdot 0.9 = 0.76 \text{ A}$.

The module can thus be a 10-watt, 12-volt unit, and the battery can be a small battery. However, if the maximum sun is significantly more than 4 hours, then the battery may overcharge, so a charge controller will be needed.

One might expect an alternative to a charge controller may be to use a larger battery. However, with an excess of 2 or more Ah/day from the module, in 30 days time, the battery will accumulate an additional 60 Ah. Only if the battery loses charge over time with no load or if it is significantly oversized, will the battery be safe from overcharge. Specifically, the *NEC* requires a charge controller whenever the PV array provides more than 3% of the battery rating in a single day. This, of course, would apply to the highest average peak sun hours of the year, whereas the present calculation has been based upon the lowest average peak sun hours of the year.

Suppose the combination of protection current and anode resistance to ground had resulted in the need for more than 12 volts. Several means of solving this problem are available. One is simply to use modules in series. Another is to use a larger anode or to use anodes in parallel. One might expect an anode with twice the surface area to have half the resistance to ground, but due to the nonlinearities of the system, this is not the case, as shown in Table 4.6.

The parallel anode solution results in a lower resistance to ground, but, perhaps not surprisingly, the resistance to ground of two identical anodes is not simply half the resistance of a single anode. The cylindrical geometry again adds a nonlinear twist to the problem, resulting in the resistance to ground of two anodes depending on the separation of the anodes. Table 4.6 shows multiple anode adjustment factors, assuming all anodes are identical and that the soil is uniform in composition. The factors in the table are multipliers for the single anode resistance to ground. Thus, for example, if the resistance to ground for a single anode is 100Ω , then the resistance to ground for 3 anodes spaced 15 ft apart will be $100 \times 0.418 = 41.8 \Omega$. This reduces the voltage required to 41.8% of that required for a single anode. It is thus a matter of calculating the life cycle cost (coming up in Chapter 5) of the three-anode system vs. the single anode system. Keeping in mind that each anode now will only carry 1/3 of the system current, the anodes should last three times longer.

A somewhat more elegant solution to the problem would involve an electronic constant current source that would provide the required current regardless of soil conditions or PV output. However, wet soil requires more current than dry soil, so the current source would need to be compensated for soil resistivity, rendering the current source design somewhat more challenging.

Whenever possible, it is advisable to make soil resistance measurements so empirical data can be used to size and locate system components properly. This eliminates many of the assumptions made and provides for greater confidence in the performance of the system. Figure 4.13 shows the final system.

Table 4.6 Multiple anode adjusting factors [9].

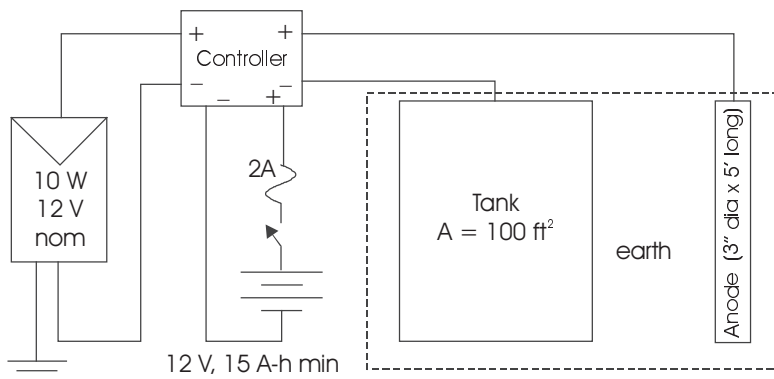
Number of Anodes	Separation of Anodes				
	5'	10'	15'	20'	25'
1	1.000	1.000	1.000	1.000	1.000
2	0.652	0.576	0.551	0.538	0.530
3	0.586	0.460	0.418	0.397	0.384
4	0.520	0.385	0.340	0.318	0.304
5	0.466	0.333	0.289	0.267	0.253
6	0.423	0.295	0.252	0.231	0.218
7	0.387	0.265	0.224	0.204	0.192
8	0.361	0.243	0.204	0.184	0.172
9	0.332	0.222	0.185	0.166	0.155
10	0.311	0.205	0.170	0.153	0.142

4.9 Example 8: A Portable Highway Advisory Sign

4.9.1 Introduction

Once upon a time, illuminated highway signs either had to be connected to the power grid or else had to be self-contained with their own portable fossil-fueled generator. Furthermore, their messages were often hard-wired, so the sign could only convey a single message. In this example, rather than determining the number of PV modules and number of batteries for a given load, the energy available for a load and the corresponding average load power will be determined. This approach is taken for several reasons, one of which is that it has not been used yet and the other being that sometimes a PV system may be limited by size or cost.

Anything to be transported on a roadway should normally be 8 ft or less in width. Assuming a sign of 8 ft width and assuming that PV modules will be mounted horizontally on top of the sign since the orientation of the sign will be

**Figure 4.13** Cathodic protection system.

random, suggests that 4 modules, each 2 ft \times 5 ft, can be used conveniently. The sign will be mounted on a trailer of standard size along with the battery pack and BOS. While it may be possible to mount additional modules elsewhere on the trailer, it is assumed that to avoid module shading and minimize damage from vandalism, only the modules on top of the sign are practical.

Since each month has different peak sun hours, each month will have different available average power for the sign. Thus, during some months, it may be possible that the sign will not be used 24 hours per day or it may be possible to convey longer or brighter messages during some months. For this example, it will be assumed that the sign will be used in the vicinity of Atlanta, GA, where freeway construction has been in progress for the past 40 years and may continue into the foreseeable future.

4.9.2 Determination of Available Average Power

If modules with 12% efficiency are used, then the modules will be able to generate approximately 12 W/ft² under full sun irradiance. The 4 modules will thus have a maximum power output of $40 \times 12 = 480$ watts, provided that they are kept clean. Assuming, however, that they will commonly be used in dusty construction sites, it is probably best to assume a 80% degradation factor due to the dust, elevated cell temperature and operation below the module V_{mp} . The maximum output is thus reduced to 384 watts. This output, of course, is only achieved if the sun is directly overhead.

To determine the available irradiance normal to the modules, it is necessary to determine the position of the sun at solar noon for the months of the year. Insolation data are available for Atlanta, GA, in Appendix A and are repeated in Table 4.7 for a fixed array with a tilt of latitude -15° . The latitude of Atlanta is approximately 33° north, so the tilt data is thus for an angle of 18°, rather than horizontal. To convert the data to horizontal, the data should be multiplied by $\cos 18^\circ = 0.95$. The data corrected for horizontal array orientation are also shown in Table 4.7. It should be noted that the correction factor is valid for the beam component of incident irradiance. Since the global irradiance also contains a diffuse component, the correction factor is a worst-case figure.

In fact, if an on-line computer were handy, one could go to www.nrel.gov and look up the figures for a horizontal surface to compare with the figures obtained by multiplying by $\cos 18^\circ$.

Table 4.7 Summary of available average monthly irradiance for Atlanta, GA (peak sun hr/day).

	Jan	Feb	Mar	Apr	May	Jun
Lat-15°	2.87	3.61	4.77	5.56	6.26	5.84
Horiz	2.73	3.43	4.53	5.28	5.95	5.55
	Jul	Aug	Sep	Oct	Nov	Dec
Lat-15°	5.90	5.83	4.69	4.84	3.69	2.95
Horiz	5.61	5.54	4.46	4.60	3.51	2.80

Next, the amount of energy available for charging batteries can be determined. Assuming a battery-charging efficiency of 90% and a wire efficiency of 98% leaves $0.90 \times 0.98 \times 384 = 339$ watts, and using a nominal system voltage of 12 V, leaves $339 \div 12 = 28.2$ A of effective charging current from the array. Assuming that 5 days of storage with deep cycle batteries capable of 80% discharge, the average number of Ah available for the display from the batteries in a 5-day period during the worst month will be $(5 \text{ days}) \times (28.2 \text{ A}) \times (2.73 \text{ hr/day}) = 385 \text{ Ah}$. The battery capacity for 5 days of storage is thus $385 \div 0.8 = 482 \text{ Ah}$, which can be obtained with four 6-V batteries, each having a capacity of 241 Ah.

Finally, the average daily power available to the sign can be computed. The assumption is that the batteries are fully charged when sign operation is begun. Under these circumstances, the batteries will discharge some on some days and charge some on other days, depending upon whether the insolation is above the monthly average or below the monthly average for the particular day. If the average daily energy used by the sign is the same as the average daily energy provided to the batteries, then the net discharge of the batteries is zero. So all that is needed is a tabulation of the average daily energy in Wh available to the batteries for each month of the year. For each day, this energy is found from

$$\text{Wh} = (\text{Effective array current}) \times (\text{battery voltage}) \times (\text{peak sun hr}), \quad (4.4)$$

where the effective array current is the current obtained after accounting for all system losses due to module degradation, battery charging efficiency and wiring losses. The average power available over a 24-hour period is simply the daily Wh divided by 24 hr. Table 4.8 tabulates the daily average power available for the 12 months of the year.

Table 4.8 Average daily power available to the sign for each month of the year.

	Jan	Feb	Mar	Apr	May	Jun
Peak sun hr	2.73	3.43	4.53	5.28	5.95	5.55
Avg power, W	38.5	48.4	63.9	74.5	83.9	78.3
	Jul	Aug	Sep	Oct	Nov	Dec
Peak sun hr	5.61	5.54	4.46	4.60	3.51	2.80
Avg power, W	79.1	78.1	62.9	64.9	49.5	39.5

With a microcontroller in the system, it is straightforward to program the unit to inform the user of the average power that will be used to implement any particular program. For that matter, the system can even be programmed to give a warning to the programmer if the average daily power is exceeded by the proposed announcement. If the sign is not programmed to use maximum available power, then the controller needs to have the capability to disconnect the PV array from the batteries.

Problems

- 4.1 For the fan example, indicate applications for which it would be desirable to have an oversized PV module and indicate when it would be satisfactory to have a smaller module that would produce a significantly lower fan speed at lower light levels. Can you envision an application for which use of a MPT would be advantageous?
- 4.2 For the alternate pumping example in Section 4.3.3, show that the values obtained for n and for V_2 are correct under the assumptions made in the example.
- 4.3 How much power could be recovered at low light levels by using an MPT on the fan of the first example in the text, assuming the MPT to be 90% efficient? Estimate the additional maximum power output that would be required of a PV array that would produce the same low-light-level power as the system with the MPT. If the additional PV cost \$5/watt, how much could you spend on the MPT to produce the same effect?
- 4.4 Prove that equations 4.1a and 4.1b are correct.
- 4.5 Determine the lamp wattage required to obtain an illumination level of 50 f-c over a 100 ft² area if a fixture is used with a CU of 0.75 and 80% of the available light reaches the work surface, the rest being absorbed by walls and other items in the space. Assume a luminous efficacy of 70 lumens/watt.
- 4.6 If the lamp of Problem 4.5 is on for an average of 6 hours per day, and if peak sun hours average 6 hours per day,
 - a. Determine the power output required for a PV array that would power the lamp, assuming 10% degradation of the PV array.
 - b. Determine a general expression for PV array power as a function of lamp operating time, assuming full utilization of the PV output.
- 4.7 For the remote cabin of Section 4.5, sketch the state of charge of the batteries for a 7-day period, assuming the batteries begin on Monday morning 80% discharged and assuming the following conditions:
 - a. three day occupancy over a weekend and average peak sun every day
 - b. two day occupancy over a weekend and average peak sun every day
 - c. three day occupancy over a weekend and 3 hours peak sun on Monday, 6 on Tuesday, 2 on Wednesday, 5 on Thursday, 6 on Friday, 2 on Saturday and 5 on Sunday.
- 4.8 For the hybrid system of Section 4.6:
 - a. Explain why the system will have 18.8 days of leeway for refueling resulting from the choice of a 1200 gal fuel tank.

- b. Suggest two good times during the year for refueling. Explain your reasons, keeping in mind that not much fuel is used in the summer.
- 4.9 For the hybrid system of Section 4.6, determine the type and amount of annual maintenance that will be required for the generator if it is a
- a. 3600 rpm gasoline generator
 - b. 1800 rpm gasoline generator
 - c. 1800 rpm diesel generator
- 4.10 For the hybrid system of Section 4.6, determine the wire size needed to carry the battery charging current from the battery charger to the batteries, assuming voltage drop is not a problem. The wire must be able to carry 125% of the charging current. Parallel conductors are allowed, provided that they are of the same size.
- 4.11 Sketch the battery system of Section 4.6 and recommend methods of wiring that will balance the current in each of the parallel sets of batteries. Keep in mind that the cell voltages of all batteries may not be exactly equal. Then make a search for batteries with higher Ah ratings to determine whether fewer than 15 parallel battery sets are possible.
- 4.12 Assuming voltage drop in wiring not to be a problem, determine the wire sizes needed to carry the currents on the dc and ac sides of the inverter of the utility interactive example of Section 4.7. You might find Table 3.7 to be useful. Note that the source circuit wiring must be capable of carrying 156% of I_{sc} of the array, and the inverter output circuit wiring must be capable of carrying 125% of the rated output current of the inverter.
- 4.13 For a soil with a resistivity of 12,000 $\Omega\text{-cm}$, and a cathode that requires 200 mA of current for protection, configure an anode system that will allow the use of a 12 volt system. Then select a battery to provide 5 days of storage and a module(s) to supply the system energy needs if the minimum insolation is 3 hr/day.
- 4.14 For a soil with resistivity of 20,000 $\Omega\text{-cm}$, and a cathode that requires 500 mA of current for protection, configure an anode system that will allow the use of a 12-volt system. Then select a battery to provide 5 days of storage and a module(s) to supply the system energy needs for minimum peak sun of 2.5 hr/day.
- 4.15 To test the soil resistivity after a large steel tank has been buried, a 6-ft-long, 4-in-diameter anode is buried about 40 ft from the tank. When a 12 V battery is connected between the anode and the tank, a current of 0.5 A flows. What is the resistivity of the soil?

- 4.16 The highway information sign is to be designed for use in Miami, FL, using the same PV panels. The sign still requires 5 days of autonomy under worst case sun conditions, so the battery requirements will need to be recalculated. Then tabulate the average daily power available to the sign for each of the 12 months of the year.
- 4.17 Redo the highway information sign example for use in Phoenix, AZ, again calculating the battery requirements and then showing the monthly average daily power availability.
- 4.18 For the highway sign of Section 4.9, determine the Ah rating of batteries that will provide 5 days of backup power for the month with the highest average daily sun hours.
- 4.19 How many days of storage will the batteries of the highway sign example of Section 4.9 provide at summer average daily power levels?

References

- [1] *1997-98 Design Guide & Catalog*, Alternative Energy Engineering, Redway, CA, 1997.
- [2] *Lighting Handbook: Reference and Application, 8th Ed.*, Illuminating Engineering Society of North America, New York, 1993.
- [3] *IES Lighting Handbook*, Illuminating Engineering Society of North America, New York, 1984.
- [4] *9200 Lamp Catalog, 22nd Ed.*, GE Lighting, General Electric Co., 1995.
- [5] *Lamp Specification and Application Guide*, Philips Lighting Co., Somerset , NJ, 1999.
- [6] www.cetsolar.com for information on LED arrays.
- [7] www.aseamerica.com for information on ASE PV modules.
- [8] www.dsireusa.org/summarytables for information on state renewable programs.
- [9] *Stand-Alone Photovoltaic Systems: A Handbook of Recommended Design Practices*, Sandia National Laboratories, Albuquerque, NM, 1995.

Suggested Reading

- Blier, F., *Fan Handbook: Selection, Application and Design*, McGraw-Hill, New York, 1998.
- NFPA 70 National Electrical Code, 1999 Edition*, National Fire Protection Association, Quincy, MA, 1998.
- Roberson, J. A. and Crowe, C. T., *Engineering Fluid Mechanics, 3rd Ed.*, Houghton Mifflin, Boston, MA, 1985.
- www.astropower.com for information on AstroPower modules.
- www.batteries4everything.com for information on a variety of batteries.
- www.fsec.ucf.edu for a wide range of information and links to other PV products and systems.
- www.sma-america.com for information on Sunny Boy inverters.
- www.xantrex.com for information on Xantrex inverters.

Chapter 5

COST CONSIDERATIONS

5.1 Introduction

The costs of a PV system include acquisition costs, operating costs, maintenance costs and replacement costs. At the end of the life of a system, the system may have a salvage value or it may have a decommissioning cost. This chapter introduces the method of life cycle costing, which accounts for all costs associated with a system over its lifetime, taking into account the time value of money. Life cycle costing is used in the design of the PV system that will cost the least amount over its lifetime. Life cycle costing, in general, constitutes a sensible means for evaluating any purchase options.

If it is necessary to borrow money to purchase an item, the cost of the loan may also need to be incorporated into the total cost of a system.

This chapter also introduces the concept of externalities. Externalities are costs that are not normally directly associated with an item. For example, it is generally agreed that acid rain can be caused by sulfur emissions from smokestacks. It is also generally agreed that acid rain can cause damage to buildings and lakes. Yet, the cost of these damages is generally not paid for directly by the entity that generates the emissions. Externalities will be considered in more detail in Chapter 9.

5.2 Life Cycle Costing

5.2.1 The Time Value of Money

The life cycle cost of an item consists of the total cost of owning and operating an item over its lifetime. Some costs involved in the owning and operating of an item are incurred at the time of acquisition, and other costs are incurred at later times. In order to compare two similar items, which may have different costs at different times, it is convenient to refer all costs to the time of acquisition. For example, one refrigerator may be initially less expensive than another, but it may require more electrical energy and more repairs over its lifetime. The additional costs of electrical energy and repairs may more than offset the lower acquisition cost.

Two phenomena affect the value of money over time. The **inflation rate**, i , is a measure of the decline in value of money. For example, if the inflation rate is 3% per year, then an item will cost 3% more next year. Since it takes more money to purchase the same thing, the value of the unit of currency, in effect, is decreased. Note that the inflation rate for any item need not necessarily follow the general inflation rate. Recently health care costs have exceeded the general inflation rate in the U.S., while the cost of most electronic goods have fallen far below the general inflation rate.

The **discount rate**, d , relates to the amount of interest that can be earned on principal that is saved. If money is invested in an account that has a positive interest rate, the principal will increase from year to year. The real challenge, then, in investing money, is to invest at a discount rate that is greater than the inflation rate.

As an example, assume an initial amount of money is invested at a rate of $100d\%$ per year, where d is the percentage rate expressed as a fraction. After n years, the value of the investment will be

$$N(n) = N_o(1+d)^n. \quad (5.1)$$

However, in terms of the purchasing power of this investment, $N(n)$ dollars will not purchase the same amount as this amount of money would have purchased at the time the investment was made. In order to account for inflation, note that if the cost of an item at the time the investment was made is C_o , then the cost of the item after n years if the inflation rate is $100i\%$ per year, will be

$$C(n) = C_o(1+i)^n. \quad (5.2)$$

One might argue that if the cost of an item increases at a rate that exceeds the rate at which the value of saved money increases, that the item should be purchased right away. Similarly, if the cost of the item increases more slowly, or, perhaps, actually decreases over time, then one should wait before making the purchase, since the cost will be less at a later time. The disadvantage of this purchasing algorithm, of course, is that the item to be purchased will not be available for use until it is purchased. Hence, the new computer that becomes less and less expensive while the invested money continues to increase, is not available for computing when it should be purchased. In other words, economics may not be the only consideration in making a purchase. Sometimes people buy things simply because they want them.

It is important to remember that choosing values for d and i is tantamount to predicting the future, since d and i fluctuate over time. Depending upon the saving mechanism, the rate of return may be fixed or may be variable. Inflation is, at best, unpredictable.

Figure 5.1 shows how the consumer price index, as a measure of inflation, the Dow Jones industrial average, as one possible measure of d , and the government prime lending rate, as a measure of the minimum borrowing interest rate, have varied over the period between 1980 and 2002. It is interesting to note how the prime lending rate is adjusted with the intent of either controlling inflation by discouraging borrowing or stimulating the economy by encouraging borrowing. The high prime lending rate in the early 1980s reflects the attempt to control high inflation in the late 1970s resulting from significant increases in energy prices during this period. The low rate in 2002 reflects the attempt to stimulate the economy and bring about a recovery of the stock market.

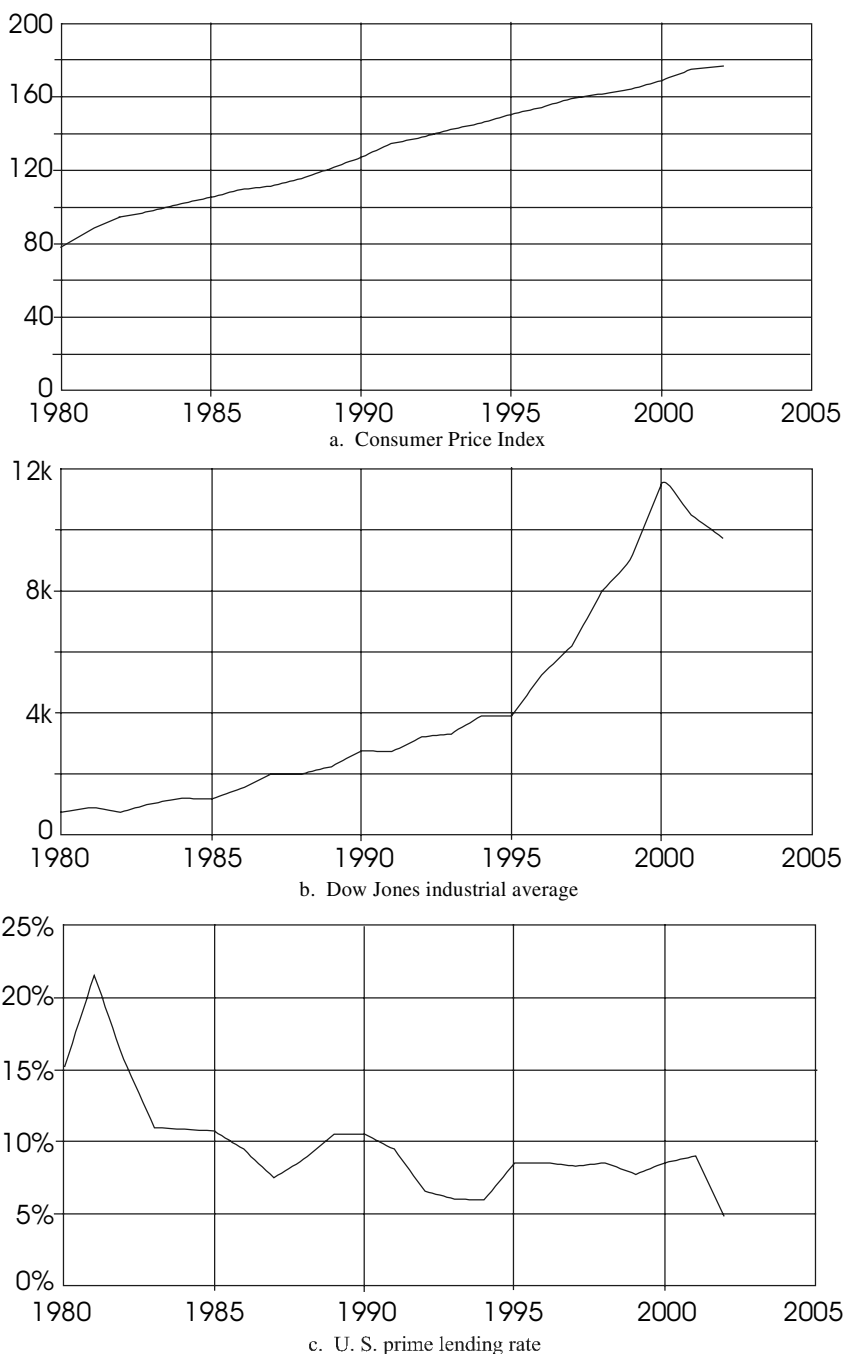


Figure 5.1 Comparison of Consumer Price Index, Dow Jones industrial average and prime lending rate, 1980-2002 [1, 2, 3].

5.2.2 Present Worth Factors and Present Worth

If $C_o = N_o$, the ratio of $C(n)$ to $N(n)$ becomes a dimensionless quantity, Pr , which represents the **present worth factor** of an item that will be purchased n years later, and is given by

$$Pr = \left(\frac{1+i}{1+d} \right)^n . \quad (5.3)$$

The present worth of an item is defined as the amount of money that would need to be invested at the present time with a return of $100d\%$ in order to be able to purchase the item at a future time, assuming an inflation rate of $100i\%$. Hence, for the item to be purchased n years later, the present worth is given by

$$PW = (Pr)C_o . \quad (5.4)$$

Sometimes it is necessary to determine the present worth of a recurring expense, such as fuel cost. Since recurring expenses can be broken down into a series of individual expenses at later times, it is possible to determine the present worth of a recurring expense by simply summing up the present worth of each of the series. For example, suppose a commodity such as diesel fuel is to be used over the lifetime of a diesel generator. It is desired to determine how much money must be invested at present at an annual interest rate of $100d\%$, under conditions of $100i\%$ annual inflation in order to purchase fuel for n years. If the first year's supply of fuel is purchased at the time the system is put into operation, and each successive year's fuel supply is purchased at the beginning of the year, the present worth of the fuel acquisitions will be

$$PW = C_o + C_o \left(\frac{1+i}{1+d} \right) + C_o \left(\frac{1+i}{1+d} \right)^2 + C_o \left(\frac{1+i}{1+d} \right)^3 + \dots + C_o \left(\frac{1+i}{1+d} \right)^{n-1} . \quad (5.5)$$

Letting $x = \left(\frac{1+i}{1+d} \right)$, (5.5) becomes

$$PW = C_o (1 + x + x^2 + \dots + x^{n-1}) . \quad (5.5a)$$

This expression can be simplified by observing that

$$\frac{1}{1-x} = 1 + x + x^2 + x^3 + \dots = \sum_{i=0}^{\infty} x^i . \quad (5.6)$$

Now, the **cumulative present worth factor** can be defined as

$$Pa = PW/C_o = \frac{1}{1-x} - \sum_{i=n}^{\infty} x^i = \frac{1}{1-x} - x^n \sum_{i=0}^{\infty} x^i ,$$

or, finally,

$$Pa = \frac{1-x^n}{1-x} . \quad (5.7)$$

It is important to recognize that (5.7) is based on the assumption that the first year's supply is purchased at the beginning of the year at a time when the fuel is at its present value. The fuel is then purchased annually with the last purchase occurring one year before the system lifetime has expired. In other words, there are n purchases of fuel, each at the beginning of the n^{th} year.

If the recurring purchase does not begin until the end of the first year, and if the last purchase occurs at the end of the useful life of the system, there will still be n purchases, but, using x again, the cumulative present worth factor becomes

$$\begin{aligned} Pa_1 &= x + x^2 + x^3 + \dots + x^n \\ &= x(1+x+x^2+\dots+x^{n-1}) = xPa . \end{aligned} \quad (5.8)$$

Since x will typically be in the range $0.95 < x < 1.05$, and since determination of i and d are at best, good guesses, and since it would be unusual to purchase an entire year's supply of many things all at once at the beginning of the year or at the end of the year, either (5.7) or (5.8) will provide a good estimate of the present worth of a cumulative expenditure. Often the values for Pr and for Pa are tabulated. Since most engineers have programmable calculators and computers, there is little point in repeating tabulated values for these expressions. Once the values for the variables have been decided upon, the present worth of quantities can be calculated. For that matter, if an engineer wanted to assume different values for d and i for different years, the same methodology could be used to determine the present worth of a quantity.

5.2.3 Life Cycle Cost

Once the PW is known for all cost categories relating to the purchase, maintenance and operation of an item, the life cycle cost (LCC) is defined as the sum of the PWs of all the components. The life cycle cost may contain elements pertaining to original purchase price, replacement prices of components, maintenance costs, fuel and/or operation costs, and salvage costs or salvage revenues. Calculating the LCC of an item provides important information for use in the process of deciding which choice is the most economical. The following example demonstrates the use of LCC.

Example 5.1. Refrigerator A costs \$600 and uses 150 kWh of electricity per month. It is designed to last 10 years with no repairs. Refrigerator B costs \$800 and uses 100 kWh of electricity per month. It is also designed to last 10 years with no repairs. Assuming all the other features of the two refrigerators are the same, which is the better buy if the cost of electricity is \$0.07/kWh? What if the cost of electricity is \$0.15/kWh? Assume a discount rate of 10% and assume an inflation rate of 3% for the electrical costs.

Solution: The solution, of course, is to perform life cycle cost analyses on each refrigerator. First note that $x = 1.03 \div 1.10 = 0.9364$. For a 10-year period, since electricity purchase begins at the time of purchase of the refrigerator, using (5.7) gives $P_A = 7.573$.

Then note that for refrigerator A, the electrical cost for the first year will be $(12 \text{ mo}) \times (150 \text{ kWh/mo}) \times (\$0.07/\text{kWh}) = \$126$ and for refrigerator B, the electrical cost for the first year will be \$84. Multiplying the first year cost by P_A , yields the PW of the electrical cost. A simple table may be constructed to compare the two refrigerators. Note that separate columns are used for the PW associated with electricity at \$0.07/kWh and electricity at \$0.15/kWh.

Table 5.1 Life cycle cost analysis for two refrigerators at \$0.07/kWh and \$0.15/kWh.

	Refrigerator A			Refrigerator B		
	First year	PW	PW	First year	PW	PW
Purchase price	\$600	\$600	\$600	\$800	\$800	\$800
Electrical cost @ \$.07/kWh	\$126	\$954		\$84	\$636	
Electrical cost @ \$.15/kWh	\$270		\$2045	\$180		\$1363
LCC		\$1554	\$2645		\$1436	\$2163

From Table 5.1 it is evident that the \$800 refrigerator has a lower LCC than the \$600 refrigerator. It is also evident that as the price of electricity is increased, the LCC of the more expensive first cost refrigerator becomes more and more attractive. Federal law requires that certain appliances, including refrigerators, have labels that disclose the energy consumption. It is not necessarily the case that the more expensive units use less electricity. One should check the labels carefully when contemplating a purchase.

Example 5.2. Compare the life cycle cost of a highway construction warning sign that is PV powered vs. using a gasoline generator to power the same sign. The system is to be capable of 24-hour-per-day operation with minimal down time. Assume the load to be 2 kWh per day with a 20-year lifetime.

To power this load with a PV system, it will take a 500-watt array of PV modules at a cost of \$4 per watt, \$900 worth of storage batteries, which need to

be replaced every 5 years, and a \$300 charge controller. Assume a system maintenance cost of \$100 per year.

Although the average power requirement is only 83 watts, it is unlikely that an 83-watt generator will be used. For the purposes of this example, assume that a 500-watt gasoline generator can be purchased for \$250. Since it is running well under rated load, a generous efficiency estimate is 2 kWh per gallon, and will thus use about 365 gallons of gasoline per year and will require frequent maintenance with an annual cost of about \$1500 for oil changes, tune-ups and engine rebuilds. Because of the heavy use, after 5 years the generator must be replaced. Assume an inflation rate of 3% and a discount rate of 10%.

Solution: For the PV system, P_r is needed for 5 years, 10 years and 15 years, using (5.3). For the generator, P_r is also needed for the generator replacement after 5 years, 10 years and 15 years. For the PV system, P_{a_1} , using (5.8) is needed for maintenance costs and P_a using (5.7) is needed for generator fuel and maintenance costs. For the given inflation and discount figures, $x = 0.9364$, $P_a = 11.50$ and $P_{a_1} = 10.77$. So Table 5.2 can now be completed.

Table 5.2 Comparison of LCCs for PV system and generator system for highway sign.

PV System			Generator System			
Component	Initial Cost	PW	Component	Initial Cost	Ann Cost	PW
Array	\$2,000	\$2,000	Generator	\$250		\$250
Controller	\$300	\$300				
Batteries	\$900	\$900	Fuel		\$550	\$6,326
Batt 5 yr	\$900	\$648	Gen 5 yr	\$250		\$180
Batt 10 yr	\$900	\$466	Gen 10 yr	\$250		\$130
Batt 15 yr	\$900	\$336	Gen 15 yr	\$250		\$93
Annual Maintenance	\$100	\$1,077	Annual Maintenance		\$1,500	\$17,250
LCC		\$5,727	LCC			\$24,229

Hence, even though the initial cost of the PV system is significantly higher, its LCC is significantly lower. Could this possibly explain the rapid deployment of these signs?

5.2.4 Annualized Life Cycle Cost

It is sometimes useful to compare the LCC of a system on an annualized basis. Dividing the system LCC by the expected lifetime of the system may appear to be the way to arrive at an annual cost. This, of course, would assume the cost per year to be the same for every year of operation of the system, which is assumed not to be the case in the original set of assumptions. Hence, to find the annualized LCC (ALCC) in present day dollars, it is necessary to divide the LCC by the value of P_a or P_{a_1} used in the PW analyses for the system components.

For the refrigerators in Example 5.1, this means dividing the LCC by 7.573 for each LCC evaluated. For the PV system of Example 5.2, the ALCC =

$\$5727 \div 10.77 = \532 , and for the gasoline generator system of Example 5.2, the ALCC = $\$24,229 \div 11.5 = \$2,107$.

5.2.5 Unit Electrical Cost

One especially valuable use of the ALCC is to determine the unit cost of electricity produced by an electrical generating system. Obviously if the electricity is to be sold, it is necessary to know the price for which it should be sold to either earn a profit or to at least know how much will be lost in the process. Once the ALCC is known, the unit electrical cost is simply the ALCC divided by the annual electrical production. If the annual electrical production is measured in kWh, then the unit electrical cost will be measured in \$/ kWh.

For the PV system of Example 5.2, the unit electrical cost is $\text{ALCC/kWh} = \$532 \div 730 = \$0.729/\text{kWh}$. For the gasoline generator system, the unit electrical cost is $\$2107 \div 730 = \$2.89/\text{kWh}$. Clearly, both of these costs far exceed the cost of utility-generated electricity, but since this is a portable application, where the sign is moved around from day to day, the cost of hooking up and disconnecting the system from utility power is impractical, at best.

5.3 Borrowing Money

5.3.1 Introduction

Sometimes the desire to own something causes the potential owner to realize that money does not grow on trees. While some money comes from paychecks, usually larger sums of money come from borrowing from banks or other lending institutions. The question at this point for the engineer-turned-economist is whether borrowed money is any different from paycheck money or money from a savings account, a mattress or other form of liquid asset. For example, if the money to purchase one of the refrigerators of Example 5.1 had to be borrowed rather than taken from a wallet, would that affect the LCC of the refrigerator?

Once again, tables are readily available for looking up the annual payments on a loan of C_0 dollars taken out at $100i\%$ annual interest over a period of n years. For that matter, it is possible to purchase a calculator that will automatically yield the answer when it has been given the terms of the loan. An engineer, of course, will want to know how the numbers are obtained.

5.3.2 Determination of Annual Payments on Borrowed Money

To satisfy this curiosity, consider Table 5.3, representing the principal, interest, total payments and principal balance at the end of the k^{th} year for repayment of an n -year loan at $100i\%$ annual interest, where C_0 represents the amount borrowed. Note that during any of the years, it is not yet known how much will be paid on the principal in order to repay all of the principal in n years. The chal-

lenge is to arrive at an appropriate formula for equal total annual payments over the period of the loan.

Table 5.3 Breakdown of portions of loan payment allocated to principal and interest.

Yr	Pmnt on Prin	Interest Payment	Total Payment	Balance of Principal
1	A_1	iC_o	$A_1 + iC_o$	$C_o - A_1$
2	A_2	$i(C_o - A_1)$	$A_2 + i(C_o - A_1)$	$C_o - A_1 - A_2$
3	A_3	$i(C_o - A_1 - A_2)$	$A_3 + i(C_o - A_1 - A_2)$	$C_o - A_1 - A_2 - A_3$
n	A_n	$i(C_o - \dots - A_{n-1})$	$A_n + i(C_o - \dots - A_{n-1})$	0

In Table 5.3, A_k represents the amount paid on the principal after the k^{th} year. To pay the principal fully in n years requires that the sum of the annual payments on principal must add up to the loan amount, C_o .

Setting the total payments of each year to be equal, yields a solution for A_1 . For example,

$$A_1 + iC_o = A_2 + iC_o - iA_1,$$

which yields

$$A_2 = A_1(1+i).$$

In general,

$$A_n = A_{n-1}(1+i) = A_1(1+i)^{n-1}.$$

Next, letting $x = (1 + i)$ and summing all the payments toward principal, yields the amount borrowed.

$$A_1 + A_1x + A_1x^2 + \dots + A_1x^{n-1} = A_1(1 + x + \dots + x^{n-1}) = C_o.$$

But (5.5a) and (5.7) have shown that

$$1 + x + x^2 + \dots + x^{n-1} = \frac{1 - x^n}{1 - x},$$

which yields

$$A_1 = \frac{C_o(1-x)}{(1-x^n)}. \quad (5.9)$$

Now all that remains is to add the interest payment for the first year to the principal payment, given by (5.9), to get the total payment for the first year, which will be equal to the total payment for each succeeding year. Proceeding yields

$$\text{ANN PMT} = \frac{C_o(1-x)}{(1-x^n)} + C_o i = C_o \left(\frac{i}{(1+i)^n - 1} + i \right).$$

Simplifying this result yields, finally,

$$\text{ANN PMT} = C_o i \left(\frac{(1+i)^n}{(1+i)^n - 1} \right). \quad (5.10)$$

Usually payments are made monthly rather than annually. In this case, one need only note that rather than n payments, there will be $12n$ payments, and the monthly interest rate will simply be the annual rate divided by 12. Doing so converts (5.10) into an equation for monthly payments. Obviously, if one wants to split hairs even more finely, (5.10) could be modified for weekly, daily or hourly payments. Equation (5.10) is also an equation that might be conveniently tabulated for various values of i and n , but again it is left to the reader to use either a computer or a programmable calculator to generate the numbers that apply to the problem at hand.

5.3.3 The Effect of Borrowing on Life Cycle Cost

Depending on the nature of a purchase, it is interesting to compare whether the cost of borrowing money will render the purchase undesirable. For example, if money is borrowed to purchase something that will provide a return on the investment, it may make economic sense to borrow the money. This is the standard criterion for commercial loans. The better the return, the better the reason to borrow the money. But what if it is necessary to borrow the money for the initial cost of a system that does not have an obvious return on investment? Does it make sense to borrow for something having a greater first cost if it results in higher loan repayment costs? Although there are several ways to evaluate the worthiness of a purchase, once again, people sometimes borrow money to purchase things that do not have a measurable monetary return on investment, such as automobiles, simply because they want them.

As a simple example, suppose it is possible to spend \$2000 on a maintenance-free system that will last for 25 years and will reduce an electric bill by a certain amount per year. The exact system might be insulation, good windows, a solar water heater, or any number of energy efficiency measures. Suppose also that money is borrowed to purchase the system and the period of the loan is 25 years. This would be the case if the system is purchased for a dwelling at the time of construction and the item is included in the 25-year mortgage. If the mortgage rate is 9%, then (5.10) shows the additional annual mortgage payments would be \$203.61. If the annual savings on the electric bill exceed \$203.61, then it is worth borrowing the money.

One should note, however, that the additional \$203.61 mortgage payment will be constant over the life of the loan. In an inflationary environment, this means that even though the electric bill savings may not be \$203.61 the first year, after a certain number of years, the annual savings may well exceed \$203.61, making the investment worth considering.

What if the money is not borrowed? What if the \$2000 is at hand and available for investing? What would be the return on investment if it is spent on one of the items of the previous example? The simple answer would say the return is equal to the resulting savings less the resulting operating or maintenance costs. This works fine for the first year, but for successive years to yield a more precise estimate, the time value of money must be taken into account. Assuming the value of the quantity saved increases at the inflation rate, i , and the discount rate is d , the present worth of the savings accrued over n years will be given by (5.5). As a result, the PW of the annual savings over n years is given by (5.7). Hence, (5.7) can be applicable in either an expenditure mode or in a savings mode. By converting costs and savings to LCC, it is easy to compare savings with costs to determine whether to make the purchase.

Assuming that a system must be acquired to do something, and assuming that the system with the least LCC has been identified, it is simply a matter of deciding whether to borrow money or to use money on hand, if, indeed, the money is on hand. If the money is not on hand, then the only option is to borrow. If the money is on hand, then the criteria is whether the lending rate is less than or more than the discount rate. If money can be borrowed at a rate less than what it can earn, then it makes sense to borrow for the acquisition and to invest the money that might have been used for the purchase. This is a choice often made by the buyer of a new automobile. Should the savings account be used or should the money be borrowed? The answer depends on the relative interest on savings vs. the interest on the loan.

5.4 Externalities

5.4.1 Introduction

What happens if something owned and operated by one entity causes damage to something owned by another entity? A quick response would be that the entity causing the damage would be liable, and that the cost of repair of the damaged property should be the responsibility of the entity doing the damage. The problem is complicated in many instances, however, when more than one entity is responsible for creating the cause of the damage, and when more than one entity suffers damage as a result of the cause. And it gets even more murky when debate ensues over whether the alleged cause is really the cause. Classic examples of such situations are the link between smoking and cancer and the link between burning of fossil fuels, acid rain and global warming.

Much debate has taken place regarding the liability of tobacco companies for alleged firsthand, smoke-induced cancer and even regarding the alleged inci-

dence of secondhand, smoke-induced cancer. Until recent large judgments against the tobacco industry, the cost of producing cigarettes did not include a component to underwrite the cost of paying the judgments. Yet, it has been argued that tobacco is the cause of billions of dollars in medical bills, none of which have been paid out of tobacco revenues. Thus, in the past, the medical bills incurred by those exposed to tobacco smoke have been treated as externalities by the tobacco industry, while in the present, these bills have become direct cost components of doing business.

There is now reasonable agreement that one cause of acid rain is the burning of fuel that contains sulfur, such as petroleum or coal. As a result, many power plants are now equipped with elaborate scrubbers that remove sulfur and other pollutants from smokestack emissions.

Although a price per pound has not been established for sulfur emissions, the Environmental Protection Agency has established limits on the amounts of various pollutants that may be contained in smokestack emissions. Limits also exist for regions, so that if a region has met its limit, then no further burning may take place unless one of the burners can be made cleaner. In some cases, when a company has not reached its emission limit, the company will sell or trade the remaining allowed emissions with another burner. As a result, monetary value is evolving for certain emissions, albeit in a bit of a roundabout way. The monetary value, however, does not relate directly to the damage done in either the form of acid rain damage or the cost of respiratory diseases. The cost of scrubbers, however, appears as a system cost during the LCC process.

Another factor that needs consideration in establishing cost is the effect of various forms of subsidies. Some subsidies may enter the picture as direct costs, while others may appear as externalities.

5.4.2 Subsidies

When performing an LCC, sometimes the cost of a component, a fuel or the operation of a system may be affected by a subsidy or subsidies. For example, the cost of military presence in a region to ensure the steady flow of a fuel from the region is never included in the selling price of the product. Mineral depletion allowances, however, can be factored into the selling price of a product. In other cases, governments have been known to offer price supports in order to ensure competitive prices in a world market. Tariffs, in effect, are a form of subsidy, since they ensure that domestic production will be sold at a profit, thus not competing directly with less costly products from outside a country.

Green pricing is a form of subsidy for the acquisition of clean energy sources. An example is when the customers of a utility express a willingness to pay extra every month to ensure that a part of their energy mix comes from renewable sources, such as photovoltaics.

Subsidies in the form of tax breaks tend to come and go on a year-by-year basis. For a few years during the 1970s, homeowners could deduct a fraction of

the cost of a domestic solar hot water system from their federal income tax. Some states initiated grant programs to encourage homeowners to install solar systems and some utilities established rebate programs for part of the cost of installing various energy conservation measures, such as more efficient air conditioning or attic insulation. Recently, several states have created buy-down programs in which rebates are offered toward the installation of PV systems.

The argument is often set forth that all competing interests must compete on a **level playing field**. The meaning is simply that with so many subsidies, some of which are obvious and others of which are hidden, it is difficult for two competing interests to engage in fair competition. This is true in many industries and particularly in the energy industry.

The reader is thus reminded that no economic analysis or comparison is complete until all forms of subsidy have been considered.

5.4.3 Externalities and Photovoltaics

The cost of an electrical generation source often excludes externalities. Subsequently, if a source is cleaner from an environmental viewpoint but has a higher LCC based on parameters considered, that source may not be chosen. A proper treatment of externalities includes not only the operating externalities, but the externalities associated with the construction and salvage or decommissioning of the facility. In both categories, photovoltaics show significant advantages over nonrenewable sources, as will be shown in Chapter 9.

Problems

- 5.1 Obtain the data for Consumer Price Index, Dow Jones industrial average and prime lending rate from references 1-3. Plot the data and attempt to fit curves to the data to show trends. For example, use Excel graphs with trendlines, equations and R^2 values added to show the “goodness of fit.” Compare the R^2 values for linear, exponential and polynomial fits to your curves.
- 5.2 Determine the present electricity cost for which the \$600 refrigerator of Example 5.1 will have the same LCC as the \$800 unit, assuming all other parameters to be the same.
- 5.3 Next time you are in an appliance store, record the first cost and annual operating costs of several refrigerators that are comparable. Then, making reasonable assumptions about discount rates, inflation rates and appliance lifetimes, compare the LCCs of the units. You might want to ask a sales-

person for information on expected lifetime and repair costs of the units, including annual maintenance contracts.

- 5.4 Use (5.10) to compare 12 equal monthly payments to one annual payment by modifying the equation to account for monthly interest rate vs. annual rate and monthly payments vs. annual payments. How does the sum of 12 monthly payments compare with a single annual payment?
- 5.5 Rework Example 5.2 for a system that uses 4 kWh per day. This will require double the PV array and double the batteries, as well as double the fuel. However, the cost of the generator will remain the same and the cost of the maintenance will remain the same. You may also assume double the cost of the charge controller.
- 5.6 Calculate a set of reasonable conditions on interest rate, term of loan and cost per installed kW, for a PV system that generates power for an average of 5 peak sun hours per day so the annual loan repayment can be recovered if the value of the electricity generated is \$0.10/kWh.
- 5.7 The value of electricity during utility peaking hours is \$0.20/kWh and the money for a utility interactive system with a 30-year expected lifetime can be borrowed at an interest rate of 7%. Calculate the installed cost per kW for the system that will result in annual loan payments equal to the value of electricity produced by the system if the electricity is produced during utility peak hours.

References

- [1] <ftp://ftp.bls.gov/pub/special.requests/cpi/cpiai.txt> for Consumer Price Index data.
- [2] <http://djindexes.com> for Dow Jones industrial average data.
- [3] <ftp://ftp.ny.frb.org/prime/Prime.txt> for prime lending rate data.

Suggested Reading

- 42 U. S. C. §7401 et. seq. (Clean Air Act).
Markvart, T., Ed., *Solar Electricity*, John Wiley & Sons, Chichester, U.K., 1994.
'National Appliance Energy Conservation Act of 1987' (PL 100-424, March 17, 1987, 101 §103).
Stand-Alone Photovoltaic Systems: A Handbook of Recommended Design Practices, Sandia National Laboratories, Albuquerque, NM, 1995.

Chapter 6

MECHANICAL CONSIDERATIONS

6.1 Introduction

Because the primary function of a photovoltaic system is to convert sunlight to electricity, often the role and importance of the mechanical aspects of the system are ignored. Most photovoltaic modules are designed to last 20 years or longer. It is important that the other components in the system, including mechanical components, have lifetimes equivalent to those for the PV modules. It is also important that the mechanical design requirements of the system be consistent with the performance requirements as well as with the operational requirements of the system.

The mechanical design of photovoltaic systems cuts across a variety of disciplines, most notably civil and mechanical engineering and, to a lesser extent, materials science, aeronautical engineering and architecture. More specifically, mechanical design involves:

- Determining the *mechanical forces* acting on the system.
- Selecting, sizing and configuring *structural members to support these forces* with an adequate margin of safety.
- Selecting and configuring *materials that will not degrade or deteriorate unacceptably over the life of the system*.
- Locating, orienting and mounting the photovoltaic array so that it has *adequate access to the sun's radiation*, produces the *required electrical output* and operates over *acceptable PV cell temperature ranges*.
- Designing an array support structure that is *aesthetically appropriate* for the site and application and provides for *ease of installation and maintenance*.

Each of these elements of the mechanical system will be discussed in more detail throughout this chapter.

6.2 Important Properties of Materials

6.2.1 Introduction

Before discussing the mechanical design process, it is useful to review the properties of materials, especially the non-photovoltaic materials that are important components of photovoltaic systems. A fairly comprehensive list of performance properties of materials in response to various stimuli is presented in Table 6.1. However, for simplicity, the properties of materials can be grouped into four general categories: electrical properties, mechanical properties, chemical properties and thermal properties [2].

Electrical properties of semiconductor materials were introduced in Chapter 3 and are discussed in more detail in Chapters 10 and 11.

The mechanical properties most important to photovoltaic systems are those associated with the strength of the structural members, including photovoltaic modules, in response to static and dynamic forces.

Table 6.1 Properties of materials [1].

Physical Properties:	Mechanical Properties:	Thermal Properties (cont.):
Crystal structure	Hardness	Specific heat Coefficient of expansion
Density	Modulus of elasticity in tension; in compression	
Melting point	Poisson's ratio	Emissivity Absorptivity
Vapor pressure	Stress-strain curve	
Viscosity	Yield strength	Ablation rate Fire resistance
Porosity	Tension	
Permeability	Compression	
Reflectivity	Shear	Corrosion and degradation in atmosphere, salt water, acids, hot gases, ultraviolet
Optical properties	Ultimate strength in tension; in shear; in bending	Position in electromotive series
Dimensional stability	Fatigue properties: smooth; notched; corrosion fatigue; rolling contact; fretting	Thermal stability Oxidation
	Charpy transition temperature	
Electrical Properties:	Fracture toughness	Biological stability
Conductivity	High-temperature creep; stress rupture	Hydrogen embrittlement
Dielectric constant	Damping properties	Hydraulic permeability
Coercive force	Wear properties: galling, abrasion, erosion	Fabrication Properties:
Hysteresis	Cavitation	
	Spalling	
Nuclear Properties:	Ballistic impact	Castability
Half life	Thermal Properties:	Heat treatability
Cross section		Hardenability
Stability	Conductivity	Formability
		Machinability
		Weldability

(From Dieter, *Engineering Design: A Materials and Processing Approach*, 2nd Ed., 1991, McGraw-Hill. Reproduced with permission of the McGraw-Hill Companies.)

The most important chemical properties are those related to material degradation and deterioration due to corrosion and exposure to ultraviolet radiation. Also of interest are the rates of chemical degradation and the associated reduc-

tion in lifetimes of various materials, such as those used for weather sealing and insulation, that are caused by repeated exposure to high operating temperatures.

The thermal properties of most concern involve thermal expansion and contraction and the resulting thermal stresses.

6.2.2 Mechanical Properties

The photovoltaic system, in particular the photovoltaic array and its structural support members, is subjected to a variety of mechanical forces -- both static and dynamic. These forces produce internal stresses and deformations. For common structural materials like steel and aluminum, there are limits to these stresses and deformations that, if exceeded, may result in failure or irreparable damage.

Stress is defined as force per unit area. Uniform normal stress occurs when a force P is normal to and distributed uniformly over a cross sectional area A . It can be calculated using the simple equation:

$$S = \frac{\text{force}}{\text{area}} = \frac{P}{A} \quad (6.1)$$

Why is the concept of stress important for the mechanical design of photovoltaic systems? Because it is the ability of a structural member to withstand stresses (i.e., forces per unit area) that determines its strength. It is the engineer's responsibility to first calculate or estimate the forces acting on the photovoltaic system and then to select and size the structural support members such that the maximum stresses experienced are well below allowable limits.

The most common static forces acting on photovoltaic arrays and supporting structures are due to the weight of the modules, mounting system and, in colder climates, snow and ice. These forces produce a combination of uniform normal, shear and bending stresses that must not be overlooked in assessing the structural integrity of the array and all of its supporting hardware. Heavy accumulations of snow and ice can produce high stress levels. However, in the overwhelming majority of cases, these types of static forces are not large enough to exceed the stress limits of the array structure.

In addition to static forces, the photovoltaic array and its support structure will experience dynamic forces, most notably wind loads. Changes in wind direction and wind speed, including the rapid changes associated with gusting, complicate the job of the structural engineer. First, the changes in wind direction often result in a structural member experiencing alternating periods of tension and compression. Consequently, the structural members must be designed not only to withstand uniform tensile stress, but also not to buckle under compression. Second, the dynamic loads may give rise to a phenomenon known as **fatigue failure**. This occurs when the stresses in a structural member alternate between tension and compression over time and can occur at stress levels considerably below those that would produce a static stress failure. Fatigue first manifests itself as cracks on the surface of the structural member, often near a

bend, angle or other location where the stress may be concentrated. Following the initiation of these surface cracks, the fracture spreads inward over the cross section of the member until the load carrying area of the member is reduced sufficiently to cause failure [2].

Figure 6.1 illustrates qualitatively the relationship between the **fatigue stress limits**, S_{max} , and the number of stress cycles experienced, N , for both ferrous (i.e., containing iron) and aluminum alloys. Note that ferrous materials, such as the steel alloys, have a well-defined **fatigue (or endurance) limit**. As long as the oscillating stresses experienced are below that limit, the number of cycles can increase indefinitely. A general rule of thumb for ferrous materials is that the fatigue limit is approximately half the tensile strength. This limit is also referred to as the **reverse fatigue limit** [2].

Fatigue is a bigger problem for aluminum and its alloys than for steel. No well-defined fatigue limit exists for aluminum. Because of this, the fatigue limit for an aluminum alloy is arbitrarily defined as a stress level for which the material can withstand a very large number of cycles (e.g., a million alternating tension and compression stress cycles).

What does this mean for the photovoltaic system design engineer? Obviously, problems with fatigue vary with geography. For areas prone to high, gusty winds, fatigue must be factored into the design. For coastal areas susceptible to hurricanes, buildings and other structures must meet stringent requirements resulting in more robust designs and higher strengths. Consequently, the stresses carried by these hurricane-tolerant buildings and structures typically will be well below the fatigue limits for the materials used.

In addition to stress, another important concept in discussing the strength of materials is **strain**, ϵ . Whereas stress is a measure of force intensity (i.e., force per unit area), strain is a measure of deformation per unit of length and can be

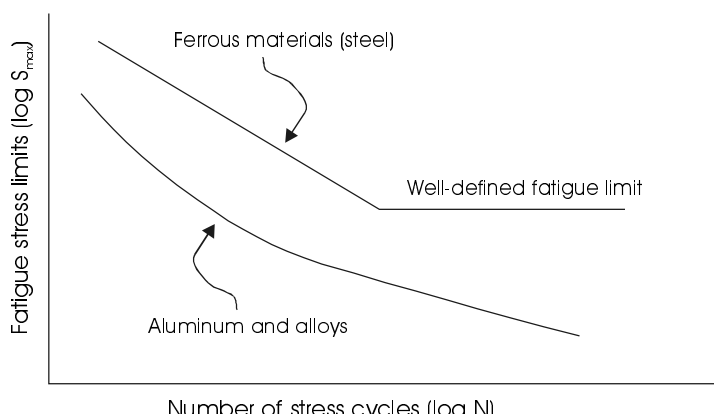


Figure 6.1 Fatigue stress vs. cycles showing a well-defined fatigue limit for ferrous metals [2].

(Figure from *Materials Engineering Science: An Introduction* by Richard W. Hanks, copyright © 1970, by Harcourt, Inc., adapted by permission of the publisher.)

defined by the equation:

$$\epsilon = \frac{\text{elongation}}{\text{length}} = \frac{\delta}{L} \quad (6.2)$$

where δ = elongation and L = length. The cause-and-effect relationship between stress and strain should be intuitive to many. The intensity of the force, i.e., stress, causes the structural member to deform, i.e., strain. However, engineers need a more useful and quantitative relationship between stress and strain.

6.2.3 Stress and Strain

Figure 6.2 shows a bar of length L and cross sectional area A . Force P acts uniformly over the cross sectional area, putting the bar in tension. The experiment is simple: gradually increase the force P from small to larger values until the bar ruptures. During the experiment, the force and the elongation will be measured continuously. Remembering that stress is simply force per unit area and strain is elongation per unit length, stress can be plotted versus strain. The resulting graph from this experiment for a typical material such as steel is shown in Figure 6.3, which should be familiar to anyone who may have studied strength of materials.

Note that the stress and resulting strain are directly proportional to each other up to a limit, appropriately named the **proportional limit**. If the force P is increased to produce stresses above the proportional limit, the stress-strain relationship is no longer linear. However, the bar may still be elastic to a slightly higher stress called the **elastic limit**. If the force P is removed at any point up to and including the elastic limit, the bar will return to its original dimensions. If the bar is stressed beyond the elastic limit, permanent deformation occurs. In addition to the elastic limit, the **yield point** is defined as the point on the stress-strain curve corresponding to a specified permanent deformation (usually when the elongation per unit length equals 0.002). The yield point is used because it is easier to determine than the elastic limit for some materials. The stress corresponding to the yield point is defined as the **yield strength**.

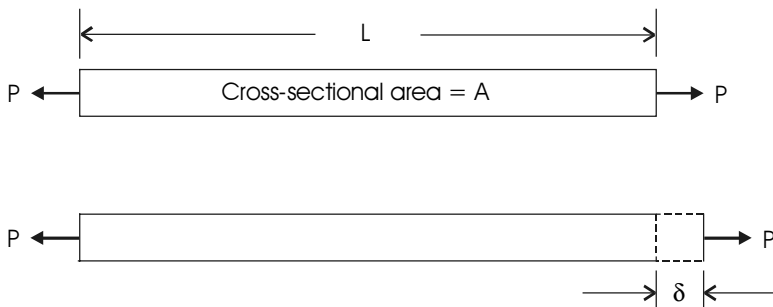


Figure 6.2 Simple pull test of a bar showing the resulting elongation.

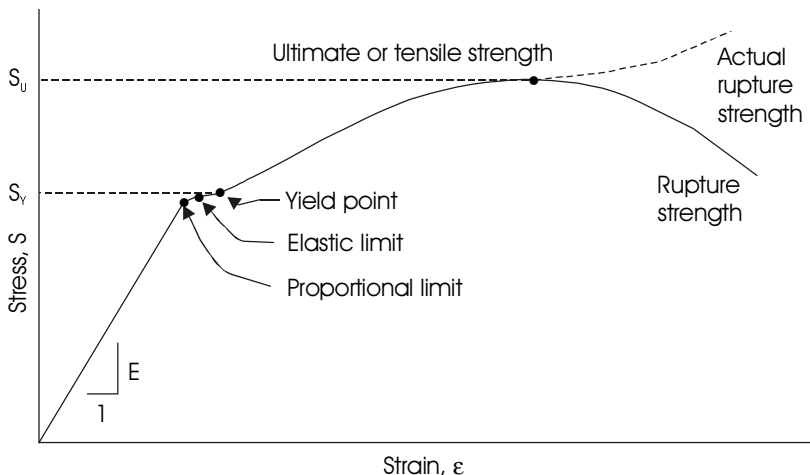


Figure 6.3 Stress-strain curve for steel.

Other key locations on the stress-strain curve include the maximum stress point on the graph, called the **ultimate tensile strength**, or, simply, the **tensile strength**, and two **rupture strengths**. The lower value for rupture strength results from using the original cross-sectional area A , while the higher value at the end of the dashed curve results from using the reduced area measured after rupture. Note that as material is stretched, its cross-sectional area decreases, resulting in higher stress for the same applied force.

In addition to the proportional limit, elastic limit, yield strength, ultimate strength and rupture strength, another important parameter obtained from the stress-strain curve is the slope of the straight-line portion of the graph from the origin to the proportional limit. This slope is defined as the **modulus of elasticity** (also known as **Young's modulus**) and is usually represented by the letter E . It represents the ratio of stress to strain in the linear portion of the graph, which is where most structural materials are designed to operate. In equation form, it can be expressed as:

$$E = \frac{\text{stress}}{\text{strain}} = \frac{S}{\varepsilon} \quad (6.3)$$

A better name for E would be modulus of stiffness. The higher the value of E , the less the material deforms for a given stress. For a spring, the spring constant is analogous to the modulus of elasticity. The higher the spring constant, the harder you have to pull it to stretch it a given amount (i.e., the stiffer it is). Equation 6.3 is known as **Hooke's law**. For most materials, the modulus of elasticity is the same for both tension and compression.

Referring to Figure 6.3 once again, the area under the stress-strain curve has special physical significance in that it is proportional to the total energy required to rupture the bar. This energy is referred to as the **toughness** of the material.

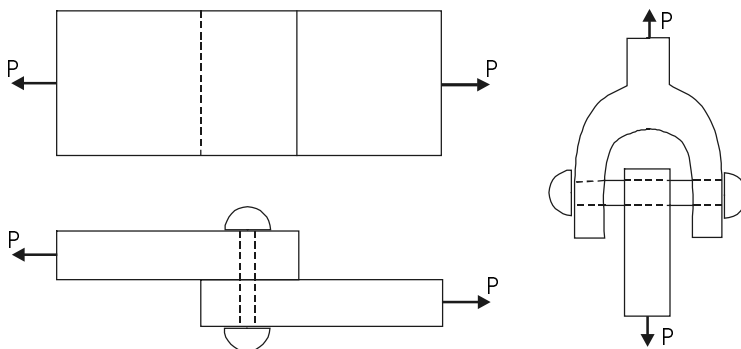


Figure 6.4 Two examples of shear loading.

For the simple case of one-dimensional, normal stress that has been discussed thus far, a useful formula for the elongation of the bar can be obtained by substituting for S (6.1) and for ϵ (6.2) into (6.3), yielding:

$$\delta = \frac{PL}{AE} . \quad (6.4)$$

This equation shows that the amount of elongation depends on the force applied, P , the dimensions of the bar (length L and area A) and the bar's material, as represented by its stiffness E .

The normal stresses considered up to this point were one-dimensional and were the result of normal forces acting uniformly over the cross-sectional area. In addition to normal forces, other forces act along or parallel to the area resisting the forces. These forces are called **shear forces**. Shear forces per unit area are called **shear, or tangential, stresses**. Figure 6.4 shows examples of structural members and fasteners subjected to forces that produce shear stresses.

In general, both normal and shear stresses are present in structural members. Like the modulus of elasticity for normal stresses, there is an analogous modulus of elasticity in shear, but it is more commonly referred to as the **modulus of rigidity** and is represented by G . Table 6.2 presents the modulus of elasticity, E , and the modulus of rigidity, G , for common structural materials.

Table 6.2 Moduli of elasticity and rigidity for structural materials [3].

Metal	E , psi	G , psi
Stainless steel, 18-8	27.6×10^6	10.6×10^6
All other steels	$(28.6\text{--}30.0) \times 10^6$	$(11.0\text{--}11.9) \times 10^6$
Cast iron	$(13.5\text{--}21.0) \times 10^6$	$(5.2\text{--}8.2) \times 10^6$
Aluminum alloys, various	$(9.9\text{--}10.3) \times 10^6$	$(3.7\text{--}3.9) \times 10^6$
Titanium (99.0 Ti), annealed bar	$(15\text{--}16) \times 10^6$	6.5×10^6

(From Avallone & Baumeister, Eds., *Marks' Standard Handbook for Mechanical Engineers*, 10th Ed., 1996, McGraw-Hill. Reproduced with permission of the McGraw-Hill Companies.)

The normal and shear stresses discussed up to this point are important and occur frequently in structural support members for photovoltaic systems. In computing these stresses, forces are assumed to be uniformly distributed over the cross-sectional areas resisting the forces. However, other forces may act on the structure and produce stresses that vary over the cross section. Examples include:

- Bending (or flexural) stresses. As an example, imagine a person standing on the end of a diving board. The top surface of the diving board would be in tension, the bottom in compression and the normal stresses along the mid-horizontal plane would be zero.
- Torsional shear stresses. Imagine the torque applied to a drive shaft of an automobile. The shear stresses across the section of the shaft vary from zero at the center to a maximum at the outer radius.
- Combined stresses consisting of axial loading, bending and torsion. All three of these types of loading may occur in various members of the photovoltaic array and support structure.

6.2.4 Strength of Materials

Referring again to Figure 6.3, the two most important values on the graph for most applications are the yield strength and the ultimate tensile strength. Although Figure 6.3 was representative of steel under tension, stress-strain curves for other materials and for different types of loading, such as compression and shear, are available [3, 4]. With access to these values, how does the engineer use them to make sure the structure is sufficiently strong?

The first thing the engineer has to decide upon is the allowable or working stress. This is the maximum safe stress that the material should carry. For photovoltaic systems, the allowable stress should be well below the yield strength and proportional limit. A common formula for computing the allowable stress is:

$$S_a = \frac{S_y}{N} \quad (6.5)$$

where S_a is the allowable stress, S_y is the yield strength in psi and N is a safety factor to compensate for any minor deviations of materials from the ideal.

For photovoltaic systems, N should be at least two to avoid accidental over-loading. In areas where fatigue may be a problem due to high, gusty winds, a higher value should be used. Also, when fatigue is a concern, the structural engineer will often choose steel over aluminum for the support structure.

As an example, suppose the structural designer wants to use an aluminum alloy with yield strength $S_y = 34,000$ psi. Using an appropriate factor of safety of $N = 2$, the allowable stress, S_a , would be $S_y/2$, or 17,000 psi. This assumes fatigue is not a concern.

Table 6.3 shows the ultimate tensile strength and yield strength for selected metals. Note that titanium is more than twice as strong as steel.

Table 6.3 Strength of common structural materials [3].

Metal	Ultimate Tensile Strength (psi)	Yield Strength (psi)
Cast iron	18,000-60,000	8,000-40,000
Wrought iron	45,000-55,000	25,000-35,000
Structural steel, ordinary	50,000-65,000	30,000-40,000
Stainless steel, 18-8	85,000-95,000	30,000-35,000
Aluminum, pure, rolled	13,000-24,000	5,000-21,000
Aluminum alloy, 17ST	56,000	34,000
Titanium 6-4 alloy, annealed	130,000	120,000

(From Avallone & Baumeister, Eds. Reproduced with permission of the McGraw-Hill Companies.)

6.2.5 Column Buckling

Often structural members used to support a photovoltaic array have one dimension, their length, which is much larger than the other dimensions. Such members or columns, if long enough and slender enough, can fail due to buckling under compressive loading. These compressive forces may be considerably smaller than those that would cause failure due to crushing. Although there is no firm rule, generally a long, slender structural member is considered to be a column if its length is more than ten times as large as its least lateral dimension. For a column made of a material with a modulus of elasticity, E, a minimum moment of inertia (of its cross-sectional area), I, and length, L, there exists a critical compressive force, P, that will cause the column to buckle. This critical load is calculated using the formula:

$$P = \frac{EI\pi^2}{L^2} \quad (6.6)$$

This equation is known as **Euler's formula** [5].

6.2.6 Thermal Expansion and Contraction

Changes in temperature cause materials to expand or contract. For example, the linear deformation of a structural member of length L can be represented by:

$$\delta_t = \alpha L \Delta T \quad (6.7)$$

where α is the coefficient of linear expansion and ΔT is the change in temperature with units consistent with the units of α .

If the deformation is allowed to occur freely, no stresses will be induced in the structure. But if this deformation is restricted or constrained, internal **thermal stresses** result. The general procedure for handling thermal stresses is as follows [5]:

- Assume the structure is relieved of all applied forces and constraints.
- Allow the temperature deformations to occur freely and calculate the expansion or contraction using (6.7).
- Show these deformations on a sketch.
- Determine the mechanical forces necessary to restore the structure to its constrained condition by solving (6.4).
- Show these forces and deformations on the same sketch used previously.
- Use the equations of static equilibrium, thermal deformation, force deformation and the definition of stress to compute all unknowns.

The computed stresses from using this procedure are the thermal stresses.

Example

Consider the case of a steel bolt in a bronze sleeve as shown in Figure 6.5. At 40°F, the sleeve fits snugly between the head of the bolt and the steel nut, but with no stress in any of the three parts. For the following dimensions and material properties, compute the thermal stresses in both the bolt and the sleeve when the temperature rises to 160°F:

D_1 = nominal diameter of bolt = inside diameter of sleeve = 1.00 in.

D_2 = outside diameter of sleeve = 1.50 in.

E_1 = modulus of elasticity for steel = 30×10^6 psi.

E_2 = modulus of elasticity for bronze = 10×10^6 psi.

α_1 = coefficient of thermal expansion for steel = 6.1×10^{-6} per °F.

α_2 = coefficient of thermal expansion for bronze = 10.1×10^{-6} per °F.

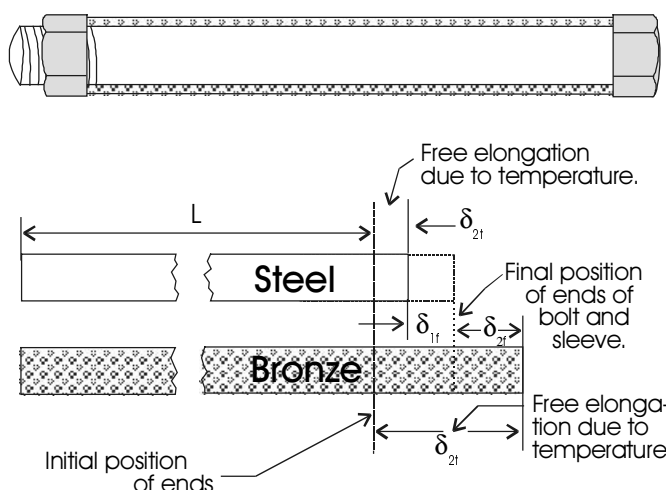


Figure 6.5 Elongations in steel and bronze due to a change in temperature.

To solve this problem, note first that the elongation of the bronze sleeve would be greater than that for the steel bolt if both were unconstrained. For any length L, these elongations could be calculated using equation (6.7). However, the bolt head and nut constrain the sleeve so that the elongations of both the sleeve and bolt must be equal. Hence, the sleeve is in compression and the bolt is in tension. Also, from the principle of action and reaction, the compressive force in the sleeve must be equal and opposite to the tensile force in the bolt.

From the sketch in Figure 6.5, the total elongations of the bolt and sleeve are, respectively:

$$\delta_1 = \delta_1(\text{thermal}) + \delta_1(\text{forces}) = \delta_{1t} + \delta_{1f} \quad (\text{steel bolt})$$

$$\delta_2 = \delta_2(\text{thermal}) - \delta_2(\text{forces}) = \delta_{2t} - \delta_{2f} \quad (\text{bronze sleeve})$$

Equating the forces, elongations and applying equations (6.4) and (6.7) yields:

$$(\alpha_1)(L)(T_2 - T_1) + PL/[(A_1)(E_1)] = (\alpha_2)(L)(T_2 - T_1) - PL/[(A_2)(E_2)]$$

The length, L, is a common term and cancels. Solving for the force, P, gives:

$$P = 3,330 \text{ lb.}$$

The normal stresses in the bolt are computed using equation (6.1) and are:

$$S_1 = 4,240 \text{ psi (tension)} \text{ and } S_2 = 3,390 \text{ psi (compression)}$$

6.2.7 Chemical Corrosion and Ultraviolet Degradation

A photovoltaic system structure that can initially withstand all anticipated mechanical and thermal stresses with an adequate margin of safety might not be a good engineering design. The engineer must also consider the environment in which the system operates and how its component materials interact with the environment and with each other. Failure of metal components by corrosion is as common as failure due to mechanical stresses.

To design for corrosion resistance, knowledge of the various forms of corrosion is necessary.

Uniform attack is the most common form of corrosion. Chemical or electrochemical reactions proceed uniformly over the entire surface area. The metal becomes thinner and thinner and eventually fails. On a tonnage basis, uniform attack is the greatest cause of metal destruction, especially steel. However, it is not particularly difficult to control through proper material selection and appropriate use of protective coatings.

Galvanic corrosion occurs because of the potential difference that exists between two dissimilar metals in contact with a corrosive or conducting solution. Of the two dissimilar metals, the less resistant, or anodic, metal is corroded relative to the more resistant, or cathodic, metal. Table 6.4 presents an abbrevi-

ated version of the galvanic series for commercially available metals and alloys. The relative position in the galvanic series depends on the electrolytic environment and on the metal's surface chemistry. To minimize galvanic corrosion, the design engineer should use similar metals or metals close to each other in the galvanic series.

Table 6.4 Galvanic series for metals and alloys [1].

Most Noble Metal (Cathodic)	
	Platinum
	Gold
	Titanium
	Silver
	316 Stainless steel
	304 Stainless steel
	410 Stainless steel
	Nickel
	Monel
	Cupronickel
	Cu-Sn bronze
	Copper
	Cast iron
	Steel
	Aluminum
	Zinc
Least Noble Metal (Anodic)	Magnesium

(Adapted from Dieter, G. E., *Engineering Design: A Materials and Processing Approach*, 2nd Ed., McGraw-Hill , 1991. Reproduced with permission of the McGraw-Hill Companies.)

The use of a small anodic metal in contact with a cathodic metal of larger surface area should be avoided. If two metals far apart in the galvanic series must be used in near contact with each other, they should be electrically insulated from each other. Coating the anodic material may not protect it, because coatings are susceptible to pinholes, causing the coated surface to corrode rapidly in contact with the large cathodic area. If a galvanic couple is unavoidable, a third metal that is sacrificial to both of the other metals may be used. Note that zinc is sacrificial to both aluminum and steel and, consequently, is often used to protect these two most common structural materials.

Crevice corrosion is an intense form that frequently occurs at design details such as holes, gasket surfaces, lap joints and crevices under bolts and rivet heads. Small quantities of stagnant liquid often form in these areas and allow this very destructive electrochemical process to occur. Unfortunately, stainless steel is especially susceptible to crevice corrosion.

Pitting is an extremely localized attack that produces holes in the metal. It is serious because it may lead to very premature failure of structural members. Pitting may require a relatively long initiation period but, once the process is started, it accelerates rapidly.

Intergranular corrosion is a localized attack along the grain boundaries of metals but not (or only slightly) over the grain faces. It is common in steel that has been heat treated at high temperatures or heat sensitized during welding. Intergranular corrosion due to welding is known as **weld decay**.

Selective leaching is the preferential removal of one or more of the alloying elements in a metal by the action of an electrolyte. The most common example of this phenomenon is the selective leaching of zinc from brass, leaving a spongy, weak matrix of copper – a process known as **dezincification**. Aluminum, iron, cobalt and chromium are also susceptible to leaching. Where and whenever selective leaching occurs, the process leaves the alloy in a weakened, porous condition.

Erosion corrosion occurs when corrosive fluid flows over a metal surface and causes the gradual wearing away of the surface. Usually the velocity of the fluid is high and mechanical wear and abrasion may be involved.

Stress corrosion cracking is caused by the combination of tensile stress and corrosion and leads to the cracking or embrittlement of a metal. The stress may result from applied forces or may be residual. Only specific combinations of alloys and the chemical environment produce stress corrosion cracking. Combinations include aluminum alloys and saltwater, some steel alloys and saltwater as well as mild steel and caustic soda. Preventing stress corrosion cracking involves selecting alloys that are not susceptible to cracking under expected operating conditions. If this is not possible, the structural members should be sized for low stress levels.

Dry corrosion involves reaction of the material directly with air. Virtually every metal and alloy reacts with the oxygen in air to form an oxide. This occurs in the absence of any liquid electrolyte and is an important form of corrosion in high temperature applications.

In addition to corrosion, ultraviolet radiation can cause degradation and deterioration of some of the exposed materials used in photovoltaic systems. These include weather-sealing materials, conduit for wiring, wire insulation, some coatings and caulking and other miscellaneous materials.

Ultraviolet radiation is that part of the electromagnetic spectrum having wavelengths between about 100 and 400 nm. The ultraviolet portion of the spectrum can be further subdivided into three regions: UV-A (315-400 nm), UV-B (280-315 nm) and UV-C (100-280 nm). UV-B and UV-C cause sunburn (erythema) and pigmentation (tanning). UV-B produces vitamin D₃. Long-term exposure to UV radiation results in loss of skin elasticity. Also, a link has been established between exposure to UV wavelengths below 320 nm and skin cancer. Because the human body is seriously affected by UV exposure, it should come as no surprise that other materials are also affected. In fact, ultraviolet radiation degrades both the optical properties and the physical properties of many materials. Consequently, the design engineer should ensure that all materials in the photovoltaic system that are exposed to sunlight are resistant to UV degradation.

6.2.8 Properties of Steel

Iron is the base element of all steels. Commercially pure iron contains only about 0.01% carbon and is relatively soft and weak. The addition of carbon significantly strengthens iron. For example, the addition of 0.80% carbon can raise the tensile strength from about 40,000 psi to 110,000 psi [6]. Steel is an alloy of iron and carbon and usually contains small amounts of manganese and other elements. There are more than 3,500 grades of steel, of which 75 percent have been developed over the last 20 years. The many different grades of steel have many different properties: physical, chemical and environmental. **Carbon steel** is steel that owes its distinctive properties to the carbon it contains. **Alloy steel** is steel that owes its distinctive properties to one or more elements other than carbon, or to the combination of these elements with carbon.

For any material, steel or otherwise, it is easy to measure its chemical composition and to determine its stress-strain curve using a pull test. The latter provides the yield strength, tensile strength, elongation and reduction in area. However, the photovoltaic engineer must not forget to consider costs, corrosion resistance and the possibility of structural fatigue as well.

Low-carbon steel is often used in the support structures for photovoltaic systems. Of the many low-carbon steel products, sheet and strip steels are becoming increasingly important and presently account for approximately 60% of the total steel production in the U.S. [3]. The relatively low cost of these steel products gives them a major advantage over more expensive aluminum, provided they can be protected adequately from corrosion.

Many different methods are used to protect steel from corrosion. In general, these protection or reduction methods include proper selection of materials, design, coatings, inhibitors, anodic protection and cathodic protection [3]. One method of protecting steel structural members is hot-dip galvanizing. Hot-dip galvanizing is a process in which thoroughly cleaned steel or iron is immersed in molten zinc and withdrawn to provide a smooth, even coating that typically has a crystalline appearance. It is by far the most widely used method for protecting steel against corrosion [6].

Zinc is a less noble metal than steel (see Table 6.4) and is sacrificed to protect the steel as part of the corrosion process. How long the zinc protects the steel depends on the thickness of the zinc coating and the environment to which the structural member is exposed. The average minimum weight of zinc coating is 1.5 ounces per square foot of surface area when hot-dip galvanized according to the specifications of ASTM A123. For highly acidic industrial atmospheres, a 1.5 ounce per square foot coating may last less than 15 years. For a rural, clean atmosphere, the same coating may last 40 years.

The largest use of zinc is for protectively coating steel. Lead is sometimes added to the zinc to produce a surface pattern called *spangle*, which is often used on unpainted surfaces. The addition of aluminum to zinc improves its corrosion protection ability. *Galfan*, which contains 5 percent aluminum and 95 percent zinc, and *Galvalume*, which contains 55 percent aluminum and 45 per-

cent zinc, are examples of zinc-aluminum coatings that effectively protect steel from corrosion [3].

Paints, lacquers, coal-tar or asphalt enamels, waxes and varnishes are all used as organic coatings for corrosion protection. However, all paints are permeable to water and oxygen to some degree. They are also subject to mechanical damage and eventually break down.

6.2.9 Properties of Aluminum

Aluminum is the second most commonly used structural material next to steel. Some of the properties of aluminum that make it attractive for use in photovoltaic systems follow:

- It is very lightweight, with a density about one-third that of steel.
- It can be fabricated into many different shapes using a variety of different methods.
- It has a wide range of properties and is available at many different tensile strengths, depending on how it is alloyed.
- It has a high strength-to-weight ratio, thus making it attractive for many applications.
- It has good corrosion resistance and can be used in a wide variety of climates and weather conditions.
- It is available in a wide variety of finishes making it attractive as an architectural metal.

Aluminum is one of the most fascinating of all the elements. It is very chemically active, with a strong affinity for oxygen. In powdered form, it is used as a fuel for solid rocket motors. How can it be that such a chemically active material is so commonly used in an unprotected form?

What makes aluminum unique is its special relationship with oxygen, which destroys other reactive metals such as sodium and seriously attacks less reactive metals such as iron. In the laboratory, most chemistry students have witnessed the spectacular reaction between sodium and the oxygen in water, in which the sodium is left unrecognizable and even more unusable. And everybody frequently encounters rusting steel. Neither of these phenomena occurs with aluminum. Rather, as soon as aluminum is produced, its surface reacts with the oxygen in the air and forms a very thin oxide layer over the entire surface. This oxide layer is hard, tenacious and not only protects the aluminum from attack by other chemicals, but also protects it from further oxidation. Because the oxide layer is transparent, it does not detract from the metal's appearance. Aluminum oxide must be removed from aluminum wire before connections are made.

Pure aluminum is relatively weak and only about one third as stiff as steel. However, aluminum can be strengthened significantly by alloying. The most common alloying additions to aluminum are copper, manganese, silicon, magnesium and zinc.

Aluminum and its alloys are divided into two major classes: wrought and cast. The wrought class is broad because aluminum can be formed by virtually every known fabrication process, including sheet and plate, foil, extrusions, bar and rod, wire, forgings and impacts, drawn or extruded tubing and others. Cast alloys are poured molten into sand (sand casting) or into high-strength steel molds (i.e., permanent molds or die casting) and allowed to solidify into the desired shape. For photovoltaic systems, wrought aluminum is more commonly used than cast aluminum. The Aluminum Association has a designation system for wrought aluminum alloys that categorizes them by major alloying additions. Table 6.5 shows the various designations.

The first digit in the series classifies the alloy by alloy series, or principal alloying element. The second digit, if different from 0, denotes modification of the basic alloy. The third and fourth digits together identify the specific alloy within the series.

Alloys in the 6xxx alloy series, which use magnesium and silicon as alloying elements, possess a combination of properties including corrosion resistance, that make them well suited for structures and architectural applications. They are also commonly used for marine applications, truck frames and bodies, bridge decks, automotive structures and furniture. From the 6xxx series, 6061 and 6063 aluminum alloys are often used as structural members for photovoltaic arrays. 6061 aluminum contains 1.0% magnesium and 0.6% silicon. For the same tempering during fabrication, 6061 aluminum alloy has higher tensile strength than 6063 aluminum, which contains 0.7% magnesium and 0.4% silicon [4]. However, 6063 aluminum has better resistance to corrosion.

Table 6.5 Designation system for wrought aluminum alloys [4].

Alloy Series	Description or Major Alloying Element
1xxx	99.00 % minimum aluminum
2xxx	Copper
3xxx	Manganese
4xxx	Silicon
5xxx	Magnesium
6xxx	Magnesium and silicon
7xxx	Zinc
8xxx	Other element
9xxx	Unused series

(From Kutz, M., *Mechanical Engineers' Handbook*, 2nd Ed, John Wiley & Sons, 1998.
Adapted by permission of John Wiley & Sons, Inc.)

6.3 Establishing Mechanical System Requirements

6.3.1 Mechanical System Design Process

Mechanical system design is the *process of selecting, sizing and configuring* a variety of structural and other components to meet predetermined design requirements. For most photovoltaic system designs, these components are usually available ‘off the shelf,’ although in some cases completely new compo-

nents may need to be developed. The challenge is to bring together *components* of the appropriate materials, geometric shapes and sizes to produce a *system* that best meets the design objectives.

The design requirements for the mechanical system consist of the following:

- Functional requirements
- Operational requirements
- Constraints
- Tradeoffs.

Developing specifications for each of the above four categories is not unique to photovoltaic system design. It is commonly used in the design of systems in general, including aircraft, satellites and other products of modern society [7]. Determining the information to include in each of the four categories is an important responsibility assumed by the systems engineer at an early stage in the design process.

6.3.2 Functional Requirements

What are the primary functions of the mechanical parts of the photovoltaic system? First and foremost, the mechanical system must be capable of carrying all expected mechanical forces with an adequate margin of safety. In fact, the most important requirement for both the mechanical and electrical design of the photovoltaic system is the safety of individuals and the protection of structures and other property that could be damaged as the result of mechanical failure. The functional requirement related to structural considerations might take several forms, such as the *specification of factors of safety, or maximum allowable stresses, or limits on deformation*. This specification will affect the materials selected, as well as the geometry and size of the structural members.

For most designs, the photovoltaic array and support structure must withstand all forces and associated stresses to which they are subjected for 20 to 30 years or longer. Often they must do so in harsh weather and chemical environments. These environments cause many materials to degrade, deteriorate and eventually fail. Consequently, the *specification of the lifetimes of the structural members and other materials* that make up the photovoltaic system is an important functional requirement. This specification will affect not only the materials selected, but also the selection of protective coatings that may be necessary to protect these materials from corrosion and other forms of environmental degradation over the anticipated life of the system.

Some photovoltaic systems track the sun, using either single or double axis tracking. The function of the tracking subsystem is to provide increased exposure to the sun's radiation. Therefore, another type of functional requirement is the *specification of the required motion of the tracking system*. This specification is especially important for concentrating arrays and affects the design of the drive mechanism for the tracker.

6.3.3 Operational Requirements

Operational requirements involve the more important aspects of the design that affect the people who install, own, operate, maintain, repair and/or service the photovoltaic system. An example of an operational requirement would be a *specification of the maximum labor hours required to assemble and install a photovoltaic system*. This type of specification is becoming increasingly important as industry tries to reduce the costs of photovoltaic system installations. It has a major effect on the simplicity of the design and the ease of assembly of the system.

A specification related to accessibility, especially accessibility to individual modules and other critical components for inspection, maintenance and repair, is another type of operational requirement. It affects the size and shape of selected mechanical components and how they are configured.

For some photovoltaic system designs, the specification of security requirements may be necessary. This type of specification is used to protect against vandalism, theft and personal injury and affects the selection and configuration of components. For example, the operational requirement to protect photovoltaic modules from flying objects has led to the frequent use of shielding on the back of small arrays for area lighting systems. Security requirements have also led the engineer to designs that include buried or tamper-proof enclosures.

Another type of operational requirement is the specification of periodic inspection and maintenance. For example, the requirement for seasonally adjusting array tilt angles affects the selection and configuration of structural support components. Anticipated rain, snow, ice, dust and the presence of birds, predisposed to target arrays with their droppings, are all examples of conditions that have affected the operational specifications for photovoltaic system designs.

6.3.4 Constraints

Invariably, the process of engineering design is constrained or limited in some way. The most common design constraint is *cost*. In the highly competitive renewable energy marketplace, it is important to keep costs to a minimum. Cost constraints have a major effect on system design. For example, aluminum may be the preferred structural material for the mechanical system because of its resistance to corrosion. But steel may be the material of choice because it is considerably less expensive, even after it has been hot-dip galvanized. Cost constraints are omnipresent and pervasive, and they challenge the ingenuity of the design engineer. Typically, the photovoltaic system must be designed and installed within a specified budget.

Another design constraint is time. Good design, in all of its creative aspects, takes precious time and sufficient time is not always available to satisfy the inner needs of the design engineer. Typically, the photovoltaic system must be designed and installed according to a specified schedule.

From time to time, the design engineer will be confronted with other types of constraints. Limited access to the sun due to existing or imminent shading (e.g.,

due to proposed construction) is commonplace. Restrictive building codes, covenants and zoning may prohibit the installation of a photovoltaic system or limit the design options. The same can be said for political, regulatory and institutional issues. And finally, the effects of weather, location and site layout often need to be considered before getting too far into the design process.

In summary, constraints are a reflection of the real world in which the engineer operates. They usually have a major effect on design decisions and, consequently, should be included in the specification of design requirements. A clear understanding of these constraints will assist the engineer in producing a better mechanical design.

6.3.5 Tradeoffs

Specifying the functional and operational requirements establishes the desired objectives for the mechanical system design. In a sense, it is a sophisticated wish list: the structure should be strong; the materials should last a long time; they should resist corrosion and other forms of degradation; and the array should have a certain orientation or possibly track the sun. In addition, the system should be easy to assemble in a short period of time; important components should be readily accessible to work on; it should be protected from vandals and thieves; and it should be easy to maintain. On the other hand, a listing of the constraints emerges: the costs are too high; the schedule cannot be met; the array must be moved to avoid shading; restrictive covenants may be violated; the grid interconnection requirements are unreasonable; and the weather is marginal for solar. In short, because of the constraints, the desired objectives cannot be met and it is time to compromise.

When the desired objectives cannot be met, the following items are subject to compromise: quality or performance, cost and schedule. There is an old saying: ‘Pick any two and trade down on the third.’ Assuming the cost and schedule constraints are rigid (they may not be), the engineer has to decide which tradeoffs in quality and performance are acceptable. Examples of tradeoffs to reduce costs and operate within budget include using steel rather than aluminum, using lower factors of safety, using lower grade steel, using less expensive corrosion inhibitors, eliminating tracking, using less expensive and probably less skilled installers and using less expensive security measures. Examples of tradeoffs to meet schedule include substituting readily available structural members for preferred parts, eliminating certain design features and using readily available labor.

6.4 Design and Installation Guidelines

6.4.1 Standards and Codes

Prior to the establishment of modern standards, structural members, nuts, bolts, screws and so on, were custom designed and manufactured. For example, one manufacturer would produce $\frac{1}{2}$ -inch bolts with 9 threads per inch, while

another would use 12 threads per inch. Some fasteners had left-handed threads and had different thread profiles. In the early days of the automobile, mechanics would lay out fasteners in a row as they were disassembled to avoid mixing them during reassembly. A lack of standards leads to a lack of uniformity and precludes efficient interchangeability of parts. It is inefficient and costly.

A **standard** is a set of specifications for parts, materials or processes intended to achieve uniformity, efficiency and a specified quality. Another important purpose of standards is to limit the number of items in the specification and thereby provide a reasonable inventory of tooling, sizes and varieties so custom parts will not be required.

A **code** is a set of specifications for the analysis, design, manufacture, construction or installation of something. The purpose of a code is to achieve a specified degree of safety, efficiency and performance or quality. It should be noted that safety codes do not imply absolute safety, which is impossible to attain. Designing a structure to withstand 120-mph winds does not mean the designer thinks 140-mph winds are impossible. It just means the designer thinks they are highly improbable.

The following organizations are involved in developing standards and codes relevant to the mechanical design of photovoltaic systems:

- Aluminum Association (AA)
- American Institute of Steel Construction (AISC)
- American Iron and Steel Institute (AISI)
- American Society of Civil Engineers (ASCE)
- American Society of Metals (ASM)
- American Society of Mechanical Engineers (ASME)
- American Society of Testing and Materials (ASTM)
- Society of Automotive Engineers (SAE).

Building codes are design, construction and installation guidelines. They are adopted and enforced by local jurisdictions to help ensure the safety of individuals and the protection of structures and other property in and around buildings. Building and electrical codes have value only if they are followed and enforced. The process begins prior to the installation of a photovoltaic system with an application for a building permit. After the installation, the building official inspects the system to determine compliance with the relevant codes. Unfortunately, many solar systems have been installed in the past without first obtaining a building permit. Most photovoltaic systems installed prior to the mid-1990s were stand-alone systems and probably would not meet present code requirements. However, with the renewed interest in photovoltaic systems for buildings as a result of financial incentive programs and government initiatives, most new systems comply with local codes. And utility-interactive photovoltaic systems are more likely to be inspected by building code officials than are stand-alone systems.

6.4.2 Building Code Requirements

The most important standard affecting the mechanical design of photovoltaic systems is entitled *Minimum Design Loads for Buildings and Other Structures* [8]. It is a standard of the American Society of Civil Engineers and is periodically updated. It provides the minimum load carrying requirements for buildings and other structures, and these requirements apply to photovoltaic systems. It is important to note that standards have meaning only when they are adopted by an enforcing jurisdiction and become part of their code. Many local jurisdictions reference parts of this ASCE standard in their building codes. However, local building codes are less uniform than local electrical codes, almost all of which use the *National Electrical Code® (NEC)*.

The basic requirements of building codes are that the photovoltaic system and any building or other structure to which it is attached, shall be designed and constructed to safely support any mechanical load or combination of loads to which they are subjected. In other words, the ASCE standard provides formulas for computing the mechanical loads from wind, snow, ice and so on. The engineer computes these loads for the conditions expected at the site of the photovoltaic system. The stresses these forces produce must not exceed the appropriately specified allowable stresses for the structural materials being used.

In addition to establishing strength requirements, building codes often limit the deformations that can occur with physical structures such as photovoltaic systems. For example, there may be restrictions on the amount of deflection or lateral drift of a structure. Such a deflection might have an adverse effect on the use of the system or attached buildings or structures. Because vibration can lead to fatigue failure, the local building code may contain provisions that address the stiffness of the structure and the associated frequencies and amplitudes of structural vibration.

6.5 Forces Acting on Photovoltaic Arrays

6.5.1 Structural Loading Considerations

Because solar energy is a relatively dilute resource, photovoltaic modules and arrays are area intensive. These large-area solar electric devices are capable of transmitting a variety of forces to themselves, their support structures, buildings and other frames or foundations to which they are mechanically attached. These forces include the dead weight of the array, the weight of array installation and maintenance people and their equipment, aerodynamic wind loading, seismic effects and the forces due to rain, snow and ice. Determining these forces under prescribed conditions can be an interesting and challenging mechanics problem.

Of the various types of forces mentioned above, aerodynamic wind loading presents the most concern. At most locations around the world, the force effects due to wind loading are much higher than the other forces acting on the struc-

ture. For example, both dead and live weight loads due to a photovoltaic array on a building are usually less than five pounds per square foot (psf). In contrast, the computed wind loads are typically between 24 psf and 55 psf, depending on location and the associated design wind speed for that location.

Because of the geographic variation in environmental conditions such as rain, snow, ice, wind speed, seismic activity, etc., local building codes tend to be much less uniform than electrical codes. Consequently, it is important for the photovoltaic systems engineer not only to become familiar with local building code requirements, but also to compute the minimum structural design loads that are relevant for a given location.

In addition to the above considerations, the design engineer must select and configure the array mounting materials so that corrosion and ultraviolet degradation are minimized. Also, if the array is mounted on a building, the structural integrity of the building must not be degraded and building penetrations must be properly sealed so that the building remains watertight over the life of the photovoltaic array.

The ASCE standard [8] provides instructions and formulas for computing the following types of loads:

- Dead loads
- Live loads
- Soil and hydrostatic pressure and flood loads
- Wind loads
- Snow loads
- Rain loads
- Earthquake loads
- Ice loads –atmospheric icing
- Combinations of the above loads.

6.5.2 Dead Loads

Dead loads consist of the weight of all the materials that are supported by the structural members, including the weights of the structural members themselves. As an example, consider a photovoltaic array mounted on the roof of a building. The modules are structurally tied together in panels using steel or aluminum structural members. The weight of the modules is carried by the structural members and transmitted to the roof structure of the building. The total dead load that the roof must carry is the combined weight of the modules, structural members used to form the panels, attachment hardware and mounting brackets. These loads can be expressed in pounds per square foot (psf) and assumed to act uniformly over the area covered by the array. Or the equations of static equilibrium can be used to determine the individual forces at each of the brackets that connect the panels to the roof. For photovoltaic systems, the dead loads are usually assumed to act uniformly over the supporting structure and are expressed in

pounds per square foot. Note that these are external loads—not internal stresses—even though similar units are used.

Dead loads for photovoltaic systems generally fall within the range of 2 to 5 psf and, even though they cannot be discounted, do not pose serious structural problems for the engineer.

6.5.3 Live Loads

Live loads associated with photovoltaic systems are those produced by individuals and their equipment and materials during installation, inspection and maintenance. In designing structures to carry live loads, the engineer may treat them as uniformly distributed loads, i.e., in psf, as concentrated loads (lb) or as a combination of uniformly distributed and concentrated loads. For photovoltaic arrays, live loads are usually assumed to be distributed uniformly and are small, on the order of 3 psf or less.

6.5.4 Wind Loads

The forces from the wind acting on photovoltaic arrays are **aerodynamic forces**. As such, their magnitudes depend partly on the properties of the atmosphere. Atmospheric properties include static pressure, temperature, viscosity and density. Of these, density is one of the more important ones affecting the mechanical forces acting on photovoltaic systems. At any given location, density is usually assumed to be constant. However, density does vary with altitude—decreasing as altitude is increased. For example, the density in the mile-high city of Denver, CO, is about 86% of the atmospheric density for Florida cities, which are only slightly above sea level. The mass density of air for the standard atmosphere at sea level is 0.00256 lb-sec²/ft⁴.

The air flowing over a photovoltaic array produces two types of forces: **pressure forces** normal to the surface and **skin friction forces** along the surface. Skin friction forces are simply surface shear forces resulting from the viscosity of the air as it contacts the surface.

Obtaining a better idea of the important relationships affecting the flow of air over structures requires some simplifying assumptions. First, assume the flow of air is **inviscid**, which implies that the viscosity of the air is zero. Next, assume that the flow of air is **incompressible**, which implies that the density of the air is constant. Finally, assume the flow of air is **conservative**, which implies that there are no other energy dissipating processes. With these assumptions, the linear momentum equation for fluid flow reduces to [9]:

$$\int \frac{1}{2} d(V^2) + \int g dz + \frac{dp}{\rho} = \text{constant} \quad (6.8)$$

where V = wind speed, g = acceleration due to gravity, z = altitude or elevation, p = static pressure and ρ = mass density. Integrating each term yields:

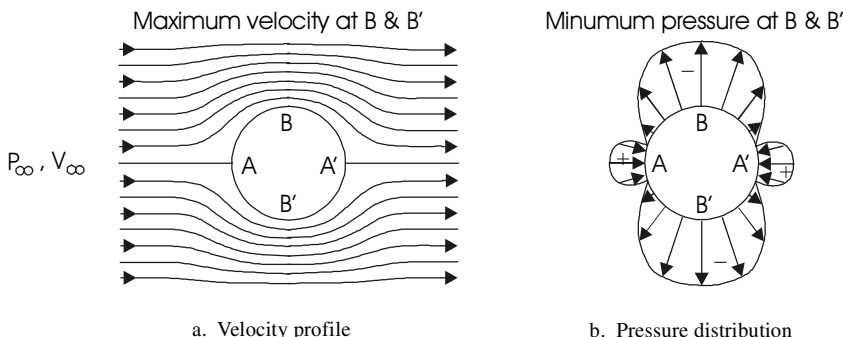


Figure 6.6 Idealized flow of air over a cylinder and the corresponding pressure distribution [10].

$$\frac{V^2}{2} + gz + \frac{p}{\rho} = \text{constant} . \quad (6.9)$$

Neglecting small changes in elevation in the vicinity of the photovoltaic system and rearranging terms yields:

$$p + \frac{1}{2} \rho V^2 = \text{constant} . \quad (6.10)$$

Whereas p is the static pressure, the term $\frac{1}{2} \rho V^2$ is referred to as the **dynamic pressure**. This very important relationship between the two variables, static pressure and velocity, is known as **Bernoulli's equation**. It shows that an increase in velocity must be accompanied by a corresponding decrease in static pressure and vice versa.

To better understand the relationship between pressure and velocity, consider the case of uniform airflow over a cylinder as shown in Figure 6.6. Air flowing along the center streamline must slow down and stop as it rams into the cylinder at point A. At this point, the speed of the air is zero and point A is called a **stagnation point**. The velocity $V_A = 0$ and the pressure P_A is a maximum and substantially higher than the free stream pressure. Figure 6.6b shows an idealized pressure distribution on the surface of the cylinder. While the maximum pressure and minimum velocity occur at point A, the minimum pressure and the maximum velocity occur at point B. The pressure at point B is less than the free stream pressure P_∞ and represents the point of maximum uplift or suction. The pressure distribution shown in Figure 6.6b for the windward side of the cylinder is appropriate, but the pressure distribution shown for the leeward side is not. In the real world, friction and turbulence come into play and cause the air to separate from the cylinder as shown in Figure 6.7. Note that this separation occurs at point C, leaving a trail of turbulent mixing downstream of the cylinder. Very little pressure recovery occurs on the right side of the cylinder, yielding a pressure distribution as shown in Figure 6.7b. This pressure distribution produces a resultant force, called **drag**, which acts to push the cylinder downstream. The

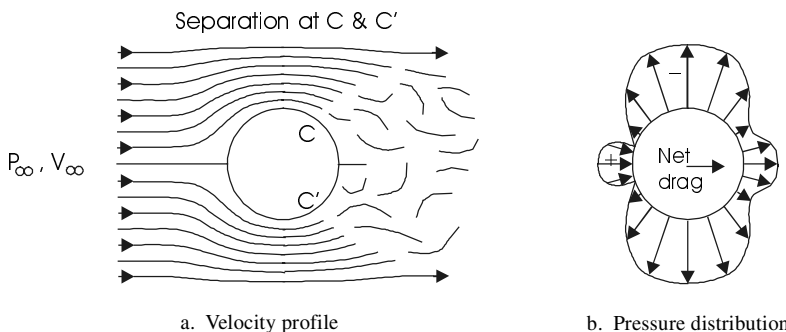


Figure 6.7 Actual air flow over a cylinder and pressure distribution, showing separation at C and C' [10].

cylinder is symmetric, but it is not streamlined. It experiences relatively high drag forces when immersed in flowing air.

Figure 6.8 shows another symmetrical body that has a streamlined shape. Streamlined bodies are shaped to reduce the separation of air, to maximize pressure recovery along their surfaces and to produce relatively low drag forces. Note that for the same shape but different orientations to the flow, quite different pressure distributions are produced. Because they are streamlined, neither airfoil produces high drag forces. However, the airfoil tilted with respect to the oncoming air experiences a significant net upward force. This upward force, perpendicular to the direction of air flow, is called **lift**. The combination of lift and drag forces produces a resultant force on the airfoil.

To continue this line of thought, next consider two flat plates, similar to photovoltaic arrays, inserted into the stream of flowing air as shown in Figure 6.9. One of the flat plates has its area perpendicular to the direction of flow, while the other is cocked at an angle to the flow. The corresponding pressure

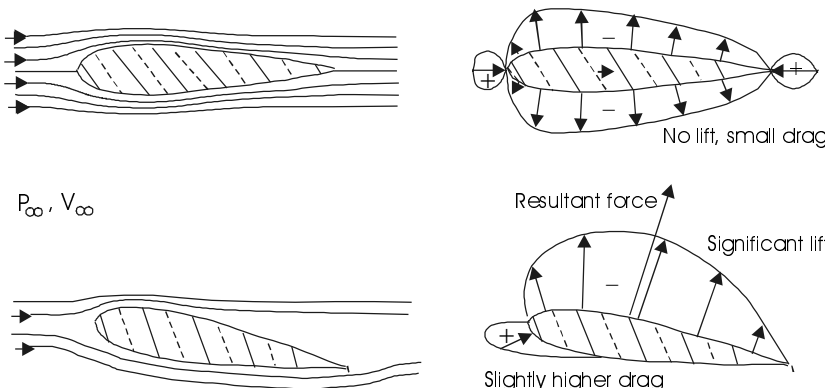


Figure 6.8 Airflow over symmetrical airfoils. The lower airfoil, which is at a positive angle of attack to the airflow, experiences significant lift [10].

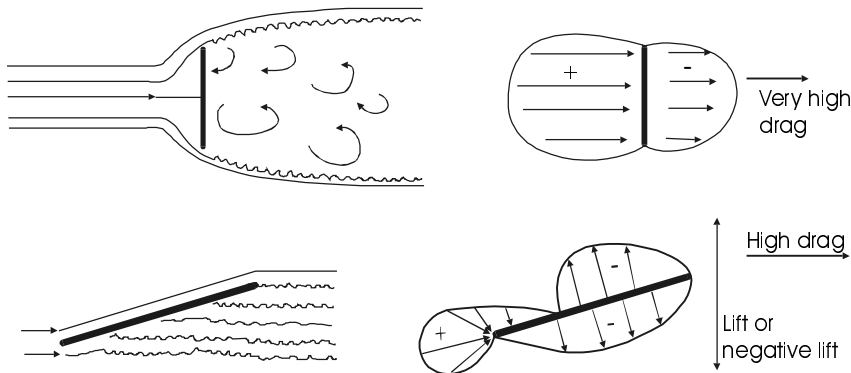


Figure 6.9 Flow over flat plates at different angles of attack to the airflow. The flat plate on the bottom may experience either an uplift or a downward force, depending on the angle of attack.

distributions are shown to the right. The vertical flat plate produces an extremely high drag force and no lift. The other flat plate, however, produces a vertical force effect, in addition to fairly high drag. Actually, the vertical component of the resultant force can act either up (lift) or down (negative lift) depending on its angle of tilt.

How does all this relate to wind loading of photovoltaic arrays and support structures? Most photovoltaic arrays are essentially large flat plates that are tilted at various angles to the direction of flow of the wind. Also, the buildings and structures to which they are attached and the terrain in their vicinity may significantly affect the flow around them. This flow often produces complex velocity and pressure distributions that, in turn, produce forces and stresses in the structural members. It should be obvious by now that the determination of wind loads on photovoltaic structures does not lend itself to theoretically derived solutions. Rather, aeronautical and civil engineers have together developed empirical formulas for estimating the structural loading resulting from exposure to various wind conditions.

At this point, it is useful to summarize the important variables and factors that affect the aerodynamic forces acting on photovoltaic arrays and structures. They include:

- Wind speed
- Effects of wind gusts
- Density of the air
- Orientation with respect to the wind direction
- Shape and surface area
- Elevation above the ground
- Effects of topographical and man-made features.

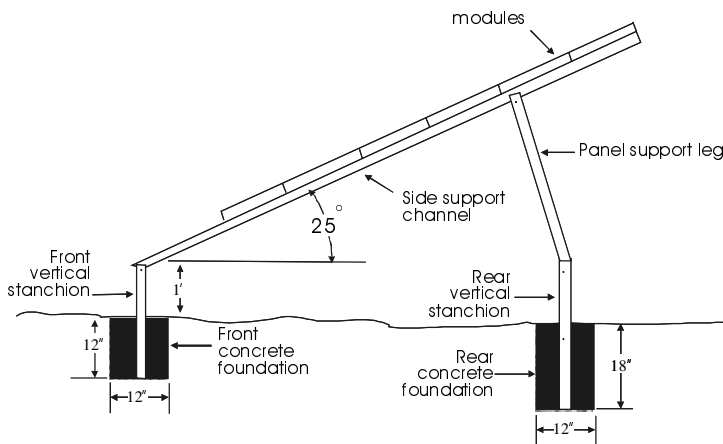


Figure 6.10 Sketch of the Hughes modular array field. This design was developed for Sandia National Laboratories [11].

The list is somewhat intimidating and shows that the best wind load analysis is not as accurate as some engineers would like. Nonetheless, with ‘ballpark accuracy’ and adequate factors of safety, good design is definitely within the engineer’s grasp.

Figure 6.10 shows a view of a modular array field designed by Hughes Aircraft Company for Sandia National Laboratories [11]. Figure 6.11 shows the *net* pressure distribution on the ground-mounted array and support structure for the combined wind and dead loads. The wind speed is 100 mph and is directed toward the front of the array. The resultant force acts down and puts structural member BC in compression. Hence, the structure must be analyzed for buckling

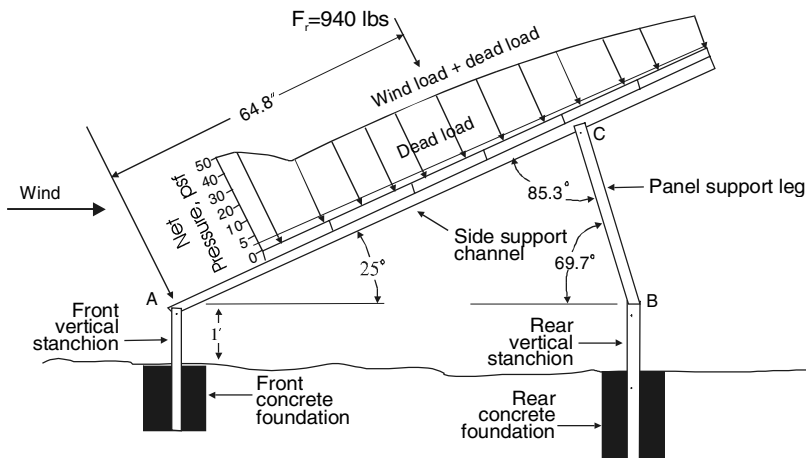


Figure 6.11 Net pressure on the array due to 100-mph winds toward the front of the array. Structural member BC is in compression.

under this loading. From the pressure distribution, based on wind tunnel testing, the forces and stresses in all the structural members can be computed.

Figure 6.12 shows the same array structure, but with the wind directed toward the back of the array. Note that the resultant force is trying to lift the array from its supports and the structural support member BC is in tension.

Work done by Boeing showed that for single arrays, the wind forces were a minimum at array tilt angles of about 20° above the horizontal [12]. Surprisingly, maximum wind forces occur at array tilt angles of 10 to 15° and again at 90° . At 10 to 15° tilt, the array acts as a reasonably efficient airfoil and large aerodynamic lift forces result. For tilt angles of 20° and higher, the air separates from the array—similar to the flow over the wing of an aircraft when it is going into a stall [13].

Ground clearance also affects wind loading. For example, it has been found that increasing the ground clearance from 2 ft to 4 ft increases the normal wind forces by 10 to 15% for an array with an 8 -ft panel height [14].

For systems consisting of multiple rows of subarrays, wind tunnel tests have shown that the interior rows experience several times less wind loading than the exterior rows [15]. Consequently, wind breaks or wind fences are sometimes used to reduce the wind loading on the exterior rows.

Because of their large exposed surface areas, their elevation off the ground and their orientation with respect to wind direction, photovoltaic arrays are often subjected to exceptionally high mechanical forces. Not only do the modules in the array have to resist these forces, but also the attachments to roofs and/or other structures must be well secured.

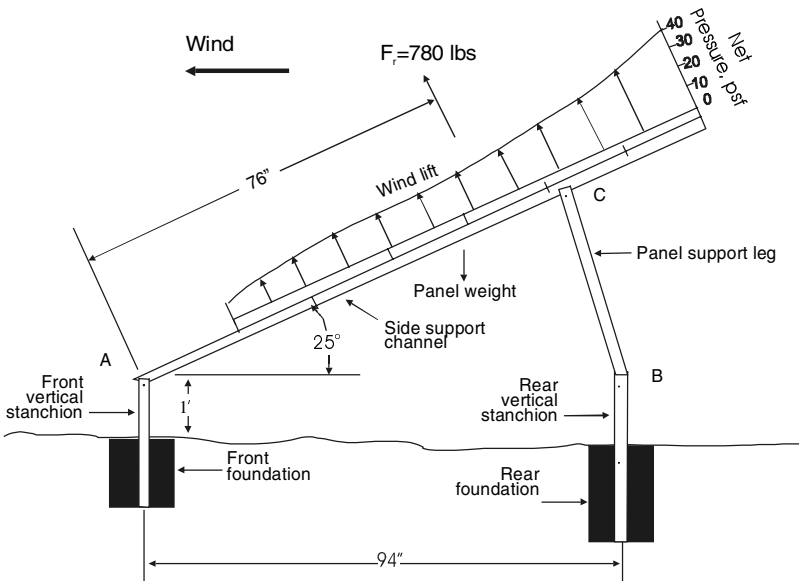


Figure 6.12 Net pressure distribution due to 100-mph winds toward the back of the array.
Structural member BC is in tension.

In designing photovoltaic arrays and structures to meet wind loads, the engineer must complete the following steps:

1. Establish the basic wind speed
2. Determine the velocity pressure
3. Determine the gust effect factor
4. Determine the appropriate pressure or force coefficient
5. Determine the wind loads on the array
6. Determine the forces acting on critical members and attachment points
7. Establish an appropriate factor of safety based on risk
8. Select structural members and attachment hardware that can carry all loads with the prescribed factor of safety.

Fortunately, the American Society of Civil Engineers has developed standards and procedures for completing the steps above [8]. For example, the ASCE has developed maps indicating the basic wind speeds throughout the U.S. (step 1); formulas, tables and charts for computing the velocity pressure (step 2); gust effect factors for various downtown, urban, rural and flatland sites (step 3); force coefficients for different shapes and structures (step 4); and equations for computing the wind loads (step 5). From these wind loads (forces per unit area) on the array, the equations of static equilibrium are used to compute the forces acting on the structural members (step 6). Knowing these forces, the engineer selects the materials, structural shapes and attachment hardware that meet all design requirements.

The ASCE procedures may be used to analyze the wind loads on standoff-mounted rooftop arrays, such as shown in Figure 6.13. Wind directions from both the front and rear of the array-roof structure should be considered, resulting in both uplifting and downward pressure distributions. Uplifting pressure is usually of greater concern because of the tensile and withdrawal forces it exerts on supporting hardware.

In the ASCE standard, the highest basic wind speed in the U.S. is 150 mph. The velocity pressure, q , is computed using the equation:

$$q = 0.00256 K_z K_{zt} K_d V^2 I \quad (6.11)$$

where: K_z = velocity pressure exposure coefficient at height z

K_{zt} = topographical factor

K_d = wind directionality factor

V = basic wind speed in mph

I = importance factor

Using the equations, tables and charts in the standard yields:

$$K_z = 0.85$$

$$K_{zt} = 1.00$$

$$K_d = 0.85$$

$$I = 1.00 \text{ and}$$

$$q = 42 \text{ psf}$$

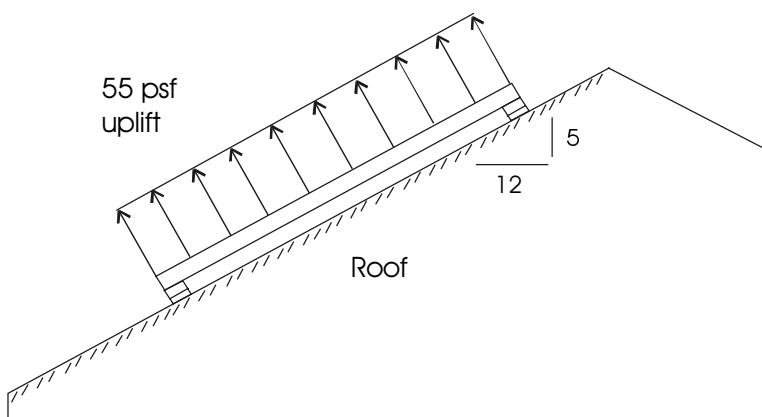


Figure 6.13 Standoff-mounted array with an uplifting pressure distribution.

The design wind pressure, p , is computed using:

$$p = q G C_f \quad (6.12)$$

where: G = gust effect factor = 0.85

C_f = force coefficient = 0.70 (for a normal gable or hip roof) and
 $p = 25 \text{ psf}$

As an example, for an array having an area of 200 sq. ft., the total uplifting (resultant) force acting on the array would be $25 \text{ psf} \times 200 \text{ sq. ft.} = 5,000 \text{ lb.}$ Knowing this resultant force, the design engineer can now determine the number of attachment points and the size of the mounting hardware necessary to safely carry this load.

Rather than computing the pressure distribution for each standoff array and roof combination, a more prudent approach is to assume a worst-case scenario for wind loading and design a mounting system capable of surviving the associated loading. Such a scenario might include maximum expected wind speeds (say 150 mph), array tilt angles that produce maximum uplifting pressure distributions (say 10 to 15°), topographical and shape effects that increase the pressure loading on the array and mounting system, and an adequate factor of safety. Using this approach and applying the methodology in the ASCE standard yields a reasonable upper limit on the design wind pressure of 55 psf.

Many manufacturers of photovoltaic modules supply structural members to support their arrays with an adequate factor of safety. In most cases, a registered professional engineer has performed a structural analysis based on a worst-case scenario such as that described above. However, such analyses are usually not site specific. Note that the array will be physically attached to and supported by a roof or some other type of structure at a specific location. It is important that the entire site-integrated system, including the attachment hardware and the roof or support structure to which the array assembly is attached, is capable of sur-

viving the worst-case scenario of wind loading—not just the array and mounting members that come with photovoltaic system package.

In summary, the largest mechanical forces acting on photovoltaic arrays and structures are due to high wind speeds. Suppliers of packaged photovoltaic systems should assume a worst-case wind loading of 55 psf (or higher) in designing their array mounting systems. Many have already done so. In addition, the entire integrated photovoltaic and building system must be able to survive the worst-case scenario of wind loading and comply with all site-specific building code requirements.

6.1.1 Snow Loads

Snow loads on photovoltaic arrays and on sloped roofs decrease as the tilt angles and slopes increase. There are three reasons for this. First, as the tilt angle increases, the component of the weight force parallel to the array surface increases relative to the component normal to the array surface, thus helping to shed the snow. Second, wind forces tend to shed the snow from the array. Third, melt water reduces the friction between the array surface and helps to shed the snow. Most photovoltaic arrays have “slippery” glass surfaces that also aid the snow-shedding process. On the other hand, obstructions and rough surfaces hinder the shedding of snow and its weight. For example, some tile roofs contain built-in protrusions or rough surfaces that prevent the snow from sliding. The snow that accumulates on arrays mounted on such roofs may be obstructed from shedding [8].

An extreme case of snow loading occurs when unusually large amounts of snow accumulate on an array at a relatively small tilt angle. However, this is rare because shallow tilt angles are uncommon in colder, snow-prone parts of the world. In most cases, snow loads on photovoltaic arrays are less than 8 psf.

6.1.2 Other Loads

The photovoltaic array and support structure may experience mechanical forces due to other loads, such as rain, ice, hydrostatic pressure and seismic activity. The latter is critical in earthquake-prone regions and the ASCE has detailed procedures for designing for seismic loads.

Foundations, footings or slabs that support photovoltaic arrays may experience uplift forces due to hydrostatic pressure in locations where ground water is close to the surface. If expansive soils are present, the hydrostatic pressures can be quite large. In such cases, the expansive soils are sometimes excavated to a depth of at least 2 ft below ground level, followed by back filling with freely draining sands and gravel.

Regardless of the location, the photovoltaic engineer is responsible for ensuring that all of the relevant loads and load combinations have been properly accounted for in the mechanical system design.

6.2 Array Mounting System Design

6.2.1 Introduction

Previous sections of this chapter discussed various properties of materials, the strength of materials, functional and operational requirements, standards and codes and the mechanical forces acting on the array and support structure. Emphasis was placed on material selection and compatibility based on concerns for structural integrity, safety and code compliance. This section focuses on those aspects of the array mounting system that affect costs, performance, maintenance and appearance.

6.2.2 Objectives in Designing the Array Mounting System

In addition to meeting structural, code and safety requirements, good design of the array mounting system should achieve the following:

- Minimizing installation costs
- Enhancing array performance
- Providing reasonable accessibility for installation and maintenance
- Making the system aesthetically appropriate for the site and application.

Minimizing Installation Costs

Both good design and good installation practices can be employed to reduce installation costs. Studies in the 1990s by Sandia National Laboratories have shown that only about half the cost of photovoltaic systems is for modules. The other half is for nonmodule components and labor, with labor being the major contributor. For example, suppose a journeyman electrician installs a photovoltaic system. The electrical contractor may charge \$75 per hour for the electrician's time. The value of reducing the number of hours for installation should be obvious. Photovoltaic manufacturers and system suppliers can reduce installation costs by doing one or more of the following:

1. *Developing packaged kits.* For about the first 2 decades of applying photovoltaics to terrestrial applications, system design was essentially customized for each installation. Since the mid to late 1990s, the trend has been to develop packaged kits that can easily be adapted to a wide variety of installations. Building applications of photovoltaics have helped to accelerate this trend. Photovoltaic system suppliers now deliver standard models, which include modules, the structural support systems, attachment hardware, batteries and inverters. Some include the module interconnect wiring, junction boxes and other balance-of-system components. The development and refinement of packaged kits should help reduce the cost of photovoltaic system installations.

2. *Minimizing the total number of parts.* A second design approach to reducing installation costs is to minimize the total number of parts included in the design. As an example, some suppliers are moving toward the use of larger

modules and fewer panels. The idea is to use less-skilled personnel to assemble and prewire panels prior to shipment to the site. This reduces the time required by more highly skilled personnel to complete the installation at the site.

3. *Minimizing part variations.* A third design approach to reducing installation costs is to minimize part variations. This concept is easily applied to the size and type of structural members, fasteners and attachment hardware. It often eliminates the need for special tooling.

4. *Designing parts to be multifunctional.* Designing systems such that some parts are multifunctional is a fourth approach to cost reduction. For example, a structural member may be used not only to carry the mechanical loads, but also to enhance the flow of air over the back surface of the array.

5. *Designing parts for multiple uses.* Structural members, brackets, attachment hardware and fasteners should be designed for possible use with different kits, model numbers and product lines.

6. *Designing for ease of assembly.* This not only reduces the time required to install systems, but also often results in higher reliability and reduced maintenance.

7. *Avoiding separate fasteners.* One popular approach to reducing installation costs is to use slotted roof brackets that allow photovoltaic modules or panels to be simply dropped into the slots. It eliminates the need for on-site attachment of nuts and bolts to connect the panels to roof brackets. Another alternative approach is to use captive fasteners.

8. *Minimizing assembly direction.* This means that parts should be designed so that they fit or can be assembled only one way—the correct way. This is common practice in many industries.

9. *Maximizing compliance in assembly.* The installer should not have to struggle to assemble the panel framework, attach the modules to the panel, or attach the panels to the support structure. To maximize compliance in assembly, the designer should avoid tolerances that are too tight. Parts should fit together with a minimum of effort.

10. *Minimizing handling in assembly and installation.* This concept follows from a number of the other items, but also includes locating holes, slots and other points of attachment to reduce handling.

In addition to the design practices suggested above [1], good installation practices can also be employed to reduce costs. Already mentioned is the practice of preassembling and prewiring panels off-site using less-expensive personnel. Another consideration for roof-mounted arrays is the number, type and placement of roof attachment points. Often this decision is made by the installer at the site, rather than by the designer, and serious tradeoffs must be considered. For example, minimizing the number of roof attachments saves time, but it also means that individual attachment points will be subjected to larger forces.

Building Integration Considerations

As the population grows and building density increases, space becomes more valuable and rooftops become more attractive locations for photovoltaic

arrays. The question arises: How can we most effectively integrate photovoltaic systems and buildings? For existing buildings, the most prudent approach is to use designs that minimize costs by incorporating the measures discussed above.

Building-integrated photovoltaic (BIPV) products are solar electric devices that replace conventional building materials. They include solar shingles, tiles, skylights, windows, overhangs, facades, and PV laminates bonded directly to metal roofing panels. They can be used on either new or existing buildings in a manner that is aesthetically pleasing and very appealing to buyers.

For broad acceptance by builders and homeowners, more BIPV products that are attractive and easily incorporated into building construction are needed. As these new building-integrated photovoltaic products achieve attractive combinations of costs and durability, they should further stimulate a growing market for rooftop applications.

However, widespread building-integrated photovoltaic applications may require more than just new BIPV products. They may also require buildings with new features that make them more receptive to photovoltaic systems. Examples include innovative roof, truss and electrical system design. In addition, the integration of on-site generation and super energy efficient buildings offers the prospect of alleviating national energy problems from both the supply and demand sides of the problem. The U.S. Department of Energy's Zero Energy Homes Program is a manifestation of the level of interest in this approach.

For new manufactured buildings, one interesting approach to building integration involves factory-installed photovoltaic systems. Approximately 30% of new housing stock in the U.S. is manufactured housing. To be effective, the manufacture of buildings in a factory requires careful planning, time-motion studies and process optimization—areas of interest to industrial engineers. Not only are the buildings manufactured quickly, but also quality control becomes an ongoing part of the process. Opportunities exist to include photovoltaic systems in the building manufacturing process. The idea is to accelerate the installation process, reduce costs and improve quality control. The complete photovoltaic system can be installed in the factory, part of it can be installed, or the manufactured building can be specially configured to more easily accept a photovoltaic system. The latter approach has been successfully demonstrated and involves installing the following items in the factory prior to shipping the building to the site: double roof trusses (to both increase load carrying ability and allow for the use of larger mounting brackets); wiring conduit from the roof through the attic and walls to the crawl space under the building; a rain-protected opening and flashing (i.e., vent stack flashing) to accommodate wiring from the array into the conduit; and a prepared, structurally enhanced location for mounting the inverter. Once the building has been delivered and set up on the site, installation of the prewired array panels, inverter and other balance-of-system components is achieved at a fraction of the time and cost of a custom installation [16].

Costs and durability of array-roof configurations

Life-cycle costing is used in economic analyses of renewable energy technologies because these technologies realize their value over time. They are usually characterized by high capital costs and low operating costs. For photovoltaic systems on buildings, the combined array-roof configuration is a major contributor to the life cycle cost. It is important that these configurations last 20 to 30 years. However, this is not always achieved without unexpected added cost. For example, asphalt shingles often have to be replaced about every ten years in warm, humid climates. The life cycle cost analysis should include the added cost of removing and re-installing the PV array when re-roofing.

The durability of some of the relatively new BIPV products is also a concern. For example, PV laminates bonded to either structural or architectural standing seam metal panels produce architecturally attractive arrays, and installation costs have been decreasing. However, the long-term durability of the bond between the laminate and the metal needs to be demonstrated [16].

6.2.3 Enhancing Array Performance

The mechanical system can affect the array performance in several ways:

- Increasing the amount of incident solar radiation
- Avoiding shading
- Allowing the array to operate at lower cell temperatures
- Protecting the array from vandalism.

Irradiance enhancement

Irradiance enhancement can be achieved by optimizing the array orientation, tracking the sun and using concentrating collectors. The optimum array orientation depends on the type of system, application and end-user. For example, to maximize annual energy production, the optimum tilt angle is about 90% of the latitude of the site and the optimum azimuth is true south for the northern hemisphere and true north for the southern hemisphere.

However, utility companies may be more interested in peak load reduction than total energy produced. Consequently, the optimum azimuth angle might point the array more closely to the west than to the south (in the northern hemisphere), since utility peak loads generally occur during summer afternoons.

Concentrating and tracking arrays work best in areas receiving a higher than average percentage of direct radiation, such as the desert southwest U.S., and may not be an attractive option in many locales. As discussed under the section on design requirements, the engineer must weigh the tradeoffs.

Shading

Closely related to irradiance enhancement is the need to avoid shading. The performance characteristics of shaded arrays varies, but photovoltaic arrays usually are more seriously affected by shading than are solar thermal collectors. Consequently, shading should be avoided to the greatest extent possible.

Array cooling

Photovoltaic modules, especially those using thick, crystalline cells, work better at lower cell operating temperatures. Consequently, the array mounting should be designed to allow air circulation along the back surface of the modules. Rack-mounted arrays typically operate at lower temperatures than other configurations. Experiments at Sandia National Laboratories show that the operating temperatures of direct-mounted arrays may be 18°C higher than the cell's nominal operating cell temperature (NOCT). For standoff-mounted arrays, a standoff height of 4 to 6 inches, with no significant obstruction to air flow, will permit adequate passive cooling of the modules.

In general, the output power of thin film materials is degraded less by high operating cell temperatures.

Protection from vandalism

Unfortunately, photovoltaic arrays are sometimes used as targets by vandals. Therefore, it may be necessary to include protection features. Back shields are often used for arrays on area lighting systems. Some of these vandal-guards do not permit adequate cooling of the array and can have a noticeable deleterious effect on performance. Back shields that allow more air circulation might be considered. For larger array fields, fencing, security lighting, motion sensors and other protection measures are sometimes employed.

6.2.4 Roof-Mounted Arrays

Photovoltaic array mounting can be categorized according to where the arrays are mounted, how they are supported and whether they have a fixed or changing orientation. Arrays can be either roof-mounted or ground-mounted. Roof-mounted arrays typically use one of four different methods of support:



Figure 6.14 Standoff-mounted array installed using slotted roof brackets. These point connections and the standoff height promote good air movement between the roof and the back surface of the modules [FSEC photo].



Figure 6.15 Spanner and J-bolt attachments provide secure anchors for roof-mounted arrays.

rack, standoff, integrated or direct. With the surge of interest in photovoltaic and building applications, better designs for each of these four roof mounting approaches are being pursued.

Standoff Mounting

Standoff arrays are mounted above and parallel to the roof surface as illustrated in Figure 6.14. Standoff mounts work well for buildings with sloping roofs. When installing a standoff-mounted array, the photovoltaic panels or subarrays are often attached to the roof using point connections—usually at or near the corners of the panels or subarrays. As a minimum, the standoff height between the roof and the bottom of the module frame should be at least three inches. Four to six inches is preferable. Lag screws that penetrate the roof rafters three to four inches may be used to fasten the mounting brackets to the roof. Spanner and J-bolt attachments, as shown in Figure 6.15, are stronger than lag bolts or lag screws and are commonly used in areas exposed to high winds.

To promote passive cooling of standoff arrays, the engineer should consider the following designs:

- Designs that allow both lateral and vertical airflow along the back surface of the modules
- Designs that induce pressure differences between air inlet and exit regions
- Arrays with larger lateral dimensions than vertical dimensions (i.e., higher aspect ratios).

Rack Mounting

Rack-mounted arrays are above and tilted with respect to the roof, as illustrated in Figure 6.16. Rack mounts work well on flat roofs and roofs with a slope of 2 in 12 or less. They may be mechanically attached to the building structure or may employ ballast to resist wind and other mechanical loads. Rack mounts are usually subjected to higher structural loads, incur higher costs for mounting hardware and are often less attractive than standoff mounts. However,

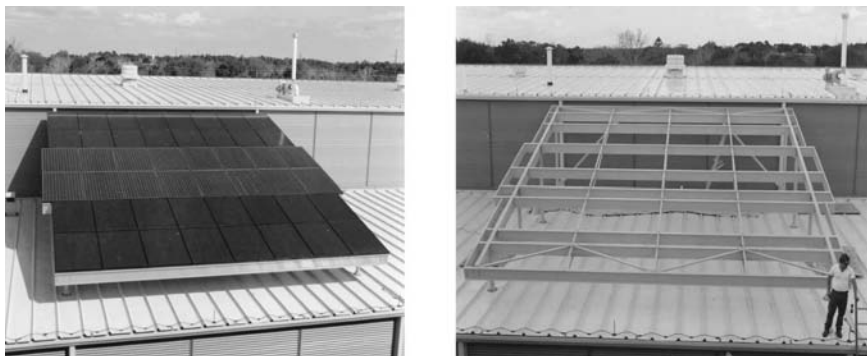


Figure 6.16 A rack-mounted array at the Florida Solar Energy Center. The robust structural system is designed to withstand category 3 hurricanes.

for the same array area, the total energy output is often higher because of better orientation and lower average operating temperatures.

Ballasted rack assemblies offer the distinct advantages of simplicity and avoidance of roof penetrations, and should be considered if acceptable by local code jurisdictions. However, most rack mountings are firmly attached to the roof substructure. These are usually point connections, although several distributed attachment methods are sometimes used. Rack-mounted arrays typically run relatively cool compared with other mounts and they can reduce heat gain through roofs. Since the primary mechanism of rack array cooling is convection from the front and back surfaces of the modules, cooling can sometimes be enhanced by locating the rack in natural air channels and by reducing obstructions to airflow, such as screens, grates and walls.



Figure 6.17 For this experimental prototype, photovoltaic modules replaced conventional roofing materials.

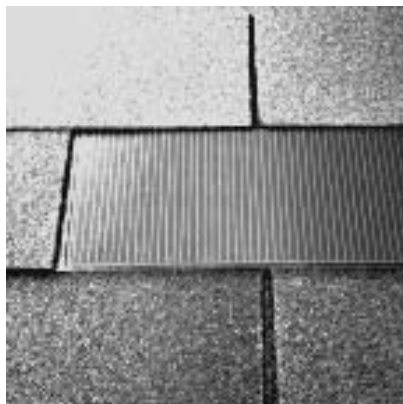


Figure 6.18 The solar shingle is installed directly on the roofing underlayment, with no air circulation below the PV laminate. It is one of a variety of new products that replaces conventional roofing materials.

Integrated Mounting

For integrated arrays, also referred to as building-integrated photovoltaics (BIPV) or integral mounting, the array replaces conventional roofing or glazing materials as illustrated in Figure 6.17. Because integrated arrays replace conventional roofing and glazing materials, they become a significant architectural feature of a building and can be aesthetically very pleasing.

Dimensional tolerances may be tighter for some integrated arrays than for standoff or rack mounts. If commercial curtain-wall glazing techniques are used, larger modules are preferable to smaller modules.

Direct Mounting

In direct mounting, the array is affixed directly to the roofing material or underlayment, with little or no airspace between the module and roof. Figure 6.18 illustrates a direct-mounted solar shingle.

Array operating temperatures for direct mounts are usually higher than for other mounting techniques. The use of direct mounting may become increasingly popular for new thin-film products that are not as sensitive to operating temperature. Some photovoltaic materials, such as solar shingles, fall into both the direct and BIPV mounting categories.

6.6.5 Ground-Mounted Arrays

Ground-mounted arrays are supported by racks, poles or tracking stands. These arrays are secured to the ground to resist uplifting caused by wind loads. All ground-mounted arrays run relatively cool because good airflow is possible over both the front and back surfaces of the modules. This cooling can be enhanced by minimizing obstructions to airflow such as shrubbery and fences.



Figure 6.19 A ground-mounted array field using rack supports.

Rack Mounting

Rack mounting is commonly used for mounting arrays on the ground. Simple structural hardware such as angles, channels and metal tubing can be used for both small and large PV arrays. Most module manufacturers and equipment suppliers offer hardware for rack mounting PV arrays on the ground. Figure 6.19 is an example of a rack-mounted array.

Pole Mounting

If the array consists of only a few modules, it can be mounted on a pole as shown in Figure 6.20. Depending on the number of modules and their height above the ground, the pole may need to be set in concrete to resist being over-



Figure 6.20 Pole-mounted arrays are often used for PV lighting systems.

turned during windy conditions. Among others, photovoltaic-powered outdoor lighting is a good application for pole-mounted arrays.

Tracking-Stand Mounting

Because tracking arrays receive more sunlight than stationary arrays, their modules produce more energy. The value of a tracking array depends on the tradeoff between additional energy produced and added cost and complexity. There are two types of trackers: active and passive. Active trackers use drive mechanisms, such as electric motors and gears, to point the array toward the sun. They may track about either one or two axes. The tracking motion may be controlled by a computer or by sun-seeking sensors.

Passive trackers normally track about only one axis and use a two-phase fluid, such as a refrigerant, that vaporizes and expands when it is heated by the sun. The expanding fluid causes the tracker to pivot toward the sun as the fluid's weight shifts from one side of the tracker to the other. An alternative design uses a hydraulic cylinder and linkage arrangement. For both tracker designs, sunshades are used to regulate the heating of the fluid and control the motion. A passive tracker is shown in Figure 6.21. Compared with a fixed-tilt array, these trackers show the greatest energy enhancement in the summer when the days are long and are less beneficial in the winter. Tracking arrays are often used for water pumping because they can produce high starting currents early in the day and because of the higher demand for water during the summer months.

6.6.6 Aesthetics

It is important for arrays on buildings to be aesthetically pleasing. They should be designed to blend into the building lines and colors. In designing



Figure 6.21 A pole-mounted array on a passive tracker at the Florida Solar Energy Center.

photovoltaic arrays for building applications, the architect and engineer should consider the following suggestions:

- Mounting the array parallel to the roof (if appropriate)
- Using the roof dimensions to establish the array aspect ratio
- Avoiding harsh contrasts and patterns
- Making the mounting hardware as inconspicuous as possible
- Avoiding shading, even if appearance suffers somewhat.

As mentioned previously, many of the new building-integrated photovoltaic products add to the architectural attractiveness of buildings.

6.1 Computing Mechanical Loads and Stresses

6.1.1 Introduction

As indicated previously, the photovoltaic array is subjected to a wide variety of mechanical influences that affect the stresses and strains in the modules, structural support members and attachment hardware. These include dead-weight loads, live loads, wind loads, and snow and ice loads. In this section, we assume a pressure distribution on the array and discuss the methods used to calculate its effects on critical elements of the support structure.

6.1.2 Withdrawal Loads

A high percentage of standoff-mounted photovoltaic arrays are attached to the roof using lag screws or bolts. The lag screw typically passes through a hole in a mounting bracket, possibly a mounting pad, shingles, waterproof membrane, sheathing and, finally, into the truss, spanner or other primary structural wood support member. The withdrawal strength of this and other attachment points is a function of the diameter of the lag screw, the length of thread embedded in the primary structural wood support, and the specific gravity of the wood. The allowable withdrawal load of lag screws and bolts per inch of embedded thread is given by [3]:

$$p = 1,800D^{3/4}G^{3/2} \quad (6.13)$$

where: p = allowable withdrawal load (lb./in.)

D = shank diameter of lag screw or bolt (in.)

G = specific gravity of oven-dry wood

Values for p computed using (6.13) include a safety factor of 4.5. This relatively high value provides added protection just in case the actual wood used may have reduced strength due to variations in specific gravity, knots, grain irregularities, holes and other defects [17].

The typical diameters of lag bolts or screws used to attach photovoltaic arrays are 1/4 in., 5/16 in. and 3/8 in., although they may be as large as 1/2 in. The specific gravities of various types of lumber can be found in the *Wood Engineering and Construction Handbook* [18]. Table 6.6 was developed using the above equation and the specific gravities for various types of lumber.

Table 6.6 Allowable withdrawal loads for lag screws and bolts.

Lumber	White Oak	Southern Yellow Pine	White Spruce	Douglas Fir
Specific gravity, G	0.71	0.58	0.45	0.41
Diameter, D (in.) ↓	Allowable withdrawal load, p (lb./in.)			
1/4	381	281	192	167
5/16	450	332	227	198
3/8	516	381	260	226
7/16	579	428	292	254
1/2	640	473	323	281

[Values for p were computed using equation (6.13) and include a safety factor of 4.5.]

Example

Assume the maximum uplifting normal pressure distribution on a standoff photovoltaic array due to wind is 55 psf. If the array panel area of 24 sq. ft. is secured by four lag screws, a) What is the withdrawal force on each lag screw, b) what depth of thread must be firmly embedded in the supporting roof truss made of white spruce for thread diameters of 1/4 in., 5/16 in. and 3/8 in., c) what is the allowable withdrawal load for a 5/16 in. x 4 in. lag screw with 3 in. of thread length, and d) what is the maximum normal pressure distribution that the four lag screws of part c can support?

- The resultant uplifting force is simply $55 \text{ psf} \times 24 \text{ sq. ft.}$, or 1,320 lb. Therefore, the withdrawal force on each lag screw is $1,320/4 = 330 \text{ lb.}$
- Using Table 6.6 for white spruce, the allowable withdrawal loads are: 192 lb./in. for 1/4 in. diameter, 227 lb./in. for 5/16 in. diameter and 260 lb./in. for 3/8 in. diameter. So the required depths of penetration into the truss are: $330/192 = 1.72 \text{ in.}$ for the 1/4 in. screw, $330/227 = 1.45 \text{ in.}$ for the 5/16 in. screw and $330/260 = 1.27 \text{ in.}$ for the 3/8 in. screw.
- Assuming all 3 in. of thread are firmly embedded in the white spruce truss, the allowable withdrawal load is $227 \text{ lb./in.} \times 3 \text{ in.} = 681 \text{ lb.}$
- Four lag screws can carry a resultant load of $4 \times 681 \text{ lb.} = 2,724 \text{ lb.}$ This corresponds to a uniform normal pressure distribution of $2,724 \text{ lb./24 sq. ft.} = 114 \text{ psf.}$

6.1.3 Tensile Stresses

In addition to withdrawal loads, uplifting pressure distributions produce tensile stresses in hardware used to secure the array to a roof or other support

structure. This hardware could be lag screws, J-bolts or threaded rods. The forces acting on the attachment hardware are computed using the equations of static equilibrium, and the tensile stresses are computed using equation (6.1).

Example

A 36 ft² photovoltaic array is secured to a roof using four 1/4 in. x 3 in. lag screws made of 304 stainless steel. The standoff-mounted array is subjected to a uniform uplifting pressure distribution of 55 psf. The allowable tensile strength of 304 stainless steel is 24,750 psi. Compute the tensile stress in the lag screws and determine if there is risk of failure in tension.

The resultant force acting on the array is 55 psf x 36 sq. ft. or 1,980 lb. Thus, $1,980/4 = 495$ lb. is the tensile force acting on each of the four lag screws. Using equation 6.1, the tensile stress is:

$$S = \frac{P}{A} = \frac{495}{0.0767} = 6,450 \text{ psi}$$

Because the computed stress is much less than the allowable tensile stress for the stainless steel, there appears to be no risk of failure in tension.

Note that the same procedure can be applied in computing the tensile stresses in J-bolts and threaded rods that are used to secure arrays to roofs or other support structures.

6.1.4 Buckling

In contrast to uplifting pressure distributions, forces distributed downward toward the plane of the array are usually not as serious a concern. However, an exception occurs when long, slender structural members are subjected to compressive forces that may result in structural instability known as buckling. In such cases, which may occur due to wind loads on rack-mounted arrays, the engineer must compute the critical buckling load using equation (6.6), which can be expanded into the following form:

$$P = \frac{EI\pi^2}{L^2} = \frac{EAr^2\pi^2}{L^2} = \frac{EA\pi^2}{(L/r)^2} \quad (6.14)$$

where: I = moment of inertia of the cross-sectional area = Ar²

A = cross sectional area of the column

r = radius of gyration of the cross sectional area

L/r = slenderness ratio of the column

Note from the above equation, larger slenderness ratios and smaller cross-sectional areas yield lower critical buckling loads. If the length L of the structural member cannot be significantly changed, the engineer should consider se-

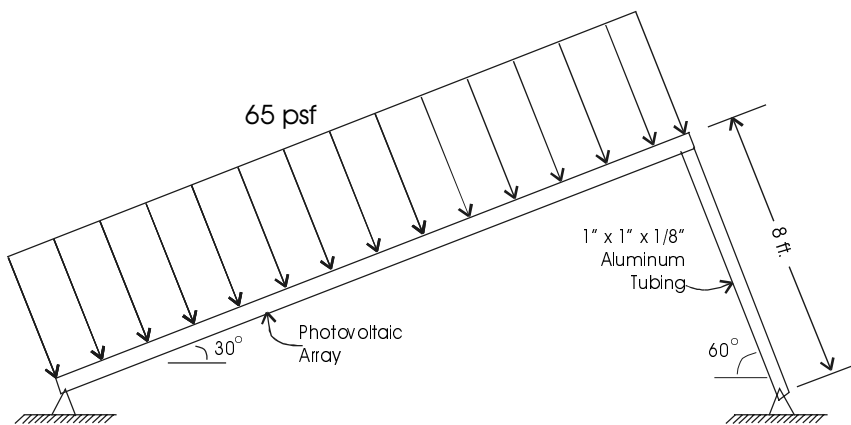


Figure 6.22 Rack-mounted array with rear support column in compression.

lecting members with cross sections having larger radii of gyration. Conceptually, the radius of gyration is a measure of an equivalent distance from a reference axis at which the entire cross-sectional area may be assumed to be concentrated to produce the same moment of inertia. The type of cross section that yields higher radii of gyration is a hollow tube in which all the cross-sectional area is distant from the axis. Consequently, hollow metal tubing is often used for column support. Radii of gyration can be either calculated or obtained from tables for steel, aluminum or other columns.

Example

Figure 6.22 shows a rack-mounted array supported by square 6063 T-6 aluminum tubing having cross-sectional dimensions of 1 in x 1 in x 1/8 in. The radius of gyration for this cross section is 0.361 in². The modulus of elasticity for the aluminum is 10 x 10⁶ psi and the cross-sectional area is 0.50 in². If the length of the rear structural support member is 8 ft. (96 in.), compute the maximum force the member can withstand without buckling.

Substituting directly into equation 6.14:

$$P = \frac{10^7 (0.50) \pi^2}{(96/0.36)^2} = 698 \text{ lb.}$$

Thus, each rear support member should not be subjected to compressive forces that approach 698 lb.

6.8 Summary

The mechanical design of photovoltaic systems is the process of selecting, sizing and configuring a variety of structural and other components to meet pre-determined design requirements. These include functional and operational re-

quirements and design constraints. Meeting the design requirements under prevailing constraints requires a weighing of alternatives and trade-offs.

The engineer must determine the mechanical forces acting on the array and select the proper materials and structural members to safely carry these loads. Photovoltaic mechanical design requires knowledge of materials, mechanics, structures and the characteristics of photovoltaic systems.

Standards, when incorporated into building codes, establish the guidelines for designing and installing photovoltaic systems.

The American Society of Civil Engineers publishes standards on design loads for buildings and other structures. These standards can be applied to solar arrays. The greatest mechanical loading on photovoltaic arrays and structures is the result of aerodynamic forces from wind. ASCE specifies the different wind speeds that should be used for design throughout the U.S.

The array mounting design should provide adequate access to the sun's radiation and allow the photovoltaic modules to operate at acceptable cell temperatures. The array should also be sufficiently accessible for installation and maintenance and aesthetically appropriate for the site and application.

Problems

- 6.1 Consider the following facts concerning a steel alloy and aluminum alloy:
a) steel is stronger, b) steel is stiffer and c) aluminum stretches much more than steel. Sketch the stress-strain curves for both on the same stress-strain graph (see Figure 6.3). Show the relative positions of the yield strength, ultimate strength and rupture strength. Also, indicate on the graphs how the moduli of elasticity compare for steel and aluminum.
- 6.2 For two bars having cross sectional areas $A_1 = 0.25 \text{ in}^2$ and $A_2 = 25 \text{ in}^2$, subjected to uniform axial forces $P_1 = 100 \text{ lb}$ and $P_2 = 1000 \text{ lb}$, compute the uniform stresses in each bar.
- 6.3 During a simple pull test of a bar, the deformation per unit length was measured at 0.000167 in/in . The corresponding stress was 5000 psi . Further in the test, the elongation per unit length and corresponding stress were 0.000667 in/in and $20,000 \text{ psi}$. If the proportional limit is $30,000 \text{ psi}$, what is the modulus of elasticity? Would this result be valid if the proportional limit was $18,000 \text{ psi}$? Explain.
- 6.4 A uniform bar has length = L and cross sectional area = A . Rather than a force P acting on the end of the bar, the only force is the uniformly distributed weight of the bar. If the total weight of the bar is W , show that the total elongation is $\delta = WL/2AE$. If its weight per unit volume is w , also show that $\delta = wL^2/2E$.

- 6.5 A steel bar having a cross sectional area of 0.5 in^2 and a length $L = 600 \text{ ft}$ is suspended vertically. The force P acting on the lower end is 5000 lb. If steel weighs $490 \text{ lb}/\text{ft}^3$ and $E = 30 \times 10^6 \text{ psi}$, find the elongation of the bar. (Hint: Use the results of Problem 6.4.)
- 6.6 A photovoltaic array is to be mounted on the roof of a nursing home, which is adjacent to a hospital. It is located in the Topeka, KS, area and is subjected to high wind loading. List at least three possible functional requirements and three operational requirements. Also identify four constraints the designer must consider. Identify the trade-offs that might be weighed.
- 6.7 Why are building codes that affect the mechanical and structural design of photovoltaic systems much less uniform throughout the U.S. than electrical codes? Explain.
- 6.8 Give two examples of cases when the design loading for the photovoltaic array and structural supports is not dominated by wind loading.
- 6.9 What conditions must be satisfied before Bernoulli's equation can be used to relate the pressure and velocity between two points in the flow field? Does a photovoltaic array meet these conditions? Explain. Why is an understanding of the Bernoulli relationship important when considering wind loading on photovoltaic systems?
- 6.10 The design wind load calculation involves the product of the wind speed, a force coefficient and an importance factor. How is the design wind speed determined? If the force coefficient (i.e., fudge factor) cannot be derived analytically, how might it be determined experimentally? The importance factor is related to the consequences of failure—the greater the consequences, the higher the factor. How would the importance factor for a PV system on a rural home compare with the application in Problem 6.6?
- 6.11 List four objectives in designing an array mounting system.
- 6.12 For a fixed-orientation array to be mounted on a south-facing roof, discuss the advantages and disadvantages of each of the four roof-mounting configurations.
- 6.13 Using Figure 6.5, assume the sleeve is made of aluminum for which $\alpha = 12.8 \times 10^{-6} \text{ per } ^\circ\text{F}$ and $E = 10 \times 10^6 \text{ psi}$. The initial temperature at which there are no stresses is 59°F , and the final temperature is 200°F . All other dimensions, properties and information are the same as in the example for Figure 6.5. Compute the stresses in both the stainless steel bolt and the aluminum sleeve at 200°F .

- 6.14 Four lag screws of 5/16 in. diameter and 3.5 in. length are used to attach an 8 ft by 8 ft standoff array to an asphalt shingle roof. The total thread length is 2.5 in. and the combined thickness of the mounting bracket, pad, shingles, roof membrane and plywood sheathing is 1.0 in. If the lag screw penetrates into the roof truss made of Southern yellow pine, what is the allowable withdrawal load on each lag screw? What is the maximum uplift loading in psf that the array can withstand?
- 6.15 A four-module photovoltaic array has an area of 40 sq. ft. and will be secured using six mounting brackets. Each bracket uses two 5/16 in. lag screws to secure the standoff-mounted array. The roof trusses are made of white spruce. The design wind load is 55 psf. What is the minimum thread penetration for each fastener?
- 6.16 A standoff-mounted array has a surface area of 50 sq. ft. and is secured to an asphalt shingle roof with four steel J-bolts of 3/8 in. diameter. If the allowable tensile stress for the steel is 40,000 psi, are the J-bolts of sufficient strength to carry a maximum uplifting wind load of 65 psf? What is the factor of safety?
- 6.17 An array of four photovoltaic modules, each with an area of 10 sq. ft., is to be mounted above and parallel to a standing seam metal roof using 6 L-brackets. The modules themselves can withstand a load of 75 psf. If it is desired to support the 75 psf uplifting load on the full array with one lag screw in each bracket, and if each bracket has an allowable withdrawal resistance of 300 lb./in., what is the minimum thread length that must penetrate the roof truss?
- 6.18 Assume the ratio of direct to total irradiance is the same for two different locations, one at 30° north latitude and one at 60° north latitude. Which location would benefit the most from a two-axis tracking array (versus a fixed-orientation array)? Explain.
- 6.19 For more effective cooling of standoff-mounted photovoltaic arrays, would you recommend higher or lower aspect ratios? Explain.
- 6.20 A rack-mounted array similar to the one in Figure 6.22 is supported at the rear by two 4-ft. columns of 6063 T-6 aluminum tubing. The modulus of elasticity of the aluminum is 10×10^6 psi. The cross-sectional area is 0.5 in² and the radius of gyration is 0.361 in. What is the moment of inertia of the cross sectional area in units of in.⁴? Compute the critical buckling load, P.

References

- [1] Dieter, G. E., *Engineering Design: A Materials and Processing Approach*, 2nd Ed., McGraw-Hill, New York, 1991.
- [2] Hanks, R. W., *Materials Science Engineering: An Introduction*, Harcourt, Brace & World, New York, 1970.
- [3] Avallone, E. A. and Baumeister, T., Eds., *Marks' Standard Handbook for Mechanical Engineers*, 10th Ed., McGraw-Hill, New York, 1996.
- [4] Kutz, M., *Mechanical Engineers' Handbook*, 2nd Ed., John Wiley & Sons, New York, 1998.
- [5] Singer, F. L., *Strength of Materials*, 2nd Ed., Harper & Brothers Publishers, New York, 1962.
- [6] Clauser, H. R., Editor-in-Chief, *The Encyclopedia of Engineering Materials and Processes*, Reinhold Publishing, New York, 1963.
- [7] Larson, W. J. and Wertz, J. R., *Space Mission Analysis and Design*, 2nd Ed., Microcosm, Inc. and Kluwer Academic Publishers, Torrance, CA, 1992.
- [8] *Minimum Design Loads for Buildings and Other Structures*, ASCE Standard, SEI/ASCE 7-02, Revision of ASCE 7-98, American Society of Civil Engineers, Reston, VA, 2003.
- [9] Bertin, J. J. and Smith, M. L., *Aerodynamics for Engineers*, 2nd Ed., Prentice Hall, Englewood Cliffs, NJ, 1989.
- [10] Hurt, H. H., *Aerodynamics for Naval Aviators*, Navweps 00-80T-80, U.S. Navy, 1960.
- [11] Modular Photovoltaic Array Field, prepared for Sandia National Laboratories, SAND83-7028, Hughes Aircraft Company, 1984.
- [12] Miller, R. D. and Zimmerman, D. K., Wind Loads on Flat Plate Photovoltaic Array Fields, Phase II Final Report, prepared for Jet Propulsion Laboratory, Contract No. NAS-7-100-954833, Boeing Engineering and Construction Company, Seattle, WA, 1979.
- [13] Marion, B. and Atmaram, G., *Preliminary Design of a 15–25 kW_p Thin-Film Photovoltaic System*, prepared for the U.S. Department of Energy, Florida Solar Energy Center, Cape Canaveral, FL, November 13, 1987.
- [14] *Wind Design of Flat Panel Photovoltaic Array Structures*, prepared for Sandia National Laboratories, SAND79-7057, Bechtel National, Inc., June 1980.
- [15] Miller, R. D. and Zimmerman, D. K., Wind Loads on Flat Plate Photovoltaic Array Fields, Phase III and Phase IV Final Reports, prepared for Jet Propulsion Laboratory, Contract No. NAS-7-100-954833, Boeing Engineering and Construction Company, Seattle, WA, April 1981.
- [16] Ventre, G.G., *A Program Plan for Photovoltaic Buildings in Florida*, prepared for the Florida Energy Office/Department of Community Affairs and Sandia National Laboratories, Florida Solar Energy Center, Cocoa, FL, FSEC-PD-2 5-99, January 1999.
- [17] *Wood Handbook—Wood as an Engineering Material*, U. S. Department of Agriculture, Forest Service, Forest Products Laboratory, Madison, WI, 1999.
- [18] Faherty, K.F. and Williamson, T.G., *Wood Engineering and Construction Handbook*, 3rd Ed., McGraw-Hill, New York, 1997.

Suggested Reading

- Building Integrated Photovoltaic Project in the 21st Century Townhouses*, Advanced Housing Technology Program, National Association of Home Builders Research Center, Inc., Upper Marlboro, MD, June 1997.
- Epstein, S. G., *Aluminum and Its Alloys*, Aluminum Association, Inc., presented at the Annual Liberty Bell Corrosion Course, sponsored by the National Association of Corrosion Engineers, Washington, D.C., September 1978.
- Healey, H., An Investigation of the Feasibility of a National Structural Certification Process, Contract Report for the Solar Rating and Certification Corporation, Healey and Associates, Merritt Island, FL, September 25, 1998.
- Hollister, S. C., *The Engineering Interpretation of Weather Bureau Records for Wind Loading on Structures*, National Bureau of Standards, Washington, D.C., November 1970.
- IEEE Recommended Practice for Qualification of Photovoltaic (PV) Modules*, IEEE Standard 1262-1995, IEEE Standards Coordinating Committee 21 on Photovoltaics, Institute of Electrical and Electronics Engineers, Inc., New York, April 12, 1996.
- Manual of Steel Construction*, 8th Ed., American Institute of Steel Construction, Chicago, 1980.
- McCluney, W. R., *Introduction to Radiometry and Photometry*, Artech House, Inc., Norwood, MA, 1994.
- Mehta, K. C. and Marshall, R. D., *Guide to the Use of the Wind Load Provisions of ASCE 7-95*, ASCE Press, Reston, VA, 1998.
- Metal Roofing, *Roofer Magazine*, July 1997.
- Orlowski, H., Corrosion protection for solar systems: methods of eliminating an old problem applied to solar components, *Heat/Piping/Air Conditioning*, July 1976.
- Photovoltaic System Design*, Course Manual, Florida Solar Energy Center, Cocoa, FL, FSEC-GP-31-86, April 1996.
- Post, H. N., Low cost structures for photovoltaic arrays, *Proc. 14th IEEE Photovoltaic Specialists Conference*, San Diego, CA, January 7-10, 1980.
- Post, H. N. and Noel, G. T., A comparative evaluation of new low-cost array field designs for grid-connected photovoltaic systems, *Proc. 19th Intersociety Energy Conversion Engineering Conference*, San Francisco, CA, August 19-24, 1984.
- Roark, R. J., *Formulas for Stress and Strain*, McGraw-Hill, New York, 1954.
- Russell, M. C. and Kern, E. C., *Stand-Off Building Block Systems for Roof-Mounted Photovoltaic Arrays*, Sandia Contract 58-8796, Massachusetts Institute of Technology, December 1985.
- Shigley, J. E. and Mischke, C. R., *Mechanical Engineering Design*, 5th Ed., McGraw-Hill , New York, 1989.
- Sick, F. and Erge, T., Eds., *Photovoltaics in Buildings: A Design Handbook for Architects and Engineers*, International Energy Agency, Paris, 1996.
- Smith, W. F., *Principles of Materials Science and Engineering*, 2nd Ed., McGraw-Hill, New York, 1990.
- Stefanakos, E. K. et al., Effect of row-to-row shading on the output of flat plate south facing photovoltaic arrays, *Solar Engineering—1986* , American Society of Mechanical Engineers, Anaheim, CA, April 13-16, 1986.
- The Design of Residential Photovoltaic Systems*, SAND87-1951, Photovoltaic System Design Assistance Center, Sandia National Laboratories, Albuquerque, NM, December 1988.

Chapter 7

STAND-ALONE PV SYSTEMS

7.1 Introduction

This chapter will introduce the design process for several complete self-contained PV systems. For each system, a life-cycle cost analysis will be made for several design options to illustrate the iterative process that leads to reasonable system cost effectiveness. The first system will be a relatively simple refrigeration system, except that the system will be designed to meet a critical need. The second system will be another mountain cabin. In this chapter, the complete cabin system will be designed, including consideration of placement of the various loads and computation of the wire sizes needed to meet the needs of the loads. A hybrid residence will then be designed, with an emphasis on the process of selecting an appropriate mix of PV and propane electrical generation. This residence will use 120 V loads as opposed to the 24 V loads of the cabin and will thus require an inverter and a more interesting control system.

In any design, the first task is normally to determine the load. Often there are several choices. For example, a choice might be made between an inexpensive incandescent lamp and a more expensive fluorescent lamp. In the first example of this chapter, a comparison will be made among systems that use two different types of refrigerators. One uses a relatively inexpensive, but somewhat inefficient, unit. The other uses a more expensive, but more efficient, unit.

The load voltage, current and power are needed for proper sizing of fuses, wires, batteries and other system components. In some cases, not all these quantities are given. For example, the specifications for a refrigerator may only give the voltage and kWh per month, or Ah per day. In these cases, it may be necessary to either calculate or estimate the other parameters.

Once the load has been determined, then the amount of battery backup needs to be determined. Some systems will not need batteries, some will have minimal storage and some will require sufficient battery storage to meet critical performance requirements in which the system must operate more than 99% of the time. It will also be the responsibility of the engineer to determine whether to use batteries that require maintenance or to use maintenance-free batteries at nearly twice the initial cost.

After battery selection, the size of the PV array must be determined. Then the electronic components of the system, such as charge controllers and inverters are selected. Finally, the balance of system components are selected, including the array mounts, the wiring, switches, fuses, battery compartments, lightning protection and, perhaps, monitoring instrumentation.

As the design process is completed for each of the following systems, general design guidelines will be presented for later use. While computer programs may be available for system design, emphasis in this chapter will instead be placed on sound, common-sense reasoning and the use of good engineering judgment.

In order to keep the design examples as realistic as possible, many of the system components described in the examples of this chapter have been found on an assortment of web sites. It is important for the reader to note that the presumed use of a particular component or web site in an example does not constitute an endorsement of the component or the company. Vendors and component availability change on a daily basis, so when a real system is designed, the designer should carry out an extensive search for the components that best meet the design goals. Hopefully the procedures for component selection outlined in this chapter will prove to be useful when the opportunity to design a real system presents itself.

7.2 A Critical Need Refrigeration System

7.2.1 Design Specifications

It is desired to provide electric power for 10 cubic feet of refrigeration for storage of medication. The medication is costly and difficult to obtain, so the system must have 99% availability. The system will be located in a village in Angola where villagers will be able to keep a careful watch on system performance so any problems will become immediately evident.

7.2.2 Design Implementation

Two implementations will be explored concurrently. The first will use a standard, 10-cubic-foot, 120 V ac refrigerator. The second will use a 10-cubic-foot, high-efficiency 24 V dc refrigerator. The ac refrigerator costs \$338 and consumes 530 kWh per year. The dc refrigerator costs \$1515 and uses 12.5 Ah per day at 90°F, with an operating current of 2.3 A at 24 V. An ac refrigerator that costs \$1900 and uses 24 Ah per day is also available, but, since it would require an inverter that would increase the overall cost beyond the dc unit that uses slightly less energy per day, it will not be considered in this example [1].

Load Determination

The first task is to determine relevant parameters for comparing the units. Since the battery capacity will be determined in Ah, it makes sense to determine the load energy requirements in Ah. Multiplication by voltage gives actual energy in Wh for the purist who notices that Ah are not proper units for energy.

To convert 530 kWh per year to Ah per day, simply divide by 365 to get kWh per day, then multiply by 1000 to get Wh per day. Finally, since the refrigerator will be supplied by an inverter with a 24 V input, dividing by 24 yields the Ah per day. However, since the inverter is used, the inverter efficiency must be accounted for by dividing the Ah per day by the inverter efficiency. Except for pure sine inverters, most modern inverters will operate at close to 95% efficiency. Using a conservative 90% figure, the daily energy use of the ac refrigerator is determined to be 67.2 Ah per day.

At this point, it should be noted that there are energy losses in the system wiring. The *National Electrical Code®* requires that overall voltage drop in a system be less than 5%. A well-designed PV system, however, will keep voltage drop in the 2% range, since the added cost of wire is nearly always less than the cost of additional PV modules to supply power lost in wiring.

Determination of Average Daily PV System Load

1. Identify all loads to be connected to the PV system.
2. For each load, determine its voltage, current, power and daily operating hours. For some loads, the operation may vary on a daily, monthly or seasonal basis. If so, this must be accounted for in calculating daily averages.
3. Separate ac loads from dc loads.
4. Determine average daily Ah for each load from current and operating hours data. If operating hours differ from day to day during the week, the daily average over the week should be calculated. If average daily operating hours vary from month to month, then the load calculation may need to be determined for each month.
5. Add up the Ah for the dc loads, being sure all are at the same voltage.
6. If some dc loads are at a different voltage, which will require a dc-to-dc converter, then the converter input Ah for these loads needs to account for the conversion efficiency of the converter.
7. For ac loads, the dc input current to the inverter must be determined and the dc Ah are then determined from the dc input current. The dc input current is determined by equating the ac load power to the dc input power and then dividing by the efficiency of the inverter.
8. Add the Ah for the dc loads to the Ah for the ac loads, then divide by the wire efficiency factor and the battery efficiency factor to obtain the corrected average daily Ah for the total load.
9. The total ac load power will determine the required size of the inverter. Individual load powers will be needed to determine wire sizing to the loads. Total load current will be compared with total array current when sizing wire from battery to controller.

The power lost in the wiring is determined by the product of the current and the voltage drop. Depending on the nature of the load, a drop in voltage may result in either a drop or a rise in current. Normally the current will drop slightly, but, in some motors with constant loads, the current will rise. If the load is an MPT, the current will also rise if the voltage drops. However, for a voltage drop of only 2%, it is reasonable to assume the load current will remain essentially constant. With this assumption, the power loss can be approximated by the product of load current at nominal load voltage and the voltage drop. Hence, a 2% voltage drop implies a 2% power loss, or, in terms of Ah, a 2% Ah loss. This loss must be added to the PV array power output requirements. Thus, a 2%

voltage drop implies a wiring efficiency of 98%, and the load Ah per day must be increased by dividing by 0.98 to account for the wiring loss.

Finally, if a system contains battery storage, the losses encountered in charging and discharging the batteries must be accounted for. As long as the batteries are not discharged or charged at a rate higher than rated by the manufacturer for full capacity performance, a 10% loss for charge and discharge is a reasonable default choice. This means the system load must be divided by 0.9 to account for the additional energy loss in the batteries. Of course, for a system without batteries, this factor need not be applied.

In the present case, to account for wiring and battery losses, the *corrected load* daily energy use becomes $67.2 \div 0.98 \div 0.9 = 76.2$ Ah/day for the ac refrigerator system. For the dc refrigerator system, the *corrected load* becomes $12.5 \div 0.98 \div 0.9 = 14.2$ Ah/day. Note that the *corrected load* is the Ah that must be supplied to the batteries so the batteries can power the *connected load*, assuming batteries are used.

Battery Selection

In Chapter 3 it was observed that the number of days of autonomy required for critical need applications depends on the location of the system. In locations with relatively high average insolation, even during the worst part of the year, less storage is needed. The number of days of autonomy required for critical and noncritical system performance is tabulated for some locations [2]. If the minimum peak sun hours over the period of operation of the load is known for a location, the number of days of autonomy can be estimated from the following formulas from Chapter 3:

$$D_{\text{crit}} = -1.9T_{\min} + 18.3 \quad (7.1a)$$

or

$$D_{\text{non}} = -0.48T_{\min} + 4.58. \quad (7.1b)$$

where T_{\min} is the minimum peak sun hours for the selected system collector tilt during any month of operation and D represents the number of storage days required, either for critical or noncritical storage. Note that these formulas are only valid for minimum peak sun hours of about one hour per day. Obviously if the sun does not shine, more than 18.3 days of storage will be needed if the system is to run more than 18.3 days.

Annual peak sun hours for selected locations are given in Appendix A. Referring to the table for Luanda, Angola, it is evident that the best annual array performance is obtained with the array tilted at the latitude (8.82° south). Note that, in the Southern Hemisphere, this means the array faces north with a tilt of 8.82° above horizontal. This gives an average daily peak sun hours of 5.03 over the year. With this tilt, the minimum peak sun hours of 3.71 occurs in July. The minimum peak sun hours for the latitude- 15° tilt (see problem 7.1) is 3.36 in July, and the minimum peak sun hours for the latitude+ 15° tilt is 3.93 in July. A

closer inspection of the table shows that the latitude+15° tilt gives a better July performance than the latitude or latitude-15° tilts. Furthermore, the latitude+15° tilt has the least annual variation in peak sun hours. This will result in a minimum of wasted PV energy production.

Since the daily load of the system is nearly constant, with somewhat higher consumption on hotter days, it makes sense to choose the latitude+15° tilt for this system, since this tilt has the largest value for the minimum peak sun hours. Hence, $T_{\min} = 3.93$ hours, and $D_{\text{crit}} = 10.83$, or approximately 11 days of storage for critical operation.

The next design choice is to determine the type of batteries to use and the allowable depth of discharge. In a critical design, deep discharge batteries allowing 80% discharge are not unreasonable, since under most conditions, the batteries will not discharge nearly this amount. Hence, the battery life will be relatively long. The daily and seasonal discharge of the batteries will be explored after the system design is completed.

Sizing of the batteries must take into account the loss of capacity under conditions of low temperature, high rate of discharge or high rate of charge. Battery size is thus determined from

$$Ah = \left(\frac{Ah}{\text{day}} \right) \left(\frac{\text{days}}{D_T D_{\text{ch}} (\text{disch})} \right), \quad (7.2)$$

where Ah/day represents the *corrected load* on the batteries, days represents the number of days of autonomy, D_T is the temperature derating factor, D_{ch} is the charge/discharge derating factor and disch is the depth of discharge expressed as a fraction. In Section 3.5.2, it was noted that lead-acid battery capacity decreases at lower temperatures and higher discharge rates. Higher charge rates also can result in greater losses.

The capacity of a battery decreases as temperature decreases. For lead-acid batteries, the capacity reduction can be approximated by the following empirical relationship, for battery temperatures between 20 and 80°F.

$$D_T = \frac{C}{C_o} = 0.00575T + 0.54, \quad (7.3)$$

where C is the battery capacity at temperature T (in °F) and C_o is the rated battery capacity at 80°F [2].

If the anticipated load will exceed the specified discharge rate for more than 10 minutes, an additional correction factor should be applied to the total corrected Ah. For example, if the battery is rated at a discharge current of 20 amperes, and the actual discharge rate will be 30 amperes, then $D_{\text{ch}} = 20/30 = 0.67$. This factor reflects the fact that there are greater I^2R losses to the internal battery resistance as the current increases, thus decreasing the energy available from the batteries to power the load.

If the battery charge rate exceeds the rated charge rate, an alternate calculation of battery capacity should be performed and compared with (7.2). Lead-acid batteries are typically designed to take 10 hours from zero charge to full charge. Hence, if 10 hours times the PV charging rate in amperes exceeds the battery capacity in Ah calculated in (7.2), it means the PV array is capable of fully charging the batteries in less than 10 hours. If this condition should occur, the battery capacity should be determined by the product of the rated charging time and the available charging current, rather than by (7.2).

In the present case, the battery capacity required would be $14.2 \times 11 \div 0.8 = 195$ Ah for the dc refrigerator and would be $76.2 \times 11 \div 0.8 = 1048$ Ah for the ac refrigerator, assuming unity values for D_T and D_{ch} and $(disch) = 0.8$. Neither situation has a charging rate that will charge the batteries in less than 10 hours or a load that will discharge the batteries in less than 10 hours.

Once the battery capacity is determined, the number of batteries in parallel required for the system is determined by dividing the total capacity required by the capacity of a single battery. Normally this computation will result in a non-integral quantity. The system designer must then decide whether to round up, to round down or to use a different battery. When the system voltage requires batteries to be connected in series as well as in parallel, rounding up or down will involve more than one battery. For example, in a 48 V system, rounding up will show a need for 4 additional 12 V batteries or 8 additional 6 V batteries. The round-up or round-down decision should thus be made carefully.

The judgment as to whether to round up or to round down should be influenced by knowledge as to whether the user of the loads can cut back on use during cloudy periods to conserve battery charge. Another factor that will influence judgment is whether at least a small amount of charging can be anticipated during periods of prolonged overcast. Professional judgment by a qualified, experienced engineer in these situations may result in savings in system cost over a system for which a computer has made the decision using unknown criteria hidden somewhere in the program. Many good PV system sizing programs are available, but the final system should always be checked by the design engineer to be sure it makes good technical and economic sense.

Batteries come in many shapes, sizes and types. Probably the first decision to make when specifying batteries is whether the owner is capable of maintaining the batteries, since maintenance-free batteries are nearly twice as expensive as flooded lead-acid batteries that require periodic testing and watering. One particular battery is a 6 V, 350 Ah flooded lead-acid unit that costs \$198 and has a life expectancy of 5 to 8 years. To obtain 195 Ah storage at 24 volts requires four of these batteries, at a cost of \$792. To obtain 1048 Ah of storage at 24 volts would require 12 of these batteries, at a cost of \$2376.

Another of the many available batteries is a 6 V, 220 Ah flooded lead-acid, deep-discharge, golf cart battery that sells for \$85 and has a 5-year life expectancy. For the 195 Ah system, four batteries are required at a cost of \$340. For

the 1048 Ah system, 20 batteries are required at a cost of \$1700. The next step is to determine which battery is a better choice.

To determine which battery is a better economic choice, it is not acceptable simply to look at the first cost. The design engineer needs to explore the life-cycle cost of the battery system. In the case of the 350 Ah unit, it is reasonable to assume an 8-year lifetime for the batteries. As a result, for a system with a 20-year lifetime, these batteries will need to be replaced only at year 8 and at year 16. The 220 Ah batteries will need to be replaced at years 5, 10 and 15. The engineer must thus estimate the average inflation rates and discount rates that will exist over the next 16 years. Using a wild guess of a discount rate of 5% and an inflation rate of 3%, a life-cycle cost analysis can be performed on the batteries, as shown in Table 7.1. The reader may wish to take a quick look at the formulas obtained in Chapter 5 for present worth, which will be used for life-cycle cost analysis in this chapter. For the PW values in Table 7.1, (5.3) is used. With the assumed values of d and i , the resulting PW formula becomes

$$PW = C_o(0.981)^n .$$

Table 7.1 Life-cycle cost analysis for 220 Ah, 5-year lead-acid batteries compared with 350 Ah, 8-year lead-acid batteries for the ac refrigerator system (1048 Ah @ 24 V).

Time	220 Ah	220 Ah PW	350 Ah	350 Ah PW
Initial Purchase	\$1,700	\$1,700	\$2,376	\$2,376
5-year replacement	1,700	1,545		
8-year replacement			2,376	2,038
10-year replacement	1,700	1,403		
15-year replacement	1,700	1,275		
16-year replacement			2,376	1,748
TOTAL LCC		\$5,923		\$6,162

Additional factors to consider when selecting batteries include the additional connections required when using larger numbers of batteries and the corresponding additional time required for installation and maintenance. Furthermore, the more connections, the greater the possibility of failure of a connection and the cost of battery cables is not negligible. On the other hand, with a smaller number of batteries, if one should fail, the system is impacted more significantly than in the case of a larger number of batteries. The weight of the battery and the difficulty of obtaining the battery may also be considered. For example, it is unlikely that the batteries for a system in Angola will be shipped from California. A local supplier with the ability to provide timely delivery and warranty service is generally more desirable. All things considered, the 350 Ah units will probably be a better choice for this system if the ac refrigerator is chosen. The choice of either of these batteries, of course, will depend upon whether someone is available to perform routine maintenance on the batteries.

Battery Selection Procedure

1. Determine the number of days storage required, depending on whether the load will be noncritical or critical. The designer may use discretion for special cases such as weekend occupancy or seasonal variations. It is possible that different seasons may have different numbers of storage days.
2. Determine the amount of storage required in Ah. This is the product of the corrected Ah per day and the number of days of storage required. This amount may vary with season. If so, list all values.
3. Determine the allowable level of discharge. Divide the required Ah by the level of allowed discharge, expressed as a fraction. For example, using 80% of total charge requires dividing by 0.8. This result is the total corrected Ah required for storage.
4. Check to see whether an additional correction for discharge rate will be needed. If so, apply this correction to the result obtained in (3).
5. Check to see whether a temperature correction factor is required. If so, apply this to the result of (3) or (4).
6. Check to see whether the rate of charge exceeds the rate specified by the battery manufacturer. If so, multiply the charging current by the rated number of hours for charging. If this number is larger than the result of (7.2), use this as the required battery capacity.
7. Divide the final corrected battery capacity by the capacity of the chosen battery. The result may be rounded up or down, depending on the judgment of the system designer. Often the result can be rounded down, provided that the system receives at least some diffuse sunlight over prolonged overcast periods.
8. If more than four batteries are required in parallel, it is generally better to consider higher capacity batteries to reduce the number of parallel batteries to provide for better balance of battery currents.

Array Sizing and Tilt

After the corrected system load in Ah has been determined for each month of the year, the PV array can be sized. Choosing an adequate number of modules without choosing more than needed to meet system requirements depends upon knowledge of average insolation conditions at the site for the months during which the system will be in use. The procedure involves determining the proper tilt to minimize the system design current and then selecting an appropriate module such that a reasonable number of modules in parallel will provide the system design current. Additional series modules may be needed if the system voltage is higher than 12 volts, depending on the module output voltage.

To determine the system design current, the corrected system load is calculated for each month of the year. It is then good practice to compute the result-

ing system design current for each month at tilt angles of latitude- 45° , latitude, and latitude+ 15° . Table 7.2 shows this calculation for the dc refrigerator in Angola, with the assumption that the corrected load is the same for all months of the year. The calculation for the ac refrigerator follows the same procedure except that the corrected load Ah per day for the ac refrigerator is used. Problem 7.6 offers the reader the opportunity to perform this calculation.

To determine the optimum design current from Table 7.2, first observe that for each array tilt, there is a maximum and a minimum value for the design current. Since the system must work under the worst of conditions, the maximum design current must be chosen for each tilt as the necessary design current. This is the amount of current that must be supplied by the PV array. Hence, if the tilt at latitude is selected, the design current will need to be 3.83 A in order to meet system load requirements in July. This also means that during the best month of the year, February, only 2.42 A is needed for design current, so the remaining current capability is wasted unless it can be put to another use. The excess current during the months with higher peak sun hours confirms the need for a charge controller to keep the batteries from being overcharged.

Table 7.2 Calculation of the design array current and array tilt for the dc refrigerator in Angola.

Mo	Corr load	Lat- 45° hr/day	Lat- 45° A	Lat hr/day	Lat A	Lat+ 15° hr/day	Lat+ 15° A
Jan	14.20	5.92	2.40	5.56	2.55	4.94	2.87
Feb	14.20	6.07	2.34	5.87	2.42	5.40	2.63
Mar	14.20	5.43	2.62	5.49	2.59	5.30	2.68
Apr	14.20	4.89	2.90	5.19	2.74	5.27	2.69
May	14.20	4.60	3.09	5.11	2.78	5.42	2.62
Jun	14.20	4.18	3.40	4.75	2.99	5.14	2.76
Jul	14.20	3.36	4.23	3.71	3.83	3.93	3.61
Aug	14.20	3.70	3.84	3.95	3.59	4.04	3.51
Sep	14.20	4.57	3.11	4.68	3.03	4.60	3.09
Oct	14.20	5.06	2.81	4.97	2.86	4.66	3.05
Nov	14.20	5.60	2.54	5.31	2.67	4.77	2.98
Dec	14.20	6.16	2.31	5.72	2.48	5.02	2.83

For the latitude- 45° tilt, the design current will be 4.23 A and for the latitude+ 15° tilt, the design current will be 3.61 A. Comparing the worst-case design currents for the three tilt angles, the smallest of the three currents is 3.61 A, which is obtained at the tilt of latitude+ 15° . Since this current will meet the system needs for all months of the year, even though it will not result in as much excess for the best month, this choice will require the minimum number of PV modules for the array and is consistent with storage calculations.

As a further exercise in array sizing, it is interesting to explore the requirements if the tilt of the array can be varied monthly or seasonally. From Table 7.2, a tabulation can be made of optimum tilt angle for each month of the year and the corresponding system design current. The result is shown in Table 7.3.

Table 7.3 Optimizing array performance by adjusting monthly tilt angles.

Mo	Jan	Feb	Mar	Apr	May	Jun
Tilt	-15	-15	0	+15	+15	+15
Hr/day	5.92	6.07	5.49	5.27	5.42	5.14
A	2.40	2.34	2.59	2.69	2.62	2.76
Mo	Jul	Aug	Sep	Oct	Nov	Dec
Tilt	+15	+15	0	-15	-15	-15
Hr/day	3.93	4.04	4.68	5.06	5.60	6.16
A	3.61	3.51	3.03	2.81	2.54	2.31

In this particular case, no saving in modules is possible, since the worst case has already been taken into account. However, if the leftover electricity generated by the PV array is put to another use, then monthly adjustment of the array tilt will provide more energy for other uses. For systems where the average load Ah varies on a monthly basis, however, this analysis may indicate cost savings by manually adjusting the array tilt either monthly or seasonally.

It may also be desirable to explore the possibility of using a tracking array mount. For a two-axis tracking array mount, the minimum peak sun hours becomes 5.14 for July. This would result in a design array current of 2.76 A, which is 0.85 A less than the design current of the nontracking system. This difference may enable the use of a module with a smaller current, so the question then is whether the added cost of the tracking mount will justify its use.

The number of modules for the system is determined by dividing the array design current by the current available from a selected module, after correcting for module degradation from aging or dirt accumulation. The derated design current of the array is the design current divided by a degradation factor, which is commonly about 0.9. Selection of modules will depend on requirements for module current and voltage at maximum power output as well as module short-circuit current and open circuit voltage. Normally, it is desirable to select a module such that the quotient of the derated design current and the module current at maximum power output will be close to an integer. If the quotient, for example, is between 3.9 and 4.1, it is easier to decide to select 4 modules than if the quotient is 3.5 or 4.5. Whereas rounding down is often possible with batteries, rounding up is generally more appropriate for PV modules.

In some cases, especially where low light or high temperature performance is desired, the designer must examine the module output curves under a range of light intensity and a range of temperature to be sure the module will have adequate output under anticipated adverse operating conditions. Note that rated module current is at the maximum power point. Usually the operating voltage of the system will be below the maximum power point voltage, so with adequate illumination, the current will be somewhere between the rated value and the short-circuit value.

For the dc refrigerator load, with a derated design current of $3.61 \div 0.9 = 4.01$ A, use of a module with a rated current of 4.4 A results in a requirement of 2

modules in series. For the dc refrigerator with two-axis tracking array mount, the derated design current is $2.76 \div 0.9 = 3.07$ A, or 2 modules in series, using modules rated at 50 W maximum power each.

The ac refrigerator, on the other hand, ends up with a fixed array design current of $76.2 \div 3.61 = 21.1$ A, which leads to a derated design current of 23.5 A. Using the 4.4 A modules in a fixed array results in the need for 10.66 modules, which rounds up to 12 modules—6 parallel sets of 2 series modules.

From a first cost perspective, if the cost of a 4.4 A module is listed as \$350, the array cost for the dc refrigerator with no tracking is \$700. If the cost of the 3.07 A module is \$250, then the array cost for the tracking configuration is \$500. For the ac nontracking case, the array cost is \$4200, assuming the use of 4.4 A modules in the array.

Array Sizing and Tilt Procedure

1. Determine the design current for each month of the year by dividing the corrected Ah load for the system each month by the monthly average peak sun hours at each array tilt angle.
2. Determine the worst-case (highest monthly) design current for each tilt angle.
3. For a fixed mount, select the tilt angle that results in the lowest worst-case design current.
4. If tracking mounts are considered, then determine the design current for one- and two-axis trackers. Note that the one-axis tracker tracks from east to west and needs to have its design currents checked for the three angles of fixed trackers.
5. Determine the derated array current by dividing the design current by the module derating factor.
6. Select a module that meets the illumination and temperature requirements of the system as well as having a rated output current and voltage at maximum power consistent with system needs.
7. Determine the number of modules in parallel by dividing the derated array current by the rated module current. Round up or down as deemed appropriate.
8. Determine the number of modules in series by dividing the nominal system voltage by the lowest anticipated module voltage of a module supplying power to the system. In this case, it is almost always necessary to round up.
9. The total number of modules is the product of the number in parallel and the number in series.

The cost of a mount for 2 modules is about \$200, while a mount for 12 modules is approximately \$600. A two-axis tracking mount for 2 modules will cost

approximately \$500. The overall first cost of array plus mount is thus relatively close for the dc refrigerator case. The choice becomes contingent on the judgment of the engineer as to whether the nontracking system or the tracking system will be more reliable over the life of the system.

Controller, Inverter and/or dc:dc Converter Selection

The dc refrigerator will require a battery charge controller as a part of the system and the ac refrigerator will require both controller and inverter to 120 V ac. Selection of any of these components is affected by the number of bells and whistles the designer feels the item should have. Many of these optional features were discussed in Chapter 3.

In the present case, relatively simple controllers are preferred because complexity sometimes leads to reliability problems. The controller must be capable of handling the battery charging current from the array as well as the current to the load. Inverters and converters need to be able to handle starting/surge currents of the loads they service. In this case, the dc refrigerator system will work fine with a simple \$100 controller, whereas the ac system will require a larger controller at a cost closer to \$200.

For a motor-driven appliance, the designer must determine whether the motor will be damaged by dc or by harmonics. Each can cause heating of the motor above its rated operating temperature. If so, the inverter must be selected to have dc and harmonic content below the limits allowed by the motor. The cost of a suitable inverter for the ac refrigerator will be about \$125.

Wire, Fuse and Switch Selection

Proper wire sizing depends on the current to be carried by the wire, but, at low voltages, primarily on the length of the wire and the resulting voltage drop. It is generally useful to lay out the system and then tabulate the lengths of the various wire runs along with the allowable voltage drops. This enables a simple calculation of the required resistance per 1000 feet of wire to keep the wire voltage drop within allowable limits. Once the resistance per 1000 feet is known, the proper wire size can be selected. The correct wire size is the larger of either the size needed to carry the rated current or the size needed to meet system voltage drop constraints.

To determine wire sizes for the array, it is necessary to recognize that under certain unusual conditions, it is possible for the reflection from cloud to focus the sunlight on an array. This phenomenon requires that the wire be able to carry the array current as enhanced by cloud focusing. To allow for cloud focusing, the array short-circuit current is multiplied by 1.25 to obtain the maximum current from array to controller. This maximum array current is then multiplied by another factor of 1.25, as required by the *NEC* for continuous operation, and wire sizes are then chosen to meet this ampacity requirement. The wiring of PV source circuits and PV output circuits must thus be capable of carrying 156% of the short-circuit current of either the source circuit or output circuit, whichever is

applicable. In later examples, operation of the wiring at elevated temperatures and/or with more than three current-carrying conductors in conduit and the resulting derating required, will also be considered.

Module manufacturers specify the value of the fuse to be installed in series with the module, and the specified value is generally very close to $1.25 \times 1.25 \times I_{SC} = 1.56 \times I_{SC}$. It is then necessary to check that the wire size is adequate to carry the fuse current. This may not be the case for short runs of wire selected on the basis of voltage drop considerations. The wire size should be increased to carry 125% of the maximum current expected, whether it is from array to controller, controller to battery or from controller to loads.

All fuses or circuit breakers used must be rated for dc use if they are to be used on dc. Fuses or circuit breakers in the line to the battery system must be located close to the batteries in order to provide protection to both the batteries and the wiring from battery to controller. Since short-circuit battery currents may exceed 5,000 A, battery overcurrent protection must have high interrupting capacity. Fuses in other lines are normally located at or near the controller.

Switches must also be capable of carrying the maximum current of any wiring. Furthermore, they must be rated for use with either ac or dc, whichever the application. They must also have an adequate voltage rating to be able to interrupt the circuit if the load is inductive. Inductive situations produce high voltages across the switch contacts when the current is suddenly interrupted.

Table 7.4 summarizes the wire, switch and fuse needs of the dc refrigerator system. Wire sizes are obtained from Table 3.7. Wire sizes are chosen to limit voltage drops to 2%. Note that the NEC does not allow wire sizes smaller than #14 for permanent wiring. The array-to-controller fuse protects the modules, whereas the other fuses protect the wiring.

Table 7.4 Summary of wire sizes and fuse sizes for dc refrigerator system.

Wire Location	Max A	One-Way Length ft	System Volts	Max Allow R, Ω	Wire Ω/kft	Wire Size	Fuse Size, A
Array to controller	6.0*	40	24	0.0800	1.000	#8	8
Batteries to controller	6.0	6	24	0.0800	6.667	#14	15
Controller to refrigerator	2.3	8	24	0.2087	13.04	#14	15

*This current is 125% of the module I_{SC} . For the 4.4A module, $I_{SC} = 4.8$ A.

Balance of System Component Selection

At this point, most of both systems have been specified. Remaining system parts will typically include a container for the batteries and sometimes, conduit, plugs and receptacles, fuse holders, surge protectors, ground rods, wire connectors, terminal lugs, etc. Depending on whether the batteries are vented or sealed, the construction of the battery compartment may be affected. The cost of BOS components will typically be about 10% of the cost of the array, depending on

whether any unusual components are needed. A more detailed analysis of BOS selection will be included in the next design example.

At this point, the two systems have been specified in sufficient detail to enable a life-cycle cost analysis. The analysis will then be completed with the block diagrams for the systems.

Life-cycle Cost Analysis

The life-cycle costs of the two refrigerator systems can now be compared. The analysis is presented in Table 7.5, using a discount rate of 5% and an inflation rate of 3%. Note that the 220 Ah battery is used for the dc refrigerator system while the 350 Ah battery is used for the ac refrigerator system, as suggested by the battery life-cycle cost analysis for the ac refrigerator. Since the 350 Ah battery far exceeds the dc system storage needs, the 220 Ah unit is used instead.

Table 7.5 Life-cycle cost comparison for dc and ac refrigerator systems.

Item	dc Refrigerator System			ac Refrigerator System		
	Cost	PW	% Tot LCC	Cost	PW	% Tot LCC
Capital Costs						
Array	\$700	\$700	14.0	\$4,200	\$4,200	31.8
Batteries	340	340	6.8	2376	2376	18.0
Array Mount	200	200	4.0	600	600	4.5
Controller	100	100	2.0	200	200	1.5
Inverter				125	125	0.9
BOS	150	150	3.0	175	175	1.3
Installation	250	250	5.0	300	300	2.3
Refrigerator	1515	1515	30.2	325	325	2.5
Subtotal		\$3,255	64.9	\$8,301	\$8,301	62.9
Operation & Maintenance						
Annual inspect	50	833	16.6	50	833	6.3
Replacement						
Battery yr 5	340	309	6.2			
Battery yr 8				2376	2038	15.5
Battery yr 10	340	281	5.6			0.0
Battery yr 15	340	255	5.1			
Battery yr 16				2376	1748	13.3
Controller yr 10	100	83	1.7	200	165	1.3
Inverter yr 10				125	103	0.8
TOTAL LCC		\$5,016	100		\$13,188	100

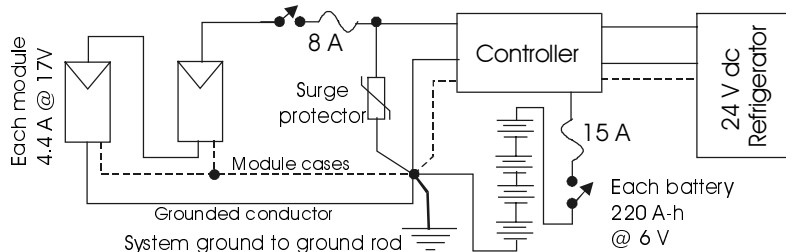
Present worth factors are obtained using the formulas from Chapter 5. A quick glance shows that the investment in the more expensive dc refrigerator results in an overall lower system cost.

It is interesting to note that the dc system has both lower capital costs as well as lower component replacement costs. In fact, it is likely that the ac refrigerator may also need replacement in less than 20 years. However, the PW of another ac refrigerator after 10 years adds only \$268 to the system LCC, so even if the ac refrigerator should fail, since it contributes only 2.5% of the LCC of the system, its replacement cost is relatively insignificant.

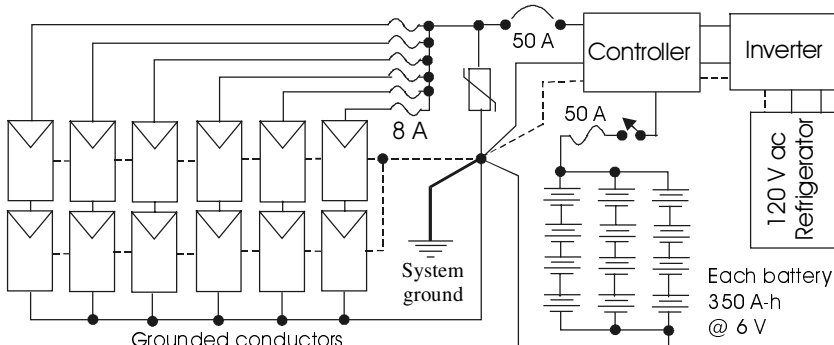
Total System Design

At this point, all system components have been selected for both refrigerator systems. It is now possible to look at the overall system design by developing system block diagrams to show the relationships of the components. Figure 7.1 shows block diagrams of both systems. Note that the controller and inverter are shown as separate units, although they could be combined into a single unit.

Since the maximum system voltage of both systems is below 50 V, grounding of the wiring is optional for systems wired in accordance with the *NEC*. However, if the system is left ungrounded, then disconnect switches must open all ungrounded conductors. It is thus generally better to establish a single point where the *grounded conductor* is connected to the *grounding conductor*. The grounded conductor carries current and is normally chosen as the negative con-



a. 12 V dc refrigerator system



b. 120 V ac refrigerator system

Figure 7.1 Block diagrams of dc and ac refrigerator systems.

ductor of the PV system. The grounding conductors do not carry current, and are used for the purpose of connecting all exposed metal system parts to ground to protect against shock hazards. As long as the grounded and grounding systems are connected at only one point, current will not flow in the grounding conductors under conditions of normal operation. Grounding conductors are shown along with the single point of connection between grounded and grounding conductors. Sizing of grounding conductors will be considered in later examples.

The ac refrigerator system schematic diagram shows the fuses in individual PV source circuits as well as a circuit breaker in the PV output circuit. In a typical installation, all the source circuit fuses as well as all the source circuit grounded conductors are run to a combiner box that houses the fuses and a busbar for connecting the grounded conductors. This busbar ensures that if the grounded conductor from one source circuit is disconnected, the grounded conductors of the other source circuits will remain connected, as required by the *NEC*. The fuses are in special holders that allow a fuse to be removed without coming in contact with either end of the fuse, since both ends of the fuseblock will be energized. Fuses and disconnects should also be included at the controller output, but are not shown in Figure 7.1.

The single grounding point is usually a terminal block with multiple set screw terminations for connecting grounded and grounding conductors. In systems that require a ground fault detection and interruption device (GFDI), the grounded conductors will generally terminate at one terminal block and the grounding conductors will terminate at a separate terminal block. The two blocks are then connected to each other through the trip mechanism of the GFDI device. Any current flowing through the GFDI device would indicate that more than one point of the grounded system is connected to the grounding system.

As a final note, the wiring of the batteries is purposely shown to have the positive and negative battery system cables diagonally opposite each other to provide for balancing of battery currents. This hookup is explored in more detail in Section 7.6.

7.3 A PV-Powered Mountain Cabin

7.3.1 Design Specifications

Figure 7.2 shows the floor plan of the cabin, located west of Denver, CO, to be outfitted with PV-powered electrical loads. The cabin will have a kitchen light, a dining room light, a light in each bedroom, a bathroom light, a living room light, a motion sensor light outside the door, a ceiling fan in each bedroom, a deep-well-water pump and a 16-cubic-foot refrigerator/freezer. The PV array will be located approximately 10 feet from the back of the cabin as shown. The 200-foot-deep well will be located 30 feet from the cabin in the same relative direction. The pump will be a submersible unit, so the total distance to the pump will be 230 feet. Provision is made for the addition of a future entertainment center when a desirable 24 V unit becomes available, or when the decision is

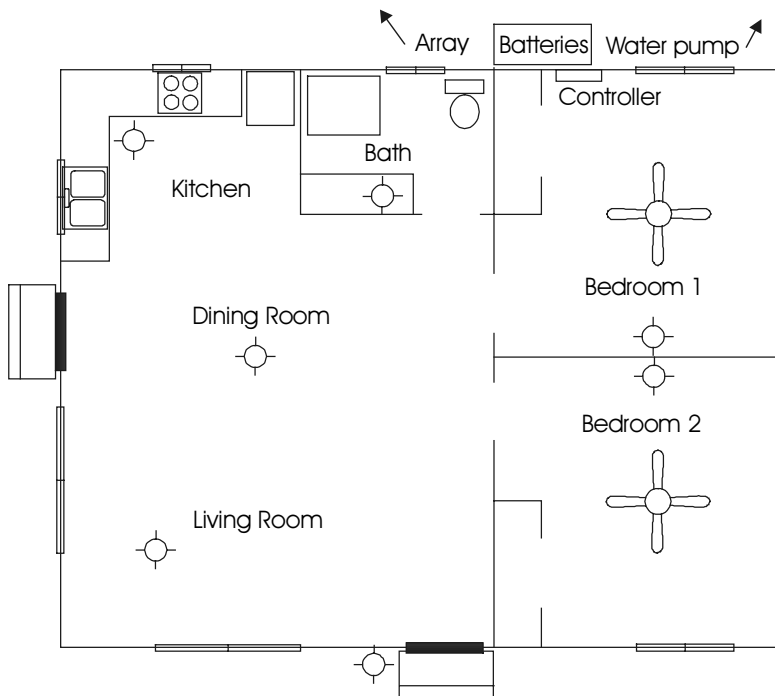


Figure 7.2 Mountain cabin floor plan and electrical layout.

made to incorporate either a 24-to-12 V dc/dc converter or a 24-to-120 V inverter to power the center.

The system loads, with the exception of the refrigerator, will operate 3 days per week to accommodate weekend use over long weekends. The refrigerator will be left on continuously in order to prevent inadvertent odor build-up in the event it should get too warm inside the unit. At least this is the stated reason. It is highly suspected that the real reason is to have cold beer ready as soon as someone arrives at the cabin.

7.3.2 Design Implementation

Design Considerations

In the recent past, stand-alone cabin systems have been designed around a 12-volt system voltage, since many 12-volt appliances and lights were on the market for use in recreational vehicles. Recently, however, 24 V dc fluorescent lights have reached the market, and 24 V water pumps, refrigerators and ceiling fans are also now available [1, 3, 4]. The PV array will be rack mounted at ground level, so the feasibility of seasonal adjustment of array tilt will be explored as a means of optimizing system performance. Also, maintenance-free,

valve-regulated lead-acid batteries will be used as a part of keeping system maintenance to an absolute minimum.

Load Determination

At this point, it should be abundantly clear that the only reasonable choice for the refrigerator/freezer will be a high efficiency dc unit. Perusal of a dc refrigerator vendor web site [1] leads to a 24 V unit that uses approximately 20 Ah/day in the winter and 25 Ah/day in the summer at a cost of only \$2419.

For the water pump, it is first necessary to determine the water needs for the cabin. This determination can be quite a wild guess unless the uses of the water are reasonably well defined. Assuming the only means of heating water is a propane stove, it is reasonable to assume that showers will not be too lengthy. However, if a solar water heater is added later, shower length may increase. A reasonable estimate for water usage might be 40 gallons per day per person, with anticipated occupancy of 4 persons. This equates to a total water requirement of 160 gallons per day. If more people use the cabin, it may be necessary to do some water rationing. In the worst case, where drinking is the only use made of the water, 160 people would still have a gallon each per day for drinking over the 3-day weekend. It is assumed that less water is used in winter, spring and fall than the 160 gallons per day of summer use.

The next step is to go to the manufacturers' catalogs or to the internet. For example, [3] and [4] list a number of different water pumps. It is not likely that a low-horsepower pump at the surface of the well will be able to lift water a distance of 200 feet on the suction side of the pump, even though it may be able to lift water this distance on the pressure side. For deep wells, normally a submersible pump is the best choice.

The first check to make on a pump to be used in a system with battery storage is whether it can pump the needed water in either a day or a week. If the pump pumps the needed water in a day, then only a 160 gallon storage tank will be needed. If it takes all week to pump the water for the weekend, then a 480 gallon storage tank will be needed. The pumping power, and, hence, the voltage and current of the pump motor, will depend on the flow rate and the lift distance. If the top of the storage tank is 10 ft above ground to provide pressure for the system, and, allowing for 5% piping losses, the equivalent lift for the pump will be $210 \times 1.05 = 220.5$ ft.

Suppose two pumps are considered. One pump will overcome a 220 ft head at 0.94 GPM when supplied with 24 V dc at a current of 4.21 A. The cost of this pump is \$604. The other pump, costing \$590, will pump 1.03 GPM @ 24 V dc and 3.85 A. The relative efficiencies of the two pumps can be determined by looking at the quotient of pumping rate to power consumed, or, since both run at the same voltage, the quotient of pumping rate and operating current. For the first pump, this ratio is 0.223, and for the second pump, the ratio is 0.268. Hence, from an efficiency perspective, the second pump is 20% more efficient.

Since a typical shower flow rate is 3 GPM, neither will be adequate for a shower, so storage will be needed. So, which is a better choice?

To answer this question for this particular application, the wire required, pump lifetime and maintenance requirements should also be considered. For the same wire size, the pump that draws 3.85 A over the 230 ft distance from the pump at the bottom of the well to the cabin will have less voltage drop than the 4.21 A pump. Thus, assuming equal maintenance costs for the pumps and equal lifetimes, the less expensive, 3.85 A pump will still be the better choice for this particular application.

To overcome the occasional hot, stuffy summer night, a dc ceiling fan is selected for each bedroom. The cost of the fan and a controller is \$178 each. The fan controllers draw 0.4 A at 24 V on high speed.

Table 7.6 Summary of monthly variation in weekly Ah loads for mountain cabin.

Load Description	Cost \$	P watts	Nov-Feb		Mar	
			Hr/ week	Ah/ week	Hr/ week	Ah/ week
Kit Light	26	30	12	15.00	10.5	13.13
BR 1 Light	30	16	6	4.00	4.5	3.00
BR 2 Light	30	16	3	2.00	3	2.00
LR Light	25	8	15	5.00	12	4.00
Fr Dr Light	48	16	1.5	1.00	1.5	1.00
DR Light	26	30	12	15.00	9	11.25
Bath Light	30	16	6	4.00	6	4.00
Refrigerator	2419	80	35	116.67	38.5	128.33
Water Pump	590	92.4	4	15.40	5	19.25
BR 1 Fan	178	9.6	0	0.00	0	0.00
BR 2 Fan	178	9.6	0	0.00	0	0.00
Entertainment	???	50	9	18.75	8	16.67
TOTALS		373.6		178.1		202.63
		Apr, Oct		May, Sep		Jun, Jul, Aug
Load Description	Hr/ week	Ah/ week	Hr/ week	Ah/ week	Hr/ week	Ah/ week
Kit Light	10.5	13.13	7.5	9.38	9	11.25
BR 1 Light	4.5	3.00	3	2.00	3	2.00
BR 2 Light	3	2.00	3	2.00	3	2.00
LR Light	9	3.00	6	2.00	6	2.00
Fr Dr Light	1.5	1.00	1.5	1.00	1.5	1.00
DR Light	7.5	9.38	6	7.50	4.5	5.63
Bath Light	5	3.33	4	2.67	3	2.00
Refrigerator	38.5	128.33	42	140.00	45.5	151.67
Water Pump	6	23.10	7	26.95	8	30.80
BR 1 Fan	3	1.20	8	3.20	24	9.60
BR 2 Fan	3	1.20	8	3.20	24	9.60
Entertainment	7	14.58	6	12.50	5	10.42
TOTALS		203.25		212.39		237.96

The remaining loads are lighting loads for each room of the cabin. Since fluorescent lights have three to five times the luminous efficacy of incandescent lights, 24 V dc fluorescent fixtures will be used throughout the cabin. Table 7.6 summarizes the average monthly variation in loads for the cabin. For each load, the average Ah/week if the load operates for n hours per day and d days per week is determined by

$$\frac{\text{Ah}}{\text{week}} = \frac{Pnd}{\eta V} , \quad (7.4)$$

where P is the load power, η is the conversion efficiency of any inverter or dc to dc converter needed to supply the load with any voltage other than the system voltage and V is the system voltage. The entries in Table 7.6 are based on 3 days per week of usage for all loads except the refrigerator, which remains on for 7 days per week and the water pump, which will pump 7 days per week, if necessary, to keep the storage tank full. The pump is controlled by a float switch in the storage tank.

It is important to note that the average Ah/week represent the weekly average, taking into account that the water pump and the refrigerator may run 7 days per week, but the other loads are only operational for 3 days per week while the cabin is occupied. The array and batteries will thus be selected to meet the average weekly system corrected loads.

The next step is to compute the system corrected loads. Using a 98% wire efficiency factor and a 90% battery efficiency factor, the corrected Ah loads for each month are obtained by dividing the load Ah/week by 0.98×0.9 . The corrected loads are shown in Table 7.7.

Table 7.7 Corrected weekly Ah loads for cabin after accounting for wire and battery losses.

Nov, Dec, Jan, Feb	Mar	Apr, Oct	May, Sep	Jun, Jul, Aug
202	230	230	241	270

Battery Selection

Since the batteries need to hold sufficient charge to power the cabin loads for a week, the batteries will not discharge in less than 10 hours. In addition, since the batteries will take a week to charge fully, the charge rate will also not be excessive. Thus, the charge and discharge derating factors will both be unity.

The factors that affect battery selection in this case are the monthly variation in average daily energy use and the monthly temperature variation of the batteries. In winter months the batteries will be colder, even though they will be in an insulated enclosure. Table 7.8 shows the calculation of required battery capacity on a monthly basis for the fluorescent-based system. It is assumed that a deep-discharge unit will be chosen with a maximum depth of discharge of 80%. Once the total battery capacity is determined, a battery can be selected that has a capacity close to an integral divisor of the total capacity. In this case, a 180 Ah,

12 V, 8-year lifetime sealed lead-acid battery costing \$300 is a reasonable choice, as indicated by the ratio of total capacity to battery capacity.

Table 7.8 Determination of system battery capacity.

Month	Jan	Feb	Mar	Apr	May	Jun
Ah/week	202	202	230	230	241	270
Temp Derate	0.80	0.80	0.85	0.90	0.95	1.00
Total Cap	316	316	338	319	317	338
# Batt	3.51	3.51	3.76	3.54	3.52	3.76

Month	Jul	Aug	Sep	Oct	Nov	Dec
Ah/day	270	270	241	230	202	202
Temp Derate	1.00	1.00	0.95	0.90	0.85	0.80
Total Cap	338	338	317	319	297	316
# Batt	3.76	3.76	3.52	3.54	3.30	3.51

The total battery capacity calculation uses (7.2) and (7.3) with the temperature derating factor as the only derating factor less than unity. The temperature derating factor is based on assumed average monthly battery operating temperatures. A check of battery requirements for each month leads to the conclusion that four batteries are needed at a total battery cost of \$1200. Note that if flooded lead-acid batteries were acceptable for this system, the battery requirements could be met by four 350 Ah @ 6 V, flooded lead-acid batteries at a total cost of \$653, confirming the earlier statement that maintenance-free batteries are approximately twice as costly as batteries that require maintenance.

Table 7.9 Determination of optimum design current and array tilt angle.

Month	Corr Load Ah/wk	Latitude-15°		Latitude		Latitude+15°	
		Hr/day	A	Hr/day	A	Hr/day	A
Jan	202	4.32	6.7	5.07	5.7	5.51	5.2
Feb	202	4.94	5.8	5.54	5.2	5.81	5.0
Mar	230	6.42	5.1	6.80	4.8	6.80	4.8
Apr	230	6.69	4.9	6.65	4.9	6.24	5.3
May	241	7.07	4.9	6.69	5.1	5.97	5.8
Jun	270	7.22	5.3	6.67	5.8	5.78	6.7
Jul	270	7.32	5.3	6.84	5.6	6.01	6.4
Aug	270	6.84	5.6	6.66	5.8	6.13	6.3
Sep	241	6.78	5.1	7.02	4.9	6.85	5.0
Oct	230	5.92	5.6	6.53	5.0	6.75	4.9
Nov	202	4.37	6.6	5.05	5.7	5.43	5.3
Dec	202	4.05	7.1	4.81	6.0	5.28	5.5
Design current for tilt		7.1		6.0		6.7	
Optimum design current				6.0			

Array Sizing and Tilt

Array sizing involves determining the optimum system design current by computing the design current for each month of the year at each of three tilt angles, then choosing the tilt angle that yields the lowest optimum design current. Since the corrected load is a weekly load rather than a daily load, but the peak sun hours are listed as daily peak sun hours, it is necessary to divide the corrected load by the peak sun hours and then by 7. This is equivalent to dividing by the weekly peak sun hours. Table 7.9 shows the results for the cabin. Note that for the specified loads, the optimum tilt angle is latitude and the optimum design current is 6.0 A. Peak sun hr/day are for Denver, CO [Appendix A].

The data in Table 7.9 can be rearranged to show the optimal array tilt angle for each month and the corresponding array current, as shown in Table 7.10. Since the corresponding design current represents the minimum allowable current for that month, the maximum of these values over the 12-month period must be chosen to provide adequate system design current for the worst month. In this case, by adjusting the tilt three times per year, the system can be optimized to obtain a design current of 5.6 A.

Table 7.10 Optimization of array by seasonal tilt adjustment (+15 = lat+15°, etc.).

Mo	Jan	Feb	Mar	Apr	May	Jun
Tilt	+15	+15	+15	-15	-15	-15
A	5.2	5.0	4.8	4.9	4.9	5.3

Mo	Jul	Aug	Sep	Oct	Nov	Dec
Tilt	-15	-15	lat	+15	+15	+15
A	5.3	5.6	4.9	4.9	5.3	5.5

The next step is to account for module degradation by dividing the optimal design current by the estimated degradation factor. In this case, 90% will again be used as a default value. The array will be located where reasonable maintenance will be possible so it will remain relatively clean. This yields derated design currents of 6.7 A for the fixed mounting system and 6.2 A for the adjustable tilt system.

If 100 W modules with a 6.2 A rated (I_{mp}) current are used, two of these modules will be adequate for the seasonably adjustable system. The fixed system will require either two 110 W modules or two 120 W modules to provide the necessary current. These modules are generally the same physical size as the 100 W modules, but have higher fill factors. Note that at a cost of approximately \$5/W, the difference in cost between the adjustable array and the fixed array is about \$100. If this \$100 is spread over the life of the system, it means a savings of about \$5/yr as a reward for making three adjustments per year. The owner will likely opt for the fixed array.

Before proceeding to controller selection, it is interesting to look at the amount of excess Ah produced by the system on a month-by-month basis, since

the array has been selected to produce adequate energy during the worst month. For the fixed array, the two modules will produce a derated current of $0.9 \times 6.7 = 6.0$ A. When multiplied by seven times the average daily peak sun hours at a latitude tilt, the average weekly Ah available from the array can be determined for each month. If the required average weekly Ah are subtracted from the available average weekly Ah, the result is the average weekly excess energy produced on a monthly basis. Table 7.11 shows this result.

Table 7.11 Average weekly excess Ah produced by the selected array for the cabin.

Mo	Jan	Feb	Mar	Apr	May	Jun
Ah	10.9	30.7	55.6	49.3	40.0	10.1
Mo	Jul	Aug	Sep	Oct	Nov	Dec
Ah	17.3	9.7	53.8	44.3	10.1	0.0

The next logical challenge for the designer is to figure out what to do with all this extra electricity. Comparison with the Ah requirements of the cabin loads shows that the spring and fall excess is approximately equal to the daily refrigerator consumption. Since it is unlikely that the cabin owner will want to bring in another refrigerator for spring and fall use only, perhaps it is more likely that the fans might be run longer. Since each fan will run for 8 hours on 3.2 Ah of electricity, each fan could be operated approximately 15 additional hours during the summer months. Doing so, however, is contingent on having sufficient battery storage to capture the additional Ah, which otherwise would have been diverted from the batteries by the controller at the point of full charge.

Another possible use for the excess electricity is to heat some water. In this case, the controller would need to divert the array output to a water heating element when the batteries reach full charge. If this is done, it is interesting to calculate the amount of heating that will take place.

Since it takes 1 Btu to raise the temperature of 1 pound of water by 1°F, and since 1 Wh is equivalent to 3.413 Btu, one need simply convert the Ah to Wh. For example, in April, the excess 49.3 Ah at a system voltage of 24 is $49.3 \times 24 = 1,183$ Wh. Since a gallon of water weighs 8.35 lb, it takes 8.35 Btu, or 2.45 Wh, to raise the temperature of a gallon of water 1°F. Hence, the leftover 1,183 Wh per week will add 4,038 Btu to a tank of water. For a 30 gallon tank, this amounts to about a 16°F temperature increase per week. For a 10 gallon tank, the increase would be 48°F per week, so that over a 4-day period of unoccupied cabin, the temperature could be raised by 27.6°F.

Another possibility would be to pump extra water. It is left as an exercise for the reader to determine the additional water that could be pumped with the leftover electricity (Problem 7.14).

It is up to the engineer to decide which use, if any, will make economic sense for this extra electricity. The determination will ultimately be dependent upon specific preferences of the cabin owner.

Controller, Inverter and/or dc:dc Converter Selection

This design will only require a charge controller. To determine controller size, maximum currents to and from the controller need to be identified. This includes current from array to controller, from battery to controller and from controller to load.

The maximum array-to-controller current is given by 125% of the short-circuit array current, to account for possible cloud focusing. The module chosen for the array has $I_{SC} = 7.2 \text{ A}$, so 125% of this value is 9.0 A.

The maximum controller-to-load current is found by dividing the total load power by the system voltage. The total load power is 373.6 W. Hence, the maximum controller to load current will be 15.6 A.

The maximum controller-to-battery current is the larger of the array-to-controller current and the controller-to-load current. The controller currents are summarized in Table 7.12. Hence, a controller with 20 A input and 20 A output will be adequate for the system.

It is also necessary to determine the desirable features for the controller. In this case, a simple unit that includes a low-voltage disconnect should be adequate. For example, a controller with three charge indicator lights can indicate whether the battery is at a low, medium or high state of charge. Temperature is desirable, since the batteries operate over a range of temperatures. A suitable controller for the system can be purchased for about \$130.

Table 7.12 Summary of controller currents for cabin.

Array to Controller	Controller to Loads	Battery to Controller
9.0 A	15.6 A	15.6 A

Wire, Fuse and Switch Selection

The next step in the design is to decide what loads will be on which circuits and then compute the proper wire sizes to limit voltage drop to the loads. Table 7.13 summarizes one possible selection of circuits along with wire sizing, wire pricing and sizing of fuses. Distances are taken from the cabin layout, taking into account the location of the loads and the location of the array, batteries, controller and distribution panel. All voltage drops are calculated at 2% based on a 24 V system voltage. Wire prices vary considerably from day to day and from one supplier to another and, particularly, upon the quantity purchased. Wire costs listed are somewhere between wholesale and retail price at the time of writing of this chapter.

The purpose of the 12 A fuse in the #10 wire from the array to controller is to protect the array from any unanticipated backfeed from the batteries. Also note that #10 wire is used between batteries and controller as well as from controller to distribution panel, even though the system is not anticipated to need wire this large. In fact, it is common practice to use even larger wire from batteries to

controller to minimize losses. Normally, however, when the larger battery cables are used, an inverter is in the system that powers relatively high wattage loads that require high inverter input currents.

Table 7.13 Summary of circuits, wiring and fusing for the cabin.

Wire location	Max A	Length, ft	Max Ω/kft	Wire Size	Wire Cost, \$	Fuse Size, A
Array to controller	9.0	15	1.3333	#10	\$6.00	12
Battery to controller	15.6	6	2.5641	#10	\$1.80	20
Controller to panel	15.6	3	5.1282	#10	\$0.90	20
Refrigerator	3.3	15	4.8000	#14	\$2.25	15
Water pump	3.9	230	0.2710	#3	\$280.60	15
Bedroom lights	1.3	20	9.0000	#14	\$3.00	15
Kit & bath lights	1.9	25	5.0087	#14	\$3.75	15
Bedroom fans	0.8	25	12.0000	#14	\$3.75	15
LR & outdoor light	1.0	52	4.6154	#14	\$7.80	15
Dining light	1.3	20	9.6000	#14	\$3.00	15
Entertainment	2.1	40	2.8800	#12	\$7.20	15

Another interesting situation that occurs in this system is the fact that the #3 wire to the pump will not fit under the circuit breaker terminal. Clever electricians, however, will be able to solve the problem. The #12 wiring to the future entertainment system is chosen over #14 just in case the system ultimately chosen will require more than 50 W. Problem 7.15 gives the reader a chance to determine the maximum load that can be connected that will keep the voltage drop less than 2%.

Switches should have the same current rating as the fuses or circuit breakers along with adequate voltage rating for the purpose. For lighting, the switches need to be rated for dc and have a voltage rating of about twice the system voltage to ensure conservative use. Fans come with fan controllers rated for the purpose. The pump will need to be controlled with a level switch in the storage tank and possibly with a time switch to limit pumping to certain hours. These switches need to be adequately rated to carry the pump motor current.

Balance of System Component Selection

Wire, switch and fuse costs are normally included in the balance of system (BOS) cost. Other items that need to be included are array mount, distribution panel(s), lightning arrestors, ground rod, battery container, battery cables, battery fuses and miscellaneous connectors and junction boxes. Most of these components, except perhaps those related to the batteries, will be used in the electrical system regardless of the source of electricity.

Once wire length and size are known, wire cost can be calculated. Fuse sizes are determined by the maximum current expected to flow in any set of wires. For the cabin, a distribution panel with dc circuit breakers rather than fuses is used to supply individual circuits to the various loads, with some doubling up of loads on a single circuit. Fuse holders are used at the battery end of the battery

connection to protect the batteries and the wire from the batteries to the controller. Lightning arrestors are important for protection of the total system and are normally located at the controller.

The array mount may take many shapes and forms, from commercially available units to homemade wooden frames. For the cabin, a commercial pole mount has been selected. A mount for 2 modules, including the support pole, will cost about \$150.

Life-cycle Cost Analysis

The final step in the cabin electrical system design is to prepare a life-cycle cost (LCC) analysis of the system. This means going to the catalogs or web pages and looking up all the prices. Many of the prices have already been reported in previous sections. The resulting LCC analysis is tabulated in Table 7.14. The analysis is based on a discount rate of 5% and an inflation rate of 3%.

One should note that the LCC analysis would normally be compared with the LCC analysis of another option, such as using a gasoline generator. Since no other system has been selected for comparison, the LCC of the system gives a reasonable estimate of the cost of the total installation, with the exception of drilling the well, the cost of plumbing and the cost of the water storage tank. It is assumed that these costs will remain the same, regardless of the system chosen to power the cabin. If an alternate system is considered, then only those components that differ between the two systems need be considered in the comparative LCC analysis.

Table 7.14 Life-cycle cost analysis for the cabin.

Item	Cost	Present worth	% LCC
Capital Costs			
Array	\$1,100	\$1,100	10.9
Batteries	1200	1200	11.9
Array mount	150	150	1.5
Controller	100	100	1.0
Loads	3570	3570	35.5
BOS	500	500	5.0
Installation	600	600	6.0
Recurring Costs			
Annual insp	50	839	8.3
Replacement			
Batteries 8 yr	1200	1029	10.2
Batteries 16 yr	1200	883	8.8
Controller 10 yr	100	83	0.8
TOTALS		\$10,054	100.0

Total System Design

Figure 7.3 shows schematically the PV system layout for the cabin. Note the locations of lightning arrestors and of ground connections. In particular, note

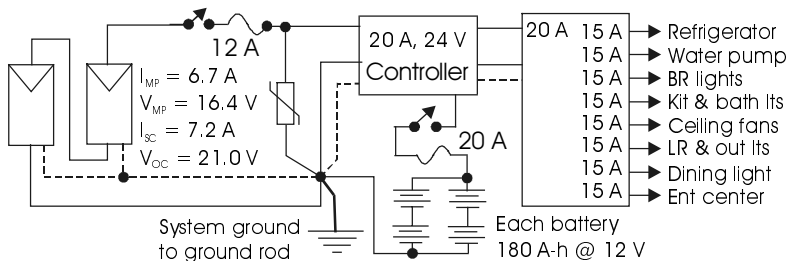


Figure 7.3 Cabin electrical system schematic wiring diagram.

that single point grounding is used at the controller. All connections to negative terminals are tied to a single point, which, in turn, is connected via the grounding electrode conductor to a ground lug wired to the ground rod of the system. *NEC* 250.166(B) states that the grounding electrode conductor should be no smaller than the largest circuit conductor, which, in this case, is the #3 copper to the water pump. However, *NEC* 250.166(C) allows a #6 Cu grounding electrode conductor because the grounding electrode is a ground rod. The grounding electrode conductor runs from the grounded/grounding terminal block to the ground rod. The equipment grounding conductors are determined by the sizes of fuses that protect the ungrounded conductors. *NEC* 250.122 allows #14 copper wire to be used as the equipment grounding conductor for circuits protected with 15 A fuses. The equipment grounding conductor between the controller and the distribution panel must be #12 copper, and if the batteries are in a metal enclosure, the enclosure must be grounded with a #12 copper wire.

7.4 A Hybrid Powered Residence

7.4.1 Design Specifications

This design example investigates the method of choosing alternate generation capacity to supplement the output of the PV array when there is a large discrepancy between month-to-month system needs vs. month-to-month PV generation capacity. If installation of a PV array to meet minimum sun availability results in significant excess generation for a number of months, then much of the PV output is wasted. In such cases, it often makes better economic sense to use a generator to supplement the PV output during the months of low PV output and size the PV to meet most of the needs during months of higher peak sun.

It has been observed in Chapter 3 that there is a significant cost increase between sizing a PV system to provide 95% of system electrical needs vs. providing 99% of system needs. Hence, use of a generator for increasing system availability from general to critical may also be cost effective.

In the present example, it is desired to power a residence near Bismarck, ND, but away from the utility grid, with a combination of PV and generator. The

residence will be occupied 7 days per week all year long. All loads will be 120 V ac as in typical residences, except that energy efficiency has been taken into account in the selection of the loads and the design of the dwelling. For example, a high efficiency refrigerator has been selected and all lighting will be fluorescent. The dwelling is designed with fans and is highly insulated with triple-pane glass in the windows. Much of the heating will be by passive solar, but propane will be used for supplemental heating, solar water heating backup and cooking. Since propane will be on site, it will also be used for the generator. The goal of the design is to arrive at a combination of PV and propane generator energy production that will result in the lowest, or, at least acceptable, LCC.

7.4.2 Design Implementation

Since PV and generator output capability come in steps, this design process will explore the LCC of several combinations of PV and generator. Up to this point little discussion of generator properties has taken place, so a part of the design discussion will deal with the selection of generators. The design process is somewhat modified from the previous examples, since the propane generator also needs to be sized and incorporated into the system. This means a more complicated system block diagram, resulting in a somewhat more challenging control problem.

Since the generator is available for PV system backup, it may seem unnecessary to incorporate batteries into the system. However, for generators to operate efficiently, they need to run at close to 90% of their output capacity. Operation of a generator at a small fraction of capacity will result in significant decrease in efficiency, as was noted in Chapter 3. Hence, batteries are used so the generator can charge them at a rate close to its capacity.

Since charging batteries too quickly tends to result in an inefficient charging process, the generator/battery system should be sized so the generator will take at least 5 hours to charge the batteries [2]. The battery selection criteria of Section 7.2 appear to present a more conservative requirement of at least 10 hours to fully charge the batteries. Actually, these criteria are not necessarily inconsistent, since the batteries will not normally be charged from full discharge to full charge. Normally the generator will charge the batteries from about 20% to about 70%. Charging the batteries from 20 to 70% in 5 hours requires a charging rate of C/10.

The bottom line, then, for batteries, is to provide a few days of storage so the charging rate will not be excessive. More storage will normally result in somewhat lower use of the generator, since the generator will not necessarily need to back up the PV array in the event of cloudy weather for a few days. Longer storage times may be desirable in areas where summers have periods of sunny days followed by periods of cloudy days. In general, fewer batteries will be used in a hybrid system since the propane generator will supplement the sun. Choice of the number of days of autonomy for the system, however, becomes more de-

pendent on other factors, such as how long it may take to implement emergency repairs on the generator.

After loads and batteries are selected, the mix of PV and propane generation is determined. Then the array size and the generator size are calculated, followed by calculation of generator fuel use and maintenance costs. Then controllers, inverters, battery chargers, fuses, wires and other BOS components are selected. After selection of all components, LCC analysis is performed on alternate system designs.

Load Determination

Table 7.15 summarizes the estimated loads for the residence by season. All loads are 120 V ac loads and the input of the inverter will be 48 V dc rather than 12 V dc in order to reduce the PV array current output requirements, thus reducing wire size from array to inverter. Note that the same number of modules will still be required, since the same total power must be produced by the array. The loads are tabulated in Ah at 48 V dc. A conversion efficiency of 95% is assumed for the inverter, so the connected loads include this figure.

Table 7.15 Estimated seasonal loads for hybrid residence.

Load Description	P, watts	Dec, Jan, Feb		Mar, Apr, May Sep, Oct, Nov		Jun, Jul, Aug	
		Hr/day	Ah/day	Hr/day	Ah/day	Hr/day	Ah/day
Kitchen Lights	80	4	7.02	3.5	6.14	2	3.51
Dining R Lights	20	2	0.88	1.5	0.66	1	0.44
Living R Lights	40	1	0.88	1	0.88	1	0.88
Family R Lights	40	4	3.51	4	3.51	3	2.63
BR 1 Lights	20	1	0.44	1	0.44	1	0.44
BR 2 Lights	20	1	0.44	1	0.44	1	0.44
BR 3 Lights	20	1	0.44	1	0.44	1	0.44
Bath 1 Lights	20	1	0.44	1	0.44	1	0.44
Bath 2 Lights	20	1	0.44	1	0.44	1	0.44
Refrigerator	100	7	15.34	7	15.34	7.5	16.44
Microwave Oven	600	0.5	6.58	0.5	6.58	0.5	6.58
TV	80	4	7.02	4	7.02	4	7.02
Stereo	60	2	2.63	2	2.63	2	2.63
Water Pump	200	1	4.39	1	4.39	1	4.39
BR 1 Fan	50	0	0	0	0	8	8.77
BR 2 Fan	50	0	0	0	0	8	8.78
BR 3 Fan	50	0	0	0	0	8	8.78
Family R Fan	50	0	0	0	0	3	3.29
Furnace Fan	200	8	35.12	6	26.32	0	0
Washer	600	0.5	6.58	0.5	6.58	0.5	6.58
Vacuum & Sm App	1200	0.5	13.16	0.5	13.16	0.5	13.16
TOTALS	3320		105.28		95.41		96.06
CORRECTED TOT	3495		119.37		108.17		108.92

It is assumed that the household will have common electric small appliances such as toasters, blenders, vacuum cleaners, hair dryers, etc. and that no more than 1200 W of small appliances will be used at any one time. It is also assumed that the fan motor of the propane furnace and the ceiling fans will not run simultaneously, but the wattage of the furnace fan equals the sum of the wattages of the ceiling fans. These assumptions may affect sizing of the generator and the wiring, depending on whether any of the load will need to be supplied by the generator while it is running to charge batteries. In this particular design example, the assumption is that the generator is used only for battery charging. Wiring, fusing and switching between batteries and inverter and between inverter and distribution panel, however, is based on the rating of the inverter as required by the *National Electrical Code*.

Battery Selection

The batteries will be reasonably well protected from the cold North Dakota winter, but will experience somewhat lower winter temperatures. The same derating schedule will be used for the North Dakota installation as was used for the Colorado cabin battery installation.

The design goal for the system will be to maximize PV energy production without experiencing unreasonably high system LCC or unreasonable waste of PV generated electricity. Noncritical battery backup is considered satisfactory for this system, with a choice of 3 days of storage to allow the sun 3 days to reappear before calling in the generator as a replacement for the sun. This period also provides time for emergency repair of the generator or other system components. If a generator is warranted (and hopefully this will be the case since this design example calls for one to be used), it will be selected to charge the batteries in 10 hours or more so there will not need to be any compensation for quick charging of the batteries. Also, with 3 days of storage, it is highly unlikely that quick discharge of the batteries will occur.

Table 7.16 Battery storage requirements for hybrid residence.

Month	Dec, Jan, Feb	Mar, Nov	Apr, Oct	May, Sep	Jun, Jul, Aug
Ah/day	119.4	108.2	108.2	108.2	108.9
Temp Derate	0.80	0.85	0.90	0.95	1.00
Total Cap Req	559.5	477.2	450.7	427.0	408.4
# Batt	12	12	12	12	12
Avail Cap	540	540	540	540	540
# Days storage	2.90	3.39	3.59	3.79	3.97

On this basis, battery capacity is shown in Table 7.16 with only temperature compensation taken into account, with an assumed depth of discharge of 80%. Table 7.16 also shows the number of batteries required if a 12 V sealed lead-acid battery with a capacity of 180 Ah is selected for the system. Note that the indi-

cated number of batteries is four times the number of necessary batteries in parallel to produce the required total Ah capacity, since the system voltage will be 48 V dc. Note also that the selection of this battery will provide more than 3 days of storage for much of the year. However, at 80% capacity rating during the winter, they will provide 97% of the capacity required for 3 days of storage. Thus, during winter months, the batteries will provide 2.9 days of storage, while in the summer they will provide nearly 4 days of storage. The total cost of the 12 batteries will be \$3600, and the expected lifetime of the batteries is 8 years.

Array Sizing

Sizing of the array for a hybrid system is generally an iterative process. The first step is to size the array for a system with no generator and then to gradually reduce the number of modules in the array while simultaneously computing the percentage of the annual energy needs provided by the PV array. The LCC of the system is computed for each proposed configuration and an optimal (or, sometimes, a suboptimal) choice is made for the number of modules in the array.

Again, the process begins with the corrected load for each month tabulated along with the peak sun hours for each month at three different tilt angles for the array. This leads to the optimum design current for a stationary array. The result is tabulated in Table 7.17.

The results of Table 7.17 show that if the PV array is sized to meet the December current requirements of 36.28 A at a tilt of latitude+15°, considerable excess energy will be produced by the array during the other months. To determine the excess, it is first necessary to select a module.

Table 7.17 Determination of design current and array tilt for hybrid residence.

Month	Corr Load	Latitude-15°		Latitude		Latitude+15°	
		Hr/day	A	Hr/day	A	Hr/day	A
Jan	119.4	2.80	42.63	3.21	37.19	3.44	34.70
Feb	119.4	4.13	28.90	4.60	25.95	4.80	24.87
Mar	108.2	4.89	22.12	5.14	21.04	5.12	21.13
Apr	108.2	5.37	20.14	5.33	20.29	5.02	21.55
May	108.2	6.14	17.62	5.82	18.59	5.21	20.76
Jun	108.9	6.50	16.76	6.03	18.06	5.26	20.71
Jul	108.9	7.06	15.43	6.62	16.45	5.84	18.65
Aug	108.9	6.69	16.28	6.51	16.73	5.98	18.21
Sep	108.2	5.44	19.88	5.61	19.28	5.47	19.78
Oct	108.2	4.23	25.57	5.61	19.28	4.69	23.06
Nov	108.2	2.82	38.36	4.59	23.57	3.39	31.91
Dec	119.4	2.59	46.09	3.20	37.31	3.29	36.28
Design current for tilt		46.09		37.31		36.28	
Optimum design current				36.28			

Using a degradation factor of 0.9 for the PV array results in a rated array current of 40.3 A to ensure the array will produce the necessary 36.28 A. Suppose a module capable of producing 6.6 A at 16.6 V, with a short-circuit current

of 7.2 A and an open-circuit voltage of 21.0 V is selected. To produce 40.3 A will require 6.1 modules in parallel, which rounds down reasonably to 6, since when charging the batteries, the modules will operate slightly below V_{mp} , which will result in a module current slightly greater than I_{mp} . To produce 48 volts will require 4 modules in series with the result of a total of 24 modules.

It is now possible to compute the contribution of the PV system to the system annual needs and to show any excess energy production. To do so, simply compute the excess monthly kWh for each month by first computing the excess Ah/day by subtracting the required Ah/day from the Ah/day capacity of the array. The Ah/day capacity of the array is the product of the derated system current, using the specific modules, and the average daily peak sun hours. Then convert the excess Ah/day to excess kWh/day by multiplying by the system dc voltage and dividing by 1000. Then multiply by the number of days in the month to get the excess kWh/month for each month.

The system annual needs can be computed by the same means, except the daily system Ah are used rather than the array daily excess Ah. For this system, the result is 1946.8 kWh/yr. Note that the 24-module array provides all the system needs except for December, where it falls short by 3.1 kWh. This amounts to the PV system's meeting 99.8% of the annual system needs. This result, of course, is based on the assumption that each 3-day interval receives three times the average daily peak sun hours. It is likely that there will be periods without sun lasting more than 3 days, so the 99.8% figure is not a realistic expectation.

Table 7.18 Monthly excess kWh capability of PV array for six array sizes.

Month	kWh Needed	Array					
		24 mod	20 mod	16 mod	12 mod	8 mod	4 mod
Jan	177.6	4.8	-25.6	-56.0	-86.4	-105.5	-133.0
Feb	160.4	69.5	31.2	-7.1	-45.5	-83.8	-122.1
Mar	161.0	110.6	65.3	20.1	-25.2	-70.4	-115.7
Apr	155.8	101.9	58.9	16.0	-26.9	-69.9	-112.8
May	161.0	115.3	69.3	23.2	-22.8	-68.9	-114.9
Jun	156.8	113.1	68.1	23.1	-21.9	-66.9	-111.8
Jul	162.1	147.6	96.0	44.4	-7.2	-58.8	-110.4
Aug	162.1	155.1	102.2	49.4	-3.5	-56.4	-109.2
Sep	155.8	125.0	78.2	31.4	-15.4	-62.2	-109.0
Oct	161.0	87.8	46.3	4.9	-36.6	-78.0	-119.5
Nov	155.8	18.2	-10.8	-39.8	-68.8	-97.8	-126.8
Dec	177.6	-3.1	-32.2	-61.3	-90.4	-119.5	-148.5
Ann PV %		99.8%	96.5%	91.7%	77.0%	51.4%	25.9%

It should be remembered that the excess kWh are assumed not to be utilized, and, hence, will not actually be produced. If they are produced, they need somewhere to go. This brings into the picture possible alternate uses, such as pumping additional water. Table 7.18 shows the excess monthly kWh produced

by the PV array for the 24-module array as well as for arrays of 20, 16, 12, 8 and 4 modules. The table also shows the percentage of annual system kWh requirements supplied by these arrays. Normally, when the PV system provides less than 95% of the system needs, an alternate source of electricity is incorporated into the system. Hence, in this case, the 20-module system should provide good system performance year around without any backup, provided that the dwelling occupants reduce energy consumption in the winter.

Generator Sizing

The generator should be sized to charge the batteries at approximately C/10 as indicated previously. At this rate of charging, the generator should be operating at approximately 80 to 90% of its rated output in order to ensure maximum generator efficiency. Hence, it is first necessary to determine what C/10 means for this system.

The first question when analyzing Table 7.16, is Which capacity should be used in determining C/10? With temperature derating applied, the batteries have a capacity of 432 Ah in the winter and 540 Ah in the summer. Since most generator operation will be in the winter, as indicated by Table 7.18, the winter capacity is the appropriate choice. Hence, 43.2 A for 10 hours will produce 432 Ah of charge.

The generator will be rated in watts. Thus, it is necessary to determine the power, rather than the Ah requirements of the batteries. This is obtained by incorporating the battery-charging voltage. For a C/10 charging rate, the battery charger output power will thus be the product of the charging voltage and the charging current, or $48 \times 1.2 \times 43.2 = 2488$ W, since the charging voltage is generally about 120% of the nominal battery voltage. If the electrical conversion efficiency of the battery charger is 90%, this would require an input power of $2488 \div 0.9 = 2764$ W to provide 43.2 A of charging current. Since the generator is to be used only for battery charging, a 2500 W generator would be a good choice, since it will run close to its rated output and will charge at a rate slightly less than C/10.

If it is desired to have the generator run part of the load while charging the batteries, or to charge at a faster rate, it would be reasonable to select the next larger size generator. However, the 2500 W unit operating at 2250 W will charge the batteries from 20% to 70% in 6.14 hours. This is normally an acceptable charge rate, especially since it will take 5/8 of 2.9 days to use this amount of charge for this particular system. Charging the batteries to only 70% allows for the PV array to top off the charge if it can. If not, and the batteries discharge to 20% again, the generator comes on again.

Generator Operating Cost

The more the generator runs, the more it will cost to operate. Generator operating cost consists of fuel cost, oil changes, tune-ups and rebuilding. To de-

termine the operating cost, then, it is necessary to determine the annual operating hours of the generator.

Since Table 7.18 already lists the monthly excess production of the PV array for six different array sizes, the monthly kWh requirements of the batteries from the generator can be determined from the months during which the PV excess is negative. All negative excesses represent PV energy shortfalls and thus represent energy to be supplied by the generator. The generator kWh output (kWh_{Gen}) needed to supply the battery kWh (kWh_{Batt}) needs is found from

$$\text{kWh}_{\text{Gen}} = \frac{\text{kWh}_{\text{Batt}} \times 1.2}{\eta} \quad (7.5)$$

where 1.2 is the ratio of charging voltage to nominal battery voltage and η is the efficiency of conversion of ac to dc in the battery charger. Battery kWh requirements from the generator are summarized in Table 7.19.

Table 7.19 Required monthly kWh to batteries from generator for six PV array sizes.

Month	kWh Needed	Array					
		24 mod	20 mod	16 mod	12 mod	8 mod	4 mod
Jan	177.6	0	25.6	56.0	86.4	105.5	133.0
Feb	160.4	0	0	7.1	45.5	83.8	122.1
Mar	161.0	0	0	0	25.2	70.4	115.7
Apr	155.8	0	0	0	26.9	69.9	112.8
May	161.0	0	0	0	22.8	68.9	114.9
Jun	156.8	0	0	0	21.9	66.9	111.8
Jul	162.1	0	0	0	7.2	58.8	110.4
Aug	162.1	0	0	0	3.5	56.4	109.2
Sep	155.8	0	0	0	15.4	62.2	109.0
Oct	161.0	0	0	0	36.6	78.0	119.5
Nov	155.8	0	10.8	39.8	68.8	97.8	126.8
Dec	177.6	3.1	32.2	61.3	90.4	119.5	148.5
Ann gen %		0.2%	3.5%	8.4%	23.1%	48.8%	74.4%

The monthly hours of generator operation can then be determined from the monthly kWh_{Gen} by the output power at which the generator is set to operate. Since most generators operate at maximum efficiency at approximately 90% of their rated output power, it will be assumed that the generator will be set to 90% of its available output power, or 2250 W. It is also reasonable to assume a battery charger conversion efficiency of 90%.

The monthly generator fuel consumption can be determined from knowledge of either the hourly fuel consumption or the fuel consumed per kWh of generation. A utility grade generator will generate approximately 12 kWh per gallon of fuel [5], but a small generator will generate considerably less, since the combustion efficiency of a small gasoline, propane or diesel engine is much less than

the efficiency of a large utility steam turbine. Table 7.20 estimates fuel consumption on the basis of a generator output of 5 kWh/gal of fuel. With a generator output of 2250 W, it will take 2.22 hours to generate 5 kWh_{Gen}, resulting in a fuel consumption rate of 0.45 gal/hr. Assuming an ac/dc conversion efficiency for the battery charger of 0.9, use of (7.5) results in 5 kWh_{Gen} providing 3.75 kWh_{Batt}. This means that in 1 hr, the generator will produce 2.25 kWh_{Gen}, which results in $3.75 \times 2.25 \div 5 = 1.69$ kWh_{Batt}, which means that it will take 0.593 hr to deliver 1 kWh to the batteries. The generator running time is thus equal to 0.593 times the kWh needed for the batteries from the generator.

Table 7.20 Monthly generator operating hours and annual fuel consumption for six PV array sizes.

Month	Battery kWh for loads	Array					
		24 mod	20 mod	16 mod	12 mod	8 mod	4 mod
Jan	177.6	0	15	33	51	69	87
Feb	160.4	0	0	4	27	50	72
Mar	161.0	0	0	0	15	42	69
Apr	155.8	0	0	0	16	41	67
May	161.0	0	0	0	14	41	68
Jun	156.8	0	0	0	13	40	66
Jul	162.1	0	0	0	4	35	65
Aug	162.1	0	0	0	2	33	65
Sep	155.8	0	0	0	9	37	65
Oct	161.0	0	0	0	22	46	71
Nov	155.8	0	6	24	41	58	75
Dec	177.6	2	19	36	54	71	88
Ann gen op hrs		2	41	97	267	563	858
Ann gen gal fuel		1	18	44	120	253	386

Generator annual operating costs can now be estimated from the maintenance information of Table 3.4, along with known fuel cost. Table 7.21 summarizes the required generator maintenance for the six PV arrays previously considered. The table entries are determined by the quotient of the annual operating hours and the specified maintenance intervals of 25 hours per oil change, 300 hours per tune-up and 3000 hours per rebuild. Once the cost of each of these items is known, the annual maintenance cost can be determined. As will soon be seen, annual maintenance costs can be an important component of the system life-cycle cost, depending upon the frequency of maintenance operations.

Table 7.21 Annual generator maintenance frequency for six PV arrays.

Item	24 mod	20 mod	16 mod	12 mod	8 mod	4 mod
Op hr/yr	2	41	97	267	563	858
Oil changes/yr	0	2	4	11	23	34
Tune-ups/yr	0	0	0	1	2	3
Yr/rebuild	>20	>20	>20	13	6	4

Controller, Inverter, Charger Selection

The controller for a hybrid system is somewhat more complicated than the controller for a conventional PV system. It must control battery charge and discharge by both the PV array and the generator. It must provide a starting signal/voltage for the generator when the batteries have discharged to a preset level and must shut down the generator when the batteries reach a preset level of charge. Proper setting of these levels is important. Too low a setting on discharge may render the batteries unable to provide starting current for the generator. Too high a setting may result in the generator's unnecessarily replacing energy that might be available from the PV array, with the PV array then being shut off with energy to spare.

The inverter for this particular system is relatively simple to specify, since it must supply all the loads of the house, which have been previously tabulated at 3320 W in Table 7.15. While it is possible to obtain separate battery charge controller, battery discharge controller, inverter and charger, it is also possible to obtain the inverter, charger, discharge controller and generator control functions in a single package. A typical utility grade sine unit that performs all these functions is rated at 4000 W with a surge rating in excess of 9000 W. It has a 120 V ac output and operates at an efficiency above 90% at output powers between 250 and 3000 W and an efficiency above 80% at powers between 100 and 250 W.

Since the average power consumption from the inverter is 239 W or less, depending upon the month of the year, this means there will be times when the inverter is operating at efficiencies less than 90%. This means higher percentage losses in the inverter when the load on the inverter is small, which means the overall system load, including inverter losses, will be somewhat higher than calculated. For example, if the inverter delivers 100 W at 80% efficiency, this means the inverter input power must be 125 W, rather than the 105 W that would result if the inverter efficiency were 95% as assumed in the connected load calculation. Over a 24-hour period, this additional 20 W loss amounts to 0.48 kWh, which must be added to the daily load on the batteries. With a daily kWh consumption of approximately 5.3 kWh, this amounts to an additional 9% load on the system. The bottom line is that, depending upon the number of modules chosen for the system, there will be less excess kWh/mo on months where the PV delivers excess kWh, and the generator will run slightly longer on the months when the PV does not provide excess kWh. To provide this additional 0.48 kWh/day, the generator will need to run an additional 17 minutes per day. Fortunately, the inverter incorporates an adjustable search mode control, so the inverter will "sleep" if the connected loads are below the sleep threshold.

Since the inverter runs on a real-time clock, it is possible to program the hours when generator operation will be permitted. It is also possible to program battery charging current so the generator will run at the design output of 2250 W. The inverter does not, however, have a built-in charge controller for input from the PV array, so a separate charge controller will be needed for the PV array to prevent the PV array from overcharging the system batteries.

Wire, Fuse, and Switch Selection

All wiring on the load side of the inverter can be done in a manner consistent with conventional 120 V residential wiring. Since the distribution panel will be running only on 120 V, it will not be acceptable to use multiwire branch circuits. A multiwire branch circuit on a 120/240 V distribution system uses a common neutral for the return path for current from circuits connected to the +120 V and to the -120 V busbars in the distribution panel. So all circuits from the distribution panel will need to have individual hot and neutral conductors. Otherwise wiring needs to comply with requirements of the *NEC* for 120 V branch circuits—requirements well known to all licensed electricians.

Table 7.22 shows the wire sizes required for array to inverter, battery to inverter, and inverter to distribution panel, assuming distances of 40 ft, 6 ft and 5 ft, respectively. Again, the maximum array-to-inverter current is 125% of the rated array short-circuit current. The battery-to-inverter current is the rated inverter output power divided by the system dc voltage *at its lowest expected value, which is normally considered to be the lowest rated inverter input voltage* and divided by the inverter efficiency. The inverter-to-panel current is determined from the rated inverter output power, divided by 120 V. Wiring must be sized to carry 125% of these rated currents. For the wiring from generator to inverter/charger, the wire must be sized to carry 115% of the rated generator output current, per *NEC*.

Table 7.22 Summary of PV circuits, wiring and fusing for the hybrid residence.

Wire location	Max A	Length, ft	Max Ω/kft	Wire Size	Fuse Size
Array to combiner	9 per source ckt*	40	1.3333	#10	12 A
Combiner to inverter	54 (6 source circuits)	3	2.9630	#6	70 A
Battery to inverter	100	6	0.8000	#2/0	150 A
Generator to inverter	20.8	20	2.88	#10	30 A
Inverter to panel	33.3	5	7.21	#8	50 A

*125% of I_{SC} of source circuit.

It is important to note that the wire size determined on the basis of voltage drop for short runs of wire may not yield a wire size that is capable of carrying the specified current. If this is the case, the wire must be selected with adequate current rating. This is the case for the combiner to inverter, battery to inverter and the inverter to distribution panel. If wires operate at temperatures in excess of 30°C, or if more than three current carrying conductors are in a conduit, the wire ampacity must be further derated. These procedures will be carried out in the examples of Chapter 8. Correct wire sizes are listed in the table.

It is also interesting to note that the load and distribution panel size calculated in this example are considerably less than the minimum service size required by the *National Electrical Code*. The local electrical inspector is the ultimate authority on the application of the *NEC*. The inspector may accept a

design certified by a registered professional electrical engineer, or the inspector may insist on wiring of adequate size to meet minimum *NEC* requirements. The concern would be that the dwelling may one day be powered by abundant utility power if the grid should be extended to the location of the dwelling.

Balance-of-System Component Selection

The BOS components will include a battery storage container, an array mount, surge protection and provisions for proper grounding of the system. Of course, the wiring from the distribution panel is also a part of the balance of the system, but its cost will not change as the mix of PV vs. propane generation is varied. The cost of the array mount and the cost of wire from array to combiner box are the only items in the BOS that will vary with the number of modules.

Life-cycle Cost Analysis

In order to determine the optimum mix of PV and generator-produced kWh, it is necessary to compute the LCC of several mixes and hope to obtain a curve that will show a minimum cost for a particular mix. However, if the system cost either increases or decreases monotonically, then no such minimum will exist. The LCC computation must take into account the costs of all system components that will vary as the generation mix is changed. This includes array cost, array mount cost, generator operating and maintenance costs and controller/inverter cost. In the ideal case, a price should be affixed to the relative environmental costs of each type of generation. While this will not be done for this example, environmental costs will be discussed in Chapter 9. In this chapter, it will simply be assumed that the less the generator runs, the less noise and air pollution will be created.

Table 7.23 shows the LCC analysis for a 24-module array with no generator and a 12-module array with a generator that must supply 23.1% of the annual energy needs. Reasonable assumptions are made for fuel cost and maintenance cost for the generator. It is assumed that propane costs \$1.50 per gallon, an oil change will cost \$5, a tune-up will cost \$50 and a rebuild will cost \$375. Array mount costs are based on the cost of typical commercial array mounts. It is assumed that the inverter for the hybrid system will be the same as the inverter for the nonhybrid system to allow for addition of a generator at a later date if desired. The installation cost is assumed to be \$1/W for the PV system plus 20% of the cost of the generator. The LCC is based on a discount rate of 5% and an inflation rate of 3%.

Figure 7.4a is a plot of LCC vs. the number of modules in the system, and Figure 7.4b is a plot of the LCC vs. the percent of annual kWh provided by the PV array. It is now up to the system owner to decide whether to spend the additional \$1808 for the convenience of the 100% PV system or to choose a compromise figure. Perhaps the biggest surprise is the LCC of the generator-only system. It must be remembered that the system also includes an inverter and batteries so the generator need not run continuously and can run at its most effi-

cient output power level. If the batteries and inverter are eliminated, the generator must run continuously and will run well below its maximum efficiency most of the time, thus significantly increasing annual fuel and maintenance costs and requiring additional cost analysis.

Table 7.23 Comparison of LCC for 24-module hybrid system and 12-module hybrid system.

Item	24-Module system			12-Module system		
	Cost	Present Worth	% Total LCC	Cost	Present Worth	% Total LCC
Capital Costs						
Array	11,880	11,880	36.2	5,940	5,940	19.2
Batteries	3,600	3,600	11.0	3,600	3,600	11.6
Array Mount	1,950	1,950	5.9	975	975	3.1
Charge controller	200	200	0.6	200	200	0.6
Inverter/Charger	3,000	3,000	9.1	3,000	3,000	9.7
Source ckt combiner	125	125	0.4	125	125	0.4
Installation	2,645	2,645	8.1	1,573	1,573	5.1
Generator	0	0	0	1,250	1,250	4.0
BOS	471	471	1.4	471	471	1.5
Recurring Costs						
Annual Insp	50	822	2.5	50	822	2.7
Generator fuel	0	0	0	179	2,944	9.5
Generator maint	0	0	0	103	1,694	5.5
Replacement						
Batteries 8 yr	3,600	3,087	9.4	3,600	3,087	10.0
Batteries 16 yr	3,600	2,646	8.1	3,600	2,646	8.5
Charge cont 15 yr	200	150	0.5	200	150	0.5
Inverter 15 yr	3,000	2,248	6.8	3,000	2,248	7.2
Gen rebuild 13 yr				375	292	0.9
TOTALS		\$32,825	100.0		\$31,017	100.0

Total System Design

Figure 7.5 shows the block diagram of the hybrid dwelling electrical system. It is assumed that the batteries will be placed in a reasonably well-insulated location so they will remain reasonably warm in the winter when they are needed the most. The array is located as close as practical to the batteries, but free of any objects that may shade the array. Based on the life-cycle cost figures, a system with 20 modules is shown. The PV array of this system supplies approximately 96% of the annual energy needs and, as indicated by Figure 7.4b, appears just at the point where system cost vs. PV availability begins to increase sharply. In this system, the PV array will provide most of the system energy needs over the period from February to October. From November to January, the generator will provide somewhere between 10.8 and 32.2 kWh/month with an annual fuel consumption of approximately 18 gallons with approximately 41 hours of operation. The generator operates only if the batteries have discharged to 20% of their capacity and then charges the batteries to 70% of capacity so any available sun-light can be used to top off the battery charge.

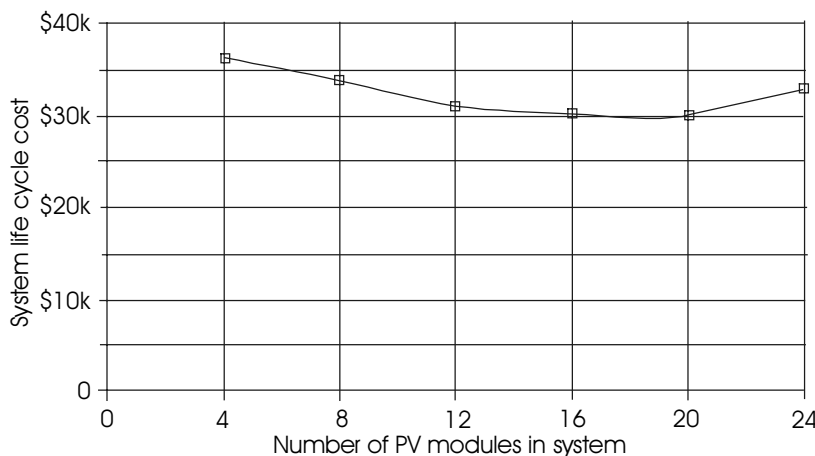


Figure 7.4a Hybrid system LCC vs. number of PV modules in system.

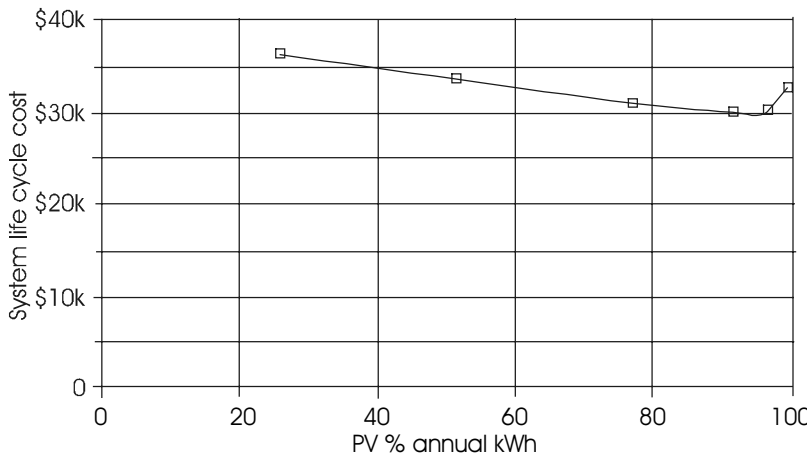


Figure 7.4b Hybrid system LCC vs. percent of annual kWh supplied by PV array.

7.5 Seasonal or Periodic Battery Discharge

When 10 or more days of autonomy are chosen for a system, it is sometimes possible to use fewer PV modules and allow the batteries to discharge to a lower state of charge for a short time instead. However, if the increased days of autonomy have been chosen for critical need purposes, then a reduction in the array size can result in compromising the critical need storage design. Furthermore, if life-cycle cost analysis is done on a system having more days of autonomy to compensate for a smaller array size, with the decreasing cost of modules, it is normally not cost-effective to replace modules with batteries, especially since the batteries will need to be replaced several times over the life of the overall system. The engineer should do an LCC analysis on any such system

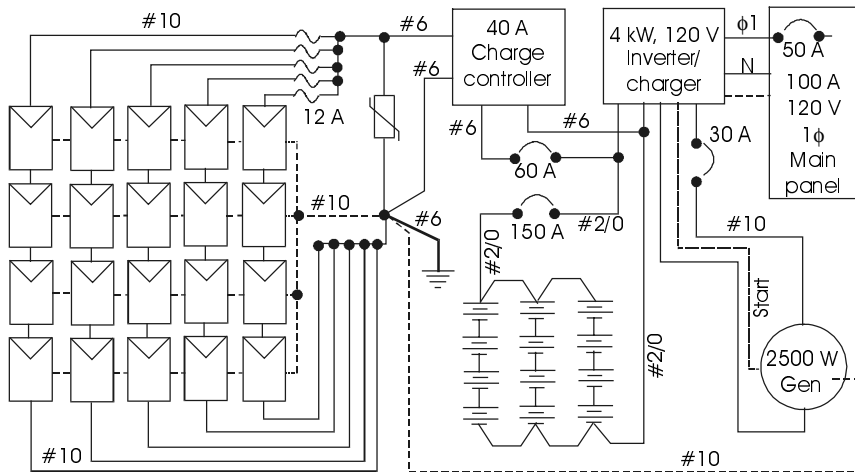


Figure 7.5 Block diagram of hybrid residence electrical system.

compared with a system with less storage and more modules to ensure the best LCC for the system.

A similar situation arises when a system is used only a few days a month. It is then possible to design a system that will store energy for, say, 25 days, and then deliver the energy for use during the remaining 5 days. This means the batteries need to provide for approximately 5 days of storage and the PV array needs to charge the batteries fully in 25 days. Actually, the array will be working for the entire month, so the batteries need not necessarily provide 5 days of storage, unless the use will be critical during periods of use. In addition, the array may be sized to provide 5 days of usage with a month of collection. This procedure is thus an extension of the procedure used in the mountain cabin example. Provided that adequate battery storage is available, the 5 days of usage may be averaged in with the 25 days of non-use for the purposes of sizing the array and the batteries.

7.6 Battery Connections

An important, but often overlooked, component of good PV system design and installation is the proper connection of batteries to ensure a balanced current flow in all batteries in the system. If connecting wires did not have resistance, the manner in which batteries are connected would be relatively unimportant. But wire does have resistance, and therefore one needs to consider this resistance when hooking up batteries. In fact, even the terminal lugs have resistance, but this resistance is more difficult to characterize, since it will depend upon the specific lug type, how tightly the lug is connected to the wire and to the battery. Connecting lug resistance will also increase over time if any corrosion should

occur at the lug. In the examples to follow, the connecting lug resistance will be assumed to be incorporated into the Thevenin equivalent (internal) resistance of the batteries.

Figure 7.6 shows three possible ways to connect eight batteries in a series-parallel configuration. If the batteries are 12-volt batteries, the system will produce 24 volts. Note that options 1 and 2 show battery-to-battery parallel connecting wires to be of equal length, and thus of equal resistance. The series-connecting wires are also of equal length. If 2/0 copper cables are used, and if $\ell_1 = \ell_2 = 1$ ft, then the cable resistance will be 0.0000967 Ω for each of these 1-ft

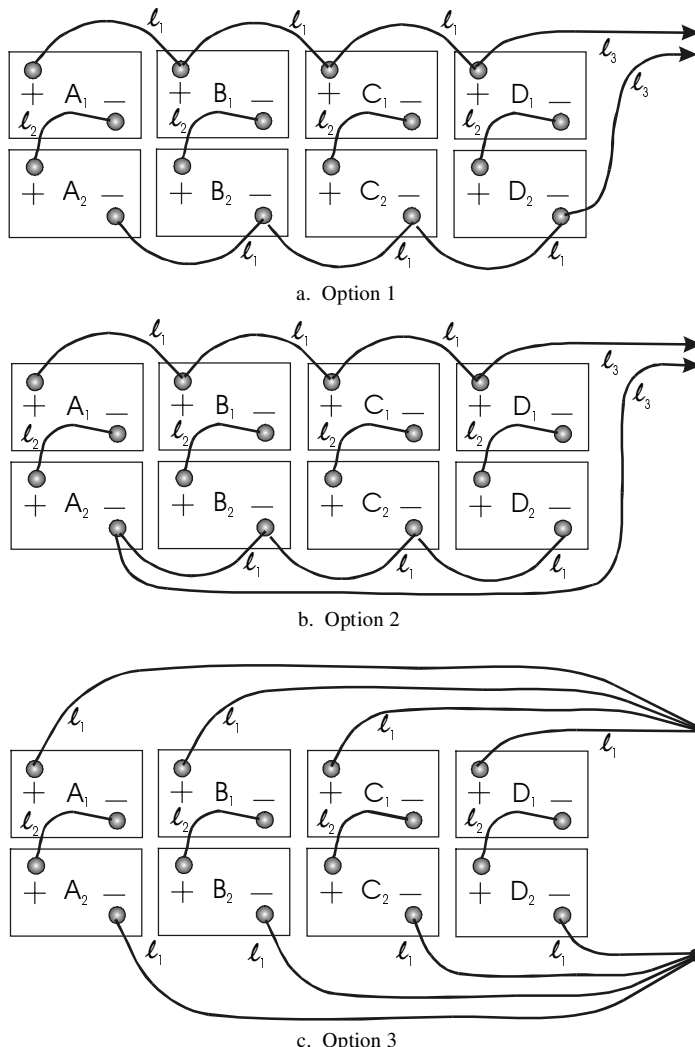


Figure 7.6 Three possible battery hookup configurations.

lengths of cable. Typically, the distance from battery to inverter input is about 6 ft. Thus, if $\ell_3 = 6$ ft, the resistance will be 0.00058Ω .

It is interesting to calculate the currents that will flow under charging and discharging conditions in the series battery strings for connection options 1 and 2 if all batteries in the system are identical. For example, consider lead-acid batteries for which the open circuit battery voltages are all 12.60 V and the Thevenin equivalent resistances of the batteries are 0.01Ω each. According to Table 3.1, this would mean the batteries are about 25% discharged. Note that these parameters suggest a possible short-circuit current of 1260 A.

Consider first the charging situation. Figure 7.7 shows the equivalent circuit for option 1. Note that if the current source negative lead is connected to point A rather than to point D, then the circuit will be equivalent to option 2. Setting $I = 60$ A as a nominal value for either charge or discharge and enlisting the assistance of a convenient network analysis program yields the results for charging and discharging for options 1 and 2 as shown in Table 7.24.

It is thus evident that option 2 should be the preferred option for several reasons. First of all, the currents are more closely balanced for all series strings of batteries. Furthermore, the charging currents are equal to the discharging currents, so even though the A and the D batteries are cycled somewhat deeper than the B and the C batteries, the starting and ending points of a full cycle of charge and discharge are the same for all the batteries. Furthermore, when the batteries are in a state of higher discharge, the cell voltage decreases and the Thevenin equivalent resistance increases such that the rate of discharge of the batteries

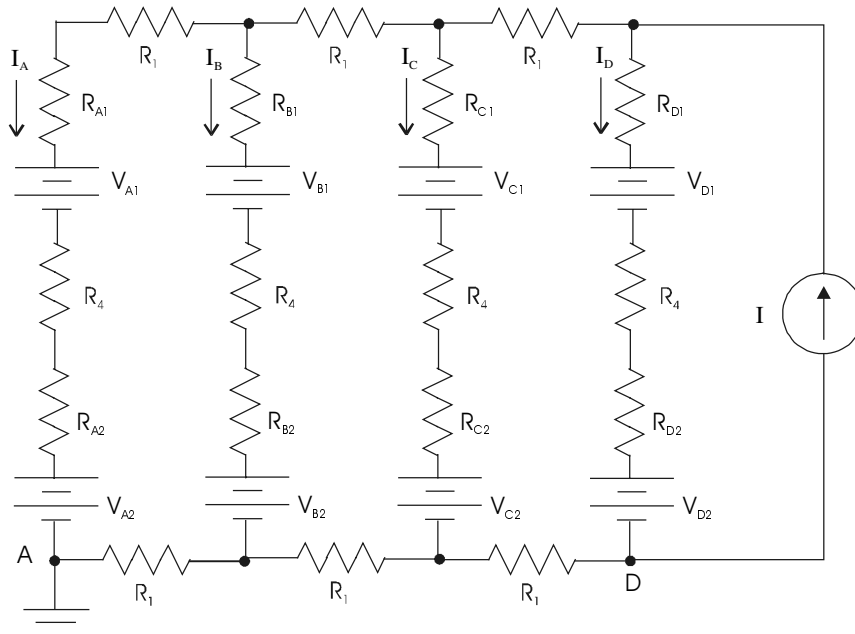


Figure 7.7 Equivalent circuit for battery connection Option 1.

tends to be self-regulated. In other words, as the batteries become more discharged than a parallel set, the batteries at higher charge supply more current to the load than the batteries at lower charge. Under charging conditions, the batteries at lower charge levels should tend to charge faster, depending on their internal resistance.

Table 7.24 Comparison of charging and discharging currents for options 1 and 2.

situation	I _A	I _B	I _C	I _D
Option 1 charge	12.36 A	15.56 A	15.83 A	16.25 A
Option 1 discharge	14.65 A	14.79 A	15.07 A	15.50 A
Option 2 charge	15.07 A	14.93 A	14.93 A	15.07 A
Option 2 discharge	15.07 A	14.93 A	14.93 A	15.07 A

The problems with the option 1 connection are also somewhat mitigated by batteries at a lower state of charge delivering less current. However, note that the charging currents are not the opposite of the discharging currents for option 1. For the A batteries, the charge rate is less than the discharge rate, while for the B, C and D batteries, the charge rate exceeds the discharge rate. After a number of cycles, this unbalance tends to result in even greater unbalance of the battery strings and can shorten the lifetimes of the batteries as a result of both overcharge and undercharge as well as uneven cycling.

Option 3 presents a somewhat different approach to equalizing battery currents. For this option, smaller wire, such as #6, is used to connect to each series battery string. The idea is to terminate the #6 ends at terminal blocks near the inverter and then use very short lengths of larger wire between the terminal blocks and the inverter. If all the lengths of wire are the same on a round-trip basis, then each string of batteries will experience the same voltage drop in the battery cabling, and currents will be exactly balanced under charge or discharge conditions. The higher resistance of the #6 wire tends to produce a current limiting effect. So if for some reason one series set tends to discharge or charge at a higher rate than another series set, the discharge or charge current will be limited by the resistance of the connecting wires, thus creating a balancing effect.

The disadvantage of option 3 is that each individual battery string will require a separate fuse or circuit breaker, similar to the source-circuit fuses in a PV array, but much larger. So in this case, there would be four battery disconnects instead of the single disconnect needed for options 1 and 2. However, it is possible that the higher resistance of the connecting wires of option 3 will limit the battery short-circuit current sufficiently that fuses or circuit breakers of a lower interrupting capacity (AIC), and thus lower cost, can be used. Recall that the interrupting capacity of an overcurrent device is a measure of the ability of the device to interrupt the circuit under short-circuit conditions, where there is a possibility that arcing may occur across open switch contacts. As a result, the overall cost of option 3 may still be attractive. However, the NEC (230.71(A)) limits the number of switches allowed to disconnect a circuit to no more than six.

An interesting approach to this problem is to use 2- or 3-pole circuit breakers, since each device has a single lever for operating the device and hence will count as a single disconnect even though it will disconnect two or three strings of batteries with a single flip of the switch handle.

In summary, the key to optimizing battery performance is proper cabling. The use of equal lengths of cables is essential. Problems 7.18-7.20 offer the reader an opportunity to explore the effect of unequal cable lengths and battery parameters on battery system charging and discharging. Option 2 is clearly better than option 1 for battery wiring, and option 3 is also potentially attractive.

Furthermore, new batteries tend to have lower internal resistance than older ones of the same type, resulting in greater unbalance of currents in parallel strings of new batteries. This generally means that if one battery is replaced, all should be replaced, probably with the exception of an early failure due to a battery defect. In any case, if not all batteries are replaced, the condition of all batteries should be carefully checked to ensure that currents are well balanced. If this is not the case, future premature failures may continue to occur. A clamp-on dc ammeter is most useful for this sort of analysis.

7.7 Computer Programs

For the computer wizard or for the person who merely wishes to minimize the computational effort involved in using a scientific calculator to optimize a design, a number of useful computer programs are available. From an engineering perspective, use of computer programs to assist in system design is essential. However, the engineer must have an idea of the limitations of the programs contemplated. The transparency of the computation process may result in the tendency to let the computer replace the creative thinking process. Herein lies the liability of computer use.

Fortunately, the computerized computation process need not be transparent to the engineer. By now, after observing the large amount of data presented in tabular form in this chapter, the engineer familiar with any spreadsheet program will quickly observe the utility of a spreadsheet in PV system analysis. In fact, the authors developed their own spreadsheets to perform the analysis of each of the systems discussed in this chapter. Generating a customized design worksheet is part of the fun of PV system analysis. It ensures that no part of the analysis process is transparent to the system designer.

One area where computer programs can be very useful is the computationally intensive determination of global radiation on surfaces at arbitrary tilt angles. The tables in Appendix A give data for three tilt angles for each location, but do not necessarily give optimal tilt for any particular system design. This is where a program such as NSol!™ by Orion Energy Corporation can save considerable computation time [6]. By varying the tilt and azimuth of the array on a computer keyboard, it is possible to optimize the match between PV output and system load requirements.

Problems

- 7.1 Offer an explanation for why a collector tilt of latitude+15° gives better summer performance in Angola. Check the peak sun hours compilations in Appendix A for other locations to see whether this phenomenon is characteristic of any other locations. Comment on the meaning of “summer” and “winter” in the tables in Appendix A.
- 7.2 Assume 10 days of autonomy are desired for a battery system, but the battery size chosen only allows for 9.2 days of storage, with a maximum depth of discharge of 80%. Then assume 12 consecutive days occur during which peak sun averages only 10% of the predicted worst-case average. What will be the state of charge of the battery system after the end of the 12th day?
- 7.3 Under what conditions of system design would the alternate formulation for battery capacity be used rather than (7.2)? Consider particularly the number of days of autonomy required.
- 7.4 At what ratio of discount rate to inflation rate would the life-cycle costs of the 220 Ah and 350 Ah battery systems in the ac refrigerator example in Section 7.2 be the same? Under what economic or other conditions would the purchase of the 350 Ah batteries be justified?
- 7.5 Calculate the life-cycle costs for the use of the 350 Ah or the 220 Ah batteries if the dc refrigerator is used in the example of Section 7.2.
- 7.6 Calculate the design array current for the ac refrigerator. Then determine the fuse and disconnect sizes for the array and for the battery system.
- 7.7 For the ac refrigerator of Section 7.2, determine the number of 4.4A modules that will be needed if tracking mounts are used. Look up the price for a tracking mount for the modules and compare the prices of modules plus mounts for tracking and fixed arrays.
- 7.8 A battery storage system is to be designed to provide a storage capacity of somewhere between 440 and 555 Ah @ 48 V at a C/20 discharge rate. Four battery types are under consideration:

Battery	Volts	Capacity	Type	Lifetime	Weight	Cost Each
A	6	220 Ah	Flooded	5 yr	56 lb	\$66
B	12	255 Ah	agm	8 yr	168 lb	\$356
C	12	180 Ah	agm	8 yr	135 lb	\$301
D	12	555 Ah	gel	12 yr	564 lb	\$1941

Assume $i = 2\%$, $d = 5\%$ and a 24-year system lifetime. Perform an LCC for the four battery types and discuss other considerations that may influence the choice of batteries. If the site were a homeowner, what would you recommend? Why? If the site were a remote communication system, what would you recommend? Why?

- 7.9 A 500 W, 120 V ac gasoline generator can be purchased for \$250 and will generate 4 kWh/gal of gasoline at 90% of full load. If the cost of gasoline is \$2.00 per gallon, and if the maintenance cycles and costs for the generator are the same as for the generator used in the hybrid system example, determine the LCC of the ac refrigerator system using the generator in place of the PV modules. The batteries and inverter remain in the system. Assume the generator needs to be replaced every 4 years.
- 7.10 Tabulate the wire, fuse and switch needs of the ac refrigerator system. Assume the same wire lengths that were used for the dc system.
- 7.11 Discuss fuse location alternatives in systems and what the fuses will protect for each location. For example, if a fuse is located at the array vs. at the controller, which gives the most system protection?
- 7.12 In the cabin example, why is a 480-gallon storage tank needed if the pump takes 7 days to pump the water needed for a 3-day weekend, assuming 160 gallon-per-day usage during the weekend?
- 7.13 Verify the wire size quoted in the text for supplying the two water pump choices for the cabin.
- 7.14 Determine the additional water that can be pumped with excess summer electricity produced by the cabin array.
- 7.15
 - a. Determine the load that can be connected to the entertainment circuit that will result in a 2% voltage drop in the branch circuit wiring.
 - b. For a 200 W load, determine the wire size that will limit the voltage drop between distribution panel and load to < 2%.
- 7.16 Show why the hybrid residence will take 5/8 of 2.9 days to use up 5 hours of charge at 2250 watts, as claimed in the text.
- 7.17 Show that the average power consumption in the hybrid residence is 239 W or less.
- 7.18 Use a network analysis program to explore the effect of unequal battery cable lengths in the distribution of currents for battery connection options 1, 2 and 3 of Figure 7.6. Solve for charging currents and discharging currents of 60 A.

- 7.19 Use a network analysis program to explore the effect of unequal open-circuit battery voltages that might be expected for charge levels of 50% and 75%. Assume, for example, that the A batteries of Figure 7.6 are charged to 50% and the rest of the batteries are charged to 75%. Then solve for the battery string currents in options 1, 2 and 3 under charge and discharge conditions.
- 7.20 Use a network analysis program to explore the effect of unequal internal battery resistances (Thevenin equivalent resistances) on the charging and discharging currents for options 1, 2, and 3 of Figure 7.6.

Design Projects

- 7.21 Develop a spreadsheet or other computer program that will enable comparative LCC analysis of a stand-alone PV system.
- 7.22 Extend your program of Problem 7.21 to include hybrid systems.
- 7.23 Write a program or develop a spreadsheet that will size a pump and wire to the pump for a PV-powered pumping system if the pumping height and daily volume are known along with the distance from the array to the pump.
- 7.24 Design your own little off-grid hide away. Specify your own loads, occupancy, peak sun and storage requirements and determine the number of batteries and the number of modules you would need to implement the system. Then specify BOS components.
- 7.25 Design you own slightly larger, off-grid hide away for a location at a latitude higher than 50° , where winter peak sun hours are significantly less than summer peak sun hours. Use winter loads such that your system will end up as a hybrid system.

References

- [1] www.AltEnergystore.com for information on dc refrigerators and other components.
- [2] *Stand-Alone Photovoltaic Systems: A Handbook of Recommended Design Practices*, Sandia National Laboratories, Albuquerque, NM, 1995.
- [3] www.SouthwestPV.com for information on PV water pumps and other dc loads.
- [4] www.windsun.com for information on 24 V dc lighting and other dc loads.
- [5] Danley, D. R., Orion Energy Corporation, Ijamsville, MD, Personal communication regarding fuel efficiency of fossil fueled generators, August, 1999.
- [6] "NSol! PV System Sizing Program, V2.8," Orion Energy Corporation, Germantown, MD, 1993-94.

Suggested Reading

NFPA 70 National Electrical Code, 2002 Edition, National Fire Protection Association, Quincy, MA, 2002.

www.batteries4everything.com for battery information.

www.unirac.com for information on array mounts.

www.zomeworks.com for information on tracking array mounts.

Chapter 8

UTILITY INTERACTIVE PV SYSTEMS

8.1 Introduction

As the cost of PV systems continues to decrease, utility interactive systems are becoming more economically viable. Furthermore, increases in consumer awareness correspond to a willingness to pay a premium price for clean electrical energy. This feedback loop, coupled with the increased demand for stand-alone systems, has resulted in a healthy demand for PV system components. And this increased demand has enabled PV module and balance of system (BOS) component manufacturers to scale up manufacturing facilities to take advantage of economies of scale to further reduce system costs.

In addition to cost reductions, the increased demand for PV systems has led to significant efforts to improve the reliability of PV system components, designs and installations. So not only are PV systems decreasing in cost, but they are increasing in reliability. While a number of electric utilities have initiated programs for installing utility interactive PV systems, the pioneering efforts of the Sacramento (California) Municipal Utility District (SMUD) and Austin (Texas) Energy have probably received the most attention in the United States.

SMUD customers participating in the PV Pioneer I program had the option of paying an extra \$4.00/month on their electric bills for which they received a 3 to 4 kW PV system installed on their roof. The system takes approximately half a day to install and is connected to the grid through a separate meter on the utility side of the grid, mounted next to the house meter [1]. Nearly 450 SMUD residential customers were participating in this program in 1998.

A new initiative, PV Pioneer II, enables the customer to own the PV system, with the PV output connected on the customer side of the revenue meter. By 2001, SMUD had installed more than 1000 PV systems, including residential, commercial, church and several larger central grid-connected PV systems. The combined output of these systems added up to more than 10 MW. In 2001, nearly 2000 SMUD customers signed letters of intent to purchase their own PV systems. SMUD has the goal of providing 20% of customer energy needs with nonhydro renewable sources by 2011 [2].

Austin (Texas) Energy is promoting the Solar Explorer program. Customers join the program by paying an additional \$3.50 per month on their electric bills. The additional revenues are used for the construction of larger PV systems that feed power into the grid. By 1999, nearly 1000 families, individuals and businesses had signed up with this program, and three larger systems had been installed in conspicuous locations [3].

On December 19, 2001, the New Jersey Board of Public Utilities issued a solicitation for \$10 million in renewable energy technology [4]. The bottom line is that consumers are demanding green energy and many states are responding to these demands.

By 1999, the technical issues associated with connecting PV systems to the utility grid had essentially been solved. In 2000, IEEE adopted Standard 929-2000. Any PV system meeting the performance criteria of IEEE Standard 929-2000, using power conditioning units (PCUs) listed under UL 1741 and installed in accordance with the current *National Electrical Code*, automatically meet all established technical performance criteria.

Although the technical problems have been solved, there are still five barriers to widespread utility interactive PV use. These barriers are 1) the high cost of PV arrays, 2) the cost of balance of system components, 3) the lack of standardization of interconnection requirements, 4) the lack of standardization of installations and accompanying training of installers and inspectors and 5) the metering of PV-generated electrical energy in a manner that fairly accounts for the value of the PV energy to the utility system [5]. Before considering the technical issues associated with small, medium and large utility interactive PV systems, the nontechnical barriers will be briefly reviewed.

The astute engineer may notice that part of the challenge in reducing the cost of PV systems involves minimizing the engineering costs associated with individual systems. While this may appear as a threat to the income of the engineer, it must be realized that if engineering costs are exorbitant, then PV systems may never come into widespread use, and the engineer may lose income for this reason. Although the next section deals with nontechnical issues, the engineer will also notice that it will be the job of engineers to work toward overcoming most of these nontechnical barriers.

8.2 Nontechnical Barriers to Utility Interactive PV Systems

8.2.1 Cost of PV Arrays

In 2002, the average cost per watt of PV modules was close to \$4.00. If 1 kW of modules were to receive 5 peak sun hours per day, they would generate a total of $(5 \text{ kWh/day}) \times (365 \text{ days/year}) = 1825 \text{ kWh/yr}$ if the array were operating at standard test conditions and if 100% of the PV-generated electricity could be delivered to the utility grid. In reality, a utility interactive PV system will deliver about 70% of its rated power to the grid, so a 1 kW array will deliver approximately 1275 kWh/yr to the utility grid. The problem, then, is to determine the amount that would need to be charged for the PV-generated electricity to pay for the system. For a PV system lifetime of 30 years, the solution is to assume the money for the PV system is borrowed over a period of 30 years and calculate the annual loan payments.

Assuming the cost of 1 kW of modules to be \$4000, with an annual interest rate on the loan of 8% and equal annual payments on the loan over the 30-year period, (5.10) can be used to determine the annual payments on the loan. The result is

$$\text{ANN PMT} = 4000 \times 0.08 \left[\frac{1.08^{30}}{1.08^{30} - 1} \right] = 355.31.$$

Paying back the loan with no profit would thus require that the annual kWh output of the modules would have to be sold for \$355.31. This amounts to $\$355.31 \div 1275 \text{ kWh} = \$0.279/\text{kWh}$. This rate is nearly triple the energy rate of most public utilities in the U.S.

Note that the annual rate to be charged is the same regardless of where the PV system is installed. Thus, if installed in an area with an average of 7 peak sun hours, the cost per kWh drops to $5/7$ of $\$0.279/\text{kWh}$, or $\$0.199/\text{kWh}$. Also note that since the loan payments will be the same over the life of the loan, the same rate per kWh can be charged over the lifetime of the system. Depending upon the inflation rate of utility-generated electricity, it is possible that the price of utility-generated electricity may at some point in time reach the value of the PV-generated electricity. Problems 1 and 2 provide the opportunity to explore what combinations of cost per module, interest rates and loan duration will result in cost-competitive PV electrical energy.

Although the value of PV-generated electrical energy appears to be more than triple the cost of electricity from the grid, in fact, it is not quite as bad as it may appear, since the time of day that the electricity is generated adds additional value to the electricity. This observation will be explored in Section 8.2.5.

8.2.2 Cost of Balance of System Components

The cost of PV modules is, of course, only part of the cost of the system. The total system cost also includes all of the array mounts, wiring, surge protection, ground fault protection, the inverter (PCU) and possibly metering or other components that may be required for the interconnection. The installation cost also must be included among the balance of system costs.

In modern systems, most of the protection mechanisms are built into the PCU, so the system can be as simple as the PV array, the PCU, the wiring between the array and PCU and the wiring from the PCU to the point of grid connection. Since the grid is essentially the storage mechanism, most of the PV system maximum power output can be used, with the exception of system losses in the wiring, inverter and modules that will normally average about 30%. The PCU will have maximum power tracking as a feature, so the system will be capable of delivering maximum output power to the grid over almost the entire range of irradiance to the system.

The economic analysis of the cost of the BOS components follows the same procedure as the economic analysis of the cost of the modules. Hence, the calculations performed in 8.2.1 must now include the balance of system costs along with the PV cost, so the combined cost is still cost competitive. Based on the experiences of SMUD, there is reason to believe that the BOS costs will also continue to decrease as experience is gained in installation, as larger quantities of PCUs are manufactured, as interconnection and installation requirements are standardized and as a fair value for PV electricity is agreed upon. And, of course, if petroleum becomes more scarce or if global warming is taken seriously, the price of fossil generation may rise to the cost of PV generation.

8.2.3 Standardization of Interconnection Requirements

Two factors dominate the interconnection process: the actual engineering costs and the paperwork. The process is further complicated by the fact that the technical requirements of utilities vary widely. The solution is straightforward. At this point in time, adequate standards have been developed to cover all of the concerns. What is thus needed is to educate all parties involved in utility interactive (grid-connected) PV installations on the validity of the IEEE, UL and NFPA codes and standards so turnkey systems can be installed by qualified installers with minimum engineering costs and minimum paperwork for small systems. It is particularly important to eliminate redundant and unnecessary interconnection requirements such as separate transformers, redundant relays, unnecessary disconnects and unnecessary meters. Larger systems may require additional engineering and paperwork, but these costs will be covered by the increased amount of energy that will be delivered by these systems.

8.2.4 PV System Installation Considerations

As of 2001, utility interactive PV system installations surpassed stand-alone systems in annual installed capacity in the U.S. [6]. As of 2002, more than 2000 utility interactive systems have been installed, thanks to incentive/buy-down programs in several states. However, only a handful of installers and inspectors were familiar with installation requirements. As the costs of PV systems continue to decline and as the costs of fossil-generated electricity continue to increase, the need for qualified PV installers and knowledgeable inspectors will very likely increase significantly.

Fortunately, a small PV installation needs to be installed only where it will not be shaded, in a manner such that it will not blow away in a strong wind, with hardware that will endure the weather over the lifetime of the system. The procedures for secure roof mounting are well known in the solar domestic water heating industry and are also applicable to PV roof mounts. Even the tilt of water heating collectors is comparable to the desirable tilt of PV arrays.

The electrical interconnection requirements for a PV system are relatively uncomplicated. Thus, electricians need to be taught how to securely mount arrays along with the *NEC* requirements for utility interactive PV installations. A single PV installer license could solve the problem, but endorsements to existing electrical contractor licenses or voluntary certification could also solve the problem of identifying qualified contractors.

Plans for PV systems can be drawn to include a variety of installation options, so the installer can submit the appropriate installation option for the proposed installation.

Finally, the building or electrical inspector needs to be apprised of the simplicity of the utility interactive PV system and the permitting process needs to be streamlined so that reasonable inspection fees can be charged.

8.2.5 Metering of PV System Output

Metering of the PV system output depends upon whether the PV system is connected on the load side or the line side of the revenue meter. The *NEC* (2002) allows for either possibility [7]. If the PV system is connected on the utility side (line side) of the meter, assuming the PV system is owned by the utility, then part of the PV output will be used by the customer, for which the customer will be billed by the utility at the standard rate. Another part of the PV output will be fed back into the grid if the customer demand is less than the PV system output. All this is transparent to the customer and to the utility. The only reason for any additional meter to record the PV system generation would be to verify that the PV system is functioning properly. The PCU, however, can be designed to fulfill this function, so a separate meter is not really needed.

If the PV system is connected on the customer side (load side) of the revenue meter, the situation changes and depends on whether the system is owned by the customer or by the utility. If the utility owns the system, then that fraction of the system output that is used by the customer does not register on the revenue meter. If there is excess PV energy, it feeds into the grid and may cause the revenue meter to run backward. Obviously this presents a more complicated situation for the utility to determine the customer usage and appropriate charges to the customer.

On the other hand, if the customer owns the PV system that is connected on the load side of the meter, then the customer's energy needs are first supplied by the PV system, with any additional demand being supplied by the utility. For that fraction of PV energy used by the PV system owner, the effect on the metering is equivalent to an energy conservation measure—the meter simply registers a lower amount of consumption. Since the system has no storage provisions, if the PV system output exceeds the demand of the owner, the excess output is transferred to the grid, possibly causing the meter to run backward. The question then arises as to whether the customer should donate this extra electricity to the utility or should be compensated for it.

The Public Utility Regulatory Policies Act of 1978 (PURPA) [8] requires that the utility pay for this electricity at the rate of its avoided cost. However, the avoided cost figure is generally established as the utility's wholesale cost of electricity, which may be significantly below the retail rate paid by the customer if an average figure is used. Furthermore, if the utility chooses to pay avoided cost, a separate metering scheme is needed to monitor that part of the PV output that is returned to the utility. Such a metering scheme adds to the cost of the installation, especially if it incorporates a time of day component.

To eliminate this added complication, more than two-thirds of the states have enacted **net metering** requirements. Net metering simply means that the utility pays the customer at the retail rate for electricity generated by the customer. Net metering makes sense because it simplifies the meter connection and the corresponding installation cost. It also provides an incentive for installation of PV systems as well as other distributed generation sources, such as wind generators.

Net metering for PV systems makes additional sense because the utility electricity displaced by PV systems is generally of high value, because it is produced during utility peaking time when more expensive utility generation is brought on line to meet utility demand. As long as the price paid by the utility for the PV output is less than the marginal cost of peaking electricity, the utility still ends up profiting by selling the electricity at its acquisition cost.

Finally, net metering makes sense because distributed generation from PV systems reduces the utility load on its transmission and distribution lines. This can reduce the need for upgrading these lines to meet increased customer load.

Currently, peak demand is generally met by utilities with gas turbine peaking generators that can be brought on line quickly. These generators are typically used less than 10% of the time to meet system peak load requirements. Although these systems are less costly on a per kW basis than large fossil or nuclear plants, the cost per kWh from these systems is quite high.

Consider, for example, a 1 MW system that has an initial cost of \$500,000. At an 8% lending rate, the annual payments on this system on a 20-year loan will be \$50,929. If the system operates 5% of the time at full load, it will generate $0.05 \times (1000 \text{ kW}) \times (24 \text{ hr/day}) \times (365 \text{ days/year}) = 438,000 \text{ kWh/yr}$. This amounts to a cost of \$0.12/kWh just to cover the cost of the loan. Fuel for gas turbine engines can add another \$0.10/kWh as an operating cost, so even if maintenance is not included, the marginal cost of peaking electricity is seen to be more than \$0.20/kWh. Thus, if a utility ends up paying \$0.09/kWh as retail rate for PV generation, it is likely avoiding a cost of \$0.20/kWh or more, especially if the PV system displaces the initial capitalization of the gas turbine generation system.

Displacing the need for the gas turbine is also an interesting consideration. What this means is that the PV system will be in operation when it is needed. This, of course, means that the PV system will be needed during peak sun hours and that the PV system will be on line during peak sun hours. Since in many areas utility demand is due to air conditioning at or near peak sun time, the first requirement is fulfilled. The second requirement is fulfilled if the PV system operates reliably every day of the year. In fact, when the value of electricity is considered, orientation of the array toward the west may result in better tracking of utility peak times by the PV output. Even though total kWh production may be less, as was noted at the end of Chapter 2 and illustrated in Figure 2.14, the overall value of the energy generated during peak hours may exceed the value of the energy generated by a directly south-facing array.

8.3 Technical Considerations for Connecting to the Grid

8.3.1 Introduction

As noted in Chapter 3, IEEE Standard 929-2000 has been developed to address the technical issues associated with utility interactive PV systems. The standard sets limits for voltage disturbances, frequency disturbances, islanding protection, power factor, harmonic distortion, reconnect after grid failure and restoration, injection of dc into the ac system, grounding and disconnects.

The quality of the output of the PCU was discussed briefly in Chapter 3. IEEE 929-2000 [9] refers to other earlier standards that were developed to insure that power supplied to the grid by small power producers meets certain standards for frequency, harmonic content and voltage level. The primary concern of IEEE 929-2000 is to guarantee that the PCU will disconnect from the utility grid if the grid loses power or strays outside established limits for voltage or frequency, even if other PV sources are connected to the grid.

UL 1741 [10] prescribes a test procedure to verify that the PCU will disconnect properly from the grid under prescribed conditions of grid voltage and frequency. Thus, any PCU listed under UL 1741 has been tested to meet the criteria established in IEEE 929.

When considering the connection of a PV source to the grid, it is important to distinguish between the electrical characteristics of a PCU and a conventional rotating generator. First of all, most utility interactive PCUs are best modeled as dependent current sources, while rotating generators appear as voltage sources. In the event of a short-circuit fault, a rotating generator can deliver a very large current, limited only by the ability of the prime mover to keep the generator rotating. Any energy stored as rotational energy can be dissipated into a short circuit as electrical energy. On the other hand, if a short circuit occurs at the output of a PCU, little more current than full-load value will flow from the PCU.

Because the PCU acts as a current source, it is easier to ensure that the PCU will meet the standards for utility interconnection. The reason is that the utility is close to being an ideal voltage source. Hence, the PCU can sense the utility voltage and frequency and inject current only if the voltage and frequency fall within prescribed limits. This same circuitry can be used to ensure that the current is injected in phase with the utility voltage. This assures a high power factor for the PCU output. The sensing circuitry has high impedance inputs and can remain connected to the utility at all times in order to monitor the voltage and frequency stability of the utility.

In addition to the areas of concern to utilities in IEEE 929-2000, the *NEC* addresses areas that relate to the safety and performance of the system from the perspective of the owner, assuming the PV system to be customer-owned and connected on the load side of the revenue meter.

The reader should keep in mind that utility interactive inverters are almost always based on conversion technology controlled by a microcontroller. Nonutility interactive units do not need nearly as sophisticated circuitry to satisfy grid connection concerns and may be based on other technologies, as discussed in Chapter 3. The microcontroller, in association with sensing circuitry, is able to measure and control many parameters associated with PCU performance.

8.3.2 IEEE Standard 929-2000 Issues

Voltage Disturbances

Table 8.1 shows voltage levels and trip times as listed in IEEE 929-2000 [9]. The voltage levels are based on limits established by ANSI C84.1 for a nominal 120 V base voltage. The percentages listed apply to other base voltage levels.

In most cases for small PV systems, the base voltage will be 120 V. The PCU needs to be designed to cease energizing the line within the number of cycles listed as occurring between the first sensed line disturbance.

Since digitally controlled PCUs can sense the line at a very high sampling rate, it is a straightforward design in hardware and software to meet these guidelines. The PCU will continue monitoring the line after the power disconnect in order to reconnect when the line has again stabilized. Note that the disconnect times listed in Table 8.1 are intended to prevent nuisance tripping when the utility is slightly out of range, provided that it returns within the prescribed limits. Once the PCU has disconnected, it must remain off line until it has confirmed that the utility has been stable for a minimum of 5 minutes.

Table 8.1 ANSI C84.1 voltage limits and IEEE 929 recommended PCU disconnect times [10,11].

Voltage	Maximum Trip Time
$V < 60$ ($V < 50\%$)	6 cycles
$60 < V < 106$ ($50\% < V < 88\%$)	120 cycles
$106 < V < 132$ ($88\% < V < 110\%$)	Normal operation
$132 < V < 165$ ($110\% < V < 137\%$)	120 cycles
$165 < V$ ($137\% < V$)	2 cycles

The set points in Table 8.1 are to be fixed in small inverters, but may be adjustable in inverters for larger systems. It should also be noted that the voltage values apply to the point of utility connection, also known as the point of common coupling (PCC) for the inverter. If the inverter is located some distance from the PCC, there may be voltage drop on the line between the inverter and the PCC. If so, compensation can be made at the inverter output, since the inverter output voltage in these cases will be higher than the voltage at the PCC.

Frequency Disturbances

IEEE 929-2000 requires that the PCU should shut down within 6 cycles if the frequency of the line voltage falls below 59.3 Hz or rises above 60.5 Hz. Once again, digital sampling enables very accurate measurement of frequency by the PCU, so the shutdown algorithm is straightforward.

Islanding Protection

A utility island occurs when a portion of the utility system containing load and operating generators is isolated from the remainder of the utility system. If the island generating source continues to feed the island during the system fault condition, the island may remain energized and several undesirable results may occur. One problem is the potential hazard to utility workers who may be working to clear the fault. It also presents a possible phasing problem when the utility comes back on line if the island source is out of phase with the utility. For these and other reasons, it is important for the PCU to disconnect from the utility if an islanding condition should occur and remain disconnected until the grid is restored to normal operation.

Normally, a single PCU will readily disconnect from the utility in the event of an islanding condition. The reason is simply that the load of the island will almost always be far more than the PCU can supply. As a result, the PCU terminal voltage will drop below the trip limits or the PCU current will exceed its rated value and the PCU will disconnect from the utility.

The greatest concern over islanding occurs when more than one PCU is in operation within the island. In this case, it is possible that they will support a feedback situation in which each PCU, sensing the combined output of the other PCUs, thinks the output of the other PCUs constitutes the grid. This possibility is enhanced under worst-case load conditions. It is thus useful to consider what might constitute worst-case load conditions.

Worst-case load conditions occur if, when the island is created by the utility fault, the island voltage does not change quickly to steady-state fault value. This will occur under two conditions: resonance at the utility frequency and island motor loads with low damping, such as grinding wheels, that continue to rotate even though power is removed from the motor.

If a circuit is at resonance with a relatively high Q, then it will continue to oscillate at its natural resonant frequency until the oscillation is ultimately damped out. As long as a motor continues to rotate, it will act as a generator and return its back emf to the grid. While induction motors are normally inefficient generators, synchronous motors are very efficient generators. The generation frequency, of course, depends on the rotation speed, so as the motor slows down, the generated frequency changes.

Circuit analysis textbooks generally prove that any parallel RLC circuit will be underdamped if it has a $Q > 0.5$. Equation (8.1) represents the response of an underdamped parallel RLC circuit.

$$v(t) = V_m e^{-\alpha t} \cos(\omega_d t + \phi), \quad (8.1)$$

where V_m is the initial amplitude, $\alpha = \frac{1}{2RC}$, $\omega_o = \frac{1}{\sqrt{LC}}$, $\omega_d = \sqrt{\omega_o^2 - \alpha^2}$ and

ϕ is a phase angle that depends upon initial energy storage in the inductor and capacitor. The Q of the circuit can be found from

$$Q = \frac{\omega_o}{2\alpha} = \omega_o RC \quad (8.2)$$

It is interesting to use (8.1) and (8.2) to calculate how long it will take for the amplitude of the voltage to decrease to the PCU trip limit as a function of Q.

The two important parameters of the equation are the exponentially decaying amplitude part, $V_m e^{-\alpha t}$, and the natural frequency, ω_d . Assuming the energized grid has a natural resonant frequency outside the trip limits, the PCU will sense the frequency departure and disconnect within the prescribed time. If the natural resonant frequency is within the trip limits, then the PCU will need to disconnect when the voltage falls outside the trip limits. For the case of the motor/flywheel

load, again, as soon as the motor speed drops enough to move the motor output frequency outside the trip limits, the PCU will trip.

Table 8.2 tabulates the number of cycles required for the amplitude of the island load voltage to decrease to 50% of its initial value. The results are obtained by setting $V_m e^{-\alpha t} = 0.5V_m$. Solving for t yields the result

$$t = \frac{\ln 2}{\alpha}. \quad (8.3)$$

But it can be shown (see Problem 8.8) that $\alpha = \pi f_o/Q$. Thus, the time for the voltage amplitude to fall to half its starting value is given by

$$t = \frac{Q \ln 2}{\pi f_o}. \quad (8.4)$$

It also can be shown that (Problem 8.9) the relationship between resonant frequency, ω_o , and natural resonant frequency, ω_d , is

$$f_o = \frac{\omega_o}{2\pi} = \frac{\omega_d}{2\pi \sqrt{1 - \frac{1}{4Q^2}}} = \frac{f_d}{\sqrt{1 - \frac{1}{4Q^2}}}. \quad (8.5)$$

So, finally, solving for t in terms of the period of the natural frequency,

$$t = \frac{Q \ln 2}{\pi f_d} \sqrt{1 - \frac{1}{4Q^2}} = \left[0.2206 \sqrt{Q^2 - \frac{1}{4}} \right] T_d. \quad (8.6)$$

Since T_d represents one cycle at the natural resonant frequency, the coefficient of T_d represents the number of cycles, N , that it takes for the voltage amplitude to decay to half its initial value.

Table 8.2 The number of cycles for the voltage to reach half the original amplitude in an underdamped, decaying, parallel RLC circuit as a function of the Q of the circuit.

Q	1	2	3	4	5	6	7	8	9	10
N	0.19	0.43	0.65	0.88	1.10	1.32	1.54	1.76	1.98	2.20

The previous analysis was based on the assumption that the utility island load had only initial stored energy. If energy continues to be added to the load in a synchronous manner, the load will continue to oscillate in a manner not very different from an electronic class C amplifier, depending upon the conduction angle of the current source. The time to decay is thus prolonged, perhaps indefinitely, depending upon the match between the load and the PCU output. So this is the worst-case condition that must be overcome.

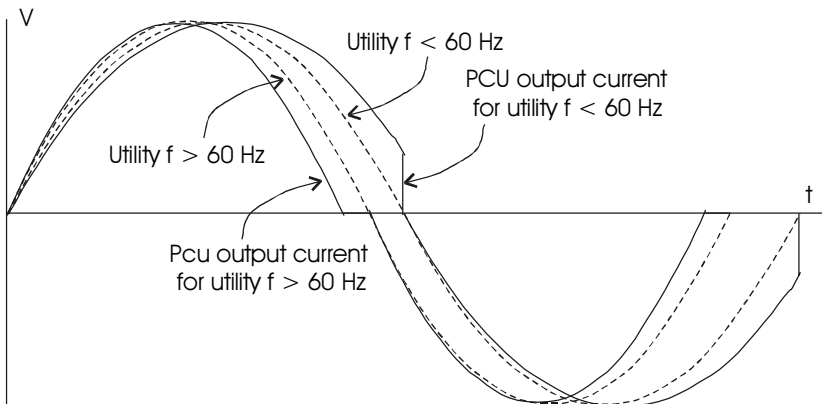


Figure 8.1 Comparison of utility voltage and PCU current for under-frequency and over-frequency utility voltage.

One means of overcoming this worst-case loading condition and still disconnecting from the load has been developed and tested by a team at Sandia National Laboratories and Ascencion Technology, Inc. [12, 13]. The procedure actually consists of two control algorithms—the Sandia Frequency Shift (SFS) and the Sandia Voltage Shift (SVS).

The SFS is a control algorithm that provides an accelerated frequency drift with positive feedback. The PCU frequency is controlled to drift away from the grid frequency unless the grid is present to lock in the PCU frequency. If the grid frequency, or island frequency, as the case may be, begins to drift either upward or downward, the control algorithm of the PCU frequency causes the PCU frequency to drift even faster in the same direction. If the grid voltage is present, then at the time of zero crossing for the grid voltage, the PCU cycle is reset to grid frequency, as shown in Figure 8.1. If the grid voltage is not present to lock in the PCU current frequency, it continues to drift away from the grid frequency until it reaches the trip point, at which the PCU disconnects as a result of its frequency being out of the allowed range.

The SVS is a similar unstable control algorithm applied to the inverter current as voltage is sensed. When voltage increases, the output current increases, and when voltage decreases, the output current decreases. An elegant means of comparing the average voltage as measured by an IIR filter with cycle by cycle voltage measurement is incorporated. The gain of the feedback loop is set so that for approximately a 1% utility voltage fluctuation, a 2% PCU current fluctuation occurs.

The combination of SFS and SVS control algorithms in a PCU has proven to provide effective means of disconnecting from the grid when multiple PCUs are connected under worst-case load conditions with $Q < 5$. The likelihood of an island load with a $Q > 5$ within the utility trip frequency range is considered to be virtually zero, so the control algorithms, combined with the voltage and fre-

quency trip limits, provide effective anti-islanding protection for the PCUs. Multiple field tests by Sandia and Ascencion Technology have verified the validity of these control algorithms for both resonant and motor loads.

Since the PCU sensing circuitry is not disconnected from the grid, when the grid is restored, the PCU is capable of monitoring the grid voltage and frequency for the time specified by IEEE 929-2000. The PCU is then either immediately reconnected at full capacity or gradually brought up to full capacity, depending on the PCU output control algorithm.

Power Factor

The rule here is simple. The PCU must operate at a power factor greater than 0.85 leading or lagging. With utility approval, it may be acceptable to operate at a leading power factor less than 0.85 to compensate for utility or building lagging power factor. This condition is easily monitored by the PCU, since voltage and current are being sensed for other purposes. It should be noted that the power factor is defined at the fundamental frequency for nonsinusoidal current delivered by the PCU.

Reconnect after Grid Failure and Restoration

IEEE 929-2000 recommends a 5-minute delay after utility grid power is restored before reconnecting the PCU to the grid. Since this is a software function, the PCU can be programmed to reconnect at any point in time the current version of IEEE 929 may require. The reason for the wait is to avoid a recurring connect/disconnect condition. Often utilities employ automatic reclosers to restore service. Many utility faults clear themselves in a short time, such as when something falls across the lines and is burned by I^2R heating. But other faults, such as downed lines resulting from accident or storm, remain faulted as the recloser tries to reset the circuit a second and a third time. If the fault remains, the utility should remain disconnected. Thus, it is desirable to have the utility grid operate in the normal range for sufficient time to ensure stability prior to reestablishing connection to the PCU.

Injection of dc Into the ac System

The PCU should not inject dc current into the ac system in excess of 0.5% of its rated ac output current under any PCU operating conditions. A number of means of preventing dc injection are available to the PCU designer. The primary reason for keeping dc out of the grid is its effect on inductive loads. With a combination of dc and ac applied to many inductors, the inductor may be driven into saturation, resulting in hysteresis losses beyond the device rating. Transformer coupling is one way to keep dc from being coupled to the grid, but it is expensive and unnecessary in view of less costly, equally reliable, other design options. Since the inverter monitors its current, it can be programmed to shut down if it should develop excessive dc in its output.

Grounding

IEEE 929-2000 recommends that the PCU and PV system be grounded in accordance with applicable codes. Grounding has been discussed in several

previous examples and will again be discussed in Section 8.3.3. Perhaps a reminder is in order that in the U.S., for systems operating over 50 V, one of the current-carrying conductors must be **grounded**. **Grounding** conductors, on the other hand, do not carry current under normal system operation, but connect the system or parts of the system to the system ground. Grounding conductors do conduct current when a ground fault occurs. The grounding conductor is the familiar round terminal on three-prong 120 V attachment caps (plug). The grounding wire is the bare wire or the green wire in electrical distribution systems, which is ultimately connected to a water pipe or a ground rod system.

Disconnects

A utility interface disconnect switch is a manual, lockable, load-break disconnect switch that is visible to and accessible to utility workers. It can be verified from a distance that the switch is open. Some utilities require such switches at the point of connection of the PV system to the utility to assure utility workers that the PV system has been disconnected. At this point, however, such switches are redundant, since any system installed in accordance with the *NEC* will have an anti-islanding inverter that will shut down when the utility is down. Furthermore, in the event that many PV systems should be connected to the grid, manually disconnecting and manually locking out all the systems will become unnecessarily time-consuming. Simply following standard grounding procedures prior to working on lines eliminates any need for manual PV disconnects. It is possible that, as utility interactive PV penetration increases, PCUs will be controllable via power line carrier signals similar to those currently in use by many utilities for demand side management purposes.

8.3.3 National Electrical Code Considerations

The *National Electrical Code* [7] is an important source of information to the PV design engineer, since it clearly defines acceptable PV system design practice. Article 690 deals exclusively with PV systems, but refers to other articles such as Article 240 on overcurrent devices, Article 250 on grounding and Article 310 on conductor ampacities. Other parts of the *NEC* also apply to specific installations or installation methods. Table 8.3 summarizes the components of *NEC* Article 690 and lists some of the other *NEC* articles that apply to PV system installations.

Most of the subsections of Article 690 are self-explanatory, so they will be left as essential pleasure reading for the reader who will be designing a PV system. A few points, however, are worthy of additional comment. The reader should realize that the intent of the following discussion is to highlight certain portions of the *NEC*. The serious system designer should consult a more comprehensive reference, such as Sand2001-0674 by John Wiles [14].

Grounding and Source Circuits

Article 690.4(c) requires that ‘connections to a module or panel shall be arranged so that removal of a module or panel from a photovoltaic source circuit does not interrupt a grounded conductor to another photovoltaic source circuit.

Sets of modules interconnected as systems rated at 50 V or less, with or without blocking diodes, and having a single overcurrent device shall be considered as a single-source circuit. Supplementary overcurrent devices used for the exclusive protection of the photovoltaic modules are not considered as overcurrent devices for the purposes of this section.”

Table 8.3 Summary of contents of *NEC®Article 690*.

Section	Contents	NEC Cross-References
I	General: Scope, Definitions, Installation, Ground-fault protection, AC modules	Article 240
II	Circuit Requirements: Maximum voltage, Circuit sizing and current, Overcurrent protection, Stand-alone systems	Articles 110, 210, 240
III	Disconnecting Means: Conductors, Additional provisions, PV equipment, Fuses, Switches and circuit breakers, Installation and service	Article 230
IV	Wiring Methods: Methods permitted, Component interconnections, Connectors, Access to boxes	Articles 310, 339, 400
V	Grounding: System grounding, Point of system grounding connection, Equipment grounding, Size of equipment grounding conductor, Grounding electrode system	Article 250
VI	Marking: Modules, AC modules, PV power source, Point of common connection	
VII	Connection to Other Sources: Identified interactive equipment, Loss of interactive system power, Ampacity of neutral conductor, Unbalanced interconnections, Point of connection	Article 230
VIII	Storage Batteries: Installation, Charge control, Battery interconnections	Articles 400, 480
IX	Systems Over 600 Volts: General, Definitions	Article 490

This statement makes two important points. First, a PV source circuit may consist of a series-parallel combination of modules, provided that the source circuit rated output voltage (i.e., V_{oc} at the lowest module operating temperature) is 50 V or less. This observation is important from the perspective of this *NEC* provision, but is also relevant in a later section on fuses and disconnects. From the grounding perspective, it simply means that all source-circuit grounds should have a common point of connection, rather than being looped together, so that if one source circuit is removed from the output circuit, the remaining source circuits will have their ground connections maintained. To facilitate compliance with this provision, source circuit combiner boxes normally include a ground busbar as well as provisions for fusing individual source circuits before their outputs are combined. This is shown in Figure 8.2.

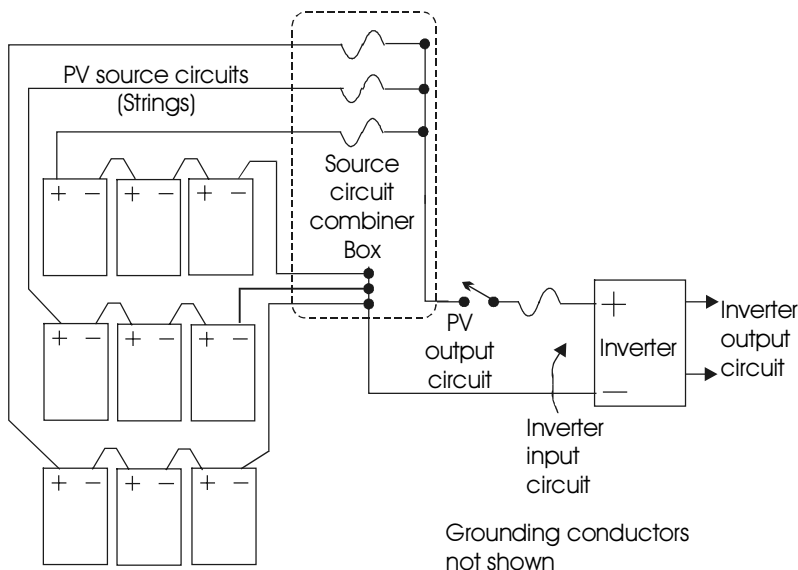


Figure 8.2 Recommended switching and fusing in PV source and output circuits.

Note first the single point of connection of the grounded conductors from each string. If any module in any string is removed, the integrity of the ground connection for the remaining strings is preserved. Also note that the individual strings may be composed of parallel modules as well as series modules, provided that the maximum string voltage is less than 50 V. Section 690.9(A) includes an exception that allows the omission of fuses in conductors provided that they are sized in accordance with 690.8(B). In 690.8(B), the required ampacity of circuit conductors is to be not less than 125% of the maximum current that will be carried. The maximum current is determined in accordance with 690.8(A) to be 125% of the rated module short-circuit current for modules in series. A further requirement of 690.9(A) for the exception to be allowed is that no external sources are connected that might produce a backfeed into the source circuit. Such backfeed might come from other parallel source circuits, batteries or an inverter.

For parallel connections, the maximum rated current is equal to the sum of the maximum rated currents that each series string contributes to the parallel combination, which equates to 125% of the sum of the individual source circuit rated short-circuit currents.

This provision is particularly useful when module short-circuit current ratings are in the 3 A range. This means, for example, that a source circuit may contain four parallel sets of 2 modules in series. The resulting source circuit will have a maximum current rating of 125% of 12 A, or 15 A at a nominal voltage of about 44 V, assuming each module has a 22 V_{OC} rating.

It is also important to distinguish the **system voltage** from the **maximum system voltage**, or **rated voltage**, since the maximum system (rated) voltage is determined under open-circuit conditions and the system voltage is determined under normal operating conditions. For example, 4 modules in series are normally needed to obtain 48 V. The open-circuit voltage of the 4 modules will usually exceed 80 V. Furthermore, *NEC* Section 690.7 requires that a temperature correction factor be applied to the module open-circuit voltage to account for the temperature dependence of cell open-circuit voltages. *NEC* Table 690.7 lists the correction factors for crystalline Si modules, for which the temperature dependence is $-2.3 \text{ mV}/^\circ\text{C}$ per cell.

For example, if the modules are to be operated where the cell temperature may drop to less than -21°C , the open-circuit voltage specified at 25°C must be multiplied by 1.25. For cells other than crystalline Si, the manufacturer must be consulted for the correction factor. The maximum system voltage for PV source and output circuits for one- and two-family dwellings may be up to 600 volts, provided that the circuits do not supply lampholders, fixtures or receptacles. Any circuits having voltages to ground in excess of 150 V must be accessible only to qualified personnel.

Note that the maximum system voltage appears between the most positive and most negative conductors of the system. For a 2-wire system, normally one will be grounded and one will be at a positive, or perhaps negative, voltage with respect to ground. Some PCUs operate with a 3-wire input from the PV output circuit, where a positive, negative and grounded conductor feed the PCU. In these cases, the system voltage is the voltage between the positive and negative conductors of the PV output circuit.

Ground Fault Protection

Kirchhoff's current law requires that the algebraic sum of the currents into a node will be zero. For a properly functioning 2-wire PV source or output circuit with one conductor grounded, any current flowing from the circuit on the ungrounded conductor will return to the circuit on the grounded conductor. For a 3-wire PV output circuit with one grounded conductor, the current in the grounded conductor will be the difference between the currents on the two ungrounded conductors. The sum of the currents entering the PCU from the PV output circuit must still equal the sum of the currents returning to the PV output circuit from the PCU.

Figure 8.3 shows how a ground fault can occur in a 2-wire PV source circuit or output circuit. The resistor, R , represents the resistance through the ground fault from the ungrounded conductor to a grounded point somewhere between the modules and the PCU. This rare event might occur if conducting material somehow became connected between the ungrounded conductor and a grounded portion of the structure, such as metal flashing or a ventilation pipe. It is conceivable that such an event might occur if insulation has been removed from the ungrounded conductor or if the insulation has degraded after exposure to ultra-violet radiation from sunlight.

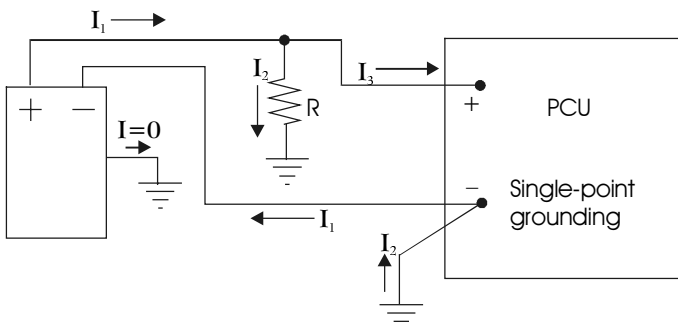


Figure 8.3 Example of ground fault.

If I_1 is the current that leaves the positive terminal of the PV source or output circuit, then I_1 must also return to the negative terminal of the same circuit. However, the current divides at R so that some of I_1 flows through the ground fault resistance and some flows to the positive input of the inverter. Since the circuit must be completed for both I_1 and I_2 , if I_2 leaves the ungrounded conductor through R , then it must return to the grounded conductor through the grounding conductor, as shown in Figure 8.3.

If the single point ground is internal to the PCU, then the PCU can be designed to sense the presence of current on the grounding conductor. Since, under normal conditions, current will not flow in the grounding conductor, the PCU will know there is a problem. One way to solve the problem is to open the grounding conductor. However, if the grounded conductor is grounded at more than one point, then opening the grounding conductor will not necessarily remove the fault, since the fault current may be able to return via any other grounded points of the grounded conductor.

Since a ground fault is very unlikely in the first place, if care is used to ensure the grounded conductor is grounded in only one place, then there will be only one path for the ground fault current to return to the grounded conductor. If this is the case, the PCU will be able to detect it and respond accordingly.

Note also that if the frames of the PV modules are grounded at a different point, this will not interfere with proper operation of the ground fault detection mechanism in the PCU. Current cannot flow through the frame ground unless there is a fault between the frame and either the grounded or ungrounded conductor of the PV modules.

If a fault occurs between the ungrounded conductor of a PV source or output circuit and a grounded structural member, it is possible that arcing may occur, presenting a possibility of fire.

Section 690-5 acknowledges this possibility and requires ground fault detection on any PV system installed on a dwelling rooftop. The ground fault detection level is not specified, but it is implied that ground fault currents on the order of one ampere are to be detected. When such a fault is detected, the ungrounded conductors of the faulted source circuit must be automatically disconnected, the

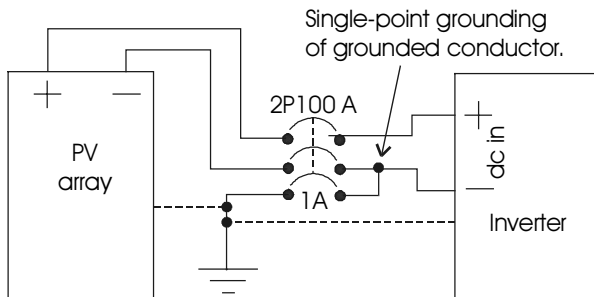


Figure 8.4 Example of ground fault detection and interruption device external to inverter.

fault current must be interrupted and an indication of the fault must be provided. If the grounded conductor must be interrupted to remove the ground fault, then all conductors must be simultaneously opened.

In the case of ac systems, ground fault protection is well defined, since the purpose is to protect humans from electrical shock. In these systems, the fault current always flows from the ungrounded conductor through the person to ground and returns to the supply along a grounding conductor or other grounded path parallel to the grounded conductor. Ground fault circuit interrupters for ac systems are thus designed to disconnect an ungrounded conductor if the difference in current between the ungrounded and grounded conductors exceeds 5 mA. The sensing may occur at the distribution panel or at an outlet.

In the case of PV source and output circuits, the sensing will take place either in the PCU or in a GFDI device at the PCU or charge controller input, depending upon whether the PV system has battery backup. Exactly how the PCU will interrupt the source or output circuit in order to remove the ground fault, however, is left to the designer of the PCU. One method of providing ground fault detection and interruption is shown in Figure 8.4. If the current in the 1 A circuit breaker between the grounded conductor and the grounding conductors exceeds 1 A, the breaker trips and the common trip causes the 2P 100A circuit breaker to trip. All breakers are dc rated.

The job of the engineer is to understand the nature of ground faults and to ascertain that ground fault protection is provided for the system in accordance with *NEC* requirements.

AC Modules

Since PV systems are inherently distributed systems, some manufacturers have introduced ac PV modules. The modules incorporate individual PCUs integral to the module. Since economy of scale has not been significant in PCU design, the cost of a PCU has been pretty much proportional to its power handling capacity. With application-specific integrated circuits and digital control, it is a straightforward design exercise to design a small, low-wattage PCU that will meet all IEEE 929 and UL 1741 requirements. The result is a module with a 120 V ac output.

The main advantage of ac modules is that they allow the system to be built in increments according to needs and budget. The main disadvantage is that each module inverter requires separate intelligence and control, increasing the cost of the system somewhat.

Other advantages include on board maximum power tracking and a 120 V ac output circuit that carries correspondingly less current, enabling wiring with smaller wire sizes with minimal voltage drop. The output of an ac module is thus considered to be an inverter output circuit and none of the dc source circuit and output circuit rules that apply to dc modules apply to ac modules. A single disconnect is allowed for the combined parallel ac output of more than one ac module, but each module must have its own connector, bolted or terminal-type disconnecting means. A single ac ground fault detector is acceptable for a group of ac modules as long as the ground fault detector will remove any ground fault that should occur.

Overcurrent Protection

NEC Article 240 provides extensive narrative on overcurrent protection. Section 690.9(A) requires that "... all photovoltaic source circuit, output circuit, PCU output circuit and storage battery circuit conductors and equipment shall be protected in accordance with the requirements of Article 240." The only exceptions to this requirement are those conductors for which Section 690.8(B) applies, as discussed earlier. Devices used on dc must have an adequate dc rating. Sometimes the dc rating is not stamped on a device, but if the manufacturer is consulted, a dc rating may be available.

Any time a fuse is energized from both directions, if the fuse is accessible to other than qualified persons, then the fuse must be disconnected from both directions independently of fuses in other PV source circuits. This situation will occur when PV source circuits are combined to form PV output circuits. In these cases, one side of a fuse is energized from one source circuit and the other side is energized from the remaining source circuits.

Connection to Other Sources

As previously mentioned, the NEC allows for PV system connection to either the line side or the load side of the revenue meter. One somewhat more subtle point is worthy of mention regarding the interconnection.

When the point of interconnection is on the load side of the revenue meter, Section 690.64(B) applies. This section allows PCU output circuits to be connected to any distribution equipment on the premises provided that 5 conditions are met.

1. Each PCU output circuit interconnection must have a dedicated disconnecting means, which will most likely be a circuit breaker.

2. The sum of the current ratings of any overcurrent devices that supply a busbar or conductor must not exceed the current rating of the conductor, except in a dwelling unit, where the combined rating of the overcurrent devices may be no higher than 120% of the rating of the busbar or conductor. The point here is

that normally a distribution panel is supplied by conductors that are rated at or below the rating of the busbars in the panel. The conductors are protected by a main circuit breaker, which, in turn, also protects the busbars in the panel.

There is no limit imposed upon the sum of the ampacities of the load circuit breakers in a distribution panel. It is not unusual, for example, for a 200 A, 40-circuit distribution panel to have the equivalent of twenty 20-A circuit breakers on each side of the line. This adds up to a total possible load on the bus of 400 A on each side of the line. This cannot normally occur, however, since the main circuit breaker will limit the current to 200 A on each side. But with an additional PV source of, say, 5 kW @ 120/240 V connected from a PCU to the bus, an additional current of 20.8 A can be supplied to each of the busbars. Since the circuit breaker at the point of utility connection normally needs to be rated at 125% of the inverter output, the next available circuit breaker will be a 2-pole, 30 A circuit breaker. Thus, if the 200 A busbars are protected by a 200 A circuit breaker in the utility feed, the overcurrent devices of sources connected to the busbars adds up to 230 A. This is unacceptable in any occupancy other than a residential occupancy. Since 230 A is less than 120% of 200 A, this connection is acceptable in a residential occupancy.

The feed from the main breaker always attaches to the top of the busbars. Depending upon the exact point of interconnection of the PCU, it is possible that portions of the busbars may carry 220.8 A until the available current is carried from the busbar by the branch circuits on the busbar. The possibility of this occurrence suggests that the PCU should be interconnected to the busbar through a circuit breaker located near the bottom of the busbar. Although this will still allow for a 220 A load on the panel, it is highly unlikely that any portion of the busbar will carry the full 220 A.

3. The interconnection point must be on the line side of all equipment having ground-fault protection, unless other ground-fault protection is provided to ensure that the equipment is ground-fault protected from all current sources.

4. ‘Equipment containing overcurrent devices in circuits supplying power to a busbar or conductor shall be marked to indicate the presence of all sources.’’ This means that if the PCU is connected into a distribution panel that is fed from a remote main disconnect at the meter location, usually outside the building, then the main disconnect should be labeled with information that a PV source is connected at the distribution panel. There is no particular safety risk from power from the PCU to maintenance personnel working on the main disconnect, since the PCU will disconnect from the line if the main is turned off. The label, however, provides an immediate explanation if the maintenance person should notice that the meter is running backwards.

5. ‘Equipment such as circuit breakers, if backfed, shall be identified for such operation.’’ Circuit breakers and fuses are bilateral, but it is important that maintenance personnel realize that the load side of a fuse or circuit breaker is connected to a source rather than a load. Technically speaking, all circuit breakers in a panel are supposed to be identified, anyway. But, in reality, they are often identified incorrectly. In other cases, the label with the identification for

circuit breakers has been degraded to the extent that it is no longer readable. In any case, the purpose of this requirement is to protect maintenance personnel from shock from the load side of a backfed circuit breaker if the circuit breaker is switched off.

In a properly functioning PV system, with an IEEE 929 compliant inverter, this requirement becomes merely a precaution against inverter failure, since IEEE 929 requires the inverter to shut down if utility power is lost. Thus, since turning off the circuit breaker removes utility power from the inverter, the inverter shuts down and no voltage is present on the load side of the backfed circuit breaker.

8.3.4 Other Issues

Aesthetics

Although not a part of Article 690, the *NEC* also indicates that all electrical work should be done in a ‘workmanlike manner.’ This addresses the importance of a professional appearance for an installation and helps to remove any potential objections to the aesthetics of the installation.

Electromagnetic Interference

The U.S. Federal Communications Commission requires that any electronic device with an electronic clock that runs at a frequency greater than 9 kHz must meet its standards for electromagnetic interference (EMI) [15]. EMI occurs in two forms—conducted and radiated. Conducted EMI is coupled directly through connections to the power line. Radiated EMI consists of radio frequency signals transmitted by the device directly to the surroundings. Both types of EMI, if sufficiently strong, can interfere with other electronic devices.

Since all modern utility interactive PCUs are microprocessor controlled, all have internal clocks that can be expected to run at frequencies in the MHz range. Hence, all are subject to the radiative and conductive emission standards as set forth in FCC Part 15 of the Code of Federal Regulations. Each unit must have a label that indicates compliance.

Conducted emission will normally not be a problem because of the low pass filters needed at the output of an inverter to average out the synthesized sinusoidal signal. High frequency currents that might otherwise be conducted to the utility interconnection are thus suppressed by this filter.

Radiated emission is caused by clock and other high frequency currents circulating in sufficiently long conductors on the printed circuit boards of the PCU. The long, sometimes looped, conductors act as antennas and radiate the clock pulse signal. These same conductors act as receiving antennas for signals from other devices. Since the clock is not sinusoidal, it contains many harmonics that spread across the spectrum. An important part of suppression of radiated emission is the PCU cover. Hence, it is important to avoid operating the PCU without its cover for prevention of electrical shock, but also for FCC compliance.

Surge Protection

PV system surge protection is not directly addressed in the *NEC* or in IEEE 929-2000. However, it is worthy of consideration. Surges may appear on either the utility line or on the PV line. Both are subject to lightning strikes, and the utility line is particularly susceptible to transients from events such as motor starting and stopping, which may cause sharp inductive voltage spikes. Most quality PCUs will provide MOV or SOV surge protection on both the dc side and the ac side of the PCU. These devices act much like bilateral zener diodes with response times measured in nanoseconds. They can bypass hundreds of joules of energy that might otherwise enter the PCU or the PV modules and damage the components. Lightning protection, as mentioned in Chapter 3, is also a wise choice for systems installed in areas with a high incidence of lightning. The idea is to dissipate any uneven charge balance between ground and the atmosphere prior to the buildup of sufficient voltage to cause arc discharge.

Mechanical Considerations

The primary consideration in the mechanical design of utility interactive photovoltaic systems is safety. This includes the safety of individuals as well as the protection of structures and other property that could be damaged as the result of mechanical failure.

Building codes are adopted and enforced by local jurisdictions to help ensure a safe environment in and around buildings. A major difference exists between the installation of utility-interactive versus stand-alone photovoltaic systems in that codes are much more likely to be enforced for the former. This is primarily because of the need to electrically connect the interactive system to the grid, which usually results in multiple inspections: a) by the electric utility service provider and b) by local code officials, which may include both electrical and building inspections. Stand-alone PV systems need only be inspected as required by local building officials.

As discussed in Chapter 6, large area arrays may present a significant wind load on a structure. They are also subject to corrosion and degradation by ultra-violet sunlight components. Furthermore, they may be subjected to other conditions such as rain, snow, ice and earthquakes. While most arrays are tested for mechanical performance, and while most array mounts have been pre-engineered to withstand the worst of loading conditions, it is still important for the engineer to determine that the specific array mounting is adequate with respect to existing structural parameters and local weather conditions. The ASCE standard procedures and formulas for computing the various types of mechanical forces should be followed. In addition to the *National Electrical Code*, the PV engineer should keep abreast of the periodic updates to *Minimum Design Loads for Buildings and Other Structures* (SEI/ASCE 7-02) [16].

Of the various types of forces mentioned above, aerodynamic wind loading generally presents the most concern. At most locations around the world, the force effects due to wind loading are much higher than the other forces acting on the structure. For example, both dead- and live-weight loads due to a photovol-

taic array on a building are usually less than five pounds per square foot (psf). In contrast, the computed wind loads are typically between 24 psf and 55 psf, depending on location and the specific array mounting configuration.

In addition to the above considerations, the design engineer must select and configure the array mounting materials such that corrosion and ultraviolet degradation are minimized. Also, if the array is mounted on a building, the structural integrity of the building must not be degraded, and building penetrations must be properly sealed such that the building remains watertight over the life of the photovoltaic array.

8.4 Small (< 10 kW) Utility Interactive PV Systems

8.4.1 Introduction

IEEE 929-2000 defines a small PV system to be rated at less than 10 kW. It is interesting to investigate what percentage of residential installations might fall outside this category.

Assuming 12% overall module efficiency, this would mean that for irradiance of 1 kW/m^2 , each square meter of PV area would generate 120 W if the modules are operating at their maximum power points. Hence, to generate 10 kW would require 83.33 m^2 of roof space, assuming the array to be roof mounted. As a rough estimate, $1 \text{ m}^2 \approx 10 \text{ ft}^2$, so the array would require approximately 830 ft^2 of roof space. For most dwellings, this area comes close to being the maximum area that may be south facing, especially if room is provided for access to the modules for maintenance. Hence, 10 kW is a reasonably practical size limit for residential PV systems.

The next question is how many kWh can the system be expected to generate? The answer depends upon the location of the system and on the overall conversion efficiency from dc array output to ac inverter output. While some areas receive upwards of 7 average daily peak sun hours over the year, other areas receive less than 4. A 10 kW PV array can thus be expected to generate somewhere between 40 and 70 kWh/day, or 1200 to 2100 kWh/mo for an annual average array output energy. Loss mechanisms, however, generally result in an overall conversion efficiency between 60 and 75%, depending on whether the system incorporates battery backup and whether a maximum power point tracking charge controller is used for systems with battery backup. Figure 8.5 shows loss mechanisms that occur between the generation of electrical power by the individual modules and final delivery of power to the utility grid.

These losses have been discussed in earlier examples, with the exception of the mismatch and dust losses. To this point, the degradation in array output has been blamed on dust only. However, since no two modules are exactly the same, when modules are combined into an array, there will be losses due to the fact that the maximum power voltages and currents of all modules will not be exactly the same for each module. Thus, if two modules are in series, they will not both necessarily operate at their maximum power currents, since the array

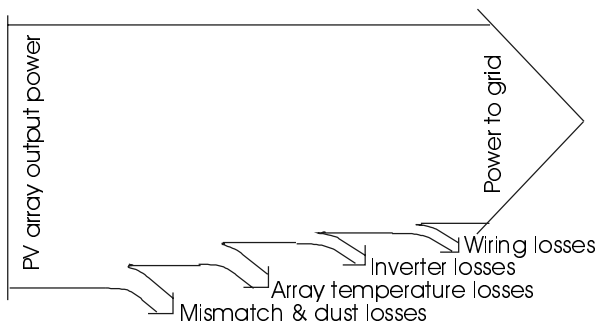


Figure 8.5 Loss mechanisms between module output and inverter output.

will operate at the overall maximum power current if the array feeds a maximum power tracking device. In a similar fashion, if two modules are in parallel, they will not necessarily have exactly the same maximum power voltage, so the overall maximum power voltage of the pair will be tracked by the maximum power tracking device. The net result is that the PV array will have less than the anticipated amount of power due to these mismatch losses. In any case, the mismatch losses can be grouped with the losses due to dirt on the modules.

If batteries are in the system, there will be battery charging and discharging losses. If the array is connected directly to the batteries, the array will operate at the battery charging voltage, which will probably be below the maximum power voltage of the array, thus resulting in additional power loss. If a maximum power point tracking charge controller is incorporated into the system, then the conversion efficiency of the MPT controller needs to be accounted for, but the array will then operate at its maximum power point.

Returning to the question of annual kWh delivered to the grid from the array, if the loss mechanisms are accounted for, it is seen that, depending upon the specific losses and on the specific irradiation data for the site, a 10 kW array can be expected to deliver somewhere between 720 and 1575 kWh/mo to the utility grid or to PV system owner loads.

Since the average residential electrical consumption is in the 1000 kWh/mo range, depending upon location once again, it appears that installation of a 10 kW PV system on every rooftop can produce sufficient kWh to exceed the demands of the dwellings upon which the PV systems are installed. Of course, the PV systems will be generating electrical energy only while the sun is shining, so if all electricity used is to be PV generated, obviously massive storage capability will be required. One way to reduce the storage needs is to reduce nighttime electrical consumption. This, of course, is contrary to most current utility marketing schemes, since it is economically beneficial to them with present generation to encourage nighttime electrical use to distribute their load more evenly.

One major advantage of distributed electrical generation on rooftops is the elimination of power plant siting concerns. Most consumers tend to be happy to install PV systems on their roofs, whether they own the system themselves or whether the system is owned by the utility. Customer surveys consistently show

customer support of cleaner generation, even if it has a premium price. If the choice becomes that of a PV system on their roof vs. a coal or nuclear plant nearby, the PV system becomes an even more attractive choice for most consumers. For those who perceive PV systems as aesthetically unappealing, it must be remembered that beauty is in the eye of the beholder.

8.4.2 Array Installation

The preferred orientation of a PV array will normally be south facing, mounted in a fixed position, tilted at 90% of latitude. This positioning will usually result in maximum annual kWh generation by the array. Depending upon the duration of utility peak load and the difference between utility peak load and utility base load, it may be desirable to mount the array with a different exposure. Although the alternate mounting may result in generation at preferred utility times, the alternate mounting will generally result in a reduction of annual kWh production. Thus, unless the utility has a preferred rate for peak electricity, it may not be worth it to the system owner to orient the array to coincide with utility peaking. In some cases a compromise can be had, especially when the roof of the dwelling has more west-facing exposure than south-facing exposure. Then some modules can be mounted with each orientation.

Arrays mounted on a roof of a residence require ground fault protection for the array output. Ground mounted arrays do not require ground fault protection, but may require protection from vandalism. Whether roof mounted or ground mounted, the mount and array assembly must meet mechanical requirements as discussed in Chapter 6.

8.4.3 PCU Selection and Mounting

It should be remembered that PCUs are not noise-free. In a manner similar to fluorescent light ballasts and other magnetic loads, the PCUs may produce a 120 Hz hum. They should thus be mounted in as practical a location as possible from an electrical and mechanical perspective, but should also not be mounted where noise will be an annoyance. Generally, mounting the PCU outdoors or in a garage or carport is acceptable. If it is mounted near an air conditioner compressor or a swimming pool pump, the PCU noise will be pretty much masked by the other noise. Fortunately the PCU is not noisy at night.

When selecting a PCU, it is important to remember to specify a utility interactive unit, since there are a wide variety of units available. Some are straight utility interactive, some can be used as utility interactive as well as stand-alone and some are intended for stand-alone use only. While a wide range of performance specifications may be available for any unit, it is important to identify those parameters that are most significant. Features to consider may include any or all of the following:

IEEE 929 and UL 1741—If the PCU has a UL 1741 listing, then it has been tested to IEEE Standard 929 and consequently complies with *NEC* requirements.

For small systems, all voltage and frequency trip points are factory preset and are not field adjustable.

Power rating—Maximum PCU output power is normally specified at an ambient temperature of 25°C. Surge power rating is less important for a utility interactive PCU, since any surges encountered in the load can generally be met by the utility. For a stand-alone PCU, surge capability is more important. Utility interactive units with battery backup act as stand-alone units if the utility disconnects, so in this case, the surge capacity becomes relevant.

Peak efficiency—It is important to note the input voltage over which the stated peak efficiency is obtained. Since the utility interactive PCU always is loaded by the utility connection, if it is designed with maximum power tracking, it will deliver maximum power to the grid over a wide range of PV input power and will operate close to peak efficiency over most of the maximum power tracking range. Modern PCUs should have peak efficiencies in excess of 90% over most of the operating range.

Maximum power point tracking range—Look for the widest possible range of input voltages over which the unit is capable of tracking maximum power.

No-load power consumption—No-load power consumption should be very low, although normally the PCU will operate at maximum power output.

Nighttime losses—If the unit operates on power supplied by the PV system, then there will be no nighttime losses. If the unit has a stand-alone mode of operation, then one can normally expect it to have a ‘sleep’ mode that consumes very little power if no loads are connected.

Warranty—Most quality PCUs carry at least a 5-year warranty. Check what the warranty covers.

Code compliance—UL 1741 listing indicates compliance with IEEE 929. It is possible to purchase PCUs that incorporate additional *NEC* compliance components, such as ground fault protection, input and output disconnects, fusible combiners for multiple string inputs, so strings will not need to be fused in a remote or difficult-to-access location and weatherproof packaging.

Data monitoring—Some PCUs provide optional data monitoring capability by digitizing system parameters and making them available on an output bus. Some monitoring is available at the PCU and some units provide for remote data logging via telephone dial-up or other communication means.

8.4.4 Other Installation Considerations

Prior to commencing the installation, since the system will very likely be inspected by both the utility and the local municipality, it is important to first complete all the necessary permitting paperwork. This may offer an excellent opportunity for the engineer to perform an educational public service by answering any questions either authority may have about the installation.

Persons not familiar with IEEE 929, UL 1741 and Article 690 of the *NEC* may be reluctant to accept the straightforward installation allowed by these codes and standards. It is possible that the most time-consuming part of the in-

stallation may be convincing the inspectors that the installation will be safe, competent and code compliant. Fortunately, electrical inspectors tend to be well versed on the *NEC* and are generally interested in new technology.

It is also conceivable that a zoning restriction on installation of rooftop solar systems on the street side of a building may exist. The permitting process may then involve a trip or two to zoning boards or town council meetings, perhaps with an attorney or a delegation of solar enthusiasts.

8.4.5 A 2.5 kW Residential Rooftop Utility Interactive PV System

PCU Selection

A number of factors may enter the decision-making process associated with installation of a residential PV system. Perhaps the area of rooftop available will be a limiting factor. Perhaps it will be budget. Unlike the decision process for stand-alone systems, the first item of consideration is not necessarily the load. In this section, a nominal 2.5 kW residential rooftop interactive system will be designed. A 2.5 kW system has been selected because an interesting 2.5 kW PCU is available and sufficient roof area is also available. The system is to be installed in a southern location where the maximum array temperature will be 60°C and the minimum array temperature will be -10°C.

The particular PCU is listed under UL 1741 and has the following operating specifications:

dc Input	Input Voltage Range	250–550 V
	Maximum Input Current	11.2 A
ac Output	Voltage	240 V 1φ
	Nominal Output Power	2200 W
	Peak Power	2500 W
	Total Harmonic Distortion	< 4%
	Maximum Efficiency	94%
General	Internal consumption in operation	≤ 7 W
	Internal consumption in standby	0.25 W
	Weight	30 kg

A particularly useful feature of this inverter is the use of the power line for transmission of data to a computer that can then be used for monitoring purposes, thus eliminating wiring for data monitoring except for sensors.

PCU Mounting

As luck would have it, the main ac distribution panel is surface mounted, with adequate space next to it for mounting the PCU. It is located where a little hum from the PCU will not annoy anyone and where it has an open space for a 2-pole circuit breaker. The weight of the PCU must be considered carefully

when the PCU is mounted and all instructions provided by the manufacturer should be followed.

Module Selection

The next step is to select an appropriate module for the system input. Working backward from the PCU input requirements, using *NEC* requirements, a set of limiting conditions can be established for the module(s). First of all, *NEC* Table 690.7 requires multiplication of V_{OC} of a Si array by 1.13 to correct for the -10°C input temperature. Thus, the maximum V_{OC} of the array at 25°C is limited to 486 V to keep the array output voltage below 550 V over the operating temperature range. The array I_{SC} must be limited so that $1.25 I_{SC}$ will be less than the PCU rated input current. Thus, $I_{SC} \leq 8.96 \text{ A}$.

Coincidentally, a certain crystalline Si module has the following operating specifications:

P_{max}	120 W
V_m	17.1 V
I_m	7.0 A
V_{OC}	21.0 V
I_{SC}	7.2 A
dimensions	26" x 56" (66 cm x 142 cm)
Bypass diodes internal to the module	

Note that if 22 of these modules are connected in series, V_{OC} for the string will be 462 V, which lies nicely within the input voltage limitations. At maximum power under standard test conditions, the string voltage will be 376 V, again, nicely within the limits of maximum power tracking. Furthermore, 125% of I_{SC} also lies nicely within the PCU input current limits. Finally, the maximum total array output power will be 2640 W. Although this power level exceeds the 2500 W rating of the inverter, this array power is acceptable, since it is at standard test conditions, and the inverter power rating applies to the inverter *output* power. With a $0.5\%/\text{ }^{\circ}\text{C}$ decrease in power for array temperatures above 25°C , and with a typical array temperature of 55°C , the array output power decreases to 2244 W. Array mismatch, dust and wiring losses may reduce the array output power by another 10%, so a more typical inverter input power will be closer to 2020 W, which is well below the inverter output power rating. With an inverter efficiency of 94%, this results in an inverter output power of about 1900 W under irradiation of 1 kW/m^2 .

Module Mounting

Normally the modules will be mounted securely in a south-facing direction several inches above and parallel to the roof slope. Several commercial array mounting kits are available for this purpose. These kits provide sufficient flexibility in the location of mounting points to ensure that the array mounts will be secured to roof trusses or to spatters that have been installed between roof trusses to provide a secure mounting for the array. The commercial kits are en-

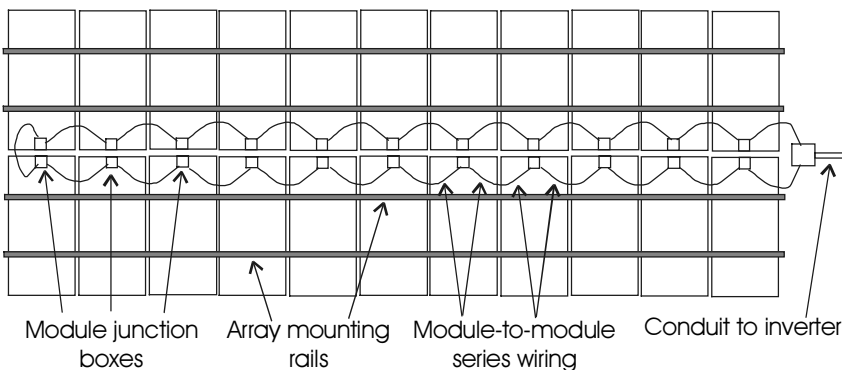


Figure 8.6 Array layout and wiring for 2.5 kW residential rooftop PV system.

gineered to meet wind load requirements and provide sufficient clearance between the array and the roof to ensure adequate cooling of the modules. If, after the modules are mounted, it will be difficult to access any of the wiring, it is a good idea to prewire such points prior to module mounting. Grounding connections sometimes fall into this category.

Assuming that the roof has sufficient area to accommodate the modules in two rows of 11 modules each, Figure 8.6 shows a convenient mounting arrangement for the modules, including the orientation of the module junction boxes for convenient wiring of the modules.

The figure shows the series-connected modules with one additional rooftop junction box at the end of the array for connecting the open wiring of the modules to the wiring in conduit to the inverter. A possible problem with the wiring as shown is that the wiring forms a rather large loop, which can act as an antenna. This may present an electromagnetic interference problem for the inverter microprocessor circuitry.

Another possible problem is the proximity of the two rows of modules. This makes it a bit more tricky to reach the junction boxes for wiring the modules. In fact, in this case, one row of modules would need to be wired and secured one at a time. Then the second row would need to be wired in the same fashion. If a space of about 30 inches can be left between the rows, it allows for much easier access to the module junction boxes and creates a better configuration to support convective cooling of the modules. This, of course, makes the loop antenna even larger in area, and it may be a good idea to run one circuit conductor along with the other conductor to reduce the loop area, even though it results in a longer conductor length and a correspondingly larger voltage drop.

Assuming a maximum wind load of 30 psf, the total wind load on the array adds up to $(30 \text{ psf}) \times (10.1 \text{ sq ft/module}) \times (22 \text{ modules}) = 6666 \text{ lb}$. If $\frac{1}{4} \text{ in} \times 3.5\text{-in}$ stainless steel lag screws are used for mounting the array supports, then each screw will support (see Table 6.6, assuming Douglas fir) $167 \times 3 = 501 \text{ lb}$, allowing for 3 in of thread actually in contact with wood. Thus, if four screws are used to secure each of the four rails, then the total holding strength will be 8016

lb, providing an overall safety factor of $8016 \times 4.5 \div 6666 = 5.4$ for the holding strength. If the array is centered on the roof, this will reduce the wind loading to a minimum and will most likely provide the most aesthetically pleasing appearance.

System Wiring

The current rating of the module wiring must be at least $1.25 \times 1.25 \times 7.2 \text{ A} = 11.23 \text{ A}$. At a temperature of 60°C , the ampacity of a conductor with 90°C rated insulation must be derated to 71%, so the module wiring must be rated at a minimum of 15.82 A at 30°C . Thus, #14 wire is adequate, since #14 with 90°C insulation is rated at 25 A at 30°C . If the array junction box is mounted 50 ft from the PCU, and if an additional 130 ft of open wiring is used between modules and the array junction box, then the equivalent 2-way distance from modules to PCU will be $(130 \div 2) + 50 = 115$ ft. Hence, if #14 copper wire is used, the resistance of the wiring from array to PCU will be 0.706Ω . At rated array current, this will produce a voltage drop of $7.0 \times 0.706 = 4.94 \text{ V}$, which is approximately 1.3% of the array output voltage. Hence, #14 Cu wire with 90°C insulation is adequate from array to PCU.

For the wiring in conduit between the array junction box and the PCU, #14 THWN-2 is readily available. However, it is possible that #14 USE-2 will not be available for the open wiring between modules. Thus, in order to meet the ultraviolet resistant requirements of the open wiring, it may be necessary to use #10 USE-2, which will lower the total wiring resistance to $0.1612 + 0.307 = 0.3231 \Omega$, which will result in a voltage drop of 2.26 V, or 0.6%. All wiring of modules and output circuit must have insulation rated at 600 V.

The wiring of the modules and the PV output circuit is particularly simple, since the wire is adequate to carry any worst-case short-circuit current. Hence, per *NEC*, the inclusion of fuses or blocking diodes in the PV source circuit is optional. Fusing of the circuit should thus be in accordance with module manufacturer recommendations, which, in this case, would mean a 12 A fuse, which is the next size above 156% of the module I_{SC} . The modules contain internal bypass diodes, so no external bypass diodes will be needed.

The wiring from PCU to the distribution panel, assuming the point of common coupling will be at the distribution panel, needs to be rated at 125% of the maximum PCU output current, or 13.02 A. Hence, #14 is also adequate to carry the PCU output current to the distribution panel, provided that the distance from PCU to distribution panel is short enough to limit voltage drop to approximately 2%. At 240 V, this allows for a distance of 75 ft. A 2-pole, 15 A circuit breaker, labeled as the point of utility connection, will be suitable for the connection to the distribution panel.

Grounding, Surge Protection and Disconnects

The PV system will require ground fault protection as well as dc and ac disconnects. The PCU is supplied with input surge protection. The negative PV output conductor should be grounded at a single point at the PCU to ensure

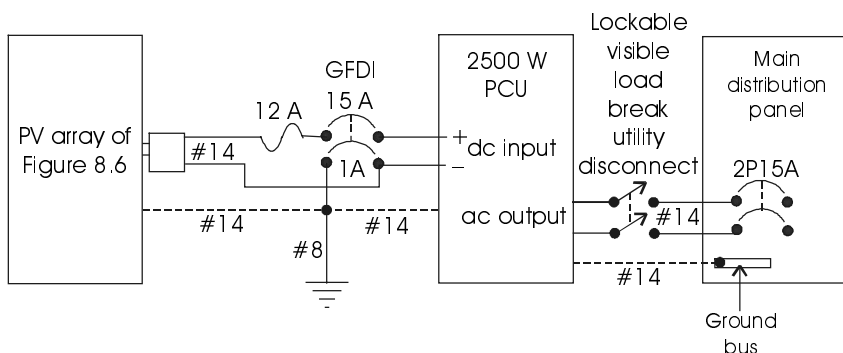


Figure 8.7 A 2 kW utility interactive residential rooftop PV system.

proper operation of the ground fault circuit. The equipment may be grounded with a grounding conductor that is the same size of the largest circuit conductor. Hence, the modules and PCU may be grounded with #14, but the grounding electrode conductor will still need to be no smaller than #8. The ac grounding conductor from the PCU can be connected to the ground bus in the distribution panel. The input will require a minimum 15 A dc disconnect rated at 600 V, and it is possible that the utility will require a lockable disconnect in a readily accessible location to disconnect the PCU output from the utility. Figure 8.7 shows a schematic diagram of the final system. Note that the dc and ac disconnects, as well as the GFDI device and dc fuse holder, are supplied with the inverter, thus reducing the number of boxes that need to fastened to the wall.

Missing in Figure 8.7 is any monitoring equipment that may be included with the system. The PCU includes the capability of monitoring PCU parameters remotely via power line carrier. PCU data can be obtained by a PC connected to any outlet in the dwelling through the ac power line of the dwelling. Additional revenue meters may be incorporated between the PCU and the point of utility connection to monitor PV output energy and at the utility service to the dwelling to monitor energy supplied to the dwelling by the utility and energy supplied to the utility by the PV system.

8.4.6 A Residential Rooftop System Using AC Modules

A recent development in PV systems is the microinverter, which is a PCU that meets UL 1741 requirements and is intended for use with a single module. The PCU is located at the module, so that, in effect, the system has no dc wiring. This eliminates the need to locate dc-rated fuses and other components. Microinverters are typically rated in the 100-to-300-watt range.

Section 690.6 notes that ‘the PV source circuit, conductors, and inverters shall be considered as internal wiring of an ac module.’ The output of an ac module is thus considered to be an inverter output circuit.

NEC 690.6(C) provides that ‘a single disconnect shall be permitted for the combined output of one or more ac modules. Additionally, each ac module in a multiple ac module system shall be provided with a connector, bolted or termi-

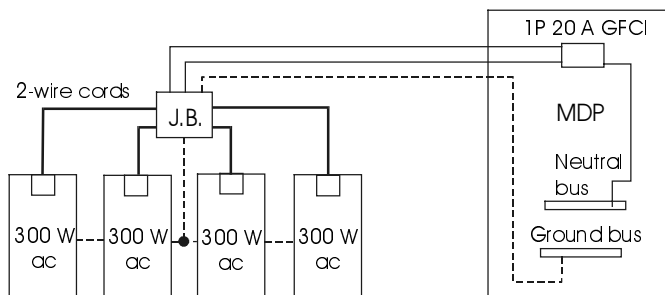


Figure 8.8 Residential rooftop system with ac modules.

nal-type disconnecting means.” Ground fault protection may use a single device for detecting ac ground faults that will disable the ac power to the ac modules. By disabling ac power to the modules from the utility connection, since the modules meet UL 1741, the module outputs are also disabled.

Of particular interest in the wiring of ac modules is the overcurrent protection requirements, which are listed in *NEC Article 240.5(B)(2)*. This particular section of the *NEC* deals with overcurrent protection of flexible cords. It specifies the length and size of flexible conductor that may be used with 20 A to 50 A branch circuits. The section provides that #18 flexible cord may be connected to a 20 A branch circuit provided that it is not longer than 50 ft. If #16 flexible cord is connected, its length must be less than 100 ft. Any length of #14 flexible cord may be connected to either a 20 A or a 30 A branch circuit.

Hence, if $1.25 \times (\text{sum of all module output currents}) < 20 \text{ A}$, then each individual module may be connected to the inverter output circuit with #18 wire, provided that the cord is less than 50 ft in length from module to the point of connection. The inverter output circuit would then be connected into the main distribution panel by backfeeding a 20 A ac ground fault circuit interrupter to provide both ground fault protection as well as protection of the conductors. Figure 8.8 shows a residential ac module system that uses 300 W ac modules connected at a single junction box with screw-type terminal strips. The combined output of the modules is then fed to the ac distribution panel with #12 wire. All cords from individual modules are UV rated.

8.4.7 A 4800 W Residential Rooftop System with Battery Storage

In some areas, it is not uncommon for utility service to be interrupted as a result of storms or other natural or unnatural events that may cause downed power lines or blown fuses. There is also mounting concern over the security of centralized power generation. In any case, whatever the reason, some utility customers, including facilities designated as storm shelters, desire to have an uninterruptible source of electric power. One way to achieve this is to install a PV system with battery backup to run emergency loads if utility power is lost.

The following system will be designed for residential use with a rooftop-mounted array in order to incorporate a GFDI device in the system, but is equally applicable for installations where the PV array is not on a residential rooftop. The system source circuits will be run from array junction boxes to source-circuit combiner boxes located 60 ft from the array junction boxes. The remaining system components will be located close to the combiner boxes, with a distance of 40 ft between the inverter and the point of utility connection in the main distribution panel. A utility lockable, visible load break disconnect switch will be located near the utility revenue meter between the inverter and the main distribution panel. A set of maintenance-free, gel cell lead-acid batteries will also be located within 6 feet of the inverter.

PCU Selection

An internet search in early 2003 for utility interactive inverters that are listed to UL 1741 that can operate in a grid-independent mode upon failure of the utility grid results in a small number of units that meet these requirements. One such unit can deliver 5500 W with a nominal 48 V dc input and a 120 V ac output. Following are specifications for input, output and general parameters of the unit:

dc Input	Input Voltage Range	44-66 V
	Maximum Input Current	137 A
ac Output	Voltage	120 V 1φ
	Rated Output Current	46 A
	Maximum Surge Current	78 A
	Total Harmonic Distortion	< 5%
	Maximum Efficiency	96%
General	Internal Consumption in Operation	20 W
	Internal Consumption in Standby	1 W
	Maximum Battery Charging Rate	75 A dc
	Weight	63 kg

The programming of the inverter is extremely flexible, allowing control of a wide range of operation modes and system variables, as will be seen as the design progresses. An important feature of the inverter is its battery-charging circuit. When the grid is up and the sun is down, the inverter will charge the batteries from the grid if programmed to do so.

Emergency Loads

Determination of emergency loads for a utility interactive system follows the same procedure as for a stand-alone system. Any difference lies in the possibility that the PV array may not be able to meet the calculated emergency load needs for a prolonged period of grid outage unless adequate PV power is available for charging the batteries when the grid is down. It is possible that space or cost limitations may limit the array power or the battery storage capacity. Since

numerous calculations of system load have been done in other examples, it will be assumed for this system that the average daily emergency load is 15 kWh/day. This emergency load will be served by an emergency distribution panel connected to the emergency output terminals of the inverter. Since the emergency loads will have priorities, if it appears that the batteries are discharging too much, it will be possible to shut down some of the lights and other loads designated as emergency loads.

Module selection

There may also be a wide selection of modules for the PV array, depending upon whether the roof may impose any geometry constraints. One module that is attractive for use in this system has the following specifications:

P_{max}	150 W
V_m	17.1 V
I_m	8.8 A
V_{OC}	20.1 V
I_{SC}	9.2 A
dimensions	37.2" x 49.4" (94.5 cm x 125.5 cm)
Bypass diodes internal to the module	

The modules will need to be connected in parallel groups of four in series to produce the nominal 48 V dc system voltage. If a total of 32 modules are used, then the rated array power will be 4800 watts, produced by eight source circuits of 4 modules each. It will be assumed that the dwelling has suitable roof geometry to accommodate this array.

An estimate of daily kWh produced by the array can be made if it is assumed that the batteries are fully charged to a gel cell float voltage of 54.4 V so all PV output power is delivered to the inverter. Normally if the array operates at a voltage below V_m , the array current will be somewhat higher than I_m . Allowing for mismatch and dust degradation, it is reasonable to assume the array will operate at a current close to $8 \times 8.8 = 70.4$ A. Multiplying this array current by the battery float voltage gives 3830 W to the inverter input, which, at 94% inverter and wiring efficiency, will deliver 3600 W to the emergency loads. Any power not delivered to the emergency loads will be delivered to the balance of the dwelling loads, and then to the utility if all the dwelling loads are satisfied. For 5 daily peak sun hours, this means the array can deliver approximately 18 kWh/day to the ac loads. This is particularly convenient, since it has already been established that the emergency loads will be approximately 15 kWh/day. The PV array is thus reasonably closely matched to the emergency loads.

Battery Selection

The question is, How many days of storage are needed for this system? In most cases, if there is a utility outage, it will be for a few hours or less. In extreme cases, the utility outage may last for a few days. It is anticipated that if one day of storage is provided, that if utility power is lost for more than a day,

the PV system will at least partially recharge the batteries each day that the utility is down. So in this case, the initial system will be designed with storage for one day, with the possibility of expanding the system if one day of storage is found to be inadequate.

Converting 15 kWh/day to Ah/day @ 48 V dc results in the need for 312 Ah of storage. Allowing for an 80% depth of discharge, this brings the storage requirements up to 390 Ah. Close to this amount of storage can be obtained by using 180 Ah @ 12 V sealed gel cell lead-acid batteries. Eight batteries will be needed to provide 360 Ah of storage.

Charge Control

With an array current of 70.4 A, two 45 A charge controllers (125% of 70.4 A) will be needed. The only time these controllers will be used by the system, will be if the grid is disconnected and if the PV system provides more energy than the emergency loads need. In this case, the controllers will need to shut down the array to prevent battery overcharge. For the rest of the time, the charge controllers should be sending all array current to the inverter. This will require careful adjustment of the charging limits on the charge controller.

The charge controllers are normally supplied with battery temperature sensors for attaching to one of the batteries to monitor battery temperature and provide automatic adjustment of charging settings to compensate for temperature.

Source Circuit Combiner Boxes

In this system, it will be convenient to use two source-circuit combiner boxes to balance the PV supply between the two charge controllers. Since there will be a total of eight source circuits, four circuits will be connected to each combiner box. Since I_{SC} of each of the source circuits is 9.2 A, and since 156% of 9.2 A is 14.35 A, the source circuits will be fused at 15 A.

Wire Sizes

Module wiring will be open, using USE-2 insulated wire, with a 28-ft total round-trip wire length between modules and junction box. Since the distance from each source circuit to the source circuit combiner box is 60 ft, and since $I_m = 8.8$ A for each source circuit, for a 48 V system, to keep the voltage drop in source circuits below 2%, the Ω/kft of the wire must be less than 0.9091. This will require that #8 copper wire be used. If #10 USE-2 wire is used for module interconnection and is then connected to the #8 wire in the rooftop junction box, the total resistance of each source circuit will be $0.12 \times 0.764 + 0.028 \times 1.21 = 0.1256 \Omega$. The overall %V.D. will thus be 2.3% under full sun conditions, which is acceptable. Use of #8 USE-2 would keep the overall %V.D. < 2%.

The final decision on wire size must also include a check on the ampacity of the proposed conductors. If two rooftop junction boxes are incorporated, and if a single conduit leads from each junction box to the source circuit combiner box, then each conduit will carry four source circuits, or eight current-carrying wires. If the maximum operating temperature of the wiring from junction box to com-

biner box is 55°C, then the #8 THWN-2 wire ampacity must be derated to 76% of 55 A = 41.8 A (*NEC* Table 310.16). The eight current-carrying wires in a single conduit require an additional 70% derating factor (*NEC* Table 310.15(B)(2)(a)), which brings the ampacity down to 29.26 A, which is still comfortably higher than the required 156% of I_{SC} . Hence the #8 and even the #10 have adequate ampacities, since the conduit fill derating would not apply to the #10 intermodule wiring.

It should be noted that although *NEC* Table 310.17 allows significantly higher ampacities for conductors in free air, and although it is tempting to use these values for the open wiring between modules, it is subject to the ampacities of Table 310.16 since the open wiring terminates in junction boxes. Since #8 wiring is used for the modules, #8 must be used for the module grounding conductors. Hence, each conduit from array junction box to source circuit combiner box will contain 9 #8 THWN-2 conductors. This means the conduit size must be at least 1", assuming that schedule 40 UV resistant PVC is used (Table C10).

With four source circuits combined in each source circuit combiner box, the PV output circuit current from each combiner box will be 125% of $4 \times I_{SC}$, or 46 A. The wire must be sized to handle 125% of this current, since the circuit must be rated for continuous duty. Thus, the ampacity of the PV output circuits must be at least 57.5 A. These circuits are inside at ground level, so no deratings apply and #6 THHN copper is the appropriate wire size.

The rated inverter output circuit current is 46 A, so the wiring from inverter output to the point of utility connection must have a minimum ampacity of 125% of this value, or 57.5 A. So again, #6 is the appropriate wire size.

Since the maximum inverter input current is 137 A, and since 125% of this current is 171 A, it is common practice, recommended by the manufacturer, to use 2/0 copper battery cables and a 175 A dc circuit breaker capable of interrupting 10,000 A as the battery fuse/disconnect.

The grounding electrode for the dc side of the PV system will be a ground rod. This means that a #6 copper wire is the appropriate grounding electrode conductor (*NEC* 250.166(C)). All other equipment grounding conductors can be #10, since the *NEC* allows #10 grounding conductors between points protected by 60A overcurrent devices (*NEC* 250.122)

Fuses, Circuit Breakers, Disconnects, GFDI and Surge Suppression Devices

The source circuit fuses have already been sized at 15 A. The PV output conductors from each source-circuit combiner box will first connect to the GFDI device, and then to individual 60 A dc circuit breakers between the GFDI device and the inverter input. Either the GFDI or the 60 A circuit breakers can serve as the disconnect for the PV output circuits. The 60 A circuit breakers provide overcurrent protection for the PV output circuits. Surge suppression devices are normally connected at the inputs to the charge controllers.

The battery disconnect has also been discussed. The load side of this disconnect is connected directly to the inverter input terminals along with the charge controller outputs.

The inverter ac input is connected to an inverter bypass switch that is used to connect utility power directly to the emergency distribution panel if the inverter needs to be shut down. The inverter ac output to the emergency panel is also connected to this switch and then to the emergency panel. A 60 A circuit breaker at the emergency panel, backfed from the inverter ac output, serves as the overcurrent protection device for the inverter ac output. A 60 A circuit breaker backfed at the main distribution panel serves as the point of utility connection and as overcurrent protection for the inverter ac input circuit. The inverter bypass switch consists of a 2-pole circuit breaker and a 1-pole circuit breaker, ganged together so that it is not possible for both circuit breakers to be simultaneously on, but it is possible for them to be on one at a time or for both to be off. When both are off, this switch serves as the disconnect between inverter and both inverter ac input and inverter ac output.

One should remember that the inverter ac output only delivers power to loads, but the inverter ac input can accommodate bilateral power flow. So if the needs of the emergency loads and battery charging are met, then excess power flows from the inverter ac input back to the point of utility connection.

Instrumentation

Normally it is desirable to monitor the state of battery charge by monitoring battery voltage and current. Monitoring of battery current normally requires a very low resistance shunt in series with the batteries. Voltage drop across this shunt is proportional to the battery current.

Since utility power may occasionally be used for battery charging, and sometimes discharging batteries may be providing power for the utility, it is somewhat more challenging to sort out where all the power flows originate and terminate. Figure 8.9 shows a block diagram of the system indicating possible power flow directions. Note that only three of the seven power flow paths are in one direction. Since it is possible for the batteries to be charged from the utility, it cannot be assumed that power from the array will be used first to charge the batteries, then to meet the needs of the emergency loads, then to feed interruptible loads, and, finally, to feed back to the utility any leftovers. It is possible that power being fed back to the utility may not be PV generated, but simply power from the batteries that had been previously charged by the utility.

Methods of measuring a sufficient number of parameters to determine all the power flows are explored in problem 8.15.

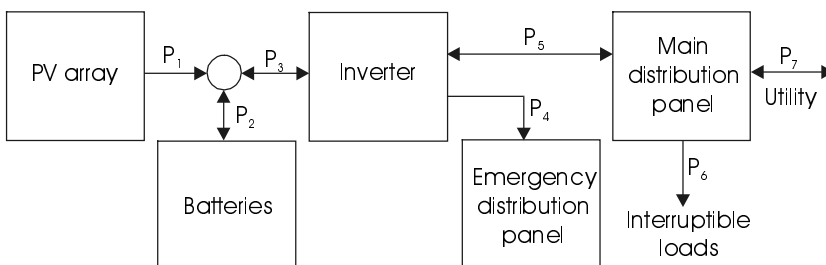


Figure 8.9 Possible power flow directions in utility interactive PV system with battery backup.

System Commissioning

Unlike the previous examples for which the inverters and systems constitute essentially “plug and play” systems, a system with battery back up will require on-site programming of the inverter and charge controllers during system start-up to ensure proper system performance.

Normally it will be desirable to have the PV system as the primary battery charger. To achieve this, the PV charge controller settings must be set to ensure full battery charge for the type of battery used in the system. Different types of batteries require different charge controller settings. The charge control settings on the inverter should be set so the batteries will charge at approximately a C/10 rate, and should be set so the batteries will not charge beyond 80%, so the PV system will finish the charging process. Alternatively, since the inverter will have a real-time clock, the inverter can be set to charge the batteries only at night if the PV system has not fully charged the batteries. Once the batteries have reached full charge, they will not normally be cycled unless a time of use sell rate is established with the utility. In this case, it may be desirable to sell energy from the batteries to the utility during utility peak time and recharge them from the utility during off-peak hours.

The “sell” voltage at the inverter input must then be set so when the batteries are fully charged, the output of the charge controllers will feed the inverter directly for conversion to ac to supply the system loads or sell back to the utility. It is important that the “sell” voltage of the inverter is set low enough to ensure that the PV charge controllers will think the batteries need charging and will feed the total PV output current to the inverter input, but not so low that the batteries will discharge to an unacceptable level to provide “sell power.”

Complete System

Figure 8.10 shows the complete system except for instrumentation connections. As a final note, at the time of this writing, the inverter selected requires an additional interface with the utility. If the reader plans to use this example as a system design, it will be necessary to check to see whether the additional interface is still required or whether a newer model is available from any of the inverter manufacturers.

Note also that the emergency panel will have both busbars connected together so it will be strictly a 120 V distribution panel. The NEC requires that it be labeled accordingly. Furthermore, the NEC requires that the sum of current ratings of all circuit breakers that supply power to a residential occupancy not exceed 120% of the current ratings of the busbars in the main distribution panel. This means that the 60 A circuit breaker from the PV system, when added to whatever main circuit breaker is connected to the utility supply to the main distribution panel, must not exceed this limit. The PV point of utility connection is shown to be located physically near the bottom of the busbar to minimize the total current at any point on the busbar.

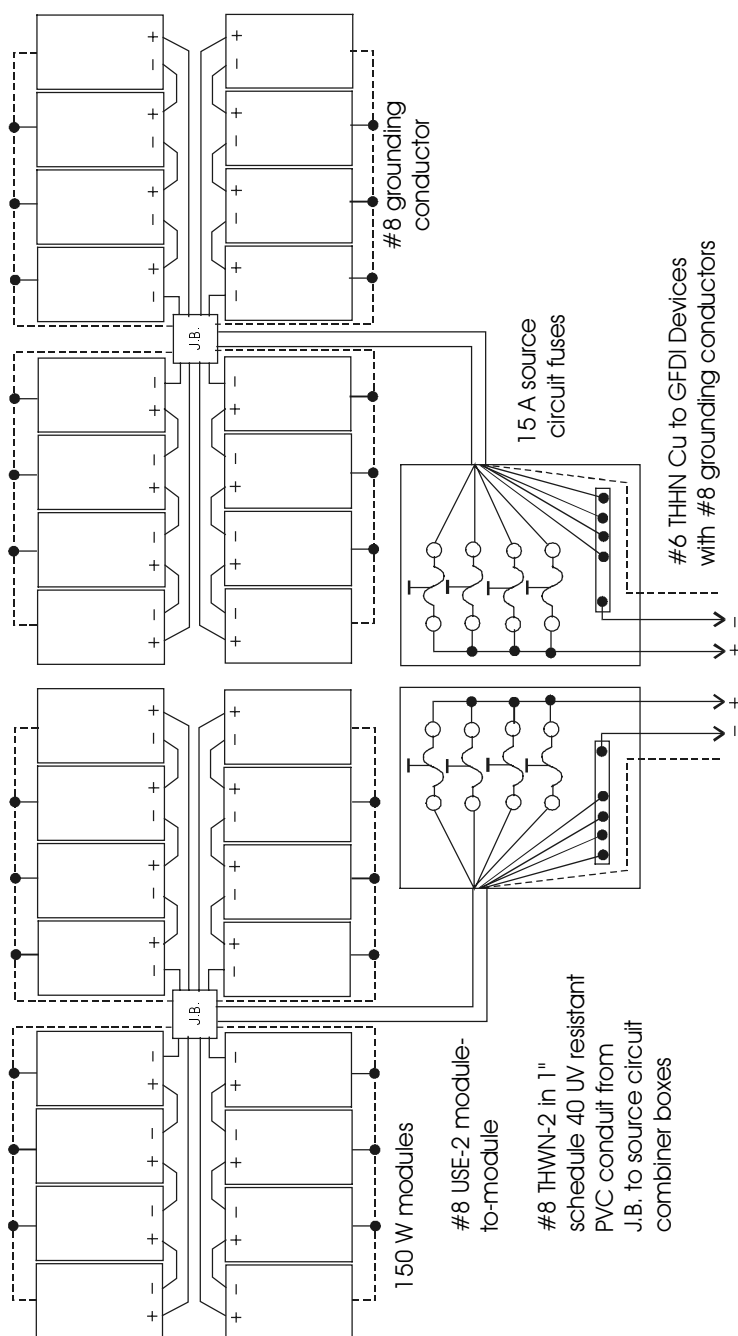


Figure 8.10a Module and source circuit combiner box wiring diagram for 4800 W residential utility interactive PV system with battery backup.

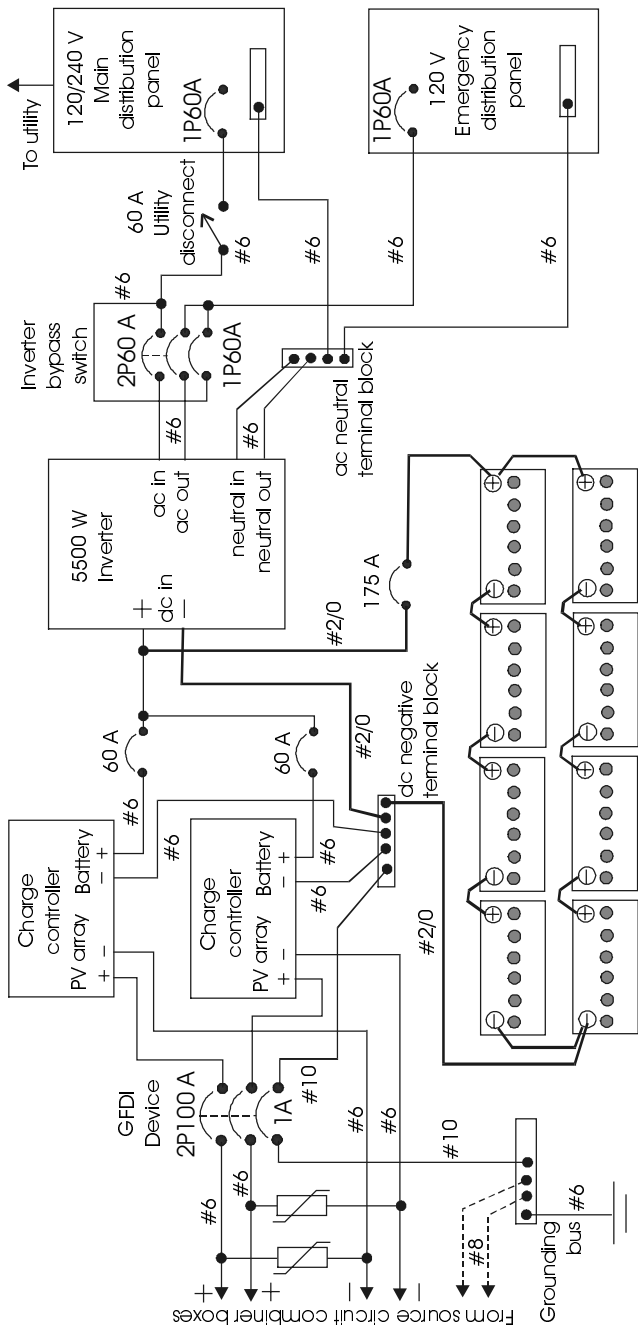


Figure 10b Continuation of wiring diagram for 4800 W residential utility interactive PV system with battery backup.

8.5 Medium Utility Interactive PV Systems

8.5.1 Introduction

All the considerations covered in Sections 8.4.1 through 8.4.4 apply to medium-sized utility interactive systems. Medium-sized utility interactive PV systems deliver power in the range of 10 kW to 500 kW.

In addition to the considerations for small systems, one must consider that medium systems may operate at higher voltages. If the system voltage is over 600 volts, then the provisions of *NEC Article 490* must be followed. While small systems must have fixed voltage and frequency setpoints, the utility may require adjustable setpoints on medium systems. In general, the larger the system, the more likely the system will incorporate custom design requirements to meet the interconnection requirements of the utility.

The exact size of a medium system will likely be determined by criteria similar to the criteria for small systems. In some cases, the available area for the array may limit the system size. In other cases, available capital may be the limiting factor. In still other cases, the choice of PCU may be the factor that determines a specific array size. Suitable locations for medium-sized systems include commercial rooftops, church rooftops and other types of institutional rooftops and parking lot or walkway canopies.

Sometimes medium sized systems are installed as retrofits and in other cases, they are installed as part of the architecture of the building as building-integrated systems. As thin-film technology continues to progress, it is likely that a wide range of building-integrated PV products will become available. For example, amorphous silicon (a-Si) cells are currently on the market in the form of an integrated roofing product. In some cases, not only do integrated PV systems add to the architectural interest of the structure, they also serve as sunshades for windows and as such provide an energy conservation feature as well as an energy generation feature.

8.5.2 A 16 kW Commercial Rooftop System

One need not drive far to observe that the amount of commercial rooftop space available for PV system installation appears to be nearly limitless. Commercial buildings, particularly in suburban areas, tend to be one-story, flat-roofed, structures, often with more than 10,000 ft² of roof space. This space is generally not shaded, since typically the building will also be surrounded by a parking area. Trees may be planted in a decorative fashion, but will generally not shade more than a small part of the roof. If the 16 kW system of this example is constructed with multicrystalline Si modules, the area required will be approximately 133 m², or 1435 ft², assuming 12% efficiency for the modules. For this example, the PV system is owned by the utility and will be connected on the utility side of the meters.

The building upon which the system is to be installed happens to have a 50 ft x 100 ft roof, with the long dimension in a north-south direction. The

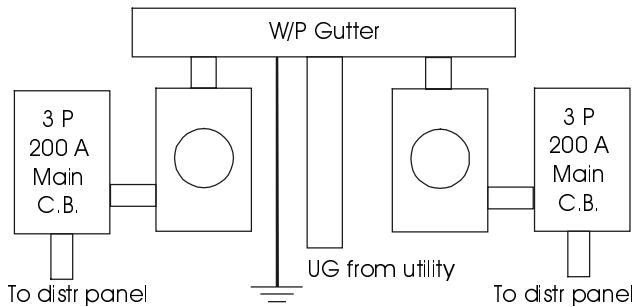


Figure 8.11 Existing electrical service diagram for 16 kW PV addition.

building is served with a 400 A, 120/208 V 3 ϕ underground utility service. It has two occupancies, one of which is a restaurant and one of which is a small specialty grocery store. Each occupancy has its own electric meter and 3 ϕ 200 A main disconnect, and all service equipment is surface mounted outdoors near the center of the building. Since there are fewer than six separate disconnects, these two disconnects serve as the main disconnect for the building. There is adequate wall space above the electrical service equipment for mounting additional PCUs, and the utility and owner have approved locating the PCUs in that space. Figure 8.11 shows the electrical riser diagram for the building.

PCU Selection

The system will be designed around a 6 kW commercially available PCU. The PCU is a single phase unit with a 120 V, 60 Hz output, that meets all UL and *NEC* requirements. Each unit weighs 74 pounds, measures 28 in x 18 in x 8 in and comes in an outdoor enclosure. Separate ac and dc disconnects are required. This means that additional boxes will need to be mounted to the wall to provide all required disconnect functions. Keeping the installation neat may pose an interesting challenge for the electrician in charge of the installation.

Operating specifications for the PCU are as follows:

dc Input	Nominal Input Voltage	± 210 V
	Minimum Operating Voltage	± 180 V
	Maximum Power Tracking Range	± 180 to 300 V
	Maximum Open-Circuit Voltage	± 300 V
	Maximum Operating Current	18 A
ac Output	Voltage	120 V
	Maximum Output Current	50 A
	Power Factor at Rated Output	> 0.98
	Peak Efficiency	96 %

Note that the PCU requires positive and negative dc supplies. Hence, the array must have a 3-wire output, with a positive, a negative and a grounded conductor, similar to the common household 120/240 V ac distribution system.

Selecting and Mounting the Array

Since the building has a flat, poured concrete roof coated with tar and gravel, roof penetrations for securing the array although possible, are not desirable. It is desired to mount the array facing south with a latitude tilt. A check on static and dynamic loading of the roof indicates that it will be acceptable to construct the frame for the PV modules so the frame can be secured to the roof with heavy weights laid across the base of the frame.

For a 16 kW system, it is convenient to use the largest possible modules. It is not unreasonable to expect that it would take somewhat longer to install 533 30-watt modules than to install 53 300-watt modules. Choosing the right module for the system to obtain as close to 16 kW output as possible consistent with PCU requirements is an interesting challenge.

First of all, the V_{OC} limits and the maximum input current limits of the PCU must be met. If the modules are to be used in an environment where the coldest temperature will be 10°F, this means the rated V_{OC} of the modules at standard test conditions must be increased by 17% per *NEC* Table 690.7. Thus, the total V_{OC} at standard test conditions of a string of modules must be less than $300 \div 1.17 = 256$ V. With an 18 A maximum input current for the PCU, this means that the combined I_{SC} of each PV output circuit (positive or negative) must be less than $18 \div 1.25 = 14.4$ A. This allows for the possibility of cloud focusing and the corresponding increase in PV output current.

Using an integral number of modules, there are only a few combinations that will produce the optimal parameters. For current, 14.4 A can be divided by 2, 3, 4 or 5 to get 7.2 A, 4.8 A, 3.6 A or 2.88 A as optimal values for I_{SC} for a selected module. For voltage, 256 V can be divided by integers of 4 or more to yield possible module V_{OC} values of 64 V, 51.2 V, 42.7 V, 36.57 V, 32 V, 28.4 V, 25.6 V, 23.3 V and 21.3 V for 4, 5, 6, 7, 8, 9, 10, 11 or 12 modules in series. At this point, then, a catalog or web search is needed to locate the most logical module for the system.

Suppose such a search is made and it is determined that the best choice of modules to meet these constraints is a module that has $V_{OC} = 62$ V, $I_{SC} = 4.8$ A, $V_m = 52.2$ V and $I_m = 4.34$ A. This means that *each leg of each phase will consist of a combination of three parallel strings of 4 series modules*. This totals 24 modules per phase and thus 72 total modules in the system. The total system maximum power output is thus $72 \times 52.2 \times 4.34 = 16,311$ W at standard test conditions. As the array temperature drops below 25°C under peak sun conditions, the array output power will increase. In any case, the chosen modules have FF = 0.76 at full sun. The only way to come closer to the rated performance of the PCU within the input operating limits of the PCU is to choose modules with a higher fill factor and to have V_{OC} equal to its maximum allowable value.

System Wiring

Since the rated voltage of each PV string exceeds 50 V, each individual string of 4 modules is considered to be a source circuit. The current rating of the

wiring of each string must be at least $1.25 \times 1.25 \times I_{SC} = 7.5$ A. Hence, #14 wire fused at 8 A is an appropriate choice.

Separate source-circuit combiner boxes are used for the positive half and the negative half of the array. The grounded conductors of each array half are joined in a junction box and the 3-wire array output is then fed to a 2-pole 30 A disconnect located near the PCU. When the source circuits are combined into the output circuit, the wire rating needs to be $1.25 \times 1.25 \times 3 \times 4.8 = 22.5$ A. Since #12 wire must be fused at no more than 20 A, #10 fused at 30 A is needed for each PV output circuit conductor.

Since the system voltage, i.e., the voltage between the negative PV output circuit conductor and the positive PV output circuit conductor, is less than 600 V, 600 V insulation is adequate and the provisions of *NEC Article 490* do not apply to this system. Since the PCU already has surge arrestors at its input and output, no additional surge protection is necessary. Grounding of the array frames is done with the largest circuit conductor, which in this case is #10. Since the array is not on a residential roof, ground fault protection is not required. The building has a lightning protection system, so the array ground can be connected into the lightning protection system ground bus.

The output circuit of each phase of the PV array is connected to each PCU through a 2-pole fused disconnect rated at 30 A, 600 V dc. The disconnect opens the ungrounded conductors of the PV output circuit. The grounded conductor is not opened when the disconnect switch is opened.

Connecting the PCU Output to the Utility

The conductors for connecting the output of the PCU to the utility must be rated for at least 125% of the PCU rated output current. In this case, the conductor rating must be at least 1.25×50 A = 62.5 A. This will require #6 Cu conductors fused at 70 A.

A convenient way to make this connection is to use a 3-pole 100 A fused disconnect, fused at 70 A per phase with dual element (time delay) fuses. Since the inverter will meet UL 1741 requirements, if any one phase requires work, or if a PCU requires repair, the fuse to the phase under repair can be removed to disconnect the phase without disconnecting the other two functioning phases.

Another reason why this is a convenient hookup is that the disconnect is readily obtainable, since it is for ac, and only one box needs to be mounted to the wall to serve the outputs of all three PCUs. This leads to a somewhat more aesthetically pleasing appearance for the back of the building. Finally, since the PV system output is to be spliced inside the gutter on the line side of the meters, only three split-bolt connectors will be needed to make the splice, unless one of the meters can be double-lugged on the line side. This means the power to the building will be shut down for a shorter time as the connection is made.

The grounding electrode conductor on the dc side will need to be #6 copper, since #6 is the largest circuit conductor. Figure 8.12 shows the wiring of the system, except for grounding conductors.

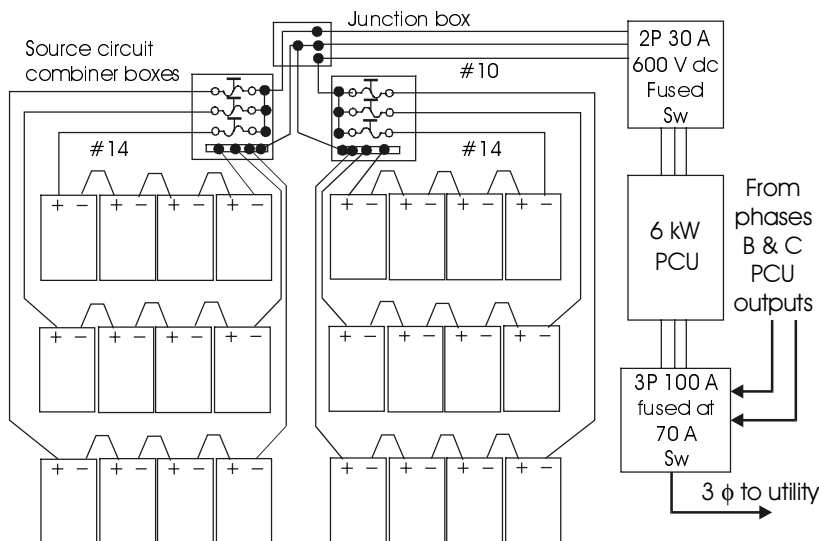


Figure 8.12 Wiring diagram for the nominal 16 kW PV system. Only phase A is shown. Phases B and C are identical to phase A and connect to the utility at the 3P 100A disconnect.

8.6 Large Utility Interactive PV Systems

8.6.1 Introduction

Large systems are defined as systems sized 500 kW and larger. To date a number of these systems have been installed. Normally they have been installed on utility property. The first system to be installed to meet this classification was the 1.0 MW system installed in 1982 by ARCO Solar at Hysperia, CA [17].

Large systems can consist of a grouping of smaller systems or can be connected as larger systems, depending upon the choice of PCU. With large systems, more coordination is needed with the utility to be sure all interconnection concerns are addressed.

8.6.2 A Large Parking Lot PV System

General Considerations

If rooftops present significant opportunities for PV generation siting, then the parking lots that serve the buildings probably present an order of magnitude greater opportunity for PV generation siting. Consider, for example, a parking lot that holds 480 automobiles, as shown in Figure 8.13. If each parking space measures approximately 9 ft × 15 ft, this means that if all stalls were to be covered with PV canopies, a total of 64,800 ft² of canopy top will be available for installation of PV modules. If the modules have an efficiency of 10%, then the system would have a peak output of 602 kW. This means that thousands of schools, factories, shopping malls, hospitals, churches, amusement parks and

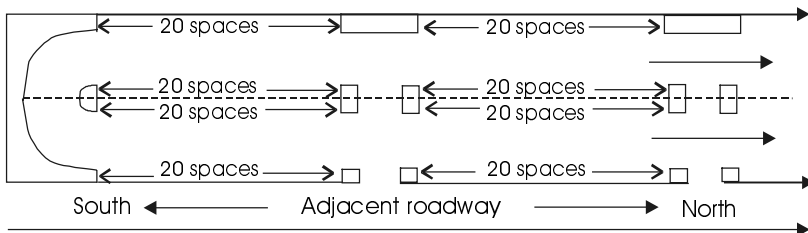


Figure 8.13 Parking lot configuration for PV installation. The lot continues to the north with groups of 80 parking spaces for a total of 480 spaces.

other similar occupancies have the siting capacity for thousands of megawatts of PV generation. In addition to generating electricity, these canopies can provide shade for the vehicles and can conceivably provide dc or ac at the proper voltage level for charging electric vehicles parked beneath them while the drivers and passengers work, learn, shop, pray or play.

At first thought it may seem reasonable for parking lot systems to be used exclusively for charging electric vehicles. However, the unpredictability of stall occupancy along with the difficulty in predicting the amount of Ah needed by an average electric vehicle suggests that a better plan for full utilization of the PV output would be to feed utility interactive inverters with MPT capability. This will ensure that the PV array will be delivering maximum power to the grid most of the time, with whatever fraction that may be needed for vehicle charging being delivered to the vehicles.

Exactly how the PV system will be configured will depend to a large extent upon how the parking lot is configured. Logically, contiguous parking spaces should be covered by contiguous PV arrays so the contiguous space will house a self-contained PV system with a PCU that feeds the grid. It is thus possible that many large systems might be comprised of a number of medium systems.

Considering that at least one type of commercially available 3- ϕ inverter is available in 50 kW and 100 kW sizes, it would be convenient to be able to break the system into either 50 kW or 100 kW subsections, all of which would tie into a main point of utility connection.

Specific Considerations

Note first that the parking lot is divided into six sections of 80 spaces, each of which consists of four groups of 20 contiguous spaces. Each group of 20 spaces measures 15 ft x 180 ft. The 602 kW divided evenly among the 480 spaces amounts to 1254 W per space, so that the total power available from each group of 20 spaces is 25,083 W. Each section of 80 spaces thus provides nominally 100 kW, provided that the arrays can be oriented for maximum output.

The lot runs in a north-south direction. This orientation will need to be taken into account when array mounts are designed, since the lot orientation presents a problem for orientation of the array in a south-facing direction.

Module Selection and Configuration

The next step is to determine a means of configuring a set of modules to provide the 25,083 W at voltage and current levels consistent with the input requirements of the PCU. The 3-phase PCU operating specifications are

dc Input	Nominal Input Voltage	325 V dc
	Minimum Input Voltage	300 V dc
	Max V_{OC}	600 V dc
	Max Power Tracking Range	300 to 600 V dc
	Max Input Current	400 A dc
	Terminals for combining 6 source circuits	
ac Output	Voltage (line-to-line)	480 V ac
	Maximum Current	125 A ac
	Power Factor at Rated Output	>0.98 .

Naturally, it would be nice if the proposed PV modules fit conveniently into the 15 ft x 180 ft space.

Before a module is selected, it should first be noted that the groups of 20 parking spaces are in the north-south direction. This complicates the process of tilting the modules at an angle in a south-facing direction, since if the modules are tilted toward the south, they may partially shade adjacent modules to the north. Furthermore, if it rains, the rain will run off the modules directly onto the drivers and passengers of the vehicles. The modules must therefore be mounted either horizontally or with a slight tilt toward the east or west. A westward tilt would be preferred, since it would optimize system output during the afternoon in the summer. The tilt also provides for somewhat better convection cooling of the modules and also enables the rain to more effectively clean the modules. Fortunately, the system is located in southern U.S., so a horizontal or slightly west-facing tilt will not significantly degrade system summer power output. From an aesthetic and structural perspective, however, the canopies over the west-facing rows, if tilted toward the west, will have the high side at the back of the parking space and the low side at the front of the space. If a means of providing adequate support can be found, along with a good argument for contemporary styling, such a configuration may still be acceptable and need not be discarded at this point of the design process.

In the emerging world of module sizes, new sizes often appear on the market. It is now assumed that after an extensive web search, or, possibly after negotiations with a manufacturer, that a module has been found with $V_{OC} = 90$ V, $I_{SC} = 4.4$ A, $V_{mp} = 70$ V, $I_{mp} = 4.0$ A, length = 6 ft, width = 5 ft and a temperature correction factor for the lowest expected temperature of 10%.

The 10% temperature factor limits the maximum of V_{OC} to $600 \div 1.1 = 545$ V. Coincidentally, 6 modules in series will have $V_{OC} = 540$ V. The 15 ft \times 180 ft space can be filled with a total of 90 modules grouped into strings of 6 modules, as shown in Figure 8.14. The 15 groups of 6 modules can be further divided into 5 groups of 3 strings of 6, also as noted in Figure 8.14.

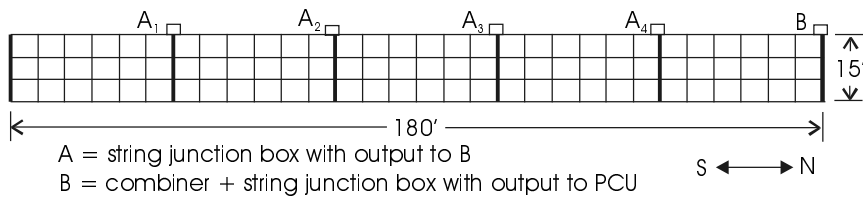


Figure 8.14 Grouping of modules in 20-parking-space canopy.

Array Wiring and Fusing

Figure 8.15 shows the grouping of the outputs of the modules. In this case, three strings of 6 modules are connected together in parallel, with a 7 A fuse in each string, since 156% of 4.4 A is 6.86 A. The derated ampacity of a #14, 90°C wire, used at 60°C will be 17.75 A, so #14 is adequate for wiring between individual modules.

When the outputs of three individual source circuits are combined, this results in circuits with a total $I_{SC} = 13.2$ A, meaning a maximum current of $13.2 \times 1.25 = 16.5$ A. The conductors from A to B thus need to be rated at 1.25×16.5 A = 20.63 A after derating for temperature and conduit fill. The maximum V_{OC} of the parallel combination will be 1.1×540 V = 594 V, so 600 V wire insulation is adequate for all wiring.

For #10 THWN-2, rated at 40 A at 25°C, a derating factor of 0.76 must be used if the wire will be exposed to ambient temperatures of 51 to 55°C. Hence, #10 THWN-2 wire has a rating of $40 \times 0.76 = 30.4$ A at 55°C as long as three or fewer current-carrying conductors are in a single conduit.

If a single run of conduit joins all of the junction boxes, then the conduit will contain two wires between A_1 and A_2 , 4 wires from A_2 to A_3 , six wires from A_3 to A_4 and eight wires from A_4 to B. NEC Table 310.15(B)(2)(a) requires derating of 80% if four to six current-carrying conductors are in the same conduit and

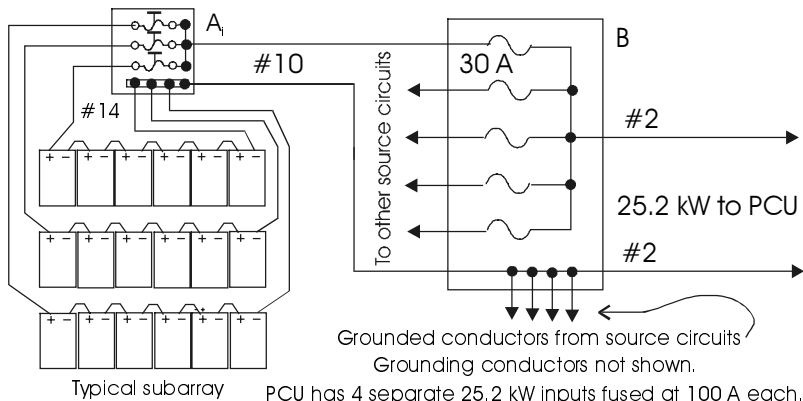


Figure 8.15 Grouping, sizing and fusing of string, source and output conductors for 20-parking-space canopies.

70% if seven to nine conductors are present. Hence, the worst case will be from A₄ to B, where the rating of the eight conductors is reduced to $0.70 \times 30.4 = 21.28$ A. Since $21.28 > 20.63$, the proposed wiring scheme with #10 THWN-2 is acceptable.

NEC Table C10 indicates the conduit size needed for the conductors. For up to 4 #10 THWN-2 conductors, $\frac{1}{2}$ in PVC is adequate. For 8 #10 THWN-2 conductors, $\frac{3}{4}$ in PVC is needed. Hence, from A₁ to A₂, $\frac{1}{2}$ in PVC may be used, while $\frac{3}{4}$ in PVC will be needed between all the other boxes.

Junction box B contains the fuses for three strings (source circuit #5) and also serves as a combiner box for the five sets of #10 wire from the 5 source-circuit sets. The three 7 A fuses in each A_i box protect the modules in each string and also limit the current in the #10 wire from A_i to box B to 21 A. However, if a short circuit occurred between box A_i and box B, nearly 65 A would be available from the four other source circuits, to flow through the short circuit. So 30 A fuses are used in B to protect the #10 conductors from the A_i boxes.

The five source circuits are combined into a single PV output circuit that is connected to the PCU input. This provides I_{SC} = 66.0 A with I_{max} = 82.52 A, which requires a current rating for the wiring of 103.15 A. This requires #2 Cu wire after derating for 40°C operation.

Checking for voltage drop, the longest run of source circuit is approximately 144 ft to the combining box at the end of the array. With an operating current of 13.2 A in each source circuit, this will result in a voltage drop of $13.2 \times (288 \div 1000) \times 1.21 = 4.6$ V for #10 Cu wire. The operating voltage of the string will be approximately 420 V, so this amounts to a 1.1% voltage drop. Since the V_{OC} of each string will not match exactly due to variations in module characteristics, the string with the highest V_{OC} should be located farthest from the combining box.

The input to the PCU is completed by duplicating the connections of the first 20 parking spaces for the remaining three sets of 20 spaces in the section of the parking lot. The input to the PCU is thus supplied by four sets of #2 wires, each of which carries a nominal current of 60 A. This results in an operating input current to the PCU of 240 A with a maximum input current of 330 A, which falls nicely within the maximum operating current specifications of the PCU. Note that the single dc input provides power for the three PCU output phases.

PCU Output Circuits

Since the output of the array is to be fed to the grid, two 100 kW 3-phase PCUs will be located together on the island connecting the west sides of the first two adjacent groups of 80 spaces. The outputs of the two PCUs will be fed to the primary of a 200 kVA, 480/13,200 V 3-phase pad mounted transformer. Two similar transformers will be located on the islands to the north to accommodate the outputs of the remaining four PCUs. The combined output of the three 200 kVA transformers is fed to the grid. The total array output current is 26.25 A per phase at 13,200 V line-to-line. Frequency and voltage trip points of the PCUs are set in accordance with specifications developed in coordination with the utility.

Array Mounts

The final step in the system design is to design array mounts that will meet cost, performance and aesthetic requirements of the system. The array mounts will support the modules and will also provide mounting space for parking lot lights to be mounted under the array so typical high-pole, parking lot fixtures will not cause shading on the modules.

In designing the array mounting system, it is first necessary to compute the mechanical forces acting on the array. These forces will then be transmitted to the array support structure and primary load-carrying members for the parking lot canopies.

The location of the system determines the types of mechanical loads that must be considered. For this system, the location is the city of Boca Raton, along the southeastern coast of Florida. For this location, only three types of loads need to be considered: dead loads due to the weight of the array and support structure, live loads associated with people and hardware during installation and maintenance of the array and wind loads. Based on experience, a good assumption is that the dead load does not exceed 5 psf and the live load does not exceed 3 psf. Consequently, it is assumed that the combined mechanical loading from both dead and live loads is 8 psf distributed uniformly over the entire array surface. It is also assumed that during installation and maintenance, concentrated live loads at any point on the support structure do not exceed 300 pounds.

For most locations, and especially for coastal Florida, the mechanical design will be largely driven by wind-loading considerations. The first step in designing photovoltaic arrays and structures to meet wind loads is to establish the basic wind speed. From ASCE 7-02 [16], the basic wind speed for Boca Raton, FL is approximately 145 mph. It is this high because South Florida is in a hurricane-prone area. For most of the noncoastal U.S., the basic wind speed is only 90 mph, creating a significantly lower wind load on arrays.

The second step in the wind analysis is to determine the velocity pressure, which is a measure of the kinetic energy of moving air. This kinetic energy can be converted into a static or design wind pressure distribution, which produces the mechanical forces acting on the array and support structure. The velocity pressure q is computed using the following equation [16].

$$q = 0.00256 K_z K_{zt} V^2 I \quad (8.7)$$

where q = velocity pressure in psf

K_z = velocity pressure exposure coefficient evaluated at height z

K_{zt} = topographic factor

V = basic wind speed in mph

I = importance factor.

The tables and figures of the ASCE Standard [16] yield $K_z = 0.85$, $K_{zt} = 1.0$, and $I = 0.87$. Therefore, for $V = 145$ mph,

$$q = 0.00256 \times 0.85 \times 1.0 \times 145^2 \times 0.87 = 39.8 \text{ psf.}$$

Note that q is a velocity pressure and not the design wind pressure acting on the array and support structure. The design wind pressure p is computed using

$$p = q G C_f \quad (8.8)$$

where p = design wind pressure in psf

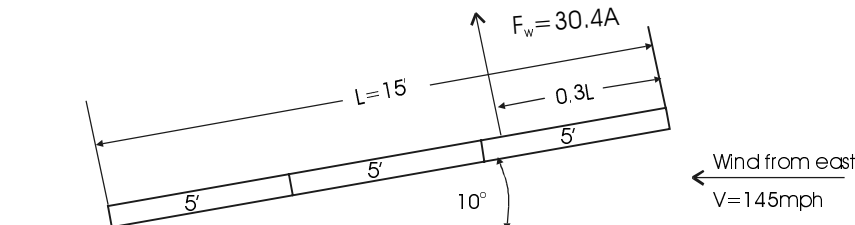
G = gust effect factor

C_f = the force coefficient for monoslope roofs over open buildings.

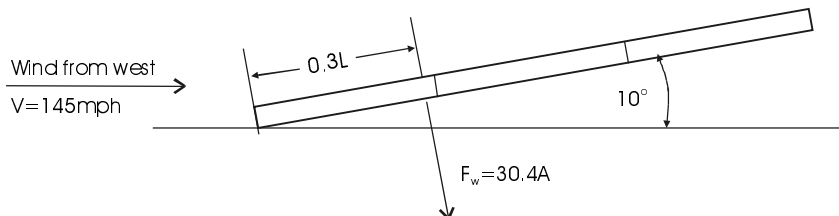
From ASCE 7-02, $G = 0.85$ and C_f is a function of the array tilt angle. For this system, the decision is made to tilt the array at an angle of 10° from the horizontal, and to have the arrays facing west. The small tilt angle significantly reduces the force coefficient and resulting design wind pressure. Facing the arrays toward the west results in the photovoltaic system feeding more electricity to the grid later in the afternoon, and helps the utility meet its large summer peak demand. For the 10° tilt angle, the corresponding force coefficient is approximately 0.9. Therefore, the design wind pressure is

$$p = 39.8 \times 0.85 \times 0.9 = 30.4 \text{ psf}$$

It is important to emphasize the sensitivity of the force coefficient and design wind pressure to the tilt angle and the aspect ratio of the array. For example,



a. Wind from the east



b. Wind from the west

Figure 8.16 Resultant forces and their centers of pressure for winds from the east and winds from the west.

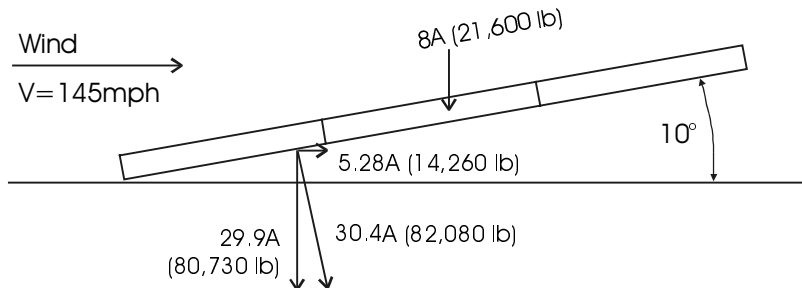


Figure 8.17 Mechanical forces acting on the PV array. The values in parentheses are for a 20-parking-space canopy.

both the force coefficient and design wind pressure for a square array tilted at 20° will be twice the values for the same array tilted at 10° ; and doubling the aspect ratio, i.e., the ratio of length to width, increases the force coefficient and design wind pressure by over 20%.

The design wind pressure of 30.4 psf does not act uniformly over the area. The actual pressure forces tend to be higher nearer the windward edge of the array. Consequently, the resultant force from this complex distribution is closer to the windward edge of the array. A good estimate of the distance from the windward edge to the location of the resultant force (or center of pressure) is 0.3 times the length of the array parallel to the wind direction [16].

Figure 8.16 shows the resultant forces, their directions and locations for winds from the east and from the west. Because of the shallow tilt angles, the array acts like an airfoil and produces an upward lift force for winds from the east, and a downward force for winds from the west.

The resultant force F_w for a 20-parking-space canopy is $30.4 \times 15 \times 180 = 82,080$ pounds, up or down depending on wind direction. The total force acting on the array and support structure includes the combination of dead loads, live loads and wind loads. Figure 8.17 shows the combined forces and their vertical and horizontal components.

Now that the forces on the array have been computed, the structural configuration for supporting the array must be determined. The primary support structure for the canopy itself will be steel columns. However, the 9 ft width of the parking spaces and the 6 ft width of the individual modules constrain the locations of the columns. The canopy is 180 ft in the north-south direction and 15

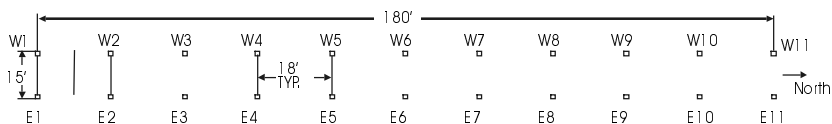


Figure 8.18 Plan view of column locations showing 11 columns along the east side and 11 columns along the west side of the canopy.

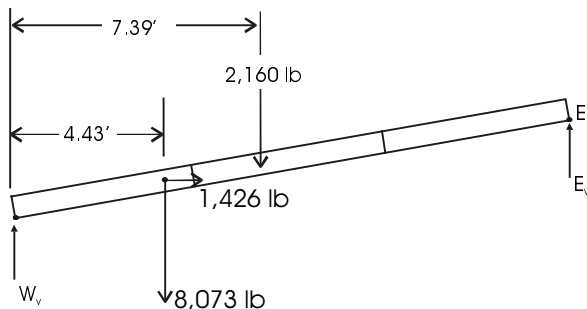


Figure 8.19 Forces acting on nine modules covering two parking spaces.

ft in the east-west direction. In the north-south direction, either 18 ft spacing (i.e., every two parking spaces) or 36 ft spacing (every four parking spaces) are options. In the east-west direction, 15 ft spacing is the logical choice. To minimize excessively long spans and heavier beams, 18 ft spacing is selected. This requires a total of 22 columns, which must be capable of carrying axial, bending and buckling loads. Figure 8.18 shows a plan view of the column locations.

Except for the end columns (E1, W1, E11, W11), any column pair such as E5, W5, must carry the mechanical forces acting over the area of 9 modules. This area is 270 ft². Figure 8.19 shows the forces acting over 9 modules that must be carried by the support column pairs.

The maximum axial forces act on the interior columns along the west side of the canopy. Static equilibrium shows that these columns should be designed to

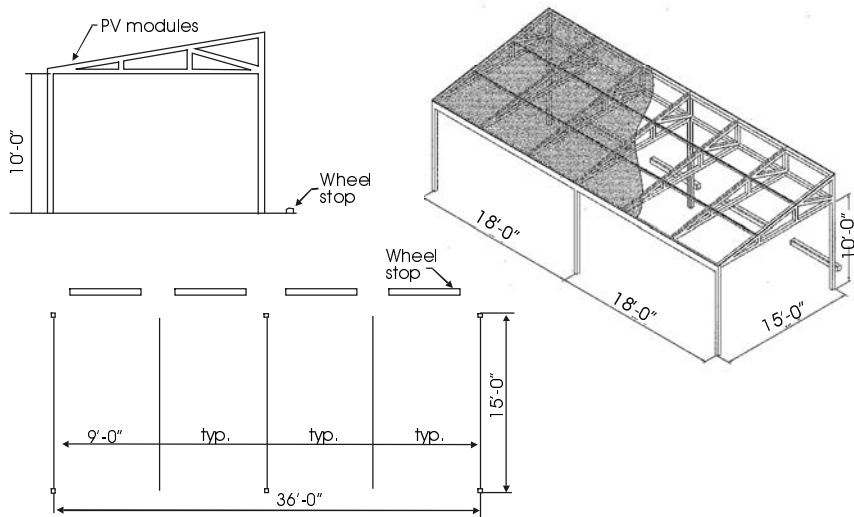


Figure 8.20 Sketch of a section of a covered parking canopy showing a typical configuration for four spaces.

safely carry approximately 6700 pounds. For this application, 4 in x 4 in square structural steel tubing with $\frac{1}{2}$ in thickness is a reasonable choice for the main structural members. The maximum axial stress in these columns is slightly greater than 1000 psi compression, and the critical buckling load is considerably higher than anything that will be experienced using the design loads. The square tubing needs to be securely anchored in reinforced concrete because this particular photovoltaic application precludes significant lateral bracing. Figure 8.20 shows a sketch of a structural configuration that might be used for the parking lot canopy.

As mentioned, the primary structural members are the square structural tubing. A horizontal structural grid is suggested at about the 10-foot height, which is the approximate height of the lower edge of the array. This will add structural stability and be useful during module installation and maintenance. Many choices exist for selecting the structural members and their attachment hardware. Some suggestions are indicated on the figure. A complete structural design and analysis are beyond the scope of the text.

Problems

- 8.1 Construct a set of tables that show the price that would need to be charged for PV-generated electricity to recover the cost of the PV modules if the modules last for 20 years and are paid for by 20-year loans at interest rates of 5 to 10% in 1% steps. Also, assume the cost per watt of module to be \$4.00, \$3.00, \$2.00 and \$1.00. The tables should be for installations in Sacramento, CA, Miami, FL, Seattle, WA and Fairbanks, AK. What combinations of interest rates and module cost will result in a cost per kWh of \$0.08 in each of the locations?
- 8.2 Repeat Problem 8.1, assuming a lifetime of 30 years for the PV system and thus a 30-year loan.
- 8.3 Using Figure 1.8, estimate how long it will take for PV-generated electricity to become cost-competitive in the locations of Problem 8.1. You may wish to determine the present electric rates in each of these locations.
- 8.4 Assume a utility interactive PV system is connected on the customer side of the revenue meter. Propose a method or methods of connecting meters so that any PV energy that is returned to the grid can be credited at a rate that is different from the retail rate. Note that this connection implies that the revenue meter should not be allowed to run backwards, since this will credit the customer at retail rates.

- 8.5 Propose a block diagram for a single meter so that power flowing in one direction can be distinguished from power flowing in the opposite direction and energy in both directions can be separately recorded.
- 8.6 Propose a block diagram for a single meter similar to the meter of Problem 8.5, but that will also be capable of recording time-of-day information along with the energy information.
- 8.7 A dc ground fault circuit interrupter senses the current on the conductor that joins the grounded conductors to the grounding conductors, as shown in Figure 8.4. If the current exceeds a predetermined amount, it will implement a disconnect function that will clear the ground fault. Think about how a ground fault might occur on a residential roof-mounted PV system and then show that the circuit of Figure 8.4 will clear the fault.
- 8.8 Show that $\alpha = \pi f_o / Q$ for a parallel RLC circuit.
- 8.9 Show that $f_o = \frac{\omega_d}{2\pi \sqrt{1 - \frac{1}{4Q^2}}}$ for a parallel RLC circuit.
- 8.10 Design a resonant (RLC) load with $Q = 5$ that will dissipate 1000 watts at 120 V (rms) at 60 Hz. Then use PSPICE or your favorite network analysis program to simulate the SFS and SVS algorithms by connecting a sinusoidal current source to the load and varying the frequency above and below 60 Hz and observing the total response (transient plus forced) as the excitation frequency moves farther away from 60 Hz.
- 8.11 For the example of Section 8.4.5, determine the maximum and minimum number of modules that can be connected in series such that their maximum power output voltage will remain in the PCU input voltage range. Assume the maximum module temperature will be 60°C and the minimum module temperature will be -15°C. Use the modules of the example.
- 8.12 Sketch two alternative mounting schemes for the modules shown in Figure 8.6. Assume that in each case, either the long dimension of the roof of Figure 8.6 or the short dimension of Figure 8.6 is inadequate to accommodate the module area as shown in the figure. Try to maximize module cooling and to minimize the length of wire in the series connection.
- 8.13 Research the recommended bulk and float settings for VRLA gel batteries and recommend settings for the bulk and float settings of the charge controllers in the example of Section 8.47. Also recommend settings for the ‘sell’ voltage of the PCU and the PCU battery charger settings.

- 8.14 Analyze the parking lot PV array of the large PV system example and provide an estimate of when (time of day and days of year) the system output will be maximum. Then provide an analysis of how the system annual output will be affected compared to a south-facing system tilted at 90% of latitude if the system is located at latitude 26°N and longitude 82°W.
- 8.15 Using the power flow diagram of Figure 8.9, show how instruments can be connected to monitor a) the power delivered by the PV array, b) the power delivered to the batteries from the PV array, c) the power delivered to the batteries from the utility, d) the power delivered to the emergency load by the PV array, e) the power delivered to the interruptible loads by the PV array and f) the power delivered to the utility by the PV array.
- 8.16 If the emergency load on the PV system of Section 8.4.7 is 30 kWh/day, determine an appropriately sized gasoline generator to provide the balance of the load not supplied by the PV system. Assume that the generator is connected to a second set of ac input terminals of the inverter and that the inverter has a battery charger that will convert the generator output to dc for battery charging with a 90% efficiency. Size the generator for a C/10 charging rate for the batteries.

Problems 8.17-8.21 are based on Figure P8.1.

The PV modules in Figure P8.1 have the following specifications under standard test conditions: $V_{OC} = 20.1$ V, $I_{SC} = 7.2$ A, $V_{mp} = 16.1$ V, $I_{mp} = 6.2$ A and $P_{max} = 100$ W. The inverter is rated at 2500 W, with 120 V ac output and an input voltage range of 22–33 V. The inverter efficiency is 92% at maximum power output.

- 8.17 If the modules are mounted with a latitude tilt in Denver, CO, estimate the annual ac kWh that will be produced by the system, assuming that all wiring is sized for overall voltage drop < 3% and that the system is functioning normally.
- 8.18 Determine all wire sizes for the system, using the following information.
- Determine wire sizes to keep individual voltage drops < 2% and overall wiring voltage drop < 4% between modules and main panel if the distances are as follows: Modules to junction box, 8 ft total wire length; junction box to source circuit combiner boxes, 40 ft (one way); combiner to charge controller, 5 ft; charge controller to inverter, 3 ft; battery total cable length, 12 ft; inverter to emergency panel, 6 ft; inverter to main panel, 30 ft.
 - Determine all maximum currents and check these wire sizes to be sure the wires have adequate ampacity to carry the maximum currents. Assume the maximum temperature of the module wiring to be 60°C, the maximum temperature between junction box and combiner box to be 45°C and the maximum temperature of all other wiring to be 30°C.

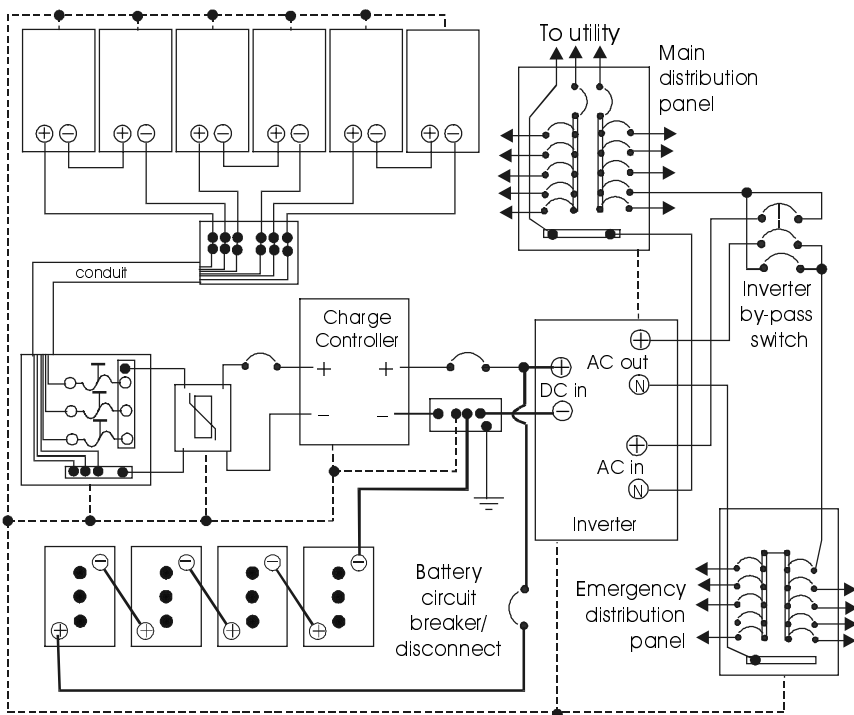


Figure P8.1 Utility interactive PV system with battery backup.

- 8.19 Determine the conduit size (Schedule 40 UV resistant PVC) necessary to accommodate the wiring between the junction box and the source circuit combiner box. Then determine the minimum allowable volume of the junction box per *NEC* based upon the wire sizes determined in Problem 8.17, if the volume of the terminal strip is 6 in³. Assume that the appropriate size grounding conductor is run with the current-carrying conductors in the conduit.
- 8.20 Determine appropriate sizes for all circuit breakers and disconnects in the system.
- 8.21 Based on the anticipated dc kWh output of the PV array to the batteries, specify the battery sizes needed to provide 1 day of storage. Keep in mind that the kWh available to the batteries from the PV array is larger than the kWh available to the ac loads from the PV array.

Design Problems

- 8.22 Specify all the components for a nominal 1500-watt ground mounted utility interactive PV system. Assume the code in effect is the most recent

- version of the *NEC*. Use a utility connection point on the utility side of the meter.
- 8.23 Specify all the components and show the design for a nominal 5000-watt residential rooftop-mounted, utility interactive PV system, based on the most recent version of the *NEC*. Connect the system on the customer side of the meter.
- 8.24 Design a 9.6 kW, customer-owned, commercial rooftop utility interactive PV system with a 120/240 V output and 30 kWh of battery backup. Specify all components and connections.
- 8.25 Design a 36 kW commercial roof-mounted PV system that will feed a 120/208 V 3 ϕ 400 A distribution panel on the customer side of the meter. Comment on the bus capacity of the distribution panel and the allowable size of the main circuit breaker on the distribution panel feeder circuit.
- 8.26 A 120 kW utility interactive system is to be installed as a parking lot canopy. It is to feed the grid with a 3-phase, 277/480 V balanced output. Draw a system diagram, showing all necessary components, including wire sizes and fuse/circuit breaker sizes and locations. Comment on your choice of whether to use a single set of inverters or multiple sets.

References

- [1] Osborn, D. E. and Collier, D. E., "Utility Business Opportunities with the Commercialization of Grid-Connected PV," Interconnecting Small PV Systems to Florida's Utility Grid, A Workshop for Florida Utilities, Cocoa, FL, October 22, 1998.
- [2] <http://SMUD.com> for more information on SMUD PV projects.
- [3] <http://www.austinenergy.com/solar-explorer/index.html> for information on Austin Energy renewable energy programs.
- [4] <http://www.bpu.state.nj.us/wwwroot/energy/rfp> for information on New Jersey Renewable Energy Technology Projects solicitation.
- [5] Wills, R. H., *The Interconnection of Photovoltaic Power Systems with the Utility Grid: An Overview for Utility Engineers*, Sandia National Laboratories, Albuquerque, NM, 1998.
- [6] Maycock, P., The world PV market production increases 36%, *Renewable Energy World*, Vol 5, No 4, July-Aug 2002, 146-161.
- [7] *NFPA 70 National Electrical Code, 2002 Edition*, National Fire Protection Association, Quincy, MA, 2002.
- [8] U.S. Senate, 95th Congress, 1st Session. Public Utility Regulatory Policy Act of 1978, Washington, D.C., Government Printing Office, 1977.
- [9] IEEE 929-2000, 'IEEE Recommended Practice for Utility Interface of Residential and Intermediate Photovoltaic (PV) Systems,' IEEE Standards Coordinating Committee 21, Photovoltaics, 2000.

- [10] UL Subject 1741, ‘Standard for Power Conditioning Units for use in Residential Photovoltaic Power Systems,’ Underwriters Laboratories Inc., 1997.
- [11] ANSI C84.1-1995, Electric Power Systems and Equipment - Voltage Ratings (60 Hertz), American National Standards Institute, New York, 1995.
- [12] Kern, G. A., Bonn, R. H., Ginn, J., and Gonzalez, S., Results of Sandia National Laboratories grid-tied inverter testing, *Proc. 2nd World Conf and Exhibition on PV Solar Energy Conversion*, Vienna, Austria, July 1998.
- [13] Kern, G. A., ‘New Techniques for Islanding Protection,’ In terconnecting Small PV Systems to Florida’s Utility Grid, A Workshop for Florida Utilities, Cocoa, FL, October 22, 1998.
- [14] Wiles, J., *Photovoltaic Power Systems and the National Electrical Code: Suggested Practices*, SAND2001-0674, Sandia National Laboratories, Albuquerque, NM, March 2001.
- [15] CFR 47, Federal Communications Commission, Rules and Regulations, Radio Frequency Devices, Part 15, 1994.
- [16] SEI/ASCE 7-02, *Minimum Design Loads for Buildings and Other Structures*, American Society of Civil Engineers, Reston, VA, Jan, 2003.
- [17] Forrester, D. L., Qualification testing for a central station, *Conference Records of 17th IEEE PV Specialists Conference*, 1019-1024, Kissimmee, FL, May 1 –4, 1984.

Suggested Reading

NESC-ANSI/NFPA C2-1993, *National Electrical Safety Code*, National Fire Protection Association, Quincy, MA, 1993.

Chapter 9

EXTERNALITIES AND PHOTOVOLTAICS

9.1 Introduction

Pollution is an insidious byproduct of civilization that threatens the quality and integrity of our air, our soils, our water and our infrastructure. The planet has a remarkable ability to cleanse itself, with significant feedback loops in place for restoration of equilibrium. One example is photosynthesis, in which the oxygen–carbon dioxide cycle is sustained by regeneration of oxygen from the carbon dioxide of respiration and oxidation. Another is digestion, in which bacteria process organic matter into a form that enables the matter to enrich soils or to nourish living bodies.

In electrical engineering terms, the feedback processes can be characterized in control terms by observing the locations of the poles of the processes. If the poles are in the left half plane, then the process is stable. If the poles are in the right half plane, then the process is unstable. Stable implies that the process will tend to correct itself. Unstable implies unbounded increase.

While many processes appear to be stable, examples of unstable processes have also been noted. In particular, increased CO₂ from nonpolar regions causes warming in the polar regions, resulting in thawing of permafrost regions, in which large quantities of CH₄, another greenhouse gas, are trapped. Liberation of the CH₄ causes additional warming, resulting in additional liberation of CH₄, and so forth. The question is whether another natural process exists to counteract this cycle. The process itself is unstable.

Human intervention is at a point where serious questions are now being asked with regard to the effects of human-generated pollutants in terms of the stability of the solutions of the process equations. One might argue that as long as the poles are kept in the left half plane, the pollution causing the appearance of the poles is at acceptable levels for the planet to sustain life. The challenge becomes one of defining acceptable limits on pollution and the resulting changes in natural cycles caused by human intervention.

9.2 Externalities

Externalities were mentioned briefly in Section 5.4 as factors resulting from energy or other manufacturing that are not incorporated directly into the selling price of a product. That is, once the smoke is out of the smokestack, it is no longer a fiscal responsibility of the smoke producer. In this chapter, externalities will be explored in greater detail. In particular, environmental effects, health and safety issues and subsidies will be discussed in the context of comparing energy produced by photovoltaic means with energy produced by other means. In general, the externalities discussed are not associated with costs that appear in a life cycle cost analysis of an energy source. The reader can expect that in the future, greater attention will be paid to those issues currently consid-

ered as externalities, as means for attaching monetary value to these issues are developed and adopted. Some readers may find the research necessary to affix monetary value to externalities of sufficient interest and challenge that they may choose to pursue this interesting and important area to a greater extent.

Perhaps one of the more challenging considerations relating to externalities is the debate as to whether they really merit consideration. Acid rain and global warming, for example, are two phenomena that have been the subjects of a great deal of discussion over the past few decades.

Acid rain is claimed to result from the emissions of sulfur and nitrogen oxides by fossil-fuel burners. As these oxides are dissolved in raindrops, they turn into weak acids that have been blamed for the changes in pH in lakes and soils and for the etching away of building structures. The scientific community has reached consensus on specific greenhouse gases that cause global warming. While it is generally accepted among the scientists that these effects really do exist, there remain skeptics who either do not believe in the phenomena or otherwise claim that insufficient information is available to confirm the cause-effect relationships with 100% certainty.

For example, Moore [1], an economist, argues that policies to reduce the emission of greenhouse gases “may be unnecessary, would be inordinately expensive and would lead to worldwide recession, rising unemployment, civil disturbances, and increased tension between nations . . .” He notes that “even if significant warming were to occur, public policymakers could, at the time it became evident, launch programs to adapt to the change, such as building dikes, increasing air conditioning, and aiding farmers and ecosystems to adjust to the new weather.” He goes on to observe that during colder periods, more people die from exposure to cold than the number who die from exposure to intense heat during warmer periods, suggesting that the potential consequences may not be as dire as predicted by those concerned about global warming.

The history of climate concern, with extensive bibliography, is nicely documented in Paterson [2]. The greenhouse properties of the atmosphere were noted as early as 1827 by Fourier, who is perhaps better known to the electrical engineer for the Fourier series. During the 19th century, discussions continued about the causes of climate change, and in 1872 the International Meteorological Organization was formed. In 1896, Arrhenius published an article in which he calculated that the temperature of the earth would rise about 5°C if atmospheric carbon dioxide were to double. In 1908 he suggested that industrial carbon dioxide emissions might result in a noticeable change in atmospheric carbon dioxide levels within the next few centuries. He continued to observe that perhaps this would be good, since it would warm up some of the cold regions of the planet and make them more useful for agricultural and other purposes. An alternative viewpoint was that there was no need for concern over carbon dioxide emissions, since the oceans would remove excess carbon dioxide and maintain the delicate balance between atmospheric oxygen and carbon dioxide.

The first formal significant consensus on global warming and its relation to the production of specific greenhouse gases probably came out of the Confer-

ence on the Physical Basis of Climate and Climate Modeling, held in 1974. The Intergovernmental Panel on Climate Change (IPCC), in its 1990 report, identified carbon dioxide, methane, chlorofluorocarbons (CFCs) and nitrous oxide as gases that will enhance the greenhouse effect and result, on the average, in an additional warming of the surface of the earth [2].

In this chapter, a general overview of relative environmental effects of energy sources is presented, followed with observations of specific areas of concern for a variety of PV sources and how to best minimize these potential adverse effects. The reader is encouraged to acknowledge that externalities must be viewed from economic as well as from political perspectives and that scientific, economic and political considerations often cause the decision-making process to become merged into a complicated maze. One need only observe the controversy over what to do with nuclear waste to appreciate the interrelationships of these three areas.

9.3 Environmental Effects of Energy Sources

9.3.1 Introduction

Although the methodology of assigning precise dollar values to carbon dioxide emission, particulate emission, nitrogen oxide emission, sulfur emission, and, in general, the adverse environmental effects of the construction, operation and decommissioning of various energy sources, it is generally possible to assign relative comparative values to most of these areas. Table 9.1 shows a matrix compiled by Baumann and Hill [3] that compares 10 negative effects for 12

Table 9.1 Relative environmental effects of a variety of renewable and nonrenewable energy sources [3].

Negligible/Significant = 1 Significant = 2 Significant/Large = 3 Large = 4	SO _x and NO _x	CO ₂	CH ₄	Health	Particulates	Heavy metals	Catastrophes	Waste disposal	Visual intrusion	Noise	Land requirements
Passive solar energy									1		
Photovoltaics					1	1		1	1		1
Wind									3	1	1
Biomass	1		3	1	1	1		1	1	1	3
Geothermal	1	1	1	1		1		2	1	1	
Hydro							2		3		3
Tidal							1		3		1
Water waves							1		1		
Coal	4	4	2	1	2	2	1	2	2	1	3
Oil	3	4	1	1	2	1	2	1	1		1
Natural gas	1	4	3	1			2		1		1
Nuclear	1	1		1			2	3	2		1

(Adapted from Baumann, A. and Hill, R., Proc 10th EC PV Solar Energy Conf, Kluwer, 1991, 834-837, with kind permission from Kluwer Academic Publishers.)

different energy sources with relative significances indicated. The observations should come as no particular surprise to anyone familiar with the listed sources.

9.3.2 Air Pollution

The U.S. Environmental Protection Agency (EPA) is required by the 1990 amendment of the Clean Air Act [4] to regulate emissions of toxic air pollutants from a published list of source categories. EPA is charged with setting standards and with establishing and promulgating rules for reducing toxic emissions to levels that meet the standards.

Each month, the EPA publishes on the worldwide web updated maps of non-attainment areas, i.e., those counties in the U.S. where certain pollutants exceed EPA limits [5]. The maps include nonattainment areas for CO, NO₂, SO₂, O₃, Pb, and particulates of diameter less than 10 μm (PM10). A glance at these maps shows that certain parts of the country have significant areas of nonattainment for several of these pollutants.

EPA also has published a list of the top 25 sources of U.S. air pollution in each of the six categories. A steel producer was at the top of the list of 25 emitters of NO₂ on the March 1999 list. The remaining 24 entries were various electrical utilities, located predominantly along the Ohio River, where coal-fired generation is a major source of electricity. The map of the U.S. shows hundreds of NO₂ emitters with annual emissions in excess of 100 tons, with emitters present in all 50 states.

Carbon monoxide is attributed mostly to steel companies, where carbon is used as a reducing agent to remove oxygen from the oxides of iron.

In March 1999, the top 25 producers of SO₂ in the United States were all electric utilities, with a total estimated production of 4.672 million tons per year. Every state in the union had SO₂ emitters except Utah.

January 2003 ozone nonattainment areas covered a significant fraction of California and a strip along the eastern seaboard from Washington, D.C., to southern Maine. Ozone is primarily a byproduct of internal combustion engines. Improving these engines or replacing much of the fleet, such as commuting vehicles with electric vehicles that run on PV-generated electricity from PV arrays in parking lots are two suggestions for reducing ozone emissions. Fuel cells as energy sources for vehicles may be another promising solution. The hydrogen for the fuel cells can be produced with PV-generated electricity.

Particulates with diameters less than 10 μm , designated as PM-10 particles, tend to remain airborne for relatively long periods of time, causing respiratory problems for anyone with sensitivities to certain particulates. Again, these contaminants were at high levels in southern California, but also, surprisingly, in the Grand Canyon area, in southern Oregon and in northern Idaho and western Montana. The 25 major fixed sources of PM-10 particles in the United States include steel mills and electric utility generators.

Although CO₂ is recognized as a greenhouse gas, its emission is not officially monitored or regulated at this time, although a move is underway to re-

duce CO₂ emissions in the U.S. to 1990 levels as a result of the 1998 Kyoto Conference [6].

Readers are encouraged to visit the EPA web site for details of current EPA programs. The World Resources Institute (WRI) maintains another web site that provides timely information on pollutants, including valuation methodologies and economic cost discussions [7]. According to WRI, the Intergovernmental Panel on Climate Change (IPCC) has calculated that to stabilize CO₂ levels at 1997 levels would require a 60% cut in emissions, maintained at that level for the next century. Readers may also wish to review their solutions to the homework problem in Chapter 1 that dealt with CO₂ emissions from burning coal and petroleum to put the CO₂ from these sources into perspective.

Air quality is not a problem limited to the United States. As developing countries continue to develop, often pollution controls take a back seat to development and the desires of the populations to have more energy at their disposal. Many of the world's larger cities have severe air pollution problems.

The World Bank [8] has tabulated pollution indices for 83 large cities around the world for 1995. In 1995, the highest levels of total suspended particulates were found in Delhi, India (415 µg/m³), with Beijing, China, and Bombay, India, following in close second and third place at 377 µg/m³ and 375 µg/m³. In contrast, Stockholm, Sweden, had a level of 9 µg/m³.

The highest levels of SO₂ occurred in Teheran, Iran (209 µg/m³). Rio de Janeiro, Brazil; Yokohama, Japan; Moscow, Russian Federation and Istanbul, Turkey also had concentrations in excess of 100 µg/m³.

The winner of the NO₂ competition was Milan, Italy, with a concentration of 248 µg/m³. Mexico City, Mexico, came in at 130 µg/m³, while Beijing, China, and Sofia, Bulgaria, both reported 122 µg/m³. New York City won the honors for the United States with 79 µg/m³. Havana, Cuba, was reported at 5 µg/m³.

For the reader who wishes to spend a year or two in the further collection of information on air pollution, on February 2, 2003, a Netscape search for air pollution data netted 758,001 responses.

9.3.3 Water and Soil Pollution

Water pollution has perhaps received the most attention in the U.S. in terms of the lowering of pH of lakes in the Finger Lakes region of New York, presumably caused by acid rain from SO₂ and NO₂ emissions in the Ohio River region. The lowering of the pH as a result of the inability of the lakes to buffer the effect of the acid rain, has been blamed for the loss of significant fish populations. This loss has, in turn, resulted in a loss of revenue to other sectors of society such as the sport fishing and tourist industries.

Other water pollution with perhaps more insidious consequences is the pollution of aquifers, lakes, rivers and streams with solid and liquid pollutants. While aquifer pollution has not been blamed on SO₂ or NO₂ or other atmospheric gases, it has been blamed on industrial solvents and other chemicals, many of which are used to support an economy with a large energy appetite.

Perhaps one of the best-known incidents in this category is the Love Canal, with many other similar sites as identified for cleanup by the EPA. At this point, the cleanup costs of these toxic waste dumps is being quantified, so these costs can be related back as externalities resulting from past waste-dumping practices.

It has been reported that soil acidification leads to permanently reduced productivity resulting from slower decomposition of humus and diminishing humus quality. Other important effects of soil acidification include leaching of alkali and alkaline metals and release of heavy metals into soils. With changing quality of the soil surrounding the roots of trees, it is believed that the trees may become more sensitive to gaseous air pollutants [9].

9.3.4 Infrastructure Degradation

A number of studies have shown that pollution causes premature degradation of infrastructure [10]. Stonework, carbon steel, nickel and nickel-plated steel, zinc and galvanized steel are all highly affected by sulfur dioxide in rain. It has been estimated that in unpolluted environments, galvanized coatings last up to three times longer, and in polluted areas galvanized transmission towers require repainting nearly twice as often. Hence, a cost figure can be attached to the restoration of structural finishes. However, assigning responsibility for the degradation is somewhat more problematic in that it is difficult to determine the mix of pollution sources that cause a specific amount of degradation to any particular site, since the origin of any pollutant at any particular time will depend on the wind direction.

9.3.5 Quantifying the Cost of Externalities

The Cost of CO₂

The cost of CO₂ can be considered in two ways: the cost of controlling CO₂ and the benefit of controlling CO₂. This method is applicable to other pollutants as well, but only CO₂ will be discussed in this section.

According to the World Resources Institute, holding CO₂ levels at 1990 levels will cost approximately 1 to 2% of the Gross Domestic Product for developed countries over the long term, with reductions below 1990 levels cost increasing to 3%. An alternate analysis, however, suggests that by reducing CO₂ levels significantly by incorporation of energy conservation measures, the cost to reduce the CO₂ levels will be less than the savings in energy costs.

If action is not taken to stop the increase of CO₂ atmospheric concentration, it has been estimated that doubling of atmospheric CO₂ will lead to an average warming of 2.5°C. According to current projections, this doubling will occur during the next century if no curtailment measures are taken. In this case, it is estimated that the damage due to the warming will reach approximately 1 to 1.5% of GDP per year in developed countries, with substantially more in island nations. If CO₂ levels continue to rise beyond the double point, the damage may come closer to 6% of GDP.

Hence, it appears certain that damage will occur if nothing is done, while it is debatable whether there will be cost or cost savings if a program to reduce

CO₂ levels is pursued. Considering that CO₂ production is also generally accompanied by the production of NO₂, SO₂ and particulates, if reduction of CO₂ is also accompanied by reduction of other pollutants, then the benefits become subject to a multiplier effect. What is also being supported here is that it may be a better strategy to focus on reducing the production of CO₂ rather than sequestering CO₂ already produced. Perhaps a carefully planned combination of these two strategies may produce the most cost-effective results.

Sequestering CO₂ With Trees

In order to quantify the cost of externalities, it is necessary to arrive at a methodology for determining the value of a ton of SO₂ or NO₂ or CO₂ or other substance. Since trees, other green plants and oceans have maintained the balance between O₂ and CO₂ over the millennia, it would seem that a tree might be valued in terms of the number of tons of CO₂ it will remove from the atmosphere in its lifetime. Since SO₂ and NO₂ generally are removed from the atmosphere by rain, which dissolves them as weak acids, presumably a price per ton can be assigned in terms of the monetary value of any damage that may result to structures or the environment from acid rain. For example, if a building requires repair more often as a result of acid rain, this is a measurable cost, provided that the increased repair costs can be documented. If the fish die in a lake as a result of acid rain and, as a result, cause a decrease in tourism to the area, this also may constitute a documented cost if the source or sources can be identified.

The cost of CO₂ and other pollutants can be measured in several ways, including the cost of repairing the damage, the cost of controlling the damage by reducing emission of pollutants and the cost of mitigating the damage, such as by absorbing the additional CO₂ by trees. Hodas (1990) [11] reported costs of \$240 per ton of carbon for removal of CO₂ from exhaust gases, with significant technical difficulty. The scrubbed CO₂ would then be liquefied and pumped to a depth of about 500 feet in the ocean, where it would then dissolve and become available for plankton and ocean vegetation. The cost of such an operation would likely be close to \$1000/kW for scrubbing and disposal. There would also be a 25% energy penalty, since the energy for the scrubbing and disposal would not be available for other end users, as well as a 22% capacity penalty and additional annual maintenance costs.

Supply, and, demand, side efficiency improvements are estimated to cost in the range of \$20 per ton of carbon avoided. Automobile efficiency increases also save 22 pounds of CO₂ per gallon not burned, with an estimated cost of \$0.53 per gallon for the effort required to increase automobile efficiency to 44 miles per gallon, assuming continued use of gasoline as a fuel.

It is estimated that the U.S. would require 1.5 billion hectares of forest to absorb its annual CO₂ emissions [11]. The problem is that the total land area of the U.S. is only 913 million hectares, and forest in Death Valley, CA, and quite a few other areas appears as an unlikely prospect.

The idea of planting trees to mitigate the effects of CO₂ generation was first attempted in a project proposed by Applied Energy Service. This project in-

volved planting approximately 50 million trees in Costa Rica to mitigate the CO₂ generated by a fossil fuel electric generator in Connecticut. The project also involved a fire protection program to save 2400 hectares of forest from fires, with an overall estimated sequestering of 387,000 metric tons of carbon per year [11].

When trees are used for CO₂ mitigation, it is necessary to consider what will be done with the trees after they mature. If they are used for firewood, then the sequestered carbon is returned to its CO₂ form. If they are used for construction, then the carbon remains sequestered. However, even if they are burned, on the assumption that something will be burned, the burning of these trees displaces burning of other trees. If the trees spared from fire are genetically diverse, then an additional value can be assigned to preservation of diversity in the biosphere.

Perhaps an even more valuable location for trees is the urban environment, particularly in tropic or near-tropic regions. Hodas [11] observes that by planting trees near buildings, the microclimate of the buildings is cooled by several degrees, thus reducing air conditioning needs and the corresponding energy required for cooling. If the energy for cooling comes from fossil-fueled generation, then the trees reduce atmospheric CO₂ directly as a result of their photosynthesis as well as indirectly by reducing the output demands and corresponding fuel requirements of the fossil-fueled generator.

The Hoff Clean Power Estimator

Hoff [12] has developed a convenient computer program, available on the internet, that estimates the annual amount of CO₂ that can be avoided as a result of using PV-generated electricity in place of electricity from fossil-fuel sources. The estimation procedure follows EPA guidelines. The program also produces an estimated net annual cost of a system on the basis of information keyed in by the person running the program. Parameters used in the calculation include local electrical rates, income taxes, incentive programs, weather data, financing details and utility load profiles.

The net annual return on investment is calculated by taking the difference between loan payments and tax and utility bill savings. While the program does not take into account an economic value for the CO₂ avoided, if an economic cost for CO₂ were to be established, the program could readily include such cost, perhaps in the form of an additional tax credit, toward the annual net cost of the PV system. While an economic value has not yet been assigned to CO₂, at the time of this writing, NO₂ and SO₂ credits can now be purchased in the U.S. If these costs, along with particulates and other air and water pollutants could be included in the Hoff Estimator, PV installations would more than likely become even more economically attractive.

Attainment Levels as Commodities

Another interesting method of assigning value to pollutants comes as a consequence of the Clean Air Act [4] and regulated attainment levels. Companies are granted a certain allowable number of pollution units for their facilities. For example, an electrical generating utility may be allowed a certain number of

tons of SO₂ emissions per year. If the utility does not generate as many tons as allowed, it may transfer the remainder of its allowed emissions to another entity. In a free enterprise society, this is not normally done as a simple, friendly gesture. Rather, air quality points are traded on the commodity exchange.

It is now possible for an individual, an organization or a company to purchase allowances for atmospheric SO₂ and NO₂ [13]. At the end of March each year, the U.S. Environmental Protection Agency holds an auction for SO₂ allowances. Anyone can bid on the allowances, and the highest bidder gets the allowance. It is also possible to purchase allowances through a commodity broker or to purchase them through various environmental groups that purchase the allowances and then do not use them. Not using the allowances results in cleaner air. It is also possible to purchase NO₂ allowances from brokers or from environmental groups, but they are not currently auctioned off by the EPA.

While this practice does not affix a price to emissions based on specific environmental costs, it at least shows that emissions do have some economic cost, and the reduction of emissions can result in economic benefit. What is interesting is that the law of supply and demand dictates the price of air quality points. If strict laws are enacted to reduce pollutants, companies end up investing in pollution control technologies, such as electrostatic precipitators and scrubbers. If these investments result in sufficient reduction in emission of pollutants, then a smaller number of air quality points will be needed and a larger number will be available. This means the price will go down.

Other related actions have also been offered by energy producers in trade for permission to operate, such as improving navigation channels to reduce the likelihood of accidental fuel spills. These added costs represent the attachment of a price to certain externalities, and, as a result, end up incorporating the costs of the externalities into the cost of the product.

Subsidies

Subsidies were included as components of direct costs of doing business in Chapter 5, since they are usually included in the reduction of the cost of a product, such as energy, to the consumer. However, unless a level playing field exists, the costs of two energy sources cannot be properly compared. A level playing field exists when all energy sources are subsidized equally on a kWh-to-kWh basis. The difficulty is the identification of all subsidies, since some are direct and others are indirect.

A direct subsidy, such as a depletion allowance, can be quantified in terms of dollars per kWh. An indirect subsidy, such as military presence, can also sometimes be quantified, but will normally not appear in the financial records of a company. The effects of favorable tax considerations and tariffs can also be quantified in either a direct or indirect manner.

Government-sponsored research and government purchase of systems or rebates or tax credits on systems are also forms of subsidy. Generally, government involvement is justified on the basis that once the subsidized industry is able to compete without subsidy, it will generate sufficient revenues to result in sufficient taxes to reimburse the government for its initial investment. In any

case, hardly an energy source exists that does not benefit to some extent from subsidies. To date, however, no one has requested a depletion allowance on sunlight, although solar access rights have been challenged in the case where one party shades another party's solar system.

9.3.6 Health and Safety as Externalities

Recent litigation against tobacco companies, resulting in the award of billions of dollars in damages to states to help reimburse the costs of tobacco-related illnesses, has shown that the cost of public health is becoming a recognized externality, with a significant price tag. Other lawsuits have also been successfully prosecuted against a variety of forms of pollution resulting from careless or indiscriminate disposal of many forms of toxic wastes. These cases confirm the linkage between public health and its economic cost.

Public safety is also at issue when energy sources are considered. The Chernobyl and Three Mile Island nuclear accidents both brought to the forefront public concern over nuclear safety. The location of large fuel tanks in highly populated areas also is of concern to public advocacy groups. Transport of various fuels is also problematic, especially when large tanker trucks are involved in accidents that result in spilling of their contents and subsequent major efforts to clean up the damage before aquifers are affected. Even in the case of renewable energy sources, concern has been expressed about the possibility of construction accidents, since installation of renewable sources tends to be more labor intensive per installed kW than conventional sources. Manufacture of the materials used in conventional generation facilities carries with it both energy costs and materials costs, along with certain levels of exposure to hazardous or toxic materials. Similar costs are associated with the manufacture of photovoltaic cells and system components. Although these costs tend to be incorporated into the production cost of the materials, when toxic waste byproducts result, they are often treated as externalities.

The balance of this chapter explores the externalities associated with the production, deployment, operation and decommissioning of PV power systems. Particular attention is paid to the environmental concerns associated with each of the phases, recognizing that in order to produce PV systems, initially other energy sources must be exploited.

9.4 Externalities Associated with PV Systems

9.4.1 Environmental Effects of PV System Production

The production phase of each PV technology can be described in terms of a production cycle, which includes potential pollutants or hazardous waste associated with each production step. Table 9.2 summarizes areas of environmental or health concern for current PV technologies that have promising possibilities for large scale production. The associated CO₂ for each technology represents the CO₂ resulting from the production of the primary energy used to produce the PV

systems, so, in effect, it represents an energy cost of production. In the future, it is conceivable that energy for PV production will come from PV sources, thus further reducing the CO₂ and other pollutants associated with the production of PV cells. This concept is feasible since PV cells over their useful lifetime will produce upwards of four times the energy expended in their fabrication. Aside from the energy cost, each technology has its own specific toxic waste areas of concern. Some concerns are common to all technologies, such as production of the materials for support structures and encapsulants for the modules.

Table 9.2 Environmental concerns associated with PV system production.

Technology	Concern	Relative Significance ^a	Relative Control Cost ^b	Control Strategy
All	Mining	Low	Lower	MSA ^c
All	Cleaning solvents	High	Higher	Recycle
All	Steel	Medium	Lower	OSHA, EPA
All	Aluminum	Medium	Lower	OSHA, EPA
All	Concrete	Medium	Lower	OSHA, EPA
All	Glass/breakage	Low	Lower	n/a
All	Encapsulants	Low	Lower	n/a
Crystalline Si	CO ₂	0.02 ^d	Lower	EPA
Multi cr Si	CO ₂	0.01	Lower	EPA
Thin film Si	CO ₂	0.005	Lower	EPA
Other thin films	CO ₂	0.004	Lower	EPA
Future cells	CO ₂	0.002	Lower	EPA
All Si cells	Silica dust	Low	Lower	OSHA, EPA
All Si cells	CH ₄	Low	Lower	Confine and recycle (C and R)
All Si cells	B ₂ H ₆	Low	Lower	C and R
All Si cells	PH ₃	Low	Lower	C and R
All Si cells	AsH ₃	Low	Lower	C and R
CIS	H ₂ Se	Low	Lower	C and R
CIS	Cd ^e	Low	Lower	C and R
CIS	Fire (Cd)	Low	Lower	None
CdTe	Cd and CdO	Low	Lower	C and R
CdTe	Te	Low	Lower	C and R
CdTe	Fire (Cd, Te)	Low	Lower	None

- (a) Compared to amount produced from equivalent amount of energy from coal-fired generation. Some items are not present in coal-fired, but are compared to other by-products of coal-fired generation such as SO₂, NO₂ and particulates.
- (b) Generally lower control costs since generally less to control.
- (c) Mine Safety Administration.
- (d) These numbers represent ratios of CO₂ to produce a kWh PV over the system lifetime to CO₂ per kWh from burning coal.
- (e) It is estimated that coal-fired stack emissions produce as much Cd per kWh as is contained in CIS per lifetime kWh. CIS Cd is recycled at end of CIS life cycle.

Perhaps the most important common denominator associated with all technologies is the material used for cleaning the cells. In all cases, high levels of cleanliness are required to maximize performance, and in some cases the solvents used are highly toxic. Fortunately these solvents have been in common use in the semiconductor industry and careful means of control are well understood within the industry. The common means of dealing with these solvents is to confine them and then recycle them.

In the case of Si PV cells, the most significant concerns are the proper handling of the dopants for n-type and p-type. Since the semiconductor industry has been handling these components effectively, the processes are well defined. Once the impurities are in the Si, the amounts are so insignificant that the doped Si is considered to be benign.

For the CIS cells and the CdTe cells, the Cd content is the primary item of concern, but since the films in these devices are generally less than $2 \mu\text{m}$ thick, the total amount of Cd and Te in these cells is very small. Another concern for CIS is the use of H_2Se for the deposit of Se into the cell, but again, the use of this highly toxic substance can be kept well under control with minimal risk of having it escape into the environment.

9.4.2 Environmental Effects of PV System Deployment and Operation

The deployment of PV systems has associated environmental and health costs similar to the deployment of other energy technologies [14]. Steel, aluminum and concrete can be expected to be part of the structures upon which the PV arrays and associated BOS components will be mounted. Hence, the production costs and associated environmental costs, such as CO production in the reduction of iron oxides, become associated with PV deployment.

Just as construction accidents occur in any construction project, it is anticipated that PV project construction will also result in construction accidents. For the most part, materials used in construction of PV facilities are nontoxic. It is thus the responsibility of the installation contractor to ensure that the workplace and work practices follow Occupational Safety and Health Administration (OSHA) rules.

Once the PV system is installed, it quietly generates pollution-free electricity any time the sun is shining. The main environmental concern associated with the operation of PV systems is if a system containing Cd or Se or Te should be exposed to fire. Analysis has shown, however, that since these materials appear in such minute quantities in thin-film PVs that anyone approaching close enough to encounter significant exposure to any of the toxins would face significantly more danger from the fire itself. For example, only 400 g of Cd are present in a 1 MW CIS PV system, whereas 5 g/m^2 of Cd are present in CdTe systems, or about 25 times the amount in CIS systems.

Other dangers associated with the installed system include, of course, the possibility of electrical shock or fire. Systems installed in accordance with the *National Electrical Code* [15] will reduce any shock or fire hazard to a mini-

mum, both for the general public as well as maintenance personnel. The fact that PV systems are inherently current limiting tends to reduce their potential to produce high-current arcing if they are inadvertently shorted. Incorporation of ground fault protection in residential rooftop systems adds further protection.

A final safety consideration for installed PV systems relates to their ability to withstand high winds. Inadequately mounted PV modules in high winds may tear loose from their mounting and become projectiles. Installations compliant with local building code wind-loading requirements present minimal risk.

9.4.3 Environmental Effects of PV System Decommissioning

Certain regulatory requirements apply to the decommissioning of PV systems. Assuming that the system will be disassembled at the end of its useful lifetime, it is then necessary to consider the destination of the disassembled components. Some of the components will require disposal according to toxic waste regulations unless they can be recycled, and other components will not be subject to quite as stringent requirements.

The Resource and Conservation Recovery Act constitutes the primary set of rules governing wastes containing Cd, Se, Pb, Cu or Ag provided that these wastes are considered to be discarded material and are not included in any specific exclusions [16]. The EPA defines the Toxicity Characteristic Leaching Procedure (TCLP) for 39 materials to determine whether waste products containing them may be classified as hazardous. Any waste product containing any of the 39 materials that yields a soluble concentration in excess of its TCLP limits is considered hazardous.

The California Hazardous Waste Control Law introduces an additional test for toxicity characterization, with two additional indicators. The Waste Extraction Test (WET) is used to identify non-RCRA toxic wastes. The WET threshold limits are defined as the Soluble Threshold Limit Concentration (STLC) and the Total Threshold Limit Concentration (TTLC), that is the total concentration of listed materials, in any form.

In terms of STLC and TTLC, it appears that CdTe modules may be characterized as hazardous in terms of TTLC and STLC for Cd. CIS modules may be subject to TTLC for Se and STLC for Se and Cd. Polycrystalline Si modules may have a problem with TTLC and STLC for Ag or Pb. In some cases, Pb and Cu may be a problem, and a-Si:H modules do not seem to have any toxicity problems [16]. If CdTe and CIS modules are recycled, they are exempt from the disposal regulations. Studies have projected recycling costs of approximately \$0.01 to \$0.04 per watt for both materials, using relatively standard separation techniques.

Problems

- 9.1 Look up the U.S. nonattainment regions on the U.S. Environmental Protection Agency web site.
- 9.2 If recycling of CdTe PV modules will cost approximately \$0.04/watt and the lifetime of a CdTe module is 20 years, what is the present value of the recycling cost for a 10 kW array?
- 9.3 Determine the prices of a ton of SO₂ and a ton of NO₂ on the commodity exchange. The EPA website lists websites and phone numbers of commodity brokers and environmental organizations that purchase and sell them.
- 9.4 If burning a gallon of gasoline produces 22 pounds of CO₂, estimate the CO₂ that your vehicle emits in a year. Compare this with the amount that would have been generated had you been driving an electric vehicle charged from a PV array or a hybrid auto or a fuel cell-powered auto. Take into account the origin of the H₂ used in the fuel cell.
- 9.5 In the CO₂ scrubbing and liquefaction scheme reported by Hodas, estimate the increase in electrical cost that would be necessary to offset the cost of the process.
- 9.6 Use the Hoff Clean Power Estimator [12] to determine for your residential zip code area:
 - a. A combination of system cost per PV watt (at STC), interest rate and loan duration that will result in a positive net annual cash flow for a PV system owner of your income level and marital status.
 - b. Assume the cost of a PV system to be \$3/watt and the annual interest rate on a 25-year loan for the PV system to be 6%. Determine the necessary value of a ton of avoided CO₂ to bring the annual system net cost to zero for your personal income and tax situation (or your hypothetical income and tax situation).

References

- [1] Moore, T. G., *Climate of Fear: Why We Shouldn't Worry about Global Warming*, the Cato Institute, Washington, D.C., 1998.
- [2] Paterson, M., *Global Warming and Global Politics*, Routledge, London, 1996.
- [3] Baumann, A. and Hill, R., *Proc. 10th EC Photovoltaics Solar Energy Conference*, Kluwer, Dordrecht, 1991, 834–837.
- [4] 42 U. S. C. § 7401 et. seq. (Clean Air Act).

- [5] wysiwyg://180//www.epa.gov/airprogm/airs/data/mapview.htm (EPA air pollution maps).
- [6] 3rd Conference of the Parties to the U. N. Framework Convention on Climate Change, Kyoto, Japan, December 1997.
- [7] http://www.wri.org/wr-96-97/ac_txt6.html (World Resources Institute).
- [8] www.worldbank.org/nipr/wdi98/tables3.12.pdf (World Bank pollution data).
- [9] Guderian, R., *External Environmental Costs of Electric Power*, Springer-Verlag, Berlin, 1990, 9–24.
- [10] Weltschev, M., *External Environmental Costs of Electric Power*, Springer-Verlag, Berlin, 1990, 25–35.
- [11] Hodas, D. R., *External Environmental Costs of Electric Power*, Springer-Verlag, Berlin, 1990, 59–78.
- [12] www.clean-power.com/estimator/ (The Hoff Clean Power Estimator Program).
- [13] <http://www.epa.gov/airmarkt/trading/buying.html> (Information on SO₂ and NO₂ commodity trading).
- [14] Markvart, T., Ed., *Solar Electricity*, John Wiley & Sons, Chichester, U.K., 1994.
- [15] *NFPA 70 National Electrical Code, 2002 Edition*, National Fire Protection Association, Quincy, MA, 2002.
- [16] Fthenakis, V. M. and Moskowitz, P. D., Emerging photovoltaic technologies: environmental and health issues update, *NREL/SNL Photovoltaics Program Review*, AIP Press, New York, 1997.

- [5] <wysiwyg://180//www.epa.gov/airprogm/airs/data/mapview.htm> (EPA air pollution maps).
- [6] 3rd Conference of the Parties to the U. N. Framework Convention on Climate Change, Kyoto, Japan, December 1997.
- [7] http://www.wri.org/wr-96-97/ac_txt6.html (World Resources Institute).
- [8] www.worldbank.org/nipr/wdi98/tables3.12.pdf (World Bank pollution data).
- [9] Guderian, R., *External Environmental Costs of Electric Power*, Springer-Verlag, Berlin, 1990, 9–24.
- [10] Weltschev, M., *External Environmental Costs of Electric Power*, Springer-Verlag, Berlin, 1990, 25–35.
- [11] Hodas, D. R., *External Environmental Costs of Electric Power*, Springer-Verlag, Berlin, 1990, 59–78.
- [12] www.clean-power.com/estimator/ (The Hoff Clean Power Estimator Program).
- [13] <http://www.epa.gov/airmarkt/trading/buying.html> (Information on SO₂ and NO₂ commodity trading).
- [14] Markvart, T., Ed., *Solar Electricity*, John Wiley & Sons, Chichester, U.K., 1994.
- [15] *NFPA 70 National Electrical Code, 2002 Edition*, National Fire Protection Association, Quincy, MA, 2002.
- [16] Fthenakis, V. M. and Moskowitz, P. D., Emerging photovoltaic technologies: environmental and health issues update, *NREL/SNL Photovoltaics Program Review*, AIP Press, New York, 1997.

Chapter 10

THE PHYSICS OF PHOTOVOLTAIC CELLS

10.1 Introduction

By this point, it is possible that the reader, now highly skilled at PV system design, might be interested in what goes on inside the PV cell during the process of converting light energy into electrical energy. This chapter is presented with the purpose of enabling the reader to become familiar with the challenges facing those engineers and physicists who spend their lives working on processes and materials aimed at reducing the cost and increasing the efficiency of PV cells. Initially, the basics of PV energy conversion are presented, followed by discussion of present limitations of cell production and some of the ideas that have emerged toward overcoming these limitations. Most readers will have already had at least an exposure to the theory of operation of the pn junction and the semiconductor diode in an electronics course, so it will be assumed that the reader will at least be familiar with the basic diode equation.

10.2 Optical Absorption

10.2.1 Introduction

When light shines on a material, it is either reflected, transmitted, or absorbed. Absorption of light is simply the conversion of the energy contained in the incident photon to some other form of energy, typically heat. Some materials, however, happen to have just the right properties needed to convert the energy in the incident photons to electrical energy.

When a photon is absorbed, it interacts with an atom in the absorbing material by giving off its energy to an electron in the material. This energy transfer is governed by the rules of conservation of momentum and conservation of energy. Since the zero mass photon has very small momentum compared to the electrons and holes, the transfer of energy from a photon to a material occurs with inconsequential momentum transfer. Depending on the energy of the photon, an electron may be raised to a higher energy state within an atom or it may be liberated from the atom. Liberated electrons are then capable of moving through the crystal in accordance with whatever phenomena may be present that could cause the electron to move, such as temperature, diffusion or an electric field.

10.2.2 Semiconductor Materials

Semiconductor materials are characterized as being perfect insulators at absolute zero temperature, with charge carriers being made available for conduction as the temperature of the material is increased. This phenomenon can be

explained on the basis of quantum theory, by noting that semiconductor materials have an energy band gap between the valence band and the conduction band. The valence band represents the allowable energies of valence electrons that are bound to host atoms. The conduction band represents the allowable energies of electrons that have received energy from some mechanism and are now no longer bound to specific host atoms.

At $T = 0 \text{ K}$, all allowable energy states in the valence band of a semiconductor are occupied by electrons, and no allowable energy states in the conduction band are occupied. Since the conduction process requires that charge carriers move from one state to another within an energy band, no conduction can take place when all states are occupied or when all states are empty. This is illustrated in Figure 10.1a.

As temperature of a semiconductor sample is increased, sufficient energy is imparted to a small fraction of the electrons in the valence band for them to move to the conduction band. In effect, these electrons are leaving covalent bonds in the semiconductor host material. When an electron leaves the valence band, an opening is left which may now be occupied by another electron, provided that the other electron moves to the opening. If this happens, of course, the electron that moves in the valence band to the opening, leaves behind an opening in the location from which it moved. If one engages in an elegant quantum mechanical explanation of this phenomenon, it must be concluded that the electron moving in the valence band must have either a negative effective mass along with its negative charge, or, alternatively, a positive effective mass and a positive charge. The latter has been the popular description, and, as a result, the electron motion in the valence band is called hole motion, where ‘holes’ is the name chosen for the positive charges, since they relate to the moving holes that the electrons have left in the valence band.

What is important to note about these conduction electrons and valence holes is that they have occurred in pairs. Hence, when an electron is moved from the valence band to the conduction band in a semiconductor by whatever means, it

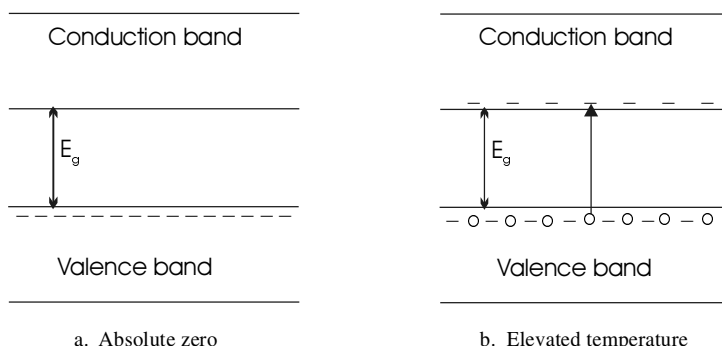


Figure 10.1 Illustration of availability of states in valence band and conduction band for semiconductor material.

constitutes the creation of an electron-hole pair (EHP). Both charge carriers are then free to become a part of the conduction process in the material.

10.2.3 Generation of EHP by Photon Absorption

The energy in a photon is given by the familiar equation,

$$E = h\nu = \frac{hc}{\lambda} \text{ (joules)}, \quad (10.1)$$

where h is Planck's constant ($h = 6.63 \times 10^{-34}$ joule-sec), c is the speed of light ($c = 2.998 \times 10^8$ m/sec), ν is the frequency of the photon in Hz and λ is the wavelength of the photon in meters. Since energies at the atomic level are typically expressed in electron volts ($1 \text{ eV} = 1.6 \times 10^{-19}$ joules) and wavelengths are typically expressed in micrometers, it is possible to express hc in appropriate units so that if λ is expressed in μm , then E will be expressed in eV. The conversion yields

$$E = \frac{1.24}{\lambda} \text{ (eV)}. \quad (10.1a)$$

The energy in a photon must exceed the semiconductor bandgap energy, E_g , to be absorbed. Photons with energies at and just above E_g are most readily absorbed because they most closely match bandgap energy and momentum considerations. If a photon has energy greater than the bandgap, it still can produce only a single EHP. The remainder of the photon energy is lost to the cell as heat. It is thus desirable that the semiconductor used for photoabsorption have a bandgap energy such that a maximum percentage of the solar spectrum will be efficiently absorbed.

Now, referring back to the Planck formula for blackbody radiation in Chapter 2 (2.1), note that the solar spectrum peaks at $\lambda \approx 0.5 \mu\text{m}$. Equation (10.1a) shows that a bandgap energy of approximately 2.5 eV corresponds to the peak in the solar spectrum. In fact, since the peak of the solar spectrum is relatively broad, bandgap energies down to 1.0 eV can still be relatively efficient absorbers, and in certain special cell configurations to be discussed later, even smaller bandgap materials are appropriate.

The nature of the bandgap also affects the efficiency of absorption in a material. A more complete representation of semiconductor bandgaps must show the relationship between bandgap energy as well as bandgap momentum. As electrons make transitions between conduction band and valence band, both energy and momentum transfer normally take place, and both must be properly balanced in accordance with conservation of energy and conservation of momentum laws.

Some semiconducting materials are classified as direct bandgap materials, while others are classified as indirect bandgap materials. Figure 10.2 shows the bandgap diagrams for two materials considering momentum as well as energy. Note that for silicon, the bottom of the conduction band is displaced in the

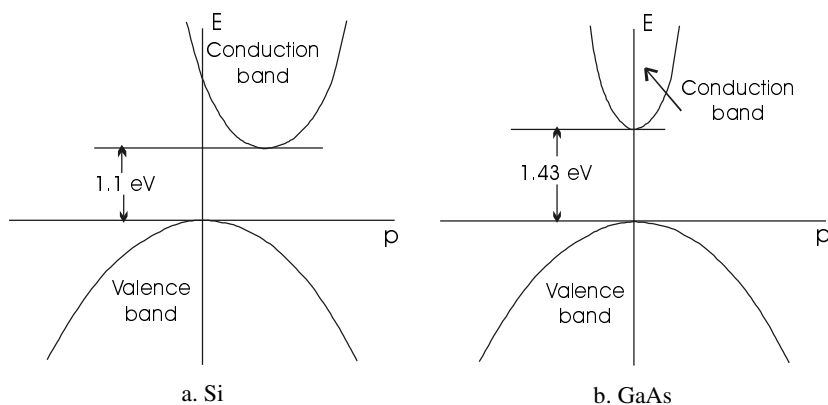


Figure 10.2 The energy and momentum diagram for valence and conduction bands in Si and GaAs.

momentum direction from the peak of the valence band. This is an indirect bandgap, while the GaAs diagram shows a direct bandgap, where the bottom of the conduction band is aligned with the top of the valence band.

What these diagrams show is that the allowed energies of a particle in the valence band or the conduction band depend on the particle momentum in these bands. An electron transition from a point in the valence band to a point in the conduction band must involve conservation of momentum as well as energy. For example, in Si, even though the separation of the bottom of the conduction band and the top of the valence band is 1.1 eV, it is difficult for a 1.1 eV photon to excite a valence electron to the conduction band because the transition needs to be accompanied with sufficient momentum to cause displacement along the momentum axis, and photons carry little momentum. The valence electron must thus simultaneously gain momentum from another source as it absorbs energy from the incident photon. Since such simultaneous events are unlikely, absorption of photons at the Si bandgap energy is several orders of magnitude less likely than absorption of higher energy photons.

Since photons have so little momentum, it turns out that the direct bandgap materials, such as gallium arsenide (GaAs), cadmium teluride (CdTe), copper indium diselenide (CIS) and amorphous silicon absorb photons with energy near the material bandgap energy much more readily than do the indirect materials, such as crystalline silicon. As a result, the direct-bandgap absorbing material can be several orders of magnitude thinner than indirect bandgap materials and still absorb a significant part of the incident radiation.

The absorption process is similar to many other physical processes, in that the change in intensity with position is proportional to the initial intensity. As an equation, this becomes

$$\frac{dI}{dx} = -\alpha I, \quad (10.2)$$

with the solution

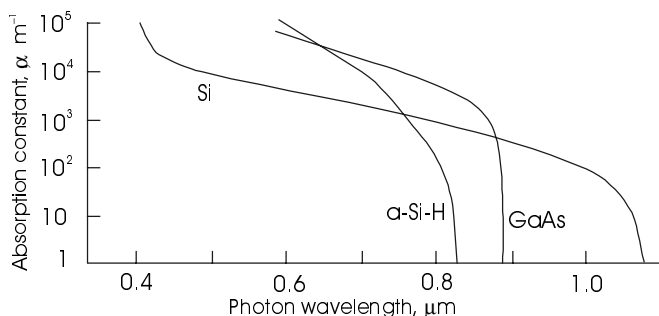


Figure 10.3 Dependence of absorption constant on wavelength for several semiconductors [1].
(Adapted from Yang, E. S., *Microelectronic Devices*, 1988, McGraw-Hill.
Reproduced with permission of the McGraw-Hill Companies.)

$$I = I_0 e^{-\alpha x}, \quad (10.3)$$

where I is the intensity of the light at a depth x in the material, I_0 is the intensity at the surface and α is the absorption constant. The absorption constant depends on the material and on the wavelength. Equation (10.3) shows that the thickness of material needed for significant absorption needs to be several times the reciprocal of the absorption constant. This is important information for the designer of a PV cell, since the cell must be sufficiently thick to absorb the incident light. In some cases, the path length is increased by causing the incident light to reflect from the front and back surfaces while inside the material until it ultimately generates an EHP. Figure 10.3 shows the dependence of absorption constant on wavelength for several materials. Observe that at energies below the bandgap energy, no absorption takes place. The material is transparent to these low-energy photons. At energies above the bandgap, the absorption constant increases relatively slowly for indirect bandgap semiconductors and increases relatively quickly for direct bandgap materials.

In any case, when the photon is absorbed, it generates an EHP. The question, then, is what happens to the EHP?

10.2.4 Photoconductors

Once an EHP is generated, it becomes a question of how long the EHP lasts before the conduction electron returns to the valence band. Remember that the creation of an EHP does not imply that the electron will remain in the conduction band and the hole will remain in the valence band. Thermal equilibrium in a semiconductor comprises a constant generation and recombination of EHPs, so that, on the average, the population of electrons and the population of holes remain constant. In fact, the product of the concentration of holes and the concentration of electrons in thermal equilibrium is a constant, which depends on temperature and the bandgap energy of the semiconductor, along with a few other

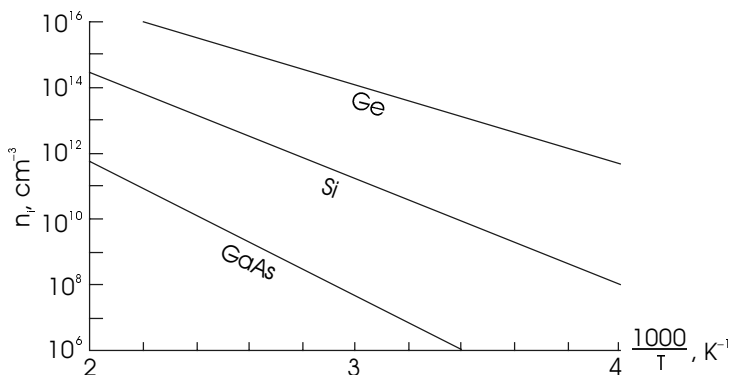


Figure 10.4 Temperature dependence of intrinsic carrier concentration for several common semiconductors [2]. (Adapted from Streetman, B., *Solid State Electronic Devices*, 4th Ed., 1995, Prentice-Hall. Reproduced with permission.)

parameters unique to each semiconductor. If n_o represents the thermal equilibrium concentration of electrons per cm^3 and if p_o represents the thermal equilibrium concentration of holes per cm^3 , then, in thermal equilibrium,

$$n_o p_o = n_i^2(T) = K T^3 e^{-\frac{E_g}{kT}}, \quad (10.4)$$

where n_i represents the intrinsic carrier concentration, K is semiconductor-material dependent, as will be discussed later, E_g is the bandgap energy, k is Boltzmann's constant and T is the temperature in K. Because of the temperature dependence of n_i , it is customary to plot n_i vs. $1000/T$ as in Figure 10.4, which shows how n_i varies with temperature for several semiconductor materials. Note that materials with smaller bandgap energies have higher intrinsic carrier concentrations. Table 10.1 shows bandgap energies and several other properties of some common semiconductors used in PV cells.

Electrons and holes generated as a result of optical absorption bring the material into a state of nonthermal equilibrium. The photon-generated excess electrons and holes remain, on the average, for a time, τ , which is defined as the excess carrier lifetime. The recombination of EHPs is a statistical process in which some EHPs recombine in times shorter than the carrier lifetime and some take longer to recombine.

EHPs, then, are subject to a generation rate, measured in number per cm^3 per sec, which is proportional to the incident photon flux, and are subject to a recombination rate that is proportional to the departure of np from its equilibrium value. Under steady state conditions, these two rates are equal.

The conductivity of a material is proportional to the density of free charge carriers, and is given by

$$\sigma = q(\mu_n n + \mu_p p), \quad (10.5)$$

where μ_n and μ_p represent, respectively, the mobility of electrons and the mobility of holes in the material. Mobility is simply a measure of how easily the particles can move around in the material when an electric field is present. Mobilities are included in the material characteristics presented in Table 10.1.

Table 10.1 Properties of several common semiconductors at room temperature [2, 3].

Material	E_g , eV	n_i , cm^{-3}	μ_n , cm^2/Vs	μ_p , cm^2/Vs	ϵ_r	Melting point, °C
Si	1.11	1.5×10^{10}	1350	480	11.8	1415
Ge	0.67	2.5×10^{13}	3900	1900	16	936
GaAs	1.43	2×10^6	8500	400	13.2	1238
CdS	2.42		340	50	8.9	1475
CdTe	1.48		1050	100	10.2	1098

Equation (10.5) clearly indicates that, if shining a light on a piece of material can create excess charge carriers, then the conductivity of the material will increase, causing a corresponding decrease in the resistance of the material. The material becomes a light-sensitive resistor. A common material used for such devices is cadmium sulfide (CdS), which is used in many of the light sensors that turn lights on after dark. The most sensitive photoconductors are materials that have long lifetimes of excess EHPs. However, if the problem is to detect short bursts of light occurring at a high repetition rate, it is necessary to have any excess population of electrons and holes quickly die out as soon as the light source is removed. The trade-off between speed and sensitivity is similar to the trade-off between bandwidth and gain for an amplifier as described by the familiar gain-bandwidth product.

Note that even though EHPs are generated in the host material, the material remains passive because the generated EHPs have random thermal velocities. This means that no net current flow results from their creation and, since no separation of charges occurs, no voltage is produced. With no resulting voltage or current, the only effect of the creation of the additional charge carriers is the reduction in resistance of the host material. The next step, then, is to figure out a way to get work out of these photon-generated charges.

10.3 Extrinsic Semiconductors and the pn Junction

10.3.1 Extrinsic Semiconductors

Up to this point, the semiconductors discussed have been intrinsic semiconductors, meaning that the populations of holes and electrons have been equal. A somewhat more formal definition of an intrinsic semiconductor takes into account differences in electron and hole mobilities and defines intrinsic semiconductors as materials for which the Fermi level energy is at the center of the bandgap. Since Fermi levels have not been discussed, and since electron and

hole mobilities are generally close enough to keep the Fermi level quite close to the center of the bandgap, the equal carrier definition will suffice for the following discussion. The reader is referred to a text on semiconductor device physics for more details on Fermi levels [1, 2].

At $T = 0$ K, intrinsic semiconductors have all covalent bonds completed with no leftover electrons or holes. If certain impurities are introduced into intrinsic semiconductors, there can be leftover electrons or holes at $T = 0$ K. For example, consider silicon, which is a group IV element, which covalently bonds with four nearest neighbor atoms to complete the outer electron shells of all the atoms. At $T = 0$ K, all the covalently bonded electrons are in place, whereas at room temperature, about one in 10^{12} of these covalent bonds will break, forming an EHP, resulting in minimal charge carriers for current flow.

If, however, phosphorous, a group V element, is introduced into the silicon in small quantities, such as one part in 10^6 , four of the valence electrons of the phosphorous atoms will covalently bond to the neighboring silicon atoms, while the fifth valence electron will have no electrons with which to covalently bond. This fifth electron remains weakly coupled to the phosphorous atom, readily dislodged by temperature, since it requires only 0.04 eV to excite the electron from the atom to the conduction band. At room temperature, sufficient thermal energy is available to dislodge essentially all of these extra electrons from the phosphorous impurities. These electrons thus enter the conduction band under thermal equilibrium conditions, and the concentration of electrons in the conduction band becomes nearly equal to the concentration of phosphorous atoms, since the impurity concentration is normally on the order of 10^8 times larger than the intrinsic carrier concentration.

Since the phosphorous atoms donate electrons to the material, they are called **donor** atoms and are represented by the concentration, N_D . Note that the phosphorous, or other group V impurities, *do not add holes* to the material. They only add electrons. They are thus designated as n-type impurities.

On the other hand, if group III atoms such as boron are added to the intrinsic silicon, they have only three valence electrons to covalently bond with nearest silicon neighbors. The missing covalent bond appears the same as a hole, which can be released to the material with a small amount of thermal energy. Again, at room temperature, nearly all of the available holes from the group III impurity are donated to the conduction process in the host material. Since the concentration of impurities will normally be much larger than the intrinsic carrier concentration, the concentration of holes in the material will be approximately equal to the concentration of impurities.

Historically, group III impurities in silicon have been viewed as electron acceptors, which, in effect, donate holes to the material. Rather than being termed hole donors, however, they have been called **acceptors**. Thus, acceptor impurities donate holes, but no electrons, to the material and the resulting hole density is approximately equal to the density of acceptors, which is represented as N_A . Figure 10.5 shows the effects of donor and acceptor impurities on the intrinsic

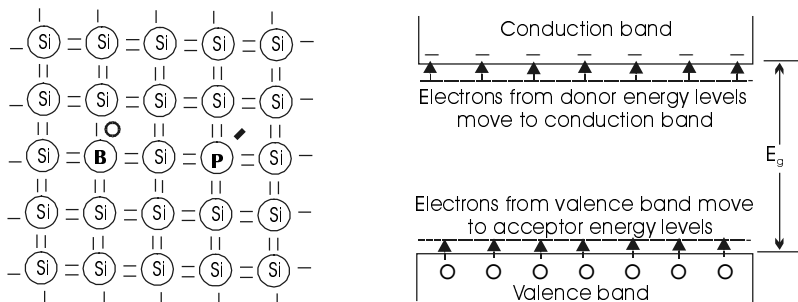


Figure 10.5 Acceptor and donor impurities in Si.

material along with the positions of the energy levels of the impurities in the bandgap of the material.

Equation (10.5) shows that adding a mere one part in a million of a donor or acceptor impurity can increase the conductivity of the material by a factor of 10^8 for silicon. Equation (10.4) shows that in thermal equilibrium, if either an n-type or a p-type impurity is added to the host material, that the concentration of the other charge carrier will decrease dramatically, since it is still necessary to satisfy (10.4). In extrinsic semiconductors, the charge carrier with the highest concentration is called the **majority carrier** and the charge carrier with the lowest concentration is called the **minority carrier**. Hence, electrons are majority carriers in n-type material, and holes are minority carriers in n-type material. The opposite is true for p-type material.

If both n-type and p-type impurities are added to a material, then whichever has the higher concentration will become the dominant impurity. However, it is then necessary to acknowledge a net impurity concentration that is given by the difference between the donor and acceptor concentrations. If, for example, $N_D > N_A$, then the net impurity concentration is defined as $N_d = N_D - N_A$. Similarly, if $N_A > N_D$, then $N_a = N_A - N_D$.

10.3.2 The pn Junction

Drift and Diffusion

When charged particles are placed in an electric field, they are exposed to an electrostatic force. This force accelerates the particles until they undergo a collision with another component of the material that slows them down. They then accelerate once again and collide again. The process continues, with the net result of the charge carrier's achieving an average velocity, either in the direction of the electric field for positive charges, or opposite the electric field for negative charges. It should be noted that this average, or *drift velocity*, is superimposed on the thermal velocity of the charge carrier. Normally the thermal velocity is much larger than the drift velocity, but the thermal velocity is completely random so the net displacement of the charge carriers is zero. Another way to

consider the thermal velocity is that at any instant, it is equally likely that a particle will be moving in any direction.

Drift current, then, is simply the component of current flow due to the presence of an electric field, and is described by the familiar equation,

$$\vec{J} = \sigma \vec{E}, \quad (10.6)$$

This is simply the vector form of Ohm's law, where J is the current density in A/cm^2 when σ is expressed in $\Omega^{-1} \text{cm}^{-1}$ and E is measured in V/cm .

Diffusion is that familiar process by which random thermal motion of particles causes them to ultimately distribute themselves uniformly within a space. Whenever particles are in thermal motion, they will tend to move from areas of greater concentration to areas of lesser concentration, simply because at any point, the probability of motion in all directions is equal. Suppose, for example that regions A and B are adjoining, as shown in Figure 10.6. Suppose also that all particles in both regions are experiencing random thermal motion and that the concentration of certain particles, z , in region A is greater than the concentration of z -particles in region B. At any instant, half the z -particles in region A will be moving toward B, and half the z -particles in B will be moving toward A. Since there are more z -particles in A, the net motion of z - particles from A to B will continue until the concentrations in A and B are equal.

If the particles are holes, this net movement from regions of greater concentration to regions of lesser concentration constitutes a flow of current that can be described in one dimension by the equation

$$J_p = -qD_p \frac{dp}{dx}, \quad (10.7a)$$

and if the particles are electrons,

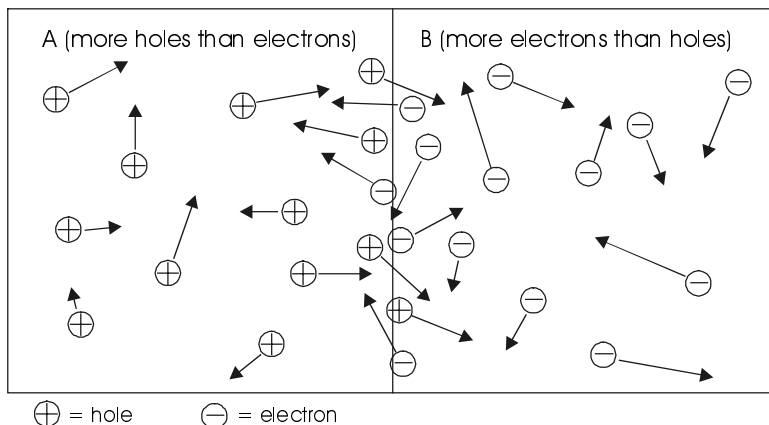


Figure 10.6 Random thermal motion and diffusion for electrons and holes.

$$J_n = qD_n \frac{dn}{dx} . \quad (10.7b)$$

In (10.7a) and (10.7b) the change in concentration with position is known as the concentration gradient and D_p and D_n are the hole diffusion constant and the electron diffusion constant, respectively. The minus sign in (10.7a) accounts for the fact that if the gradient is negative, the holes flow in the positive x-direction. The lack of the minus sign in (10.7b) accounts for the fact that if electrons flow in the positive x-direction, the associated current is in the negative x-direction. In each case, $q = 1.6 \times 10^{-19}$ coulomb.

At this point, all that is necessary is to make two additional observations. The first observation is that donor and acceptor atoms become donor and acceptor ions when they give up their electron or hole to the host material. These ions are fixed in position in the host by covalent bonds. The second observation is that in either n-type material or in p-type material, any point in the material will have charge neutrality. That is, the net charge present at any point is zero due to positive charges being neutralized by negative charges. However, when n-type and p-type materials are joined to form a pn junction, something special happens at the boundary.

Junction Formation and Built-In Potential

Although n-type and p-type materials are interesting and useful, the real fun starts when a junction is formed between n-type and p-type materials. The pn junction is treated in gory detail in most semiconductor device textbooks. Here, the need is to establish the foundation for the establishment of an electric field across a pn junction and to note the effect of this electric field on photo-generated EHPs.

Figure 10.7 shows a pn junction formed by placing p-type impurities on one side and n-type impurities on the other side. There are many ways to accomplish this structure. The most common is the diffused junction.

To form a diffused pn junction, the host material is grown with impurities, so it will be either n-type or p-type. The material is either grown or sliced into an appropriate thickness. Then the material is heated in the presence of the opposite impurity, which is usually in the form of a gas. This impurity will diffuse into the host material at a level that exceeds the host impurity level, but will only penetrate a small distance into the host material, depending on how long the host material is left at the elevated temperature. The result is a layer of material of one dominant impurity on top of the remainder of the material, which is doped with the other dominant impurity.

When the two materials are brought together, the first thing to happen is that the conduction electrons on the n-side of the junction notice the scarcity of conduction electrons on the p-side, and the valence holes on the p-side notice the scarcity of valence holes on the n-side. Since both types of charge carrier are undergoing random thermal motion, they begin to diffuse to the opposite side of

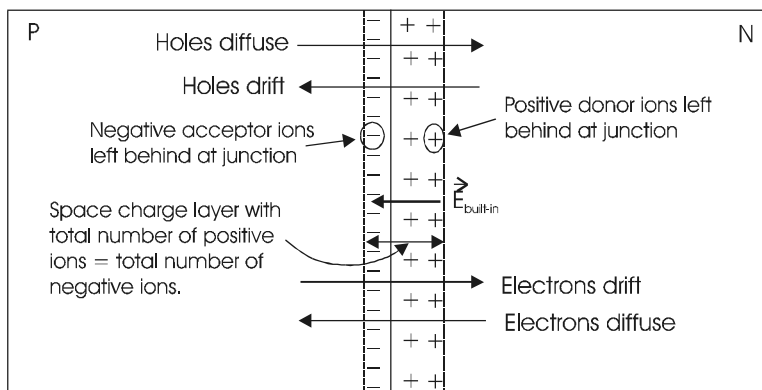


Figure 10.7 The pn junction showing electron and hole drift and diffusion.

the junction in search of the wide open spaces. The result is diffusion of electrons and holes across the junction, as indicated in Figure 10.7.

When an electron leaves the n-side for the p-side, however, it leaves behind a positive donor ion on the n-side, right at the junction. Similarly, when a hole leaves the p-side for the n-side, it leaves a negative acceptor ion on the p-side. If large numbers of holes and electrons travel across the junction, large numbers of fixed positive and negative ions are left at the junction boundaries. These fixed ions, as a result of Gauss' law, create an electric field that originates on the positive ions and terminates on the negative ions. Hence, the number of positive ions on the n-side of the junction must be equal to the number of negative ions on the p-side of the junction.

The electric field across the junction, of course, gives rise to a drift current in the direction of the electric field. This means that holes will travel in the direction of the electric field and electrons will travel opposite the direction of the field, as shown in Figure 10.7. Notice that for both the electrons and for the holes, the drift current component is opposite the diffusion current component. At this point, one can invoke Kirchhoff's current law to establish that the drift and diffusion components for each charge carrier must be equal and opposite, since there is no net current flow through the junction region. This phenomenon is known as the law of detailed balance.

By setting the sum of the electron diffusion current and the electron drift current equal to zero and recalling from electromagnetic field theory that

$$E = -\frac{dV}{dx}, \quad (10.8)$$

it is possible to solve for the potential difference across the junction in terms of the impurity concentrations on either side of the junction. Proceeding with this operation yields

$$-q\mu_n n \frac{dV}{dx} + qD_n \frac{dn}{dx} = 0, \quad (10.9a)$$

that can be rewritten as

$$dV = \frac{D_n}{\mu_n} \frac{dn}{n}. \quad (10.9b)$$

Finally, recognizing the Einstein relationship, $D_n/\mu_n = kT/q$, which is discussed in solid state physics textbooks, and integrating both sides from the n-side of the junction to the p-side of the junction, yields the magnitude of the built-in voltage across the junction to be

$$V_j = \frac{kT}{q} \ln \frac{n_{no}}{n_{po}}. \quad (10.10a)$$

It is now possible to express the built-in potential in terms of the impurity concentrations on either side of the junction by recognizing that $n_{no} \approx N_D$ and $n_{po} \approx (n_i)^2/N_A$. Substituting these values into (10.10a) yields, finally,

$$V_j = \frac{kT}{q} \ln \frac{N_A N_D}{n_i^2}. \quad (10.10b)$$

At this point, a word about the region containing the donor ions and acceptor ions is in order. Note first that outside this region, electron and hole concentrations remain at their thermal equilibrium values. Within the region, however, the concentration of electrons must change from the high value on the n-side to the low value on the p-side. Similarly, the hole concentration must change from the high value on the p-side to the low value on the n-side. Considering that the high values are really high, i.e., on the order of $10^{18}/\text{cm}^3$, while the low values are really low, i.e., on the order of $10^2/\text{cm}^3$, this means that within a short distance of the beginning of the ionized region, the concentration must drop to significantly below the equilibrium value. Because the concentrations of charge carriers in the ionized region are so low, this region is often termed the **depletion region**, in recognition of the depletion of mobile charge carriers in the region. Furthermore, because of the charge due to the ions in this region, the depletion region is also often referred to as the **space charge layer**. For the balance of this text, this region will simply be referred to as the junction.

The next step in the development of the behavior of the pn junction in the presence of sunlight is to let the sun shine in and see what happens.

The Illuminated pn Junction

Equation (10.3) governs the absorption of photons at or near a pn junction. Noting that an absorbed photon releases an EHP, it is now possible to explore what happens after the generation of the EHP. Those EHPs generated within the pn junction will be considered first, followed by the EHPs generated outside, but near, the junction.

If an EHP is generated within the junction, as shown in Figure 10.8 (points B and C), both charge carriers will be acted upon by the built-in electric field. Since the field is directed from the n-side of the junction to the p-side of the junction, the field will cause the electrons to be swept quickly toward the n-side and the holes to be swept quickly toward the p-side. Once out of the junction region, the optically generated carriers become a part of the majority carriers of the respective regions, with the result that excess concentrations of majority carriers appear at the edges of the junction. These excess majority carriers then diffuse away from the junction toward the external contacts, since the concentration of majority carriers has been enhanced only near the junction.

The addition of excess majority charge carriers to each side of the junction results in either a voltage between the external terminals of the material or a flow of current in the external circuit or both. If an external wire is connected between the n-side of the material and the p-side of the material, a current, I_p , will flow in the wire from the p-side to the n-side. This current will be proportional to the number of EHPs generated in the junction region.

If an EHP is generated outside the junction region, but close to the junction (with ‘close’ yet to be defined, but shown as point A in Figure 10.8), it is possible that, due to random thermal motion, either the electron, the hole, or both will end up moving into the junction region. Suppose, for example, that an EHP is generated in the n-region close to the junction. Then suppose the hole, which is the minority carrier in the n-region, manages to reach the junction before it recombines. If it can do this, it will be swept across the junction to the p-side and the net effect will be the same as if the EHP had been generated within the junction, since the electron is already on the n-side as a majority carrier. Similarly, if an EHP is generated within the p-region, but close to the junction, and if the minority carrier electron reaches the junction before recombining, it will be swept across to the n-side where it is a majority carrier. So what is meant by close?

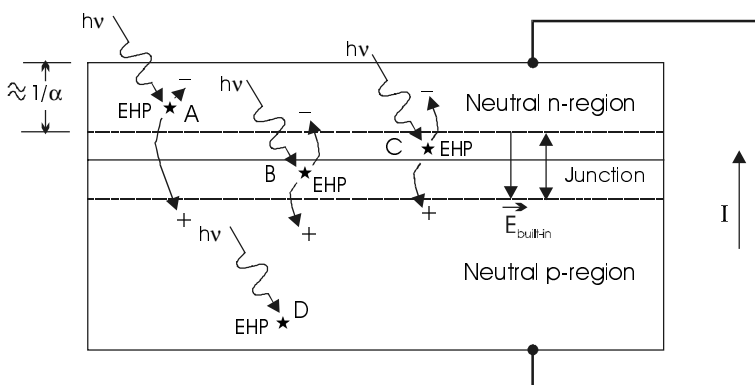


Figure 10.8 The illuminated pn junction showing desirable geometry and the creation of electron-hole pairs.

Clearly, the minority carriers of the optically generated EHPs outside the junction region must not recombine before they reach the junction. If they do, then, effectively, both carriers are lost from the conduction process, as in point D in Figure 10.8. Since the majority carrier is already on the correct side of the junction, the minority carrier must therefore reach the junction in less than a minority carrier lifetime, τ_n or τ_p .

To convert these times into distances, it is necessary to note that the carriers travel by diffusion once they are created. Since only the thermal velocity has been associated with diffusion, but since the thermal velocity is random in direction, it is necessary to introduce the concept of minority carrier diffusion length, which represents the distance, on the average, which a minority carrier will travel before it recombines. The diffusion length can be shown to be related to the minority carrier lifetime and diffusion constant by the formula

$$L_m = \sqrt{D_m \tau_m} , \quad (10.11)$$

where m has been introduced to represent n for electrons or p for holes. It can also be shown that on the average, if an EHP is generated within a minority carrier diffusion length of the junction, the associated minority carrier will reach the junction. In reality, some minority carriers generated closer than a diffusion length will recombine before reaching the junction, while some minority carriers generated farther than a diffusion length from the junction will reach the junction before recombining.

Hence, to maximize photocurrent, it is desirable to maximize the number of photons that will be absorbed either in the junction or within a minority carrier diffusion length of the junction. The minority carriers of the EHPs generated outside this region have a higher probability of recombining before they have a chance to diffuse to the junction. If a minority carrier from an optically generated EHP recombines before it crosses the junction and becomes a majority carrier, it, along with the opposite carrier with which it recombines, is no longer available for conduction. Furthermore, the combined width of the junction and the two diffusion lengths should be several multiples of the reciprocal of the absorption constant, α , and the junction should be relatively close to a diffusion length from the surface of the material upon which the photon impinges, to maximize collection of photons. Figure 10.8 shows this desirable geometry. The engineering design challenge then lies in maximizing α , as well as maximizing the junction width and minority carrier diffusion lengths.

The Externally Biased pn Junction

In order to complete the analysis of the theoretical performance of the pn junction operating as a photovoltaic cell, it is useful to look at the junction with external bias. Figure 10.9 shows a pn junction connected to an external battery with the internally generated electric field direction included. If (10.10a) is recalled, taking into account that the externally applied voltage, with the exception

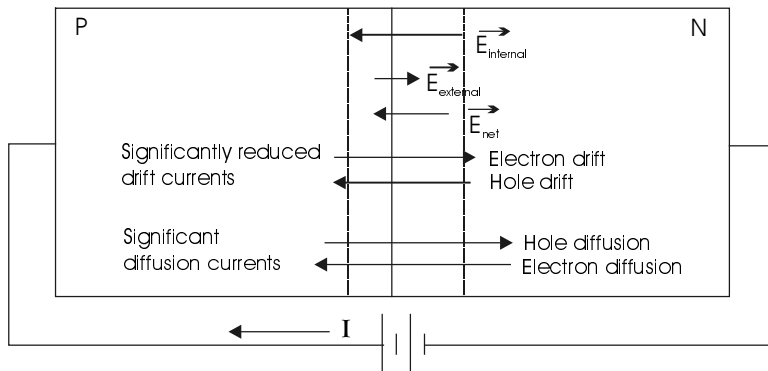


Figure 10.9 The pn junction with external bias.

of any voltage drop in the neutral regions of the material, will appear as opposing the junction voltage, the equation becomes

$$V_j - V = \frac{kT}{q} \ln \frac{n_n}{n_p}. \quad (10.12)$$

Note that the only difference between (10.12) and (10.10a) is that the electron concentrations on the n-side and on the p-side of the junction are no longer expressed as the thermal equilibrium values. This will be the case only when the externally applied voltage is zero. However, under conditions known as low injection levels, it will still be the case that the concentration of electrons on the n-side will remain close to the thermal equilibrium concentration. For this condition, (10.12) becomes

$$V_j - V = \frac{kT}{q} \ln \frac{N_d}{n_p}. \quad (10.13)$$

Since V_j can be calculated from (10.10b), the quantity of interest in (10.13) is n_p , the concentration of minority carriers at the edge of the junction on the p-side. Equation (10.13) can thus be solved for n_p with the result

$$n_p = N_D e^{-\frac{q(V_j-V)}{kT}} = N_D e^{\frac{-qV_j}{kT}} e^{\frac{qV}{kT}}. \quad (10.14)$$

Next, note that the thermal equilibrium value of the minority carrier concentration occurs when $V = 0$. If the excess minority carrier concentration is now defined as $n_p' = n_p - n_o$, and if n_o is subtracted from (10.13), the result is

$$n_p'(0) = n_p(0) - n_o(0) = N_D e^{\frac{-qV_j}{kT}} \left(e^{\frac{qV}{kT}} - 1 \right) = n_{po} \left(e^{\frac{qV}{kT}} - 1 \right). \quad (10.15)$$

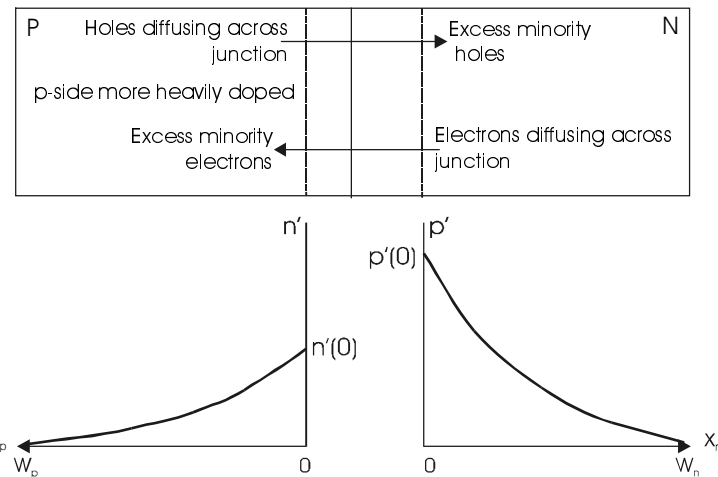


Figure 10.10 Excess minority carrier concentrations in neutral regions of pn junction device.

What happens to these excess minority carriers? They diffuse toward a region of lesser concentration, which happens to be away from the junction toward the contact, as shown in Figure 10.10.

If the contact is a few diffusion lengths away from the junction, it can be shown, by solving the well-known continuity equation, that the distribution of excess minority electrons between the junction and the contact will be

$$n'_p(x_p) = n'_p(0) \cosh \frac{x_p}{L_n} - n'_p(0) \operatorname{ctnh} \frac{w_p}{L_n} \sinh \frac{x_p}{L_n}. \quad (10.16)$$

A similar expression can be obtained for the concentration of excess minority holes in the neutral region of the n-side of the device. To obtain an expression for the total device current, (10.7) is used for each side of the device, noting that the gradient in the total carrier concentration is given by the gradient of the excess carrier concentration, since the spatial variation in the excess concentration will far exceed any spatial variation in the equilibrium concentration. Combining the results for electron and hole currents yields the total current in the device as it depends on the externally applied voltage along with the indicated device parameters. The result is, if A represents the cross-sectional area of the pn junction and adjoining regions,

$$I = I_n + I_p = qA \left(\frac{D_n n_{po}}{L_n} \operatorname{ctnh} \frac{w_p}{L_n} + \frac{D_p p_{no}}{L_p} \operatorname{ctnh} \frac{w_n}{L_p} \right) \left(e^{\frac{qV}{kT}} - 1 \right). \quad (10.17)$$

Equation (10.17) is, of course, the familiar diode equation that relates diode current to diode voltage. Note that the current indicated in (10.17) flows in the

direction opposite to the optically generated current described earlier. Letting $qA(\text{nasty expression}) = I_o$ and incorporating the photocurrent component into (10.17) finally yields the complete equation for the current in the PV cell to be

$$I = I_\ell - I_o \left(e^{\frac{qV}{kT}} - 1 \right). \quad (10.18)$$

Those readers who remember everything they read will recognize (10.18) to be the same as (3.1). Note that the current of (10.18) is directed out of the positive terminal of the device, so that when the current and voltage are both positive, the device is delivering power to the external circuit.

10.4 Maximizing PV Cell Performance

10.4.1 Introduction

Equation (10.18) indicates, albeit in a somewhat subtle manner, that to maximize the power output of a PV cell, it is desirable to maximize the open-circuit voltage, short-circuit current, and fill factor of a cell. Recalling the plot of (10.18) from Chapter 3, it should be evident that maximizing the open-circuit voltage and the short-circuit current will maximize the power output for an ideal cell characterized by (10.18). Real cells, of course, have some series resistance, so there will be power dissipated by this resistance, similar to the power loss in a conventional battery due to its internal resistance. In any case, recalling that the open-circuit voltage increases as the ratio of photo current to reverse saturation current increases, a desirable design criteria is to maximize this ratio, provided that it does not proportionally reduce the short-circuit current of the device.

Fortunately, this is not the case, since maximizing the short-circuit current requires maximizing the photocurrent. It is thus instructive to look closely at the parameters that determine both the reverse saturation current and the photocurrent. Techniques for lowering series resistance will then be discussed.

10.4.2 Minimizing the Reverse Saturation Current

Beginning with the reverse saturation current as expressed in (10.17), the first observation is that the equilibrium minority carrier concentrations at the edges of the pn junction are related to the intrinsic carrier concentration through (10.4). Hence,

$$p_{no} = \frac{n_i^2}{N_D} \quad \text{and} \quad n_{po} = \frac{n_i^2}{N_A}. \quad (10.19)$$

So far, no analytic expression for the intrinsic carrier concentration has been developed. Such an expression can be obtained by considering Fermi levels,

densities of states, and other quantities that are discussed in solid-state devices textbooks. Since the goal here is to determine how to minimize the reverse saturation current, and not to go into detail of quantum mechanical proofs, the result is noted here with the recommendation that the interested reader consult a good solid-state devices text for the development of the result. The result is

$$n_i^2 = 4 \left(\frac{2\pi kT}{h^2} \right)^3 \left(m_n^* m_p^* \right)^{\frac{3}{2}} e^{-\frac{E_g}{kT}}, \quad (10.20)$$

where m_n^* and m_p^* are the electron effective mass and hole effective mass in the host material and E_g is the bandgap energy of the host material. These effective masses can be greater than or less than the rest mass of the electron, depending on the degree of curvature of the valence and conduction bands when plotted as energy vs. momentum as in Figure 10.2. In fact, the effective mass can also depend on the band in which the carrier resides in a material. For more information on effective mass, the reader is encouraged to consult the references listed at the end of the chapter.

Now, using (10.11) with (10.19) and (10.20) in (10.17) the following final result for the reverse saturation current is obtained.

$$I_o = \left(4qA \left(\frac{2\pi kT}{h^2} \right) \left(m_n^* m_p^* \right)^{\frac{3}{2}} e^{-\frac{E_g}{kT}} \right) \times \left(\frac{1}{N_A} \sqrt{\frac{D_n}{\tau_n}} \operatorname{ctnh} \frac{\ell_p}{\sqrt{D_n \tau_n}} + \frac{1}{N_D} \sqrt{\frac{D_p}{\tau_p}} \operatorname{ctnh} \frac{\ell_n}{\sqrt{D_p \tau_p}} \right). \quad (10.21)$$

Since the design goal is to minimize I_o while still maximizing the ratio I_c/I_o , the next step is to express the photocurrent in some detail so the values of appropriate parameters can be considered in the design choices.

10.4.3 Optimizing Photocurrent

In Section 10.3.2, the photocurrent optimization process was discussed qualitatively. In this section the specific parameters that govern the absorption of light and the lifetime of the absorbed charge carriers will be discussed, and a formula for the photocurrent will be presented for comparison with the formula for reverse saturation current. In particular, minimizing reflection of the incident photons, maximizing the minority carrier diffusion lengths, maximizing the junction width and minimizing surface recombination velocity will be discussed. The PV cell designer will then know exactly what to do to make the perfect cell.

Minimizing Reflection of Incident Photons

The interface between air and the semiconductor surface constitutes an impedance mismatch, since the electrical conductivities and the dielectric constants of air and a PV cell are different. As a result, part of the incident wave must be reflected in order to meet the boundary conditions imposed by the solution of the wave equation on the electric field, E, and the electric displacement, D.

Those readers who are experts at electromagnetic field theory will recognize that this problem is readily solved by the use of a quarter-wave matching coating on the PV cell. If the coating on the cell has a dielectric constant equal to the geometric mean of the dielectric constants of the cell and of air and if the coating is one-quarter wavelength thick, it will act as an impedance-matching transformer and minimize reflections. Of course, the coating must be transparent to the incident light. This means that it needs to be an insulator with a bandgap that exceeds the energy of the shortest wavelength light to be absorbed by the PV cell. Alternatively, it needs some other property that minimizes the value of the absorption coefficient for the material, such as an indirect bandgap. Several of these coatings are listed in Table 10.2.

It is also important to realize that a quarter wavelength is on the order of 0.1 μm . This is extremely thin, and may pose a problem for spreading a uniform coating of this thickness. And, of course, since it is desirable to absorb a range of wavelengths, the antireflective coating will be optimized at only a single wavelength. Despite these problems, coatings have been developed that meet the requirements quite well.

Table 10.2 Some antireflective coatings useful in PV cell production [3].

Material	Index of Refraction
Al_2O_3	1.77
Glasses	1.5 –1.7
MgO	1.74
SiO	1.5 –1.6
SiO_2	1.46
Ta_2O_5	2.2
TiO_2	2.5 –2.6

(Adapted from Hu, C. et al., *Solar Cells From Basic to Advanced Systems*, McGraw-Hill, 1983.
Reproduced with permission of the McGraw-Hill Companies.)

An alternative to antireflective coatings now commonly in use with Si PV cells is to manufacture the cells with a textured front surface, as shown in Figure 10.14. Textured front and back surfaces and their contribution to the capture of photons will be discussed later in this section in conjunction with Figure 10.14. The bottom line is that a textured surface acts to enhance the capture of photons and also acts to prevent the escape of captured photons before they can produce EHPs. Furthermore, the textured surface is not wavelength dependent as is the antireflective coating.

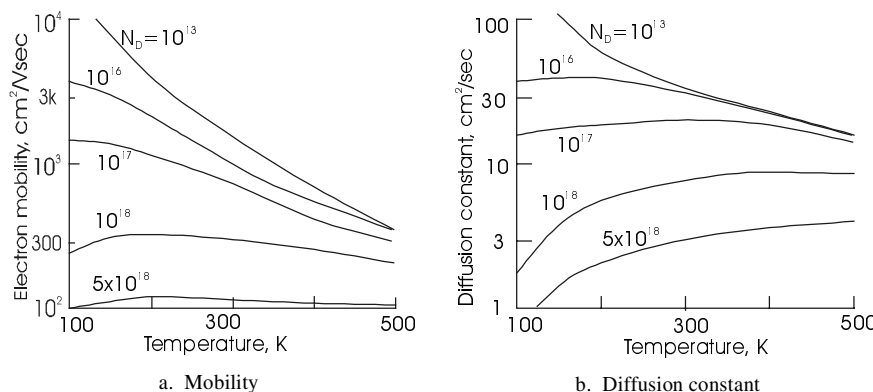


Figure 10.11 Temperature and impurity dependence of electron mobility and diffusion constant in silicon.

Maximizing Minority Carrier Diffusion Lengths

Since the diffusion lengths are given by (10.11), it is necessary to explore the factors that determine the diffusion constants and minority carrier lifetimes in different materials. It needs to be recognized that changing a diffusion constant may affect the minority carrier lifetime, so the product needs to be maximized.

Diffusion constants depend on scattering of carriers by host atoms as well as by impurity atoms. The scattering process is both material dependent and temperature dependent. In a material at a low temperature with a well-defined crystal structure, scattering of charge carriers is relatively minimal, so they tend to have high mobilities. Figure 10.11a illustrates the experimentally determined dependence of the electron mobility on temperature and on impurity concentration in Si. The Einstein relationship shows that the diffusion constant is proportional to the product of mobility and temperature. This relationship is shown in Figure 10.11b. So, once again, there is a trade-off. While increasing impurity concentrations in the host material *increases* the built-in junction potential, increasing impurity concentrations *decreases* the carrier diffusion constants.

The material of Figure 10.11 is single crystal material. In polycrystalline or amorphous material, the lack of crystal lattice symmetry has a significant effect on the mobility and diffusion constant, causing significant reduction in these quantities. However, if the absorption constant can be made large enough for these materials, the corresponding decrease in diffusion length may be compensated for by the increased absorption rate.

When an electron and a hole recombine, certain energy and momentum balances must be achieved. Locations in the host material that provide for optimal recombination conditions are known as recombination centers. Hence, the minority carrier lifetime is determined by the density of recombination centers in the host material.

One type of recombination center is a crystal defect, so that as the number of crystal defects increases, the number of recombination centers increases. This

means that crystal defects reduce the diffusion constant as well as the minority carrier lifetime in a material.

Impurities also generally make good recombination centers, especially those impurities with energies near the center of the bandgap. These impurities are thus different from the donor and acceptor impurities that are purposefully used in the host material, since donor impurities have energies relatively close to the conduction band and acceptor impurities have energies relatively close to the valence band.

Minority carrier lifetimes also depend on the concentration of charge carriers in the material. An approximation of the dependence of electron minority carrier lifetime on carrier concentration and location of the trapping energy within the energy gap is given by

$$\tau_n = \frac{n \left[n + p + 2n_i \cosh \frac{E_t - E_i}{kT} \right]}{CN_t(np - n_i^2)}, \quad (10.22a)$$

where C is the capture cross section of the impurity in cm^3/sec , N_t is the density of trapping centers and E_t and E_i are the energies of the trapping center and the intrinsic Fermi level. In most materials, the intrinsic Fermi level is very close to the center of the bandgap. Under most illumination conditions, the hyperbolic term will be negligible compared to the majority carrier concentration and the excess electron concentration as minority carriers in p-type material will be much larger than the electron thermal equilibrium concentration. Under these conditions, for minority electrons in p-type material, (10.22a) reduces to

$$\tau_n \approx \frac{1}{CN_t}. \quad (10.22b)$$

Hence, to maximize the minority carrier lifetime, it is necessary to minimize the concentration of trapping centers and to be sure that any existing trapping centers have minimal capture cross sections.

Maximizing Junction Width

Since it has been determined that it is desirable to absorb photons within the confines of the pn junction, it is desirable to maximize the width of the junction. It is therefore necessary to explore the parameters that govern the junction width. Perhaps the reader recalls similar discussions in a previous electronics class.

An expression for the width of a pn junction can be obtained by solving Gauss' law at the junction, since the junction is a region that contains electric charge. Solution of Gauss' law, of course, is dependent upon the ability to express the spatial distribution of the space charge in mathematical, or, at least, in graphical form. Depending on the process used to form the junction, the impurity profile across the junction can be approximated by different expressions. Junctions formed by epitaxial growth or by ion implantation can be controlled to

have impurity profiles to meet the discretion of the operator. Junctions grown by diffusion can be reasonably approximated by a linearly graded model. The interested reader is encouraged to consult a reference on semiconductor devices for detailed information on the production of various junction impurity profiles.

The junction with uniform concentrations of impurities is convenient to use to obtain a feeling for how to maximize the width of a junction. Solution of Gauss' law for a junction with uniform concentration of donors on one side and a uniform concentration of acceptors on the other side yields solutions for the width of the space charge layer on each side of the junction. The total junction width is then simply the sum of the widths of the two sides of the space charge layer. The results for each side are

$$W_n = \left[\frac{2\epsilon N_A}{qN_D(N_A + N_D)} \right]^{\frac{1}{2}} (V_j - V)^{\frac{1}{2}} \quad (10.23a)$$

and

$$W_p = \left[\frac{2\epsilon N_D}{qN_A(N_D + N_A)} \right]^{\frac{1}{2}} (V_j - V)^{\frac{1}{2}}. \quad (10.23b)$$

Before combining these two results, it is interesting to note that the width of the junction on either the p-side or on the n-side depends on the ratio of the impurity concentrations on each side. Again, since Gauss' law requires equal numbers of charges on each side of the junction, the side with the smaller impurity concentration will need to have a wider space charge layer to produce enough impurity ions to balance out the impurity ions on the other side. The overall width of the junction can now be determined by summing equations (10.23a) and (10.23b) to get

$$W = \left[\frac{2\epsilon(N_D + N_A)}{qN_A N_D} \right]^{\frac{1}{2}} (V_j - V)^{\frac{1}{2}}. \quad (10.24)$$

At this point, it should be recognized that the voltage across the junction due to the external voltage across the cell, V , will never exceed the built-in voltage, V_j . The reason is that, as the externally applied voltage becomes more positive, the cell current increases exponentially and causes voltage drops in the neutral regions of the cell, so only a fraction of the externally applied voltage actually appears across the junction. Hence, there is no need to worry about the junction width becoming zero or imaginary. In the case of photovoltaic operation, the external cell voltage will hopefully be at the maximum power point, which is generally between 0.5 V and 0.6 V for silicon.

Next, observe that, as the external cell voltage increases, the width of the junction decreases. As a result, the absorption of photons decreases. This sug-

gests that it would be desirable to design the cell to have the largest possible built-in potential to minimize the effect of increasing the externally applied voltage. This involves an interesting trade-off, since the built-in junction voltage is logarithmically dependent on the product of the donor and acceptor concentrations (see 10.10b), and the junction width is inversely proportional to the square root of the product of the two quantities. Combining (10.10b) and (10.24) results in

$$W = \left[\frac{2\epsilon(N_D + N_A)}{qN_D N_A} \right]^{\frac{1}{2}} \left(\frac{kT}{q} \ln \frac{N_A N_D}{n_i^2} - V \right)^{\frac{1}{2}}. \quad (10.25)$$

Note now that maximizing W is achieved by making either $N_A \gg N_D$ or by making $N_D \gg N_A$. For example, if $N_A \gg N_D$, then (10.25) simplifies to

$$W = \left[\frac{2\epsilon}{qN_D} \right]^{\frac{1}{2}} \left(\frac{kT}{q} \ln \frac{N_A N_D}{n_i^2} - V \right)^{\frac{1}{2}}, \quad (10.26a)$$

or, if $N_D \gg N_A$, then

$$W = \left[\frac{2\epsilon}{qN_A} \right]^{\frac{1}{2}} \left(\frac{kT}{q} \ln \frac{N_A N_D}{n_i^2} - V \right)^{\frac{1}{2}}. \quad (10.26b)$$

Another way to increase the width of the junction is to include a layer of intrinsic material between the p-side and the n-side as shown in Figure 10.12. In this **pin** junction, there are no impurities to ionize in the intrinsic material, but the ionization still takes place at the edges of the n-type and the p-type material. As a result, there is still a strong electric field across the junction and there is still a built-in potential across the junction. Since the intrinsic region could conceivably be of any width, it is necessary to determine the limits on the width of the intrinsic region.

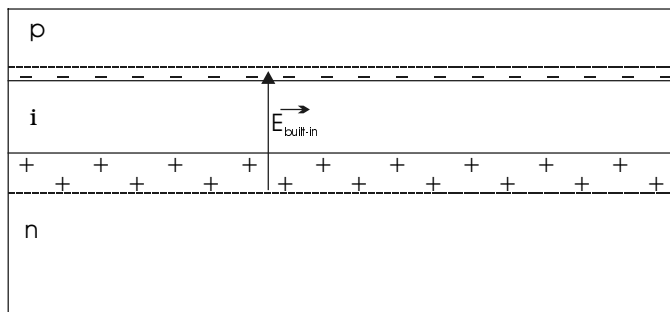


Figure 10.12 The pin junction.

The only feature of the intrinsic region that degrades performance is the fact that it has a width. If it has a width, then it takes time for a charge carrier to traverse this width. If it takes time, then there is a chance that the carrier will recombine. Thus, the width of the intrinsic layer simply needs to be kept short enough to minimize recombination. The particles travel through the intrinsic region with a relatively high drift velocity due to the built-in electric field at the junction. Since the thermal velocities of the carriers still exceed the drift velocities by several orders of magnitude, the width of the intrinsic layer needs to be kept on the order of about one diffusion length.

Minimizing Surface Recombination Velocity

If an EHP is generated near a surface, it becomes more probable that the minority carrier will diffuse to the surface. Since photocurrent depends on minority carriers' diffusing to the junction and ultimately across the junction, surface recombination of minority carriers before they can travel to the junction reduces the available photocurrent. When the surface is within a minority carrier diffusion length of the junction, which is often desirable to ensure that generation of EHPs is maximized near the junction, minority carrier surface recombination can significantly reduce the efficiency of the cell.

Surface recombination depends on the density of excess minority carriers, in this case, as generated by photon absorption, and on the average recombination center density per unit area, N_{sr} , on the surface. The density of recombination centers is very high at contacts and is also high at surfaces in general, since the crystal structure is interrupted at the surface. Imperfections at the surface, whether due to impurities or to crystal defects, all act as recombination centers.

The recombination rate, U , is expressed as number/cm²/sec and is given by

$$U = cN_{sr}m', \quad (10.27)$$

where m' is used to represent the excess minority carrier concentration, whether electrons or holes, and c is a constant that incorporates the lifetime of a minority carrier at a recombination center. Analysis of the dimensions of the parameters in (10.27) shows that the units of cN_{sr} are cm/sec. This product is called the **surface recombination velocity**, S . The total number of excess minority carriers recombining per unit time and subsequent loss of potential photocurrent, is thus dependent on the density of recombination centers at the surface and on the area of the surface. Minimizing surface recombination thus may involve reducing the density of recombination centers or reducing the density of minority carriers at the surface.

If the surface is completely covered by a contact, then little can be done to reduce surface recombination if minority carriers reach the surface, since recombination rates at contacts are very high. However, if the surface is not completely covered by a contact, such as at the front surface, then a number of techniques have been discovered that will result in passivation of the surface. Silicon

oxide and silicon nitrogen passivation are two methods that are used to passivate silicon surfaces.

Another method of reducing surface recombination is to passivate the surface and then only allow the back contact to contact the cell over a fraction of the total cell area. While this tends to increase series resistance to the contact, if the cell material near the contact is doped more heavily, the ohmic resistance of the material is decreased and the benefit of reduced surface recombination offsets the cost of somewhat higher series resistance. Furthermore, an E-field is created that attracts majority carriers to the contact and repels minority carriers. This concept will be explored in more detail in Section 10.5.2.

A Final Expression for the Photocurrent

An interesting exercise is to calculate the maximum obtainable efficiency of a given PV cell. Equation (10.3) indicates the general expression for photon absorption. Since the absorption coefficient is wavelength dependent, the general formula for overall absorption must take this dependence into account. The challenge in design of the PV cell and selection of appropriate host material is to avoid absorption before the photon is close enough to the junction, but to ensure absorption when the photon is within a minority carrier diffusion length of either side of the junction. Figure 10.13 shows a typical photon absorption profile for the n-region and the p-region of a cell with the p-region at the surface.

Since direct bandgap materials tend to have larger absorption constants than indirect materials such as Si, it is relatively straightforward to capture photons in these materials. In Si, however, several clever design practices are used to increase absorption. Since some photons will travel completely across the cell to the back of the cell without being absorbed, if the back of the cell is a good reflector, the photons will be reflected back toward the junction. This is easy to do, since the back contact of the Si cell covers the entire back of the cell. How-

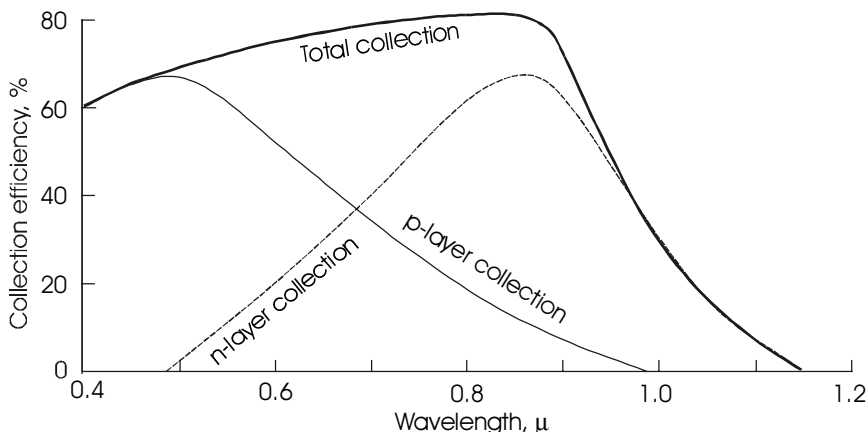


Figure 10.13 Photon collection efficiency vs. wavelength and location in cell for a typical PV cell with p-layer at the surface [1]. (Adapted from Yang, E. S., *Microelectronic Devices*, 1988, McGraw-Hill. Reproduced with permission of the McGraw-Hill Companies.)

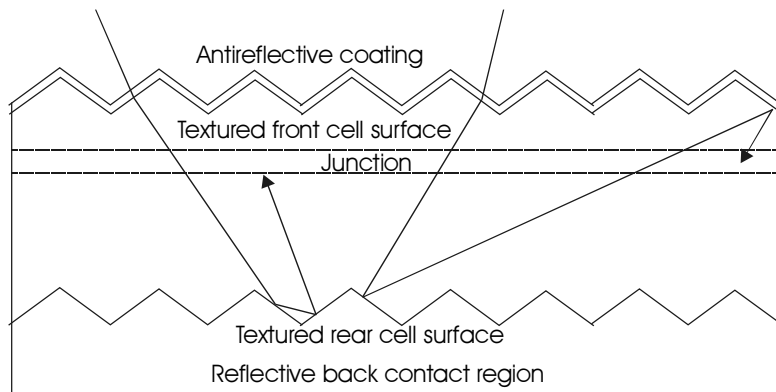


Figure 10.14 Maximizing photon capture with textured surfaces.

ever, rather than having a smooth back surface that will reflect photons perpendicular to the surface, the back surface is textured so the incident photons will be scattered at angles, thus increasing the path length.

The front of the cell, however, can be covered with an antireflective coating to maximize transmission of photons into the material. Hence, a similar scheme is necessary to keep the photons in the material if, after bouncing off the back surface, they are still not absorbed. Once again, a textured surface will enhance the probability that a photon will undergo internal reflection, since the dielectric coefficient, and, hence, the index of refraction of the host material, is greater than that of the antireflective coating. This is analogous to when ripples on water prevent a person below the surface from seeing anything above the surface. When the surface is smooth, it is possible to see objects above the water, provided that the angle of view is sufficiently close to the perpendicular. Figure 10.14 shows a cell with textured front and back surfaces and the effect on the travel of photons that enter the host material.

The foregoing discussion can be quantified in terms of cell parameters in the development of an expression for the photocurrent. Considering a monochromatic photon flux incident on the p-side of a p⁺n junction (the + indicates strongly doped), the following expression for the hole component of the photocurrent can be obtained. The expression is obtained from the solution of the diffusion equation in the neutral region on the n-side of the junction for the diffusion of the photon-created minority holes to the back contact of the cell.

$$\Delta I_{\text{hp}} = \frac{qAF_{\text{ph}}\alpha L_p}{\alpha^2 L_p^2 - 1} \left[\frac{S \cosh \frac{w_n}{L_p} + \frac{D_p}{L_p} \sinh \frac{w_n}{L_p} + (\alpha D_p - \frac{1}{2}) e^{-\alpha w_n}}{S \sinh \frac{w_n}{L_p} + \frac{D_p}{L_p} \cosh \frac{w_n}{L_p}} - \alpha L_p \right]. \quad (10.28)$$

It is assumed that the cell has a relatively thin p-side and that the n-side has a width, w_n . In (10.28), F_{ph} represents the number of photons per cm^2 per second per unit wavelength incident on the cell. The effect of the surface recombination velocity on the reduction of photocurrent is more or less clearly demonstrated by (10.28). The mathematical whiz will immediately be able to determine that small values of S maximize the photocurrent, and large values reduce the photocurrent, while one with average math skills may need to plug in some numbers.

Equation (10.28) is thus maximized when α and L_p are maximized and S is minimized. The upper limit of the expression then becomes

$$\Delta I_{\ell p} = -qAF_{ph}, \quad (10.29)$$

indicating that all photons have been absorbed and all have contributed to the photocurrent of the cell.

Since sunlight is not monochromatic, (10.28) must be integrated over the incident photon spectrum, noting all wavelength-dependent quantities, to obtain the total hole current. An expression must then be developed for the electron component of the current and integrated over the spectrum to yield the total photocurrent as the sum of the hole and electron currents. This mathematical challenge is clearly a member of the nontrivial set of math exercises and is not included as a homework problem. Yet, some have persisted at a solution to the problem and have determined the maximum efficiencies that can be expected for cells of various materials. Table 10.3 shows the theoretical optimum efficiencies for several different PV materials.

Table 10.3 Theoretical conversion efficiency limits for several PV materials at 25°C. [4, 5]

Material	E_g	η_{max}
Ge	0.6	13%
CIS	1.0	24%
Si	1.1	27%
InP	1.2	24.5%
GaAs	1.4	26.5%
CdTe	1.48	27.5%
AlSb	1.55	28%
a-Si:H	1.65	27%
CdS	2.42	18%

10.4.4 Minimizing Cell Resistance Losses

Any voltage drop in the regions between the junction and the contacts of a PV cell will result in ohmic power losses. In addition, surface effects at the cell edges may result in shunt resistance between the contacts. It is thus desirable to keep any such losses to a minimum by keeping the series resistance of the cell at a minimum and the shunt resistance at a maximum. With the exception of the cell front contacts, the procedure is relatively straightforward.

Most cells are designed with the front layer relatively thin and highly doped, so the conductivity of the layer is relatively high. The back layer, however, is generally more lightly doped in order to increase the junction width and to allow for longer minority carrier diffusion length to increase photon absorption. There must therefore be careful consideration of the thickness of this region in order to maximize the performance of these competing processes.

If the back contact material is allowed to diffuse into the cell, the impurity concentration can be increased at the back side of the cell, as illustrated in Figure 10.15. This is important for relatively thick cells, commonly fabricated by slicing single crystals into wafers. The contact material must produce either n-type or p-type material if it diffuses into the material, depending on whether the back of the cell is n-type or p-type.

In addition to reducing the ohmic resistance by increasing the impurity concentration, the region near the contact with increased impurity concentration produces an additional electric field that increases the carrier velocity, thus producing a further equivalent reduction in resistance. The electric field is produced in a manner similar to the electric field that is produced at the junction.

For example, if the back material is p-type, holes from the more heavily doped region near the contact diffuse toward the junction, leaving behind negative acceptor ions. Although there is no source of positive ions in the p-region, the holes that diffuse away from the contact create an accumulated positive charge that is distributed through the more weakly doped region. The electric field, of course, causes a hole drift current, which, in thermal equilibrium, balances the hole diffusion current. When the excess holes generated by the photo-absorption process reach the region of the electric field near the contact, however, they are swept more quickly toward the contact. This effect can be viewed as the equivalent of moving the contact closer to the junction, which, in turn, has the ultimate effect of increasing the gradient of excess carriers at the edge of the junction. This increase in gradient increases the diffusion current of holes away

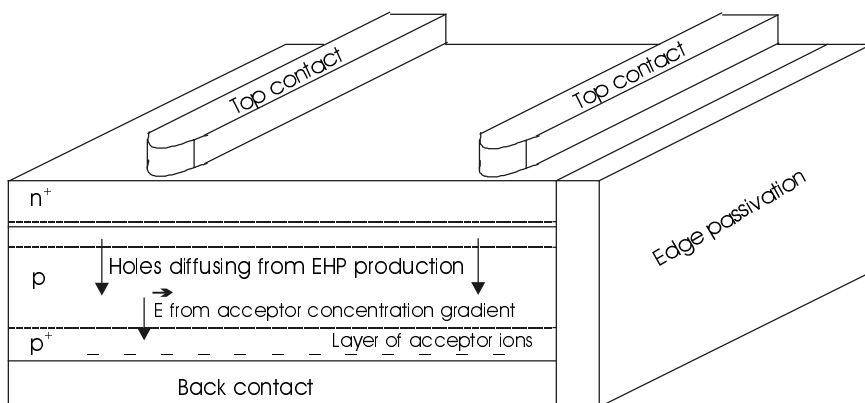


Figure 10.15 PV cell geometry for minimizing losses from cell series and shunt resistance..

from the junction. Since this diffusion current strongly dominates the total current, the total current across the junction is thus increased by the heavily doped layer near the back contact.

At the front contact, another balancing act is needed. Ideally, the front contact should cover the entire front surface. The problem with this, however, is that if the front contact is not transparent to the incident photons, it will reflect them away. In most cases, the front contact is reflecting. Since the front/top layer of the cell is generally very thin, even though it may be heavily doped, the resistance in the transverse direction will be relatively high because of the thin layer. This means that if the contact is placed at the edge of the cell to enable maximum photon absorption, the resistance along the surface to the contact will be relatively large.

The compromise, then, is to create a contact that covers the front surface with many tiny fingers, as shown in Figure 10.15. This network of tiny fingers, which, in turn, are connected to larger and larger fingers, is similar to the configuration of the capillaries that feed veins in a circulatory system. The idea is to maintain more or less constant current density in the contact fingers, so that as more current is collected, the cross-sectional area of the contact must be increased. This subject is covered in more detail in the next chapter.

Finally, shunt resistance is maximized by ensuring that no leakage occurs at the perimeter of the cell. This can be done by nitrogen passivation or simply by coating the edge of the cell with insulating material to prevent contaminants from providing a current path across the junction at the edges.

10.5 Exotic Junctions

10.5.1 Introduction

Thus far, only relatively simple junctions have been considered. PV cell performance can be enhanced significantly by incorporating a variety of more sophisticated junctions, including, but not necessarily limited to: graded junctions, heterojunctions, Schottky junctions, multijunctions and tunnel junctions. This section provides an introduction to these junctions so the reader will better understand the various junction types in the specific devices to be presented in the next chapter.

10.5.2 Graded Junctions

All the formulations to this point have related to the abrupt junction, in which the impurity concentration is constant to the junction and then abruptly changes to the opposite impurity concentration. While these junctions do exist, graded junctions are more common in materials for which the junction is fabricated by diffusion of impurities from the surface. The fabrication process for obtaining a linearly graded impurity profile as shown in Figure 10.16 will be discussed in some detail in the next chapter.

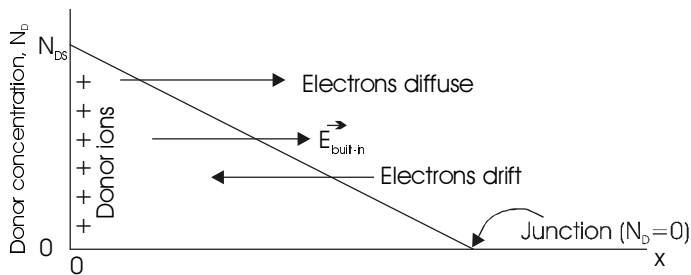


Figure 10.16 Diffusion and drift directions and electric field resulting from linearly decreasing impurity profile.

The significance of the graded junction is that majority carrier transport beyond the junction is improved by an additional electric field component resulting from the decreasing impurity concentration from surface to junction, as shown in Figure 10.16. The origin of this electric field component is the same as the origin of the additional field near the back contact when the back metallization is allowed to diffuse into the back of the cell. Each impurity atom donates either an electron or a hole and becomes ionized. If there is a gradient in impurity concentration, then the mobile carriers will diffuse in the direction of the gradient, leaving behind fixed impurity ions that serve either as the origin or termination of electric field lines.

An expression for the electric field in terms of the impurity concentration can be obtained by equating the diffusion current to the resulting drift current needed to balance the net current to zero when no external circuit is available for current flow. Assuming the majority carriers to be electrons in a heavily doped surface region, setting the sum of electron drift and diffusion current to zero results in

$$q\mu_n nE + qD_n \frac{dn}{dx} = 0, \quad (10.30)$$

which can be solved for E with the result

$$E = -\frac{D_n}{\mu_n} \frac{1}{n} \frac{dn}{dx} = -\frac{kT}{q} \frac{1}{N_D} \frac{dN_D}{dx}. \quad (10.31)$$

This additional E-field provides a drift component to the electron flow away from the junction toward the contact that effectively increases the velocity of the electrons toward the contact, resulting in lower resistive losses in the electron transport process toward the contact. Problem 10.7 provides an opportunity for calculation of the E-field present if the impurity concentration decreases linearly from surface to junction.

10.5.3 Heterojunctions

One of the problems identified with the optical absorption process is the absorption of higher energy photons close to the surface of the cell. Most of the EHPs generated by these higher energy photons are lost to recombination when they are created more than a diffusion length from the junction.

This phenomenon can be mitigated to some extent by the use of a heterojunction. A heterojunction is simply a composite junction comprised of two materials with closely matched crystal lattices, so the bandgap near the surface of the material is greater than the bandgap near the junction. The higher bandgap region will appear transparent to photons with lower energies, so these photons can penetrate to the junction region where the bandgap is less than the incident photon energy. In the region of the junction, they can generate EHPs that will be collected before they recombine.

Heterojunctions are sometimes made between two n-regions or two p-regions as well as between n-region and p-region. The behavior of the heterojunction is dependent upon the crystal lattices, work functions, impurity doping profiles and energy band properties of each semiconductor material, to the extent that discussion of any particular junction would probably not be applicable to a different junction. Readers interested in specific junctions, such as Ge:GaAs or Al-GaAs:GaAs, will be able to obtain more information from journal and conference publications.

In some cases, materials cannot be made either n-type or p-type. Use of a heterojunction with a material that can be made to complete a pn junction is another important use of heterojunctions. For example, p-type CdS is yet to be produced. But a thin n-type CdS layer on top of a CIS structure will produce a pn junction effect, so CdS is often used as a part of a thin film structure to produce a thin, heavily doped n-region near the front surface of the cell.

10.5.4 Schottky Junctions

Sometimes, when a metal is contacted with semiconductor material, an ohmic contact is formed and sometimes a rectifying contact is formed. It all depends on the relative positions of the work functions of the two materials. Figure 10.17 shows situations where the work function of the metal, $q\phi_m$, is greater than that of the n-type semiconductor, $q\phi_s$, and where the work function of the metal is less than that of the n-type semiconductor material. The work function is simply the energy difference between the Fermi level and the vacuum level and the Fermi level is that energy where the probability of occupancy by a mobile carrier is 0.5. For the semiconductor, the energy difference between the bottom of the conduction band and the vacuum level is designated as $q\psi_s$.

When the metal and semiconductor are joined, electrons flow either from metal to semiconductor or from semiconductor to metal, depending on which has the higher Fermi level. In the case where $q\phi_s < q\phi_m$, as indicated in Figure 10.17a, electrons will flow from semiconductor to metal in a manner similar to

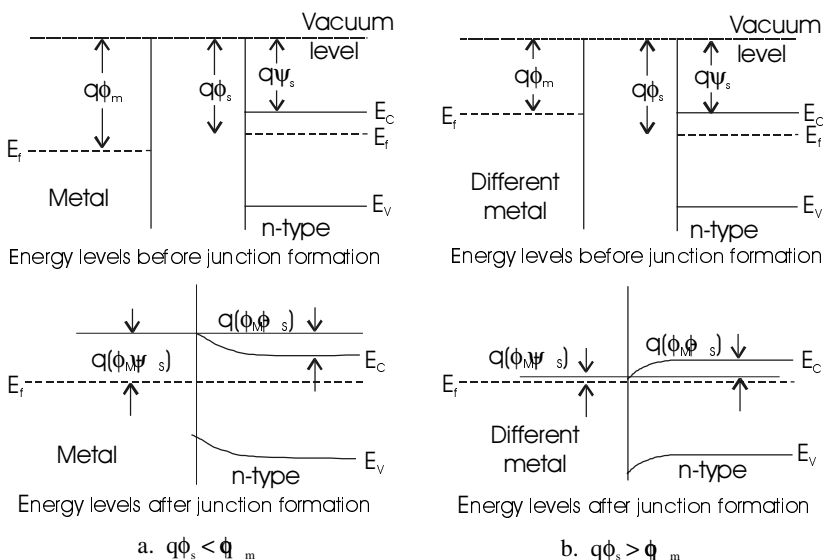


Figure 10.17 Energy levels in metal semiconductor junctions.

diffusion across a pn junction from n-type to p-type. As the electrons leave, they leave behind positive donor ions, just as in the pn junction. Since the materials are in contact, at the point of contact the probability of electron occupancy must be the same for each material, which requires the Fermi levels of each material to align. Since the semiconductor surface in contact with the metal is depleted of electrons, the Fermi level must move farther away from the conduction band, because, as the Fermi level moves closer to the conduction band, more electrons will appear in the conduction band and vice versa.

The donor ions on the n-side of the contact thus become the origin of an electric field directed from the semiconductor to the metal. This field causes a drift of electrons from metal to semiconductor to balance the diffusion from semiconductor to metal. Note that holes cannot diffuse from metal to semiconductor, since the metal supports only electrons. Thus, the built-in potential is only about half what it might be if holes could also diffuse across the junction.

In Figure 10.17b, where $q\phi_s > q\phi_m$, the electrons diffuse from the metal to the semiconductor, thus increasing the concentration of electrons on the semiconductor side of the junction. This diffusion, in effect, causes the equivalent of heavier doping of the n-type semiconductor and enables current to flow easily in either direction across the junction. This is therefore an ohmic junction, whereas the junction of Figure 10.17a is a rectifying junction. External contacts to a PV cell need to be ohmic to prevent unnecessary voltage drop at the contact, whereas the rectifying contacts are useful for other purposes.

For the rectifying junction, a positive external voltage from metal to semiconductor reduces the built-in field, enabling the electrons that have diffused to the metal to continue flowing in the external circuit, as shown in Figure 10.18a.

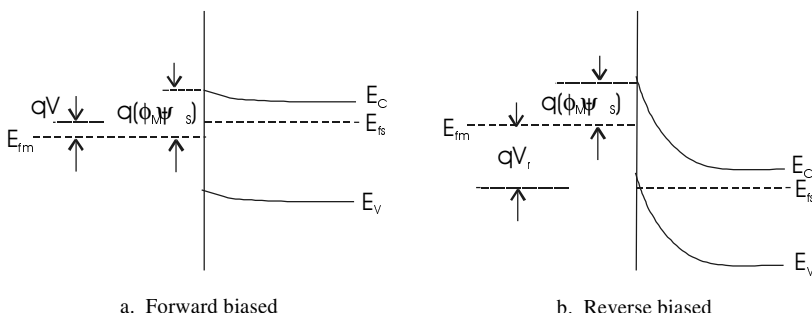


Figure 10.18 The rectifying metal-n-type semiconductor junction under forward biased and reverse biased conditions.

Note that as the Fermi level on the semiconductor side is drawn closer to the conduction band, more electrons can diffuse to the metal, resulting in significant current flow from metal to semiconductor. The reduced built-in field reduces drift components in the opposite direction in a manner similar to the forward bias condition of a conventional pn junction.

When the external voltage is negative, the built-in field is as shown in Figure 10.18b. Although this might be expected to result in significant electron flow from metal to semiconductor, this does not occur, since the metal electrons must overcome the barrier between the metal Fermi level and the semiconductor conduction band. Only a few of the metal electrons are sufficiently energetic to do so, so the result is a relatively small reverse saturation current, and thus a rectifying contact. The contact is rectifying even though the relatively strong E-field in the semiconductor region would be capable of enhancing drift current if replacement mobile charges were available.

For PV action, photons need to generate EHPs on the semiconductor side of the junction within a minority carrier diffusion length of the junction, so the minority carrier can be swept out of the region to the other side of the junction by the built-in field.

It has been shown that, if the semiconductor material is n-type and $q\phi_m < q\phi_s$, the junction becomes ohmic, with bidirectional current conduction. When the semiconductor is p-type, the opposite is true. That is, for $q\phi_m > q\phi_s$, the contact is ohmic and for $q\phi_m < q\phi_s$, the contact is rectifying.

These conditions must thus be met when ohmic contacts are to be made to semiconductor materials. This is why certain metals such as Mo, Al and Au are acceptable for ohmic contacts on some materials but not on others.

The Schottky barrier junction is relatively straightforward to fabricate, but is not very efficient as a PV cell since it has a relatively smaller open-circuit voltage than a conventional pn junction due to diffusion currents flowing in only one direction across the junction. On the other hand, the lower voltage drop across the junction when it is conducting results in lower power dissipation, making the Schottky diode convenient for use as a blocking diode.

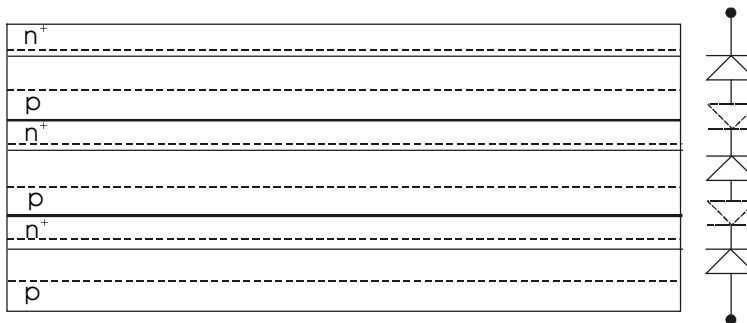


Figure 10.19 Three junctions in tandem (series), showing opposing pn junctions.

10.5.5 Multijunctions

Since photon energy is most efficiently absorbed when it is near the bandgap, a clever way to absorb more photons is to stack junctions of different bandgaps. By starting near the front surface with a relatively larger bandgap material, the higher energy photons can be absorbed relatively efficiently at this junction. Then a smaller bandgap junction, perhaps followed by an even smaller bandgap junction, will enable lower energy photons to be absorbed more efficiently. Since the junctions are in series, they must produce equal currents.

Figure 10.19 shows three junctions in series, each of somewhat different material in order to achieve three different bandgaps. The illustration may seem very logical, but there is a bit of a problem that is encountered when more than one junction is connected in series. That is simply the fact that, although the p-to-n direction of the first junction may be forward biased, this makes the n-to-p junction between the first and second pn junctions become reverse biased. The reverse bias across these junctions causes unnecessary voltage drop equivalent to the drop across blocking diodes inserted in strings of PV modules. Hence, a means must be devised to eliminate the effect of these reverse-biased junctions. Fortunately the tunnel junction can eliminate this problem.

10.5.6 Tunnel Junctions

Tunnel junctions take advantage of the Heisenberg uncertainty principle, i.e.,

$$\Delta p \Delta x \geq \hbar , \quad (10.32)$$

where Δp and Δx are, respectively, the uncertainty in particle position and the uncertainty in particle momentum, and \hbar is Planck's constant divided by 2π . In a tunnel junction, the junction width is so extremely narrow, that with relatively small uncertainty in particle momentum, it cannot be specified with certainty that the particle is on one side or the other side of the junction. This phenomenon is

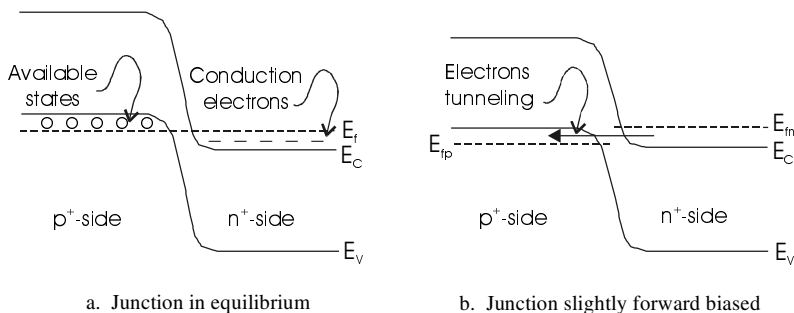


Figure 10.20 Tunnel junction showing conditions necessary for tunneling.

known as quantum-mechanical tunneling. The process takes place without any change in energy, since the particle essentially tunnels through the potential barrier produced by the tunnel junction. Noting (10.24), it is evident that if impurity concentrations are very large on each side of the junction, the junction width will be quite small and the built-in potential will be relatively large, according to (10.10b). As the junction is forward biased, the junction width becomes even smaller, per (10.24). Tunneling occurs when the electrons in the conduction band on the n-side rise to energy levels adjacent to empty states on the p-side, provided that the junction is sufficiently narrow, as illustrated in the energy band diagram of Figure 10.20.

Thus, the multiple pn junctions of the multijunction configuration can be accomplished by incorporating p^+n^+ tunnel junctions between each junction to eliminate the reverse-biased pn junctions. This is shown in Figure 10.21.

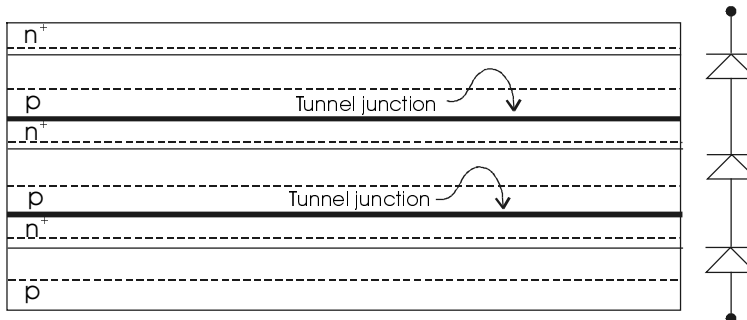


Figure 10.21 Separation of multiple pn junctions with tunnel junctions.

Problems

- 10.1 What can be said about the bandgap of glass? Why is silicon opaque? For what range of wavelengths will silicon appear transparent?
- 10.2 Given the arguments about direct vs. indirect bandgap materials and the ability of these materials to absorb photons, offer an argument about the optimal bandgap structure of a material that will *emit* photons efficiently. Note that photon emission involves a transition of an electron from the conduction band to the valence band.
- 10.3 What would the bandgap need to be for an infrared LED? What about a red LED? What about a green LED? What about a blue LED? Would you expect the materials with these bandgaps to be direct bandgap materials or indirect bandgap materials?
- 10.4 Compare the average thermal velocity of an electron, v_{th} , at room temperature, if $\frac{1}{2}mv_{th}^2 = \frac{1}{2}kT$, where m is the electron mass, k is Boltzmann's constant and T is the absolute temperature, with the drift velocity of an electron having a mobility of $10^3 \text{ cm}^2/\text{volt}\cdot\text{sec}$ in an electric field of 1000 V/cm. The drift velocity equals the product of the mobility and the electric field. At what electric field strength will the drift velocity equal the thermal velocity?
- 10.5 Use (10.9b) to solve for the concentration of electrons as a function of position between the neutral n-side edge of the junction and the edge of the neutral p-side of the junction. Plot this concentration function on a logarithmic scale along with the concentration of ionized impurities in the space charge layer.
- 10.6 Solve for the concentration of holes in the space charge layer. Show that in the space charge layer in thermal equilibrium, that $np = n_i^2$ at every position, x .
- 10.7 Show that (10.10b) can also be obtained by setting the net hole current across the junction equal to zero.
- 10.8 If a material has $\mu_n = 8600 \text{ cm}^2/\text{volt}\cdot\text{sec}$, $\mu_p = 400 \text{ cm}^2/\text{volt}\cdot\text{sec}$ and $\tau_n = \tau_p = 10 \text{ ns}$, would you design a PV cell with the light incident on the n-side or the p-side of the material? Approximately what should be the distance between the edge of the space charge layer and the back contact? Explain why.
- 10.9 Show that (10.24) results from adding (10.23a) to (10.23b).

- 10.10 Show that combining (10.10b) and (10.24) results in (10.25).
- 10.11 Assume $N_A = 10^{20} \text{ cm}^{-3}$ and $N_D = 10^{17} \text{ cm}^{-3}$. Assume room temperature.
- Calculate the built-in junction potential for Si and GaAs.
 - Calculate the junction width for Si and for GaAs under short-circuit conditions.
- 10.12 Use (10.30) to calculate the electric field in the n-region adjacent to the junction if the donor concentration is given by $N_D(x) = N_S(1 - bx)$, where x is distance measured from the surface of the cell and b is a constant.
- 10.13 Calculate the widths of the following abrupt junctions in Si at room temperature with no external bias applied.
- $N_A = 10^{16}$ and $N_D = 10^{20}$.
 - $N_A = 10^{21}$ and $N_D = 10^{21}$.
- Next, calculate the widths of each junction if a forward bias of 0.3 V is applied, with all the external voltage appearing across the junction. Sketch the energy band picture for part b.

References

- [1] Yang, E. S., *Microelectronic Devices*, McGraw-Hill, New York, 1988.
- [2] Streetman, B. G., *Solid State Electronic Devices*, 4th Ed., Prentice Hall, Englewood Cliffs, NJ, 1995.
- [3] Hu, C. and White, R. M., *Solar Cells: From Basic to Advanced Systems*, McGraw-Hill, New York, 1983.
- [4] Rappaport, P., *RCA Review*, Vol 20, September 1959, 373-379.
- [5] Zweibel, K., *Harnessing Solar Power*, Plenum Press, New York, 1990.

Chapter 11

PRESENT AND PROPOSED PV CELLS

11.1 Introduction

In the last chapter, the basic theory of PV cells was presented without regard to any specific cell technology. This chapter will cover some of the fabrication processes associated with current cells along with discussions of the operation of a variety of cells, some of which are commonly in use and others of which are still in the experimental phases.

Progress in PV research and development is moving so rapidly that by the time this chapter is in print, much of it will likely be outdated. Hence, in addition to introducing the reader to technologies of the early 2000s, it is also the goal of this chapter to provide the reader with the intellectual tools needed to read and understand current literature. Many of the sources of current information on PV technology are listed in the reference section of the chapter.

In general, cell fabrication begins with the refining and purification of the cell base material. After extremely pure material is available, then the pn junction must be formed. In some multiple-layer cells, more than one junction is formed along with various fascinating isolation steps. The single crystal silicon cell has made its mark on history. Whether it will continue to make its mark on the future will depend on reducing the amount of energy consumed in the production of the cell. Its fabrication and characteristics will be discussed first. During the discussion of the single crystal silicon cell, important processes, such as crystal growth and diffusion will be discussed. These basic processes in many cases are applicable to the fabrication of other types of PV cells. Important new developments in crystalline Si cell technology are centered around the thin Si cell, which will also be discussed.

Perhaps the most promising future PV cells will consist of thin films. Certain materials have direct bandgaps with energies near the peak of the solar spectrum, along with relatively high absorption constants and the capability of being fabricated with pn junctions. These films are not single crystal devices, so there are limitations to carrier mobilities and subsequent device performance. However, in spite of the non-single-crystal structures, laboratory conversion efficiencies in excess of 20% have been achieved [1].

Thin films are advantageous because only a minimal amount of material is required to deposit a film with a thickness of 1 or 2 μm . Figure 11.1 shows the photon current vs. optical path length for common thin film materials. Note that within 1 to 2 μm all the materials approach photon current saturation, whereas crystalline Si requires significantly greater thickness for full photon absorption. Examples of thin film PV cells that are currently under serious consideration are amorphous silicon (a-Si), copper indium (gallium) diselenide (CIGS) and cadmium telluride (CdTe). At the time of this writing, a-Si and CIGS modules are in commercial production and CdTe modules are undergoing commercial scale

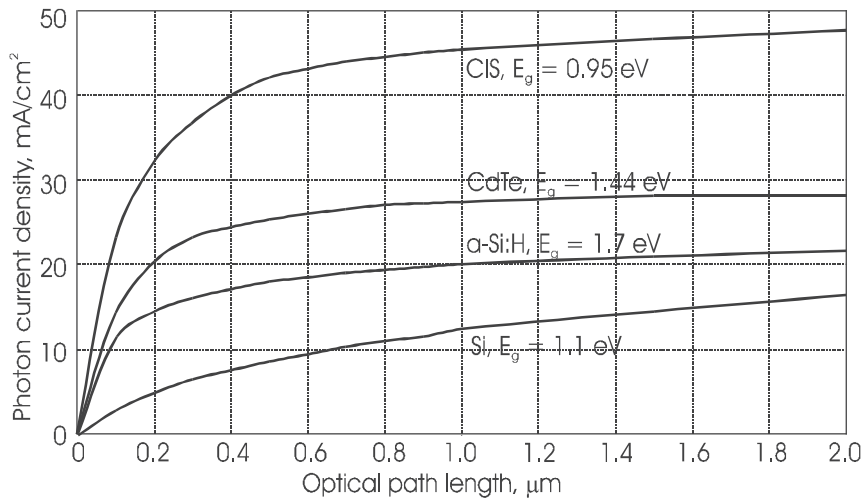


Figure 11.1 Photon current vs. optical path length for thin film materials, compared with crystalline silicon, standard test conditions [2].

testing. Gallium arsenide has been used for high-performance cells and has also been the subject of thin film experimentation.

Availability of cell component materials is also of interest if many gigawatts of PV power are to be obtained from any technology. Discussion of each technology includes commentary on the availability, production, refining and purification of the cell component materials. Of all the thin film materials, availability of indium may become a limiting factor in the production of CIS PV cells, but this limit will not be approached until 200 gigawatts of cells have been produced. Annual production of In would limit CIS cell production to about 4 gigawatts per year. For comparison purposes, 2001 worldwide electrical generation capacity is approximately 3365 gigawatts [3]. Other thin film materials, although scarce, are sufficiently abundant for the production of many gigawatts of PV cells at reasonable cost, provided that certain production shortcomings that limit cell performance can be overcome.

11.2 Silicon PV Cells

The first silicon PV cells were of the single crystal variety. Single crystal cells are the most efficient and most robust of the silicon PV cell family, but are also the most energy intensive in their production. For this reason, other varieties of silicon cells have been developed. Polycrystalline cells are somewhat less efficient, but are less energy intensive. Amorphous silicon cells are even less energy intensive, but tend to have stability problems and are still less efficient. However, amorphous silicon is a direct bandgap material with an energy gap larger than pure silicon, so it has a much larger absorptivity than crystalline silicon with peak absorption at a wavelength closer to the peak of the solar

spectrum and is thus a suitable material for thin film cells. The instability mechanism in amorphous silicon is reasonably well understood and means for overcoming the instability are now in common use. Additional efficiency increases have been achieved for amorphous silicon by the use of multijunction cell structures.

Thin Si cells represent a compromise between crystalline cells and amorphous cells. These relatively recent introductions to the Si cell family use novel techniques for photon capture and minimization of top surface area blocked by contacts. Good efficiencies have been achieved in lab scale devices.

11.2.1 Production of Pure Silicon [4]

The first thing that must be done in the production of a silicon cell is to find some silicon. Although nature has not seen fit to leave behind large quantities of relatively pure silicon in a form similar to the large deposits of carbon that have been mined for many years and burned in furnaces and worn on fingers, silicon has been provided in abundant quantities mixed with oxygen. Indeed, more than half the crust of the earth is composed of this silica compound, so all that is needed is to mine it and remove the oxygen.

Of course, this is not done with zero energy. Separation of oxygen from silicon is quite energy intensive, requiring the reduction of SiO_2 with carbon in a carbon arc furnace. Regrettably, the CO_2 byproduct of this process is a greenhouse gas, so the production of pure Si for PV cells begins with the production of a greenhouse gas along with the silicon. Fortunately, over the lifetime of the cell, the amount of CO_2 from the reduction process is significantly less than the amount of CO_2 that would be produced if fossil fuels were used instead of PV cells to generate the same amount of electrical energy. The energy cost of this step is approximately 50 kWh/kg of silicon, and the result is metallurgical grade silicon, which is only about 99% pure.

A purity of 99% means impurity levels of 1 part in 100. This means that additional refining needs to take place, since the purity of electronic grade silicon needs to be in the neighborhood of 1 part in 10^7 or so, depending on how efficient the cell is to be. Unwanted impurities lead to crystal defects and trapping levels that affect the cell output. Hence, the next step in the refining process is to react the metallurgical grade silicon with either hydrogen or chlorine to form either SiH_4 (silane) or SiHCl_3 (trichlorosilane).

The more common reaction is to combine the Si with HCl in a fluidized bed reaction. This reaction, however, produces a combination of Si-H-Cl compounds, such as SiH_2Cl_2 , SiHCl_3 and SiCl_4 along with chlorides of impurities. Each of these liquids has its own boiling point, so it is relatively straightforward to use fractional distillation to separate the SiHCl_3 from the other components. Although it looks simple on paper, the energy required in this step is relatively high. The next step is to remove the silicon from the trichlorosilane. This is done by reacting the trichlorosilane with hydrogen at a high temperature, producing polycrystalline silicon and HCl, at an energy cost of close to 200 kWh/kg of silicon. At this point, the silicon achieves the electronic grade level of purity.

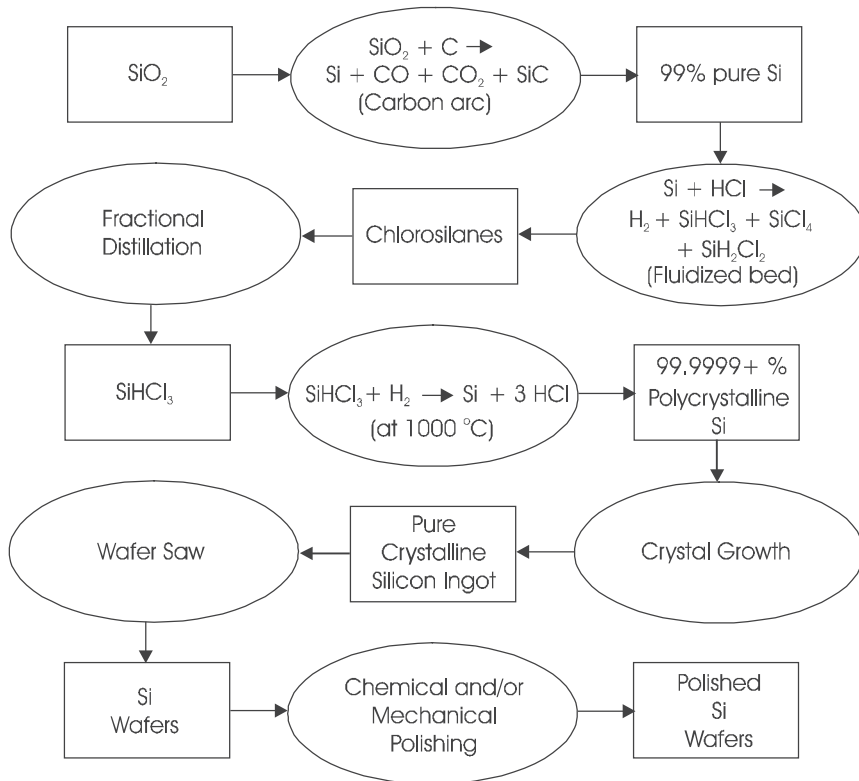


Figure 11.2 Production of single crystal silicon wafers from sand [5].
(Adapted from Ciszek, T. F., 1988, © IEEE.)

11.2.2 Single Crystal Silicon Cells

Fabrication of the Wafer

To produce single crystal silicon from the polycrystalline material, the silicon must be melted and recrystallized. This is done by dipping a silicon seed crystal into the melt and slowly withdrawing it from the melt with a slight twisting motion. As the silicon is pulled from the melt, it reaches a somewhat higher purity level since the remaining impurities tend to remain behind in the melt. Under properly controlled conditions for solidification and replenishment of the melt, crystals as large as 4 to 6 inches in diameter and 3 to 5 feet long can be readily grown.

To produce n-type or p-type crystals, boron or arsenic can be introduced to the melt in whatever quantities are needed to produce the desired doping levels. Other type III or type V materials may also be introduced, but generally the diffusion constants or activation energies of these materials are less desirable from a PV performance perspective. Indium, for example, is a group III impurity, but at room temperature, because of the higher activation energy of indium, a sig-

nificant percentage of the indium atoms do not ionize and donate holes to the host crystal. Phosphorous is a group V impurity that has satisfactory ionization properties, but also has a higher diffusion constant in silicon, so that if the host material is heated, phosphorous atoms will migrate in the host material at a faster rate than arsenic atoms.

Special saws are then used to cut the ingots into wafers. Since circular wafers mounted in a module leave a large amount of empty space between the wafers, often times the edges of the wafers are trimmed to make the wafers closer to square. The wafers are approximately 0.01 inch thick and are quite brittle. The sawing causes significant surface damage, so the wafers must next be chemically etched to restore the surface. In order to achieve the textured finish as described in the last chapter, it is possible to use a preferential etching process, so that after etching, the wafer surface is textured and relatively defect free. Again, the wafering process is quite energy intensive.

Fabrication of the Junction [6]

The next step in the production of the single crystal silicon cell is to create the pn junction. In electronic semiconductors, pn junctions can be created by diffusion, epitaxial growth and ion implantation. These methods work fine for junctions having areas in the 10^{-12} m^2 range, but for PV cells with junction areas in the 10^{-2} m^2 range, the time it takes to produce a given area of junction becomes very important. Hence, due to cost constraints, pn junctions in crystalline silicon PV cells are made primarily by diffusion.

Impurity atoms diffuse into silicon in a manner similar to the diffusion of holes and electrons across regions of nonuniform impurity density. The concentration as a function of distance from the surface, x , and time is determined by the solution of the familiar diffusion equation

$$\frac{\partial N}{\partial t} = D \frac{\partial^2 N}{\partial x^2}, \quad (11.1)$$

where N represents the density of the impurity and D is the diffusion constant associated with the specific impurity. It should be noted that D is highly temperature dependent, especially close to the melting temperature of the host material. At room temperature, diffusion is negligible, but in the neighborhood of 1000°C , diffusion becomes appreciable.

The solution to (11.1) depends upon the boundary conditions imposed on the impurity. Most diffusion processes begin by holding the surface concentration of impurities constant for a fixed time. Then the impurity source is removed so the total number of impurities now remains constant, equal to the number of impurity atoms that diffused into the host during the constant surface concentration step of the process. The first step, known as the **predeposition**, leads to the well-known complimentary error function solution, i.e.,

$$N(x, t) = N_0 \operatorname{erfc} \frac{x}{2\sqrt{Dt}}, \quad (11.2)$$

where N_o is the concentration of impurities at the surface of the wafer. Suppose the substrate is uniformly doped p-type material and the impurities being diffused are n-type. The net impurity concentration at any depth, x , then, is the difference between the n-type and the p-type concentrations, or,

$$N(x,t) = N_o \operatorname{erfc} \frac{x}{2\sqrt{Dt}} - N_A . \quad (11.3)$$

When the net impurity concentration is positive, the material is n-type, and when the net impurity concentration is negative, the material is p-type. The junction is located where the net impurity concentration is zero, which represents the transition between n-type and p-type. The depth of the junction can thus be determined by setting $N(x,t) = 0$ and solving for x , yielding the result

$$x = 2\sqrt{D} \operatorname{erfc}^{-1} \frac{N_A}{N_o} . \quad (11.4)$$

This will not normally be the final junction depth, since after the predeposition step, the impurity concentration at the wafer surface is close to the solid solubility limit for the host material, which shortens the minority carrier diffusion length in this region. This preliminary junction depth estimate is useful, however, because it leads to a determination of the amount of time needed in the predeposition step to produce a junction at a depth less than the final desired junction depth, which will ultimately be 5 to 10 times the initial junction depth.

To reduce the surface concentration, a **drive-in** diffusion is carried out next. The drive-in diffusion is simply the continued application of heat to the material after the supply of the surface impurity is removed. The result is that the impurity continues to diffuse from the region of greater concentration to the region of lesser concentration. The impurity concentration is given, to a good approximation, by the solution of the diffusion equation under conditions of constant impu-

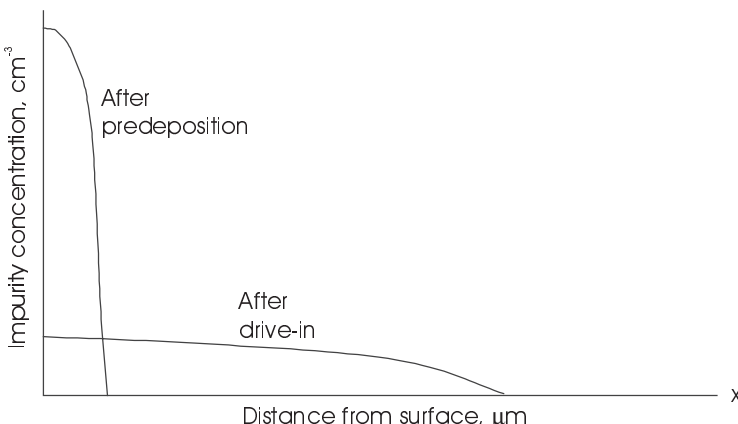


Figure 11.3 Concentrations of impurities after two diffusion steps.

rities per unit area. The assumption is that all of the impurities diffused into the material during the predeposition step remain at the surface of the material. The number of impurities per unit area can be determined by integrating (11.3) from the surface into the material. While the actual distance of travel of the impurities is less than 1 μm , the integration is performed from 0 to infinity to yield

$$Q(t) = \int_0^{\infty} N(x, t) dx = 2N_o \sqrt{\frac{Dt}{\pi}} . \quad (11.5)$$

After the drive-in step, the net impurity concentration is represented fairly accurately by the Gaussian distribution function,

$$N(x, t) = \frac{Q}{\sqrt{\pi Dt}} e^{-\frac{x^2}{4Dt}} - N_A . \quad (11.6)$$

This expression can now be solved for the junction depth by again setting $N(x, t) = 0$. The solution is left as an exercise for the reader (Problem 11.2). It is thus a straightforward matter to control the diffusion of impurities into the wafer to produce a junction at any desired depth from the surface. Since it is desirable to have the junction within a minority carrier diffusion length of the surface, the depth can be set to achieve this goal. Note that (11.3) through (11.6) also enable the cell designer to control the impurity concentration profile on the n-side of the junction. Figure 11.3 shows the impurity concentrations after the two diffusion steps have been completed.

Contacts

After creating the pn junction, the next step is to affix contacts to the cell. If the intent is to fabricate contacts that will last as long as the rest of the cell, then alligator clips are somewhat inadequate. It is necessary to affix contacts that are low resistance ohmic contacts that will remain in good contact with the cell through extreme temperature cycling. The contact material must lend itself to bonding of connecting wires so the cell can be integrated into a module.

The back contact covers the entire cell and is commonly made of evaporated aluminum that is annealed by heating the material after evaporation. The annealing process causes the aluminum to diffuse slightly into the silicon, creating a strong bond that will not break under thermal cycling. Since aluminum is a group III element, it also acts as a p-type donor and produces a heavily doped p-region adjoining the contact. This heavily doped p-region creates an impurity gradient that produces a resulting electric field that accelerates holes toward the back contact.

The front contact is considerably more challenging for several reasons. First of all, if the front contact is opaque to light, then it will block photons from entering the cell and being absorbed. This means the area of the front contact must be minimized. On the other hand, if the area is too small, then the resistance of the contact increases. Since the junction is only a small distance below the front

surface, if the contact material is annealed, it is possible that it will diffuse into the silicon and short out the junction. For that matter, even if the contact does not diffuse across the junction initially, this can occur over time under operation at higher temperatures and shorten the lifetime of the cell. Hence, the design constraints on the front contact are that it must be small, ohmic and present low series resistance while not threatening the junction.

The series resistance at the front contact of a cell depends on the distance the charge carrier must travel through the host material to the contact in addition to the resistance of the contact itself. The conductivity of a material is given by

$$\sigma = q(\mu_n n + \mu_p p). \quad (11.7)$$

It is convenient to consider the resistance between two points on an ohms-per-square basis. Figure 11.4 shows a piece of material with dimensions $\ell \times \ell \times t$. The resistance between the two ends of the material is given by

$$R = \frac{1}{\sigma} \frac{\ell}{\ell t} = \frac{1}{q(\mu_n n + \mu_p p)t} \text{ ohms/square.} \quad (11.8)$$

For a typical thin n-type silicon region with $n \approx 10^{20} \gg p$, $\mu_n \approx 100$ and a junction depth of approximately $1 \mu\text{m}$ ($=t$), the resistance per square becomes $R = 6.25 \text{ ohms}$.

Now suppose two contacts are each 2 cm long and spaced 0.5 cm apart, as shown in Figure 11.5. The problem is to approximate the resistance between bulk and contact. Since the worst-case resistance is from the midpoint between the two contacts, the longest distance to a contact is 0.25 cm. Over the 2 cm distance, a total of eight squares, each 0.25 cm on a side, can be inserted between the midpoint and one of the contacts and another eight can be inserted between the midpoint and the other contact. Hence, there are the equivalent of

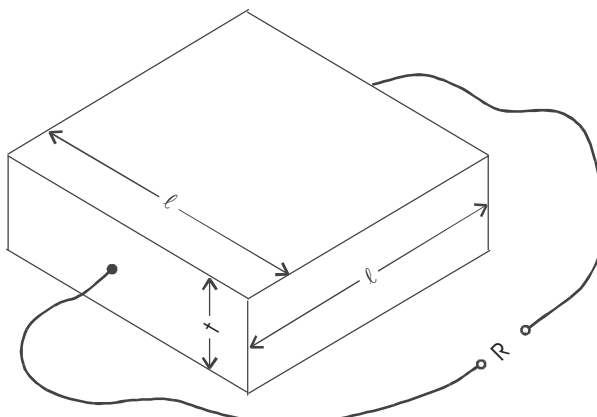


Figure 11.4 Determination of resistance per square.

16 squares in parallel, each of which has a resistance of 6.25 ohms. The resulting resistance of the 16 parallel squares is thus $6.25 \div 16 = 0.39$ ohm.

Suppose further that the cell is approximately 10 cm in diameter and generates a total of 2.5 A under standard illumination. Assuming uniform generation of current, this means that each square cm generates approximately 0.032 A. Since the area between the two contacts is 1 cm², approximately 32 mA is generated in this region that needs to be carried by the contacts after it reaches the contacts. In general, a contact will be collecting current from both sides, so that each cm of contact length will collect approximately 16 additional mA of current, if the spacing is maintained at 0.5 cm.

An estimate of the power loss to the series cell resistance can be obtained from the worst-case resistance and the total current flowing through this resistance, with the result that $P = I^2R = 0.4$ mW. The power generated in this region, assuming a maximum power voltage of approximately 0.55 V, is $P = IV = 0.032 \times 0.55 = 16.5$ mW. Hence, approximately 2.4% of the power generated is lost to the ohmic resistance of the cell between the generation point and the contact in this worst-case example. Since most of the charge carriers have a smaller distance of travel to the contact, the resistance experienced will be less, and the overall power loss will be less than 2% between bulk and contact.

To determine power losses in the contacts, it is necessary to determine the resistance of the contact. Aluminum has a bulk resistivity, ρ , of 2.7×10^{-6} ohm-cm. Assuming a contact with typical thickness of 50 μm and width of 100 μm , the resistance per centimeter length is $R = \rho/A = 0.054$ ohms/cm. Hence, the contact with 2 cm length will have a resistance of 0.108 ohm.

Since the current in the contact increases linearly from zero at the beginning to 32 mA at the end, the average current in the contact is 16 mA. However, to more accurately express the ohmic losses in the contact, the losses should be integrated over the length of the contact. Choosing any point, x , along the contact, the current at point x will be $I(x) = 0.016x$, and the differential resistance of this portion of the contact will be $0.054dx$ ohm, since the resistance of the

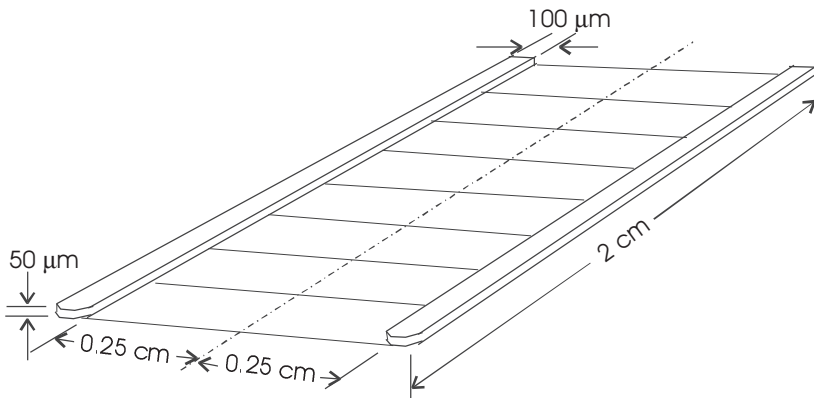


Figure 11.5 Determination of resistance between bulk and contacts.

contact is 0.054 ohm/cm of length. The result of this calculation is

$$P = \int_0^2 d(I^2 R) = \int_0^2 (.016x)^2 .054dx = 3.7 \times 10^{-5} \text{ watts.} \quad (11.9)$$

This is only about 10% of the power loss over the cell surface. Hence, most of the series resistance is due to the surface resistivity of the bulk cell material. However, if the contact is only 5 μm thick, the resistance increases by a factor of 10 and the power loss is comparable to the bulk losses. These calculations illustrate a means that may be used to determine optimal spacing between top contacts as well as the dimensions of the top contacts to keep power losses to a minimum while still enabling maximum photon absorption.

As the current in the contacts continues to increase, the cross-sectional area of the contact must increase to enable the contact to carry the total current within acceptable voltage drop limitations. This is analogous to the circulatory system of plants, in which leaves contain capillaries that extend over the leaf to provide transport for nutrients.

The front contacts can be fabricated by several means, including evaporation in a vacuum chamber or silk screening with a paste. For fine lines, the lines may be defined with photoresist as is done in the production of small geometry electronic semiconductors.

If aluminum is the contact material, in order to make an ohmic contact to the n-type material, it is necessary to anneal the contact for approximately 5 minutes at a temperature of approximately 450°C. To prevent transport of the aluminum through to the junction, it is advisable to use a small percentage of silicon in the aluminum or to first evaporate a very thin ($\approx 0.01 \mu\text{m}$) layer of titanium or chromium to act as a barrier to the aluminum diffusing into the junction.

Antireflective Coating

After affixing the contacts to the material, an antireflective coating may be applied to the cell, normally by evaporation, since the coating must be so thin. A quarter wavelength coating has a thickness of approximately 0.15 μm . These coatings are commonly used for photographic lenses to increase their speed by reducing reflection and simultaneously increasing transmission. Typical coatings are listed in Table 10.2. As long as the photon wavelength is relatively close to the quarter-wavelength constraint, transmission in excess of 90% can be achieved for the cell surface.

Because antireflective coatings optimize transmission at only one wavelength, textured cell surfaces are becoming more common for enhancing light trapping over the full spectrum.

Modules

The cells must then be mounted in modules, with interconnecting wires or metal foil strips. The interconnects are typically ultrasonically bonded to the cell contacts. The cells are then mounted to the module base and encapsulated

with a glass or composite. The encapsulant must be chosen for long life in the presence of ultraviolet radiation as well as possible degradation from other environmental factors. Depending on the specific module environment, such as blowing sand, salt spray, acid rain or other not-so-friendly environmental component, the encapsulant must be chosen to minimize scratching, discoloration, cracking or any other damage that might be anticipated. Earlier encapsulants, such as ethylene vinyl acetate (EVA), tended to discolor as a result of exposure to high levels of ultraviolet radiation and higher temperatures. Other encapsulants had a tendency to delaminate under thermal stresses. Modern materials now seem to have overcome these problems [7].

After the cells are encapsulated in modules, they are ready to produce electricity very reliably for a long time, normally in excess of 20 years.

11.2.3 Multicrystalline Silicon Cells

At this point, it should be clear that the production of single crystal Si cells is highly energy intensive. The large amount of energy used in the wafering process includes the single crystal Si lost when the crystals are sawed into wafers. Further loss occurs if the round wafers are trimmed to approximate a square to fill a greater percentage of a module with cells. The question arises whether a means can be conceived for growing single crystal wafers or perhaps a compromise can be achieved by manufacturing wafers that approximate single crystal material. To date, at least three methods have been explored and developed for the production of multicrystalline PV cells—crucible growth, the EFG process and string ribbon technology.

One compromise involves pouring molten Si into a crucible and controlling the cooling rate. The result is not single crystalline material, since no seed crystal is used, but the multicrystalline Si obtained by this process has a square cross-section and is sufficiently close to the single crystal ideal that efficiencies in the range of 15% can be obtained. It is still necessary to saw the ingots into wafers, but the wafers are square, so no additional sawing is needed, as was the case with the round Si ingots. This process increases the production rate per kg of material by reducing the kerf loss.

Another method of producing multicrystalline Si is the edge-defined film-fed growth (EFG) method [8]. The EFG process involves pulling an octagon tube, 6 m long, with a wall thickness of 330 μm , directly from the Si melt. The octagon is then cut by laser along the octagonal edges into individual cells. Cell efficiencies of 14% have been reported [9].

The third method of producing multicrystalline Si cells involves pulling a ribbon of Si, or dendritic web, from the melt. The difficulty in this process is controlling the width of the ribbon. To do so, high-temperature string materials are used to define the edges of the ribbon. The string materials are pulled through a crucible of molten Si in an Ar atmosphere after the attachment of a seed crystal to define the crystal structure of the ribbon. The nonconducting string material has a coefficient of thermal expansion close to that of Si, so dur-

ing the cooling process, the string material will not affect the Si crystallization process. A lab cell efficiency of 16.2% has been achieved and an efficiency of 15.4% has been achieved for an 80 cm² cell [10].

Essentially the same processes are used with the multicrystalline wafers that are used with the single crystal wafers. Multicrystalline modules are characterized by the cells' completely filling the modules, with the cells' having a sort of speckled appearance resulting from the departure from single crystal structure. Since the multicrystalline cells still maintain the basic crystalline properties, the 1.1 eV indirect bandgap results in the need for thicker cells with surface texturing to provide for maximum photon capture, as in the case of single crystal cells.

Since multicrystalline cells are currently in the production phase, it is reasonable to project efficiency increases and cost per watt reductions as research and development progresses.

11.2.4 Buried Contact Silicon Cells

In 1984, a team of University of New South Wales researchers led by Green and Wenham achieved a breakthrough in buried contact Si cells that has now been licensed to a number of firms worldwide [11]. The technology consists of multiple layers of alternate n-type and p-type material, each on the order of 1 μm in thickness, interconnected by laser-cut grooves in which the metal contacts are buried. Figure 11.6 shows the processing sequence for the cell.

Processing begins with an insulating substrate or superstrate (1), upon which are sequentially deposited a dielectric layer and then alternating p-type and n-type layers of Si, followed by another dielectric layer (2). Next, thin grooves are laser cut into the structure, followed by heavy doping of the walls of the grooves to provide contacts for all of one type of layer (n or p) (3). After another laser grooving, which overlaps the previous groove in some regions, the groove walls are doped to the opposite polarity to form contacts for the remaining layers (4). The second groove is formed so that some of the grooves have n-type walls and some have p-type walls, whereas other grooves have n-type material on one wall and p-type on the other wall. The final step is metallization of the grooves with an alloy of Ni/Cu/Ag. This step connects all n-layers in parallel, connects all p-layers in parallel and also provides a series connection between n- and p-layers of adjacent cells (5) so no external wiring is needed to connect series cells.

The buried contact cell takes advantage of the use of thin layers of Si with the advantage of the buried contacts' obscuring significantly less surface area than contacts deposited on the surface. Furthermore, since the buried contacts also serve as interconnects between cells, the interconnect processing step can be streamlined with an extra bonus of more reliable contacts.

Perhaps the most interesting feature of the buried contact thin Si cell is the fact that the stacked layers of p- and n-type Si are connected in parallel, rather than in series as is common with many tandem cells. After the EHPs are generated in the vicinity of any of the pn junctions, the current flow direction is horizontal from the n-region to the n+ -region and from the p-region to the p+ vertical region and then to the buried contacts. The collection efficiency of such a

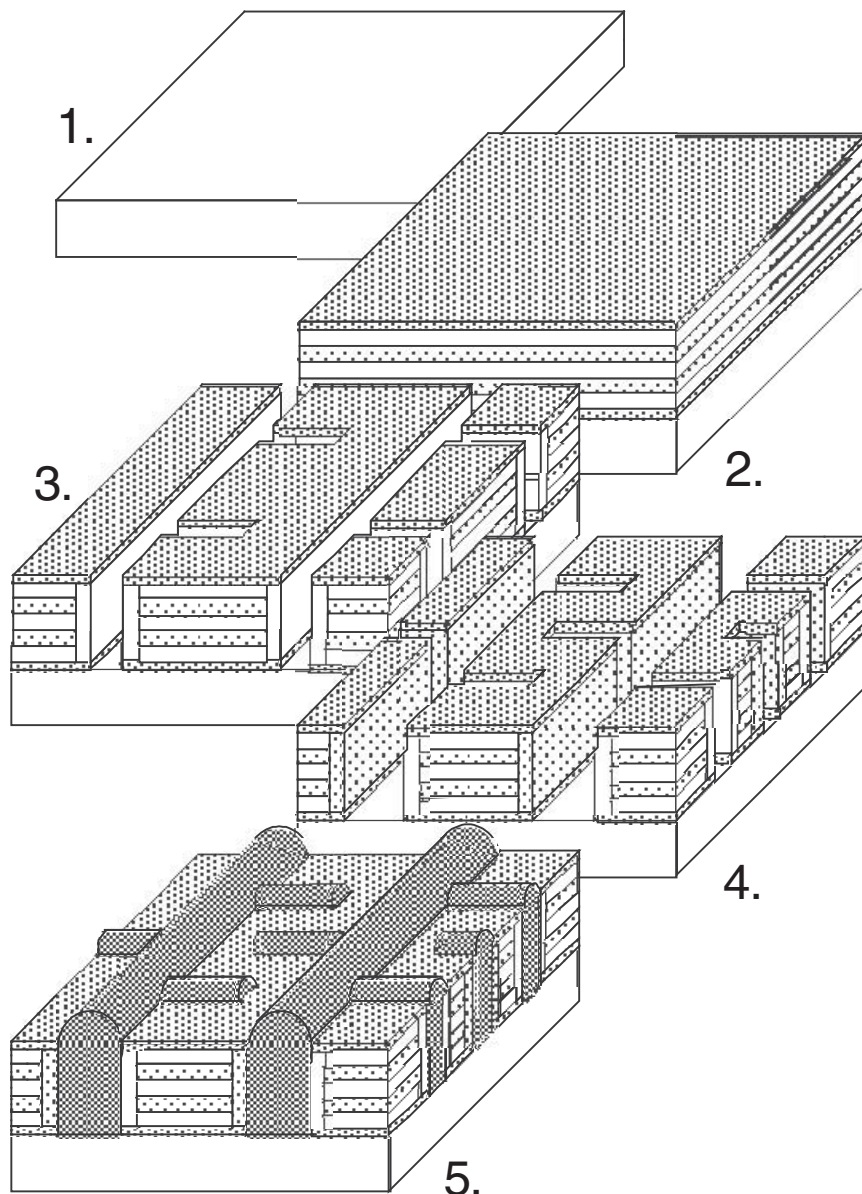


Figure 11.6 Processing sequence for buried contact thin Si cell. (Courtesy of M. Green.)

configuration is very high, since any photon-generated EHPs are generated within a diffusion length of a junction. Furthermore, since the junctions are so close, the material need not be nearly as good as for thicker cells. With the

elimination of the ingot and wafer processing steps, processing costs are reduced significantly. With the parallel conduction paths to the contacts, charge carriers tend to migrate to the paths of least resistance, leading to high fill factors.

An efficiency of 24.7% has been reported for a device with this cell structure and a flat plate module with an efficiency of 22.7% has been reported [12].

11.2.5. Other Thin Silicon Cells

A series of papers describing advances in this crystalline Si cells were presented at the IEEE 29th Photovoltaic Specialists Conference in 2002. Thin crystalline cell technology has been pursued with the hope that cell efficiency can be improved through the use of crystalline Si and that cell manufacturing cost can be lowered by using less material in the construction of the cell. A number of processes, including thin Si on ceramics [13], thin film crystalline silicon on glass (CSG) [14], and epitaxial growth of Si on existing crystalline Si with subsequent removal of the epitaxially grown cell from the existing Si substrate (the PSI Process) [15] are described in the Conference Proceedings.

The CSG process has produced modules of areas in the range of 480–900 cm² since 1998. Efficiencies have risen from 2% in 1999 to 8% in 2002. The structure consists of textured glass, antireflective coating, n⁺pp⁺ structure, resin insulator and metallization that dips into the structure from the back surface to form back and front cell contacts. The front contact does not require a transparent conducting oxide (TCO), so losses from the TCO are eliminated. TCOs will be discussed in more detail later in this chapter.

The modules consist of cells that are monolithically connected, and due to isolated metal interconnects that produce a fault-tolerant structure, performance of the module is not degraded as the size is scaled up. The production cost of this module in May of 2002 was \$1.95/W. Projections suggest a possible reduction of cost to \$1/W as the production process is improved.

Progress in the area of thin silicon cells over a relatively short period since 1997 suggests that the reader may expect to see continued developments and improvements of cells of this type.

11.2.6 Amorphous Silicon Cells

Amorphous silicon has no predictable crystal structure. Its atoms are located at more or less random angles and distances from each other. As a result, many of the potential covalent bonds in the silicon are not completed. These incomplete bonds cause a large number of equivalent impurity states in the bandgap and the noncrystalline nature of the material results in very low values for electron and hole mobilities. The impurity states would typically result in trapping of mobile carriers, so the combination of impurity states and diminished transport properties at first rendered amorphous silicon as a rather poor semiconductor material.

But persistent solid-state physicists confirmed that the incomplete bonds could be passivated with hydrogen, thus significantly reducing the number of

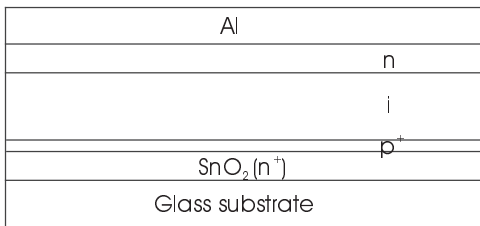


Figure 11.7 Basic a-Si:H cell structure.

impurity states in the bandgap, and that with n-type and p-type materials, a pn junction could be formed. Furthermore, by incorporating an intrinsic layer between p⁺ and n-type material, a reasonable EHP generation region could be created with reasonable transport properties resulting from minimized impurity scattering in the passivated intrinsic material. Another positive feature of the a-Si:H system is that it has a direct bandgap close to 1.75 eV, resulting in a high absorption coefficient and qualifying a-Si:H as a good potential candidate for a thin film photovoltaic material.

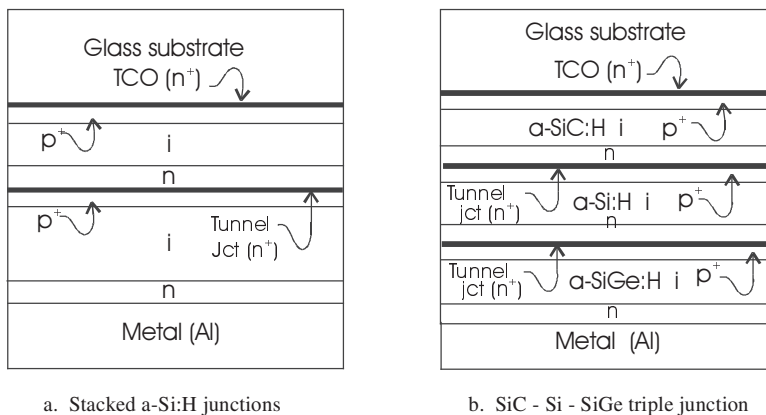
Fabrication

Figure 11.7 shows the structure of a basic a-Si:H cell. Fabrication of the cell begins with the deposition of a transparent conducting oxide layer on a glass substrate. The TCO, typically n⁺ SnO, constitutes the front contact of the cell. Next, a very thin layer of p⁺ a-Si:H is deposited, usually by plasma decomposition of SiH₄. The degenerate n-type TCO and the degenerate p-layer form a tunnel heterojunction. After the p⁺ layer, a slightly n-type intrinsic layer is deposited, followed by a stronger n-layer and finally a back contact, usually of Al, is deposited.

Initial operation of the basic cell with a relatively wide intrinsic layer was found to result in cell degradation when the cell was operated under sunlight conditions. The degradation was accounted for by the Staebler-Wronski effect, which explains the degradation in terms of increased density of scattering and trapping states in the intrinsic layer in proportion to photon exposure.

To mitigate the effects of the wider i-layer, cells were designed with narrower i-layers, but stacked, as shown in Figure 11.8a. These stacked cells require inclusion of tunnel junctions to prevent the blocking action of the pn junctions of adjacent cells, as discussed in Section 10.5.6. These cells have shown improved long-term performance.

The concept of stacked cells has been extended one step further by recognizing that C and Ge also bond reasonably well with a-Si to produce either a-SiC:H or a-SiGe:H. The C alloy has a higher bandgap, thus enhancing absorption in the blue range, while the Ge alloy has a smaller bandgap, thus enhancing absorption in the infrared range. The net result is an overall performance improvement over the a-Si:H cell. The structure is shown in Figure 11.8b, noting again the need for tunnel junctions between cell layers.



a. Stacked a-Si:H junctions

b. SiC - Si - SiGe triple junction

Figure 11.8 Stacked a-Si:H with Si only and with SiGe and SiC layers.

Another interesting variation in cell structure is shown in Figure 11.9, where a stainless steel substrate has been used to produce a flexible cell. United Solar has produced rolls of a-Si cells for use in roofing and other building integrated applications using this technology [16]. Figure 11.9 also shows a-Si on a very lightweight polymer substrate, about 2 mils thick, that has been proposed for extraterrestrial applications where minimal weight is important and where stresses on the structure are minimal [17]. Both types of cell have been reported to have efficiencies in the 10% range.

United Solar produces the cell on stainless steel by a proprietary roll-to-roll process. Note that the back surface incorporates an Al/ZnO textured film between the n-layer and the stainless steel to enhance photon trapping. The bandgap of a a-SiGe:H cell is dependent upon the fraction of Ge in the mix. In this structure, the top a-Si:H intrinsic layer has a bandgap of approximately 1.8 eV. The middle a-SiGe:H cell has a Ge fraction of approximately 15% in the intrinsic layer, resulting in a bandgap of approximately 1.6 eV, and the bottom a-SiGe:H cell has an intrinsic layer Ge fraction of approximately 45%, resulting in a bandgap for this layer of approximately 1.4 eV[18].

The challenge in creating the PV-on-polymer structure is keeping the polymer from deforming during heating portions of the processing. To do so, the process involves using a silicone gel between the bottom of the polymer and a heat sinking material, so the polyimide can be protected from heat stresses.

Cell Performance

Table 10.3 shows a theoretical maximum efficiency for a-Si of 27%, whereas in the late 1990s, large scale efficiencies for a-Si devices were reported in the 10% range, with lab cell stable efficiencies for triple junction devices of approximately 14% [19]. Considering that initial efficiencies of only a few percent were achieved, these efficiencies represent significant progress.

With the worldwide efforts in place to continually improve cell processing, along with the incorporation of novel and practical applications that can justify

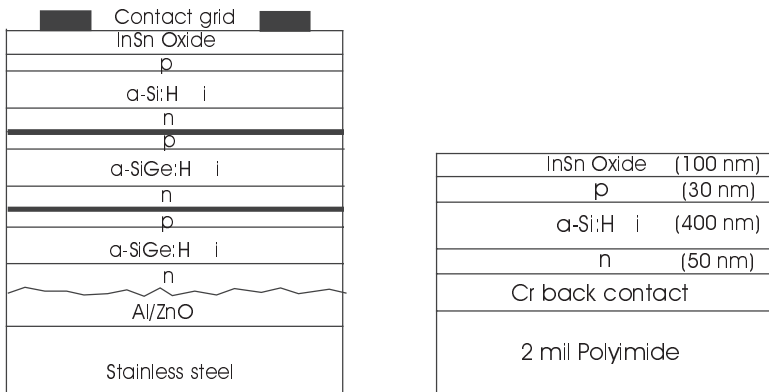


Figure 11.9 a-Si:H cell on stainless steel and polymer substrates [16, 17]. (Adapted from Guha et al., 607, and Huang et al., 699, *Proc. 26th IEEE PV Spec. Conf.*, 1997, ©1997 IEEE.)

the use of cells with efficiencies in the 8 to 10% range, continued progress can be expected with amorphous and thin film silicon cells.

When cells are stacked, they must be designed so absorbing layers produce equal photocurrent, since the layers are approximately ideal current sources connected in series. The increased efficiency of stacked (series) cells is thus due to more complete photon capture, with EHPs being effectively separated at the junctions, resulting in higher overall cell open-circuit voltages resulting from the combined series junctions.

Overall cell efficiency is also limited by the wavelength range over which the ARC will effectively minimize reflections, since the ARC optimal thickness is 1/4 wavelength. This limits the number of effective series junctions.

11.3 Gallium Arsenide Cells

11.3.1 Introduction

The 1.43 eV direct bandgap, along with a relatively high absorption constant, makes GaAs an attractive PV material. Historically high production costs, however, have limited the use of GaAs PV cells to extraterrestrial and other special purpose uses, such as in concentrating collectors. Production of pure gallium arsenide requires first the production of pure gallium and pure arsenic. The two materials are then combined to form GaAs. Most modern GaAs cells consist of thin films of GaAs grown on substrates such as Ge by an assortment of film growth processes.

11.3.2 Production of Pure Cell Components

Gallium [20]

Gallium was predicted by Mendeleev and first discovered by spectroscopic analysis by Lecoq de Boisbaudran in 1875. De Boisbaudran then separated out

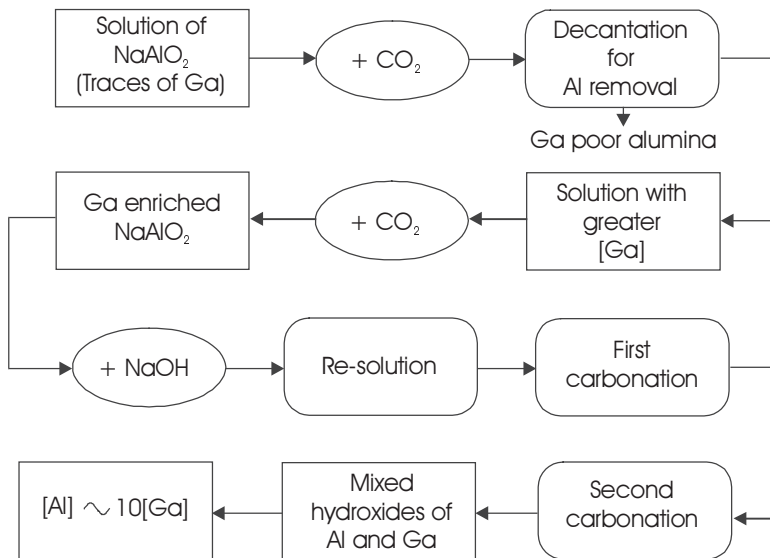


Figure 11.10 The Beja process (Pechiney) for the manufacture of gallium [20].

(Adapted from *Kirk-Othmer Encyclopedia of Chemical Technology*, 2nd Ed.

© 1968 John Wiley & Sons, Inc. Adapted by permission of John Wiley & Sons, Inc.)

Ga from its hydroxide by electrolysis in the same year. Ga is a metal, which liquefies just above room temperature, but has a very high boiling point. It is found as a trace element in diaspore, sphalerite, germanite, bauxite and coal, all of which contain Zn, Ge or Al, in addition to the Ga. In fact, coal flue dusts can contain up to 1.5% Ga, although most contain less than 0.1%. The relative abundance of Ga is comparable to the abundance of Pb and As, but the percentage composition of Ga in any naturally occurring mineral rarely exceeds 1%. The most important source of Ga is bauxite, even though this ore only contains 0.003 to 0.01% Ga.

Gallium can be extracted by many different methods, depending on the host material. For example, in bauxite, the weight ratio of Al to Ga is approximately 8000:1. In the Bayer process for Al extraction, bauxite is first mixed with a NaOH solution. The solution is autoclaved, diluted and decanted, at which point a red mud is removed from the material. Decomposition follows, which results in removal of hydrated alumina along with extracts having Al:Ga ratios of approximately 200:1. This Al:Ga mixture is then subjected to evaporation and is again mixed with NaOH and fed back into the mixing, autoclave, dilution, decantation and decomposition steps again.

When Al:Ga ratios of about 200:1 are reached in the sodium aluminate, the sodium aluminate solution can be subjected to processes such as the Pechiney process, which is shown in Figure 11.10. In the Pechiney process, which was invented by Beja and came into use after World War II, the sodium aluminate solution is reacted with CO₂ in several stages. In the first stage, much of the

soda and alumina are precipitated. This leaves a liquor enriched in Ga, from which Ga-rich alumina is obtained. This alumina is again dissolved in NaOH and fractional carbonation is repeated. The final product, after enough fractional carbonation steps, is a mixed oxide with adequate Ga content to enable electrolytic deposition of Ga from the NaOH solution.

Semiconductor grade Ga, with a purity of 99.999+%, is obtained by a variety of physical and chemical processes. These methods include chemical treatments with acids or gases at high temperatures, physicochemical methods, such as filtration of fused metal, heating in vacuum, dissolving again and subjecting to further electrolysis or crystallization as monocrystals. It is also possible to react Ga with Cl, fractionally distill the solution until the desired purity is reached, then recover the Ga and reconvert it to metal.

Arsenic [21]

Arsenic has been known since 1250 A.D. In 1649 Schroeder published two methods of preparing the element. Arsenic is found in many forms in nature, including sulfides, arsenides, sulfarsenides, oxides and arsenates. The most common source of As is FeSAs. When FeSAs is heated, the As sublimes, leaving FeS behind. Arsenic oxidizes rapidly if heated and, along with its compounds, is very poisonous. Arsenic is typically marketed in its arsenic trioxide form, which can be obtained at various purity levels by resublimation. This form is most commonly used in the manufacture of insecticides.

Semiconductor grade As can be obtained by reducing a chemically purified compound with a highly pure solid or gas. One such highly pure form is arsine (AsH_3), which is also highly poisonous and requires very special precautions. If elemental As is desired, the AsH_3 can be decomposed by heating, resulting in highly pure elemental As. A large percentage of use of As in semiconductors involves the decomposition of AsH_3 at high temperatures.

Germanium [20]

The existence of Ge was predicted by Mendeleev in 1870, and it was isolated by Winkler in 1886. Only a small number of minerals contain Ge in appreciable quantities, including $(\text{AgGe})\text{S}$, $(\text{AgSnGe})\text{S}$, $(\text{CuZnAsGe})\text{S}$ and $(\text{CuFeAsGe})\text{S}$. Most Ge, however, is recovered from Pb-Zn-Cu ores in Africa.

The recovery process involves heating the ore under reducing conditions. This vaporizes Zn and Ge so they can be oxidized and collected. The fumes are then leached with H_2SO_4 and the pH is then gradually increased. As the pH increases to 3, Ge is 90% precipitated, whereas Zn begins to precipitate at pH of 4. If Zn and Ge are both precipitated at a pH of 5, a 50:1 Zn:Ge ratio solution will produce a Zn-Ge precipitate containing close to 10% Ge. If MgO is used as the base, then a Mg-Ge precipitate containing about 10% Ge is obtained.

The next step is to react the precipitate with strong HCl, which causes GeCl_4 to form. The GeCl_4 can then be fractionally distilled and reacted with H_2O to form GeO_2 . The GeO_2 can then be reduced with H_2 to obtain pure Ge. The resulting Ge can then be zone refined to obtain semiconductor grade Ge.

11.3.3 Fabrication of the Gallium Arsenide Cell

Crystalline gallium arsenide is somewhat more difficult to form than silicon, since gallium and arsenic react exothermally when combined. The most common means of growing GaAs crystals is the liquid encapsulated Czochralski (LEC) method. In this method, the GaAs crystal is pulled from the melt. The melted GaAs must be confined by a layer of liquid boric oxide. The trick is to create the GaAs melt in the first place. Several means have been developed, such as first melting the Ga, then adding the boric oxide, and then injecting the As through a quartz tube [22].

Most modern GaAs cells, however, are prepared by growth of a GaAs film on a suitable substrate. Figure 11.11 shows one basic GaAs cell structure. The cell begins with the growth of an n-type GaAs layer on a substrate, typically Ge. Then a p-GaAs layer is grown to form the junction and collection region. The top layer of p-type GaAlAs has a bandgap of approximately 1.8 eV. This structure reduces minority carrier surface recombination and transmits photons below the 1.8 eV level to the junction for more efficient absorption.

A number of other GaAs structures have been reported recently, including cells of other III-V compounds. Figure 11.12 shows a cascaded AlInP/GaInP/GaAs structure grown by molecular beam epitaxy (MBE) [23] and an InP cell fabricated with the organo-metallic vapor phase epitaxy process (OMVPE) [24].

The epitaxial growth process involves passing appropriate gases containing the desired cell constituents over the surface of the heated substrate. As the gases contact the substrate, the H or CH₃ attached to the In or P or Ga are liberated and the In, P or Ga attaches to the substrate. Hence, to grow a layer of p-type InP, a combination of trimethyl indium, phosphine (for P) and diethyl zinc (for acceptor impurities) are mixed in the desired proportions and passed over the heated substrate for a predetermined time until the desired layer thickness is obtained. The process is repeated with different mixes of gases to form the other layers at the desired thickness.

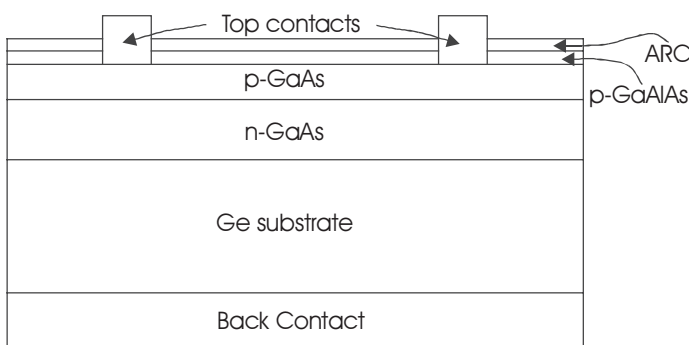
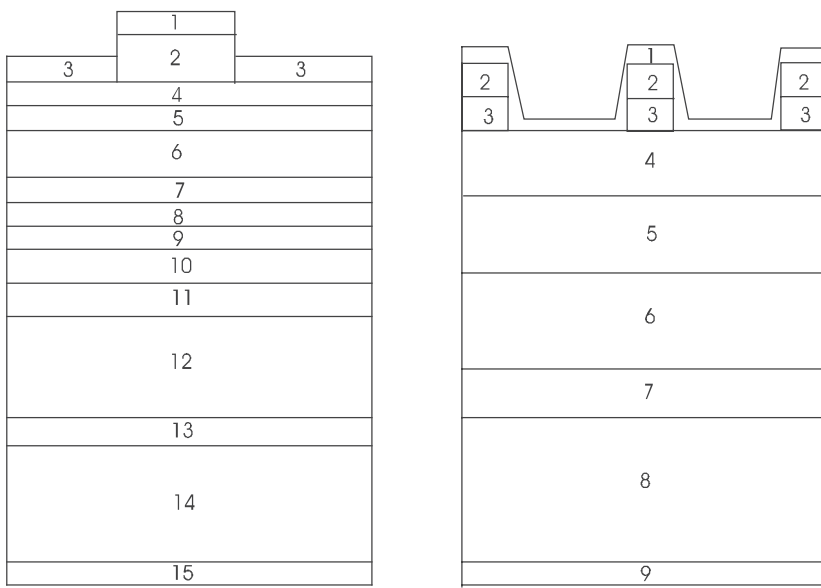


Figure 11.11 Structure of a basic GaAs cell with GaAlAs window and passive Ge substrate.



a. AlInP/GaInP/GaAs cell [16]

b. InP cell [17]

Figure 11.12 Cascaded AlInP/GaInP/GaAs cell and InP cell. Properties of the regions of the cells are summarized in Table 11.1. (Adapted from Lammasniemi, et al., 823, and Hoffman, et al., 815, Proc 26th IEEE PV Spec Conf, 1997. © 1997 IEEE.)

Table 11.1 Summary of composition of regions of cells of Figure 11.12.

Region	AlInP/GaInP/GaAs cell			InP cell		
	Material	Thickness	Doping	Material	Thickness	Doping
1	Au/Ni/Ge	contact		MgF ₂ /ZnS	110–55 nm	ARC
2	SiO ₂ /SiN _x	ARC		Au-Ge	2–3 μm	front grid
3	GaAs	600 nm	n=8E18	InGaAs	0.1–0.5 μm	
4	AlInP	25 nm	n=2E18	InP	50–100 nm	p=1E18
5	GaInP	75 nm	n=1–4E18	InP	100–200 nm	p=1E17
6	GaInP	400 nm	p=5–500E16	InP	1.5–4.0 μm	n=1E17
7	AlInP	25 nm	p=5E18	InP	250–500 nm	n=1E18
8	GaAs	10 nm *	p=1E20	InP	400 μm	n>1E18
9	GaAs	10 nm *	n=8E18	Au-Ge	contact	
10	GaInP	50 nm	n=2E18			
11	GaAs	100 nm	n=1E18			
12	GaAs	3500 nm	p=1E17			
13	GaInP	100 nm	p=1E19			
14	GaAs	substrate				
15	Au/Pt/Ti	contact				

* Tunnel junction

GaAs cells remain expensive to fabricate and are thus used primarily for extraterrestrial applications and in concentrating systems.

11.3.4 Cell Performance

Cells fabricated with III-V elements are generally extraterrestrial quality. In other words, they are expensive, but they are high-performance units. Efficiencies in excess of 20% are common and efficiencies of cells fabricated on more expensive GaAs substrates have exceeded 34% [25].

An important feature of extraterrestrial quality cells is the need for them to be radiation resistant. Cells are generally tested for their degradation resulting from exposure to healthy doses of 1 MeV or higher energy protons and electrons. Degradation is generally less than 20% for high exposure rates.

Extraterrestrial cells are sometimes exposed to temperature extremes, so the cells are also cycled between -170 and $+96^{\circ}\text{C}$ for as many as 1600 cycles. The cells also need to pass a bending test, a contact integrity test, a humidity test and a high temperature vacuum test, in which the cells are tested at a temperature above 140°C in vacuum for 168 hours [26].

Fill factors in excess of 80% have been achieved for GaAs cells. Single cell open-circuit voltages are generally between 0.8 and 0.9 V.

The design of stacked cells depends upon the air mass under which the device is intended to operate. In order to ensure equal photon-generated current in each absorption layer, layer thickness needs to be adjusted for the air mass under which operation is anticipated, because air masses do not attenuate the entire spectrum proportionately, as shown in Figure 2.2.

In particular, if a cell absorbs efficiently at $\lambda = 0.9 \mu\text{m}$, significantly more photons are available at this wavelength at AM0 than at AM1. Thus, for operation at AM1, the absorber width would need to be increased to generate a photocurrent comparable to that which a narrower layer would generate at AM0. This consideration is particularly important when optimizing cell performance at AM0, but can also be relevant for cells designed for use in regions where exposures to AM 1.5 or AM 2.0 may occur for long periods of cell operation.

The bottom line is that III-V cells are excellent extraterrestrial performers, and it appears that continued research will improve performance, reduce mass and reduce cost of the cells. Whether III-V cells will be able to compete with other technologies for terrestrial applications will depend on the degree of future improvements in all technologies. This mystery will likely unfold before the eyes of any reader born after the fabrication of the first commercial PV cell.

11.4 Copper Indium (Gallium) Diselenide Cells

11.4.1 Introduction

The first CIS PV cell was reported in 1974 by a group at Bell Laboratories [27]. Copper indium diselenide was chosen as a potential photovoltaic material because of its attractive direct bandgap (1.0 eV), its very high optical absorption

coefficient and its potentially inexpensive preparation. Furthermore, the cell components are available in adequate quantities and the manufacturing, deployment and decommissioning of the technology fall within acceptable environmental constraints.

While current technology involves the use of Cd as a cell component, the total quantity is relatively small, and efforts are underway to identify alternate, less toxic, materials to replace the Cd. The challenge with CIS, as with other thin film technologies, is to prepare a cell with appropriate electric field for collection of photon-generated, electron-hole pairs. Then ohmic contacts need to be affixed, with the front contact being highly conducting, but transparent to incident photons. The final device structure must be stable and must be encapsulated to ensure long module lifetime.

Unlike Si, which has been studied intensely for decades and is well-understood by the scientific community, the fundamentals of CIS are less well-understood. For example, energy bands in Si have been studied extensively and detailed explanations are available in nearly any solid-state devices text. CIS, on the other hand, rarely receives mention. As basic research on the properties of CIS leads to increased understanding of the fundamental properties of the material, chances for significant device improvement will be enhanced.

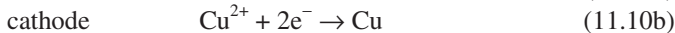
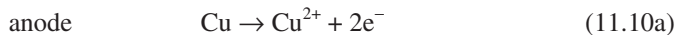
Current estimates for large-scale production of CIS devices suggest the possibility of producing devices for \$1.00/watt or less [28]. Achieving these production costs requires improving cell efficiency as much as possible in order to lower area-related costs. Frames, glass, encapsulants, array mounts and sometimes the cost of land itself all fall into this category.

11.4.2 Production of Pure Cell Components

Copper [29]

Of all the elements used in the production of semiconductors, copper is probably the most abundant. It is known from prehistoric times. It occasionally occurs in pure form in nature, but also occurs in many minerals, such as cuprite, malachite, azurite, chalcopyrite and bornite. The sulfides, oxides and carbonates are the most important sources of Cu. The refining process involves smelting, leaching and electrolysis. Since Cu is used in so many applications, and is found in so many locations in so many different compounds, many different methods of Cu refining have been developed. The reader is referred to reference [29] for examples.

Copper can be refined to semiconductor grade by electrolysis of a solution of copper sulfate and sulfuric acid. The anode is made of approximately 99% pure Cu and the solution is maintained so that almost everything that plates out on the cathode is Cu. The chemical reactions at anode and cathode are



Although it appears that this process is exclusively moving Cu from anode to cathode, it is also moving elements such as oxygen, sulfur, arsenic, antimony, bismuth, lead, nickel, selenium, tellurium, gold and silver from anode into solution. Oxygen is generally the most common impurity in the anode Cu, in the form of Cu₂O. As the Cu₂O moves into the solution, it reacts with the sulfuric acid to form CuSO₄ and H₂O along with Cu, which precipitates into the slime along with most of the other elements from the anode which do not dissolve. This loses half the Cu to the slime, but the slime then can be reprocessed.

Only the silver will dissolve, but addition of HCl or NaCl to the solution will precipitate the silver. Hence, only the CuSO₄ is left in solution for migration to the cathode, with the net result that the Cu plates out onto the cathode.

The slime thus contains compounds such as Cu₂S, Cu₂Se, Ag₂S and Ag₂Se, all of which may be of interest in further refining operations for recovery of any of the other elements. In the meantime, the Cu on the cathode will be very pure if the solution is properly controlled.

Indium [30]

Indium is most commonly found with zinc, but is also found with iron, lead and copper ores. Little use was made of In until it was found to be useful in certain semiconductors. Most commercial In is now obtained from the flue dusts and residues from smelting lead and zinc. As late as 1924, less than an ounce of pure In existed, even though it is rather widely scattered throughout the world, albeit in very small concentrations in host minerals. The price of highly pure In is in the neighborhood of \$100 per ounce.

Several means of extracting In from its natural states are available. In the presence of lead and zinc, the material can be melted and treated with chlorine gas or other chlorine source. This removes the Zn and In as chlorides, provided that the temperature is low enough to prevent evaporation of the In. The chloride slag is then leached with dilute sulfuric acid, which causes the In to precipitate along with Zn dust. The next step is to melt the In-Zn mixture and remove the Zn with Cl.

Indium is refined to semiconductor grade by further physical or chemical separation techniques, such as zone refining and fractional distillation of liquid In compounds.

Selenium [31]

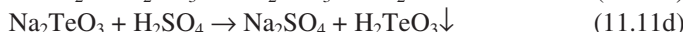
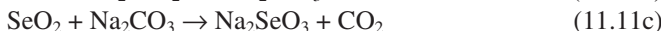
Selenium is a group VI element, and, as a result, is very similar to sulfur in many of its chemical properties, which accounts for its common occurrence with CuS. In its natural form, it combines naturally with 16 other elements and is a major component of 39 mineral species and a minor component of another 37 mineral species. Since Se is always combined with other elements, such as S, there are no identified "reserves" of Se. Certain native plant species preferentially absorb Se, and are sometimes indicators of the presence of the element. Elemental Se is relatively nontoxic, but many Se compounds are very poisonous. Selenium is recovered primarily from the anode muds from the refining of

copper. It is also recovered from flue dusts from processing copper sulfide ores. The price of high-purity Se is about \$4 per ounce.

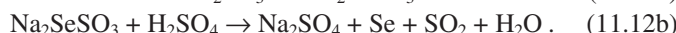
A number of methods of recovery of Se are available, depending on the starting material and the desired end products. One method is to first eliminate the Cu in Cu ores through either aeration with H_2SO_4 or by first oxidizing the mud and then reacting with H_2SO_4 in a leaching process. The H_2SO_4 causes the Cu to precipitate out of solution, leaving the Se behind in the mud for smelting with soda and silica. The initial product of this smelting process contains only about 1% Se, but most of the Fe, As, Sb and Pb are eliminated.

The molten charge is then oxidized with air. This volatilizes the Se, which is then caught in a scrubber and combined again with soda to produce a Se-rich soda slag. The slag is then subjected to a precious metal recovery process, leaving a slag that is leached with water and filtered, yielding sodium selenite and sodium tellurite alkaline liquor.

When the pH of the liquor is reduced to 6.2 by adding acid, the Te precipitates as tellurous acid, leaving the selenium behind in the sludge. Additional acid, followed by sulfur dioxide, precipitates Se as an amorphous sludge. This Se is washed, dried and reduced to a powder after boiling with steam. At this point, the Se is relatively pure, but still contains some Te. The chemical reactions take place with Se and Te both included in the first three reactions, prior to precipitation of the Te in the fourth reaction. After separation of the Se, the Te can be prepared in a similar fashion. The process will yield both Se and Te, both of which will require further refining for purities in excess of 99.99%.



One method of achieving high purity Se is to dissolve the Se from the previous process in hot sodium sulfite, wherein Te and many other impurities do not dissolve. The solution is then filtered and acidified with sulfuric acid to again liberate the Se. This distillation process is repeated several times until the Se is ultimately highly purified, at which point it is formed into shot for transport and storage. The two final reactions are



The purity of the higher purity final Se products is generally verified spectrographically, with commercial grade having purity of better than 99.0%, high-purity grade having purity in excess of 99.99%, and ultra-high purity with a purity as high as 99.9999%.

Cadmium [32]

Cadmium was discovered in 1817 [20] by Friedrich Stromeyer in zinc carbonate and by K. S. L. Hermann in a specimen of zinc oxide. The common denominator is that cadmium is commonly found embedded in zinc compounds, although cadmium sulfide is found in Scotland, Bohemia and Pennsylvania.

Since zinc is routinely refined, the leftover cadmium from the process is generally recovered, mixed with carbon and redistilled to yield an enriched dust. This process is repeated several times. Then hydrochloric acid is mixed with the cadmium dust, and zinc is added, resulting in the precipitation of the cadmium. After several repetitions of this process, electrolysis is finally used to deposit the final material. Cadmium is a group II metallic element, and along with solutions of its compounds, is highly toxic.

Sulfur [33]

Sulfur is abundant in the crust of the earth, both in elemental and combined forms. Elemental sulfur tends to occur in layers above salt domes. Abundant supplies of elemental sulfur have been discovered in many locations around the world. It has been used for thousands of years in many applications.

Elemental sulfur is generally recovered by pumping superheated water down a well to melt the sulfur, after which the molten sulfur is extracted from the well. The elemental sulfur is then generally reacted with a suitable element to enable the sulfur to be carried in a gaseous state for vapor deposition onto a substrate.

Molybdenum [34]

Molybdenum, a group VI metal, is an important metal for making ohmic contacts, particularly as the back contact in a CIS cell. The metal was first prepared by P. J. Hjelm in 1782. It has high strength, high corrosion resistance and is often used in alloys, particularly in the production of stainless steel. It retains its strength at high temperatures better than most other metals.

Most Mo is mined in the U.S., Canada and Chile. Molybdenum occurs principally in MoS_2 , but the concentration of MoS_2 in ores is rather small. About a ton of ore must be mined, crushed and milled to recover about 4 pounds of Mo. After the ore is crushed, the MoS_2 is recovered in relatively high concentration by floatation.

Roasting then drives off the sulfur and oxidizes the Mo to MoO_3 . Reduction with H_2 at high temperature yields Mo in powder form with purity in the 99% range. The powder can be reacted with halogens to form compounds such as MoF_6 and MoCl_5 , which are suitable for vapor phase deposition of Mo.

11.4.3 Fabrication of the CIS Cell

While it is possible to produce both n-type and p-type CIS, homojunctions in the material are neither stable nor efficient. A good junction can be made, however, by creating a heterojunction with n-type CdS and p-type CIS.

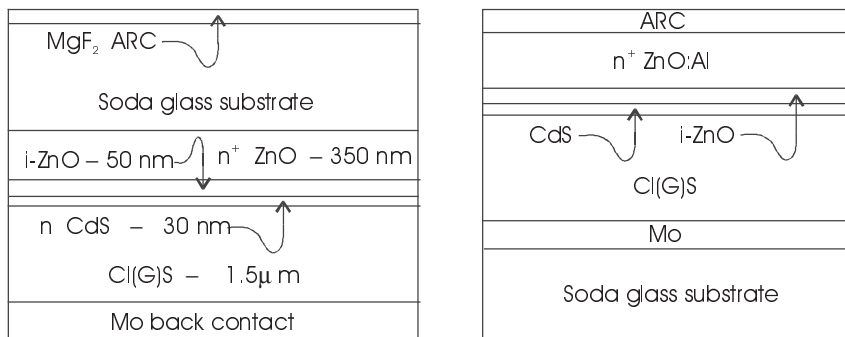


Figure 11.13 Typical CIGS thin-film structures [35, 36]. (Adapted from Ullal et al., *Proc 36th IEEE PV Spec Conf*, 1997, 301, ©IEEE.)

The ideal structure uses near-intrinsic material near the junction to create the widest possible depletion region for collection of generated EHPs. The carrier diffusion length can be as much as 2 μm , which is comparable with the overall film thickness. Figure 11.13 shows a basic $\text{ZnO}/\text{CdS}/\text{CIGS}/\text{Mo}$ cell structure, which is in popular use at the time of this writing. Again, CIGS technology is advancing rapidly as a result of the Thin-Film Photovoltaics Partnership Program, so by the time this paragraph is read, the structure of Figure 11.13 may be only suitable for history books and general discussion of the challenges encountered in thin-film cell development.

Nearly a dozen processes have been used to achieve the basic cell structure of Figure 11.13. The processes include rf sputtering, reactive sputtering, chemical vapor deposition, vacuum evaporation, spray deposition, and electrodeposition. Sometimes these processes are implemented sequentially and sometimes they are implemented concurrently.

In the physical vapor deposition (PVD) process, which was used to achieve a record laboratory cell efficiency, the constituent elements are deposited under a relatively high vacuum of 10^{-6} Torr. In the PVD process, the four elements can be simultaneously evaporated, they can be sequentially evaporated followed by exposure to Se or they can be sequentially evaporated in the presence of Se. The soda lime glass substrate is maintained between 300 and 600°C during the evaporation process.

The front ohmic contact is straightforward, and ZnO generally works well. The trick is to achieve sufficiently high conductivity without absorbing any of the incident photons. Often the ZnO is applied in two layers. The layer on the glass is fairly strongly n -type, with a very thin intrinsic layer in contact with the CdS . The more heavily doped layer has high conductivity, in the neighborhood of 4 Ω/square , and the narrow intrinsic layer acts as a passivation layer between the thin CdS layer and the TCO, but is narrow enough to allow efficient transport of electrons to the TCO.

11.4.4 Cell Performance

When new technology PV cells are developed, normally small area cells are fabricated first to determine whether it appears practical to extend the technology to larger area cells and modules. At the time of this writing, the highest performance achieved for a CIGS laboratory cell was 18.9% [25]. Scaling up to the production of minimodules with areas up to 100 cm^2 resulted in decrease in efficiency to 13% and further scaling up to 4 ft^2 modules generally resulted in efficiencies less than 10%. In March, 1999, Siemens Solar reported a 3651 cm^2 CIGSeS module with an efficiency confirmed by NREL of 12.1% [25].

Clearly, the challenge in module development is to overcome the factors that result in degradation of cell performance and clearly these challenges are being undertaken ambitiously. To do so requires understanding of the factors that cause the degradation. Some of these considerations include general device design, contact grid design, antireflection coatings and the sheet resistance of window layers.

An example of the trade-offs involved in scaling up a technology is the ZnO transparent contact. For a laboratory scale device with an area of 1 cm^2 or so, the ZnO layer can be relatively thin, with a sheet resistivity of $15\text{ }\Omega/\text{square}$, since the relatively small current from the cell will experience minimal voltage drop through this contact. The thin window absorbs a minimal amount of incident radiation so the CIS absorber layer can achieve maximum conversion efficiency. However, as the cell is made larger, the sheet resistance of the TCO must be reduced to prevent voltage drop at the contact and corresponding degradation of fill factor and cell efficiency. The price paid for lower sheet resistance is a greater amount of absorption of incident photons by the transparent contact.

Series connection of cells can also cause cell performance degradation. Figure 11.14 shows how individual cells have been replaced by minimodules that are monolithically connected. This monolithic connection process eliminates the need for separate fabrication processes for interconnecting cells.

After deposition of the Mo, it is scribed to separate adjacent cells, creating cells with a length of about 4 ft and a width of a fraction of an inch. Next, after deposition of the CIS cell components, the CIS is scribed. Finally, after deposition of the TCO, the TCO and CIS are scribed. While this process may appear to be straightforward, it can also be appreciated that the first cut needs to remove all of the Mo, but none of the glass. The second and third cuts must leave the Mo intact. Considering thickness of a few μm or less for these layers, the process falls somewhat short of being classified as trivial.

By incorporating Ga into the CIS mixture, the bandgap of the material can be increased beyond 1.1 eV. This movement of the bandgap energy closer to the peak of the solar spectrum increases conversion efficiency in this wavelength region and leaves lower energy photons for capture by the free carrier absorption process in the transparent conducting oxide (TCO) layer while the higher energy photons are converted to EHPs. The result is increasing the cell open-circuit voltage from approximately 0.4 V to as high as 0.68 V, with fill factors ap-

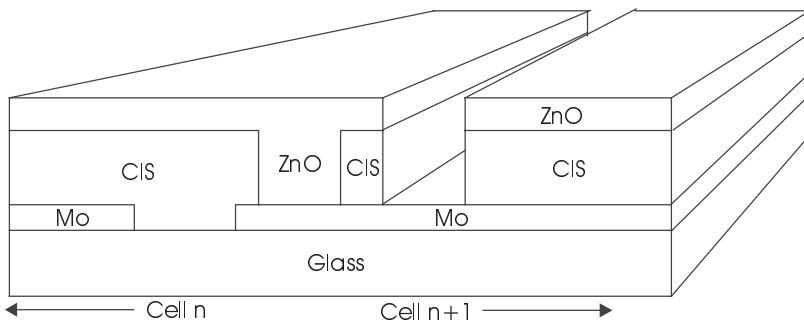


Figure 11.14 Siemens monolithic method of series cell connection [37].

proaching 80% for laboratory cells. Experiments with adding sulfur to the selenium have also resulted in cell performance improvements.

Transient Effects

Unlike the a-Si cells, the CIS cells have shown good long-term outdoor stability, with interesting recovery behavior for cells that have been light-starved. Siemens Solar (now Shell Solar) 4 ft² modules have been tested for 7 years with evidence of minimal module degradation over time. Earlier modules (1990) had aperture efficiencies in the neighborhood of 7%; a 2002 module achieved an efficiency of 7.4% on a metal foil substrate [25] and a conventional CIGS module attained an efficiency of 13.6% [38].

Exposure to more intense light has actually caused efficiencies to increase. Exposure to elevated temperatures has resulted in loss of efficiency, but light soaking has restored the modules to original efficiency levels.

11.5 Cadmium Telluride Cells

11.5.1 Introduction

In theory, CdTe cells have a maximum efficiency limit close to 25%. The material has a favorable direct bandgap and a large absorption constant, allowing for cells of a few μm thickness. By 2001, efficiencies approaching 17% were being achieved for laboratory cells, and module efficiencies had reached 11% for the best large area (8390 cm^2) module [25]. Although tellurium is not as abundant as other cell components, cadmium and tellurium are both available in sufficient quantities for the production of many gigawatts of array. The amount of cadmium poses a possible fire hazard and some concern at the time of decommissioning of the modules, as indicated in Chapter 9. Analysis of the concerns, however, has shown that the Cd of the cells would be recycled at decommissioning time and that the danger of burns from any fire far exceeds the danger of contact with any Cd released from heating of the modules. Means for recycling CdTe modules exist that result in recovery of glass, CdCO_3 , electrolytically refined Te and clean EVA at a cost of less than \$0.04 per watt [39].

At the time of this writing, CdTe modules are undergoing large-scale testing, but are not yet commercially available. Progress toward commercialization is rapid, and it is likely that by the time this paragraph is bound by a hard cover, commercial CdTe modules will be available. Purification of all of the components of the CdTe cell have been discussed so far except the Te. After a brief summary of the extraction and purification of Te, cell fabrication and cell performance will be discussed.

11.5.2 Production of Pure Tellurium [33]

Tellurium is a group VI metallic element, which was discovered by Muller in Transylvanian gold ore in 1782 and first extracted and identified by M. H. Klaproth in 1798. It is found as tellurides of copper, lead, silver, gold, iron and bismuth and is widely distributed over the surface of the earth, although its percentage in the earth's crust is very small. The primary sources of tellurium for production are leftovers from copper and lead refining, where tellurium and selenium both appear in very small quantities.

When copper is produced by electrolysis, the tellurium is precipitated along with other impurities in the copper to become a sludge at the anode. Several alternative chemical means are then used to separate the tellurium from the other impurities in the sludge. The first step is to produce tellurium dioxide, which precipitates out of solution while the other impurities remain dissolved. Alternatively, other impurities may first be precipitated, leaving behind higher concentrations of tellurium in the form of tellurous acid. If the oxide is produced, then the oxide is reduced to form elemental tellurium.

Elemental tellurium remains contaminated with iron, copper, tin, silver, lead, antimony and bismuth and can be further purified by low pressure distillation, where the heavier metals remain in the residue. Selenium, however, is volatile and remains a contaminant in the distilled tellurium. Further purification can be achieved by dissolving the tellurium in strong nitric acid. Diluting and boiling hydrolyzes the tellurium to a precipitate form. The precipitate is separated, washed, dissolved in hydrochloric acid and reduced with sulfur dioxide.

This relatively pure tellurium can be brought to the ultrahigh purity state by zone refining in an inert gas atmosphere, and single crystals can be grown by either the Czochralski or Bridgman methods.

Tellurium is classified as “probably” toxic and reasonable care is recommended in its handling.

11.5.3 Production of the CdTe Cell

Figure 11.15 shows a typical CdTe cell structure. The cell begins with a glass superstrate with a transparent, conducting, oxide layer about $1\text{ }\mu\text{m}$ thick, a thin CdS buffer layer about $0.1\text{ }\mu\text{m}$ thick, a CdTe layer a few μm thick and a rear contact of Au, Cu/Au, Ni, Ni/Al, ZnTe:Cu or (Cu, HgTe).

The TCO layer has been fabricated with SnO_x, InSnO and Cd₂SnO₄. The

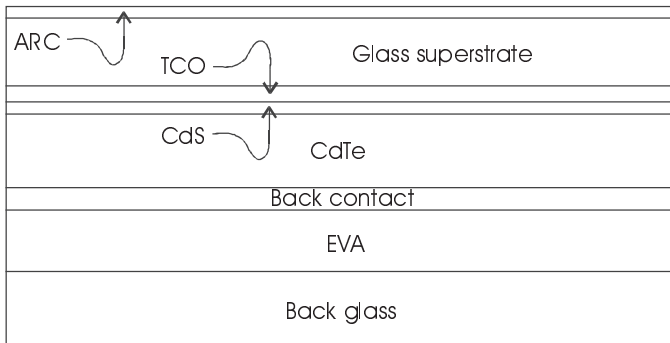


Figure 11.15 Basic structure of a CdTe PV cell [35]. (Adapted from Ullal et al., *Proc 26th IEEE PV Spec Conf*, 1997, 301, © 1997 IEEE.)

Cd_2SnO_4 has been shown to exhibit better conductivity and better transparency [40] than the other TCOs and may end up as the preferred TCO. The Cd_2SnO_4 layer is deposited by combining CdO and SnO_2 in a 2:1 proportion in a target material, which is then deposited by means of radio frequency magnetron sputtering onto the glass superstrate.

The thin n-type CdS layer has been deposited by the metal organic chemical vapor deposit (MOCVD) process as well as by other thin film deposition techniques. The layer needs to be annealed prior to deposition of the CdTe in order to reduce CdS surface roughness, thus reducing defects on the CdS/CdTe boundary. This is normally accomplished in air at approximately 400°C for about 20 minutes.

An interesting challenge exists with regard to the CdS layer, since the layer is so thin. During deposition of the CdTe or subsequent heat treatment of the cell, intermixing of the CdS and CdTe can occur at the boundary. This can result in junctions between the CdTe and the TCO layer, which causes significant reductions in cell open-circuit voltage. Several methods of minimizing this mixing have been proposed [41].

Numerous methods have been used to deposit the CdTe layer, including atmospheric pressure chemical vapor deposition (APCVD), atomic layer epitaxy (ALE), close-spaced sublimation (CSS), electrodeposition (ED), laser ablation, physical vapor deposition (PVD), screen printing (SP), spray, sputtering and MOCVD [25]. The CdTe layer is subjected to a heat treatment in the presence of CdCl_2 for about 20 minutes at about 420°C. This treatment enhances grain growth in the CdTe layer to reduce grain boundary trapping effects on minority carriers. Nonheat-treated CdTe cells tend to have open-circuit voltages less than 0.5 V, while after heat treating, V_{OC} can exceed 0.8 V.

Another important step in optimizing cell performance is to ensure stability of the back contact. Before the back contact is applied, the CdTe is etched with nitric-phosphoric (NP), resulting in a layer of elemental Te at the back CdTe surface. The elemental Te produces a more stable contact between the p-type CdTe and the back metal [42].

Final processing of modules involves encapsulation of the back of the cell with a layer of EVA between the metallization and another layer of glass.

11.5.4 Cell Performance

No fewer than nine companies have shown an interest in commercial applications of CdTe. As of 2001, depending on the fabrication methodology, efficiencies of close to 17% had been achieved for small area cells ($\approx 1 \text{ cm}^2$), and 11% on a module with an area of 8390 cm^2 [25]. Sufficient experience has been logged with large-scale production to identify areas in which improvement is needed [43]. These areas include improving the design, operation and control of a CdTe reactor; increasing the understanding of the fundamental properties of CdTe films; maintaining uniformity of materials and device properties over large areas, including the interdiffusion of CdTe and CdS and the back contact; obtaining stability of the back contact and addressing any environmental concerns over Cd. Since Te availability may limit cell production, increasing performance with thinner layers of CdTe is also desirable. Reducing the thickness of the CdTe layer to $0.5 \mu\text{m}$ will allow for four to five times the cell area, provided that efficiency can be maintained or increased. Just as in the case of other thin-film arrays, area-related costs limit the minimal cost per watt of CdTe arrays, so increase in efficiency is important to minimize cost per watt.

Fill factors for lab cells have been obtained in the 65- to 75% range [44], with the slope of the cell J-V curve at V_{OC} in the range of $5 \Omega\text{-cm}^2$. Short-circuit current densities upward from 25 mA/cm^2 have been obtained by using a thin buffer layer of CdS along with a thin insulating TCO layer between the heavily doped TCO and the CdS layer [25].

Experimental CdTe arrays in sizes up to 25 kW have been deployed in California, Ohio, Tunisia, Colorado and Florida for testing purposes [25]. Two 25 kW arrays are in use at Edwards Air Force Base in California as a power source for electrolysis of water to provide H_2 for fuel cells. Two 10 kW arrays are connected to utility grids and are reported to be performing very well. No degradation has been observed for the first 2 years of operation.

11.6 Emerging Technologies

11.6.1 New Developments in Silicon Technology

While progress continues on conventional Si technology, new ideas are also being pursued for crystalline and amorphous Si cells. The goal of Si technology has been to maintain good transport properties, while improving photon absorption and reducing the material processing cost of the cells. When the thickness of Si is reduced, some sort of substrate material is required to maintain sufficient physical strength for the cell. Two substrates that seem to show promise are ceramic and graphite, both having led to cell efficiencies in the 10% range [45]. Diffusion of contaminants such as Mg, Mn and Fe from ceramic substrates has been shown to limit performance of Si on ceramics, and methods of introducing

barrier layers at the Si-ceramic interface have been shown to limit the introduction of contaminants into the Si [46]. It is likely that these and other versions of thin Si cells will continue to attract the attention of the PV community.

Another interesting opportunity for cost reduction in Si cell production is to double up on processing steps. For example, a technique has been developed for simultaneously diffusing boron and phosphorous in a single step, along with growing a passivating oxide layer [45].

As an alternative to the pn junction approach to Si cells, MIS-IL (Metal insulator semiconductor inversion layer) cells have been fabricated with 18.5% efficiency [47]. The cell structure is shown in Figure 11.16. The cell incorporates a point-contacted back electrode to minimize the rear surface recombination, along with Cs beneath the MIS front grid and oxide window passivation of the front surface to define the cell boundaries. Further improvement in cell performance can be obtained by texturing the cell surfaces.

The MIS-IL cell uses the top SiO_x layer as a tunnel junction. The presence of positive charges in the SiO_x layer creates the electric field from oxide to p-Si, thus creating the inversion layer at the top of the p-type material. This field then separates the EHPs just as the E-field at a pn junction separates the carriers.

Other groups have worked on cells with both contacts on the back, in order to eliminate the shadowing of the front surface by the front contacts [44]. The ACE Designs project, funded by the European Community, resulted in the development of three types of rear contact Si cells—metallization wraparound (MWA), metallization wrap-through (MWT) and emitter wrap-through (EWT). A laser-grooved, buried grid process (LGBG) applied to the MWA technology is estimated to have the best potential for lowest cost rear contacted cells [48].

New developments in surface texturing may also simplify the process and result in additional improvement in Si device performance. Discovery of new substrates and methods of growing good quality Si on them is also an interesting possibility for performance improvement and cost reduction for Si cells.

Another idea that has been investigated is to combine crystalline and amorphous Si into a tandem cell arrangement to take advantage of the different band-gaps of the two materials in increasing absorption efficiency [49]. Recent work in Japan has produced a 1cm^2 tandem cell with an open-circuit voltage of 1.4 V,

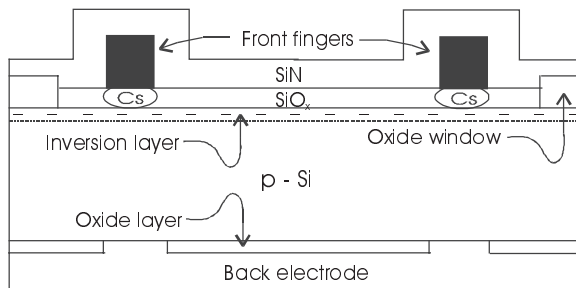


Figure 11.16 Structure of an MIS-inversion layer Si cell [47]. (Adapted from Metz, et al., Proc 26th IEEE PV Spec Conf, 1997, 31, ©1997 IEEE.)

a fill factor of 71.9% and an efficiency of 14.5% [50]. The cell is composed of a textured transparent conducting oxide on a glass substrate, followed by an a-Si:H cell, an interlayer, a microcrystalline Si cell and a back contact/reflector. The interlayer is incorporated to produce some reflection of the incident photons back into the a-Si to better match the current densities of the two cells.

Work also continues on dendritic web Si. Current standard dendritic web cell thicknesses are 100 μm . Recent reports describe 70 μm cell thickness, with cell efficiencies up to 14.1% [51].

Still another interesting process for producing crystalline, thin-film Si cells involves the epitaxial growth of very thin crystalline cells on existing crystalline cells [52]. The growth takes place at a temperature that does not melt the existing cell, and thus the epitaxially grown cell can be “peeled” off the existing cell and mounted on its own substrate, usually glass. By fabricating the new cell on a cell with a textured surface, the new cell also will have a textured surface. The overall thickness of the epitaxially grown cell is less than 20 μm , and the epitaxial growth process is convenient for adding n-type impurities and then switching to p-type impurities to produce the pn junction of the cell. The thin layers justify epitaxial growth as the mechanism for cell production.

Since new ideas will continue to emerge as interest in Si PV technology continues to grow, the interested reader is encouraged to attend PV conferences and to read the conference publications to stay up-to-date in the field.

11.6.2 CIS-Family-Based Absorbers

Figure 11.17 shows the theoretical maximum efficiency of a solar absorber as a function of bandgap. Table 11.2 shows the bandgaps of a family of CIS-type materials. Much is yet to be learned about inhomogeneous absorbers and composite absorbers composed of combinations of these various materials. The possibility of multijunction devices is also being explored.

Efficiency of large-area devices is critically dependent on spatial uniformity

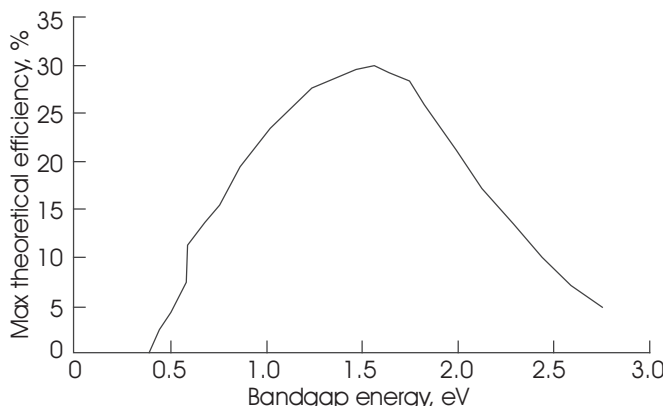


Figure 11.17 Theoretical maximum PV cell efficiency vs. bandgap [53].

of the absorber layers and electrodes as well as on the performance of cell interconnects. Hence, with any of the listed absorber possibilities, the key to performance will be in the engineering of reliable and reproducible module processing techniques.

Even an issue as mundane as the quality and cleanliness of the glass substrate can have a significant effect on module performance. Polishing the glass with CeO₂ has been shown to increase module performance [54]. Furthermore, it appears that if a certain amount of Na diffuses from the glass to the absorber, the absorber performance is increased [53].

Table 11.2 Bandgaps of CIS-related materials [54].

Material	Bandgap
CuInSe ₂	1.05 eV
AgInSe ₂	1.24 eV
CuInS ₂	1.56 eV
CuGaSe ₂	1.67 eV
AgGaSe ₂	1.69 eV
AgInS ₂	1.95 eV
CuGaS ₂	2.33 eV
AgGaS ₂	2.56 eV

Meanwhile, work is underway to reduce the material usage in the production of CIS modules in order to further reduce production costs. Examples of reduction of material use include halving the width of the Mo contact layer, reduction in the use of H₂S and H₂Se and a reduction in ZnO, provided that a minimum thickness can be maintained [55].

11.6.3 Other III-V and II-VI Emerging Technologies

It appears that compound tandem cells will receive appreciable emphasis in the III-V family of cells over the next few years. For example, Ga_{0.84}In_{0.16}As_{0.68}P_{0.32}, lattice matched to GaAs, has a bandgap of 1.55 eV and may prove to be an ideal material for use under AM0 conditions, since it also has good radiation resistance [56]. Cells have been fabricated with Al_{0.51}In_{0.49}P and Ga_{0.51}In_{0.49}P window layers, with the best 1 cm² cell having an efficiency of just over 16%, but having a fill factor of 85.4%. The best performing window was the AlInP.

Mechanical stacking of materials having different lattice constants has also been proposed [57]. Performance modeling of a proposed 26-layer, 4-junction device based on GaInP, GaAs, GaInAsP and GaInAs has shown the possibility of 35.3% conversion efficiency.

Cell efficiencies can be increased by concentrating sunlight on the cells. Although the homojunction cell efficiency limit under concentration is just under 40%, quantum well (QW) cells have been proposed to increase the concentrated efficiency beyond the 40% level [58]. In QW cells, intermediate energy

levels are introduced between the host semiconductor's valence and conduction bands to permit absorption of lower energy photons. These levels must be chosen carefully so they will not act as recombination centers, however, or the gains of EHPs from lower energy incident photons will be lost to the recombination processes. Laboratory cells have shown higher V_{OC} resulting from a decrease in dark current for these cells. Intense study is underway with the goal of understanding the electronic processes that take place within these cells [59].

11.6.4 Other Technologies

Thermophotovoltaic Cells

To this point, discussion has been limited to the conversion of visible and near infrared spectrum to EHPs. The reason is simply that the solar spectrum peaks out in the visible range. However, heat sources and incandescent light sources produce radiation in the longer infrared regions, and in some instances, it is convenient to harness radiated heat from these processes by converting it to electricity. This means using semiconductors with smaller bandgaps, such as Ge. More exotic structures, such as InAsSbP, with a bandgap of 0.45-0.48 eV have also been fabricated. The InAsSbP can be fabricated as p-type and n-type. The pn junction is grown on a substrate of InAs [60].

Intermediate Band Solar Cells

In all cells described to this point, absorption of a photon has resulted in the generation of a single EHP. If an intermediate band material is sandwiched between two ordinary semiconductors, it appears that it may be possible for the material to absorb two photons of relatively low energy to produce a single EHP at the combined energies of the two lower energy photons. The first photon raises an electron from the valence band to the intermediate level, creating a hole in the valence band, and the second photon raises the electron from the intermediate level to the conduction band. The trick is to find such an intermediate band material that will "hold" the electron until another photon of the appropriate energy impinges upon the material. Such a material should have half its states filled with electrons and half empty in order to optimally accommodate this electron transfer process. It appears that III-V compounds may be the best candidates for implementation of this technology. Theoretical maximum efficiency of such a cell is 63.2% [61].

Supertandem Cells

If a large number of cells are stacked with the largest bandgap on top and the bandgap of subsequent cells decreasing, the theoretical maximum efficiency is 86.8% [62]. A 1 cm^2 4-junction cell has been fabricated with an efficiency of 35.4%. The maximum theoretical efficiency of this cell is 41.6% [63]. Perhaps one day one of the readers of this paragraph (or one of their great-great grandchildren) will fabricate a cell with the maximum theoretical efficiency.

Hot Carrier Cells

The primary loss mechanism in PVcells is the energy lost in the form of heat when an electron is excited to a state above the bottom of the conduction band of a PV cell by a photon with energy greater than the bandgap. The electron will normally drop to the lowest energy available state in the conduction band, with the energy lost in the process being converted to heat. Hence, if this loss mechanism can be overcome, the efficiency of a cell with a single junction should be capable of approaching that of a supertandem cell. One method of preventing the release of this heat energy by the electron is to heat the cell, so the electron will remain at the higher energy state. The process is called *thermoelectronics* and is currently being investigated [62].

Optical Up-and Down-Conversion

An alternative to varying the electrical bandgap of a material is to reshape the energies of the incident photon flux. Certain materials have been shown to be capable of absorbing two photons of two different energies and subsequently emitting a photon of the combined energy. Other materials have been shown to be capable of absorbing a single high-energy photon and emitting two lower energy photons. These phenomena are similar to up-conversion and down-conversion in communications circuits at radio frequencies.

By the use of both types of materials, the spectrum incident on a PV cell can be effectively narrowed to a range that will result in more efficient absorption in the PV cell. An advantage of this process is that the optical up-and-down converters need not be a part of the PV cell. They simply need to be placed between the photon source and the PV cell. In tandem cells, the down-converter would be placed ahead of the top cell and the up-converter would be integrated into the cell structure just ahead of the bottom cell.

Organic PV Cells

Even more exotic than any of the previously mentioned cells is the organic cell. In the organic cell, electrons and holes are not immediately formed as the photon is absorbed. Instead, the incident photon creates an *exciton*, which is a bound EHP. In order to free the charges, the exciton binding energy must be overcome. This dissociation occurs at the interface between materials of high electron affinity and low ionization potential [63]. Photoluminescence is related to this process. Just to end this chapter with a little chemistry, the reader will certainly want to know that one material that is a candidate for organic PV happens to be poly{2,5-dimethoxy-1,4-phenylene-1,2-ethenylene-2-methoxy-5-(2-ethyl-hexyloxy)-1,4-phenylene-1,2-ethenylene}, which goes by the nickname M3EH-PPV. Whether M3EH-PPV will dominate the PV market one day remains to be seen. So far efficiencies of this very challenging technology have been in the 1% range.

11.6.5 Summary

Regardless of the technology or technologies that may result in low-cost, high-performance PV cells, it must be recognized that the life cycle cost of a cell depends on the cell's having the longest possible, maintenance-free lifetime. Thus, along with the developments of new technologies for absorbers, development of reliable encapsulants and packaging for the modules will also merit continued research and development activity.

Every year engineers make improvements on products that have been in existence for many years. Automobiles, airplanes, electronic equipment, building materials and many more common items see improvement every year. Even the yo-yo, a popular children's toy during the 1940s and 1950s, came back with better-performing models. Hence, it should come as no surprise to the engineer to see significant improvements and scientific breakthroughs in the PV industry well into the next millennium. The years ahead promise exciting times for the engineers and scientists working on the development of new photovoltaic cell and system technologies.

Problems

- 11.1. Assume a PV module is to have dimensions of 1 ft x 4 ft. Also assume that 4-inch round cells are available.
 - a. Calculate the percentage of the module area that will be covered with circular cells.
 - b. Assume 6-inch diameter cells are available so they can have their edges sawed to produce cells that are 4 inches across. Calculate the percentage fill of these "squared up" cells.
 - c. What is the percentage loss of material in the "squaring up" process?
 - d. Repeat b and c for 5-inch diameter cells.
- 11.2. Determine the expression for the depth of the junction after the drive-in diffusion step.
- 11.3. Sketch the impurity distribution profile between the junction and the back contact of a single crystal silicon cell to show how the annealed aluminum of the back contact creates an accelerating E-field.
- 11.4. What volume and weight of tellurium is needed to produce a square meter of CdTe thin film with a thickness of $1.5 \mu\text{m}$? Assume the Cd and Te occupy equal volumes within the film.

11.5. What volume and weight of indium is required to fabricate a 1 MW PV CIS array if the CIS layer thickness is 1.5 μm , assuming that 18% of the layer volume is due to the In. Assume an array efficiency of 10% and standard test conditions.

References

- [1] Ullal, H., et al., *Proc. 29th IEEE PV Spec. Conf.*, 2002, 472–7 .
- [2] Tarrant, D. E. and Gay, R. R., *Research on High Efficiency, Large Area CuInSe₂ - Based Thin Film Modules, Final Technical Report*, NREL, Golden, CO, April 1995.
- [3] <http://www.eia.gov/pub/international/> (Worldwide electrical generation capacity data.)
- [4] Markvart, T., Ed., *Solar Electricity*, John Wiley & Sons, Chichester, U.K., 1994.
- [5] Ciszek, T. F., *Proc. 20th IEEE PV Spec Conf.*, 1988, 31.
- [6] Streetman, B. G., *Solid State Electronic Devices*, 4th Ed., Prentice Hall, Englewood Cliffs, NJ, 1995.
- [7] Bohland, J., Accelerated aging of PV encapsulants by high intensity UV exposure, *Proc. 1998 Photovoltaic Performance and Reliability Workshop*, Cocoa Beach, FL, November 3–5, 1998.
- [8] www.ase-international.com (For information on EFG process)
- [9] Rosenblum, A.E., et al., *Proc. 29th IEEE PV Spec. Conf.*, 2002, 58–61.
- [10] Hanoka, J. I., *Proc. 29th IEEE PV Spec. Conf.*, 2002, 66–69.
- [11] Green, M. A. and Wenham, S. R., Novel parallel multijunction solar cell, *Applied Physics Letters* 65, 1994, 2907.
- [12] Green, M. A., *Proc. 29th IEEE PV Spec. Conf.*, 2002, 9–14.
- [13] DelleDonne, E., et al., *Proc. 29th IEEE PV Spec. Conf.*, 2002, 82–85.
- [14] Basore, Paul A., *Proc. 29th IEEE PV Spec. Conf.*, 2002, 49–52.
- [15] Brendel, R., et al., *Proc. 29th IEEE PV Spec. Conf.*, 2002, 86–89.
- [16] Guha, S., Yang, J., et al., *Proc. 26th IEEE PV Spec. Conf.*, 1997, 607–610.
- [17] Huang, J., Lee, Y., et al., *Proc. 26th IEEE PV Spec. Conf.*, 1997, 699–702.
- [18] Guha, S., and Yang, J., *Proc. 29th IEEE PV Spec. Conf.*, 2002, 1070–1075.
- [19] Yang, J., Banerjee, A., et al., *Proc. 26th IEEE PV Spec. Conf.*, 1997, 563–568.
- [20] Standen, A., Executive Ed., *Kirk-Othmer Encyclopedia of Chemical Technology*, 2nd Ed., Vol 10, John Wiley & Sons, New York, 1968.
- [21] Standen, A., Executive Ed., *Kirk-Othmer Encyclopedia of Chemical Technology*, 2nd Ed., Vol 2, John Wiley & Sons, New York, 1968.
- [22] Williams, R., *Modern GaAs Processing Methods*, Artech House, Norwood, MA, 1990.
- [23] Lammansniemi, J., et al., *Proc. 26th IEEE PV Spec. Conf.*, 1997, 823–826.
- [24] Hoffman, R., et al., *Proc. 26th IEEE PV Spec. Conf.*, 1997, 815–818.
- [25] Kazmerski, L. L., *Proc. 29th IEEE PV Spec. Conf.*, 2002, 21–27.
- [26] Brown, M. R., et al., *Proc. 26th IEEE PV Spec. Conf.*, 1997, 805–810.
- [27] Shay, J. L., Wagner, S., and Kasper, H. M., *Applied Physics Letters*, 27, No. 2, 1975, 89.

- [28] Wiedeman, S., et al., *Proc. 14th NREL PV Program Review*, AIP Conf. Proceedings 394, Lakewood, CO, 1996, 133–142.
- [29] Standen, A., Executive Ed., *Kirk-Othmer Encyclopedia of Chemical Technology*, 2nd Ed., Vol 6, John Wiley & Sons, New York , 1968.
- [30] Standen, A., Executive Ed., *Kirk-Othmer Encyclopedia of Chemical Technology*, 2nd Ed., Vol 11, John Wiley & Sons, New York, 1968.
- [31] Standen, A., Executive Ed., *Kirk-Othmer Encyclopedia of Chemical Technology*, 2nd Ed., Vol 17, John Wiley & Sons, New York, 1968.
- [32] *The Encyclopedia Britannica*, 15th ed., Encyclopedia Britannica, Inc., Chicago, IL, 1997.
- [33] Standen, A., Executive Ed., *Kirk-Othmer Encyclopedia of Chemical Technology*, 2nd Ed., Vol 19, John Wiley & Sons, New York , 1968.
- [34] Standen, A., Executive Ed., *Kirk-Othmer Encyclopedia of Chemical Technology*, 2nd Ed., Vol 13, John Wiley & Sons, New York, 1968.
- [35] Ullal, H. S., Zweibel, K. and von Roedern, B., *Proc. 26th IEEE PV Spec. Conf.*, 1997, 301–305.
- [36] Carlson, D. E., et al., *Proc. 25th IEEE PV Spec. Conf*, 1996, 1023–1028.
- [37] Tarrant, D. E. and Gay, R. R., *Thin-Film Photovoltaic Partnership Program—CIS-based thin film PV Technology. Phase 2 Technical Report, October 1996–October 1997*, NREL report NREL/SR-520-24751, Golden, CO, May 1998.
- [38] Konagai, M., *Proc. 29th IEEE PV Spec. Conf.*, 2002, 38–43.
- [39] Bohland, J., et al., *Proc. 26th IEEE PV Spec. Conf.*, 1997, 355–358.
- [40] Wu, X., Sheldon, P., et. al, *Proc. 26th IEEE PV Spec. Conf.*, 1997, 347–350.
- [41] McCandless, B. E. and Birkmire, R. W., *Proc 26th IEEE PV Spec. Conf.*, 1997, 307–312.
- [42] Levi, D. H., et al., *Proc. 26th IEEE PV Spec. Conf.*, 1997, 351–354.
- [43] Birkmire, R. W., *Proc. 26th IEEE PV Spec. Conf.*, 1997, 295–300.
- [44] Zhou, C. Z., et al., *Proc. 26th IEEE PV Spec. Conf.*, 1997, 287–290.
- [45] Krygowski, T., Rohatgi, A., and Ruby, D., *Proc 26th IEEE PV Spec. Conf.*, 1997, 19–24.
- [46] Slaoui, A., et al., *Proc. 29th IEEE PV Spec. Conf.*, 2002, 90–93.
- [47] Metz, A., et al., *Proc. 26th IEEE PV Spec. Conf.*, 1997, 31–34.
- [48] Schönecker, A., et al., *Proc. 29th IEEE PV Spec. Conf.*, 2002, 106–109.
- [49] Kuznicki, Z. T., *Proc. 26th IEEE PV Spec. Conf.*, 1997, 291–294.
- [50] Yamamoto, K., et al., *Proc. 29th IEEE PV Spec. Conf.*, 2002, 1110–1113.
- [51] Meier, D. L., et al., *Proc. 29th IEEE PV Spec. Conf.*, 2002, 110–113.
- [52] Brendel, R., et al., *Proc. 29th IEEE PV Spec. Conf.*, 2002, 86–89.
- [53] Granata, J., Sites, J. R. and Tuttle, J. R., *Proc. 14th NREL PV Program Review*, AIP Conf. Proceedings 394, Lakewood, CO, 1996, 621–630.
- [54] Tarrant, D. E. and Gay, R. R., *Research on High Efficiency, Large Area CuInSe₂ Modules, Final Technical Report*, NREL, Golden, CO, April 1995.
- [55] Weiting, R., *Proc. 29th IEEE PV Spec. Conf.*, 2002, 478–483.
- [56] Jaakkola, R., et al., *Proc. 26th IEEE PV Spec. Conf.*, 1997, 891–894.
- [57] Sharps, P. R., et al., *Proc. 26th IEEE PV Spec. Conf.*, 1997, 895–898.
- [58] Barnham, K. W. J. and Duggan, G., A new approach to high-efficiency multi-band-gap solar cells, *J. Appl. Phys.* 67, 1990, 3490–3493.
- [59] Corkish, R. and Honsberg, C., *Proc. 26th IEEE PV Spec. Conf.*, 1997, 923–926.
- [60] Khvostikov, V. P., et al., *Proc. 29th IEEE PV Spec. Conf.*, 2002, 943–946.
- [61] Luque, A., et al., *Proc. 29th IEEE PV Spec. Conf.*, 2002, 1190–1193.

- [62] Green, M. A., *Proc. 29th IEEE PV Spec. Conf.*, 2002, 1330–1334.
- [63] Zahler, J. M., et al., *Proc. 29th IEEE PV Spec. Conf.*, 2002, 1029–1032.

Suggested Reading

- Brown, K. E., et al., *Proc. 29th IEEE PV Spec. Conf.*, 2002, 1186–1189.
- Goetzberger, A., *Proc. 26th IEEE PV Spec. Conf.*, 1997, 1–6.
- Hu, C. and White, R. M., *Solar Cells, From Basic to Advanced Systems*, McGraw-Hill, New York , 1983.
- Mahan, A. H., et al., *Proc. 14th NREL PV Program Review*, AIP Conf. Proceedings 394, Lakewood, CO, 1996, 27–32.
- Tuttle, J.R., et al., *Proc. 14th NREL PV Program Review*, AIP Conf. Proceedings 394, Lakewood, CO, 1996, 83–105.
- Weast, R. C., Ed-in-Chief; Lide, D. R., Ed.; Astle, M. J., Assoc. Ed.; Beyer, W. H., Assoc. Ed.; CRC *Handbook of Chemistry and Physics*, 70th Ed., CRC Press, Boca Raton, FL, 1990.

Appendix A

AVERAGE DAILY IRRADIATION FOR SELECTED CITIES

The U. S. data in the following tables has been compiled by the National Renewable Energy Laboratory. Data outside the U. S. has been compiled by Sandia National Laboratories. Average daily irradiation in kWh/m² is tabulated for each month of the year, including annual averages, for an assortment of orientations, including:

1. Fixed, south-facing arrays tilted at latitude -15° , latitude and latitude $+15^{\circ}$.
2. Single axis east-west tracking mounts tilted at three angles.
3. Horizontal and vertical mounts (U. S. data only).
4. Double axis tracking mounts.

The following cities are included, listed alphabetically by state, then by country. For 34 additional listings, the reader is encouraged to consult *Stand Alone Photovoltaic Systems, A Handbook of Recommended Design Practices*, by Sandia National Laboratories, Albuquerque, New Mexico. Appendix B lists the NREL and several other web sites that provide irradiation information.

1. Fairbanks, Alaska
2. Sacramento, California
3. Denver, Colorado
4. Miami, Florida
5. Atlanta, Georgia
6. Boston, Massachusetts
7. Albuquerque, New Mexico
8. Bismarck, North Dakota
9. Austin, Texas
10. Seattle, Washington
11. Luanda, Angola
12. Buenos Aires, Argentina
13. Melbourne, Australia
14. Shanghai, Peoples Republic of China
15. Paris-St. Maur, France
16. New Delhi, India
17. Tokyo, Japan
18. Nairobi, Kenya
19. Mexico D. F., Mexico
20. Stockholm, Sweden

Fairbanks, AK Average Daily Peak Sun Hours, kWh/m² Latitude: 64°49' N Longitude: 147°52' W

	Month	Jan	Feb	Mar	Apr	May	Jun	Jul	Aug	Sep	Oct	Nov	Dec	Avg
Array tilted at Latitude -15°	Fixed Array	0.7	2.2	4.5	5.6	5.7	5.7	5.4	4.5	3.4	1.9	1.0	0.2	3.4
	1-Axis Tracker	0.7	2.6	5.7	7.7	8.2	8.3	7.6	6.0	4.4	2.2	1.1	0.2	4.6
Array tilted at Latitude	Fixed Array	0.7	2.4	4.7	5.6	5.3	5.2	4.9	4.2	3.4	2.0	1.1	0.3	3.3
	1-Axis Tracker	0.8	2.7	5.9	7.7	8.0	8.0	7.4	5.8	4.4	2.3	1.2	0.3	4.5
Array tilted at Latitude +15°	Fixed Array	0.8	2.5	4.7	5.3	4.6	4.5	4.3	3.8	3.2	2.0	1.1	0.3	3.1
	1-Axis Tracker	0.8	2.8	5.8	7.4	7.6	7.6	6.9	5.5	4.2	2.3	1.2	0.3	4.4
Horizontal Array		0.1	0.8	2.3	4.0	5.1	5.6	5.1	3.7	2.3	1.0	0.3	0.0	2.5
Vertical South-facing Array		0.8	2.5	4.5	4.9	4.1	3.9	3.7	3.3	3.0	2.0	1.1	0.3	2.8
2-Axis Tracking Array		0.8	2.8	5.8	7.7	8.4	8.7	7.9	6.0	4.4	2.3	1.2	0.3	4.7

Sacramento, CA Average Daily Peak Sun Hours, kWh/m² Latitude: 38° 31'N Longitude: 121° 30'W

	Month	Jan	Feb	Mar	Apr	May	Jun	Jul	Aug	Sep	Oct	Nov	Dec	Avg
Array tilted at Latitude -15°	Fixed Array	2.6	3.9	5.2	6.5	7.3	7.6	7.8	7.5	6.7	5.3	3.3	2.4	5.5
	1-Axis Tracker	3.0	4.7	6.6	8.6	10.1	10.8	11.2	10.4	9.1	6.8	4.0	2.8	7.3
Array tilted at Latitude	Fixed Array	2.9	4.2	5.4	6.3	6.8	7.0	7.2	7.2	6.9	5.7	3.7	2.7	5.5
	1-Axis Tracker	3.3	4.9	6.7	8.5	9.8	10.3	10.8	10.2	9.2	7.1	4.3	3.0	7.4
Array tilted at Latitude +15°	Fixed Array	3.1	4.3	5.2	5.9	6.0	6.0	6.3	6.5	6.6	5.8	3.9	2.9	5.2
	1-Axis Tracker	3.4	5.0	6.6	8.2	9.2	9.7	10.1	9.8	9.0	7.2	4.5	3.2	7.2
Horizontal Array		1.9	3.0	4.3	5.9	7.2	7.9	7.9	7.0	5.7	4.0	2.4	1.7	4.9
Vertical South-facing Array		2.7	3.6	3.8	3.6	3.0	2.7	2.9	3.6	4.5	4.6	3.4	2.6	3.4
2-Axis Tracking Array		3.4	5.0	6.7	8.6	10.2	11.0	11.4	10.4	9.2	7.2	4.5	3.2	7.6

Denver, CO Average Daily Peak Sun Hours, kWh/m² Latitude: 39°45'N Longitude: 104°52'W

	Month	Jan	Feb	Mar	Apr	May	Jun	Jul	Aug	Sep	Oct	Nov	Dec	Avg
Array tilted at Latitude -15°	Fixed Array	3.8	4.6	5.4	6.1	6.2	6.6	6.3	5.9	5.1	4.0	3.5	5.4	
	1-Axis Tracker	4.8	5.9	7.0	8.1	8.4	9.1	9.1	8.6	7.9	6.7	5.0	4.4	7.1
Array tilted at Latitude	Fixed Array	4.4	5.1	5.6	6.0	5.9	6.1	6.1	6.0	5.6	4.6	4.2	5.5	
	1-Axis Tracker	5.2	6.2	7.2	8.0	8.1	8.8	8.7	8.4	7.9	7.1	5.5	4.9	7.2
Array tilted at Latitude +15°	Fixed Array	4.8	5.3	5.6	5.6	5.2	5.2	5.3	5.5	5.8	5.7	4.8	4.5	5.3
	1-Axis Tracker	5.5	6.4	7.1	7.7	7.7	8.2	8.2	8.0	7.8	7.1	5.7	5.2	7.1
Horizontal Array		2.4	3.3	4.4	5.6	6.2	6.9	6.7	6.0	5.0	3.8	2.6	2.1	4.6
Vertical South-facing Array		4.5	4.6	4.3	3.6	2.8	2.6	2.7	3.2	4.0	4.6	4.4	4.3	3.8
2-Axis Tracking Array		5.6	6.4	7.2	8.1	8.5	9.4	9.2	8.6	8.0	7.1	5.7	5.3	7.4

Miami, FL Average Daily Peak Sun Hours, kWh/m² Latitude: 25°48'N Longitude: 80°16'W

Month		Jan	Feb	Mar	Apr	May	Jun	Jul	Aug	Sep	Oct	Nov	Dec	Avg
Array tilted at Latitude -15°	Fixed Array	4.1	4.7	5.5	6.2	5.9	5.5	5.7	5.6	5.1	4.7	4.2	3.9	5.1
	1-Axis Tracker	5.2	6.1	7.0	7.9	7.4	6.6	7.0	6.9	6.2	5.9	5.2	4.9	6.4
Array tilted at Latitude	Fixed Array	4.7	5.2	5.7	6.1	5.6	5.1	5.4	5.5	5.1	5.1	4.7	4.5	5.2
	1-Axis Tracker	5.7	6.4	7.2	7.8	7.2	6.3	6.7	6.7	6.2	6.1	5.6	5.4	6.5
Array tilted at Latitude +15°	Fixed Array	5.0	5.4	5.6	5.7	5.0	4.5	4.8	5.0	4.9	5.1	4.9	4.9	5.1
	1-Axis Tracker	5.9	6.5	7.1	7.5	6.7	5.9	6.3	6.4	6.1	6.2	5.8	5.7	6.3
Horizontal Array		3.5	4.2	5.2	6.0	6.0	5.6	5.8	5.6	4.9	4.4	3.7	3.3	4.8
Vertical South-facing Array		4.1	3.9	3.4	2.6	1.9	1.6	1.7	2.1	2.7	3.5	3.9	4.1	3.0
2-Axis Tracking Array		6.0	6.6	7.2	7.9	7.4	6.7	7.1	6.9	6.2	6.2	5.9	5.8	6.7

Atlanta, GA Average Daily Peak Sun Hours, kWh/m² Latitude: 33° 39' N Longitude: 84° 36' W

Month		Jan	Feb	Mar	Apr	May	Jun	Jul	Aug	Sep	Oct	Nov	Dec	Avg
Array tilted at Latitude -15°	Fixed Array	3.4	4.2	5.1	6.0	6.2	6.3	6.1	5.9	5.3	4.9	3.8	3.2	5.0
	1-Axis Tracker	4.2	5.3	6.5	7.7	7.9	8.0	7.6	7.4	6.6	6.2	4.7	3.9	6.3
Array tilted at Latitude	Fixed Array	3.8	4.6	5.3	5.8	5.8	5.8	5.7	5.7	5.4	5.2	4.2	3.7	5.1
	1-Axis Tracker	4.5	5.5	6.6	7.6	7.7	7.6	7.3	7.2	6.7	6.4	5.0	4.3	6.4
Array tilted at Latitude +15°	Fixed Array	4.1	4.7	5.1	5.4	5.2	5.1	5.0	5.2	5.1	5.3	4.5	3.9	4.9
	1-Axis Tracker	4.7	5.6	6.5	7.3	7.2	7.1	6.8	6.9	6.5	6.5	5.2	4.5	6.2
Horizontal Array		2.6	3.4	4.5	5.7	6.2	6.4	6.2	5.7	4.8	4.1	2.9	2.4	4.6
Vertical South-facing Array		3.5	3.7	3.5	3.0	2.4	2.2	2.2	2.7	3.2	4.0	3.8	3.5	3.1
2-Axis Tracking Array		4.8	5.7	6.6	7.7	8.0	8.1	7.7	7.4	6.7	6.5	5.3	4.5	6.6

Boston, MA Average Daily Peak Sun Hours, kWh/m² Latitude: 41° 40'N Longitude: 71° 10'W

	Month	Jan	Feb	Mar	Apr	May	Jun	Jul	Aug	Sep	Oct	Nov	Dec	Avg
Array tilted at Latitude -15°	Fixed Array	3.0	3.8	4.6	5.2	5.7	6.0	5.7	5.0	4.1	2.8	2.5	4.5	
	1-Axis Tracker	3.6	4.7	5.7	6.5	7.3	7.7	7.8	7.3	6.3	5.0	3.4	2.9	5.7
Array tilted at Latitude	Fixed Array	3.4	4.2	4.7	5.0	5.3	5.5	5.6	5.5	5.1	4.3	3.1	2.9	4.6
	1-Axis Tracker	3.9	5.0	5.9	6.5	7.1	7.4	7.5	7.1	6.4	5.2	3.6	3.2	5.7
Array tilted at Latitude +15°	Fixed Array	3.6	4.3	4.6	4.7	4.7	4.8	4.9	5.0	4.9	4.4	3.3	3.1	4.4
	1-Axis Tracker	4.1	5.1	5.8	6.2	6.6	6.9	7.0	6.8	6.2	5.2	3.7	3.4	5.6
Horizontal Array		1.9	2.7	3.7	4.7	5.6	6.1	6.1	5.4	4.3	3.0	1.9	1.6	3.9
Vertical South-facing Array		3.4	3.9	3.7	3.1	2.8	2.6	2.8	3.1	3.5	3.6	3.0	2.9	3.2
2-Axis Tracking Array		4.1	5.1	5.9	6.6	7.4	7.9	7.9	7.3	6.4	5.3	3.8	3.4	5.9

Albuquerque, NM Average Daily Peak Sun Hours, kWh/m² Latitude: 35° 03' N Longitude: 106° 37' W

	Month	Jan	Feb	Mar	Apr	May	Jun	Jul	Aug	Sep	Oct	Nov	Dec	Avg
Array tilted at Latitude -15°	Fixed Array	4.6	5.4	6.3	7.3	7.7	7.8	7.4	7.2	6.6	5.9	4.8	4.3	6.3
	1-Axis Tracker	5.9	7.1	8.3	10.0	10.6	10.8	9.9	9.5	8.8	7.9	6.3	5.5	8.4
Array tilted at Latitude	Fixed Array	5.3	6.0	6.5	7.2	7.2	7.1	6.9	6.9	6.8	6.5	5.5	5.0	6.4
	1-Axis Tracker	6.5	7.5	8.6	9.9	10.3	10.4	9.5	9.3	9.0	8.3	6.8	6.1	8.5
Array tilted at Latitude +15°	Fixed Array	5.8	6.2	6.5	6.6	6.3	6.1	6.0	6.3	6.5	6.6	5.9	5.5	6.2
	1-Axis Tracker	6.9	7.7	8.5	9.5	9.7	9.7	8.9	8.9	8.8	8.4	7.1	6.5	8.4
Horizontal Array		3.2	4.2	5.4	6.8	73.7	8.1	7.5	6.9	5.9	4.7	3.5	2.9	5.6
Vertical South-facing Array		5.2	5.1	4.5	3.7	2.8	2.4	2.5	3.2	4.2	5.1	5.2	5.1	4.1
2-Axis Tracking Array		6.9	7.7	8.6	10.0	10.8	11.1	10.0	9.5	9.0	8.4	7.2	6.6	8.8

Bismarck, ND Average Daily Peak Sun Hours, kWh/m² Latitude: 46°46'N Longitude: 100°45'W

	Month	Jan	Feb	Mar	Apr	May	Jun	Jul	Aug	Sep	Oct	Nov	Dec	Avg
Array tilted at Latitude -15°	Fixed Array	3.1	4.0	5.0	5.6	6.1	6.5	6.8	6.4	5.3	4.2	2.9	2.6	4.9
	1-Axis Tracker	3.7	4.9	6.3	7.3	8.3	8.9	9.5	8.7	7.0	5.3	3.4	3.0	6.4
Array tilted at Latitude	Fixed Array	3.5	4.4	5.2	5.5	5.7	5.9	6.3	6.1	5.4	4.5	3.2	3.0	4.9
	1-Axis Tracker	4.0	5.2	6.4	7.3	8.0	8.6	9.2	8.5	7.0	5.5	3.7	3.3	6.4
Array tilted at Latitude +15°	Fixed Array	3.7	4.5	5.1	5.1	5.1	5.1	5.5	5.5	5.1	4.5	3.4	3.2	4.7
	1-Axis Tracker	4.2	5.3	6.4	7.0	7.6	8.0	8.6	8.1	6.8	5.5	3.9	3.5	6.3
Horizontal Array		1.7	2.6	3.8	4.9	6.0	6.6	6.8	5.8	4.2	2.8	1.7	1.4	4.0
Vertical South-facing Array		3.7	4.2	4.3	3.7	3.3	3.1	3.4	3.7	3.9	3.9	3.2	3.1	3.6
2-Axis Tracking Array		4.2	5.3	6.5	7.4	8.4	9.2	9.7	8.7	7.0	5.5	3.9	3.6	6.6

Austin, Texas Average Daily Peak Sun Hours, kWh/m² Latitude: 30° 18'N Longitude: 97° 42'W

	Month	Jan	Feb	Mar	Apr	May	Jun	Jul	Aug	Sep	Oct	Nov	Dec	Avg
Array tilted at Latitude -15°	Fixed Array	3.7	4.4	5.2	5.6	5.8	6.4	6.7	6.5	5.7	5.0	4.1	3.5	5.2
	1-Axis Tracker	4.6	5.6	6.6	7.1	7.3	8.3	8.7	8.5	7.3	6.5	5.1	4.4	6.7
Array tilted at Latitude	Fixed Array	4.2	4.8	5.4	5.5	5.5	5.9	6.2	6.3	5.8	5.4	4.6	4.0	5.3
	1-Axis Tracker	5.0	5.9	6.7	7.0	7.1	8.0	8.4	8.3	7.3	6.8	5.5	4.8	6.7
Array tilted at Latitude +15°	Fixed Array	4.4	5.0	5.3	5.1	4.9	5.1	5.4	5.7	5.5	5.5	4.8	4.3	5.1
	1-Axis Tracker	5.2	6.0	6.6	6.7	6.7	7.4	7.8	7.9	7.2	6.8	5.7	5.0	6.6
Horizontal Array		3.0	3.8	4.7	5.4	5.9	6.6	6.8	6.3	5.2	4.4	3.3	2.8	4.9
Vertical South-facing Array		3.8	3.8	3.4	2.7	2.1	1.9	2.0	2.6	3.3	4.0	4.0	3.8	3.1
2-Axis Tracking Array		5.2	6.0	6.7	7.1	7.4	8.5	8.9	8.5	7.4	6.9	5.7	5.1	7.0

Seattle, WA Average Daily Peak Sun Hours, kWh/m² Latitude: 47° 27' N Longitude: 122° 18' W

	Month	Jan	Feb	Mar	Apr	May	Jun	Jul	Aug	Sep	Oct	Nov	Dec	Avg
Array tilted at Latitude -15°	Fixed Array	1.5	2.3	3.5	4.6	5.4	5.7	6.1	5.6	4.7	3.0	1.7	1.3	3.8
	1-Axis Tracker	1.6	2.7	4.2	5.6	6.9	7.3	8.2	7.3	5.8	3.6	1.9	1.4	4.7
Array tilted at Latitude +15°	Fixed Array	1.6	2.5	3.6	4.4	5.1	5.2	5.7	5.4	4.7	3.2	1.8	1.4	3.7
	1-Axis Tracker	1.8	2.8	4.3	5.5	6.7	7.0	7.9	7.2	5.9	3.7	2.0	1.5	4.7
Horizontal Array	Fixed Array	1.7	2.5	3.5	4.1	4.5	4.5	4.9	4.9	4.5	3.2	1.8	1.4	3.5
	1-Axis Tracker	1.8	2.8	4.2	5.3	6.3	6.6	7.4	6.8	5.7	3.7	2.0	1.5	4.5
Vertical South-facing Array		1.0	1.7	2.8	4.1	5.3	5.8	6.1	5.2	3.8	2.2	1.2	0.8	3.3
2-Axis Tracking Array		1.5	2.2	2.8	3.0	3.0	2.8	3.1	3.4	3.4	2.7	1.7	1.3	2.6
		1.8	2.9	4.3	5.6	7.0	7.5	8.3	7.4	5.9	3.7	2.0	1.5	4.9

Luanda, AngolaAverage Daily Peak Sun Hours, kWh/m²

Latitude: 8° 49'S Longitude: 13° 13'W

Month	Array tilted at Latitude – 15°		Array tilted at Latitude		Array tilted at Latitude + 15°		2-Axis Tracking Array
	Fixed Array	1-Axis Tracker	Fixed Array	1-Axis Tracker	Fixed Array	1-Axis Tracker	
Jan	5.92	7.62	5.56	7.20	4.94	6.28	7.67
Feb	6.07	7.83	5.87	7.66	5.40	6.96	7.84
Mar	5.43	7.02	5.49	7.19	5.30	6.89	7.20
Apr	4.89	6.19	5.19	6.68	5.27	6.76	6.79
May	4.60	5.61	5.11	6.34	5.42	6.70	6.73
Jun	4.18	5.01	4.75	5.80	5.14	6.27	6.34
Jul	3.36	4.17	3.71	4.78	3.93	5.11	5.14
Aug	3.70	4.75	3.95	5.21	4.04	5.36	5.37
Sep	4.57	5.96	4.68	6.21	4.60	6.08	6.23
Oct	5.06	6.66	4.97	6.60	4.66	6.11	6.69
Nov	5.60	7.27	5.31	6.93	4.77	6.11	7.30
Dec	6.16	7.87	5.72	7.36	5.02	6.33	7.95
Ann Avg	4.96	6.33	5.03	6.50	4.87	6.25	6.77

Buenos Aires, ArgentinaAverage Daily Peak Sun Hours, kWh/m²

Latitude: 34° 58'S Longitude: 58° 48'W

Month	Array tilted at Latitude – 15°		Array tilted at Latitude		Array tilted at Latitude + 15°		2-Axis Tracking Array
	Fixed Array	1-Axis Tracker	Fixed Array	1-Axis Tracker	Fixed Array	1-Axis Tracker	
Jan	7.13	9.80	6.58	9.24	5.77	8.05	9.85
Feb	6.49	8.72	6.19	8.52	5.62	7.74	8.74
Mar	5.45	7.02	5.47	7.20	5.21	6.89	7.22
Apr	4.46	5.50	4.75	5.97	4.80	6.03	6.07
May	3.57	4.07	4.02	4.64	4.25	4.90	4.91
Jun	2.93	3.13	3.39	3.67	3.65	3.96	4.01
Jul	3.24	3.57	3.70	4.14	3.95	4.42	4.45
Aug	4.11	4.98	4.48	5.51	4.60	5.66	5.67
Sep	5.07	6.38	5.19	6.68	5.06	6.52	6.70
Oct	5.90	7.86	5.71	7.80	5.27	7.21	7.91
Nov	6.47	8.90	6.02	8.46	5.33	7.44	8.92
Dec	7.12	9.85	6.51	9.18	5.65	7.88	9.94
Ann Avg	5.16	6.65	5.17	6.75	4.93	6.39	7.03

Melbourne, AustraliaAverage Daily Peak Sun Hours, kWh/m²

Latitude: 37° 49'S Longitude: 144° 58'E

Month	Array tilted at Latitude – 15°		Array tilted at Latitude		Array tilted at Latitude + 15°		2-Axis Tracking Array
	Fixed Array	1-Axis Tracker	Fixed Array	1-Axis Tracker	Fixed Array	1-Axis Tracker	
Jan	7.15	9.95	6.60	9.39	5.78	8.19	9.99
Feb	6.37	8.63	6.07	8.44	5.51	7.68	8.65
Mar	3.96	5.38	3.94	5.53	3.74	5.30	5.54
Apr	4.14	5.06	4.41	5.49	4.45	5.55	5.58
May	3.51	3.93	3.96	4.49	4.20	4.74	4.76
Jun	3.13	3.32	3.65	3.90	3.96	4.22	4.27
Jul	3.31	3.61	3.80	4.19	4.08	4.48	4.51
Aug	3.72	4.37	4.05	4.85	4.17	4.99	4.99
Sep	4.61	5.89	4.72	6.17	4.59	6.04	6.19
Oct	5.36	7.27	5.18	7.22	4.77	6.68	7.32
Nov	5.37	7.62	5.01	7.25	4.45	6.39	7.63
Dec	5.93	8.45	5.45	7.88	4.77	6.78	8.51
Ann Avg	4.71	6.21	4.74	6.23	4.54	5.92	6.50

Shanghai, ChinaAverage Daily Peak Sun Hours, kWh/m²

Latitude: 31° 17'N Longitude: 121° 28'E

Month	Array tilted at Latitude – 15°		Array tilted at Latitude		Array tilted at Latitude + 15°		2-Axis Tracking Array
	Fixed Array	1-Axis Tracker	Fixed Array	1-Axis Tracker	Fixed Array	1-Axis Tracker	
Jan	3.38	3.74	3.82	4.31	4.06	4.59	4.62
Feb	3.07	3.55	3.28	3.92	3.33	4.02	4.03
Mar	4.27	5.54	4.35	5.80	4.23	5.67	5.82
Apr	4.85	6.58	4.70	6.53	4.34	6.04	6.62
May	5.34	7.38	4.99	7.02	4.45	6.17	7.40
Jun	4.69	6.63	4.33	6.17	3.83	5.29	6.69
Jul	5.82	8.01	5.38	7.53	4.74	6.54	8.06
Aug	5.99	8.04	5.72	7.84	5.20	7.11	8.05
Sep	5.20	6.72	5.22	6.90	4.98	6.61	6.91
Oct	4.38	5.37	4.66	5.83	4.71	5.89	5.93
Nov	3.47	3.90	3.88	4.45	4.08	4.70	4.72
Dec	3.11	3.35	3.57	3.92	3.84	4.22	4.27
Ann Avg	4.46	5.73	4.49	5.85	4.32	5.57	6.09

Paris-St. Maur, FranceAverage Daily Peak Sun Hours, kWh/m²

Latitude: 48° 49'N Longitude: 2° 30'E

Month	Array tilted at Latitude – 15°		Array tilted at Latitude		Array tilted at Latitude + 15°		2-Axis Tracking Array
	Fixed Array	1-Axis Tracker	Fixed Array	1-Axis Tracker	Fixed Array	1-Axis Tracker	
Jan	1.77	1.77	2.06	2.06	2.24	2.24	2.24
Feb	2.47	2.54	2.75	2.82	2.91	2.94	2.94
Mar	3.75	4.56	3.90	4.79	3.88	4.69	4.81
Apr	4.32	6.02	4.25	5.99	4.04	5.54	6.06
May	5.01	7.39	4.78	7.05	4.41	6.22	7.41
Jun	5.37	8.04	5.05	7.50	4.61	6.45	8.10
Jul	5.14	7.66	4.87	7.21	4.47	6.28	7.69
Aug	4.59	6.60	4.45	6.46	4.18	5.87	6.62
Sep	3.95	5.04	4.02	5.19	3.93	4.98	5.20
Oct	2.74	3.01	2.95	3.27	3.02	3.31	3.33
Nov	1.71	1.71	1.95	1.95	2.11	2.11	2.11
Dec	1.56	1.56	1.83	1.83	2.02	2.02	2.02
Ann Avg	3.53	4.66	3.57	4.68	3.49	4.39	4.88

New Delhi, IndiaAverage Daily Peak Sun Hours, kWh/m²

Latitude: 28° 35'N Longitude: 77° 12'E

Month	Array tilted at Latitude – 15°		Array tilted at Latitude		Array tilted at Latitude + 15°		2-Axis Tracking Array
	Fixed Array	1-Axis Tracker	Fixed Array	1-Axis Tracker	Fixed Array	1-Axis Tracker	
Jan	5.04	6.38	5.83	7.38	6.28	7.87	7.92
Feb	6.37	8.09	7.04	8.97	7.31	9.23	9.24
Mar	7.05	8.60	7.31	9.02	7.18	8.83	9.05
Apr	7.12	9.23	6.94	9.17	6.42	8.50	9.30
May	7.38	9.83	6.87	9.36	6.08	8.25	9.86
Jun	6.76	9.15	6.19	8.53	5.38	7.32	9.23
Jul	4.50	6.31	4.20	5.94	3.75	5.17	6.34
Aug	5.53	7.44	5.30	7.27	4.83	6.60	7.46
Sep	5.66	7.23	5.70	7.44	5.46	7.13	7.45
Oct	6.09	7.34	6.57	7.99	6.69	8.09	8.13
Nov	5.62	7.49	6.43	8.56	6.88	9.05	9.08
Dec	4.87	6.06	5.73	7.11	6.26	7.68	7.77
Ann Avg	6.00	7.76	6.18	8.06	6.04	7.81	8.40

Tokyo, Japan
 Average Daily Peak Sun Hours, kWh/m²
 Latitude: 35° 41'N Longitude: 140° 14'W

Month	Array tilted at Latitude – 15°		Array tilted at Latitude		Array tilted at Latitude + 15°		2-Axis Tracking Array
	Fixed Array	1-Axis Tracker	Fixed Array	1-Axis Tracker	Fixed Array	1-Axis Tracker	
Jan	2.95	3.14	3.34	3.63	3.55	3.87	3.90
Feb	3.22	3.64	3.47	4.03	3.53	4.14	4.15
Mar	3.42	4.52	3.47	4.74	3.35	4.64	4.76
Apr	3.63	5.21	3.50	5.18	3.23	4.80	5.25
May	3.81	5.61	3.58	5.34	3.21	4.71	5.62
Jun	3.32	5.03	3.09	4.69	2.76	4.03	5.08
Jul	3.68	5.47	3.43	5.15	3.07	4.48	5.49
Aug	3.80	5.49	3.62	5.37	3.30	4.88	5.50
Sep	2.99	4.28	2.96	4.40	2.80	4.23	4.41
Oct	2.56	2.98	2.67	3.24	2.65	3.27	3.29
Nov	2.63	2.79	2.92	3.19	3.06	3.37	3.39
Dec	2.68	2.76	3.08	3.24	3.31	3.50	3.54
Ann Avg	3.22	4.24	3.26	4.35	3.15	4.16	4.53

Nairobi, Kenya
 Average Daily Peak Sun Hours, kWh/m²
 Latitude: 1° 18'S Longitude: 36° 45'E

Month	Array tilted at Latitude – 15°		Array tilted at Latitude		Array tilted at Latitude + 15°		2-Axis Tracking Array
	Fixed Array	1-Axis Tracker	Fixed Array	1-Axis Tracker	Fixed Array	1-Axis Tracker	
Jan	6.93	8.57	6.46	8.08	5.67	7.02	8.62
Feb	7.14	8.95	6.89	8.73	6.29	7.92	8.96
Mar	6.41	8.17	6.49	8.35	6.26	7.98	8.37
Apr	5.32	6.78	5.65	7.29	5.75	7.36	7.40
May	4.40	5.51	4.86	6.21	5.13	6.55	6.57
Jun	4.13	5.09	4.66	5.88	5.02	6.34	6.41
Jul	3.46	4.37	3.81	4.98	4.02	5.32	5.35
Aug	4.02	5.19	4.30	5.68	4.42	5.83	5.84
Sep	5.26	6.80	5.42	7.08	5.33	6.91	7.09
Oct	5.80	7.44	5.69	7.37	5.32	6.81	7.48
Nov	5.93	7.49	5.60	7.12	5.01	6.26	7.52
Dec	6.52	8.06	6.03	7.52	5.24	6.44	8.15
Ann Avg	5.44	6.87	5.49	7.02	5.29	6.73	7.31

Mexico D. F., MexicoAverage Daily Peak Sun Hours, kWh/m²

Latitude: 19° 33'N Longitude: 99° 18'W

Month	Array tilted at Latitude – 15°		Array tilted at Latitude		Array tilted at Latitude + 15°		2-Axis Tracking Array
	Fixed Array	1-Axis Tracker	Fixed Array	1-Axis Tracker	Fixed Array	1-Axis Tracker	
Jan	4.32	5.06	4.90	5.85	5.23	6.23	6.27
Feb	6.24	7.39	6.86	8.17	7.11	8.40	8.41
Mar	7.71	9.51	7.99	9.96	7.86	9.74	9.99
Apr	6.22	8.07	6.07	8.02	5.64	7.41	8.13
May	5.93	7.84	5.57	7.45	4.97	6.56	7.86
Jun	4.94	6.66	4.58	6.20	4.06	5.32	6.72
Jul	4.92	6.64	4.60	6.24	4.10	5.42	6.67
Aug	5.43	7.19	5.22	7.02	4.78	6.37	7.20
Sep	5.00	6.51	5.04	6.69	4.84	6.41	6.70
Oct	4.45	5.67	4.82	6.15	4.87	6.22	6.26
Nov	4.50	5.29	5.06	6.04	5.36	6.38	6.40
Dec	4.51	5.54	5.23	6.49	5.68	6.99	7.07
Ann Avg	5.36	6.78	5.50	7.04	5.38	6.79	7.31

Stockholm, SwedenAverage Daily Peak Sun Hours, kWh/m²

Latitude: 59° 21'N Longitude: 17° 57'E

Month	Array tilted at Latitude – 15°		Array tilted at Latitude		Array tilted at Latitude + 15°		2-Axis Tracking Array
	Fixed Array	1-Axis Tracker	Fixed Array	1-Axis Tracker	Fixed Array	1-Axis Tracker	
Jan	1.43	1.43	1.67	1.67	1.81	1.81	1.81
Feb	2.46	2.47	2.76	2.76	2.91	2.91	2.91
Mar	3.85	4.63	4.02	4.85	3.99	4.74	4.86
Apr	4.12	5.82	4.05	5.77	3.82	5.34	5.86
May	5.17	8.16	4.91	7.76	4.52	6.83	8.18
Jun	5.45	8.94	5.12	8.33	4.67	7.14	9.03
Jul	5.27	8.51	4.98	8.00	4.56	6.95	8.56
Aug	4.57	6.79	4.42	6.62	4.13	6.00	6.80
Sep	3.46	4.42	3.52	4.53	3.42	4.34	4.54
Oct	2.09	2.20	2.25	2.38	2.30	2.41	2.43
Nov	1.09	1.09	1.25	1.25	1.34	1.34	1.34
Dec	1.05	1.05	1.24	1.24	1.35	1.35	1.35
Ann Avg	3.33	4.63	3.35	4.60	3.24	4.26	4.81

Appendix B

A PARTIAL LISTING OF PV-RELATED WEB SITES

The following web sites represent a small sample of the hundreds of web sites that list information on solar and renewable energy. The skilled web surfer will be able to find many more useful sites in a relatively short time. Listing of a web site in this appendix does not constitute any endorsement by the authors or publisher. Also, since web sites change continually, not all sites listed may exist at the time of reading of this appendix.

Irradiance Data	http://rredc.nrel.gov/solar/pubs/ http://rredc.nrel.gov/solar/old_data/nsrdb/redbook/sum2/ http://wrdc-mgo.nrel.gov/ http://solstice.crest.org/renewables/solrad/	
PV System Components	http://www.shellsolar.com	(module manufacturer)
Manufacturers and Distributors	http://www.asepv.com http://www.kyocera.com http://www.astropower.com http://www.sharpusa.com http://www.evergreensolar.com http://www.bpsolar.com http://sma-america.com http://www.xantrex.com http://www.omnion.com http://www.realgoods.com http://www.SouthwestPV.com http://www.windsun.com http://www.solardirect.com http://www.alt-energy.com http://www.eco-web.com http://www.poweriseverything.com http://www.altenergystore.com http://desotoenergy.com http://www.cetsolar.com http://www.mayberrys.com http://www.batteries4everything.com (batteries) http://www.unirac.com (array mounts) http://www.zomeworks.com (array mounts)	(module manufacturer) (module manufacturer) (module manufacturer) (module manufacturer) (module manufacturer) (module manufacturer) (inverters, etc.) (inverters, etc.) (inverters, etc.) (retail distributor) (retail distributor) (retail distributor) (retail distributor) (retail distributor) (retail distributor) (retail distributor) (retail distributor) (retail distributor) (generator distributor)
Organizations, Energy Data and Utility PV Projects	http://www.austinenergy.com http://www.smud.org http://www.bpu.state.nj.us http://www.eia.doe.gov/emeu/aer http://www.sandia.gov http://www.dsireusa.org	(utility) (utility) (state regulator) (energy information) (research lab) (state programs)

Environmental Sites	http://www.epa.gov/air/data/index.html http://www.wri.org/wr-96-97/ac_txt6.html http://www.worldbank.org http://www.clean-power.com http://www.epa.gov/airmarkt/trading/buying.html
Financial Information Sites	ftp://ftp.bls.gov/pub/special.requests/cpi/cpiai.txt http://djindexes.com ftp://ftp.ny.frb.org/prime/Prime.txt

In addition to the sites listed, the following site, maintained by the Florida Solar Energy Center, contains an extensive list of links to a wide range of energy-related activity. General categories of the links available include:

Codes, Standards and Accreditation - Organizations and Associations
Colleges and Universities
Electrical, Construction and Labor - Unions, Organizations and Associations
Electric Utilities, Organizations and Research Centers
Electric Vehicles, Wind and Hydroelectric Energy Systems
Electrical, Electronic, Mechanical and Industrial Equipment
Energy Efficiency and Renewable Energy-Related Directories and Link Lists
Energy-Efficient Lighting, Appliances, Equipment and Building Supplies
Hoff's Clean Power Estimator
International Governments and Organizations
National Laboratories and Research Institutes
Photovoltaic Systems, Components and Engineering
Renewable Energy Education and Training
Renewable Energy-Related Non-Governmental Organizations, Associations and Information
Renewable Energy-Related Government Agencies, Departments and Laboratories
Space, Meteorological and Ocean Information
Software and Computer
Science, Technology and Consumer Information
Solar Thermal Equipment - Domestic Water and Pool Heating and Desalination
Solar Radiation Data and Instruments
State of Florida - Government, Departments and Organizations
U.S. Federal - Government, Departments and Organizations
Water World

For information on any of these areas, go to

<http://www.fsec.ucf.edu>

Appendix C **DESIGN REVIEW CHECKLIST**

The purpose of this textbook has been to prepare the engineer for the design of photovoltaic systems. The purpose of this Appendix is to provide a checklist against which the system designer can verify that sufficient information has been provided in the design to meet the needs of whoever is given the tasks of design review, installation, inspection, operation and maintenance of the designed system. To this end, the Florida Solar Energy Center has developed a *Design Review Checklist and Reporting Form*. Following is a list of the items on the Checklist that should be addressed in any grid-connected system design. The complete form, with space for comments on compliance, is available on the FSEC website (www.fsec.ucf.edu).

If design projects are assigned for a course that uses this book, it is recommended that the designs contain the information listed in this appendix.

I. System Documentation

A complete system documentation package is a fundamental requirement for system approvals. As a minimum, the system documentation package should include the following items. This information should be delivered to the end-user upon completion of the installation.

1. System description and specifications.
2. Lists and specifications for parts and equipment supplied and not supplied with any package system.
3. Electrical diagrams and schematics with all items in the following section on electrical design.
4. Mechanical drawings with all items in the following section on mechanical design.
5. System installation and checkout procedures.
6. Safety instructions and hazard warnings for installation, operation and maintenance of the system.
7. Owner's operating instructions.
8. Owner's manuals, specification sheets and warranty information for individual major system components.

II. Electrical Design

The electrical system design must be consistent with the latest version of the *National Electrical Code* and should, as a minimum, provide a system schematic diagram that includes the following information. Local code enforcement officials may require an engineering seal on the electrical prints.

1. Description of methods and materials for wiring of the PV modules, panels and arrays.

2. Specification of appropriate types, sizes, ratings and locations for all system conductors.
3. Specification of the appropriate types, sizes, ratings and locations for conduit, wireways and junction boxes to be used in the installation.
4. Specification of appropriate ratings and locations for required overcurrent devices.
5. Specification of appropriate ratings and locations for required disconnect devices.
6. Specification of requirements, conductors and locations for equipment and system grounding.
7. Specification of and diagrams for the methods and equipment required to interface the PV system output with the electric utility grid.

III. Mechanical Design

Methods for the safe, secure and durable attachment of PV arrays to rooftops or other support structures is an essential part of a complete design package. Local code enforcement officials may require a mechanical engineer to seal the mechanical prints. The prints, as a minimum, should include the following information on mechanical components of the system.

1. For rooftop mounting, guidelines for locating and orienting the array on the rooftop.
2. Guidelines for the mechanical assembly of modules and panels.
3. Specification of hardware for proper mechanical assembly of modules and panels.
4. Diagrams and procedures for making structural attachments to roofs.
5. Specification of hardware for making structural attachments to roofs.
6. Description of appropriate methods of weathersealing rooftop attachment points.
7. Independent test results or engineering approval that the array mounting system design is capable of withstanding maximum forces anticipated for the location of the system (e.g., wind, snow or earthquake loads.)

IV. PV Modules and Array

Information should be provided that verifies that the PV modules proposed for the system have been properly listed, along with performance data for the modules. As a minimum, the following information should be supplied.

1. Module performance test results from an independent test laboratory.
2. Indication of compliance with IEEE 1262, IEC 61215 or 61646 module qualification tests.
3. Indication of compliance with UL 1703 or equivalent product safety testing.

V. Power Conditioning Equipment and Batteries

As a minimum, the following information should be provided for inverters, chargers, charge controllers, batteries and other power processing equipment.

1. Compliance of inverter with UL 1741 and IEEE 929-2000 if used in a grid connected system.
2. Evidence that voltage operating windows under temperature extremes are acceptable.
3. Verification that charge controller set points are appropriate for the system batteries that are selected.
4. Locations for power conditioning equipment and batteries that are consistent with appropriate codes.